Ground Gas Source, Migration and Hazard: A Conceptual Model

Christopher J. Teasdale

Thesis submitted in fulfilment of the requirements for the degree of Doctor of Philosophy in the Faculty of Science, Agriculture and Engineering

December 2016

Newcastle University, Newcastle upon Tyne, UK, NE1 7RU

In loving memory of my father
Maurice Leslie Teasdale
(3^{rd} August 1944 – 19^{th} November 2015)

Declaration

I hereby certify that this work is my own, except where otherwise acknowledged, and that it has not been previously submitted for a degree at this or any other university.

Christopher J. Teasdale

21st December 2016

Acknowledgements

I would like to gratefully thank my supervisors, Dr Jean Hall, Prof. David Manning (School of Civil Engineering and Geosciences, Newcastle University) and John Martin (TerraConsult Ltd) for their support and guidance throughout my time at Newcastle University. I am indebted to them for their time, knowledge and expertise.

I would like to acknowledge EPSRC and TerraConsult Ltd for their financial support and for the training that TerraConsult Ltd has provided during my research. I would particularly like to thank Graham Boultbee for passing on his expertise and for the great camaraderie in the field.

The laboratory and workshop staff at Newcastle University has been a major contributor to the project by constructing a borehole in the laboratory in order to test carbon dioxide and methane diffusion. I would like to thank Robert Hunter, David Innes, David Dick, and Matthew Johnson for helping with the design and construction of the borehole. I am especially grateful for their time and patience. Other members of staff I would like to thank for their support are Stuart Patterson, William Cragie and Philip Green.

I am especially grateful to Paul Donohoe for his guidance with GC-MS analysis. Furthermore, I would like to thank him for conducting the IR-MS analyses of samples. Other members of staff that I would like to acknowledge for their guidance are Bernard Bowler, David Earley and David Race. Additional IR-MS analyses of samples were conducted at the University of California Davis Stable Isotope Facility, CA, USA by Richard Doucett and I would like to acknowledge this invaluable contribution to the research.

Lastly, on a personal level, I would like to say a big thank you to Mhari Barnes, Emma Bell, Matthew Cracknell, Peter Gilbert, Christopher Iliffe, Elizabeth Lewis, Samantha Mahaffey, Douglas Richardson, Katherine Rothwell, Luke Smith, Charlotte Spencer-Jones and David Walker, whose friendship and banter over beer / coffee / tea / cake / pizza has kept me sane and has got me here today.

Abstract

For the first time in human history the global atmospheric CO_2 concentration has surpassed 400 ppm and is projected to reach 600–800 ppm by A.D. 2100. A positive feedback in average global temperatures relating to an increase in CO_2 levels in the upper atmosphere has been well-documented. With a global warming potential 25 times that of CO_2 over 100 years, CH_4 is also considered to be a significant greenhouse gas. Understanding and managing the exchange of CO_2 and CH_4 between the geosphere and atmosphere as a part of the global carbon cycle is consequently an important geotechnical engineering challenge of the 21st Century.

A conceptual model of ground gas dynamics in the near-surface was developed with wider implications for the geotechnical engineering industry activities in the near-surface and deep subsurface. Evidence was collated from historic gas monitoring data, high temporal frequency gas monitoring data, stable isotope analysis, and modelling and measuring gas transport mechanics in order to compile a conceptual model.

Historic ground gas monitoring of landfill sites provided an extensive data resource. Routine point measurement of CH_4 and CO_2 in the sub-surface has not enabled gas transport mechanisms to be fully understood. Emission events may be overlooked by this method. By monitoring gases at high temporal frequency (up to every three minutes) this study has attempted to resolve the relationship between ground gases and the atmosphere. As a result, barometric pumping was proven to be a major control on CH_4 and CO_2 emissions from the near-surface.

Data yielded from a high temporal frequency gas monitoring campaign in 2013, showed that an average pressure gradient of -0.7 mbar/hr was sufficient to induce a gas release from the near-surface comprising 40.1% CH_4 and 7.9% CO_2. The cycling of air and ground gases was shown to be rapid, often occurring over three hours or less. Crucially, only air was present in the test borehole for 70% of the period indicating the fragility of point measurement strategies.

Gas source is an important aspect of regulation. For sites with multiple anthropogenic environments and/or complex geology could have multiple ground gas sources. In the event of gas emission or leaks, liability is critical. Stable isotope ratio analysis was used to differentiate between biogenic and thermogenic gas sources. Gases were sampled from municipal landfill sites in Greater Manchester and Cheshire, UK, that indicated multiple gas sources.

Landfill flare gas CH_4 yielded $^{13}\delta C_{CH_4}$ −65.0‰ and δD_{CH_4} −319‰ while perimeter monitoring wells produced $^{13}\delta C_{CH_4}$ −55.0‰ and δD_{CH_4} −173‰ which compared with mineshaft vent gas CH_4 which yielded $^{13}\delta C_{CH_4}$ −50.5‰ and δD_{CH_4} −208‰. This suggested that CH_4 originating from underlying Coal Measures had been transported via the weathered top-surface of the bedrock or via a fault and had mixed with landfill gas in the perimeter monitoring wells. At the Greater Manchester site, gas sources were differentiated and it was proven that coal gas was an environmental hazard in the locality.

Gas transport was modelled by diffusion using Fick's Law. A novel approach to measuring gas transport was conducted using a specially designed 'artificial borehole' experimental apparatus. A closed-system, the artificial borehole data indicate that gas transport was diffusive when subject to an additional 50 mbar pressure in addition to ambient pressure. Fick's Law was shown to predict CO_2 diffusion transport curves between t = 0 and t = 4 hr. Diffusion was shown to be an efficient process initially. However, the data did not fit the model after t = 24 hr and uniform concentration was achieved through the apparatus at t = 168 hr (1 week). Consequently, advective transport may supersede diffusive transport. When the apparatus was sand-filled, the data showed that diffusion efficiency was reduced due to an increase in tortuosity of CO_2 transport path.

These components were used to develop a widely-applicable conceptual model of ground gas dynamics in the near-surface. The data presented here have far-reaching implications for industry, policy makers and regulators; particularly concerning hydraulic fracturing ('fracking'), and carbon capture and storage (CCS). The methodology for high temporal frequency gas monitoring is recommended to establish baseline gas concentration, establish the effect of industry on the natural system and to detect and quantify any leak and migration of CH_4 and CO_2. Combined with knowledge of site geology it should be possible to predict lateral gas transport in the near-surface environment.

Contents

List of Figures

List of Tables

Chapter 1

Introduction

1.1 Carbon Dioxide and Methane Gases in the Environment

Understanding the gas exchange of carbon dioxide (CO_2) and methane (CH_4) between the geosphere and atmosphere is of paramount importance to managing future human-made emissions of these gases. Since the advent of industrialisation in the 18^{th} Century, human activities have caused atmospheric concentrations of CO_2 to increase at an accelerating pace. The pre-industrial concentration of atmospheric CO_2 was 280 ppm and subsequently increased to an excess of 390 ppm by the early 21^{st} Century (Solomon et al., 2007). As recently as 2013, the daily atmospheric CO_2 concentration was recorded at 400 ppm for the first time (Jones, 2013). The global CO_2 concentration is projected to reach between 600 and 800 ppm by A.D. 2100 (Solomon et al., 2007).

A well-documented association has been established between the rise in CO_2 levels in the Earth's atmosphere and global climate change. Practical effects resulting from extraction and burning of fossil fuels include an increase in extreme weather events such as heat waves, droughts, heavy rainfall, flash flooding, and global sea level rise (Hansen et al., 2016). Owing to the persistence of CO_2 in the atmosphere over thousands of years (Archer, 2005), undesirable effects of climate change may irreversibly be locked-in. Owing to its longer residence time in the upper atmosphere, CH_4 has a global warming potential 25 times that of CO_2 when compared over 100 years (Scheutz et al., 2009). Additionally, CH_4 possesses a stronger molar absorption coefficient for infrared radiation than CO_2 (Solomon et al., 2007).

The Kyoto Protocol (1997), an international treaty with the aim of reducing greenhouse gases in the atmosphere, was estimated to cost the UK in 2010 between £6.2 billion (1.1% GDP) and £17.4 billion (3.1% GDP) with respect to its com-

pliance with its 2012 emissions target (Jones, 2008). In December 2015, the Paris Agreement was sealed by the United Nations Framework Convention on Climate Change (UNFCCC) and was opened for signatories on 22nd April 2016. An extension of the Kyoto Protocol, its focus is to accelerate and intensify the actions and investments required for a sustainable low carbon future. Governments agreed to ensure a global average temperature below 2°C above pre-industrial levels and aimed to limit the increase to 1.5°C (to significantly reduce the risks and impacts of climate change). Governments also agreed that global carbon emissions should peak as soon as possible, and to undertake rapid reductions thereafter in accordance with the best available science (European Commission, 2016). With a target to reduce carbon emissions by at least 40% by A.D. 2030, in March 2015, the EU was the first major economy to submit its intended contribution to the new agreement (European Commission, 2016). Not only does curbing global CO_2 emissions present a major environmental challenge for the 21st Century, it also requires a significant political and economic impetus.

A key unknown in CO_2 accounting is the gas exchange between the soil (defined here as the unsaturated zone, thus encompassing unconsolidated deposits as well as biologically-active soils) and the atmosphere. Figure 1.1 clearly demonstrates the environmental challenge. Over the ten year period 2005–2014, net atmospheric growth of CO_2 was 16 ± 0.4 Gt C/yr (Le Quéré et al., 2015).

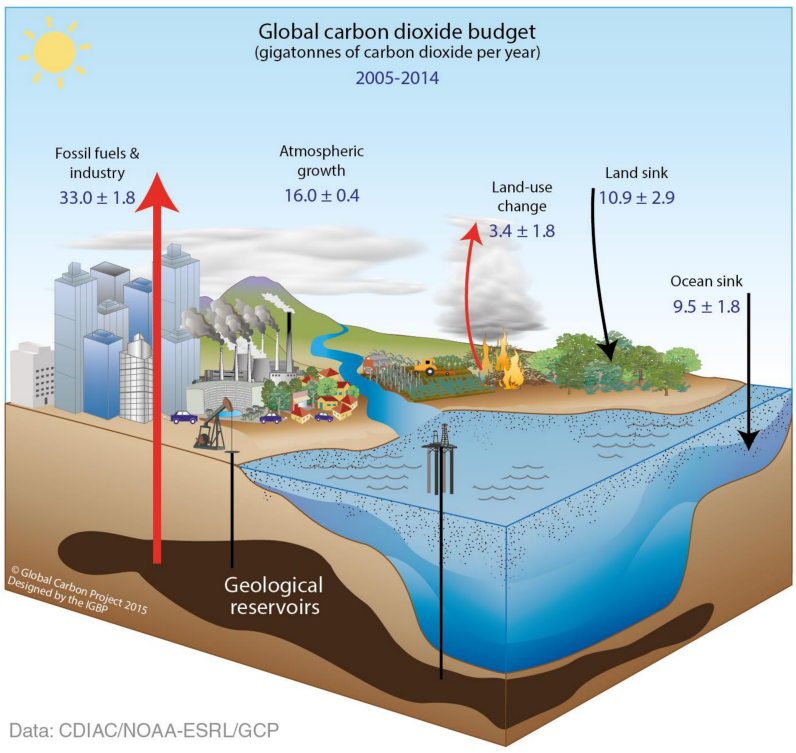

Figure 1.1: Global Carbon Dioxide Budget 2005 – 2014 (from Le Quéré et al. (2015))

The atmospheric carbon pool is 750 Gt C while organic carbon to a depth of 1 m amounts to 1,500 Gt C (Schlesinger and Andrews, 2000). Additionally, land-plant biomass accounts for $\sim$ 500 Gt C (Smith, 2004), mostly below ground within root systems. This combined terrestrial plant-soil system has a resultant annual 120 Gt C exchange with the atmosphere (Smith, 2004). By comparison, the oceans dominate as a carbon reservoir at $\sim$ 39,000 Gt C (Batjes, 1996). However, the net exchange with the atmosphere is only 90 Gt C/yr (Schlesinger and Andrews, 2000). Consequently, the soil-carbon pool has the potential to be more reactive in the short-term as it can more readily be influenced by human activity through management of land use.

To understand gas exchange between the geosphere and atmosphere, it is essential that the knowledge-base of ground gas dynamics is enhanced and expanded. The identification and quantification of baseline conditions along with natural and anthropogenic feedbacks to baseline conditions are key parameters in understanding the exchange of CO_2 between the geosphere and atmosphere. As the carbon terrestrial sink arguably presents the greatest potential to be engineered to mitigate against rising atmospheric CO_2 levels, it is crucial to understand the mechanisms that form this component of the global carbon cycle.

Gas is a natural component of the geological subsurface, occurring within rock pores and fractures, and migrating in response to pressure gradients (i.e. generally to the surface, unless trapped). Geological gases have a wide range of compositions, depending on their origin. CO_2 and CH_4 are formed naturally as a consequence of the decomposition (diagenesis) of organic matter within sediments and sedimentary rocks. In deep sediments, if geological factors are right, these gases accumulate in reservoirs which form the target of petroleum exploration. Unconventional sources of natural gas include shale gas, tight gas and coal bed CH_4 (McGlade et al., 2013). Production from these sources may require artificial fracturing, and there are concerns that 'fracking' may cause gases to leak to shallow groundwater systems or to escape to the atmosphere through the soil (Davies, 2011; Davies et al., 2012).

In addition to considering geological gas as a resource, Carbon Capture and Storage (CCS) procedures require injection of CO_2 into deep formations where it is to be stored (Bachu, 2003; Bachu et al., 2007; Eccles et al., 2012). Endorsed by the Intergovernmental Panel on Climate Change (IPCC) and the UNFCCC (D'Alessandro et al., 2010), underground storage in aquifers and deep formations is technically feasible and under favourable conditions, CO_2 may be retained for millions of years (Abu-Khader, 2006; Wilson et al., 2003). Nonetheless, there are accompanying risks of leaks as well as blowouts that can endanger human life (Wilson et al., 2003). Ad-

ditionally, pumping CO_2 into deep geologic formations at high pressure may induce minor earthquakes as well as contaminating local groundwater stocks (White et al., 2003).

In this context, there is a need to understand the initial ground conditions to relate any perturbations incurred from engineering activities. Furthermore there is a need to detect and monitor any displacement of ground gases to enhance public perception and acceptance of these geotechnical engineering enterprises. Therefore, the development of methodologies and strategies to accurately detect and measure CH_4 and CO_2 in the unsaturated zone originating from deeper geology is a key environmental concern. The value of studying this compartment of the land carbon sink is particularly important when considered in the wider global carbon cycle and climate forcing resulting from atmospheric growth of CO_2.

The Research Gap

In the context of the hydraulic fracturing and CCS industries, there is a clear need to identify baseline ground conditions before engineering works begin. Work into the development of detection, measurement and quantification of CH_4 and CO_2 ground gases is required. Furthermore, research is required to determine the period of time that best establishes baseline conditions. Once baseline conditions have been confidently characterised, any changes to the system during and after engineering works may readily be identified. The on-going monitoring of these facilities is essential for a positive public perception and approval.

Further enhancement of the understanding of the dynamic ground gas regime may be achieved through the determination of gas transport mechanics. A robust methodology is required to test these dynamics. This could be used to predict changes to the ground gas regime on geologic time-scales and ultimately the hazard posed by ground CH_4 and CO_2 for a given locality.

Importantly, there are differing schools of thought on the terrestrial carbon sink: soil scientists concerned with the top metre of organic material and geotechnical engineers concerned with the deeper geology. Each prioritise the factors that control CH_4 and CO_2 exchange between the geosphere and atmosphere differently. Also, the time-scales examined by soil scientists may be diurnal, weekly, monthly or seasonal as opposed to geotechnical engineers that may be examining changes over thousands of years. Therefore, there is a need to review and link the perceptions between these schools of thought.

1.2 Aim and Objectives

The aim of this research was to develop a widely-applicable conceptual model that characterises the source, lateral transport and hazard of naturally occurring CO_2 and CH_4 along with CO_2 and CH_4 contained within engineered environments such as municipal landfills in the near-surface. It was an ambition that the conceptual model should be able to characterise baseline conditions and predict flux of CO_2 and CH_4 from the unsaturated zone in response to natural and anthropogenic perturbations to the system.

The specific research objectives were as follows:

- To undertake a literature review encompassing the chemical, physical and hazardous properties of ground gases; sources of ground gases; gas migration and emission; and historic incidents of gas emissions;
- To establish a baseline of CO_2 and CH_4 concentration in the near-surface ground gas environment and natural variations in response to meteorological conditions;
- To analyse historical data for sites in NW England of comparable geologies that overlie the Bowland-Hodder Shales where shale gases may be exploited in the future and extend these data sets forward to gain a comprehensive understanding of baseline conditions;
- To capture and interpret high temporal frequency gas monitoring at municipal landfills for which historic data point-measurement data exist;
- To develop methodologies for high temporal frequency ground gas monitoring for municipal landfills that could be applied to other engineered environments;
- To sample landfill gases from municipal landfill sites with suspected multiple gases sources and analyse by stable isotope ratios to determine gas origin. Subsidiary objectives relating to stable isotope analysis were:
  - To compare methodologies of stable isotope analysis;
  - To determine the effective storage time of samples kept in evacuated containers;
- To investigate the mechanics of gas transport in the near-surface ground gas environment by undertaking a series of laboratory-based experiments that synthesise conditions encountered at the research municipal landfill sites, and;
- To develop and design a widely-applicable ground gas conceptual model outlining source, migration and hazard based upon the findings of this research.

Scope of Research

The data presented in this thesis are not intended to be an exhaustive collation of the available historic and current ground gas data. Only data originating from municipal landfill sites was examined. Data from other engineered environments such as abandoned mine shaft vents, carbon sequestration sites, hydraulic fracturing sites, etc, were not considered. An emphasis was placed on the research and development of existing and new methodologies for the detection and measurement of ground gases. In this endeavour, the establishment of longer term trends was confined to the finite resources of this project. The monitoring of ground gases was curtailed by the availability of equipment and the time constraints of the research. Novel data presentation approaches were developed to ease interpretation and comparison between different borehole characteristics and between different sites. Gas transport mechanics were modelled on the assumption of diffusive flow according to Fick's Law. However, other mechanistic and statistical approaches could have been adopted or examined. These are also outside the scope of this research. It was intended that once the methodologies presented in this thesis had been established and refined, that they could be used to expand the database in future research.

1.3 Thesis Structure

Chapter 2 – Literature Review

This thesis begins with detailing the literature concerning ground gas hazards, sources, migration and emission risks along with case studies of historic incidents of uncontrolled ground gas release that have resulted in damage to property, injury or death.

Chapter 3 – The Research Sites

As was stated in the objectives, the research sites were specifically chosen for their location within future shale gas exploration in the UK. Their geology is crucial for examining ground gases and their geologies are outlined in Chapter 3.

Chapter 4 – Review of Historic Gas Monitoring Data

Chapter 4 reviews the historic gas monitoring data from the research sites update to 30th June 2015. The data were derived from point measurement of ground gases using portable monitors such as the GA2000 (Geotechnical Instruments (UK) Ltd) and GFM435 (Gas Data Ltd). Some data sets were 20 years old and provided a

useful database. This chapter uses a novel approach to representing multiple gas concentrations in ternary diagrams to ease interpretation of gas composition. An initial conceptual model was designed based on these data.

Chapter 5 – High Temporal Frequency Data

Building from Chapter 4, Chapter 5 examines the high temporal frequency data collected from the research sites. It builds on the conceptual model design initially proposed in Chapter 4. The high temporal frequency data demonstrated the 'breathing' of the ground during sharp falls in atmospheric pressure resulting in the release of CH_4 and CO_2. These data are related back to the historic gas monitoring data reviewed in Chapter 4.

Chapter 6 – Determination of Gas Source

Arising from the historic data review, it was apparent that multiple gas sources may have been present at one of the research sites. Chapter 6 details a methodology for sampling of ground gases from monitoring wells, analytical analysis of gases by GC-MS and compound specific IR-MS. Likely gas sources based on 'gas signatures' are deduced from stable isotope ratios.

Chapter 7 – Gas Transport Mechanics

Chapter 7 presents experimental data derived from a 'artificial borehole' experimental rig. The rig was designed to simulate a geotechnical engineered borehole typically used to monitor ground gases and groundwater levels. The aim of the 'artificial borehole' testing was to investigate gas transport mechanics in the unsaturated zone.

Chapter 8 – Conceptual Model

Adjustments and refinements were made to the conceptual model design based upon evidence collected from each chapter. A final design is presented and discussed in Chapter 8. Data were contrasted with data from the existing literature. The methodologies for gas monitoring presented in this thesis were related to industry applications with respect to the importance of time-scale and changes in a dynamic system. An emphasis was placed on the implications arising from the presented data and the conceptual model for the industrial sector.

Chapter 9 – Conclusion

A summary of the work conducted in this thesis is given in Chapter 9 along with the wider implications for industry and recommendations for expansion and progression of this research in the future.

1.4 Outline Methodology

In order to meet the objectives of this project, investigations were conducted into four principal threads of research. Each may be compartmentalised into their own methodology sections and are summarised below.

Research Sites and Historic Gas Monitoring Data Compilation

Municipal landfills provide useful engineered environments with a plentiful source of CH_4 and CO_2 gases to research and develop methodologies for quantifying ground gases. It is these methodologies that could also be applied to the regulation of hydraulic fracturing and CCS. A requirement of landfill regulation is the monitoring of ground gases through an array of internal and perimeter monitoring wells. A range of geotechnical instruments to monitor ground gases is commercially available for contractors to meet these regulation obligations.

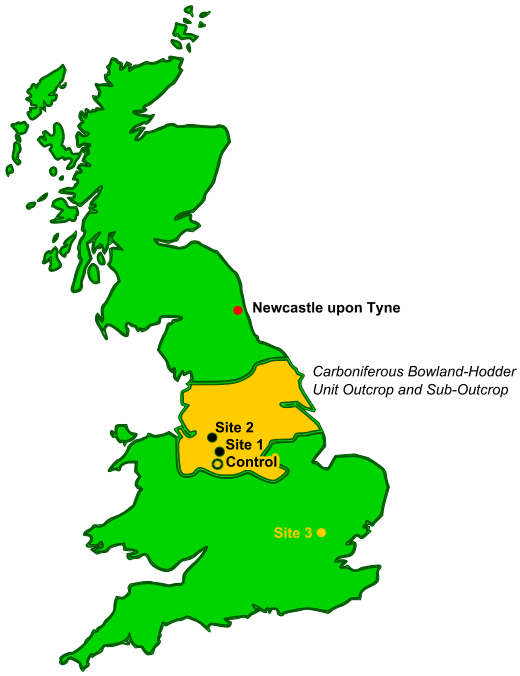

Figure 1.2: Location of the Bowland-Hodder Outcrop and Sub-Outcrop within the British Isles and the Position of the Research Sites within the Future Potential Shale Gas Exploration Area (adapted from Andrews (2013))

Data derived from routine monitoring of landfill sites form an extensive database that can be examined and reviewed. In some instances, landfill monitoring data extend over a 20 year period. Landfill sites were selected due to the presence of a thick layer of unconsolidated Quaternary deposits where lateral gas transport could readily be tracked. The majority of the research sites were located within the future Shale Gas exploration area in the UK (Figure 1.2). Consequently, the research presented in this thesis is pertinent in the wider context of hydraulic fracturing, CCS, the global carbon cycle, and mitigation of future human-made CO_2 emissions.

The data used in this study have been derived from peripheral monitoring of landfill sites and similar artificial environments. The variation of landfill gas composition within a landfill was not directly considered. Instead, the emphasis was placed on gas compositions in boreholes designed to monitor possible migration of landfill gas into the surrounding ground. At these sites there is a regulatory requirement for monitoring ground gases both outside and inside the site, providing a substantial database that extends many years. Historically, gas composition was measured in accordance with regulatory requirements using hand-held gas monitors. Measurements were made using a Geotech UK GA2000 Landfill Gas Analyser until 2012, after which, a Gas Data Ltd GFM435 Landfill Gas Analyser was used.

The graphical approach presents compositional data compared in terms of the measured CH_4, CO_2 and O_2 content normalised to nitrogen (assuming N_2 to be the balance, i.e. 100 - (Σ CH_4 + CO_2 + O_2)), in a ternary plot. This allowed the relative proportions of CH_4 and CO_2 to be compared irrespective of any dilution by air, the O_2/N_2 ratio indicated whether this had occurred and the extent to which O_2 had been removed. In a plot of this type, 'end member' compositions could be identified so that an array of observed data points could be explained as mixtures of gases from different sources. Therefore, the characteristics of one borehole may be compared with another (Teasdale et al., 2014).

High Temporal Frequency Gas Monitoring Data Capture

GasClam®, developed by IonScience Ltd and distributed through ShawCity Ltd, is a high-frequency, continuous, fully automated ground gas monitor. It is capable of a maximum sample rate frequency of every three minutes. Like traditional hand-held monitors, it measures CH_4, CO_2, O_2 as well as H_2S and Volatile Organic Compounds (VOCs). Additionally, it is capable of measuring ambient temperature, ambient pressure, borehole pressure, pressure difference and water depth. However, the model used for this research was not equipped with the water depth gauge. Importantly, the GasClam has been used to monitor ground gas concentrations by

Cuadrilla Resources Ltd during Shale Gas exploration in Lancashire, UK during the time-frame of this research (Wadey-Leblond, 2012).

During data capture, the GasClam was set to take a sample of all parameters every thirty minutes. A major problem with point measurement instruments is the disruption of ground conditions within a monitoring well. Therefore, the GasClam was set to vent closed mode, as per manufacturer guidelines. Spent samples were purged into the borehole. An analysis of the data was produced and contrasted with the historic point measurement data.

Stable Isotope Analysis of Gas Samples

Gas samples were collected from monitoring wells on research municipal landfill sites and from abandoned mine shaft vents. Flared landfill gas and mine shaft vent gases were used as reference gases. Samples were subject to Compound-Specific Isotope-Ratio Mass Spectrometry (IRMS) analysis. The results demonstrated distinctive 'isotopic signatures' depending on gas source, thereby permitting the differentiation of gas origin.

Simulation of Gas Transport Mechanics

Gas transport was modelled according to Fick's Law of Diffusion. The modelled data were used as a benchmark to compare experimental results against. A 3 m high 'artificial borehole' was constructed in order to test gas transport mechanics. Gas standards were injected into a reservoir at the base of the apparatus and the progress of gas transport was monitored by sampling of gas through sample ports located at regular intervals up the side of the apparatus. Samples were stored in 12 ml exetainers prior to analysis. The concentration of CH_4 and CO_2 at a given distance from source and at a given time was calculated through GC-MS analysis of samples. Compilation of results yielded transport curves for specific times after the start of each experiment. These data were interpreted in the context of diffusion models.

Chapter 2

Literature Review

2.1 Introduction

This chapter introduces the chemical, physical and hazardous properties of common hazardous ground gases in the context of this project. It will discuss the anthropogenic and natural sources of these gases and how they are generated in the near-surface regime. Strategies for monitoring these gases during ground investigations and a review of the current literature examining the migration and emission of ground gases from the vadose zone will also be examined.

2.2 Chemical and Physical Properties of Common Hazardous Ground Gases

A summary of the chemical and physical properties of hazardous gases commonly found in the ground that are of importance to this investigation is provided in Table 2.1.

Property	**Methane**	**Carbon Dioxide**	**Carbon Monoxide**	**Hydrogen Sulphide**	**Hydrogen**
Chemical Formula	CH_4	CO_2	CO	H_2S	H_2
Molecular Weight	16	44	28	34	2
Melting Point (°C)	-184	Sublimes at	-205	-85	-259.14
Boiling Point (°C)	-164	-78.5	-191	-61	-252.87
Density (kg/m^3)	0.71	1.98	1.25	1.53	0.085
Solubility in H_2O at STP (mg/l)	25	1,450	21.4	4,100	1.62 at 21°C
Viscosity (Ns/m^2)	1.03×10^{-5}	1.4×10^{-5}	1.66×10^{-5}	1.0×10^{-5}	8.7×10^{-6}
Diffusion Coefficient in Air (m^2/s at STP)	1.5×10^{-5}	1.39×10^{-5}	1.96×10^{-5} at 9°C	1.76×10^{-5}	6.1×10^{-5}

Table 2.1: Chemical and Physical Properties of Hazardous Ground Gases (adapted from Hooker and Bannon (1993))

2.2.1 Methane

Methane is a colourless, odourless and flammable gas that occurs naturally in the environment following the anaerobic degradation of organic material. It is the most abundant organic compound in the Earth's atmosphere and is formed in many different environments (Wilson et al., 2006). It has a very low solubility in water at Standard Temperature and Pressure (STP). Its solubility increases proportionally with increasing temperature (Buryakovsky et al., 2005). Chemically inert, CH_4 does not readily react with other substrates but is known to react violently with chlorine (Cl_2) and bromine (Br_2) gases in the presence of direct sunlight at STP.

Due to its absorbance and emission of solar radiation in the thermal range of the infrared spectrum, it is considered to be an important greenhouse gas. With a global warming potential (GWP) 25 times greater than CO_2 over 100 years, its emission to the atmosphere is considered to be one of the greatest environmental challenges of the 21st Century (Nosalewicz et al., 2011; Scheutz et al., 2009). However, with a lifetime of 12±3 years in the atmosphere, the 20-year time horizon GWP value of 56 is a more realistic assessment (UNFCCC, 2015). It is this larger value that authors such as Howarth et al. (2011) argue should be quoted when referring to CH_4 GWP.

2.2.2 Carbon Dioxide

Like CH_4, CO_2 is a colourless and odourless gas. It is used as the benchmark from which other greenhouse gas GWPs are derived. As such it is assigned a GWP value of 1. However, its lifetime in the atmosphere is variable, unlike CH_4 which is more stable (UNFCCC, 2015). It is formed naturally by aerobic and anaerobic degradation of organic materials, action of acid water in carbonate rocks, and respiration of soil bacteria (Hooker and Bannon, 1993). At high concentrations it has a slight acidic taste. Due to its higher density than air, CO_2-rich gas mixtures tend to accumulate in low-lying areas. Unlike CH_4, it is non-combustible and is highly soluble in water. In solution it forms a corrosive liquid as it reacts with water to yield carbonic acid (H_2CO_3) as pH values descend below 6.4 (Drever, 1997) (Figure 2.1).

Local variations in atmospheric CO_2 concentration are known to occur. Oxidation and combustion of organic materials and plant respiration will lead to a localised inflation of CO_2 concentration. Conversely, photosynthesis of plants can lead to a localised reduction of CO_2 concentration. The global atmospheric concentration of CO_2 has increased from around 280 ppm at the advent of industrialisation to a present day excess of 390 ppm (Solomon et al., 2007) and is a major greenhouse gas.

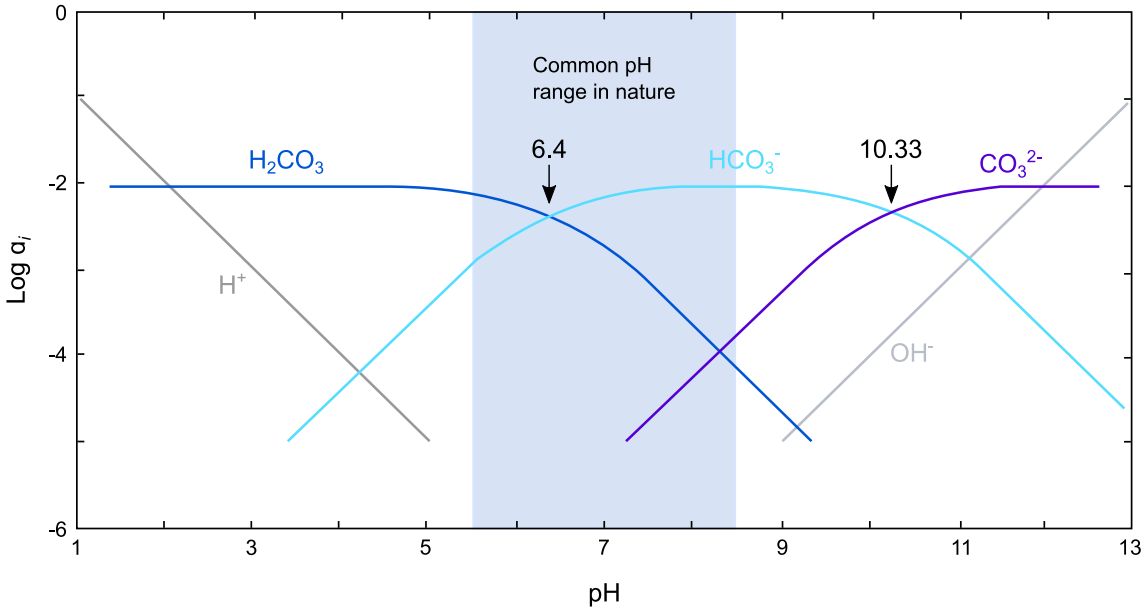

Figure 2.1: Activities of Different Species in the Carbonate System as a Function of pH (from Drever (1997))

2.2.3 Carbon Monoxide

Unlike CO_2, CO is explosive in air. It is produced as a consequence of the incomplete combustion of organic materials and is commonly formed after explosions of flammable gas or coal dust (Hooker and Bannon, 1993). In landfill waste it can also be produced by the reduction of CO_2 by nascent H_2. It is soluble in alcohol and benzene (C_6H_6) and slightly soluble in H_2O. It is a colourless, toxic, flammable, odourless and tasteless gas.

2.2.4 Hydrogen Sulphide

A colourless gas, H_2S has a characteristic, potent, 'rotten egg' smell at low concentrations (< 1 ppm). However, it becomes odourless at concentrations > 50 ppm due to anaesthesia of olfactory sense. It is readily soluble in H_2O and organic solvents such as petroleum. Decomposition of sulphur-containing organic matter generates H_2S. It can be found in the vicinity of sewage treatment plants. SO_4^{2-}-reducing bacteria obtain energy by oxidising organic matter or H_2 with sulphates (SO_4^{2-}) and produce H_2S. This commonly occurs in low-O_2 environments such as standing water. Other anaerobic bacteria produce H_2S by digesting amino acids containing SO_4^{2-} (Appels et al., 2008).

2.2.5 Hydrogen

A colourless, odourless and tasteless gas, H_2 is slightly soluble in aqueous and alcoholic solutions. Although non-toxic, it is combustible. In the ground it is formed by the chemical reaction between H_2O and a finely divided metal (e.g. Al) (Czech and Troczynski, 2010).

2.3 Hazardous Properties of Ground Gases

A summary of the hazardous properties of common ground gases is given in Table 2.2.

Property	**Methane**	**Carbon Dioxide**	**Carbon Monoxide**	**Hydrogen Sulphide**	**Hydrogen**
Hazard	Flammable and explosive	Toxic	Flammable, explosive and toxic	Flammable, explosive and toxic	Flammable and explosive
Lower explosive or flammable limit (% v/v in air)	5.0	Non-combustible	12.5	4.3	4.0
Upper explosive or flammable limit (% v/v in air)	15.0	Non-combusible	74.2	45.5	74.0
Work place 8 hour long-term exposure limit (ppm)	Non-toxic	5,000	30.0	5.0	Non-toxic.
Work place 15 min short-term exposure limit (ppm)	Non-toxic	15,000	200	10.0	Non-toxic.
Environmental assessment levels for air ($\mu g/m^3$)			350 short-term, 10,000 long-term	140 short-term, 150 long-term	

Table 2.2: Hazardous Properties of Ground Gases (adapted from Hooker and Bannon (1993) and Wilson et al. (2009))

Gaseous emissions originating from contaminated land or natural sources may constitute short-term and long-term hazards depending on the gas composition, geological conditions and proximity to a receptor. Hazards are categorised as: flammability and explosion risk, physiological effects, odour and plant toxicity and are discussed blow.

2.3.1 Flammability and Explosion Risk

The greatest risk posed by CH_4 is its fire and explosion hazard. It forms an explosive mixture with air when its concentration is between 5% v/v and 15% v/v (Cashdollar et al., 2000). Above 15% the flammability of CH_4 decreases. However, limits of flammability are affected by the composition of a mixture of gases, strength of ignition source, temperature, pressure and the nature of the surroundings (Card, 1995). Air has a diluting effect and can cause a gas composition to fall into the flammable range (Card, 1995).

If O_2 concentration is reduced, the limits of CH_4 flammability are reduced. For example, in air (O_2 20.9% v/v) the lower and upper explosive limits of CH_4 are as quoted from Hooker and Bannon (1993) above. However, at 13.45% v/v O_2, the lower and upper explosive limits of CH_4 are 6.5 and 7% v/v respectively (Wilson et al., 2006). At 13.45% v/v O_2, CH_4 is incapable of propagating a flame (Hooker and Bannon, 1993).

Carbon dioxide has a similar limiting effect on the flammability of CH_4. The range of volume of CH_4 which is explosive is narrowed and when the proportion of CO_2 reaches 25% v/v, the flammability of CH_4 is completely suppressed (Hooker and Bannon, 1993). If the ratio of CO_2 to CH_4 is greater than 3.5, the mixture will not be flammable if mixed in any proportion with air (Card, 1995).

Hydrogen forms explosive mixtures with air in the range 4 to 75% v/v H_2 (Cashdollar et al., 2000). Due to its low ignition energy and wide limits of flammability, H_2 is considered to be one of the most dangerous flammable gases. Likewise, CO and H_2S are flammable over a wide range when mixed in air.

Beresford (1989) states that there are three conditions that must be fulfilled in order for an explosion to take place: a source of flammable gas or vapour, an enclosed space in which the gas or vapour can accumulate, sufficient air for a flammable mixture and a source of ignition. A flammable gas mixture or vapour burns rapidly when ignited. If confined, the deflagration generates high explosive overpressures.

2.3.2 Physiological Effects

Physiological hazards of chemicals are dependent on the toxicity, degree, nature and length of exposure. Detrimental effects may occur on both short-term and long-term time-scales. Local effects are produced at the point of contact with the body whereas systemic effects are those produced by the chemical or its metabolites on a whole range of bodily functions, often removed from entry into the body (Hooker and Bannon, 1993).

In a confined space, the effect of the accumulation of CH_4 and/or associated gases will be to displace air and reduce the total concentration of O_2 in the atmosphere. Detrimental physiological effects of an atmosphere deficient in O_2 will vary with length of exposure and between individuals. The effects of reduced O_2 concentration are described in Table 2.3.

Oxygen % by Volume in Air	**Physiological Effect**
19–21	Normal range of concentration in the atmospheric air.
16	Faster, deeper breathing, slight impairment of judgement.
10–16	Initial signs of anoxia leading to emotional upsets and abnormal fatigue upon exertion.
6–10	Nausea, vomiting, unconsciousness, collapse may occur.
< 6	Convulsions, gasping respiration, death.

Table 2.3: Effects of Reduced Oxygen Concentration (from Edwards (1989))

Methane

Although a low toxicity gas, CH_4 can cause asphyxia due to the displacement of O_2. Symptoms of O_2 starvation develop at 33% v/v CH_4 and at 75% v/v CH_4, fatality can occur within minutes.

Carbon Dioxide

Carbon dioxide is classified as a highly toxic chemical. Physiological effects of depleted O_2 arising from elevated CO_2 are more severe by comparison with O_2 reduction resulting from elevated CH_4 concentration (Wilson et al., 2006). Carbon dioxide adversely affects the respiratory and central nervous systems (Card, 1995). Near instantaneous physiological effects are incurred as a consequence of the high solubility of CO_2 and rapid diffusion into the blood (Jensen, 2004).

Shortness of breath and headache are symptomatic of 3% v/v CO_2. The severity of these symptoms increases at 5 to 6% v/v CO_2. Headache, visual distortion, tremors and rapid loss of consciousness are diagnostic of 10 to 11% v/v CO_2 exposure. Fatality occurs at concentrations in excess of 22% v/v CO_2 (Hooker and Bannon, 1993).

Carbon Monoxide

Like CO_2, CO is classed as a highly toxic chemical. It has a much greater affinity for haemoglobin than O_2. Prevention of O_2 transport around the body is incurred by the formation of carboxyhaemoglobin. Negative effects upon human health are dependent on the initial concentration of CO in the blood, the concentration in the air,

the length of time of exposure and the level of activity of the individual. At concentrations of greater than 40% carboxyhaemoglobin seizures and coma are common, above 60% carboxyhaemoglobin unconsciousness and death is likely (Omaye, 2002). Symptoms of milder poisoning (> 20%) include headaches, dizziness, confusion and nausea (Omaye, 2002).

Hydrogen Sulphide

H_2S is graded a highly toxic chemical. It is particularly potent as its odour is detectable at concentrations less than 0.025 ppm, yet toxic effects as a result of high concentrations can be reached almost without warning as olfactory fatigue occurs around 100 ppm (Beauchamp et al., 1984). A summary of physiological effects in humans with increasing H_2S concentration is given in Table 2.4.

Concentration ppm	**Physiological Responses**
0.003–0.02	Odour threshold.
3–10	Obvious unpleasant odour.
20–30	Strong offensive odour ('rotten eggs').
30	Sickening sweet odour.
50	Conjunctival irritation.
50–100	Irritation of respiratory tract.
100–200	Loss of smell ('olfactory fatigue').
150–200	Olfactory paralysis.
250-500	Pulmonary oedema.
500	Anxiety, headache, ataxia, dizziness, stimulation of respiration, amnesia, unconsciousness.
500–1,000	Respiratory paralysis leading to fatality, immediate collapse, neural paralysis, cardiac arrhythmias, death.

Table 2.4: Human Physiological Responses to exposure of H_2S (adapted from Beauchamp et al. (1984); Reiffenstein et al. (1992))

Hydrogen

Hydrogen is categorised as a non-toxic, simple asphyxiating gas.

2.3.3 Odour

The major constituents of most soil gases are not odorous with the exception of H_2S. Despite this, the characteristic 'ripe and fruity' odour associated with the decomposition of waste is resultant from the reaction between short-chain fatty acids (known as 'volatile fatty acids') and methyl, ethyl, propyl, and butyl alcohols (Christensen et al., 1992). Common fatty acids such as valeric acid and butyric

acid are products of carbohydrate degradation along with alcohols, aldehydes and ketones. Fang et al. (2012) reported values of 0.0173 ppm and 0.0116 ppm for butyric and valeric acid respectively in a gas extraction well for a closed landfill. This far exceeded the odour threshold values (measured by the triangle odour bag method) of 0.00019 ppm and 0.000037 ppm for butyric and valeric acid respectively according to Nagata and Takeuchi (2003). However, caution should be taken with these figures as there are multiple methods for the measurement of odour threshold and data reported in the literature can vary by up to four orders of magnitude (Pullen, 2007).

The release of odorous gases may be intermittent and dependent on weather conditions and is therefore a long-term nuisance (Card, 1995). Odours may cause nausea and may increase the perception of adverse health effects (Wilson et al., 2006). Adequate dilution and dispersion is the most effective measure to render a gas odourless. In-ground protection measures that can be employed include: passing the gas over activated carbon to absorb odours prior to release, the use of deodorants, and active abstraction of gas and flaring to burn and destroy odours (Card, 1995). In practice, membranes in conjunction with in-ground venting to dilute and disperse gas may be the easiest and most effective solution.

2.3.4 Plant Toxicity

Research increasingly suggests that there is a correlation between high concentrations of CH_4 and CO_2 in the soil and vegetation necrosis, especially in areas surrounding landfill sites (Barry, 1986). During periods of prolonged waterlogging, impeded gas exchange leads to high partial pressure of CO_2 in the root zone, with adverse effects on root growth and metabolism (Boru et al., 2003; Kırmızı and Bell, 2012).

Additionally, where the O_2 content of the soil is low, the conversion of CH_4 to CO_2 may be incomplete and intermediate products such as methanol CH_3OH, formaldehyde (HCHO) and formic acid (HCO_2H) may be present. These chemicals can remain in the soil and exhibit phytotoxic effects to plants (Card, 1995). Gases associated with landfill gas that are known to be highly toxic to plants include H_2S, ammonia (NH_3), benzene (C_6H_6), ethylene (C_2H_4), acetaldehyde (CH_3CHO) and thiols (-R-SH) (Kanol and Zetther, 1990).

2.4 Sources of Ground Gases

Methane, CO_2, radon (Ra) and volatile organic vapours (VOCs) occur naturally in the environment. Buried organic matter has the potential to generate CH_4, CO_2 and associated trace gases. There are numerous sources derived from anthropogenic and natural sources that are compiled in Table 2.5.

Sources that are derived from the degradation of organic material principally comprise CH_4 as the dominant hazardous gas. Methane is the most abundant organic compound in the Earth's atmosphere and is synthesised in many different environments. Under aerobic conditions, CH_4 is readily oxidised to CO_2 as it is biochemically reactive. Therefore, CO_2 is often associated with the presence of CH_4, but it can also be generated directly (Wilson et al., 2006).

Source	**Origin**	**Methane**	**Carbon Dioxide**	**Other Gases**
		Anthropogenic		
Landfill Sites	Microbial decay of organic materials derived from the disposal of putrescible materials.	20–65%	15–40%	Several hundred trace organic gases (maybe odorous or toxic) (generally make up < 1% total volume).
Made Ground	Microbial decay of organic materials contained in reworked natural ground containing demolition and other wastes.	0–20%	0–10%	
Foundry Sands	Microbial decay of waste materials from the foundry process (phenolic binders, dextrin, coal dust, wood rags, paper).	Up to 50%	15–40%	Trace organic gases (generally < 1% of the total volume) (maybe odorous and/or toxic).
Sewage Sludge, Dung, Cess Pits/Heaps	Microbial decay of organic materials.	60–75%	18–40%	Trace organic gases (generally < 1% total volume) (maybe odorous and/or toxic).
Burial Grounds (Including Cemeteries)	Microbial decay of organic materials contained within human/animal remains.	20–65%	15–40%	

Source	**Origin**	**Methane**	**Carbon Dioxide**	**Other Gases**
Industrial, Chemical, Petroleum Sites or Manufacturing	Organic vapours derived from leaks or spills from storage, processing and disposal areas.	30–100%	2–8%	Trace organic gases (generally < 1% total volume) (maybe odorous and/or toxic).
Natural Gas (Supply Pipes)	Leakage from bulk pipeline transportation of natural gas.	90–95%	0–9.5% (CO_2 not present in mains gas, but may be oxidised following leak).	1–27% C_2-C_4 alkanes. 4.7% CO.
		Natural		
Soil	Physical, chemical and biological transformations of rock during weathering.	< 2 ppm	350 ppm	
Coal Measures Strata	Burial of vegetation under high temperatures and pressures, liberating gases as a by-product of mining activities.	< 1–90%	0–6%	4 – 13% C_2-C_4 alkanes. 0 – 10% CO. Production of H_2S possible but rarely in hazardous concentrations.
Peat/Bog Areas	Gas formed by the microbial decay of accumulated plant debris under anaerobic conditions.	10–90%	0–5%	
Alluvium (Organic Rich Sediments)		0–5%	0–10%	
Radon-Emitting Rocks	Decay of naturally occurring uranium with soils and rocks.	Variable	Variable	0 – 1000 Bq/m^3 Ra gas. Higher concentrations of gas up to 4,000,000 Bq/m^3 have been recorded in SW England.
Carbonate Rich Strata	Dissolution of calcium carbonate ($CaCO_3$) by acidic water.	Variable	1–6%	
Other geological sources (e.g. oil and gas fields, oil shale, volcanic)	These are not especially relevant to the UK but are relevant in some countries.			

Table 2.5: Sources and Origins of Hazardous Gases (adapted from Hooker and Bannon (1993); Wilson et al. (2006))

2.4.1 Landfill Processes

Although many anthropogenic sources are listed in the preceding summary including made ground, foundry sands, sewage sludge and burial grounds, this section will primarily review the microbial processes associated with landfill as the data used in this research concerns UK landfill sites. While each of these sources will have its own set of microbial processes, those pertaining to the unique situation of landfills are discussed here. Other anthropogenic sources of CH_4 and CO_2 result from failures in engineering and include, for example, leaks associated with petroleum sites or natural gas supplies.

Little consideration had been given to landfill construction, microbial processes that generate gases and potential gas emissions until around the early 1970s. A pioneering study of the time by Farquhar and Rovers (1973) collated the limited resources available and introduced new ideas and concepts to the field. Subsequent studies have tended to use this work as a foundation.

Farquhar and Rovers (1973) separated decomposition of waste into two stages, namely The Non-Methanogenic Stage' and 'The Methanogenic Stage'. The two stages were further subdivided into four phases, 'Phase 1: Aerobic', 'Phase 2: Anaerobic Non-Methanogenic, 'Phase 3: Anaerobic Methanogenic Unsteady' and 'Phase 4: Anaerobic Methanogenic Steady'. Using information on the decomposition of sewage sludges and the destruction of organic material in soil as a basis, the term 'anaerobic decomposition' was defined as the attack of a mixed micro-biological culture on complex organic material in the absence of O_2. The changing composition of gases over time is demonstrated in Figure 2.2.

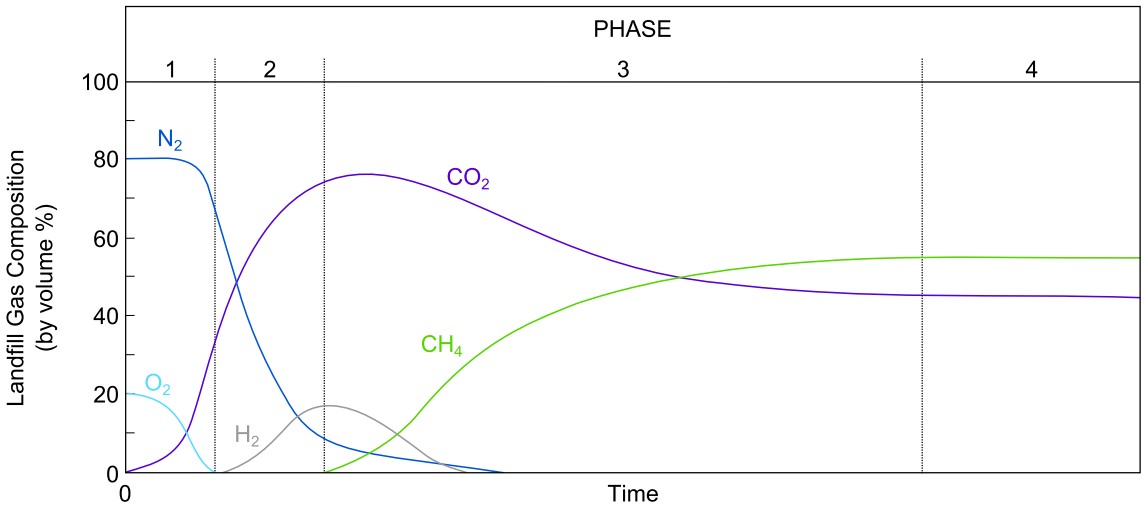

Figure 2.2: Sanitary Landfill Gas Production over Time (from Farquhar and Rovers (1973))

'The Non-Methanogenic Stage'

Typically, municipal wastes are comprised of 40–50% cellulose, 10–15% lignin, 12% hemicellulose and 4% protein (Barlaz et al., 1989). In this initial stage, complex polymers (e.g. cellulose, hemicellulose, starch and protein) are converted to lower molecular weight, soluble monomers (e.g. sugars and amino acids) by hydrolysis catalysed by extra cellular enzymes (Farquhar and Rovers, 1973; Bareither et al., 2013). Although the micro-organisms expend more energy than is immediately recovered during hydrolysis, the organic material is subsequently modified for use in energy yielding reactions. Therefore, hydrolysis is not likely to be a rate limiting step in decomposition (Farquhar and Rovers, 1973; Toerien and Hattingh, 1969).

Fermentation of these monomers to alcohols and carboxylic acids (e.g. acetate, propionate and butyrate), H_2 and CO_2 with further acetogenesis of H_2 and CO_2 to acetate, creates the substrates and chemical and microbial equilibrium required for methanogenesis (Zehnder, 1978). Acetic acid (CH_3COOH) is largely identified by researchers as the predominant acid in the organic acids produced in this stage (Farquhar and Rovers, 1973). However, it is disputed whether the microbial flora are facultative or strictly anaerobic (Farquhar and Rovers, 1973). Bareither et al. (2013) noted that for efficient and balanced waste decomposition, CH_4-producing *Archaea* (i.e. methanogens) are critical as they are responsible for the terminal step in the anaerobic decomposition process.

'The Methanogenic Stage'

Acetotrophic and hydrogenotrophic decomposition constitute the two primary pathways of methanogenesis (Zinder, 1993). These pathways differ as acetotrophic methanogenesis involves the consumption of acetate whereas H_2 and CO_2 or formate are consumed in hydrogenotrophic methanogensis (Zehnder, 1978). The reactions occurring during this stage involve the cleavage of CH_3COOH into CH_4 and CO_2 and the reduction of CO_2 through the addition of H_2 to form CH_4 and H_2O. In Figure 2.2, these processes are achieved in Phases 3 and 4.

Methanogenic archaea, common inhabitants of soil and sewage, are active micro-organisms at this stage. Although energy is captured by micro-organisms during this stage, there is very little synthesis of new cell material (Farquhar and Rovers, 1973). *Archaea* are phylogenetically related prokaryotes distinct from *Bacteria*. Woese and Fox (1977) determined that the ribosomal RNA sequences of *Archaea* were unlike those of *Bacteria* and eukaryotes. Methanogens differ from bacterial species as O_2 causes necrosis, they produce unusual enzymes and have different cell walls.

Multiple studies have identified methanogens associated with both acetotrophic and hydrogenotrophic degradation pathways (e.g. Huang et al. (2002); Calli et al. (2006)). However, the environmental, operational and material factors that induce the dominance of acetotrophic vs hydrogenotrophic methanogenesis are complex and are not well understood (Bareither et al., 2013; Semrau, 2011).

Simultaneously, N_2 and H_2S gases may be produced during anaerobic decomposition. Following the depletion of O_2, denitrification (a microbial process) can occur when nitrate ions (NO_3^-) are reduced while acting as terminal electron acceptors. Sulphate ions (SO_4^{2-}) also act as terminal electron acceptors and are reduced by SO_4^{2-}-reducing micro-organisms to produce H_2S (Farquhar and Rovers, 1973). These reactions tend to proceed at neutral or weakly alkaline pHs. As organic acids are degraded, the pH increases to near neutral conditions and is buffered by the bicarbonate (HCO_3^-) system (Bozkurt et al., 2000). A large redox buffering capacity is provided by the organic matter in waste. Therefore, reducing conditions may prevail for extended periods of time (Bozkurt et al., 2000). A progression of pH and redox potential along with changing landfill gas composition with time as conceptualised by Bozkurt et al. (2000) is shown in Figure 2.3. Other gases produced during this stage in negligible concentrations are ethane (C_2H_6), propane (C_3H_8) and phosphine (PH_3) (Farquhar and Rovers, 1973).

While the 'Non-Methanogenic Stage' sees the production of H_2, the 'Methanogenic Stage' sees the total consumption of H_2. The rate of consumption is thought to exceed the rate of production as methanogenesis proceeds at a much faster rater than the preceding reaction. Therefore, H_2 is generally not found with CH_4 (Farquhar and Rovers, 1973). The main gases produced during this stage include CO_2, CH_4, H_2, H_2S and N_2 (Farquhar and Rovers, 1973). Additionally, trace volatile organic compounds (VOCs) accounting for $< 1\%$ of gaseous emissions, are produced from the volatilisation of compounds contained within the waste and during decomposition of the wastes (Allen et al., 1997b). Landfill gases contain VOCs in the following six classes of compounds: saturated and unsaturated hydrocarbons, acidic hydrocarbons and organic alcohols, aromatic hydrocarbons, halogenated compounds, sulphur compounds (e.g. carbon disulphide) and inorganic compounds (Allen et al., 1997b).

Environmental Factors Affecting the Production of Gas

Major environmental factors that affect the anaerobic production of CH_4 in the methanogenic stage are summarised from Farquhar and Rovers (1973) in this section.

- Most micro-organisms require moisture for activity. This includes methanogenic archaea and it is likely that activity increases with moisture content. Moisture

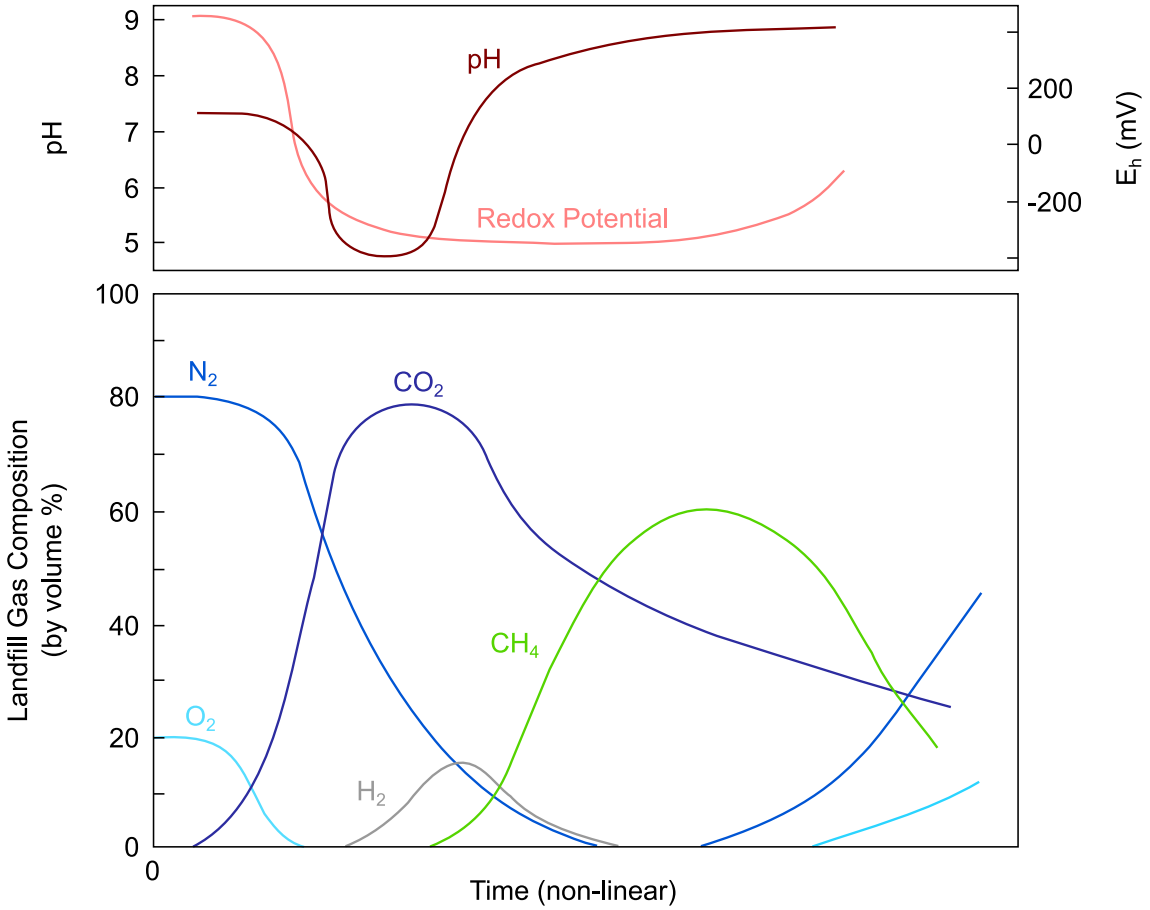

Figure 2.3: Landfill Gas Composition over Time against pH and Redox Potential (from Bozkurt et al. (2000))

content is generally in excess of 90% of wet sludge weight in digesters where methanogenic archaea perform well.

- Micro-organisms require a very specific pH range for optimal production of gas. For example, sewage sludge digestion was reported to be optimised between pH 6.4 and 7.2 (Kotze et al., 1969). Similarly, Skinner (1968) defined a tolerant range in soil from pH 5.5 to 9.0.
- Bicarbonate (HCO_3^-) buffers the system as organic acids are degraded. Kotze et al. (1969) observed that a HCO_3^- alkalinity of 2,000 mg/l expressed as calcium carbonate ($CaCO_3$) and an ammonium ion (NH_4^+) concentration in excess of 100 mg/l expressed as NH_3 were required for maximum CH_4 production.
- A Redox potential in the negative range (generally less than -200 mV) is required for CH_4 production.
- Three temperature ranges have been identified for anaerobic decomposition:
  - Thermophilic range with temperatures > 44°C.
  - Mesophilic range with temperatures between 20 and 44°C.
  - Psychrophilic range with temperatures < 20°C.

Generally, the trend is for rates of decomposition to increase with temperature up to 55°C. Beyond this temperature, decomposition rates decline dramatically. Additionally, decomposition rates are sensitive to abrupt changes in temperature as small as 1 to 2°C.

- Pressures in excess of 2,413 mbar were found to have no negative effect on CH_4 production (Skinner, 1968).
- Varying amounts of nutrients (dependent on waste deposits) will affect the rates of decomposition, gas production and the relative proportions of CH_4 and CO_2 in the gas. An optimal ratio of C to N of 16:1 was reported by Kotze et al. (1969).

Composition of Landfill Gas over Time: The Four Phases

Farquhar and Rovers (1973) first postulated four phases for the composition of landfill gas over time (Figure 2.2). The first phase of landfill gas production is the aerobic phase. Decomposition of waste takes place aerobically with the consumption of O_2 present in the refuse at the time of placement. Carbon dioxide is produced in approximate molar equivalents to consumed O_2 with little displacement of N_2 (Farquhar and Rovers, 1973). Although O_2 is initially available in the pores serving as an oxidising agent, the initial supply is very limited and may be depleted after only a few days (Bozkurt et al., 2000).

Phase 2 begins after the depletion of O_2. It is during this phase that anaerobic activity becomes the dominant process. An increase and peak in CO_2 concentrations occurs and there is some H_2 production. Due to the observed boom in CO_2 evolution, there is a dramatic displacement of N_2. The notable time-lag for the commencement of the production of CH_4 after anaerobic conditions have been achieved may be as a consequence of the need for enough CO_2 in solution to act as a proton acceptor. Overall, the anaerobic phase is characterised by a rapid polymer hydrolysis and a sharp decline in redox potential (Farquhar and Rovers, 1973; Bozkurt et al., 2000). Measured peak CO_2 concentrations by volume typically lie in the range 50–70% and may take between 10 to 40 days to be achieved (Farquhar and Rovers, 1973).

Defined as the unsteady phase due to the concentration of CH_4 increasing to a relatively constant terminal value ($\sim 60\%$), Phase 3 begins at peak H_2 concentration of $\sim 20\%$. During the initial part of this phase, the concentration of H_2 reduces to 0%. The rapid decay of H_2 is attributed to *Methanogenic archaea* which appears to be capable of using H_2 at a very rapid rate (Farquhar and Rovers, 1973). Both CO_2 and N_2 reach terminal values during this phase. Declining from a peak value of $\sim 80\%$, CO_2 concentration terminates around 40% while the N_2 concentration

becomes negligible (Farquhar and Rovers, 1973).

Early research suggested that the time taken for completion of Phases 1 to 3 was between 180 and 500 days. For example, Ramaswamy (1970) reported a time of 180 days for completion of the first three phases, Rovers and Farquhar (1972) reported a time of 250 days, while Beluche (1968) disclosed a time of 500 days. However, great care needs to be taken with these figures as all are based on laboratory experiments conducted with cylinders filled with refuse to simulate landfill. Conditions may, therefore, be atypical of those in real landfills. Experiments are also not to the same scale as real landfills. Therefore, the time taken for Phases 1 to 3 to reach completion may be years to decades depending on the nature, volume and availability of substrate.

The composition of gases produced in Phase 4 and the rate of production remain steady at their peak. However, this does not eliminate the possibility of variations in gas production due to environmental changes and it does not take into account the possibility of long-term variations due to nutrient depletion or the accumulation of inhibitory materials (Farquhar and Rovers, 1973). On the whole, CH_4 concentration will remain steady between 50 and 70% while CO_2 will stabilise between 30% and 50% (Farquhar and Rovers, 1973). Within this range, Kotze et al. (1969) reported a gas composition of 66% CH_4 and 34% CO_2 during the digestion of sewage sludge.

Small volumes of N_2 and H_2S may also be present. If the concentration of CH_4 is substantially below 50% by volume, it is likely that production is being retarded, especially if H_2 is detected (Kotze et al., 1969). Abrupt changes in gas composition are usually indicative of some change in environmental conditions (Farquhar and Rovers, 1973).

Building on from the initial analysis of landfill gas production over time by Farquhar and Rovers (1973), Kjeldsen et al. (2002) confirmed the initial four phases using data collected over 30 years and theorised future gas compositions (Figure 2.4). At the time of writing, the period supposed by Kjeldsen et al. (2002) extended beyond the 30-year post-closure monitoring period prescribed for landfills in the United States. Continuing on from the 60% CH_4 and 40% CO_2 attained at the end of Phase 4, Kjeldsen et al. (2002) proposed a further four phases. All study landfill sites were in Phase 4 of Figure 2.4. Phase 5 had not yet been achieved in any of the landfills as N_2 is absent. These phases were termed, 'Methane Oxidation', 'Air Intrusion' and 'Carbon Dioxide'. Phases 5 and 6 may be viewed as intermediate phases between the stable methanogenic phase and the carbon dioxide phase. Upon the carbon dioxide phase being attained, the landfill becomes aerobic. In Phase 8, atmospheric conditions are achieved.

Throughout the stable methanogenic phase, the gas production rate is continuously decreasing (Kjeldsen et al., 2002; Karthikeyan and Joseph, 2006). During the later stages of gas generation when rates are reduced, it is possible for air to be sucked into a landfill owing to over-pumping for landfills with an active gas extraction system. This is not the case for landfills that do not have an active gas extraction and utilisation system. Barometric pressure changes alone will drive air intrusion through a small elevated gas pressure into the upper waste layers (Kjeldsen et al., 2002).

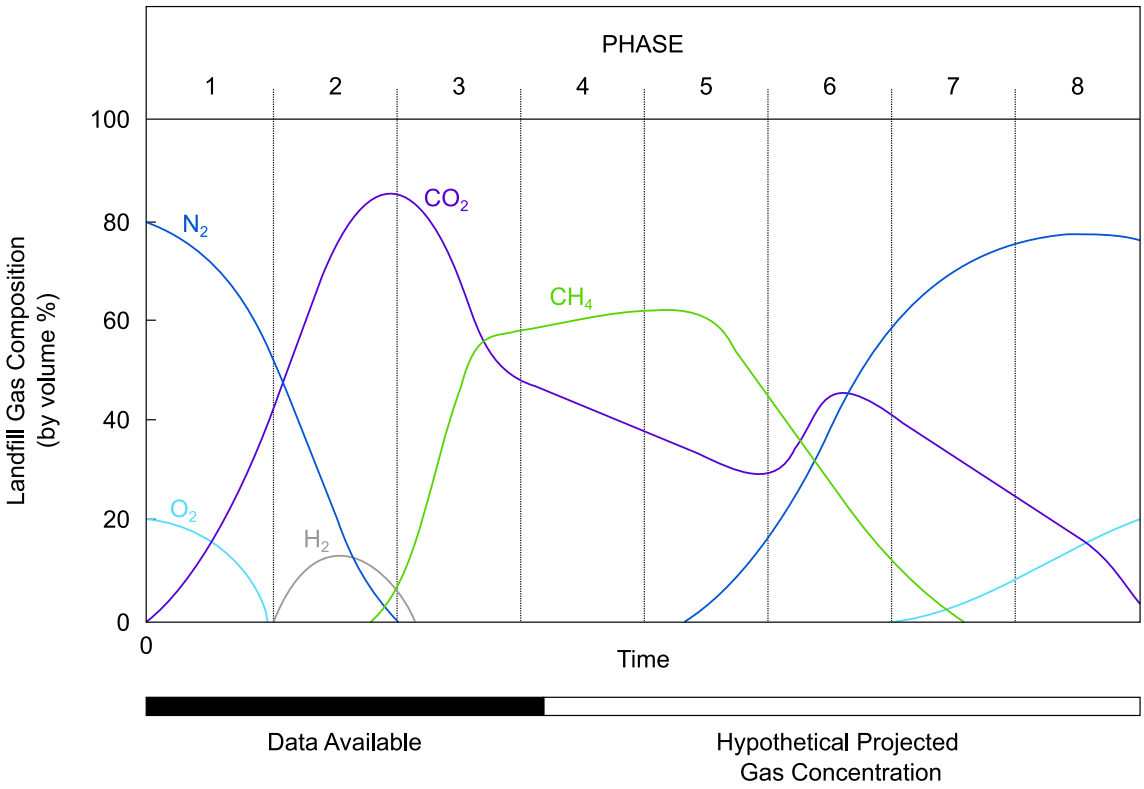

Figure 2.4: Sanitary Landfill Gas Production over Time (from Kjeldsen et al. (2002))

If a landfill has a tight cover and open gas vents (assuming that active gas extraction and gas flaring has ceased), air intrusion may be local and of minor importance. However, for landfills with more permeable covers, O_2 intrusion at high barometric pressure or due to diffusion will promote oxidation of CH_4 that is still being produced. Therefore, via these mechanisms, an insignificant part of landfill waste will be intruded by air and CH_4 oxidation will predominantly take place in the cover soil or in waste surrounding gas vents (Kjeldsen et al., 2002).

The following phase is hypothesised to be 'air intrusion'. This phase will result from the continual decrease of CH_4 production and air intruding through the cover soil into the waste mass. At some point during this phase, all of the CH_4 produced will be oxidised. Thus, the concentration of CO_2 will increase as it is produced in

the CH_4 oxidation reaction. Also, N_2 concentration will increase as a result of air intrusion. However, O_2 concentration will remain negligible as it is rapidly consumed in the reaction of CH_4 oxidation. Overpressure in a landfill will reduce to zero as CH_4 production declines (Kjeldsen et al., 2002).

Phase 7, in which CO_2 concentration will exceed CH_4 concentration, is termed 'carbon dioxide' phase by Kjeldsen et al. (2002). Oxygen intruding landfill at this point in time will be consumed for oxidation with any residual CH_4, organic materials and reduced inorganic species. By Phase 7, aerobic conditions are re-established allowing refuse oxidation as some lignocelulosic substrate is more degradable under oxic conditions compared to anoxic conditions (Kjeldsen et al., 2002). Carbon dioxide production has been observed in conjunction with a decrease in pH in refuse and harbour sediments (Revans et al., 1999; Calmano et al., 1993). This phase has also been called the humic phase (Bozkurt et al., 1999).

The exchange of air between landfill and atmosphere is governed by the diffusion, wind-induced exchange, natural convection and barometric pumping (Bozkurt et al., 1999). A *diffusional transport* is driven by concentration differences between landfill and atmosphere. Landfill gas components are exchanged for atmospheric components by this mechanism. An important parameter is the diffusivity of gas in the landfill cover and the waste layers. Saturation by water places a crucial role in this. An engineered cap often includes a clay layer with a very low gas diffusivity at normal water content. If waste layers are saturated with water, gas diffusion is not active because diffusion through water is 10,000 times lower than air (Kjeldsen et al., 2002). Diffusion is also significantly reduced by the presence of a plastic flexible membrane layer (Kjeldsen et al., 2002).

Wind speed plays a minor role in air intrusion into landfill (Bozkurt et al., 1999). A pressure gradient is created between atmosphere and landfill that causes air to flow through a landfill. However, the magnitude is governed by the wind speed and the permeability of the cover and waste layers. Natural convection processes induced by changes in temperature, air humidity, gas concentration (CO_2/O_2) also play a minor role in air intrusion into landfill.

Principally, if a landfill's cover has a lower permeability than the waste layers and if the cover is defective with cracks or has open gas vents, changes in barometric pressure will pump gases in or out of a landfill through such openings (Kjeldsen et al., 2002). The direction of flow will depend on the direction of the pressure change (Gebert and Gröngröft, 2006). Passive venting was used by Christensen et al. (2000) as a remedial technology to remove volatile pollutants from sandy unsaturated layers covered by clay. During this investigation, it was shown that

barometric pressure changes led to a significant exchange of air through the installed screen wells (Christensen et al., 2000).

It is important to note that the changes in landfill gas composition post Phase 4 proposed by Kjeldsen et al. (2002), are based solely on theory. At the time of writing the review, Kjeldsen et al. (2002) had access to only 30 years of landfill gas monitoring data as monitoring had only been a requirement from the early 1970s. By the early 2000s, most landfills were still in the stable methanogenic phase. Likewise, the sites used in this study were still in the anaerobic stable methanogenic phase. Therefore, the proposed later stages, while important, are not necessarily crucial to the research presented here.

2.4.2 Coal Measures Strata

Primarily, this research is concerned with CH_4 and CO_2 evolved from landfill processes as described in the previous section. However, the underlying strata also provides a natural source of these gases. Most importantly, Coal Measures strata can be a significant source of CH_4 at depth, particularly where mining operations have previously taken place. The amount of CH_4 that may emanate from Coal Measures depends on the 'Coal Rank'.

Compared with mineral material that generally constitutes most rock types, coal is comprised of plant debris which is a far more fragile material. On burial, plant debris is exposed to elevated heat and pressure that induces changes in composition and properties. Sometimes referred to as 'organic metamorphism', the 'rank' of a coal is a measure of how much change has occurred. Based upon composition and properties, coals are assigned to a rank progression that corresponds to the amount of change that has occurred (Table 2.6) (King, 2015).

Underlying Coal Measures are postulated to be the second most likely source of ground gas after landfill in this research. Accordingly, an appreciation of the likely quantity emanating from underlying strata as prescribed by 'coal rank' is required. The majority of research sites are located in the NW of England in Cheshire and Greater Manchester (historically Cheshire). Coal Measures in this area date from the Westphalian Stage of the Carboniferous Period (358.9–298.9 MA). Deposits extend beneath much of the Cheshire Basin and the county to depths greater than 1,200 m (Norton et al., 2006).

Multiple coalfields cross the county borders. The North Wales (Flintshire) Coalfield constitutes generally easterly dipping (structurally complex), Pennine Lower-Middle Coal Measures. With an average gas seam content of 8.4 m^3 CH_4 t^{-1}, these sequences mainly contain medium volatile coking coal (Norton et al., 2006). The

Rank	Properties	Carbon Content (dry ash basis)
Peat	An organic sediment of recently accumulated to partially carbonised plant debris en masse. It is transformed into a rock by burial, compaction and coalification	$< 60\%$
Lignite	The lowest rank of coal, a peat that has been transformed into rock. The rock is a brown-black coal and sometimes contains recognisable plant structures. In Europe, Australia and UK, some low-level lignites are called 'brown coal'	60–70%
Sub-bituminous	Subjected to a greater level of organic metamorphism than lignite. Some O_2 and H_2 is driven off by the metamorphism. This loss produces a richer carbon content. Based on heating value (8,300–13,00 British Thermal Units), sub-bituminous coal may be sub-divided into 3 ranks, A, B and C.	70–77%
Bituminous	By far the most abundant rank of coal as it accounts for $\sim 50\%$ of coal produced in the United States. Owing to an increased level of organic metamorphism compared with sub-bituminous coal, it has a higher carbon content. The bituminous coal rank is sub-divided into 'low volatile bituminous', 'medium volatile bituminous' and 'high volatile bituminous'.	77–87%
Anthracite	The highest rank of coal, with the highest carbon content. It also generally has the highest heating value per ton on a mineral matter free basis. Often, on the basis of carbon content it is subdivided into 'semi-anthracite' and 'meta-anthracite'. In the UK, the dominant source of anthracite is located in the NW of the South Wales Coalfield (British Geological Survey, 2010)	$> 87\%$

Table 2.6: Coal Rank (adapted from King (2015))

coalfield dips under the western margins of the Cheshire Basin. Comprising an average gas content of 9.0 m^3 CH_4 t^{-1}, the South Lancashire Coalfield contains Pennine Lower-Middle Coal Measures of high to medium volatile rank bituminous coals. This coalfield is concealed beneath the northern area of Cheshire and was heavily worked in this area (Norton et al., 2006). Finally, the North Staffordshire Coalfield outcrops in the SE of Cheshire. Like the South Lancashire Coalfield, it contains Pennine Lower-Middle Coal Measures with high to low volatile rank bituminous coals and has an average gas seam content of 8.0 m^3 CH_4 t^{-1} (Norton et al., 2006). Consequently, a high CH_4 contribution may be expected in areas formerly mined, or where the head of the bedrock is heavily weathered or the bedrock contains major faults.

2.4.3 Bowland-Hodder Shale and Shale Gas

Bowland-Hodder Shale

According to the British Geological Survey (BGS), the Bowland Shale formation dates from the Carboniferous Period, specifically dating from the Asbian Substage (337.5–333 MA) to the Yeadonian Substage (315.5–314.5). It is a mainly dark grey fissile and blocky mudstone that is weakly calcareous. It has subordinate sequences of interbedded fossiliferous limestone and sandstone that are more or less discrete bands. In the locality (Furness and Settle areas), the formation is thick-bedded, blocky to sub-fissile, dark grey and black, organic-rich mudstone. It has subordinate beds of dark grey siltstone, sandstone and pale brown dolomitic limestone. Bands of marine deposits are also present. The formation shows an upward decrease in carbonate turbidites with an associated increase in siliciclastic sandstone turbidities.

Generally, the formation is between 120 m and 620 m deep from the surface. It thickens in a north-easterly direction along the axis of the Central Lancashire High, from about 22 m in the Roddlesworth Borehole to 102 m thickness in th Boulsworth Borehole. In the study area, the upper boundary is defined as the base of the Millstone Grit (over most of the Pennine Basin). In Staffordshire and the East Midlands, the upper boundary is the base of the Morridge Formation. The base of the formation (lower boundary) is defined as upon the Pendleside Limestone Formation in the Craven Basin, on the Widmerpool Formation in North Wales, and on the Hodderense Limestone Formation in the south of the Isle of Man. It is interpreted as the first appearance of black mudstone above variegated mudstones or fine-grained limestones.

Shale Gas

Following burial, in conventional oil and gas accumulations, hydrocarbons are generated from shales comprising source rock. These hydrocarbons migrate from the source rock, through carrier beds over geological time and accumulate in porous reservoirs (typically sandstone or carbonate) in discrete traps. However, for unconventional hydrocarbon accumulations, such as shale gas, the opposite is true as shales act as both source and reservoirs. The extensive basin centres consequently become exploration targets (Andrews, 2013).

Gas may be present in two components, either adsorbed onto kerogen or clay particles, or present as free gas in pore spaces and natural fractures. Predominantly, shale is comprised of very fine-grained clay particles deposited in a thinly laminated texture. Layers of re-deposited limestone or thin clastic beds within the

shale sequence also produce shale gas. The clay particles fall out of suspension and are interspersed with organic matter (the rock's total organic content (TOC)). At depth, these strata are compressed under pressure, expelling the pore water that results in the low-permeability layered shale rock. This relates to the nature of the sediment's very fine-grained and laminar particles and not the overall rock composition which is layered. Each layer is an effective barrier to fluid migration and in this composite layering, an effective vertical seal is achieved.

Compared with conventional gas sources, typical shales have a very low matrix permeability (<0.1 mD in shales compared with >1 mD in conventional sandstone reservoirs) (Andrews, 2013). In shale, hydrocarbon gases are effectively trapped and are unable to flow or be extracted without anthropogenic intervention. Migration of gases to conventional traps may only occur on geologic time-scales.

2.4.4 Source Quantification

By far the most practical tool at the researcher's disposal to identify CH_4 and CO_2 source is the utilisation of carbon isotopes. Carbon has three isotopes, ^{12}C, ^{13}C and ^{14}C. Carbon-12 is the most abundant (98.89%) and most stable isotope, followed by Carbon-13 (1.11% abundance) and Carbon-14 which is the heaviest and most unstable isotope (active) with abundance 1×10^{-10}% (Hitchman et al., 1989). Identification of source works on the principle of determining the relative proportions of each isotope or ratios (e.g. $^{13}C/^{12}C$) in each source giving a characteristic 'signature' or 'fingerprint' dependent on source. This process is particularly beneficial for contractors where issues of ownership and mitigation are apparent. A clear advantage of stable isotope analysis over radiocarbon dating is that due to the abundances of ^{12}C and ^{13}C, ratios may be easily determined with a relatively simple mass spectrometer in less time and at a fraction of the cost of ^{14}C measurements (Hitchman et al., 1989).

Stable Isotope Analysis

A key concept in the use of stable isotopes to determine gas source is that CH_4 formed biochemically in landfills (biogenic source) will be depleted in the heavier ^{13}C and ^{2}H (D) isotopes as microbes discriminate against these isotopes (i.e. lower, or more negative ^{13}C and ^{2}H) compared with thermogenic (e.g. geogenic) CH_4 (Kerfoot et al., 2013). Biogenic gas is defined as gas that has been synthesised by methanogenic organisms whereas thermogenic gas is defined as gas formed deeper in the Earth from buried organic material at high temperature and pressure. For the

purposes of this project, gas present at the research sites originating from deeper geology is referred to as geogenic gas. Residual CH_4 will be depleted in ^{13}C while evolved CH_4 will have a greater proportion of ^{12}C (Coleman et al., 1981). Consequently, CH_4 oxidised to CO_2 by microbes will also be enriched in the lighter carbon isotope.

According to Hitchman et al. (1989) thermogenic sources will generally have a $^{13}\delta C_{CH_4} > -60‰$ while $^{13}\delta C_{CH_4} < -60‰$ generally indicates a biogenic gas origin. Bergamaschi et al. (1998) reported values of $^{13}\delta C_{CH_4}$ from thermogenic sources in the range -25‰ to -60‰ while Raco et al. (2014) reported $^{13}\delta C_{CH_4}$ from biogenic sources in the range -46.1‰ to -66.3‰ in a study of landfill gas fractionation factor limits. Although the figures reported by Raco et al. (2014) broadly agree with the rule proposed by Hitchman et al. (1989), there is scope for $^{13}\delta C_{CH_4}$ and δD_{CH_4} values obtained from biogenic and thermogenic sources to overlap. Therefore it is accepted that source identification by stable isotopes is not necessarily a clean-cut process. It is assumed that values plotting between end-member populations are gas mixtures. Further data quoted in the literature is provided in Table 2.7 and pictorially represented in Figure 2.5.

Already there have been many studies into the characterisation of naturally occurring (geogenic) CH_4, particularly in China, using stable isotope analysis. A prominent example is Dai et al. (2012) who reported a range of $^{13}\delta C_{CH_4}$ values between $-36.9‰$ and $-30.8‰$ and δD_{CH_4} values between $-173‰$ and $-155‰$ in the Sichuan Basin in eastern Sichuan Province. One of the most important on-shore gas-producing areas in China, the main source rocks include: Lower Cambrian Marine Shales, Lower Silurian Marine Mudstones, Lower Permian Marine Pelitic Carbonates, Upper Permian Marine-Terrigenous Coal Measures, Upper Triassic Terrigenous Coal Measures and Lower Jurassic Lacustine Mudstones (Dai et al., 2009).

The rocks encountered here encompass both older and younger rocks in terms of geological age than those encountered in NW England where the research sites are located. The Coal Measures contained in this basin are younger than those in NW England which are Carboniferous, Westphalian in age. Nevertheless, multiple studies consistently indicate that geogenic CH_4 is enriched in both $^{13}\delta C_{CH_4}$ (-39.0 to $-29.0‰$) and δD_{CH_4} (-257 to $-114‰$) when compared with biogenic source counterparts (-66.3 to $-46.1‰$ $^{13}\delta C_{CH_4}$ and -329 to $-254‰$ δD_{CH_4}).

However, determination of source by stable isotope analysis may not be as clean-cut as the data reported here indicate. For example, Zazzeri et al. (2015) illustrated that an active colliery in Nottinghamshire, UK, yielded a $^{13}\delta C_{CH_4}$ value of $-51.2 \pm 0.3‰$. Conversely, closed colliery values contained more positive $^{13}\delta C_{CH_4}$ values in

Source	$^{13}\delta C_{CH_4}$ ‰ Min	$^{13}\delta C_{CH_4}$ ‰ Max	δD_{CH_4} ‰ Min	δD_{CH_4} ‰ Max
		Biogenic		
Zazzeri et al. (2015)	-60.2 ± 1.4	-55.2 ± 0.6	Not reported	Not reported
Raco et al. (2014)	-66.3	-46.1	-329	-291
Kerfoot et al. (2013)	-63.2	-47.2	-299.6	-253.7
Widory et al. (2012)	-60.0 ± 0.2	-46.7 ± 0.2	-316 ± 3.4	-267 ± 4.9
Bergamaschi et al. (1998)	-60.3 ± 2.3	-57.4 ± 1.7	-310 ± 5	-299 ± 10
Bergamaschi and Harris (1995)	-62.3	-55.3	-326.8	-292.1
		Thermogenic		
Zazzeri et al. (2015)	-36.3 ± 0.3	-30.9 ± 1.4	Not reported	Not reported
Hu et al. (2014)	-33.7	-29.7	-118	-114
Ni et al. (2014)	-39.0	-37.7	-257	-250
Kerfoot et al. (2013)	-36.46	-29.91	-197.4	-193.7
Dai et al. (2012)	-36.9	-30.8	-173	-155
Dai et al. (2007)	-39.0	-29.0	Not reported	Not reported

Table 2.7: Typical Stable Isotope Ranges Reported in Literature for Biogenic and Thermogenic Sources

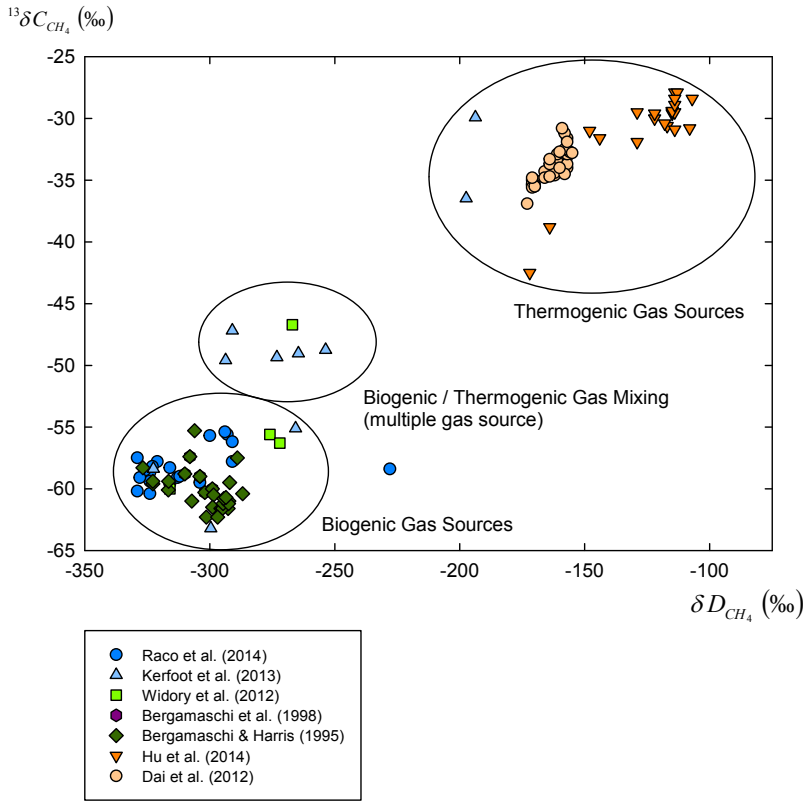

Figure 2.5: δD_{CH_4} versus $^{13}\delta C_{CH_4}$ Plot Indicating Biogenic and Thermogenic Gas Populations

the range -33.3 ± 1.8‰ to -30.9 ± 1.4‰ (Zazzeri et al., 2015). The open colliery $^{13}\delta C_{CH_4}$ value trespassed the range more commonly associated with landfill while the

closed colliery values were more in alignment with the natural gas values reported in Sichuan Province, China by Dai et al. (2012).

Radiocarbon Dating

Unlike stable isotope analysis which relies on multiple variables and an intrinsic knowledge of landfill processes and microbiology, radiocarbon dating works solely on the radioactive decay of ^{14}C. Carbon-14 has a relatively short half-life of 5,730 years. Accordingly, geological sources of CH_4 are depleted in ^{14}C by virtue of their great age while modern biogenic sources contain ^{14}C that reflects contemporary atmospheric ^{14}C levels (Muir et al., 2015; Fellner and Rechberger, 2009).

By convention 100% modern carbon (100 pMC) is defined as $0.7549\times$ ^{14}C activity of the internationally recognised oxalic acid II standard SRM-4990C (1340.07 pMC) (Muir et al., 2015). With respect to ^{13}C this is normalised to $-25‰$ (Muir et al., 2015). A peculiarity arising from nuclear weapons testing in the 1950s and early 1960s means that present day ^{14}C is currently $\sim$104 pMC (Hua et al., 2013; Muir et al., 2015). Rising from 97 pMC pre-1950, ^{14}C activity in the northern hemisphere peaked at $\sim$200 pMC in 1963. Excess ^{14}C entering the oceans and biota, and through dilution by fossil fuel burning has reduced ^{14}C atmospheric abundance (Hua et al., 2013; Muir et al., 2015).

Few studies into determination of ^{14}C in biogenic and geogenic gas sources have been undertaken by comparison with $^{13}\delta C/^{12}\delta C$ studies. This is likely to be due to the high cost of analysis meaning it is not always commercially viable. For known gas sources, ^{14}C determination is not likely to enhance the scientific knowledge. Therefore, the use of radiocarbon dating may be best used for unknown or mixed gas sources where $^{13}\delta C/^{12}\delta C$ analysis has not clarified the gas origin.

A recent study by Palstra and Meijer (2014) examined the $^{13}\delta C$ and ^{14}C values obtained from biogas and natural gas samples. Two results were reported for $^{13}\delta C_{CO_2}$ (‰), the CO_2 in the raw biogas samples and the CO_2 resulting from the combustion of pretreated biogas samples and natural gas samples. Biogenic gas sources included in this study were, maize, onions, landfill ($\times 2$), organic waste, municipal sewage sludge, sugar beet, and manure and vegetables while natural gas (geogenic) sources included Norway Gas, North Sea Gas and Groningen Gas.

Values for $^{13}\delta C_{CO_2}$ after combustion (i.e. $^{13}\delta C_{CH_4}$) were in the range $-61.24‰$ to $-28.55‰$ with mean $-49.37‰$ while $^{13}\delta C_{CO_2}$ values in the raw biogas samples ranged from $-5.55‰$ to $+30.45‰$ with mean $+11.99‰$ (Palstra and Meijer, 2014). These figures were typical of biogenic gas sources and were in good agreement with other stable isotope data. The raw samples show more positive $^{13}\delta C_{CO_2}$ values than

$^{13}\delta C_{CH_4}$ values indicating an enrichment in ^{12}C. The results reported by Palstra and Meijer (2014) are shown in Figure 2.6.

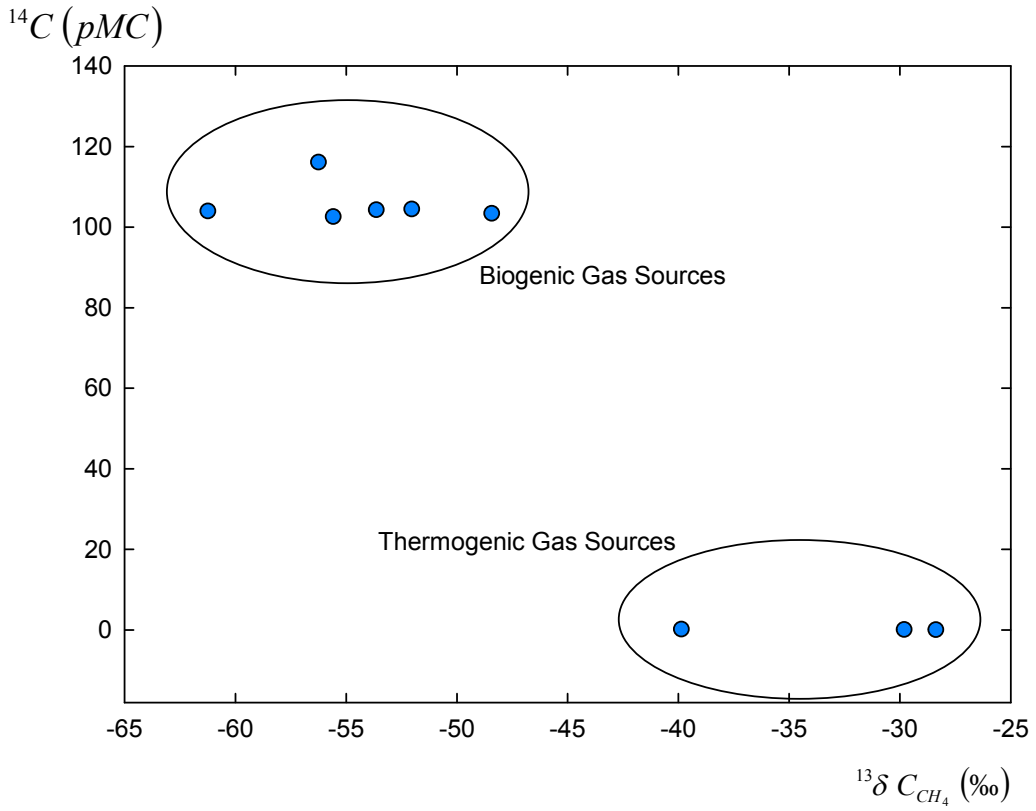

Figure 2.6: ^{14}C (pMC) versus $^{13}\delta C_{CH_4}$ (‰) Plot from Palstra and Meijer (2014) Indicating Biogenic and Thermogenic Gas Populations

Mean values for ^{14}C for raw biogenic source samples and post CH_4 combustion samples were 105.0% and 105.2% respectively (Palstra and Meijer, 2014). By comparison, Norway Gas ^{14}C was 0.18%, North Sea Gas ^{14}C was 0.10% and Groningen Gas ^{14}C was 0.05% (Palstra and Meijer, 2014). It can be clearly proven that the biogenic sources contain ^{14}C indicative of contemporary atmospheric ^{14}C levels while geogenic sources are depleted in ^{14}C, a clear distinction between sources.

In the UK, this approach was used alongside stable isotope analysis in the aftermath of the Loscoe Landfill Explosion in March 1986 (Williams and Aitkenhead, 1991). The identification of the gas source was complicated due to underlying shallow coal seams in the vicinity. However, radiocarbon dating of samples in conjunction with stable isotope analysis proved that the gas that caused the explosion had emanated solely from the landfill (Williams and Aitkenhead, 1991). Further information on this case study may be found in Section 2.6.

2.5 Gas Migration and Emissions

Perhaps one of the greatest challenges of this research was to detect, measure and ascribe a mechanism of gas migration in the unsaturated zone. Discussed here are potential migration mechanisms and mathematical modelling of these mechanisms. Also discussed are factors that permit migration of gases including landfill design factors, geological pathways, hydrological and meteorological controls. Lastly, the detection and measurement of CH_4, CO_2 and associated ground gases by commercially available equipment is reviewed in this section.

2.5.1 Migration Mechanisms and Mathematical Modelling

The important factors governing the migration of gases in the subsurface are gas solubility (Henry's Law), gas viscosity (Darcy's Law) and gas diffusion (Fick's Law). The latter of which is more closely associated with groundwater modelling. Additionally, gas solubility is variable and is influenced by temperature, pressure and salting-out effects. For example, it is known that CO_2 is 58 times more soluble in H_2O than CH_4 at standard temperature and pressure (STP) (Hooker and Bannon, 1993). Under favourable conditions, a proportion of CO_2 migrating away from municipal landfills or equivalent sources will be lost from the system due to its high solubility. Therefore, the fate of CO_2 in a given system is an important consideration.

Gas Solubility

Depending on the pressure, temperature and the concentration of other gases and minerals in the groundwater, CH_4 and CO_2 do not always exist in gaseous form in the subsurface. Pressure has the most dominant effect on CH_4 dissolution in H_2O. The solubility of gas in water increases with pressure as governed by Henry's Law:

$$P_b = x_b \cdot K_b \tag{2.1}$$

Where:
P_b = Partial pressure of the gas (dimensions of pressure e.g. Pa, atm, mbar).
x_b = Mole fraction of solute (dimensionless).
K_b = Henry's Law constant (dimensions of pressure).

Using this equation it can be shown that air-saturated water at 10°C in equilibrium with air at normal atmospheric pressure (1 atm) will contain 4.78×10^{-5} mg of CH_4 per litre of H_2O (equivalent to 6.70×10^{-5} ml STP CH_4 per litre of H_2O).

When the partial pressure of CH_4 reaches 1 atm at 10°C, the H_2O in equilibrium saturation will hold 29.9 mg of CH_4 per litre of H_2O (equivalent to 41.9 ml STP CH_4 per litre of H_2O).

Temperature Effects

With increasing temperature, the solubility of most gases decreases until the solvent reaches a critical temperature. In the case of CH_4, solubility in H_2O declines from 0 to 100°C but increases by a factor of 20 between 100 and 350°C (Drummond, 1981). Air-saturated H_2O at 25°C and atmospheric pressure will contain 3.56×10^{-5} mg CH_4 per litre of H_2O (Hooker and Bannon, 1993).

Pressure Effects

The solubility of most gases is proportional to increasing pressure. The solubility of most gases is a linear function of pressure. The mass of gas dissolved by a given volume of solvent is proportional to the partial pressure of the gas with which it is in equilibrium, which is an alternative expression of Henry's Law.

Salting-out Effects

Solubility of gases is often presented with respect to deionised water. However, natural waters usually contain varying amounts of dissolved salts which act to lower the solubility of gases (Hooker and Bannon, 1993). Setschenow (1889) states that at constant temperature, the logarithm of gas solubility is a linear function of salt concentration.

Gas Viscosity

Viscosity is defined as the internal resistance of a fluid to flow (Amyx et al., 1960). It is a function of temperature, pressure and molecular weight. When estimating the rate of flow of fluids through rocks and sediments, knowledge of the viscosity of fluids is a prerequisite. Under a pressure gradient, gases may move by viscous flow through a porous medium such as sediment or rock. Flow rates can be estimated using Darcy's Law:

$$Q_v = \left(\frac{K_i \cdot \gamma \cdot A \cdot i}{\mu}\right) \cdot C \tag{2.2}$$

Where:
Q_v = Flow of gas (m^3/s) through area A.
K_i = Intrinsic permeability of material through which gas or vapour is flowing.

γ = Unit weight of gas (N/m^3).
μ = Viscosity of gas (Ns/m^3).
A = Area of migration perpendicular to migration direction (m^2).
i = Pressure gradient along migration route.
C = Concentration of gas or vapour.

The Darcy equation is based on the intrinsic permeability of the soil or rock through which a gas is flowing. It is expressed differently from the common equation for Darcy's Law which is specific to the flow of water through the ground and is based on the saturated hydraulic permeability of the ground (Wilson et al., 2009). The theory assumes laminar, uncompressible gas flow and does not make any provisions for chemical or biogeochemical reactions that may occur along the migration route (Wilson et al., 2009). There are instances where it is necessary to calculate the viscosity of a gas mixture. For example, landfill gas, a mixture of CH_4 and CO_2 in the approximate ratio 3:2.

Gas Diffusion

Gases may also move in the sub-surface by molecular diffusion which requires the presence of a concentration gradient. Gas flows from an area of high concentration to an area of low concentration. In accordance with Fick's Law, the rate of mass transfer of a gas or vapour by diffusion can be estimated as follows:

$$E = A\,(C_{source} - C_{g^0})\,D^{eff}/L \tag{2.3}$$

Where:
E = Rate of mass transfer due to diffusion (g/d).
A = Area through which migration occurs (m^2).
C_{source} = Concentration of gas being considered at source (g/m^3).
C_{g^0} = Concentration of gas being considered at limit of migration (g/m^3).
D^{eff} = Effective diffusion coefficient in the medium being considered (m^2/d).
L = Distance over which migration occurs (m).

Gas diffusion coefficients vary according to the type of porous medium and the degree of saturation (Hooker and Bannon, 1993).

Fick's Law assumes that isobaric conditions are prevalent, there is no pressure driven flow, relatively low concentration of gas and high soil permeability (Wilson et al., 2009). Additionally, it is assumed that diffusion only occurs in one direction, diffusion coefficient is constant (although it varies with concentration and temper-

ature) and it excludes the effect of Knudsen diffusion (where the scale length of a system is comparable to or smaller than the mean free path) and non-equimolar diffusion.

2.5.2 Landfill Design Factors

Since the late 1950s' discovery that groundwater is contaminated by landfill leachate, two separate landfill design concepts have evolved: natural attenuation (for non-hazardous industrial and municipal waste) and containment (for hazardous industrial waste) (Bagchi, 2004). Older landfills (pre-1970) tend to be of the natural attenuation type. A brief summary of their design factors is given in this section.

Natural Attenuation Landfills

Natural attenuation landfills work on the principle that leachate (and gas) percolating through the landfill base will be purified (attenuated) in the underlying unsaturated soil zone and groundwater aquifer (Bagchi, 2004). However, studies have shown that small natural attenuation landfill facilities comprising less than 40,000 m^3 waste volume may impact groundwater quality (Friedman, 1988). Consequently, natural attenuation may be considered high risk due to the uncertainty in prediction of contaminant loading and quantification of leachate attenuation mechanisms (McBean et al., 1995). More recently, the regulation trend has moved towards maximising containment and removal of leachate before release to the environment (McBean et al., 1995).

Mechanisms of attenuation include: adsorption, biological uptake, cation and anion exchange, dilution, filtration, and precipitation. All mechanisms with the exception of dilution may be operative in the unsaturated zone while all mechanisms with the exception of biological uptake may be operative in an aquifer (Bagchi, 2004).

The unsaturated zone is a potential buffer that may protect groundwater through various physical, chemical and biological processes that alter the nature and quantities of contaminants arriving at the water table as a function of time (McBean et al., 1995). An ideal situation for a natural attenuation facility would be to have uniform, moderately textured soil (soils with moderate amounts of silt and clay). Furthermore, a substantial thickness between the bottom of the facility and the top-surface of the groundwater is desirable (McBean et al., 1995). These soils are advantageous as they encompass a relatively large surface area with a moderate to low water flow rate.

At the opposite end of the spectrum, heavily textured soils (e.g. tight clays)

would not provide a good location for natural attenuation landfills as they do not allow a sufficient passage rate of leachate. In these circumstances, there would be a risk of a build up of leachate head within the site unless provision was made for removal and treatment(McBean et al., 1995). Biological uptake of contaminants and precipitation reactions are influenced by the degree of saturation of the unsaturated zone. Higher levels of saturation lead to less available O_2 for biological activity. Ensuing anaerobic conditions would lead to bacterial growth. Bagchi (2004) noted that the worst case scenario is for the soil to be fully or nearly saturated, therefore, attenuation should be focused on biological uptake under similar conditions.

Containment-Type Landfills

Containment-type landfills are engineered to a much higher standard with the aim of significantly reducing discharge into underlying hydrogeologic environments. Improvements in engineering standards have increased since the 1970s with multiple layering strategies and geosynthetic materials now commonplace. Soils comprising a high percentage of clay-sized particles are most frequently used and often serve as a primary barrier to liquid and gas movement (McBean et al., 1995). Leakage through the base of a containment landfill is theoretically unavoidable. Leachate is partitioned into two fractions: (1) a laterally transported to collection pipes and stored in leachate tanks fraction, and (2) a small portion that percolates through the liner (Bagchi, 2004).

However, a major problem with using clays is that significant variation in permeability can be observed as a result of relatively small changes in other properties. For example, a change of 2 to 3% in moisture content can result in a permeability change by an order of magnitude (Dixon and Murray, 1998). Additionally, faults in liners can cause permeability to exceed design calculations. Cracks and fissures in soil liners caused by improper placement procedures, or punctures and incomplete sealing of the seams of flexible membrane liners can compromise performance (McBean et al., 1995).

Leachate leakage through a properly constructed liner is not high. However, there is an issue of longer-term integrity of synthetic layers in continuous contact with landfill leachate (McBean et al., 1995). Data provided by Gordon et al. (1989) suggests that leakage through a clay liner reduces over time (due to a decrease in liner permeability). Multiple-layered liners are generally considered to be a more robust approach to prevent contaminant migration. A double-lined landfill is called a composite lined landfill and comprises a synthetic membrane overlying a clay liner (Bagchi, 2004). Specific site conditions will determine the minimum thickness of

these layers. An important consideration is that transport may be governed by advective (pressure gradient) or diffusive flow (concentration gradient). Of these two processes, Quigley et al. (1988) showed that diffusion was the more important mechanism owing to the low permeability and porosity of clays.

2.5.3 Hydrological and Meteorological Controls

There are a number of hydrological and meteorological controls on gas transport in the sub-surface. The controls include: soil saturation, rainfall, temperature, pH, atmospheric pressure, wind velocity. The influences on gas migration are discussed in this section.

Atmospheric Pressure and Wind Velocity

Perhaps the most significant meteorological control on gas transport in the sub-surface is the influence of atmospheric pressure. There are numerous studies and reviews reporting an inverse relationship between atmospheric pressure gradient and gas emission/migration, including: Christophersen and Kjeldsen (2001); Christophersen et al. (2001); Czepiel et al. (2003); Poulsen et al. (2003); Gebert and Gröngröft (2006); Scheutz et al. (2009); Gebert et al. (2011); Rachor et al. (2013); and Delkash et al. (2016). It is important to note that wind is induced by atmospheric pressure gradients. Emission and dispersion of CH_4 and CO_2 from a sub-surface source will be dependent upon wind velocity.

In a study of passive landfill gas emission, Gebert and Gröngröft (2006) showed that gas flow was driven by variations in atmospheric pressure. They asserted that advective gas flow reversed more than once daily and that atmospheric pressure changes below 1 mbar were enough to induce immediate changes in flow direction. Furthermore, Gebert and Gröngröft (2006) determined that diurnal variations in atmospheric pressure up to 4 mbar controlled gas flow direction, but were often superimposed by longer-term pressure changes associated with atmospheric highs and lows.

This corroborated the work of Czepiel et al. (2003), who reported a significant inverse relationship between gas emission and atmospheric pressure gradient. A linear regression yielded a correlation coefficient, r^2, of 0.95 from landfill gas emission data (Czepiel et al., 2003). Additionally, Pedersen (2010) observed that the scale of the pressure gradient governed the magnitude of the emission. For instance, a shallow negative pressure gradient over a long period of time was noted to result in a lower positive pressure in the landfill (Pedersen, 2010). Conversely, Christophersen

et al. (2001), did not find a strong correlation between pressure gradient and gas emissions ($r^2 = 0.37$). Although the correlation was statistically significant ($P < 0.001$), Christophersen et al. (2001) argued that barometric pressure was not the most important controlling factor on gas emissions.

Building on earlier work, Gebert et al. (2011) proposed a simplified matrix to assess the relative importance of different factors. For gas transport governed by diffusion, soil temperature is a heavy influence. Time-scales are monthly reflecting seasonal variability. Also, in terms of diffusion transport, Gebert et al. (2011) noted that soil moisture impacted gas balance on shorter time-scales such as hourly and weekly, but also increased towards seasonality. By comparison, the authors noted that wind and changes in barometric pressured affected gas transport predominantly on very short time-scales such as hours or minutes.

Contrasting to these observations, Gebert et al. (2011) stated that when gas transport was dominated by advection, barometric pressure fluctuations had a higher impact on gas composition across all scales. The significance of soil moisture and soil temperature was lower under advection transport control. By extension, wind velocity and associated near-surface pressure changes were assumed to influence gas composition at sites of advective transport (Gebert et al., 2011). These observations relating to pressure gradients were also supported by Rachor et al. (2013) and Delkash et al. (2016).

Soil Temperature and Saturation

Greenhouse gas production in soil is directly affected by soil temperature and moisture due to effects on micro-organisms and root activity (Smith et al., 2003). Gas diffusivity is inversely proportional to soil water content and controls the movement of gases to and from the atmosphere. With increasing height of water table, CH_4 is driven towards the surface while CO_2 is dissolved into the groundwater due it being 58 times more soluble in water than CH_4 (Hooker and Bannon, 1993). As emissions of CO_2 resulting from soil respiration are 10–15 times greater than from fossil fuels, soils and vegetation are considered to be the principal sources from which CO_2 enters the atmosphere (Raich and Schlesinger, 1992).

For depths of 2, 5 and 10 cm, Davidson et al. (1998) reported corresponding diurnal temperature responses (Q_{10}) for CO_2 fluxes of 2.2, 2.7 and 4.2. With increasing depth, there is a decrease in diurnal temperature variation (Davidson et al., 1998). According to Smith et al. (2003), the release of CO_2 from soil organic matter by heterotrophic respiration and autotrophic root respiration, generally increases exponentially with temperature. Additionally, greater microbial activity (and con-

sequent CO_2 production and emission) rate in the uppermost layers of soil will be expected due to greater effect of diurnal temperature changes (Smith et al., 2003).

Soil water content (particularly water-filled pore space) is another variable that affects soil respiration rates (Xu and Qi, 2001). As soil dries, a critical point is reach at which microbial activity is inhibited and respiration decreases (Smith et al., 2003). In very wet soils, aeration is restricted due to a high proportion of the pores being filled with water. Under these conditions, respiration is also constrained and CO_2 flux decreases. This affect is not as prominent as when water shortage is the limiting factor (Smith et al., 2003).

From a soil science perspective, depth of water table also has an important effect on soil respiration. For example, Davidson et al. (1998) showed that water table effects O_2 supply to the decomposer microflora that are a major control on CO_2 emission in high latitudes in soils with thick organic layers. It is for this reason that afforestation as a potential mitigation strategy for fossil fuel emissions of greenhouse gases has become a topical issue following the Kyoto Protocol (Smith et al., 2003).

2.5.4 Detection and Measurement

Commercially, there is a wide range of equipment and instrumentation available for the detection and measurement of CH_4 and CO_2 in the sub-surface. In particular, there is a healthy industrial market for landfill gas monitors with multiple manufacturers producing instruments. Although designed specifically for the monitoring of landfill gas, many of these instruments may be adapted for use across a wide-range of applications including natural emissions, shale gas exploration, hydraulic fracturing 'fracking' and Carbon Capture and Storage (CCS). Traditionally, hand-held point-measurement monitors were the primary choice for gas measurement and regulation compliance. However, in more recent years there has been a move towards high temporal frequency monitoring (for example, Wadey-Leblond (2012)). A review of the available techniques is given in this section and is divided into point measurement monitoring and high temporal frequency monitoring.

Point Measurement Monitoring

In the UK, the two main manufacturers of hand-held portable, point measurement landfill gas analysers are Geotechnical Instruments (UK) Ltd and Gas Data Ltd. Both companies produce a range of products. Currently Geotech UK models include, 'GA5000 Portable Landfill Gas Analyser,' 'GEM5000 Portable Landfill Gas Extraction Monitor,' 'BIOGAS 5000 Portable Biogas Analyser,' 'BIOGAS 300 and

GA3000 PLUS Fixed Landfill Gas and Biogas Analysis Systems,' 'AP Autopumps range for landfill pumps, leachate pumps and condensate pumps,' and 'ATEX dipmeters for leachate and liquid level monitoring'.

Similarly, Gas Data Ltd produce an array of products that include, GFM Series Portable Gas Analysers, GFM Series Portable Gas Flow Meters, Fixed Gas Analysis Systems and Wastewater & Sewage Management. The GFM Series Portable Gas Analysers currently include, 'GFM436' (for site investigation, landfill and compliance), 'GFM426' (portable landfill gas extraction monitor), 'GFM406' (multichannel portable gas analyser) and 'GFM225' (CO_2 detector and security analyser). At the time measurements were taken the most recent models available to the author were Geotech UK's GA2000 (equivalent to GA5000) and Gas Data Ltd's GFM435 (equivalent to GFM436).

Flow Measurement

Borehole flow is the mass movement of gas in a borehole. Usually, it is expressed as either being in the positive direction (venting) or negative direction (sucking). Flow is heavily related to atmospheric pressure and to the mass production of gas in a landfill. Under conditions of falling atmospheric pressure, it is usual to anticipate a positive borehole flow as the negative pressure gradient will allow gas to move upwards towards the surface. Therefore, if air pressure is rising, we expect negative borehole flow.

Another way to describe borehole flow would be to analyse the difference between borehole pressure and air pressure. If the borehole pressure is less than the atmospheric pressure, a positive pressure gradient is formed and positive borehole flow conditions exist. If the borehole pressure is greater than the atmosphere, however, a negative pressure gradient exists and the borehole is said to be under negative borehole flow conditions.

Changes in the flow readings can be used as a useful indicator that a change has occurred within a landfill. However, this requires that measurements are reproducible. Care needs to be taken to ensure that samples are taken by the same procedure each time. If flow readings do show change, it can be used to inform the operator that further investigations are required.

Flow rates are also subject to changes in atmospheric pressure. If atmospheric pressure is falling, the user might anticipate a positive borehole flow reading and vice versa. Therefore, it is essential to monitor during pressure fall and pressure rise and record absolute atmospheric pressure in order for any flow readings obtained to have any context and significance.

Manufactured by ShawCity UK Ltd, the GFM435 portable landfill gas monitor is Monitoring Certification Scheme (MCERTS) and ATEX approved. It is optimised for site investigation and peripheral landfill monitoring.

Gas flow rates from a ground borehole are measured using a miniature thermal dispersion flow transducer. This device is bidirectional and carries the following calibration specification.

- In the borehole out-flow direction (or venting/positive flow) 0 to 100 l/hr (or 0 to 2.78×10^{-5} m^3/s).
- In the borehole in-flow direction (or sucking/negative flow) 0 to -60 l/hr (or 0 to -1.67×10^{-5} m^3/s (Gas Data UK Ltd, 2012).

The instrument's internal transducer pipe connections are sized so that the instrument itself presents negligible impedance to the gas flow. Typical impedance measurements are less than 50 Pa at 100 l/hr. In the field, the instrument is connected to a borehole valve by a 0.6 m length bore hose that has an internal diameter of 0.003 m.

The purpose of a field measurement is to assess the rate of discharge of gas from a venting borehole and the consequential change of gas pressure in the borehole.

The pressure indication (dp) is a cross calibration of gas flow to pressure at the borehole end of the sample tube. That is, the pressure indicates is the pressure difference between the gas in the entrance of the sample tube and atmosphere whilst the gas is flowing. Consequently, the flow reading is a dynamic measurement. Over time, the pressure reading from the GFM435 will reduce as gas from the borehole is exhausted through the instrument. This concept is generally accepted as a good analogy for a borehole venting to the atmosphere.

However, the calibration for dp is only valid when the sample tube specified by the manufacturer is employed. Validation of the data is compromised if the sample tube length or diameter is altered, or if any inline filter is incorporated. Furthermore, annual recalibration of the flow and pressure channels is recommended by the manufacturer as a field instrument is subject to damaging events such as dirt/water ingress, over/under range flow surges, shock, extremes of temperature.

A miniature thermal dispersion pressure transducer that is equipped with the GFM435 is preferable to a digital manometer as a digital manometer does not permit gas flow and therefore takes a static pressure reading only. It is argued that this is not analogous to a venting borehole.

A complicating factor is that a capped landfill, with air-tight sealed boreholes will build up static pressure. This pressure is related to the rate of gas generation.

However, it is also heavily influenced by gas permeability, thickness of cover and preferential pathways that may exist. Geotechnical Instruments (UK), the manufacturer of GA2000 argue that the pressure in a borehole, and thus a landfill, cannot be used as an indication of gas generation rate (Riley, 2009).

Under equilibrium conditions, gas generation within a landfill is balanced by the loss of gas. In these circumstances, there will be no gas flow into or out of the borehole as the borehole pressure will be the same as the pressure in the landfill. When a flow measuring instrument is connected to the borehole and the tap is opened, the equilibrium conditions described above are disrupted. Gas will be forced out of the borehole as the pressure in the borehole will equilibrate with atmospheric pressure.

With the borehole tap opened, the system is opened to the atmosphere and the borehole will consequently reach near atmospheric pressure. As the landfill will be at a higher pressure, the low pressure borehole acts as a sink for the high pressure gas in the landfill. In other words, a flow of gas will enter the borehole from the surrounding landfill. Factors including internal landfill pressure, permeability of waste, existence of preferential pathways, moisture content and water table will affect the measured flow. It is argued that without a restriction applied to the flow, a reading will not be a true indication of the gas generation within a landfill (Riley, 2009).

Therefore, the GA2000 is fitted with a restrictor to gas flow (Riley, 2009). Less gas is removed from the borehole and accordingly, the pressure within the borehole is not as reduced as much as before. Also, the equilibrium state of the landfill is not as disrupted as much.

This method, known as the restricted flow method yields lower values for the measured flow. Arguably, this 'low flow' alternative method does no suffer as much from the gas sink effect as the open flow method (Riley, 2009).

An advantage of this restricted flow method is that restrictor in the instrumentation's system is the limiting factor. The measured flows will be independent of any other parameters such as pipe length and internal diameter. Flow readings are, therefore, more reproducible and allows the operator to compare readings taken over long timescales and identify any changes over the lifetime of the landfill. However, as discussed, it is not possible to determine absolute gas generation rate from a landfill by this approach.

A summary of the manufacturers specifications is provided in Table 2.8.

Specification	GA2000	GFM435
Manufacturer	Geotechnical Instruments (UK) Ltd	Gas Data Ltd
Flow Transducer	Restricting flow transducer (unknown restriction factor and whether the restriction is arbitrary).	Bidirectional thermal dispersion flow transducer (does not limit flow and is equipped with pressure indication facility).
Calibration Range	0 to 20 l/hr ± 0.3% (unable to measure negative borehole flow).	0 to 100 l/hr (positive borehole flow). 0 to -60 l/hr (negative borehole flow).

Table 2.8: Landfill Gas Analyser Manufacturer Flow Measurement Specifications

High Temporal Frequency Monitoring

At the present time, GasClam®, developed by IonScience Ltd and distributed through ShawCity Ltd is the first and so far only ground gas monitor in the UK facilitating the automated capture of long-term, high frequency data. It is capable of a sample rate frequency of every three minutes. Like traditional hand-held monitors, it measures CH_4, CO_2, O_2 as well as H_2S and Volatile Organic Compounds (VOCs). Additionally, it is capable of measuring ambient temperature, ambient pressure, borehole pressure, differential pressure and water depth. However, the model used for this research was not equipped with the water depth gauge. Crucially, the GasClam has been used to monitor ground gas concentrations by Cuadrilla Resources Ltd during Shale Gas exploration in Lancashire, UK during the time-frame of this research (Wadey-Leblond, 2012).

Unlike the hand-held equivalent instruments that quantify flow, the GasClam does not. Instead, the ambient pressure and borehole pressure are recorded. A differential between these two pressures is calculated. When the differential pressure is positive, ambient pressure is less than borehole pressure. Under these conditions, there is a mass movement of gas (CH_4 and CO_2 from borehole to atmosphere). A greater differential results from a steep decline in atmospheric pressure. Conversely, a negative differential results from atmospheric pressure being greater than borehole pressure. When these conditions prevail, air enters a borehole from the atmosphere.

Summary of Technical Equipment Specifications

A summary of the specifications of the three landfill gas analysers is provided in Table 2.9. The method used to quantify gases along with calibration range, accuracy and resolution is provided.

Specification	GA2000	GFM435	GasClam
CH_4	Infrared 0–100% v/v (Accuracy 0.5% < 70% 1.5% > 70%)	Infrared 0–100% v/v (Accuracy 0.2% at 5.0% 1.0% at 30.0%)	Infrared 0–100% v/v (Resolution 0.5% < 50% 1.0% > 50%)
CO_2	Infrared 0–100% v/v (Accuracy 0.5% < 60% 1.5% > 60%)	Infrared 0–100% v/v (Accuracy 0.1% at 10.0% 3.0% at 50.0%	Infrared 0–100% v/v (Resolution 0.5% < 50% 1.0% > 50%)
O_2	Electrochemical 0–25% v/v (Accuracy 1.0%)	Electrochemical 0–25% v/v (Accuracy 0.5%)	Electrochemical 0–25% v/v (Resolution 0.1%)
H_2S	Electrochemical 0–1,000 ppm (Accuracy 2% f.s.)	Electrochemical 0–1,500 ppm (Accuracy 5% f.s.)	Electrochemical 0–100 ppm (Resolution 1 ppm)
CO	Electrochemical 0–1,000 ppm (Accuracy 2% f.s.)	Electrochemical 0–1,000 ppm (Accuracy 5% f.s.)	Electrochemical 0–1,000 ppm (Resolution 1 ppm)
VOCs	N/A	N/A	Photoionisation Detector 0–4,000 ppm (Resolution 1 ppm)
Atmospheric Pressure	Pressure Transducer 700–1200 mbar (Accuracy 5 mbar)	Pressure Transducer 800–1200 mbar (Accuracy 1 mbar)	Piezoelectric 800–1200 mbar (Resolution 1 mbar)
Borehole or Differential Pressure	Pressure Transducer −500–500 mbar (Accuracy 4 mbar)	Pressure Transducer −100–300 Pa	Piezoelectric 800–1200 mbar (Resolution 1 mbar)
Temperature	External Probe −10.0–75.0°C (Accuracy 0.5°C)	External Probe −10.0–100°C (Accuracy 0.5°C)	Internal Chip −5.0–12.0°C (Resolution 1.0°C)

Table 2.9: Landfill Gas Analyser Manufacturer Specifications

2.6 Historic Incidents

Despite the widespread presence of CH_4 and CO_2 gases in the sub-surface, incidents that have resulted in damage/destruction of property, injury or death have been mercifully few and far between. However, a number of incidents concerning landfill, mine workings and coal gas in the UK during the 1980s and 1990s has led to an increase in public awareness, helped develop the knowledge-base of mechanisms in the sub-surface and tightened regulation. Crucially, this has resulted in improved engineering techniques and more rigorous engineering practises which has improved worker and public safety.

2.6.1 Abbeystead, Lancashire, UK, 1984

The Abbeystead disaster occurred on 23rd May 1984 during a public demonstration of a new water pumping facility provided by the North West Water Authority

(NWWA). Eight people were killed instantly with a further eight succumbing to their injuries later. A further 26 people received non-fatal injuries. The valve house was extensively damaged in the explosion (Orr et al., 1991; HSE, 1985). This constituted one of the worst explosions involving CH_4 derived from shale gas in the British Isles.

Although the cause of ignition was never identified, it was determined that CH_4 had been displaced from stagnant water in a void formed at the end of a tunnel in the preceding 17 days before the explosion (Carson and Mumford, 2007). When pumping resumed for the demonstration on the evening of 23rd May 1984, as the water levels rose in the tunnel, it forced out the CH_4/air mixture in the void through the air valves located above the access end of the tunnel and into the sealed vent chamber. From the vent chamber the gas was free to flow through the large open vent pipe into the valve house (Orr et al., 1991).

Investigations following the incident involved geological surveys to determine potential sources of gases and reservoirs along with analysis of gas and water samples to identify the source. The main conclusions were (from Orr et al. (1991)):

- Isotopic analysis showed that the CH_4 was derived from source rocks at considerable depth (i.e. shale gas).
- The CH_4 was migrating upwards to a trap at the level of the tunnel, most likely at a constant rate.
- A possible mechanism for CH_4 migration was by 'gas-lift pump' as CH_4 is insoluble in water at high pressure.
- CH_4 entry was concentrated mainly near to the axis of an anticline about 2.0–2.5 km distant.
- In dissolved and free gas form, the long-term average rate of CH_4 egress from the tunnel was 8 kg/day.
- Water entry was predominantly from the Abbeystead (southern) limb of the anticline.
- Inversely proportional to barometric pressure, CH_4 inflow varied and responded to other factors such as transfer rate and previous operating history.
- It was estimated that $\sim 50\%$ of CH_4 entered the tunnel as a free gas.

An important aspect of this case was that there were no associated former mine workings in the vicinity. The void where the explosion occurred was operational and had not been decommissioned. The CH_4 gas that had caused the explosion was derived from a deep geological source. It was postulated that because the long-term rate of entry of CH_4 did not vary significantly between 1984 and 1991, the

source reservoir was of considerable capacity. Therefore, the lower trap in the reef deposits in the Carboniferous Bowland shales at a depth of 1,000 m was identified as the most likely reservoir (Orr et al., 1991). This is of crucial significance to the research presented here as most of the research sites are located above the Bowland-Hodder unit in NW England. Furthermore, this is a likely future area of shale gas exploitation.

2.6.2 Loscoe, Derbyshire, UK, 1986

By far the most prominent example in geotechnical engineering is the Loscoe explosion in Derbyshire, UK which occurred on 24th March 1986. Landfill gas (60% CH_4:40% CO_2) migrated laterally 70 m from Loscoe landfill resulting in the destruction of one residential property and injuring the three occupants of the building (Williams and Aitkenhead, 1991). To determine the cause of the explosion, Derbyshire County Council commissioned the British Geological Survey to carry out investigations involving assessment of the geology, determination of soil gas composition, review migration mechanisms and pathways, and examine meteorological effects (Aitkenhead and Williams, 1986).

A specific chain of events and a series of coincidences was found to have caused the explosion. A summary of the data and evidence is provided below (from Williams and Aitkenhead (1991)):

- The landfill was a former brick clay quarry. It received inert waste between 1973 and 1982. In 1984, part of the site was lightly covered with permeable material. A clay layer to cap the site was added shortly before the explosion in 1986. Landfills of this age were generally engineered to much lower specifications and did not require any basal lining.
- Precursors in 1983 included the necrosis of vegetation (trees and lawn) in the garden of the destroyed property. Additionally, the soil became warm, dried out, crumbled and a white fibrous mould was observed. Adjacent properties experienced the same phenomena and unpleasant odours.
- As a precaution, British Coal installed a stand-pipe with a flame trap to vent soil gas to the atmosphere after a 0.5 m hole exposed muddy water bubbling with gas which contained 50% of the lower explosive limit of CH_4.
- Analysis of the gas indicated that it was more likely to have been evolved from rotting material rather than a burning coal seam.
- The local geology is comprised of Middle Coal Measures strata of Westphalian age that crops at or near the surface. The Middle Coal Measures comprise

coal, mudstones, siltstones and sandstones around the broad and shallow Shipley Syncline. At Loscoe, the beds dip 5°to 11°in a general south-easterly direction with no faults or minor folds. Despite mudstones having the lowest permeability, the gently inclined interbedded rock sequence allowed the lateral, unrestricted migration of landfill gas. However, a thin surface layer ($\sim$ 1 m) of clay comprising Head and glacial till restricted movement of gas to the surface except where breached by excavations such as those for building foundations or underground service trenches.

- Gas movement by diffusive flow modelled by Fick's Law was dismissed as too inefficient. Working on the basis of an initial 60% CH_4 concentration at the landfill boundary and a diffusion coefficent of CH_4 in unsaturated sandstone of 3×10^{-6} m^2/s, it would require a period of 26 years to achieve a 5% CH_4 concentration 100 m distant. These figures were far beyond the parameters observed for the explosion.
- On the morning of the explosion, a deep Atlantic depression was crossing the UK resulting in an atmospheric pressure drop of 40 mbar in 10 hours. The explosion occurred after a fall of 20 mbar. However, the mechanism of movement is more complex. The investigators considered whether the gas was free to escape uniformly or whether it escaped from a specific point, i.e. where the surface clay is breached. Other factors that needed to be considered were the volume of the rock containing the gas and the gas diffusivity in that medium. None of these factors were known with any accuracy at Loscoe. An approximation was calculated to prove the barometric pressure mechanism using the following assumptions:

  - No CH_4 was initially present under the floor.
  - Influx of gas resulted only from the atmospheric depression.
  - The volume of the underfloor space was estimated to be 120 m^3 (10 m $\times$ 12 m $\times$ 1 m).
  - The explosion took place at the lower explosive limit of CH_4 in air (5%).
  - The volume of CH_4 required to have entered the underfloor space would have been 6 m^3 (5% of 120 m^3).
  - Landfill gas contains 60% CH_4, the volume of gas required to have been expelled from the ground was 10 m^3.
  - If expelled in 5 hours (during the depression), the flux would have at least needed to be 2 m^3/hr.
  - If CH_4 was already present in the sandstone beneath the underfloor space, this flux could have easily been achieved by a 40 mbar change in pressure,

given that sandstone is more permeable to landfill gas than to water.

- Gas samples from the soil were consistent with landfill gas (CH_4:CO_2 60%:40%). Gas derived from the stand-pipe was separated into CH_4 and CO_2. Radiocarbon (^{14}C) analysis of CH_4 recorded a ^{14}C value of 125%, indicating a modern source such as landfill and not the underlying coal strata. Additionally, the mains gas was ruled out as the source of the explosion as C_2H_6 normally present in the mains supply at 3–4% v/v with a CH_4:C_2H_6 ratio of about 25:1 was not present in the soil gas in the same proportions. Furthermore the mains gas CO_2 content of $< 0.5\%$ was much lower than the soil gas CO_2 content of 40%.

A landmark case, Loscoe set a precedent and brought new knowledge to geotechnical engineering that resulted in tighter regulation and higher specification engineered systems. An important issue outlined by the incident was gas source and responsibility. The evidence documented by Williams and Aitkenhead (1991) proved that it was the landfill operator who was responsible for the explosion and not the Coal Board or Gas Supplier.

Furthermore, little consideration had previously been given to potential migration of gas off site from landfills. Therefore, conceptual site models take into greater account the geology and hydrogeology of a site as well as changes induced by meteorology. Conceptual models are tailored for each location and take into account a greater depth and breadth of factors. In conjunction with a robust conceptual site model, monitoring of the site by means of gas monitors and boreholes are now employed to a maximum for optimum regulation and public perception of safety. Indeed, gas monitors have become a new industry over the last 25 years with multiple manufacturers offering a range of instruments across the market.

Additionally, landfill engineering specifications are much higher compared with the 1960s and 1970s. Usually, landfills contain a sophisticated basal lining system and cap to prevent/minimise migration of gases and leachates off site as much as possible. A typical basal lining may comprise engineered clays and low density flexible membranes to contain gases and leachates. Landfill caps may typically utilise a thick clay (1 m) and restoration soils.

2.6.3 Arkwright Town, Derbyshire, UK, 1988

Incidents involving gases, particularly CH_4 associated with mine workings have been well documented from the early days of mining in the UK. Between 1851 and 1980, there were no fewer than 186 major explosions in British coal mines attributed to firedamp (explosive concentration of CH_4 5% v/v – 15% v/v) resulting in $\sim$ 10,000

fatalities (Turton, 1981). An incident concerning firedamp occurred at Arkwright Town, Derbyshire in late 1988.

On 9th November 1988, more than 40 families were evacuated by the local authority after CH_4 was found to be seeping into houses. Following the closure of Arkwright Colliery in early 1988, groundwater levels began to rebound forcing CH_4 from underground voids. Entry into private premises was believed to be through cracks that had been caused by subsidence. As a precaution, the settlement was completely demolished in 1995 and relocated a safe distance from the former colliery workings (Hall et al., 2005).

2.6.4 Widdrington, Northumberland, UK, 1995

Blackdamp, a mixture of N_2, CO_2 and water vapour gases that displaces O_2, is particularly associated with abandoned mine workings. Due to its greater density than air, it is often located in low-lying areas such as natural depressions in topography and man-made ditches for underground services. On 11th February 1995, it claimed the life of 60-year-old, Donald Tollett at the Kava Furniture Factory, Widdrington, Northumberland. The factory, a private premises, was located in former colliery buildings. On bending over to attend to a collapsed collie dog, Mr Tollett also collapsed and died as a result of asphyxiation (Hall, 2007).

The abandoned mine workings were identified as the source of the gas. A number of conditions were attributed to the timing of the gas release (from Hall (2007)):

- Steady barometric pressure conditions for several days prior to the incident followed by a sudden fall in pressure.
- A positive pressure was established by a sufficient build-up of gas within the mine workings.
- Pumping cessation from the old mine workings had lead to groundwater rebound.
- The drift entrance was not a gas-tight seal.
- Above the drift entrance there was little or no ventilation in the buildings that lead to an accumulation of gas.

As a result of this fatality, remedial steps were taken to minimise future risk at the site. This included the excavation of the top 5 m of drift which was backfilled with a clay-rich material. Meanwhile the drift entrance was completely sealed in concrete and a vent pipe was installed (Hall, 2007).

A similar incident occurred near Barnsley, South Yorkshire in 1998 when 22-year-old Christopher Noonan suffocated while laying sewer pipes in a trench. It was later

identified that blackdamp had leaked into the trench from a nearby disused colliery. In December 2000, Barnsley Council admitted to two breaches in health and safety regulations by not properly appraising the risk posed by mine gas when the work was planned in the vicinity of a former colliery. The authority was subsequently fined £20,000 at Sheffield Crown Court (Humphries, 2001).

Chapter 3

The Research Sites

3.1 Introduction

This chapter introduces the three research sites and control site from which data were collected for this project. A description of location, geology and hydrogeology are given for each site and in relation to anticipated movement of gas in the unsaturated zone. The sites were selected as the underlying geology included a thick unsaturated zone (confined by glacial clays) through which CH_4 and CO_2 gases could be transported. Figure 3.1 indicates their approximate locations within the UK.

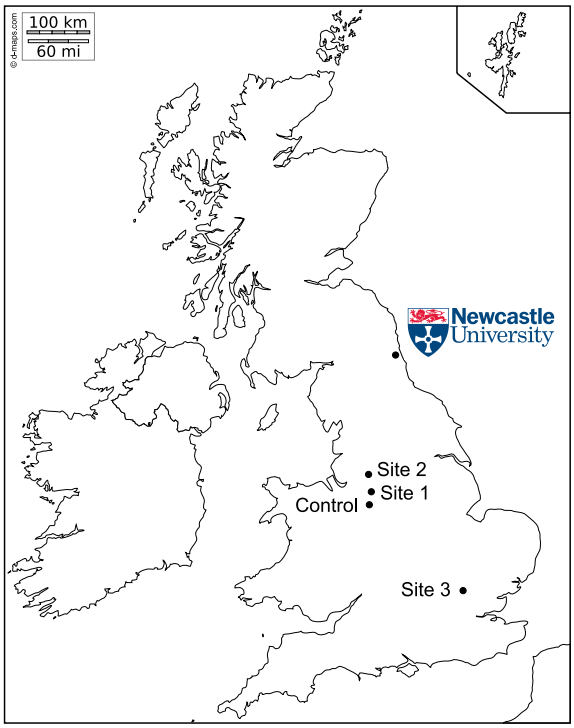

Figure 3.1: Outline Map of the UK Showing Approximate Locations of the Sites (Map from d-maps.com (2015))

3.2 Site 1

3.2.1 Site Location and Description

Figures 3.2 and 3.3 indicate the location of Site 1 within Cheshire, UK. The entrance to the site is located at 53.269397 °N, -2.174366 °E or OS grid reference SJ 885 747.

Figure 3.2: Aerial Photograph Showing the Location of Site 1 within Cheshire, UK

A former sand quarry, the site was progressively filled with inert waste starting from 1968. According to the Environment Agency (2010b), inert waste is defined as that which does not undergo any significant physical, chemical or biological transformation. Inert waste does not dissolve, burn or otherwise physically or chemically react, biodegrade or adversely affect other matter that it comes into contact. It does not likely give rise to environmental pollution or harm human health.

Over half of the quarry void was filled by 1991. In order to allow reclamation of the quarry and to raise the level to the surrounding land, tipping of solid non-biodegradable wastes (e.g. soils, sands, clay, clean brick and stone) commenced in 1998. By 2003, landfilling operations had ceased, at which point, gas monitoring of the site began. As it is the oldest landfill site studied, it is also the least engineered.

Generally undulating in nature, the adjacent land slopes gently downward in a northerly direction. To the north and east, the site is bounded by pasture, while the south and west boundaries are bordered by residential dwellings and gardens. Consequently, there is a potential receptor of any uncontrolled gas migration.

Figure 3.4 clearly shows how the array of monitoring well installations was designed to capture movement of landfill gas away from the landfill. Boreholes 06/17 and 06/18 provide the nearest indication of any imminent danger of environmental hazard to human life resulting from migration of landfill gas.

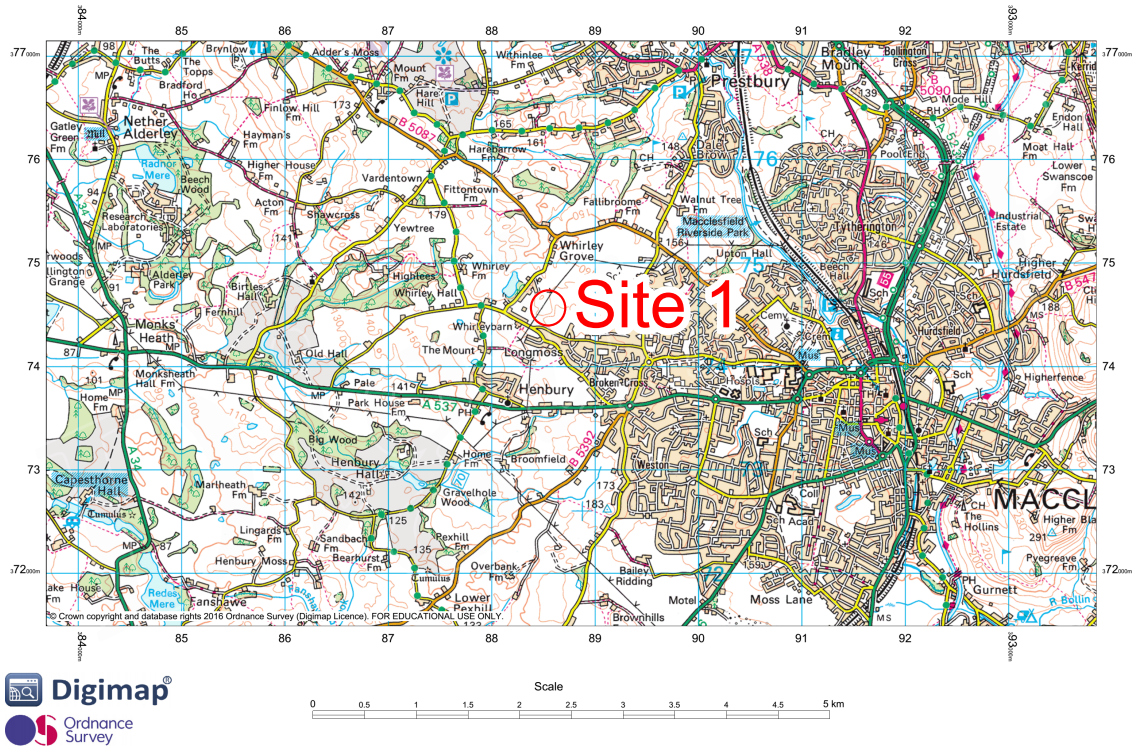

Figure 3.3: Ordnance Survey Map Indicating Location of Site 1 (from Ordnance Survey (2015b))

3.2.2 Geology and Hydrogeology

Figure 3.5 shows schematic geological cross-sections of Site 1. The underlying solid geology consists of the Permo-Triassic Tarporley Siltstone Formation, which dips in a westerly direction. Glacial drift deposits of varying thickness overly the Permo-Triassic bedrock. The rock-head lies approximately 30 m below ground level. Immediately overlying the bedrock is an impermeable layer of Lower Boulder Clay that varies in thickness. This in turn is overlain by the Middle Sands which is generally in excess of 15.2 m thick (Martin, 2005). During quarry operations, it was the Middle Sands that were commercially excavated. Capping the Middle Sands is an upper layer of Boulder Clay that is between 0.9 m and 3.6 m thick.

The Environment Agency classes the Middle Sands as a Secondary A aquifer and the underlying bedrock as a Secondary B aquifer (Environment Agency, 2010a). Overall, these are grouped in the Environment Agency's Minor Aquifer Low Groundwater Vulnerability Zone (Environment Agency, 2010a). The geological memoir

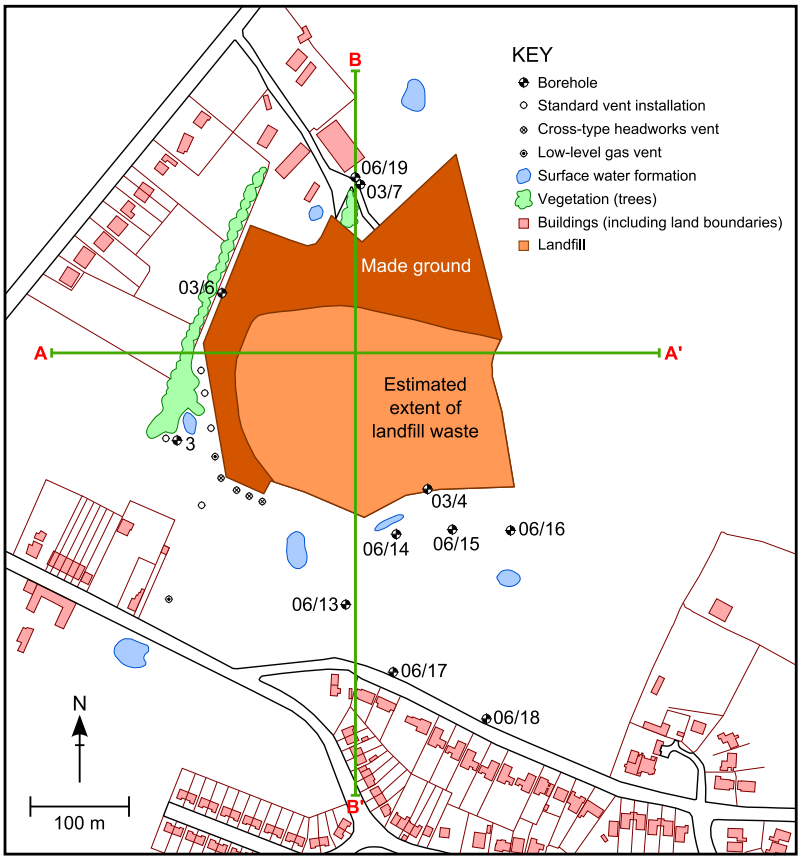

Figure 3.4: Map of Site 1 Showing the Locations of Monitoring Boreholes (from Martin (2005))

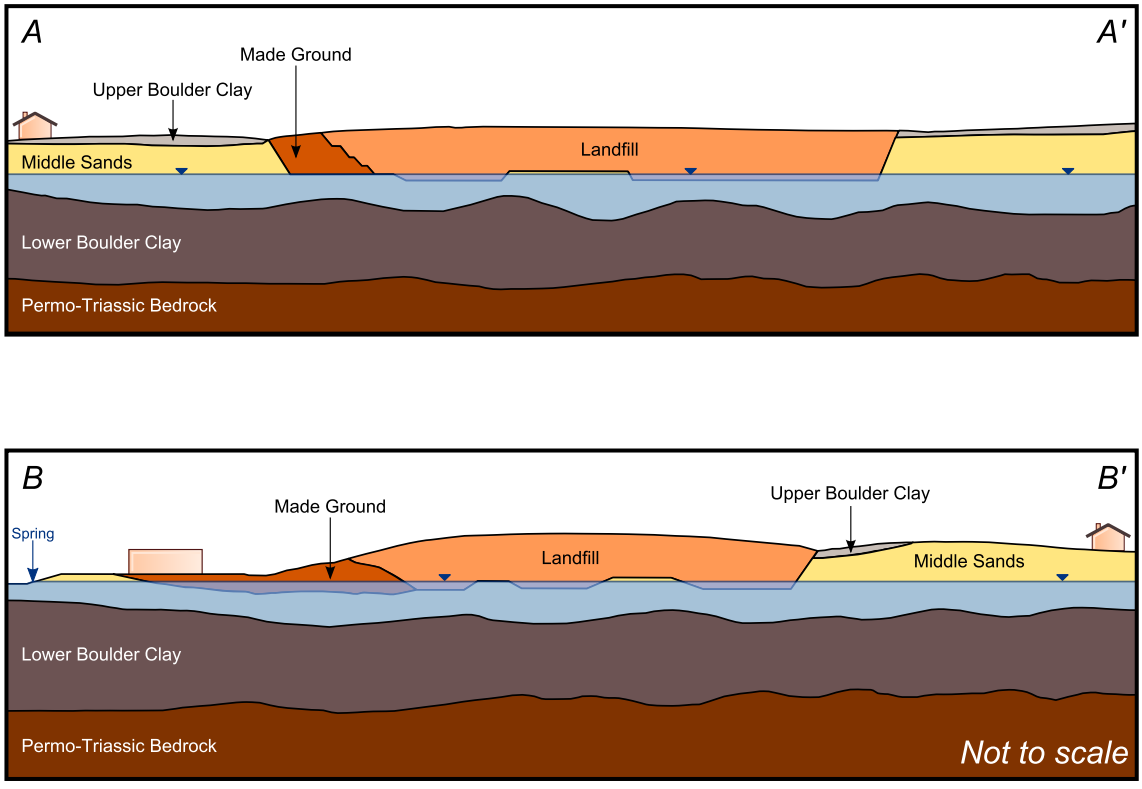

Figure 3.5: Cross Sections of Site 1 Showing Geological Relationships (from Martin (2005))

(Evans, 1968) suggests that the groundwater level limited the quarry base, which was 12.2 m below the original ground surface. A number of springs occurring around 163 m A.O.D. (Ordnance Datum is defined by the Ordnance Survey as Mean Sea Level (MSL) at Newlyn, Cornwall between 1915 and 1921) can be identified from local maps within the vicinity of the site. This spring line occurs where the topography drops below the contact between the Lower Boulder Clay and the Middle Sands.

The monitoring well installations are approximately 30 m to 35 m in depth (with boreholes 03/7 and 06/19 to the north of the site being notable exceptions at 10 m depth). Response zones of all boreholes are confined to the Middle Sands. Slotted pipe allows gases to permeate from the Middle Sands (generally middle 15 m section of the installation). Plain pipe is used up to 5 m depth with at least a 1 m bentonite seal. Therefore, all gases measured in these wells are assumed to originate from the Middle Sands.

3.3 Site 2

3.3.1 Site Location and Description

Figure 3.6: Aerial Photograph Showing the Location of Site 2 within Greater Manchester, UK

Figures 3.6 and 3.7 indicate the location of Site 2 within Greater Manchester, UK. The entrance to the site is located at 53.383231 °N, -2.179737 °E or OS Grid Reference SJ 881 873.

Site 2 is a fully engineered containment landfill facility that was constructed in phases within the footprint of a former brick clay quarry. The site occupies

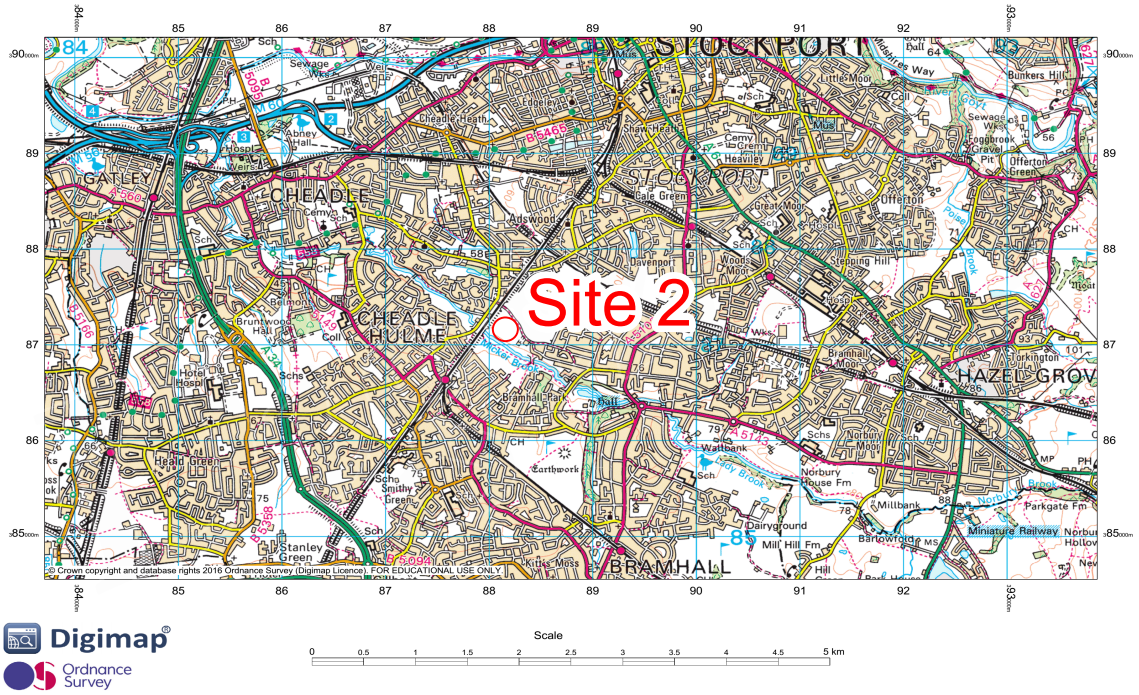

Figure 3.7: Ordnance Survey Map Indicating Location of Site 2 (from Ordnance Survey (2015a))

just over 6 ha, is dome-shaped in relief, stands a maximum 75 m A.O.D. and is approximately 350 m long by 150 m wide. Household, commercial, construction and industrial wastes were permitted to be deposited during operations.

Landfill construction was in four phases (1A, 1B, 2A and 3). After installation of a composite liner, landfilling would commence in that area of the quarry void and construction of the next phase would begin. Each phase was separated by an engineered bund, designed to minimise the movement of any leachate produced at the site. Landfilling took place over a 5 year period from July 1998 to October 2003. The landfill cap specification features a 2.0 mm high-density polyethylene (HDPE) flexible membrane liner (FML) over a 1.0 m thick clay layer. This is overlain with a 1.0 m layer of restoration soils (Jowett and Martin, 2008). A summary of landfill construction is contained in Table 3.1.

Landfill Phase	Start Date	Completion Date
Phase 1A	July 1998	September 1999
Phase 1B	September 1999	October 2000
Phase 2	October 2000	December 2001
Phase 3	December 2001	October 2003

Table 3.1: Construction history of Site 2

To the north east of the site is a former landfill area operated by a different authority. It is understood that this site was not constructed with formal contain-

ment engineering. Instead, it relies on the natural clays to attenuate potentially polluting emissions. This site is older having obtained its licence for the tipping of domestic and commercial waste in a former clay pit in 1979. By 1989, high levels of CH_4 emissions were recorded. An active ventilation system was installed to mitigate against this. In 1995, landfill gas barriers were installed along the perimeter of this landfill site. However, the specifications of these installations are unknown.

Figure 3.8 shows the array of monitoring boreholes on the perimeter of the landfill facility. None of the boreholes are situated within the landfill waste as they are designed to capture gas concentration on the perimeter only. Consequently, there should be no high concentrations ($> 10\%$) of CH_4 and CO_2 due to the high specification of the landfill liner. Any concentration that exceeds this is hypothesised to originate from the underlying geology or the nearby older landfill.

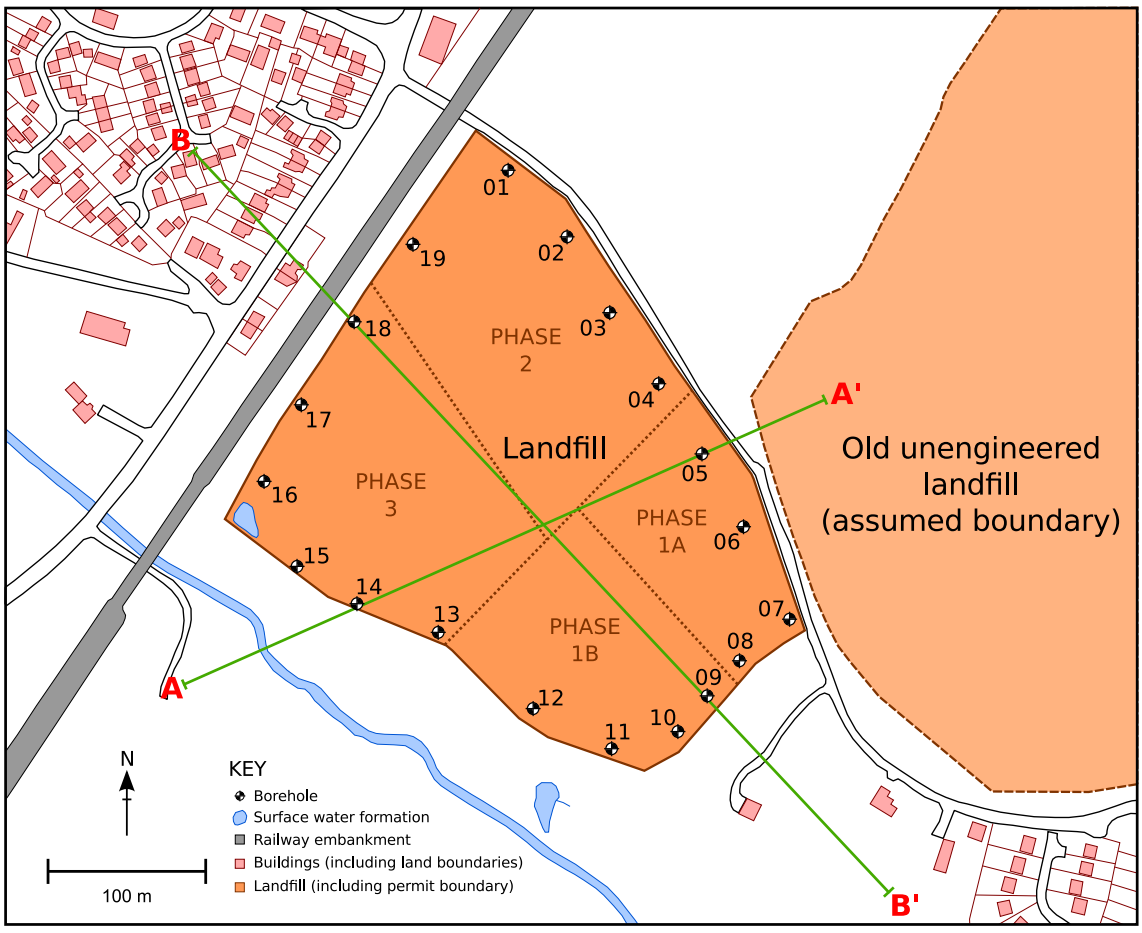

Figure 3.8: Map of Site 2 Showing the Locations of Monitoring Boreholes (from Jowett and Martin (2006))

3.3.2 Geology and Hydrogeology

In a regional context, Site 2 is located on the northern boundary of the Cheshire Basin. Permo-Triassic mudstones and sandstones overly Westphalian (Carbonifer-

ous) Coal Measures at depth (Figure 3.10) (Taylor, 1963). Faults in this area tend to be orientated north-south, affecting both the Permo-Triassic and Carboniferous deposits. The whole area is overlain by Glacial Till. Borehole logs indicate that the Glacial Till across the site is composed of a firm to stiff, dark brown, silty clay with occasional sand and gravel, and occasional lenses of fine sand (Jowett and Martin, 2008). The thickness of this clay is between 5.5 and 19.0 m.

Site 2 immediately overlies sandstones of the Permo-Triassic Sherwood Sandstone Formation. Aligned below the west portion of the site and running approximately NNW-SSE, the Cheadle Heath Fault has downthrown the Wilmslow Sandstone to the east of the fault, alongside rocks of the older Pebble Beds Group to the west. The beds dip slightly in a westerly direction (Jowett and Martin, 2006).

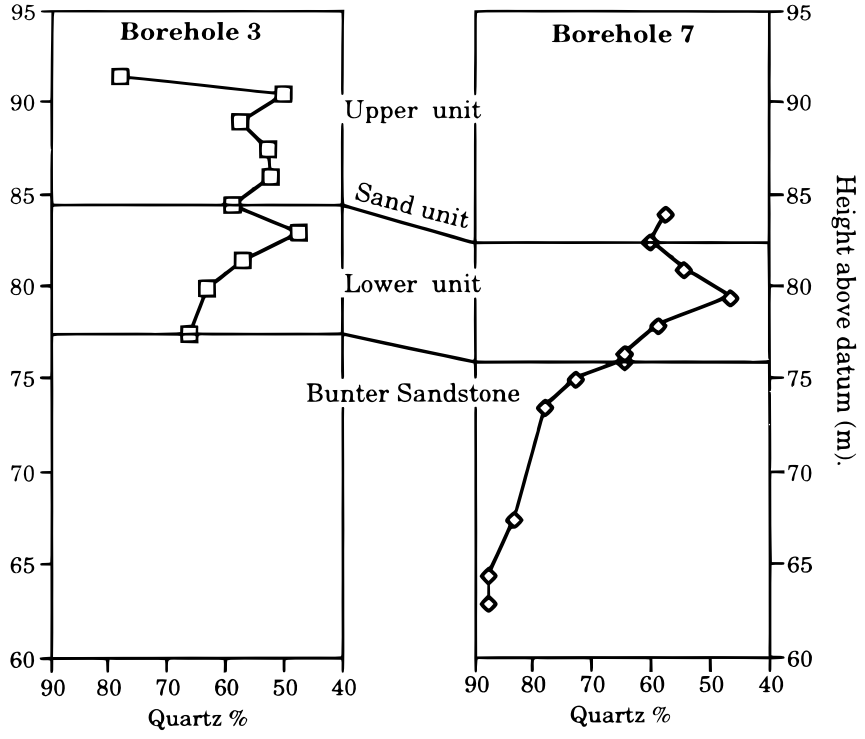

Figure 3.9: Quartz Content (%) at Increasing Depth (from Barlow (1996))

In an earlier study of Boulder Clay as a model brick-clay raw material at Site 2, Barlow (1996) demonstrated that there is no clear boundary between the Lower Boulder Clay, 'lower unit' and the Permo-Triassic bedrock, 'Bunter Sandstone' (now known as Sherwood Sandstone Group) (Figure 3.9). As the inferred boundary is crossed ($\sim$ 75 m A.O.D.), the Quartz (SiO_2) content increases from $\leq 57 \geq 45\%$ to $\leq 90\%$. This is a strong indication that the top-surface of the Permo-Triassic bedrock is heavily weathered. Consequently, this may present many conduits for gas (particularly CH_4) migration from the underlying Lower Pennine Coal Measures.

The Sherwood Sandstone Formation is classified as a principal aquifer by the Environment Agency due to its high inter-granular and/or fracture permeability (Environment Agency, 2010a). Consequently, it is grouped in the Major Aquifer, High Groundwater Vulnerability Zone. However, the site is not located within a Source Protection Zone (SPZ) of any major abstractions (Environment Agency, 2010a).

Regional groundwater flow is shown to be from SSE to NNW and the piezometric surface at the site is $\sim$ 57.0 m A.O.D. according to British Geological Survey (BGS) Records (Allen et al., 1997a; Jowett and Martin, 2006). Flow is thought to be in hydraulic continuity with a water course to the west of the site. Groundwater strikes were made at $\sim$ 45.0 m A.O.D. within the sand and gravel unit at the base of the superficial deposits (Jowett and Martin, 2006). Generally, groundwater levels are higher in boreholes to the NE of the site (BHs 01, 04 and 07) than those to the SW (BHs 11, 13 and 16). This appears to confirm the direction of groundwater flow.

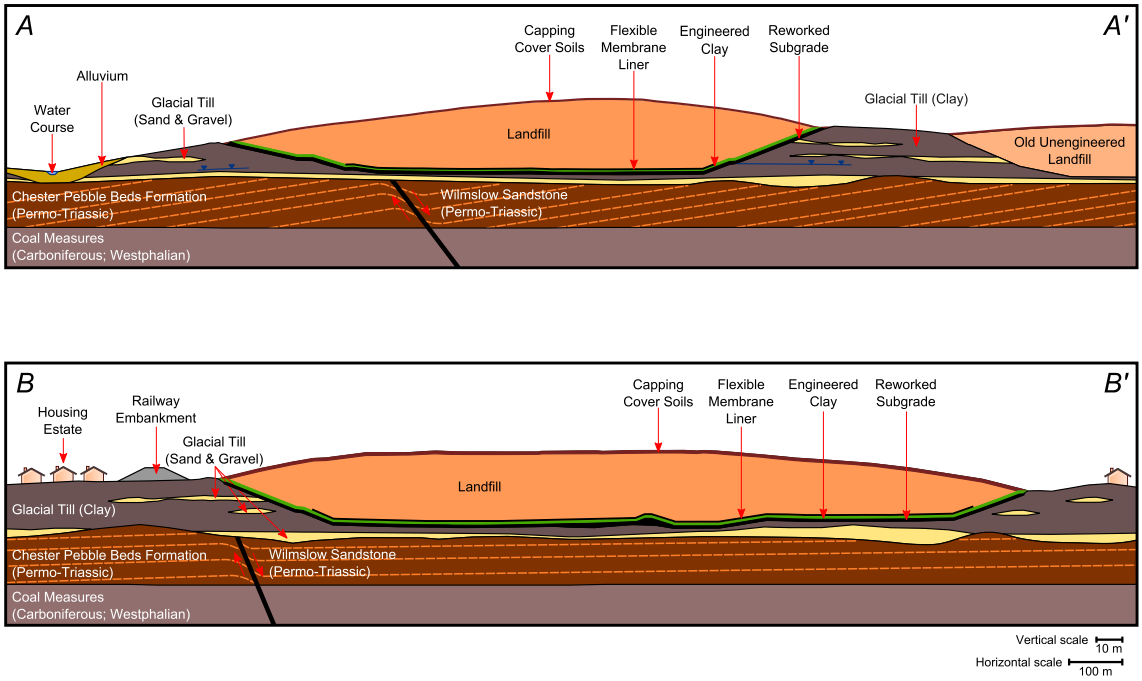

Figure 3.10: Cross Sections of Site 2 Showing Geological Relationships (from Jowett and Martin (2006))

3.4 Site 3

3.4.1 Site Location and Description

Unlike Sites 1 and 2 which are located in NW England, Site 3 is located in Hertfordshire, SE England (Figure 3.11). The entrance to the site is located at 51.825381 °N, -0.054558 °E or OS Grid Reference SJ 881 873.

The aerial photograph indicates that the surrounding area has mixed land use including residential, industrial works, leisure (golf course) and agricultural land. It is bounded to the west and south by primary A-roads.

The site is a permitted landfill facility situated within the footprint of a sand and gravel quarry covering an area of $\sim$ 55 Ha (Jowett, 2011). It comprises two separate areas of landfill (A and B). Landfill operations in Area A were completed in 1997. As of 2011, operations in Area B were still ongoing. At its highest point, the site is $\sim$ 90 m A.O.D. (Jowett, 2011).

The site was landfilled in phases (cells). Specifications for the construction and capping of Area A are given in Tables 3.2, 3.3 and 3.4.

Figure 3.11: Aerial Photograph Showing the Location of Site 3 within Hertfordshire, UK

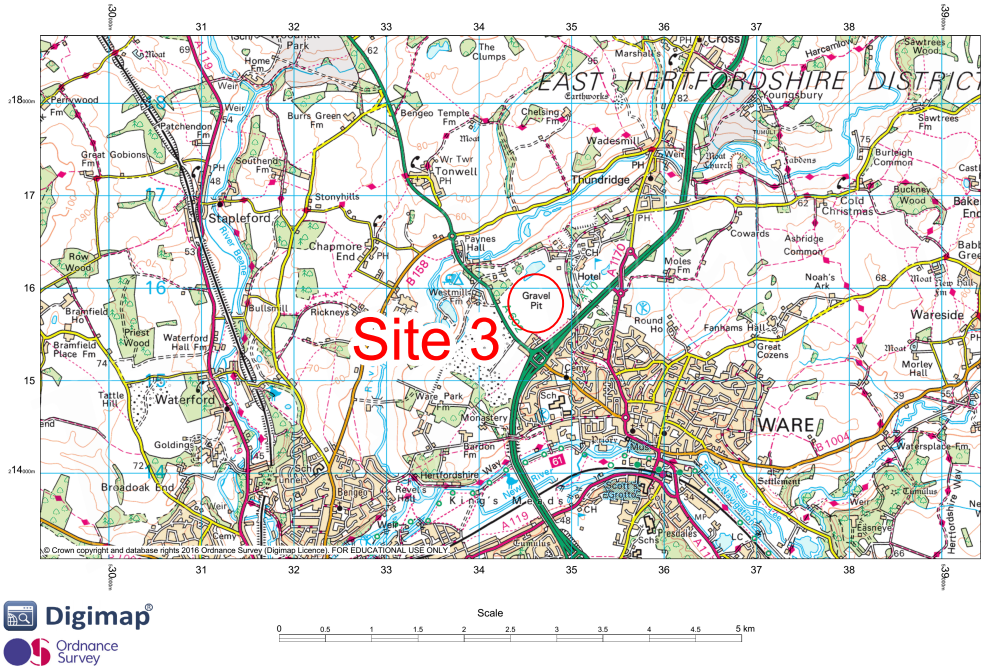

Figure 3.12: Ordnance Survey Map showing Location of Site 3 (from Ordnance Survey (2015c))

Cell	Basal Design	Side-wall Design	Construction Date
0	Basal layer of site-won clay placed to a minimum thickness of 2 m.	No specific design engineering.	1983
1	Basal layer of engineered clay constructed using won materials.	Engineered clay side-wall constructed to a height of 4 m.	N/A
2	Basal layer of engineered clay constructed using won materials.	Engineered clay side-wall constructed to a height of 4 m. Remainder of side-wall (adjacent to A-road) constructed using inert wastes.	N/A
3	Basal layer of engineered clay constructed using site won materials.	Engineered clay side-wall constructed to a height of 4 m.	N/A
4	From bottom up • 1 m thickness engineered clay placed to achieve a permeability of 1×10^{-9} m/s. • Geo-textile separator. • Drainage blanket.	Lower 4 m section: • 1 m thickness of engineered clay place to achieve a permeability of 1×10^{-9} m/s. Upper side-wall: • 1 m thickness of engineered clay place to achieve a permeability of 1×10^{-9} m/s. • Geo-textile separator. • 1.5 mm thick Linear Low Density Polyethylene (LLDPE) Flexible Membrane Liner (FML) anchored at top and lower side-wall. • Geo-textile separator.	Base: 1998 Side-wall: 2000 Cell 4/5 tie-in: 2000
5	Basal layer of engineered clay constructed using site won materials.	Minimum 2 m thickness of quarry overburden left in situ.	1995

Table 3.2: Site 3 Area A Construction Specification (from Jowett (2011))

Plans indicate that the base of Area A landfill cells ranges from 52 m A.O.D. to 59 m A.O.D. and at the highest point, the wastes attain a thickness of $\sim$ 34 m. Approximate phase dates (where available) are given in Table 3.3. Capping of Area A landfill cells was phased between 1997 and 2004 using a range of engineering designs. A summary is provided in Table 3.4.

Landfill Cell	Approximate Start Date	Approximate Completion Date
0	1983	Not available
1	Not available	1999/2000
2	Not available	1999/2000
3	Not available	Prior to 2000
4	Circa 1999/2000	2003
5	1995	1997

Table 3.3: Site 3 Area A Construction Dates (from Jowett (2011))

Area of Landfill	**Cap Design**	**Year Capped**
Cell 0	Thickness of cover soils	N/A
Cell 1 - Crown	From top to bottom: • 1 m thickness of restoration soils. • Geo-textile separator. • 1 mm thick Very Flexible Polyethylene (VFPE) Flexible Membrane Liner (FML). • Geo-textile separator. • 300 mm blinding layer.	September 1999
Cell 1 - NE side slope	Thickness of cover soils (installed as a temporary cap).	2000
Cell 2 - Crown	From top to bottom: • 1 m thickness of restoration soils. • Geo-textile separator. • 1 mm thick VFPE FML. • Geo-textile separator. • 300 mm blinding layer.	September 1999
Cell 2 - SE side slope	Thickness of cover soils (installed as a temporary cap)	2000
Cell 3 - Crown	From top to botton: • 1 m thickness of restoration soils. • Geo-textile separator. • 1mm thick VFPE FML. • Geo-textile separator. • 300 mm blinding later.	September 1999
Cell 3 - SE side slope	Thickness of cover soils (installed as a temporary cap).	2000
Cell 4 - lower slope adjacent to primary road	From top to bottom: • Restoration soils. • Lapped Geo-synthetic Clay Liner (GCL). • 300 mm blinding layer.	2003
Cell 4 - crown	From top to bottom: • 300 mm topsoil. • 700 mm subsoil. • Geo-textile separator. • 1 mm thick LLDPE FML. • 300 mm blinding layer.	2004
Cell 5	Thickness of cover soils	Oct/Nov 1997

Table 3.4: Cap Design and Construction Dates for Site 3, Area A (from Jowett (2011))

Area B at Site 3 is permitted to accept non-hazardous domestic, industrial and commercial wastes. Like Area A, this area has a phased construction and is divided into individual cells. As of June 2011, landfilling activity was still on-going.

The cells have been designed and constructed with a fully engineered containment lining system. For the liner base and lower 2 m of the outer side-walls, the specification is as follows (top to bottom):

- 0.5 m thick leachate drainage blanket (40 mm gravel) extended along liner base and 3 m up side-wall;
- 80 mm thick layer of Dense Asphaltic Concrete (DAC);

- 60 mm thick 'Asphaltic Binder Layer';
- 200 mm thickness of 'Type 1' sub-base;
- Geotextile separator;
- 0.5 m thick engineered clay liner compacted so as to achieve a permeability of less than 1×10^{-9} m/s.

The internal bunds along the cell boundaries also carry this specification. A similar design (with the exception of the lower engineered clay liner, which is absent) is also used for the upper sections of the outer side-walls. The landfill base is $\sim$ 50 m A.O.D. at its deepest point in Area B. Additionally, the interface lining system (ILS) to be constructed against Area A will comprise 1 m engineered clay 1×10^{-9} m/s and HDPE. Construction dates for the Area B cells, along with the beginning and end of waste depositing are provided in Table 3.5.

Landfill Cell	Construction Data	Landfilling Start Date	Landfilling Completion Date
Cell 1	2003/2004	July 2004	September 2005
Cell 2	2004/2005	September 2005	October 2006
Cell 3	2005/2006	October 2006	September 2007
Cell 4	2006/2007	September 2007	February 2009 (Partly capped)
Cell 4B	2008	September 2009	Still taking waste
Cell 5	2008	February 2009	August 2010
Cell 6 (South)	2010	July 2010	Still taking waste
Cell 7 (South)	2010	July 2010	Still taking waste

Table 3.5: Site 3 Area B Construction and Landfill Operations (as of 2011) (from Jowett (2011))

The cap design for all cells in Area B of Site 3 is as follows (top to bottom):

- 200 mm topsoil;
- 300 mm subsoil;
- Geo-textile separator;
- 1 mm thick LDPE FML;
- 200 mm regulating layer.

A map of Site 3 showing the array of perimeter gas monitoring boreholes is given in Figure 3.13. Each borehole is divided into six to eight sealed (with bentonite) response zones. Thus, it is possible to extract a gas profile of the ground with increasing depth at Site 3.

Two older landfills (licences granted in 1977 and 1984) are located to the west and north of the development, respectively. The contractor of the current development is not aware of any landfill gas issues arising from these sites (Jowett, 2011). Therefore, these sites are assumed to have a 0% gas input for the purposes of this analysis.

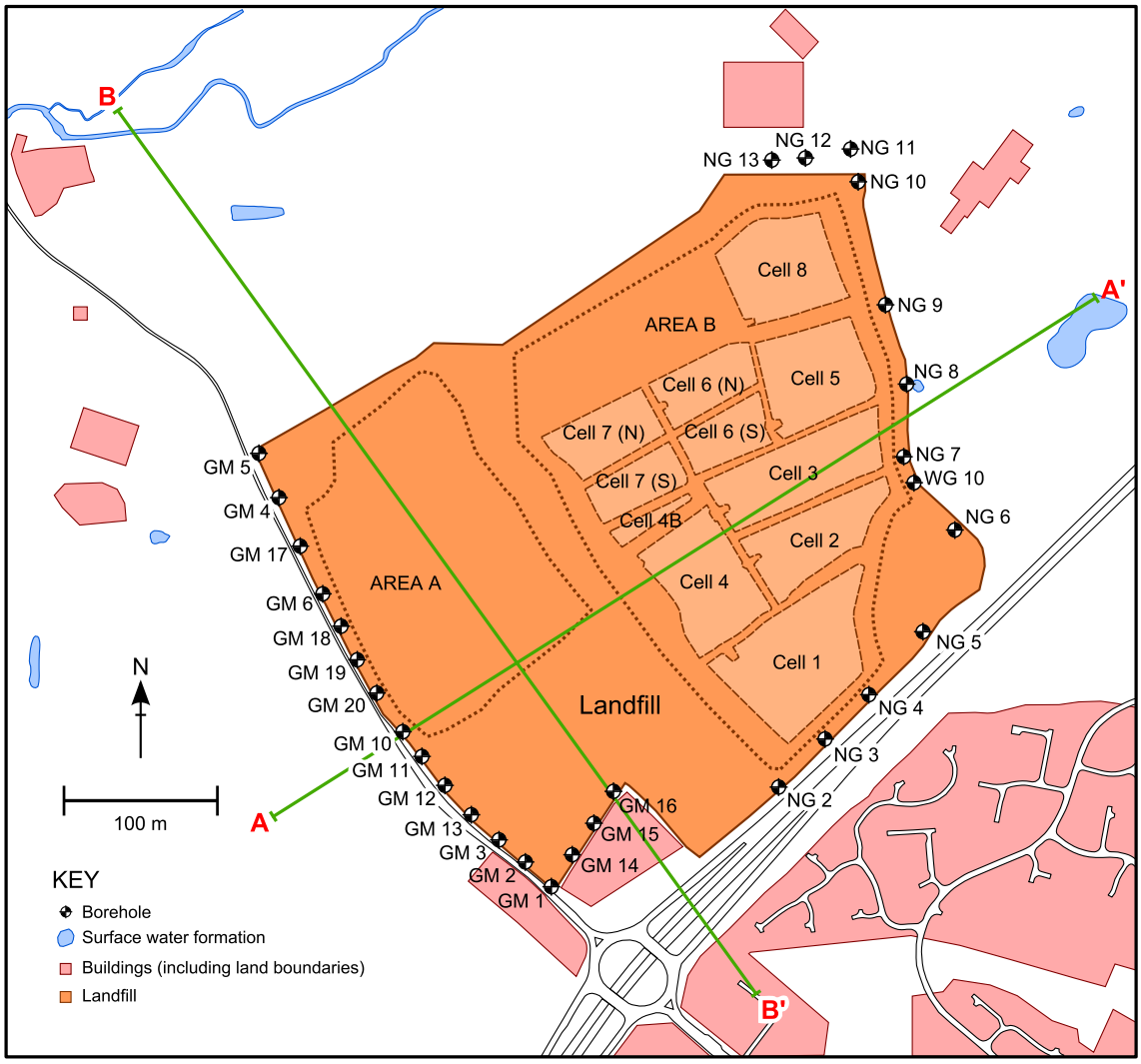

Figure 3.13: Map of Site 3 Showing Locations of Monitoring Boreholes (from Jowett (2011))

3.4.2 Geology and Hydrogeology

Regionally, Site 3 is located on the northern limb of the London Basin. It is situated over solid strata of the Cretaceous Upper Chalk Unit. This encompasses both the Upper Chalk and Middle Chalk Formations. A nearby deep boring indicates that the Upper Chalk is 55.8 m thick while the Middle Chalk is 69.2 m thick (Sherlock et al., 1924). The uppermost 7 m is described as a soft white chalk with many flints (Sherlock et al., 1924). Taking the form of a broad, gentle synclinal fold orientated NE – SW, the local strata are assumed to dip gently to the SE (Jowett, 2011).

Overlying the bedrock, superficial deposits are present across the site and generally comprise Glacial Clay (which outcrops across the western half and eastern edge) and Glacial Gravel (which is present at the surface as a linear strip running from north to south). These deposits are absent in the north-western corner of the site, causing the Upper Chalk to outcrop in this area. The Glacial Clay is generally

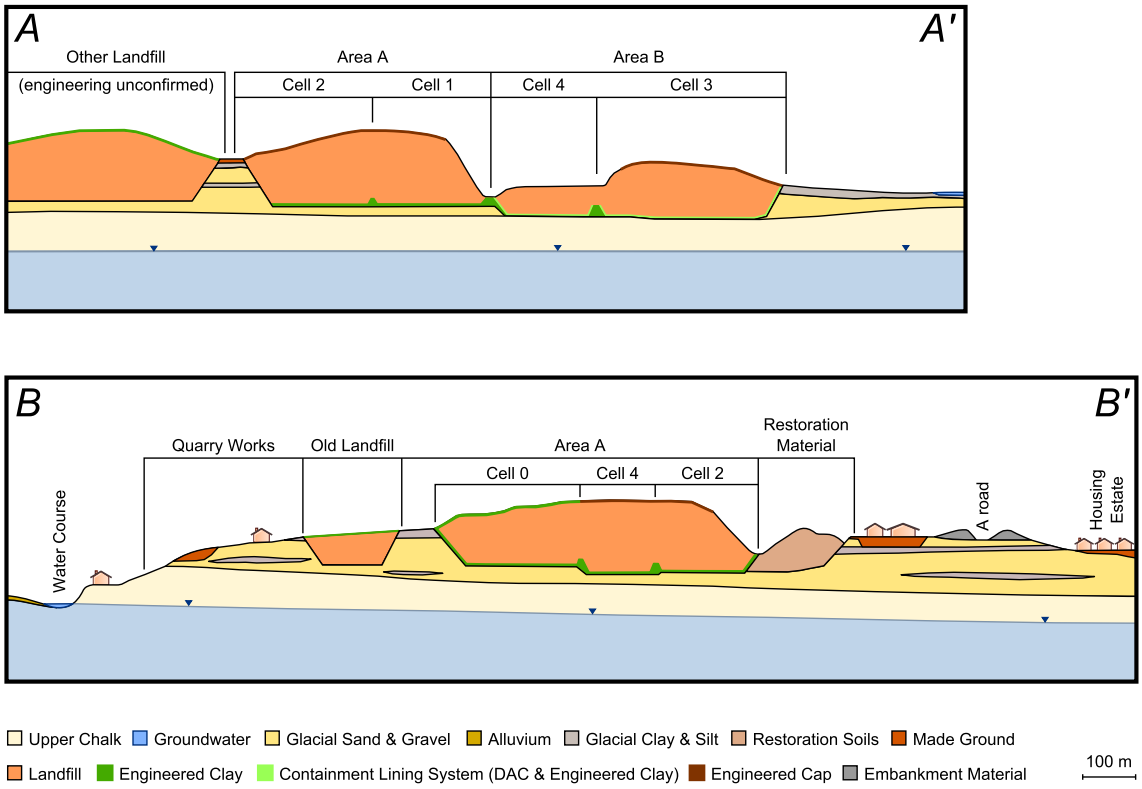

Figure 3.14: Cross Sections of Site 3 Showing Geological Relationships (from Jowett (2011))

1 to 5 m thick, while the Glacial Gravel is typically 10 to 22 m thick (Jowett, 2011).

The Environment Agency defines the Upper Chalk as a principal aquifer and as such is grouped in the 'Major Aquifer Intermediate Groundwater Vulnerability Zone'. Additionally it is in the 'Outer Zone (Zone 2) Groundwater Source Protection Zone' which defines the site as being a source of groundwater for public consumption that is at risk of contamination. The Outer Zone (Zone 2) is specifically defined as a 400 day travel time from a point below the water table. The superficial deposits are classified as an unproductive strata (Environment Agency, 2010a). With dual porosity and dual permeability, the Upper Chalk also comprises a thick unsaturated zone (30 m) (Gooddy et al., 2007). Although the solid geology differs significantly from Sites 1 and 2, the presence of a thick unsaturated zone makes Site 3 highly analogous to Sites 1 and 2.

According to the BGS hydrogeological map for the area between Cambridge and Maidenhead (Cradock-Hartopp et al., 1984), local groundwater flow is shown to be in a general southerly direction towards a major water course that lies to the north of the site (Jowett, 2011). Dedicated groundwater monitoring boreholes on the northern boundary have recorded groundwater levels in the range 38 m A.O.D. to 42.5 m A.O.D. while monitoring boreholes on the south-eastern boundary of the site have recorded groundwater levels in the range 34 m A.O.D. to 37 m A.O.D..

This would indicate that groundwater generally flows to the SE. However, there are some monitoring boreholes on the south-eastern boundary that consistently record groundwater levels in excess of 40 m A.O.D. that contravene this trend (Jowett, 2011).

3.5 Control Site

3.5.1 Site Location and Description

A control site in Cheshire was selected to obtain monitoring data from a location with similar geological character but without the possible influence of sanitary landfill operations or underlying Coal Measures. This site is an operational silica sand quarry, with a permit dating from 1997. This permit was extended in 2008 to an extra 11.8 ha and is anticipated to last until 2018 with full restoration completed by 2020 (WBB Minerals Ltd, 2008). Due to the phased extraction of sand, the site has been progressively restored. The borehole used as a control is located to the SE of the quarry. Slopes have already been restored in this area and it is anticipated that any exchange between ground gas and the atmosphere via working faces $\sim$ 10 m distant should be effectively sealed by boulder clay used in restoration.

Figure 3.15: Aerial Photograph Showing the Location of the Control Site within Cheshire, UK

Figures 3.15 and 3.16 show the site within the context of the surrounding landscape which includes pastoral and arable fields. The site is also in close proximity to an urban area (3.7 km from centre). The entrance to the site is located at 53.157035 °N, -2.258843 °E or Ordnance Survey grid reference SJ 827 622.

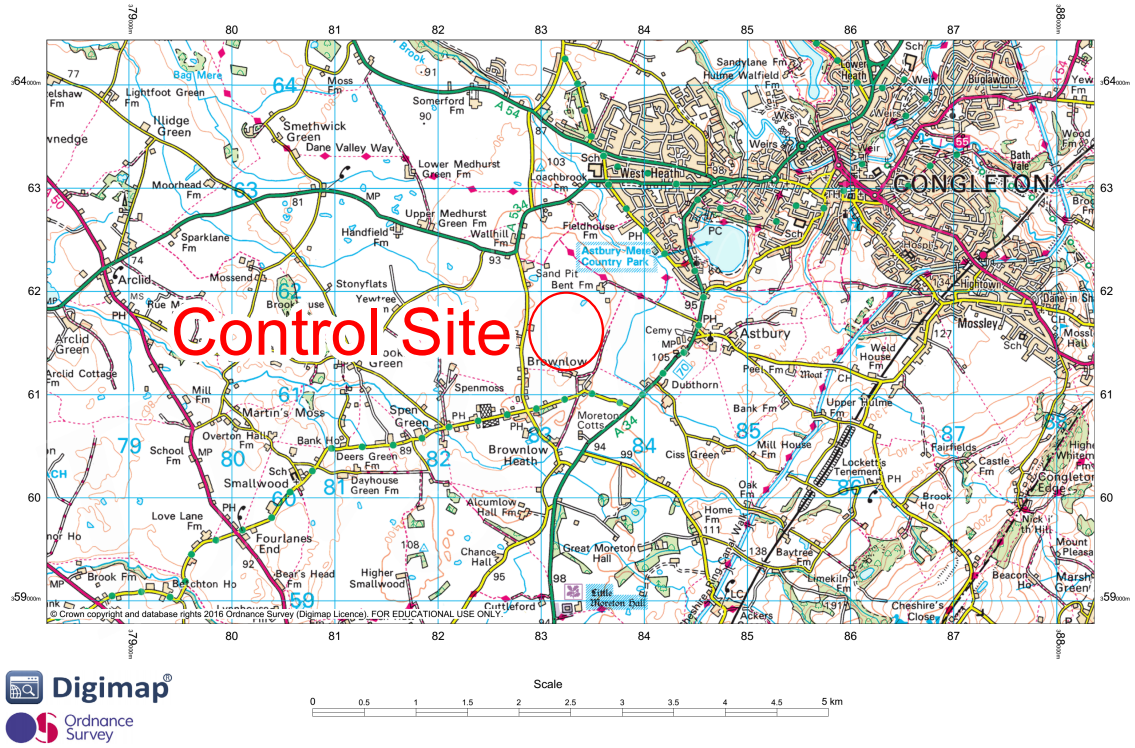

Figure 3.16: Ordnance Survey Map Showing Location of Control Site and Location of Control Borehole (from Ordnance Survey (2015b))

3.5.2 Geology and Hydrogeology

The Control Site has a similar geology to Site 1 (Figure 3.5). 0.5 m of topsoil is underlain by 3.8 m of Upper Boulder Clay which in turn is underlain by approximately 26 m of Middle Sands. The deeper geology consists of a thicker layer of Lower Boulder Clay (> 10 m) capping the Permo-Triassic bedrock. Slightly differing from Site 1, the Permo-Triassic bedrock is a part of the Sidmouth Mudstone Formation and dates from the Early–Late Triassic Epoch (British Geological Survey, 2015). Like Site 1, the Permo-Triassic bedrock is classed by the Environment Agency as a Secondary B aquifer while the superficial deposits are classified as a Secondary A aquifer (Environment Agency, 2010a). Although a major aquifer, the site is grouped in the Low Risk Groundwater Vulnerability Zone by the Environment Agency.

Chapter 4

Review of Historic Gas Monitoring Data

4.1 Data Compilation

The data used in this study have been derived from peripheral monitoring of landfill sites and similar artificial environments. The variation of landfill gas composition within a landfill is not directly considered. Instead, the emphasis is placed on gas compositions in boreholes designed to monitor possible migration of landfill gas into the ground that surrounds landfill. At these sites there is a regulatory requirement for monitoring ground gases both outside and inside the site, providing a substantial database that extends back many years. For the three sites considered, the data extends back to 2003, 1998 and 1995 (Sites 1, 2 and 3, respectively). All sites provide data in excess of ten years and in the case of Site 3, twenty years.

Historically, gas composition has been measured in accordance with regulatory requirements using hand-held gas monitors, as frequently as daily (Site 2) to as infrequently as quarterly (Site 1). Measurements were made using a Geotech UK GA2000 Landfill Gas Analyser until 2012, after which, a Gas Data Ltd GFM435 Landfill Gas Analyser was used. A limitation due to the change of instrumentation over a period of several years is that data sets may not be directly comparable.

Both gas monitoring instruments employ a dual beam infra-red absorption method to quantify the concentration of CH_4, CO_2 and O_2 in a flowing gas. The balance is assumed to be N_2. However, the instruments differ in their measurement of borehole flow. The GA2000 Landfill Gas Analyser's pressure transducer is equipped with a set resistor that minimises flow. It is argued by the manufacturer that this will more closely reflect true borehole conditions as the act of opening a borehole valve will disrupt equilibrium conditions. Conversely, the GFM435 Landfill Gas Analyser's

pressure transducer does not carry this specification.

Key limitations arising from a point measurement strategy as adopted here are summarised as follows:

- Data are discontinuous and thus identifying diurnal, seasonal and annual trends is difficult.
- It is difficult to determine how gases present in a borehole interact with changing atmospheric conditions (such as atmospheric pressure, wind speed/velocity, temperature and rainfall)
- It is not possible to determine how underground conditions (such as depth of water table, temperature and microbial activity) affect the production and emission of CH_4 and CO_2 gases.
- It is important to know whether or not a borehole is venting to the atmosphere or absorbing atmospheric gases. The action of opening a borehole valve to the atmosphere induces a pressure gradient and disturbs equilibrium conditions. Therefore, any data capture by hand-held portable gas monitors may be skewed.

4.2 Data Representation and Interpretation

The graphical approach used in this chapter presents compositional data compared in terms of the measured CH_4, CO_2 and O_2 content normalised to nitrogen (assuming N_2 to be the balance, i.e. 100 - (Σ CH_4 + CO_2 + O_2)), in a ternary plot. This allows the relative proportions of CH_4 and CO_2 to be compared irrespective of any dilution by air, the O_2/N_2 ratio indicating whether this has occurred and the extent to which O_2 has been removed, as N_2 can be regarded as non-reactive (Bergamaschi and Harris, 1995). In a plot of this type, 'end member' compositions can be identified so that an array of observed data points can be explained as mixtures of gases from different sources. Therefore, the characteristics of one borehole may be compared with another (Teasdale et al., 2014).

4.3 Site 1

4.3.1 Data

Spatial Composition

Figure 4.1 shows the gas composition recorded over a period of eleven years taking a transect of Boreholes 03/4, 06/14 and 06/17 at Site 1 (Figure 3.4). Borehole 03/4

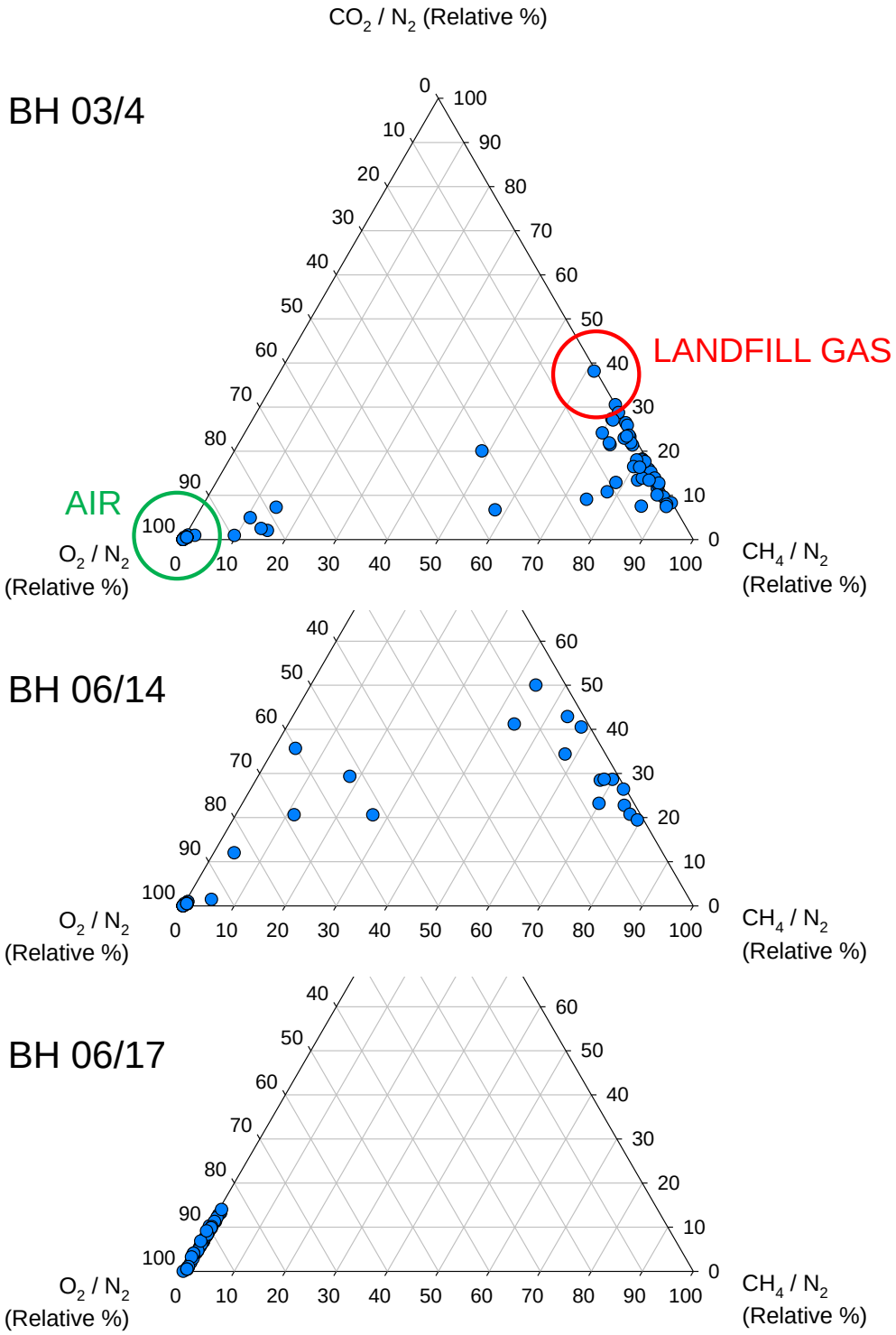

Figure 4.1: Gas Compositions for Monitoring Wells, Site 1 (29/01/2004 – 08/05/2015), Indicating (Figure 4.1a) Expected Plotting Positions of Landfill Gas and Air

located on the southern boundary of the landfill produced a CH_4-rich gas signature (70:30 CH_4/CO_2) which is attributed to landfill gas (typically 60:40 CH_4/CO_2). This is due to its close proximity to the edge of the landfill. The higher proportion of CH_4 to CO_2 (80:20) may be accounted by scrubbing of CO_2 from the system (i.e.

dissolution in groundwater). Additionally, wastes containing fats (triglycerides), typically produce a landfill gas in the ratio of 70:30 CH_4:CO_2.

Twelve years after closure, Borehole 03/4 still produces this composition of gas which provides evidence that there is enough substrate for methanogenic bacteria to produce CH_4 and CO_2. This also indicates that the gas is able to migrate through the unconsolidated Quaternary deposits due to the absence of an engineered landfill liner. Values recorded at 100% O_2/N_2 correspond to air. This occurs when air has entered the borehole from the atmosphere, thereby diluting or displacing the landfill gas. There is some evidence of mixing between landfill gas and air at this location, but this was observed on few occasions (points between the two end member compositions).

Borehole 06/14, located approximately 25 metres south of the landfill perimeter shows a more diffuse scatter of data. While there is still a strong indication of the presence of landfill gas, the proportion of CH_4 is lower (Figure 4.1b), suggesting the possibility of mixing with a more O_2-rich gas, or removal of CH_4 by biological processes. However, Boreholes 06/15 and 06/16 (Appendix B, Figures E.5 and E.6) also located approximately 25 m away from the landfill southern boundary show no presence of landfill gas. As indicated previously, these boreholes have response zones in the underlying unconsolidated sands; it is therefore expected that these boreholes should also show evidence of landfill gas presence. This could be attributed to preferential pathways in the subsurface such as fissures or uncharted fractures and faults. Local variations in the water table that drives the migration of gas could also be a factor.

Borehole 06/17, located more than 100 m away from the landfill and closest to nearby housing, records no landfill gas (Figure 4.1c). Likewise, Borehole 06/18 also located approximately 100 m south of the landfill records no landfill gas (Appendix B, Figure E.7). The 100% O_2/N_2 value indicates that only air is ever present in these boreholes. As these two boreholes have consistently shown the same gas concentration relationships throughout nine years, it is reasonable to conclude that CH_4 and CO_2 do not migrate over 100 m through the unconsolidated Quaternary deposits at Site 1. Therefore, CH_4 and CO_2 encroachment into residential properties is not an imminent danger.

Boreholes 03/7 and 06/19 (Appendix B, Figures E.3 and E.8) located less than 2 m apart on the northern boundary of the site show very different gas compositions. Borehole 03/7 shows a landfill gas/air mix while Borehole 06/19 shows a CO_2-air mix. It is postulated that because the older Borehole, 03/7, was engineered to a lower standard, a gas-tight seal was not achieved and the landfill gas has leaked into

this borehole via the made ground that covers the north of the site. The data from these boreholes is consequently not discussed.

Flow

As was set out in the introductory commentary of this Chapter, accurately quantifying borehole flow (l/hr) is inherently difficult as opening a borehole valve induces a pressure gradient that alters the equilibrium conditions of the ground. However, it is possible, as a bare minimum, to categorise the borehole flow measured by hand-held portable gas monitors as positive or negative. Positive borehole flow may be described as the flow that is induced when borehole pressure is greater than atmospheric pressure. Conversely, negative borehole flow conditions result from atmospheric pressure that is greater than borehole pressure. When these conditions prevail, the net movement of gases will be from atmosphere to borehole (ground). Positive borehole flow is of utmost importance as when this condition exists, there will be a net movement of gases from borehole (ground) to atmosphere. If these conditions exist, it is also likely that due to the pressure gradient, gases may migrate within the sub-surface. Figure 4.2 categorises samples according to positive or negative borehole flow for Boreholes 03/4, 06/14 and 06/17.

Figure 4.2a and Figure 4.2b clearly show that in the majority of cases of landfill gas, positive borehole flow conditions exist. Therefore, when these samples were taken, CH_4 and CO_2 were being emitted to the atmosphere in the landfill gas ratio. Only one sample from Borehole 06/14 indicating a landfill gas ratio was taken under negative borehole flow conditions.

Statistics in Table 4.1 show positive and negative borehole flow incidence in relation to gas composition sampled in these boreholes. Gas mixtures ($< 50\%$ O_2) were assumed to be landfill gas while $\sim 0\%$ CH_4 and CO_2 samples were assumed to be air (no LFG).

In Boreholes 03/4 and 06/14, landfill gas samples were recorded predominantly during positive borehole flow conditions (80.0% and 63.2% respectively). By comparison, the occurrence of landfill gas measured during negative borehole flow conditions was far less (21.6% and 2.8% for Boreholes 03/4 and 06/14 respectively). When negative borehole conditions exist, it is more likely for no landfill gas to be present in a borehole and for air to enter from the atmosphere. The high percentages for no landfill gas measured under negative flow conditions for Boreholes 03/4 and 06/14 (78.4% and 97.2% respectively) strongly indicate this.

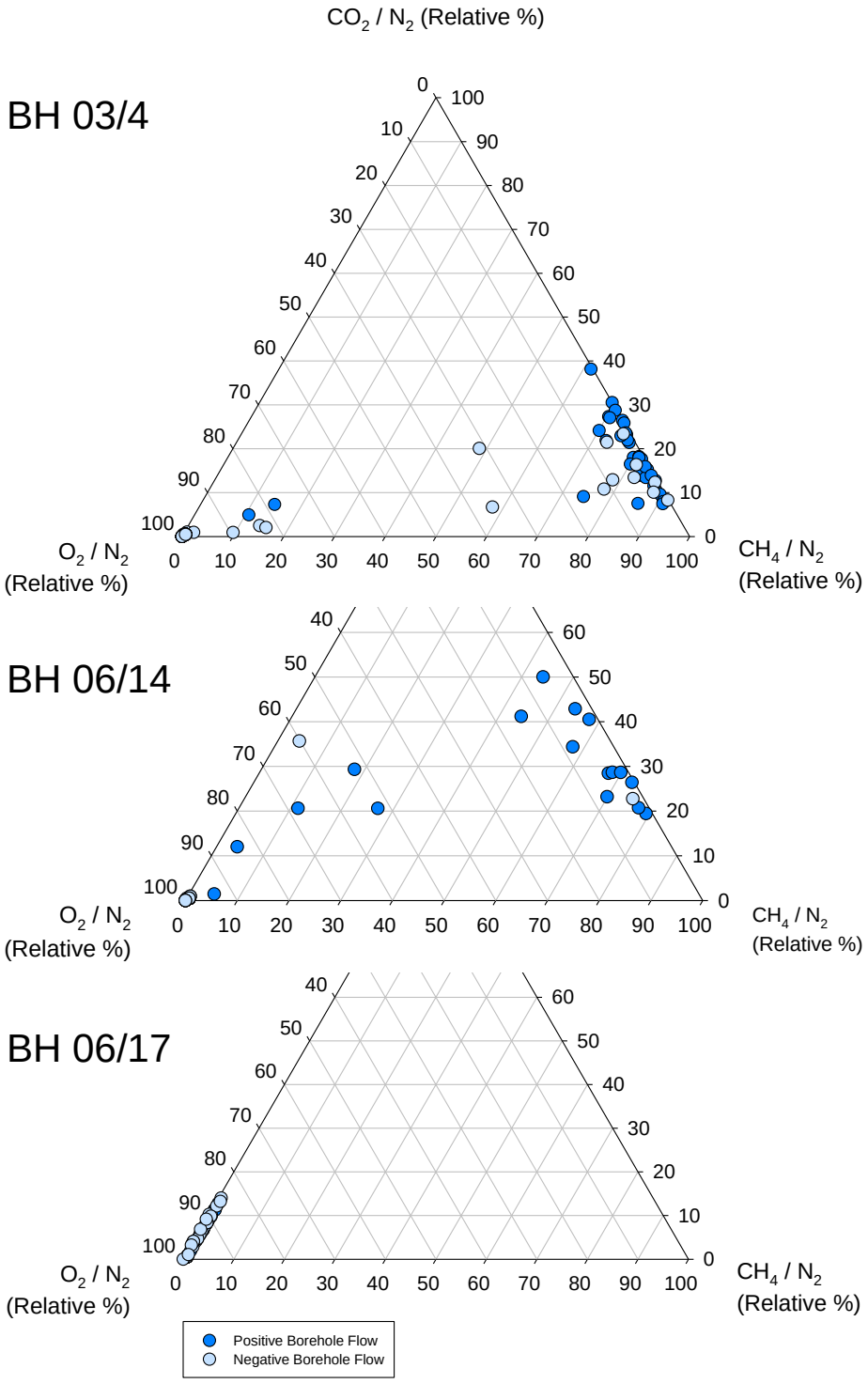

Figure 4.2: Gas Compositions for Monitoring Wells, Site 1 (29/01/2004 – 08/05/2015), Indicating Incidence of Positive and Negative Borehole Flow

However, with only 91 data points for Borehole 03/4 and 55 data points for Boreholes 06/14 and 06/17 over an eleven-year and nine-year-period respectively, the point measurement strategy is not comprehensive enough to draw any firm conclusions. There is a strong indication, however, that atmospheric pressure conditions

play a key role in the emissions of gases from the sub-surface.

Borehole Identification	Positive Flow		Negative Flow	
	% No LFG	% LFG	% No LFG	% LFG
BH 03/4	20.0	80.0	78.4	21.6
BH 06/14	36.8	63.2	97.2	2.8
BH 06/17	100.0	0.0	100.0	0.0

Table 4.1: Percentage of Samples Containing Landfill Gas (LFG) Recorded during Positive and Negative Borehole Flow at Site 1

Seasonal

Gas mixtures with $< 50\%$ O_2/N_2 were classified as LFG, while samples composed of $> 50\%$ O_2/N_2 and $\sim 0\%$ CH_4/N_2 and CO_2/N_2 were classified as No LFG. The seasons were defined as Winter, 1st December – 28/29th February; Spring, 1st March – 31st May; Summer, 1st June – 31st August; Autumn, 1st September – 30th November.

Weakening air pressure over the Atlantic between late September and early March, accompanied with a westerly jet stream, brings low air pressure weather systems, known as depressions, across the British Isles. The busiest period of this winter storm season tends to be between December and February. For example, the winter of 2013/14 was exceptionally stormy. With at least 12 deep depressions crossing the UK in rapid succession between 5th December 2013 and 12th February 2014, this was the stormiest period of weather recorded in the UK for 20 years and the wettest winter since 1914/15 (Lewis et al., 2015). During this period, a deep Atlantic depression occurred on 23rd – 25th December 2013. This storm with a central low pressure of 927 mbar, recorded a low pressure in the British Isles of 936.4 mbar at Stornoway, Western Isles (Kendon and McCarthy, 2015).

A rapid decrease in air pressure from stable or average conditions (1013 mbar) as a result of a low pressure weather system is likely to cause a release in CH_4 and CO_2 from the near-surface ground gas environment. Over the summer months, more settled weather conditions prevail as stable high pressure (> 1020 mbar) dominates. All this means that the period between October and March is more likely to yield emissions of CH_4 and CO_2 from the ground. Therefore, it was hypothesized that the Autumn and Winter months (i.e. 1st September – 28/29th February) would present the greatest occurrence of landfill gas.

The data present a scenario that appears to show that for boreholes where landfill gas is sometimes present (BH 03/4 and 06/14), two-thirds of data points contain no

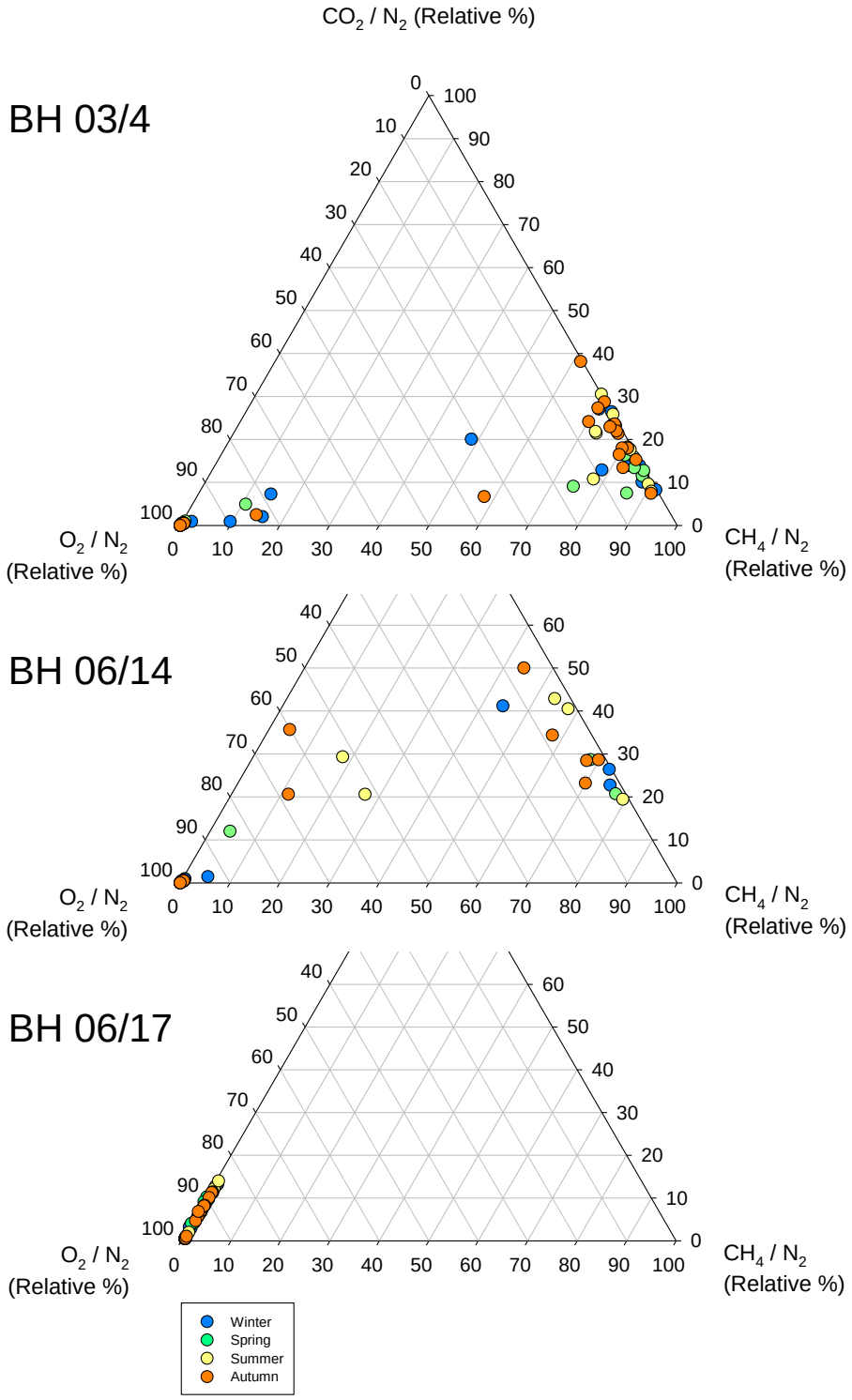

Figure 4.3: Seasonal Gas Compositions for Monitoring Wells, Site 1 (29/01/2004 – 08/05/2015)

landfill gas, irrespective of season that the data were recorded (Figure 4.3). The only significant deviation from this pattern is the autumn data for BH 03/4 where the proportions of landfill gas versus no landfill gas are reversed. Landfill gas samples for this season were represented by 68% of data points. This was in accordance with the anticipated greater occurrence of emissions of CH_4 and CO_2 resulting from increased

likelihood of unstable atmospheric conditions. However, there is insufficient evidence to prove the theory. Further data recorded at high frequency throughout several years in multiple monitoring wells would be required. Furthermore, high frequency data would require the recording of multiple variables such as atmospheric pressure, borehole pressure, ambient temperature, borehole temperature, depth to water table for the data to be of good enough quality for interpretation.

Borehole	Winter		Spring		Summer		Autumn	
Identification	% No LFG	% LFG	% No LFG	% LFG	% No LFG	% LFG	% No LFG	% LFG
BH 03/4	62.5	37.5	65.2	34.8	52.6	47.4	32.0	68.0
BH 06/14	76.9	23.1	85.7	14.3	70.0	30.0	72.2	27.8
BH 06/17	100.0	0.0	100.0	0.0	100.0	0.0	100.0	0.0

Table 4.2: Percentage of Samples Containing Landfill Gas (LFG) Recorded Seasonally at Site 1

4.3.2 Key Trends and Interpretations

The key trends and interpretations that can be extracted from Site 1 are summarised as follows:

- In very close proximity to an unlined landfill still in the 'methanogenic stage', gas composition is predominantly 'landfill gas' (i.e. 70:30 CH_4/CO_2).
- Under positive borehole flow conditions, 80% of samples contain landfill gas in close proximity to the landfill.
- Gas composition constituting landfill gas is observed on fewer occasions at a distance of 25 m from the landfill.
- No landfill gas is recorded 100 m from the landfill.
- The unconsolidated drift geology in which the landfill is situated, accompanied with a lack of basal liner due to the landfill's age, has allowed landfill gas to migrate at least 25 m to the south. This assumes that no uncharted preferential pathways exist.
- The point measurement data are too sparse in order to draw any firm conclusions about seasonality of gas measurements.

4.4 Site 2

4.4.1 Data

Spatial Composition

At Site 2, which overlies Coal Measures, monitoring wells are located around the landfill perimeter only. Additionally, the collected gases evolved from all three landfill cells are flared. The composition of the flared gas is also measured and provides a useful reference to compare the composition of gases in the perimeter boreholes on the site.

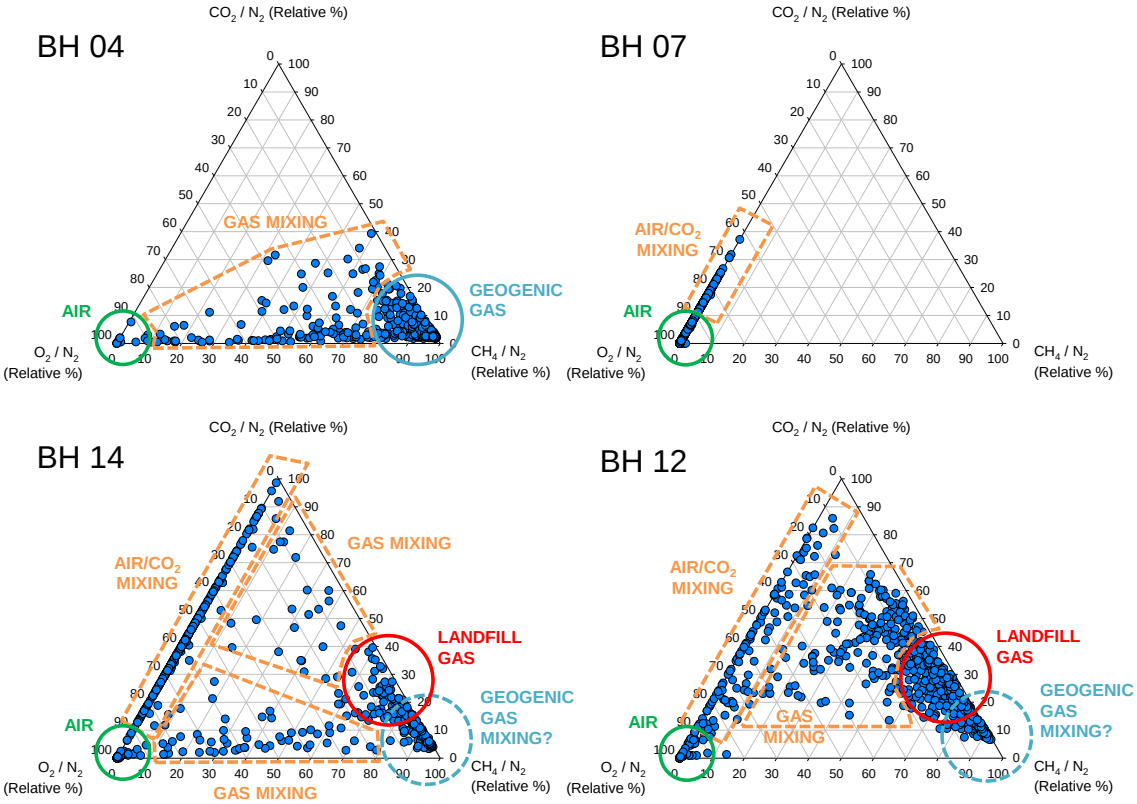

Figure 4.4: Site 2 Borehole Gas Compositions (28/02/1997 – 29/06/2015)

From hand-held monitor generated data, the CH_4/N_2 ratio frequently exceeds 80%, suggesting a geogenic gas influence arising in at least two boreholes (BH 04 and BH 14).

Examining the composition of gas present in BH 04 at Site 2, it is apparent that it is very different from the flared gas composition (Figure F.16) which shows an expected landfill gas signature (60:40 CH_4:CO_2) with few points representing air. Likewise, when contrasted against BH 03/4, Site 1 (Figure 4.1a) that shows a CH_4–rich landfill gas (70:30 CH_4/CO_2) mixed with air, it is clear that this CH_4 has a

different origin, independent of the landfill waste. The most probable explanation is that CH_4 has degassed from an underlying coal seam in the Coal Measures. The weathered top-surface of the Permo-Triassic bedrock (Barlow, 1996) in conjunction with a fault running NNW–SSE through the western portion of the site (Jowett and Martin, 2006) provides many potential conduits for gas migration from the lower sub-layers.

Furthermore, from the inception of monitoring of this borehole on 13th August 1998, the high-value percentage of CH_4 has been present and has persisted throughout the 17 years of monitoring. Not only are the proportions of gas concentrations inconsistent with landfill gas, they do not appear to follow the physiology of the production of landfill gas. After initial aerobic conditions, anoxic conditions prevail and methanogenic production of CH_4 and CO_2 begins. To begin with CO_2 concentration exceeds that of CH_4. With the loss of H_2, CH_4 concentration increases and reaches a terminal value of 60–70% and surpasses CO_2 as the dominant gas produced in landfills. Historic investigations have shown that it typically takes between 180 and 250 days for this phase to be achieved (Farquhar and Rovers, 1973). Therefore, it is unexpected for BH 04 to have achieved a concentration of CH_4 at least above 50% before a minimum of six months had elapsed.

The evidence based on gas composition and biogeochemistry of landfill is not sufficient to prove the origin of the gas in BH 04. Stable isotope analysis and radiocarbon dating (^{14}C) would aid this point. A geogenic gas would be expected to be completed depleted in ^{14}C owing to the relatively short half-life of 5,730 years of ^{14}C (Muir et al., 2015) and the great age of the Carboniferous rock (298.9–358.9 million years) from which it was exuded.

On inspection, BH 14 (Figure 4.4) presents an array of different gas compositions compared with BH 04. Air and landfill gas end members are identifiable. However, there could be a geogenic mixing component as CH_4 concentration reaches 80% or greater on multiple occasions. Additionally, there is a CO_2 component which has varying degrees of dilution by air (concentrations range from 0–100% CO_2). Data points between these identifiable clusters represent a complex mixing pattern.

Like BH 14, the BH 12 (Figure 4.4) ternary plot also appears to have identifiable air, air–CO_2 mixing and landfill gas clusters. Likewise, there may be a geogenic mixing component. However, landfill gas appears to be the dominant gas present in this borehole. Boreholes 12 and 14 have the most variable gas compositions observed for Site 2 with CH_4/N_2 and CO_2/N_2 ratios both approaching 100% (Figure 4.4). This does not exclude mixing of air and landfill gas at Site 1. As Site 1 was monitored far more infrequently than Site 2, mixing of CH_4 and air was observed on fewer

occasions. Site 2 is very different from Site 1 where gas composition was almost exclusively air or landfill gas (with some mixing in between). Boreholes at Site 2 demonstrate a more complex pattern. The greater mixing of gases is most likely to be due to multiple sources of gases and the geological characteristics of the site that are consistent with a geogenic gas derived from the underlying Coal Measures.

Borehole 07 demonstrates a similar gas composition to BH 06/17 at Site 1. The gas appears to be predominantly air with a small concentration of diluted CO_2 (10–30% v/v range). A similar gas composition is present in boreholes 01, 02, 03, 05, 06, 08, 09, 10, 11, 13, 15, 16, 17, 18 and 19 (Appendix C, Figures F.1–F.15). These boreholes show a greater mixing of CO_2, and in some instances, this is up to 100% CO_2/N_2. However, some boreholes appear to show a gradient between landfill gas and air end-member populations; particularly BH 10 (Appendix C, Figure F.8). This is likely to be an artefact of the opening and closing of different landfill phases during the five years of operations. Boreholes 9, 13 and 17 (Appendix C, Figures F.7, F.10 and F.13) show an incomplete gradient.

Flow

Flow data for Site 2 has not been historically recorded and is not discussed in this review.

Seasonal

The greater frequency of point measurement recording and greater period of time encompassed by Site 2 means that it is possible to identify some seasonality in the data. In particular, BH 14 shows some interesting periodicity (Figure 4.5). The time intervals selected in Figure 4.5 are arbitrary and are based on the dominant gas present in BH 14 to illustrate the rapid changes in composition.

From inception until 17th June 2004, the gas composition was a CO_2–air mixture. The composition changed dramatically for the six month period 24th June 2004 to 19th January 2005 to be more landfill/geogenic in nature. The time-lag for the change in composition is only a week. This could coincide with the closure of Phase 3 of the landfill in October 2003. However, the change in composition is not gradual and is more like an on/off switch. Therefore, the change in composition could be related to the opening of a preferential pathway that previously did not exist. A five month period of CO_2–air mixing follows between 26th January 2005 and 20th June 2005. Once again, this is replaced with a period of what appears to be landfill gas between 29th June 2005 and 24th October 2005. Subsequently, CO_2–air mixing conditions dominate between 31st October 2005 and 8th June 2006. From the first

occurrence of CH_4 in this borehole on 24th June 2004, the cycling between CO_2–air and landfill gas composition appears to occur on approximate six month periods that correspond with summer and winter. It could be that CH_4 appears in this borehole in the summer months when groundwater levels are sufficiently low enough to allow it to accumulate as CH_4 is highly insoluble in water. Unfortunately, groundwater data was not provided for Site 2. Therefore, it is not possible to make any conclusions.

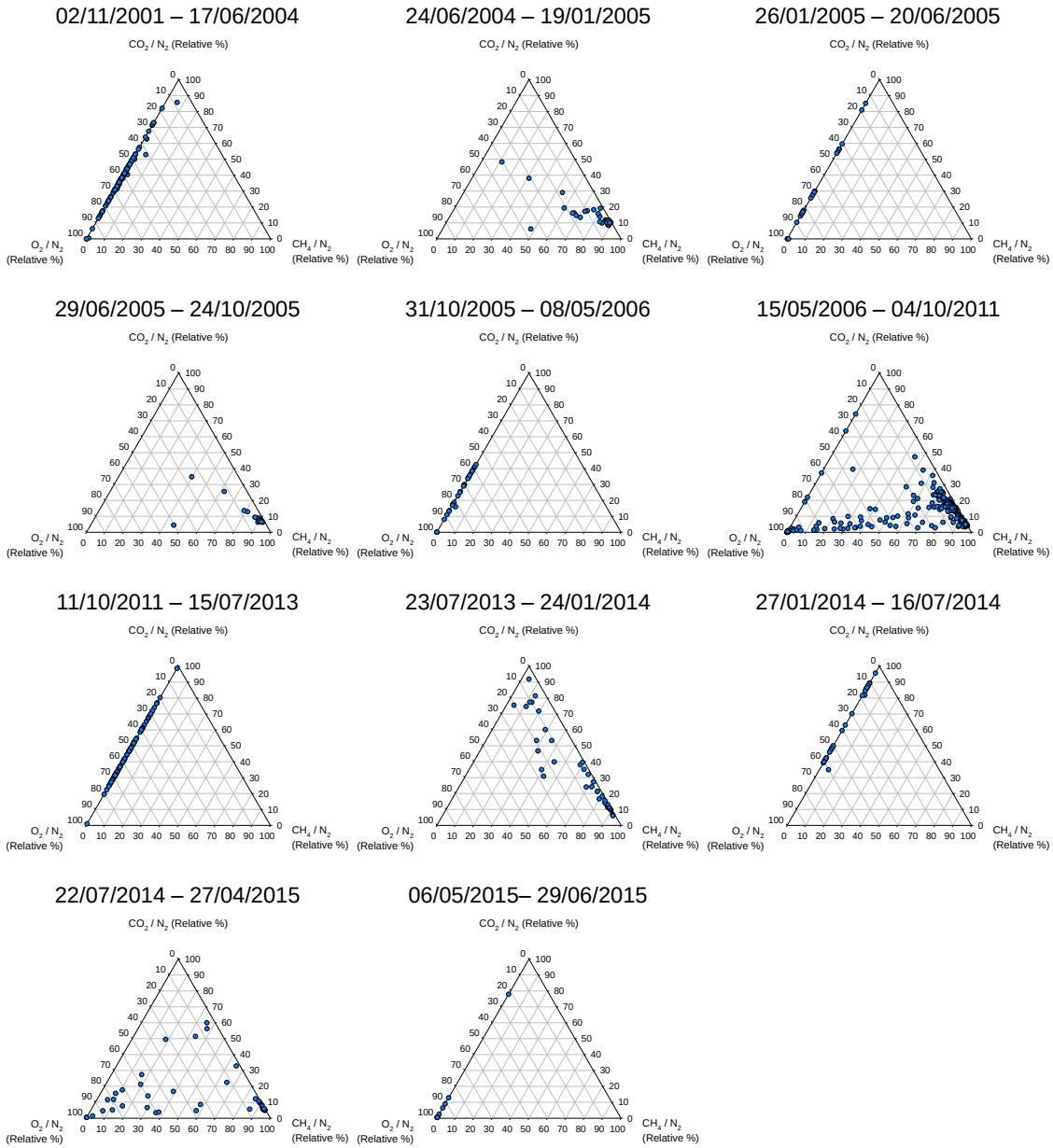

Figure 4.5: Gas Composition for BH 14, Site 2 (02/11/2001 – 29/06/2015)

This periodicity is disrupted between 15th May 2006 and 4th October 2011 when the gas composition was predominantly landfill in nature. It is possible that there was some geogenic influence as CH_4/N_2 exceeded 80% while O_2/N_2 and CO_2/N_2

approached 0% on many occasions. Between air and landfill gas a diffusion gradient with many points exists. CO_2–air gas mixture is observed on few occasions during this five year period.

A pattern similar to prior to 15th May 2006 exists post 4th October 2011 until the end of the data set on 29th June 2015. However, on the occasions when CH_4 does appear in BH 14, the clustering of data points around the landfill gas ratio is less obvious and there appears to be a much greater variation in the mixing of CH_4, CO_2 and O_2. Furthermore, the seasonality does not appear to be strictly summer/winter as it did prior to 2006. Variations in groundwater in accordance with exceptionally dry or wet years could account for this. In the absence of groundwater data, no firm conclusion can be drawn. It is thought that variation in groundwater depth, in conjunction with a preferential pathway, is the most likely cause for the changes in gas composition observed in this monitoring well. The changing nature of the gas composition during the period 22nd July 2014 to 27th April 2015 may reflect a change or decrease in the available substrate, assuming CH_4 is solely landfill derived.

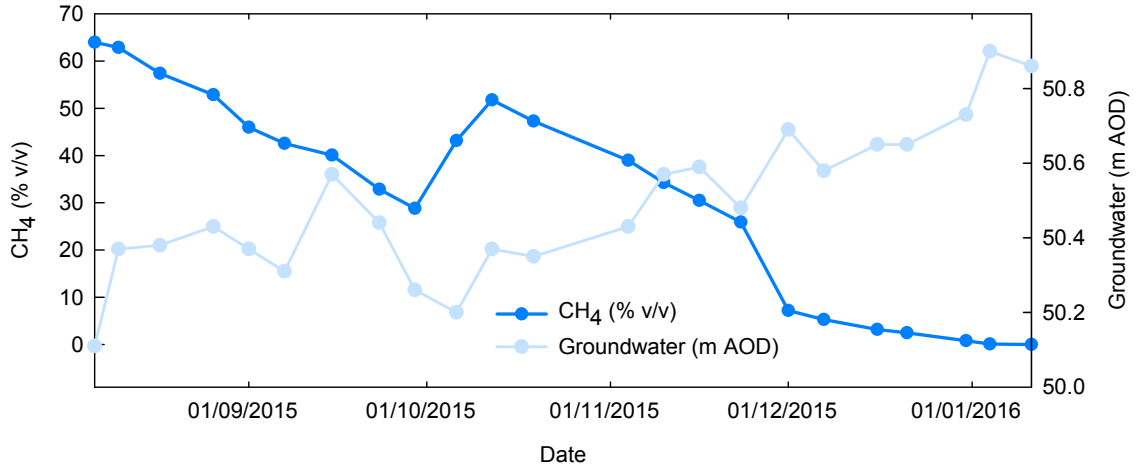

Figure 4.6: Site 2 BH 14 CH_4 Concentration against Groundwater Depth (06/08/2015–11/01/2016)

Following on from the historic monitoring period, the contractor monitored the groundwater depth in relation to CH_4 concentration (Figure 4.6). It does appear to confirm that over a five month period between August 2015 and January 2016, the CH_4 concentration recedes from 64.0% to 0% as the groundwater level rises from 50.11 m AOD to 50.86 m AOD. A groundwater depth change of only 0.75 m is enough to reduce the CH_4 concentration to 0% from landfill concentration. This suggests that a preferential pathway is available to CH_4 as the groundwater level drops in the summer months. However, longer-term data over many seasons and years would be required to confirm the theory. An analysis of these data shows that there is a weak

to good correlation between groundwater depth and CH_4 concentration (Figure 4.7).

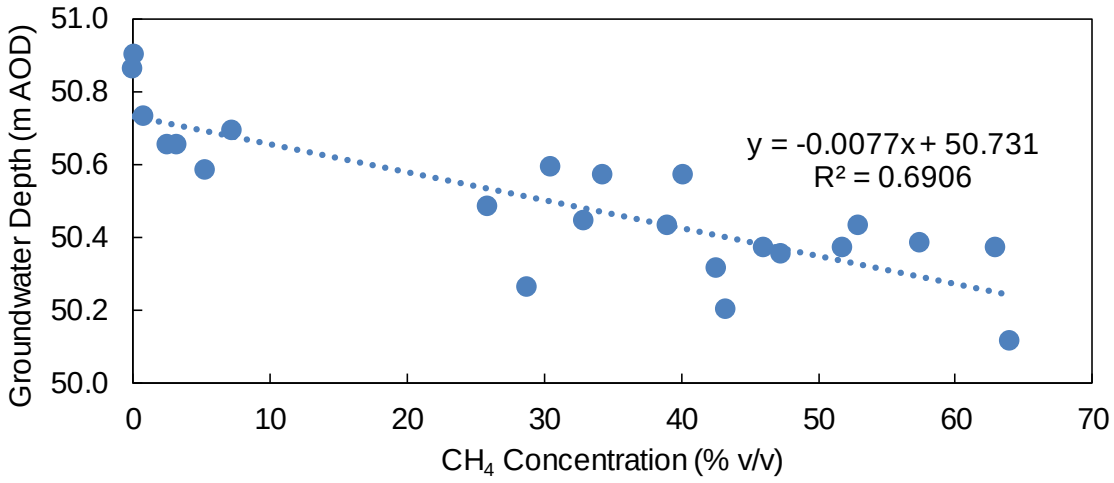

Figure 4.7: Site 2 BH 14 CH_4 Concentration against Groundwater Depth

By comparison, BH 12 shows a progression in gas composition that closely relates to the work of Farquhar and Rovers (1973) (Figure 4.8 and Appendix Figure F.18). From inception in 1998 until Spring 2002, the gas composition recorded the majority of the time was air with CO_2 mixed (up to 80%). On multiple occasions a mixture of CH_4, CO_2 and O_2 is observed. The composition of this tri-gas mixture is extremely variable and random. However, from Spring 2002 onwards, the gas composition present in this borehole is refined to the classic landfill gas ratio (60:40–70:30 CH_4/CO_2). On increasingly fewer occasions during the period 2002–2006 only air is observed. The mixing of air with CO_2 is also reduced during this four year period.

From 2007–2009, only landfill gas is observed in BH 12. The CH_4 component in this gas increases to the point that the ratio of CH_4:CO_2 exceeds 90:10. It is possible that this is the influence of an external geogenic source as has been previously discussed. Certainly, it is irregular for landfill gas.

This trend continued into the period 2010–2012. This period also saw the reintroduction of O_2 into the gas mixture and the air/CO_2 gas mixture is observed. Likewise, the period 2013–2015 is similar but with more air/CO_2 gas mixture observations than the previous three years. As for the latter years of BH 14, this could be evidence for the changing nature or reduction in the available substrate contained in the landfill for the production of CH_4. Unlike BH 14, BH 12 appears to show no seasonality in the data and closely mimics the graph of gas production versus time proposed by Farquhar and Rovers (1973).

Borehole 10 gas composition also indicates changing composition over time. Like

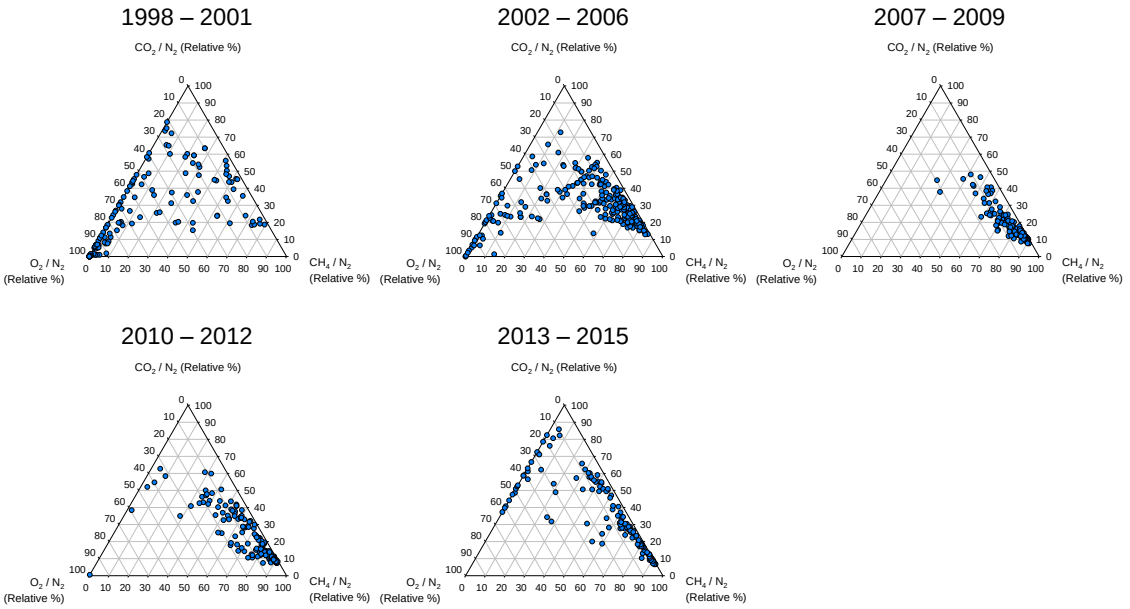

Figure 4.8: Gas Composition for BH 12, Site 2 (13/08/1998 – 29/06/2015)

BHs 12 and 14 landfill gas, air and air/CO_2 gases can be identified. Unlike BH 12, the mixing of CH_4 and CO_2 does not exceed the ratio 50:50. Like BH 14, BH 10 also exhibits some periodicity in the data. The landfill gas ratio is first achieved in 2000, around eighteen months after Phase 1B of the landfill was completed. The data for the first three years (1998–2000) show a gradient from air towards landfill gas (Figure 4.9).

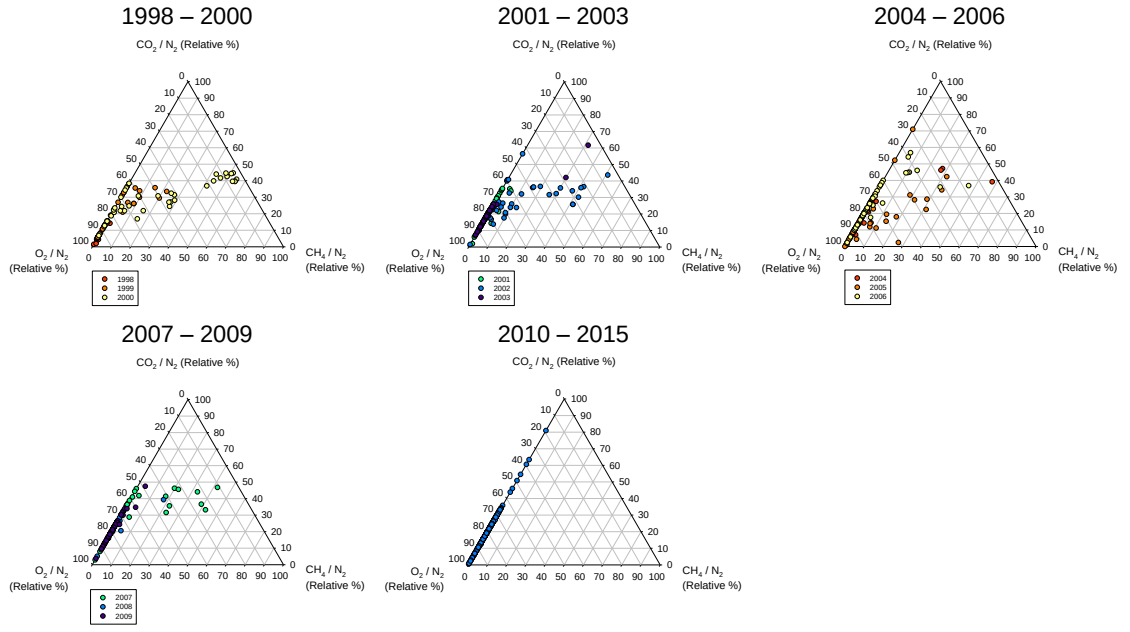

Figure 4.9: Gas Composition for BH 10, Site 2 (13/08/1998 – 29/06/2015)

The gradient identified between 1998 and 2000 is repeated again 2001–2003, 2004–2006 and to a lesser extent 2007–2009. After 2010 only air is present with mixing of CO_2 up to 80%. These fluctuations could be attributed to seasonal fluxes in groundwater. However, in the absence of groundwater data it is not possible to say for certain. Unlike BH 14, it appears more likely that the occurrence of landfill gas is an artefact of the closure of different phases of landfill. Once capped, routes of migration are cut off. This is more consistent with the data shown here, particularly after 2010 when no landfill gas has been recorded.

4.4.2 Key Trends and Interpretations

The key trends and interpretations resulting from Site 2 are outlined as follows:

- Air, landfill gas, and air/CO_2 mixing can be identified in multiple boreholes at Site 2.
- The proportions of CH_4, CO_2 and O_2 in BH 04 are not consistent with landfill gas and may relate to a gas of geogenic origin via the fault underlying the site and the weathered top surface of the bedrock.
- Boreholes 12 and 14 contain air and landfill gas. The ratio 70:30 CH_4/CO_2 is exceeded in both boreholes and in some instances is as great as 90:10 CH_4/CO_2. It is possible that there is a geogenic mixing component in these boreholes.
- Although much can be interpreted from compositional data, stable isotope analysis coupled with radiocarbon dating may differentiate gas origin and corroborate the compositional data plotted in the ternary diagrams.
- Boreholes 10 and 14 show longer term periodicity in the data. In the case of BH 10 it is more likely that this is attributed to the closing of landfill cells while BH 14 may be seasonal. However, there are insufficient data to prove this. In the absence of groundwater data, analysis of weather data may be used to investigate this further.
- The acquisition of high frequency data over a long period of time may resolve seasonal trends.

4.5 Site 3

4.5.1 Data

At Site 3, there are two series of boreholes, 'GM' and 'NG'. The GM Series begins in 1995 and captures gas from the first area of the landfill to be filled (Area A) while the NG Series begins in 2003 and captures gas from Area B of Site 3. Area B is younger and engineered to a higher standard than Area A. Multiple response zones that are sealed from each other are monitored in the GM Series boreholes and the data from these boreholes form the analysis of this section. Data from the NG Boreholes are given in Appendix D, Figure G.14. No CH_4 is present in any of these boreholes. Only air with small concentrations of CO_2 is present. Typical CO_2 values range 0.1–20% with some observations up to 60%.

Spatial

Advantageously, the GM Series boreholes at Site 3 are split into air-tight, multiple response zones. Unlike Site 1 and Site 2, it is possible to obtain a profile of gas composition within the unsaturated zone. Furthermore, the data set begins in 1995, and thus, a comprehensive historic data set of 20 years exists. The only slight disadvantage is that the geology is different from Sites 1 and 2, and the Control Site. However, the chalk is permeable and porous, meaning its properties are not too dissimilar from the Middle Sands that dominate Site 1 and the Control Site, and to a lesser extent, Site 2.

Of particular interest are boreholes GM 5 (located NW corner of Site 3) and GM 14 (located SW corner of Site 3) (Figure 4.10). These boreholes show a clear progression from 100% CO_2 to air (100% O_2/N_2) from the bottom to the top of the boreholes. There are several explanations as to why this trend has been observed.

First of all, it could be as simple that this is an observation of stratification of the gas column. CO_2 is heavier than CH_4 and air. Therefore, it could be possible that if gases separate, CO_2 concentrates at depth by virtue of its higher relative atomic mass. Other boreholes that show a varying ratio of CO_2/N_2 to O_2/N_2 are GM 1, 2, 3, 15 and 16 (Appendix D, Figures G.1, G.2, G.3, G.9 and G.10). Unlike GM 5 and 14, these boreholes do not show a clear progression between end members with decreasing depth in the ternary diagrams. Therefore, other scenarios are more likely.

As stratification is an unlikely conclusion to be drawn from the data, diffusive and/or advective flow are considered as flow mechanisms. Point measurement data such as the data presented here are not substantial enough to confirm whether

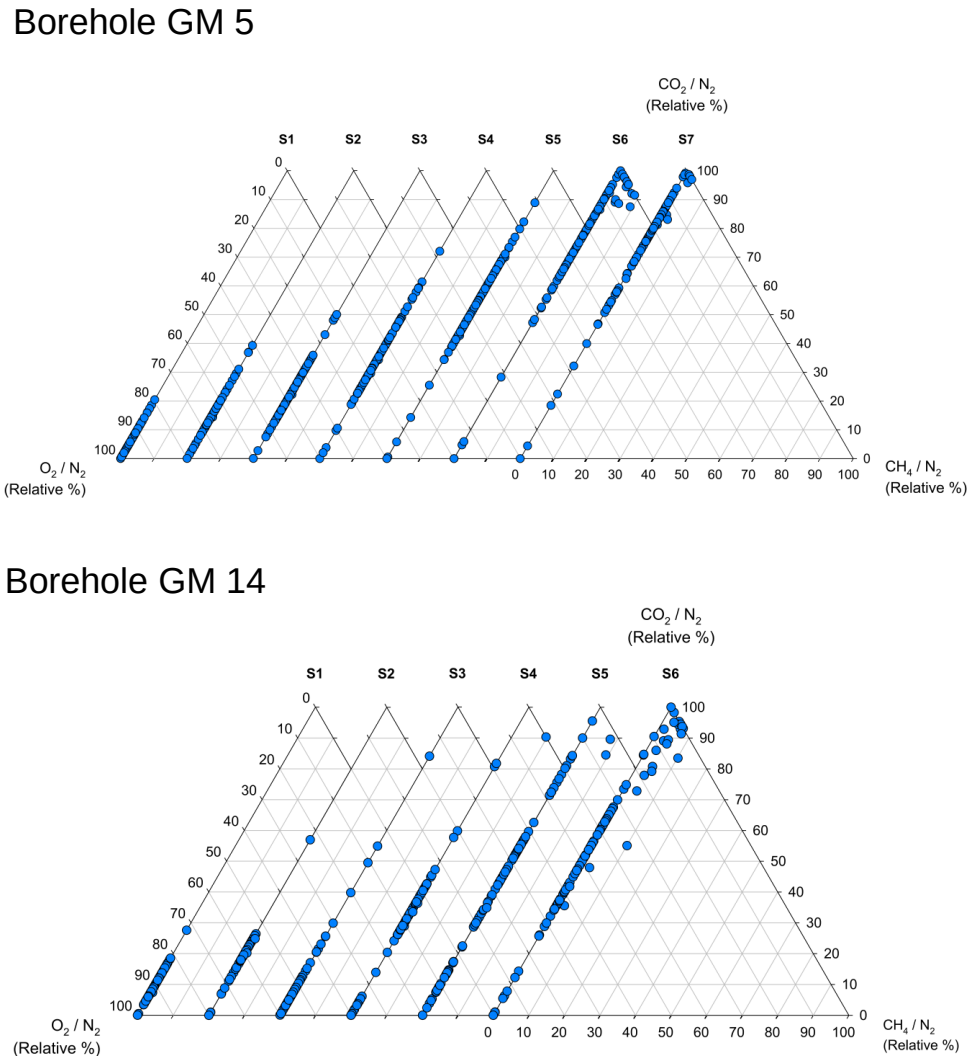

Figure 4.10: Gas Composition for BH GM 5 & 14, Site 3 (21/02/1995 – 18/05/2015)

diffusive, advective (or a combination of both) is the correct mechanism of flow. The data certainly suggests that there are mechanisms at play that warrant further investigation by mathematical modelling and laboratory-designed experiments.

Like boreholes GM 5 and 14, borehole GM 10, located on the western boundary (Figure 4.11), also shows a difference in gas composition in accordance to depth. At depth, landfill gas is the predominant gas. With decreasing depth, a gradient towards air forms (S4 and S5). However, S2 shows a more complicated mixing of gases with values approaching 100% CO_2/N_2 ratio. There is clear mixing between 100% O_2/N_2 and CO_2/N_2 as well as between 100% CO_2/N_2 and CH_4/N_2 that is not present in any other response zone. It appears to be anomalous to the trend as S1 clearly shows that predominant gas is air with varying dilution of CO_2 (multiple data points approach 50% CO_2/N_2 with 50–90% CO_2/N_2 observed on fewer occasions).

Adjacent to borehole GM 10 on the western boundary of the site, borehole GM 20 also shows a similar progression from landfill gas at depth to air in the shallow layers of the ground. Unlike GM 10, the composition of landfill gas present in GM 20 tends to show a mixing with CO_2 so that the ratio of CO_2/CH_4 exceeds 50:50 and on occasion 100% CO_2/N_2 is achieved. The S2 response zone, which is the second shallowest, shows a large and complex mixing of all three gases that appears to be random.

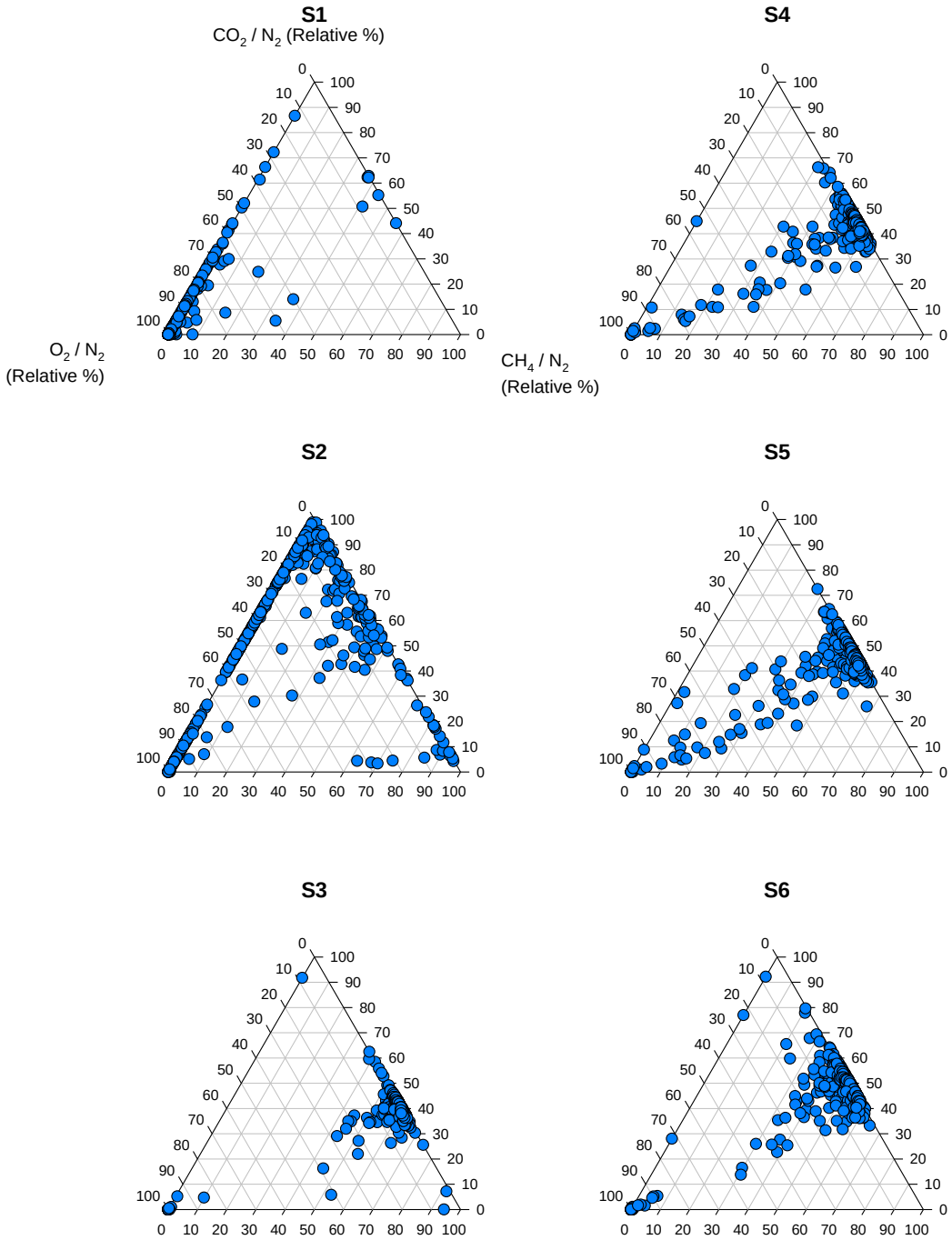

Figure 4.11: Gas Composition for BH GM 10, Site 3 (29/10/1998 – 18/05/2015)

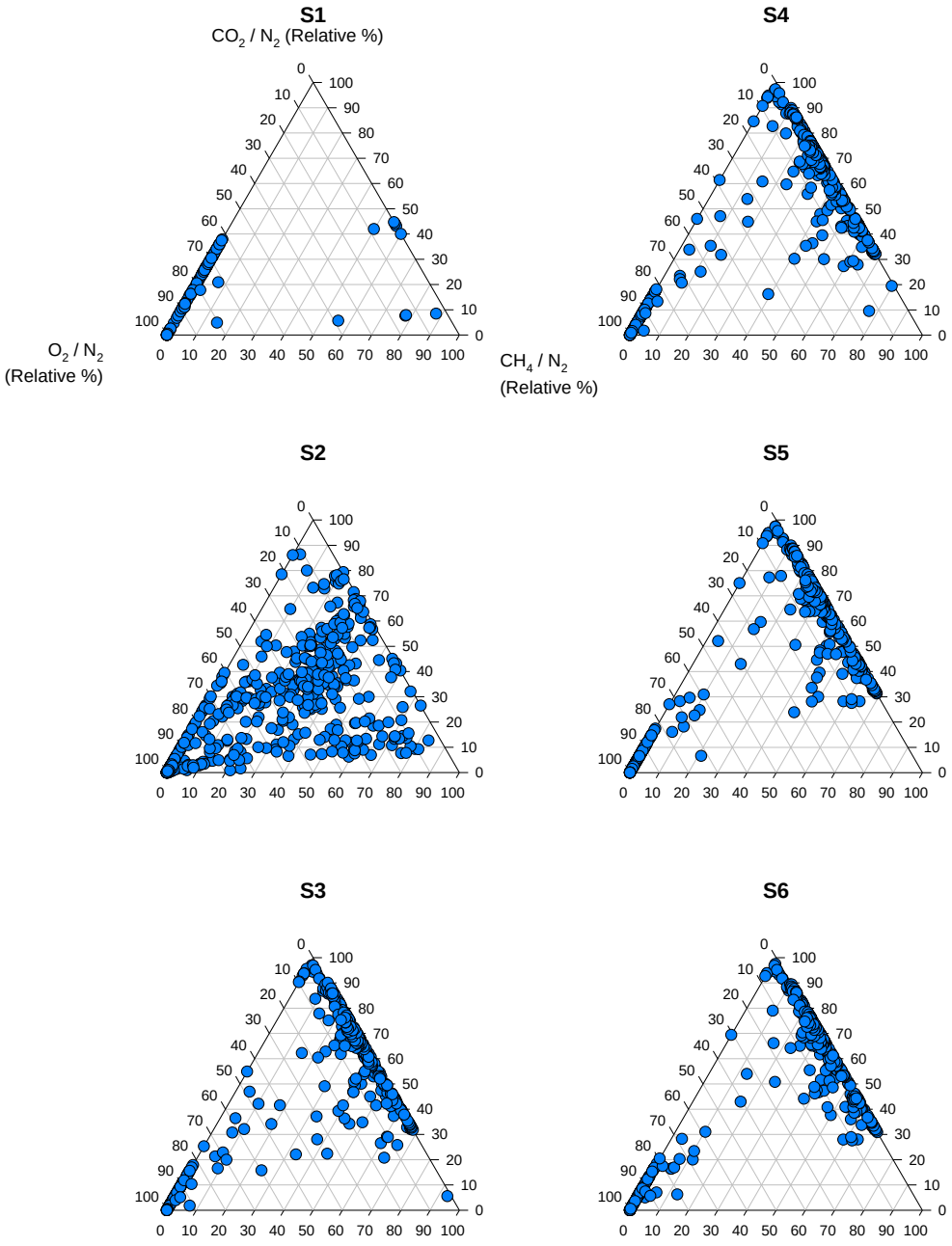

Figure 4.12: Gas Composition for BH GM 20, Site 3 (12/11/1998 – 18/05/2015)

Flow

Flow data for Site 3 have not been historically recorded and are not discussed in this review.

Seasonal

The apparent randomness in the observed data suggests that seasonal trends are not dominant. The limitations of point measurement data shown for Site 1 and Site 2, also apply to Site 3. Seasonal data are not discussed in this review.

4.5.2 Key Trends and Interpretations

The key trends and interpretations that can be extracted from Site 3 are outlined as follows:

- Like Sites 1 and 2, populations in the gas composition can be identified as air and landfill gas as well as CO_2 diluted in air with varying mixtures in between.
- There is not enough detail in the data to know what ground conditions and atmospheric conditions (if any) caused evolution of landfill gas.
- In Area A of this landfill, the grade of engineering (operations opened 1983) is such that landfill gas is monitored in perimeter boreholes.
- Without boreholes located further away from the landfill it is unknown how far gas has migrated, although the road that bounds the west of the site may act as barrier.
- Area B (operations commenced 2003) is engineered to a much higher standard. Boreholes located on the landfill perimeter in this area (NG boreholes) show absence of landfill gas. Containment of gas on site has been successful.
- GM boreholes with multiple, air-tight response zones show changing composition in gas with depth. There is some evidence of CO_2 dilution in air with greatest concentration of CO_2 at depth, gradually moving towards air composition nearer to the surface in boreholes GM 5 and 14.
- The data are insufficiently detailed to make conclusions about the mechanisms that have caused these patterns to be observed. Mechanisms postulated include stratification of gas column, diffusive flow and advective flow. It is thought that controlled laboratory experiments could examine gas migration processes.

4.6 Initial Conceptual Model Design

The conclusions drawn from the compositional data from the three research sites can be demonstrated in an initial conceptual model design (Figure 4.13). The basic design of the conceptual model outlines the principal migratory routes that the compositional data showed. No assumptions about mechanistic movement have been made as the compositional data do not include that level of detail. No H_2S, CO or VOCs were recorded during the historic monitoring and were therefore excluded from the conceptual model. However, it is acknowledged that from time to time, these gases may be present in particulate amounts.

Some assumptions about underlying geology and associated abandoned mine

workings have been included to account for the data from Site 2 which showed a CH_4-rich source in BH 04. Therefore, the initial design includes coal seams in the Carboniferous geology and an abandoned, dewatered mine void. However, as the data presented here are solely from perimeter monitoring of landfill sites, further evidence to substantiate gas source would be required.

Evidence from Site 1 suggests that in unconsolidated Quaternary Deposits such as Middle Sands, CH_4 and CO_2 are able to traverse short distances. Certainly, CH_4 and CO_2 are recorded 25 m distant from landfill, but not 100 m. It is unknown if preferential pathways exist. However, the Middle Sands are considered to be largely homogeneous. Gases escape to the atmosphere through the top soil via cracks in the surface such as those created by plant roots. If CH_4 accumulates in a high concentration, necrosis of vegetation will occur as was observed in the lead up to the Loscoe Explosion in 1986. If the consolidated material is capped by a layer of Boulder Clay, flow of gases will be impeded and forced to migrate around the clay owing to its impermeable properties.

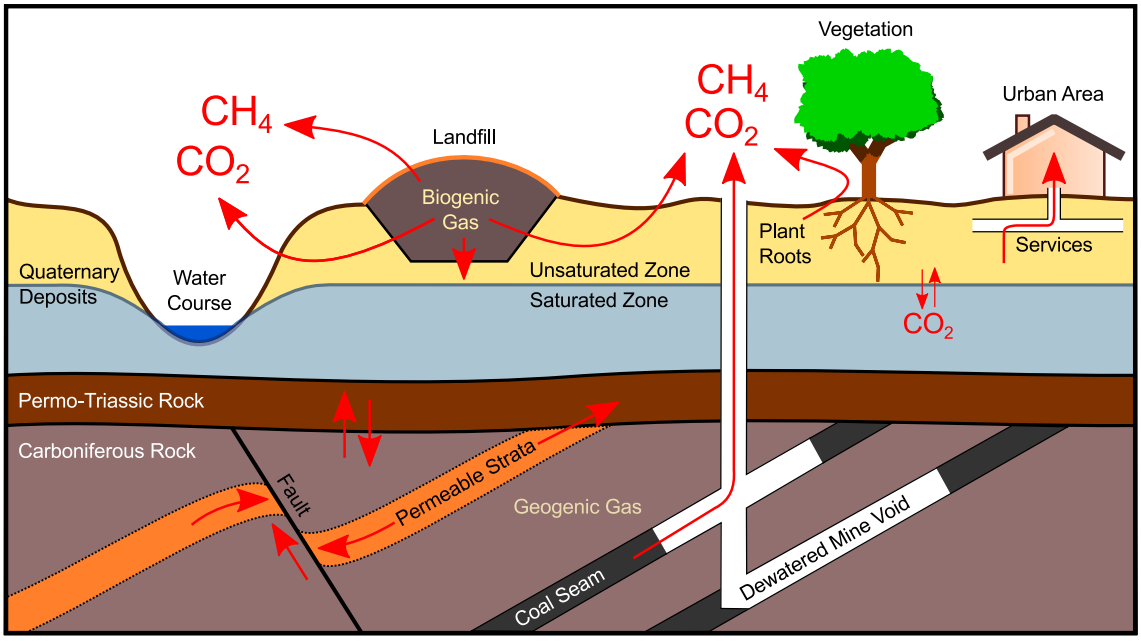

Figure 4.13: Initial Conceptual Model Design

Further evidence from Site 1 indicates that atmospheric pressure could be a control on the release of CH_4 and CO_2 gases from ground to atmosphere. Likewise, the high solubility of CO_2 in water has to be considered. Seasonal changes in groundwater surface are anticipated and are considered to be an effective method of 'scrubbing' CO_2 from the system by dissolution. This process is reversible and so a dynamic equilibrium exists between landfill input and groundwater exchange in the unsaturated zone.

Faults, fractures and fissures may act as conduits of gas transport in the sub-surface. Multiple perimeter monitoring wells at Site 2 showed a gas mixing component that suggested a geogenic origin (BHs 04, 12 and 14). In these boreholes the ratio of CH_4:CO_2 exceeded 90:10. The complex geology of Site 2 that included a fault underlying the landfill was thought to act as a major gas transport channel. Quantification of the SiO_2 content of the sand showed a non-linear change across geologic boundaries (as shown in Figure 3.9). The inference was that the top-surface of the bedrock was heavily weathered, also permitting the transport of gases between strata. Additionally, layers of permeable and porous strata act as 'conductors' of CH_4 and CO_2.

Although the key routes of gas migration have been outlined in this initial conceptual model, it does produce further research questions. These questions are:

- What are the controlling atmospheric and ground conditions that result in the release of CH_4 and CO_2 from the ground to the atmosphere;
- What mechanism(s) drive gas transport in the sub-surface, and;
- Is there a robust approach to quantifying and differentiating the source of CH_4 and CO_2 in the sub-surface.

The following chapters aim to answer these questions and move towards adding to the depth knowledge in these areas. Refinements will be made to the conceptual model design as data adds to the knowledge and the robustness of the model.

Chapter 5

High Temporal Frequency Data

5.1 Data Compilation

5.1.1 GasClam

GasClam®, developed by IonScience Ltd and distributed through ShawCity Ltd, is a high-frequency, continuous, fully automated ground gas monitor. It is capable of a maximum sample rate frequency of every three minutes. Like traditional hand-held monitors, it measures CH_4, CO_2, O_2 as well as H_2S and Volatile Organic Compounds (VOCs). Additionally, it is capable of measuring ambient temperature, ambient pressure, borehole pressure, pressure difference and water depth. However, the model used for this research was not equipped with the water depth gauge. Importantly, the GasClam has been used to monitor ground gas concentrations by Cuadrilla Resources Ltd during Shale Gas exploration in Lancashire, UK during the time-frame of this research (Wadey-Leblond, 2012).

5.1.2 Monitoring Schedule and Specification

The GasClam was deployed at Site 1 between 18th February 2013 and 25th November 2013, and at Site 2 between 8th July 2014 and 5th January 2015. During data capture, the GasClam was set to take a sample of all parameters every thirty minutes. As has been previously discussed, a major problem with point measurement instruments is the disruption of ground conditions within a monitoring well. Therefore, the GasClam was set to vent closed mode, as per manufacturer guidelines. Spent samples were purged into the borehole. A second GasClam supplied by IonScience carrying the 0–5% CH_4 and CO_2 infrared channels was used at the Control Site between 3rd February and 17th February 2014. A complete monitoring schedule is provided in Table 5.1.

GasClam s/n	Site 1	Site 2	Control Site
000237/05/12	**BH 03/4**	**BH 04**	**BH 96G**
	18/02/2013–25/02/2013	08/07/2014–18/09/2014	19/12/2013–02/01/2014
	12/04/2013–19/04/2013	**BH 08**	
	22/07/2013–25/07/2013	18/09/2014–02/10/2014	
	29/07/2013–25/11/2013	**BH 12**	
	BH 03/6	13/10/2014–09/11/2014	
	19/07/2013–22/07/2013	**BH 14**	
	25/07/2013–29/07/2013	10/11/2014–05/01/2015	
000049/09/09	**BH 03/4**		
	19/07/2013–22/07/2013		
	25/07/2013–29/07/2013		
	BH 03/6		
	22/07/2013–25/07/2013		
	29/07/2013–01/08/2013		
000041/12/09			03/02/2014–17/02/2014

Table 5.1: Gas Monitoring Schedule (18/02/2013 – 05/01/2015)

5.1.3 Scope

Despite the advantage of high temporal frequency data over point measurement data, there are limitations within the scope of this research. Only one GasClam was used due to financial constraint. Ideally, every perimeter monitoring well on a given site would need to be fitted with a GasClam (or equivalent) instrument in order for data sets to be directly comparable. In the industrial sector, this would constitute a large financial investment. Consequently, the scope of this chapter is to demonstrate the GasClam's capabilities, to analyse high temporal frequency data, to resolve the relationship between gas emissions and atmospheric conditions, and to contextualise this with the historic monitoring data. Average pressure changes were calculated by subtracting minimum pressure (mbar) from maximum pressure (mbar) divided by time (hr). Boreholes that were consistently dry or showed little annual variation in groundwater depth were selected to eliminate the effect of hydrometric pumping on the data.

5.2 Preliminary Data

5.2.1 Site 1 BH 03/4

Initial readings were made at Site 1, BH 03/4, between 18th February and 25th February 2013, and 12th April and 19th April 2013. This particular borehole was selected as the primary research borehole as it has been historically dry. Therefore,

there is no contribution to gas emissions from hydrometric pumping. Initial results from the GasClam are shown in Figure 5.1.

During the period 12th April to 19th April 2013 there were three emission events of CH_4 and CO_2. Concurrently, O_2 dropped to 0% from atmospheric concentration (20.9%). On 13th April, the atmospheric pressure dropped 4 mbar in 4 hours 15 minutes (0.94 mbar/hr) and this was enough to induce an emission of CH_4 and CO_2. This emission event lasted a period of 24 hours as the air pressure stabilised at 1005 mbar for 20 hours. At its peak, CH_4 concentration was 35.5% while CO_2 concentration was 2.3% on 14th April. Of note, the decrease in concentration of O_2 mirrored the increase in CH_4 concentration.

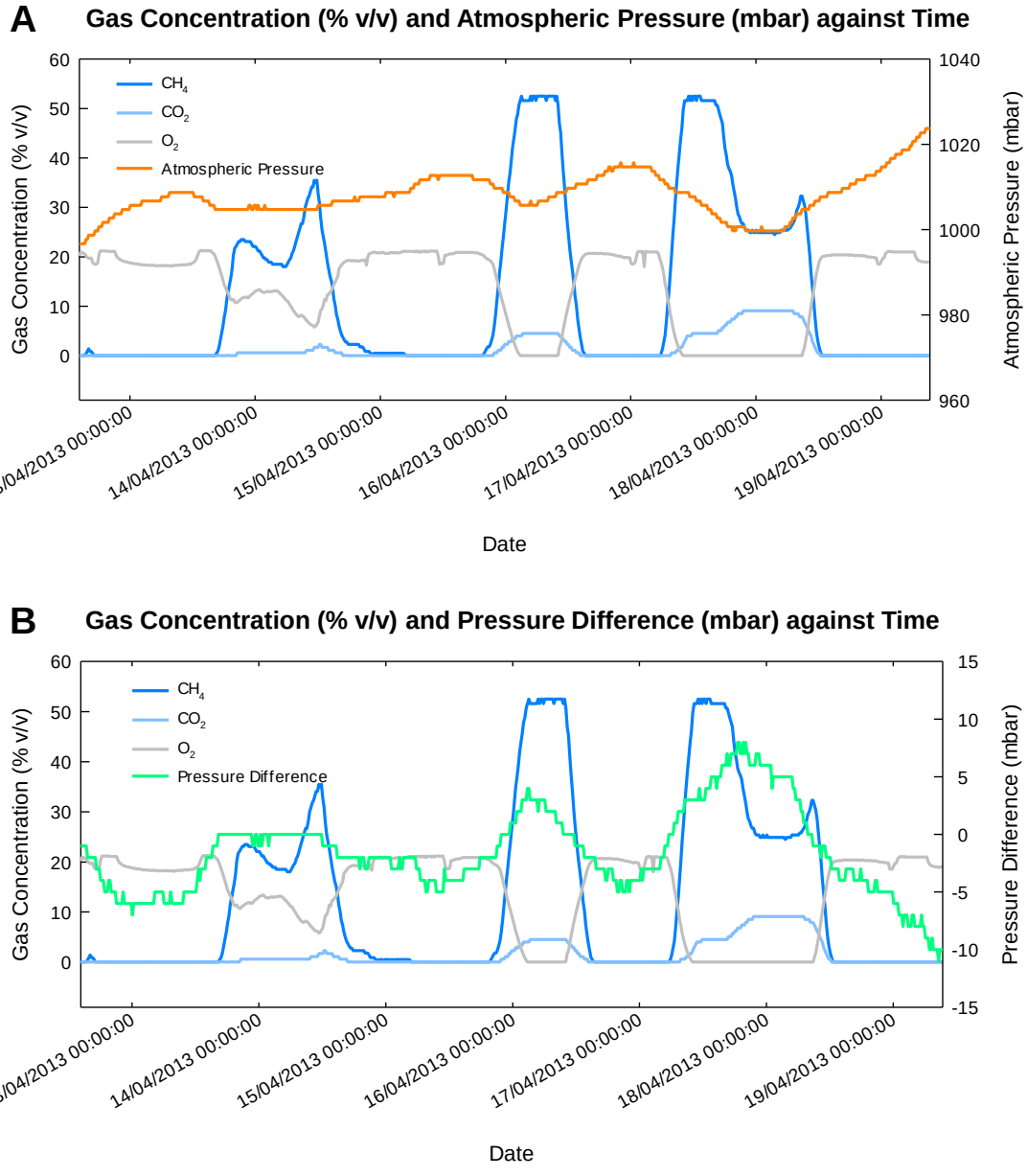

Figure 5.1: Preliminary GasClam Data BH 03/4 (12/04/2013 – 19/04/2013)

There is a secondary peak in CH_4 at 32.3% which could also relate to interference in the signal or a purging problem. The secondary CH_4 peak corresponds to a simultaneous decrease in CO_2 concentration. This may indicate reduction of CO_2 to CH_4. Alternatively, it could be a result of the lower buoyancy of CO_2. As the atmospheric pressure increases, CO_2 is removed from the borehole ahead of CH_4 which may account for the secondary spike on 18th April 2013.

Further emission events occurred on 16th April and 17–18th April. Both events were induced by a decline in atmospheric pressure. The event beginning 16th April occurred in response to a 7 mbar drop in atmospheric pressure over a 9 hour period (0.78 mbar/hr) and produced a peak CH_4 concentration of 52.5% and CO_2 concentration 4.5%. The third event beginning 17th April was a result of a drop in atmospheric pressure by 16 mbar over a 19 hour period (average 0.84 mbar/hr). This emission event also peaked at 52.5% CH_4 and 9.1% CO_2 while O_2 concurrently fell to 0% from 20.9%.

Atmospheric pressure conditions are critical to the behaviour of BH 03/4, Site 1. As the atmospheric pressure drops, the internal pressure of the borehole increases. That is, a pressure gradient is induced that causes the movement of gases from the borehole to the atmosphere. During the first emission event, the pressure difference increased from -7 to 0 mbar, during the second there was an increase from -5 to 4 mbar, and during the third there was an increase from -5 to 8 mbar. Correspondingly, the greatest change in internal borehole pressure was resultant from the largest negative atmospheric pressure gradient. This appears to confirm the close relationship between ground conditions and atmospheric conditions.

However, there are observable problems with the high temporal frequency data generated by the GasClam. During the first emission event of 13–14th April, there is a clear splitting of the CH_4 peak. This does correspond to a proportional displacement of O_2. It would be anticipated that O_2 would drop to 0% with no mixing of CH_4 and CO_2.

Furthermore, the second emission event results in flat or 'clipped' peaks of CH_4 (52.5%) and CO_2 (4.5%). Similarly, a 'clipping' effect takes place during the third emission event. Initially these concentrations are the same magnitude as the previous event. However, there is an offsetting effect as CO_2 increases to 9.1% while CH_4 decreases to 24.9%. This could be a result of interference in the CH_4 channel from other small-chain alkanes such as ethane (C_2H_6) and propane (C_3H_8). There is a secondary peak in CH_4 at 32.3% which could also relate to interference in the signal or a purging problem.

At the start of the monitoring period commencing 19th July 2013, a second GasClam (serial number *000049/09/09*) was hired from ShawCity Ltd to verify the results from GasClam *000237/05/12*.

The results from Gas Clam *000049/09/09* are very different in nature from GasClam *000237/05/12*. Where split peaks were previously observed due to an assumed purging issue, asymmetric peaks are observed. Furthermore, the data recorded in July 2013 (preceded by two weeks of stable and high atmospheric pressure), indicates that for BH 03/4, Site 1, a very unstable regime exists. Changes in pressure difference of no more than 1 mbar appear to be enough to induce gas emission.

There are interesting comparisons to be made with GasClam *000237/05/12* data. Peak CH_4 concentration was 49.7% and peak CO_2 concentration was 5.9%. The CH_4 peak was similar in magnitude to GasClam *000237/05/12* that recorded peak CH_4 52.5% (2.8% difference). The peak concentration of CO_2 was lower by 3.2% v/v. Although the CO_2 peak appears to be clipped, there is no clipping at different concentrations without displacement of O_2 (unlike the data from GasClam *000237/05/12*) which suggests that the data are more reliable. Also, there is no 'noise' produced in the O_2 channel, unlike the data output from GasClam *000237/05/12*.

A particular point of interest is the sustained CH_4 and CO_2 emission over the three day period between 26th July 2013 and 28th July 2013. The data imply that the slow fall in atmospheric pressure (1009–999 mbar) over three days is sufficient to sustain gas emission. Over this period, the pressure difference increased from -1 mbar to 3 mbar. This could indicate the high sensitivity of the system to small changes in atmospheric pressure.

5.2.2 Site 1 BH 03/6

Both GasClam *000237/05/12* and *000049/09/09* were trialled in BH 03/6 at Site 1. The data outputs from both GasClams showed a very different scenario from BH 03/4. Changes in gas composition appear to be independent from changes in atmospheric pressure. Examining the pressure difference data it becomes clear as to why this has occurred. The range in recorded pressure difference is from -1 to 1 mbar. These subtle changes in the pressure difference appear to be external of atmospheric pressure changes.

Assuming nil influence from hydrometric pumping (fluctuations in groundwater depth), the changes in gas composition could be attributed to a borehole leak. That is, an air tight seal has not been achieved (with bentonite) leading to intrusion of air at random intervals. The effect of air mixing with the landfill gases is to dilute CH_4 (peak concentration 0.9% and 1.9% recorded by GasClam *000237/05/12* (Figure

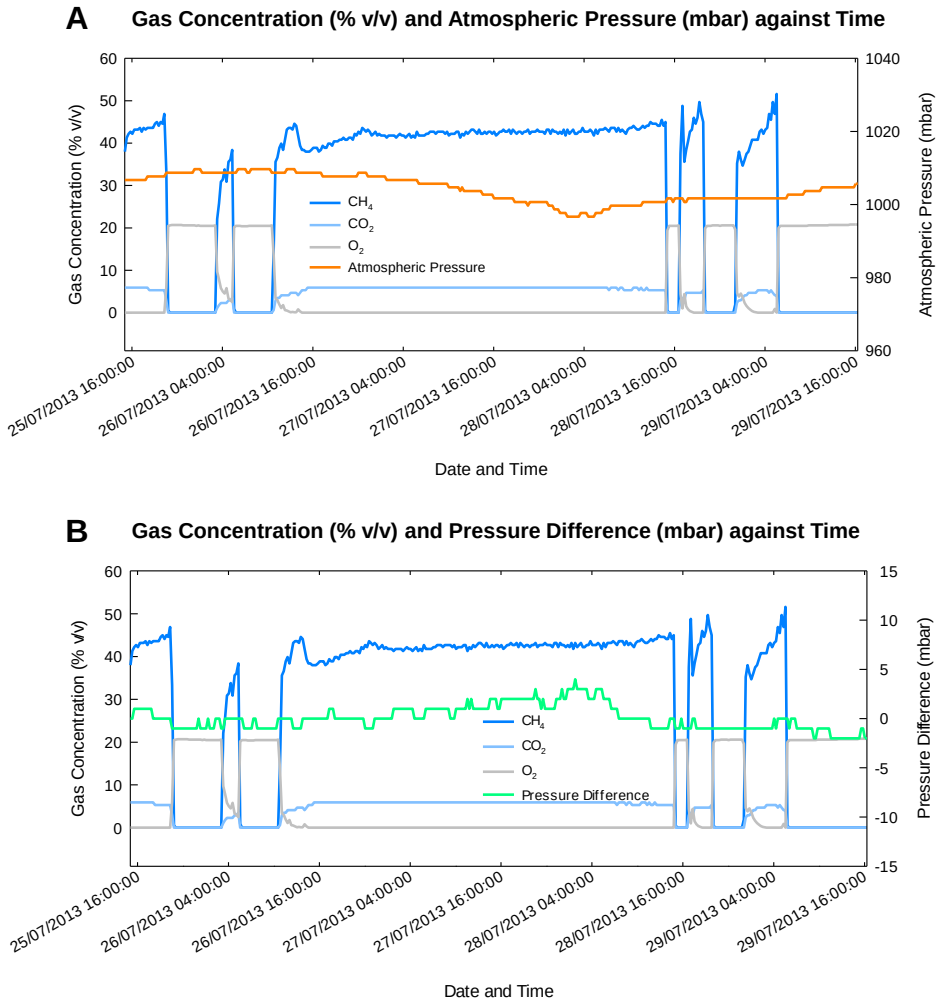

Figure 5.2: GasClam *000049/09/09* Data for BH 03/4 (25/07/2013 – 29/07/2013)

5.3a and Figure 5.3b) and GasClam *000049/09/09* (Figure 5.3c and Figure 5.3d) respectively). In contrast the CO_2 concentration peaks at similar concentration to BH 03/4 (12.4% and 10.6% GasClam *000237/05/12* and GasClam *000049/09/09* respectively). This could be owing to the heavier relative mass of CO_2 compared with air and CH_4. If a leak does exist, it is more likely that any CH_4 present will quickly diffuse into the atmosphere.

Further evidence to suggest a defective seal in the installation comes from the historic gas monitoring data. Historically, during periods of rapidly decreasing atmospheric pressure, BH 03/4 has registered high gas flow rates whereas BH 03/6 has recorded nil or negative gas flow rates. For example on 24th January 2007, BH 03/4 recorded a gas flow rate of 19.11 l/hr whereas BH 03/6 only recorded a flow rate of 0.2 l/hr. Likewise, a similar scenario was recorded on 29th August 2012 when BH 03/4 flow rate was 28.6 l/hr and BH 03/6 flow rate was below the detection limit of the instrument (< 0.1 l/hr).

The data from both GasClams appears to corroborate this theory. In particular, the lack of change in borehole pressure relative to changes in atmospheric pressure is indicative that the borehole installation has a malfunctioning seal. Another explanation could be that owing to preferential pathways, BH 03/6 has a smaller reservoir of gas available to it. Therefore, it was decided to discount further data capture from BH 03/6.

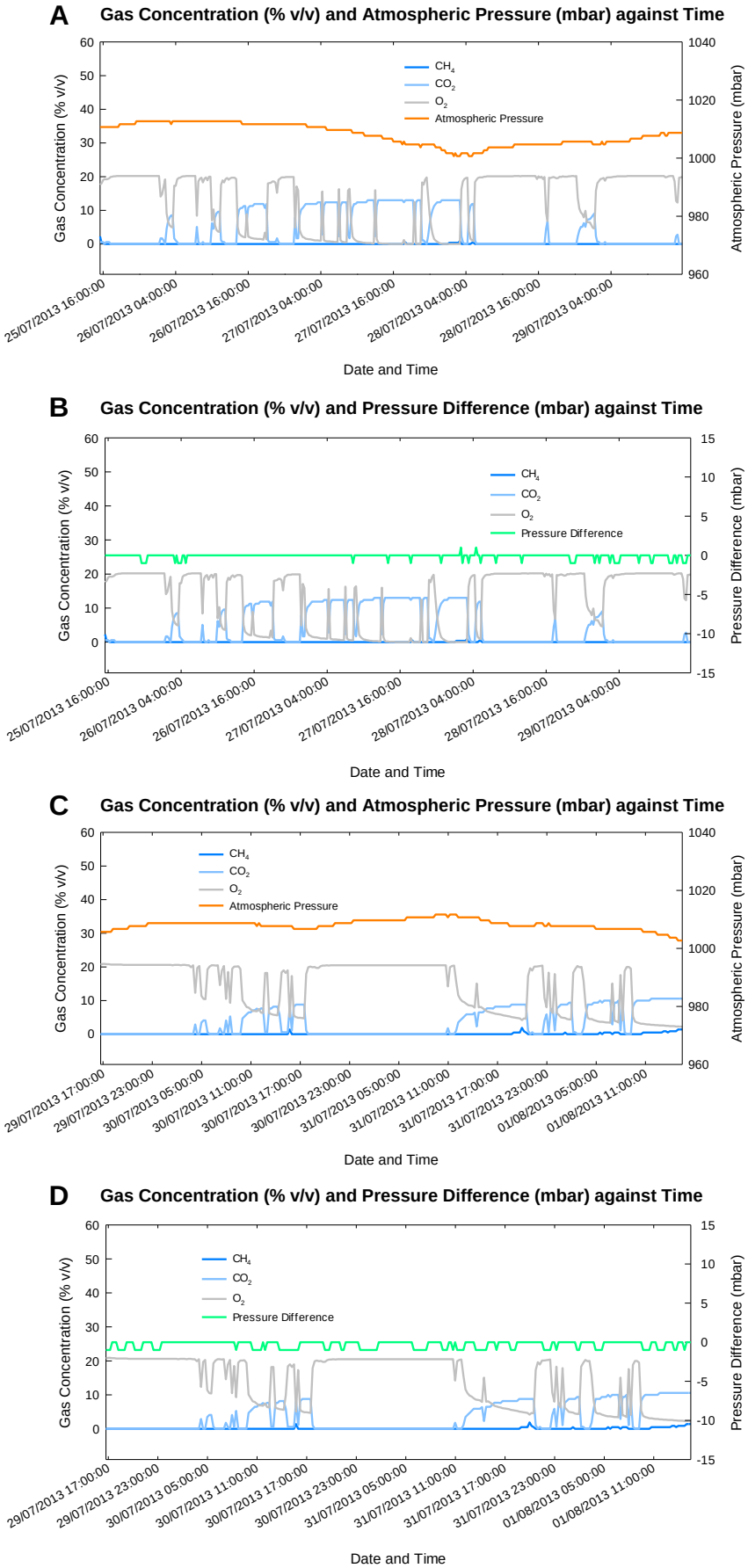

Figure 5.3: Comparison of GasClam *000237/05/12* (Figures 5.3a and 5.3b) and *000049/09/09* (Figures 5.3c and 5.3d) Data for Site 1 BH 03/6 (25/07/2013 – 01/08/2013)

5.3 Site 1

5.3.1 Temporal Changes and Effect of Barometric Pressure

Figure 5.4 shows the period 29th October 2013 to 12th November 2013 captured by GasClam *000237/05/12* in BH 03/4.

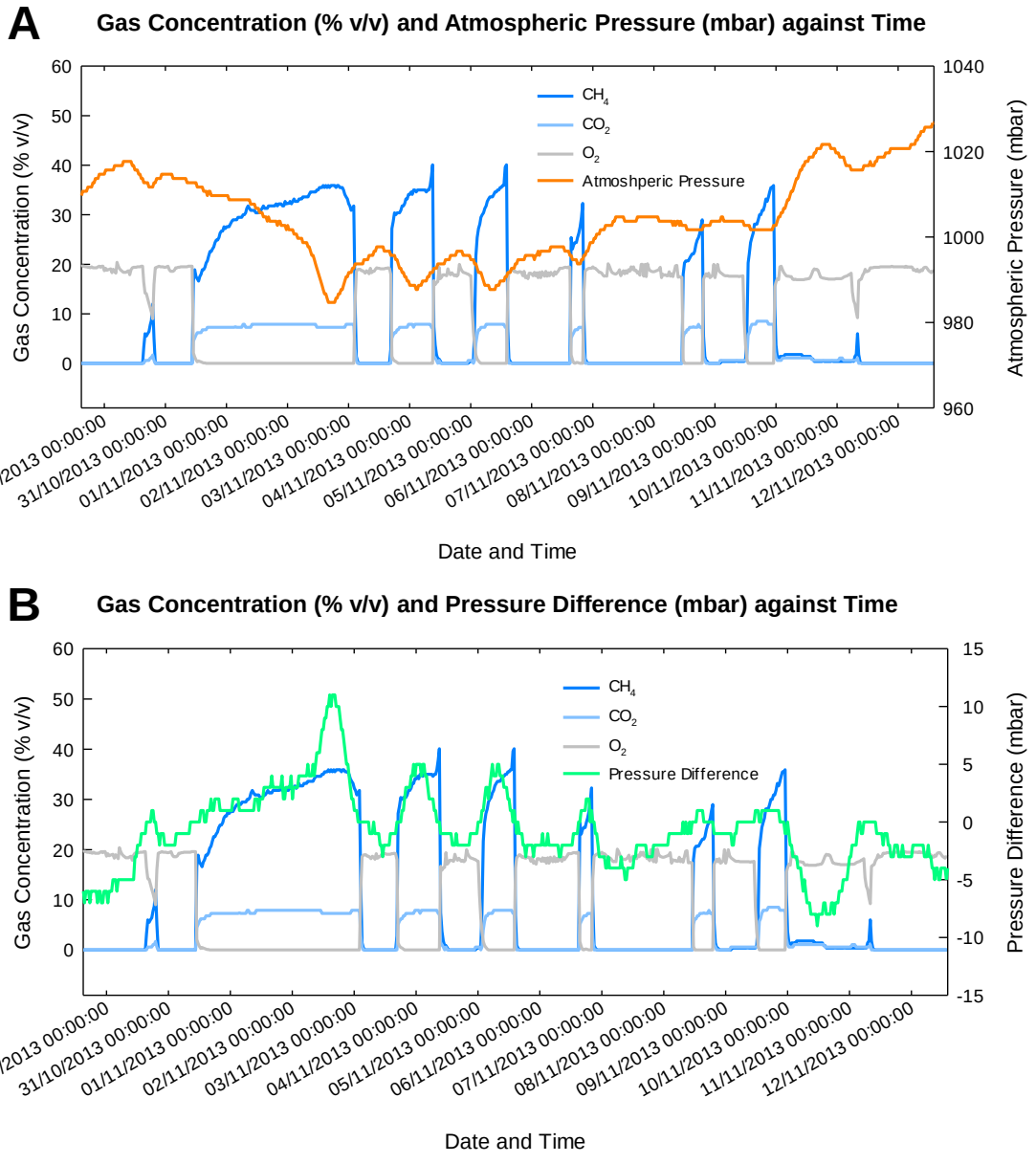

Figure 5.4: Site 1 BH 03/4 High Temporal Frequency Gas Data (29/10/2013 – 12/11/2013)

There were three prominent successive rises and falls in atmospheric pressure that occurred on 2nd, 3rd and 5th November 2013. The falls had average gradients of 1.55 mbar/hr, 0.71 mbar/hr and 0.81 mbar/hr with peak low pressure intensities of 985 mbar, 988 mbar and 988 mbar respectively. With each fall, corresponding peak concentrations of CH_4 (up to 40.1%) and CO_2 (up to 7.9%) were observed,

the balance was assumed to be N_2. As CH_4 and CO_2 appeared in the borehole, O_2 concentration decreased to 0% from atmospheric concentration ($\sim$ 20%).

For the observed borehole, the change in gas composition is very sensitive to changes in atmospheric pressure. A pressure drop of little more than 3 mbar over a 2–4 hr period can induce CH_4 and CO_2 to emanate into the borehole from the surrounding ground. The concentrations of CH_4 and CO_2 were lower than the expected composition of landfill gas, but were not corrected for dilution by air and N_2.

Additionally, when the time series data are plotted against pressure difference (the pressure difference between atmosphere and borehole) (Figure 5.4b), it is clear that under positive pressure conditions (i.e. the borehole was 'blowing'), CH_4 and CO_2 concentrations were elevated within the borehole. Conversely, when negative pressure conditions existed, O_2 only (i.e. air) was measured in BH 03/4.

Peak pressure difference was recorded at 11 mbar, 5 mbar and 5 mbar on 2nd, 3rd and 5th November 2013, respectively. Not only was there a time lag between peak pressure difference and peak CH_4 concentration in the borehole, but the peak concentration appeared to be proportional to peak pressure difference. Further emission events on 6th, 8th and 11th November 2013 yielded peak CH_4 concentrations of 32.3%, 29.0% and 6.0% respectively while peak pressure difference was 2 mbar, 1 mbar and 0 mbar, respectively for the three events. An anomaly to this pattern occurred on 9th November 2013 when peak CH_4 was recorded at 35.3% against a peak pressure difference of 1 mbar. A more substantial data set encompassing all seasons would be required to assess this. A summary of emission events between 29th October and 12th November 2013 is recorded in Table 5.2.

Event Date	**Peak CH_4** (%)	**Peak CO_2** (%)	**Average Gradient** (mbar/hr)	**Peak Pressure Difference** (mbar)
02/11/2013	35.9	7.9	−1.55	11
03/11/2013	40.1	7.9	−0.71	5
05/11/2013	40.1	7.9	−0.81	5
06/11/2013	32.3	7.3	−0.72	2
08/11/2013	29.0	7.9	−0.26	1
09/11/2013	35.3	8.5	−0.25	1
11/11/2013	6.0	1.1	−0.71	0

Table 5.2: BH 03/4 Gas Emission Events (29/10/2013 – 12/11/2013)

The data indicate high temporal variability. The periodicity of the cycling of gases can be as short as a few hours to as long as a few days. For the two week period presented in Figure 5.4 for BH 03/4, only air (O_2 + N_2) was present for 70%

of the monitoring period. Thus, there is a high probability that if the borehole had been monitored using a hand held gas monitor (point measurement), an emission event would not have been recorded. To be certain of the ground gas regime for a site where CH_4 and CO_2 are likely to pose a hazard, a high temporal resolution data set may be required. Furthermore, a longer statutory monitoring period could be necessary to identify any longer-term seasonal variations in the ground gas regime.

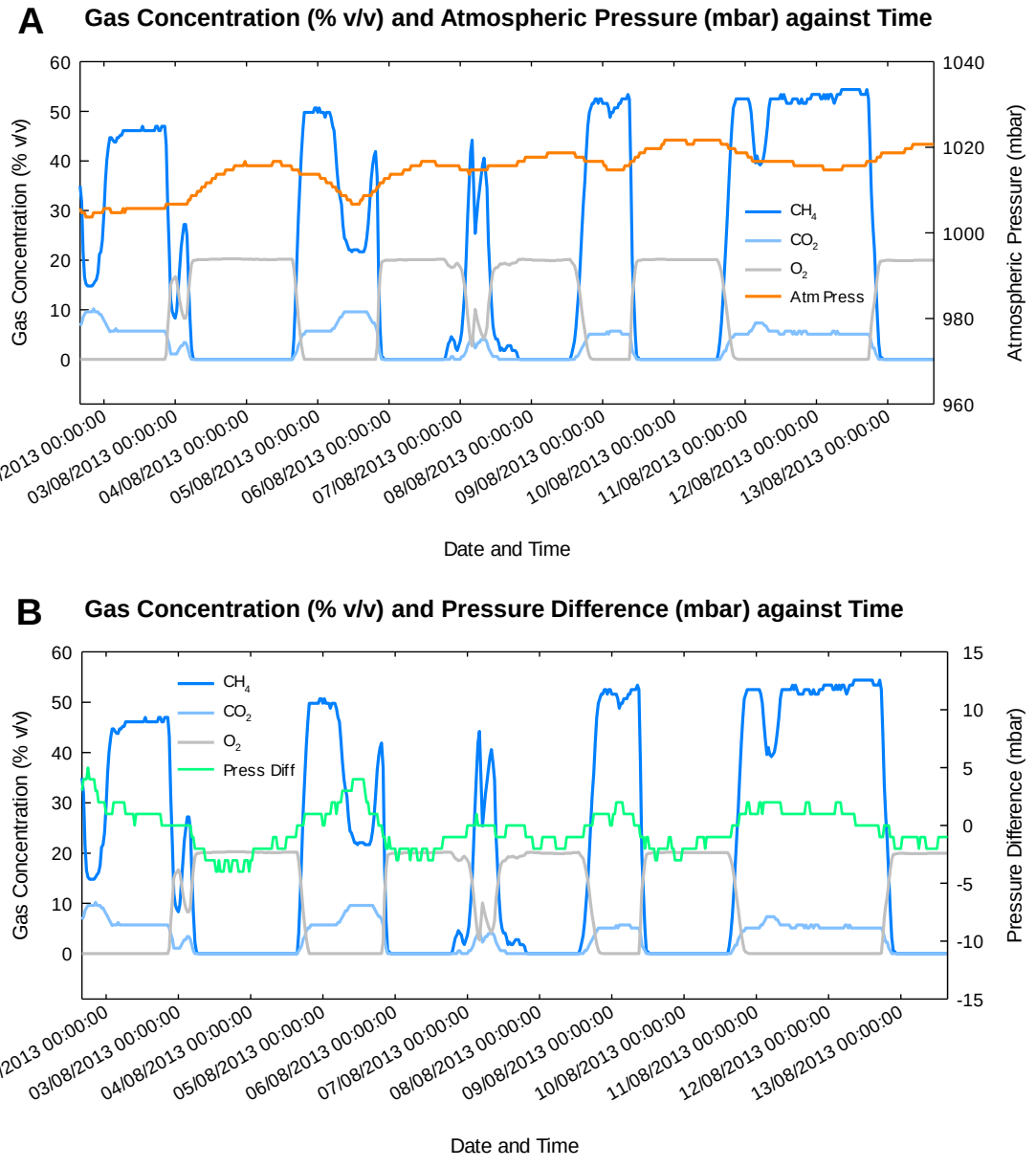

Figure 5.5: Site 1 BH 03/4 High Temporal Frequency Gas Data (01/08/2013 – 13/08/2013)

By comparison, the two week period commencing 1st August 2013 is shown in Figure 5.5. Typical conditions of the summer months, high (> 1010 mbar) and stable atmospheric pressure, prevailed during this period. Yet, there were five clear

emission events of CH_4 and CO_2 gases from BH 03/4. These events occurred, 1st – 3rd August, 4th – 5th August, 7th August, 8th – 9th August, and 10th – 12th August 2013.

Examination of the atmospheric pressure data indicates that small dips in pressure were enough to induce these gas emission events. As with the November 2013 (Figure 5.4) data, as CH_4 and CO_2 appear in the borehole, O_2 concentration dips from atmospheric (20.9%) to 0%. The transition period for CH_4 and CO_2 to displace O_2 usually took place over a matter of hours ($\sim$ 4 hr). Unlike the November 2013 data, peak CH_4 concentration was recorded at the higher value of 54.4% while CO_2 peak concentration was 10.2%. This may be related to the higher temperatures recorded in August 2013 (average 15.6°C) compared with November 2013 (average 6.8°C). As gases expand with increasing temperature, this could aid transport through the unconsolidated sands underlying the site.

A summary of emission events and related pressure gradients and pressure differences is given in Table 5.3.

Event Date	**Peak CH_4** (%)	**Peak CO_2** (%)	**Average Gradient** (mbar/hr)	**Peak Pressure Difference** (mbar)
01–03/08/2013	47.0	10.2	−0.54	5
04–05/08/2013	50.7	9.6	−0.42	4
07/08/2013	40.6	4.5	−0.17	1
08–09/08/2013	53.4	5.7	−0.36	2
10–12/08/2013	54.4	7.4	−0.20	2

Table 5.3: BH 03/4 Gas Emission Events (01/08/2013 – 13/08/2013)

Both the August and November data sets indicate that the steeper the rate of decline in atmospheric pressure, the greater the resultant pressure difference. In August the average gradient was −0.37 mbar while in November the average gradient was −0.72 mbar. This appeared to follow usual UK weather patterns of more settled conditions in the summer months and more turbulent conditions in the autumn months. Interestingly, despite the overall weaker gradients observed in August, the peak concentration of CH_4 and CO_2 were far higher than in November. As previously mentioned, this could be attributed to the warmer average temperatures in August compared with November.

However, there are some 'issues' with the data. On numerous occasions, the CH_4 peak is split to such an extent that it cannot be attributed to 'noise' in the data. The most prominent examples occurred between 01:00 and 19:00 BST on 5th August 2013, and between 02:00 and 05:00 BST on 11th August 2013. On these

occasions when the CH_4 concentration dipped, it was offset by a small increase in CO_2 concentration. On 5th August the CO_2 concentration increased from 5.7% to 9.6% while on 11th August it increased from 5.1% to 7.4%. This could be evidence for the oxidation of CH_4 to CO_2 in the borehole. It could also just as likely be interference in the CH_4 channel from other short-chain alkanes such as ethane C_2H_6 and propane C_3H_8, or it could be a simple purging issue. Throughout the data set generated between 19th July 2013 and 25th November 2013 there are numerous examples of this phenomenon as shown in Appendix E. Further testing would be required to determine if CH_4 oxidation is being observed or whether the peak splitting is due to instrument error.

5.3.2 Comparison with Historic Gas Monitoring Data

To contextualise the high temporal frequency data with the historic gas monitoring data, the gas data presented in Figure 5.4 for BH 03/4 was normalised to N_2 and converted to a ternary plot as prescribed in Chapter 4. The ternary plot for the historic gas monitoring data is shown in Figure 5.6a and the high temporal frequency data is presented in Figure 5.6b.

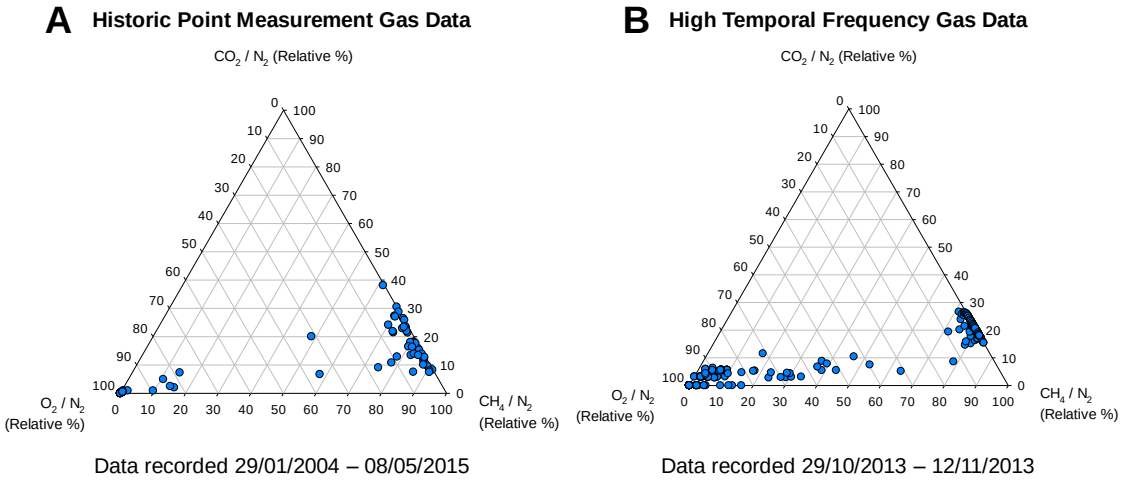

Figure 5.6: Site 1 BH 03/4 High Temporal Frequency Gas Data Comparison with Historic Gas Monitoring Data

The ternary plot derived from the high temporal frequency data captured between 29th October 2013 and 12th November 2013 clearly show gas compositions previously identified from the historic gas monitoring data in Chapter 4. Landfill gas is indicated by a cluster of data points around the 70:30 CH_4/N_2:CO_2/N_2 ratio and air indicated by 100% O_2/N_2. The high temporal frequency data demonstrate more fully the gradient that exists between the two populations of gas compositions.

More importantly, the high temporal frequency data recorded over only a two week period clearly reproduce the same gas compositions as the historic gas monitoring data using a point measurement strategy over an eleven year period. Importantly, the high temporal frequency data recorded over only a two week period clearly reproduce the same gas compositions as the historic gas monitoring data using a point measurement strategy over an eleven year period. This is significant as 100% of the variability in gas composition over eleven years is actually observed on much shorter timescales. The high temporal frequency data set provides evidence that point measurement strategies are likely to miss CH_4 and CO_2 gas emission events for this borehole.

It is possible to demonstrate a direct comparison between the historic gas monitoring data and the high temporal resolution data recorded by GasClam *000237/05/12* as shown in Figure 5.7. Data recorded by point measurement for the decade 2004–2013 and the year 2013 are shown in Figures 5.7a and 5.7b. It is important to note that for Site 1 routine monitoring had been reduced to quarterly measurements in 2008, so only four measurements were made in 2013. As it happened for that year, no emissions of CH_4 and CO_2 were recorded.

However, as can be seen from the high temporal frequency data recorded by GasClam *000237/05/12*, it can be demonstrated that the populations of the different gas compositions recorded over ten year period 2004–2013 can occur on much shorter time scales. To clearly illustrate this point data from a specific day (Figure 5.7e), within a specific week (Figure 5.7d), within a specific month (Figure 5.7c) were selected. Clearly on other days, it is a more likely scenario that only air would be present in the borehole. As previously mentioned, for the period 29th October 2013 – 12th November 2013, 70% of the monitoring period was characterised by air. What the data for 14th November 2013 clearly demonstrate is that within a 24 hour period, it is possible for the gas composition to change from air to landfill gas (70:30 CH_4/N_2:CO_2/N_2) and vice versa. Therefore, it could be regarded that this virtually renders the historic point measurement data acquired over ten years as obsolete.

Further data recorded from BH 03/4 for the period 19th July to 25th November 2013 is provided in Appendix E. Although the data presented here strongly indicate an intrinsic link with fluctuations in atmospheric pressure, it is important to note that the data set is not substantial enough to affirm this point. Further investigation over several years and seasons would be necessary to confirm the trends identified here.

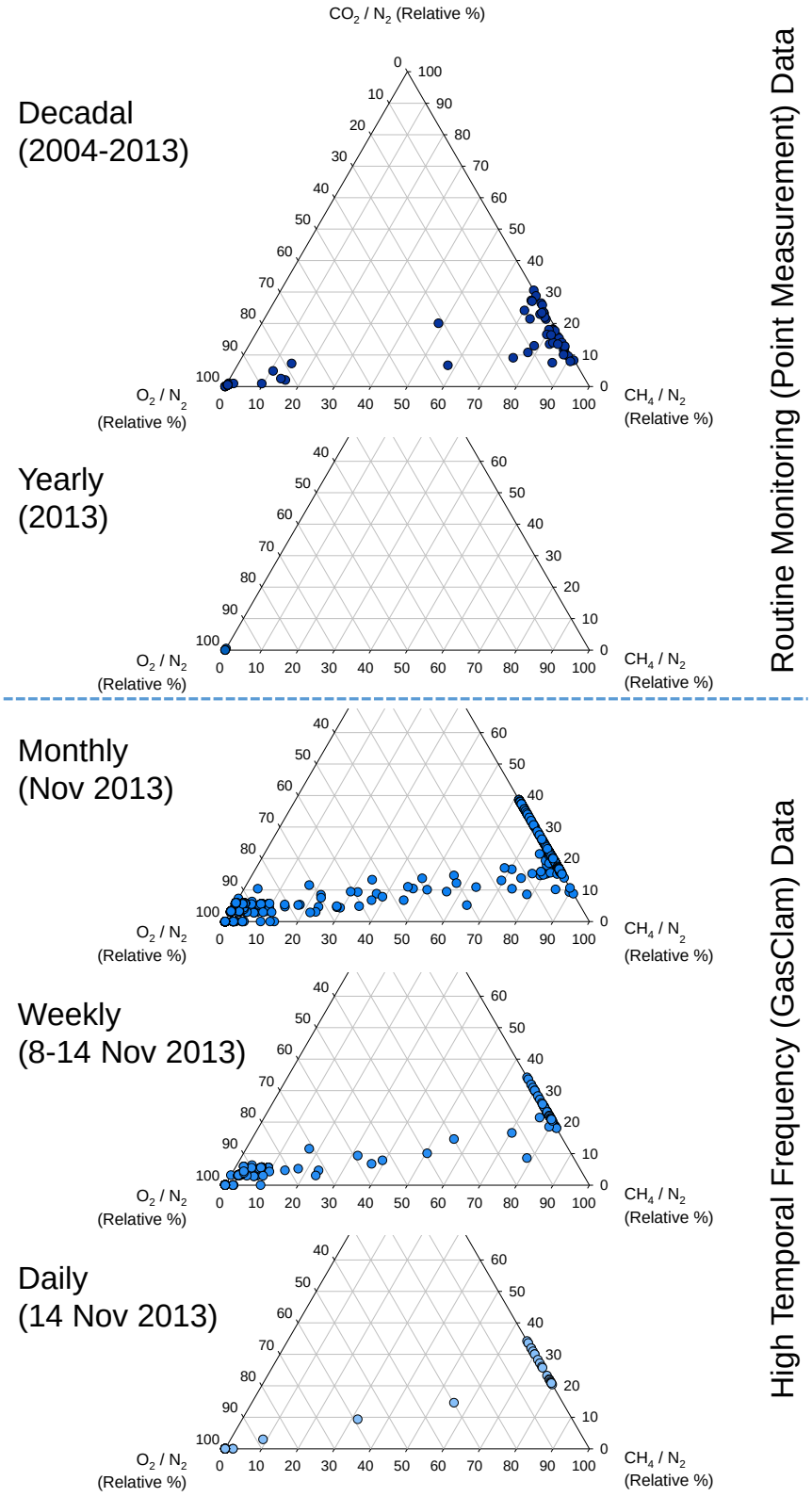

Figure 5.7: Comparison of Historic Point Measurement Data and High Temporal Frequency Data

5.4 Site 2

5.4.1 Temporal Changes and Diurnal Effects

Figure 5.8 illustrates the changing gas composition for BH 04, Site 2 for the period 8th July to 21st July 2014. Historically, this borehole had demonstrated a CH_4-rich gas composition continually from the inception of site activities in August 1998.

Strikingly, the data set produced for BH 04, Site 2, shows a completely different trend from Site 1, BH 03/4. The changing concentrations of CH_4 and CO_2 gases are not reflected in the changing atmospheric pressure. The pressure difference only varies between -1 and 0 mbar and appears to make no contribution to the changes observed in gas composition in BH 04.

When one examines the temperature data (Figure 5.8c), it is clear that the gas present in this particular borehole is changing on a diurnal timescale. CH_4 and CO_2 are inversely proportional to temperature while O_2 is directly proportional to temperature. Temperature tended to peak around 7 pm each day during the two week period. This could be a result of the metal headworks of the borehole having an insulating effect. Similarly, temperature tended to reach its lowest around 7 am each day. At this time of day, CH_4 and CO_2 concentrations peaked.

Unlike Site 1 where O_2 varied between 0% and 20.9%, the range of O_2 concentration recorded for BH 04, Site 2, was between 7.4% and 13.3% (a very narrow range of 5.9%). At no time was pure air present in the borehole and at no time was landfill gas (70% CH_4:30% CO_2). The prevailing gas composition was a mixture of CH_4 and O_2. When O_2 concentration is plotted along with temperature (Figure 5.9), the relationship between the gas composition and temperature is resolved. As the periodicity is over 24 hours, it is assumed that the cycling of gases is diurnal.

Furthermore, as the atmospheric pressure decreases (Figure 5.9), the relationship between O_2 concentration and temperature weakens. As the pressure increases and stabilises, the relationship between O_2 concentration and temperature strengthens once more. While atmospheric pressure may not have a direct impact on the gas composition as it appears to do at Site 1 (where its influence was more analogous to an on/off switch), it certainly appears to weaken the relationship between gas concentration and temperature as it is decreases.

Although the presence of CH_4 and CO_2 is persistent in BH 04, the fluctuations in concentration of these gases continue to vary on a diurnal timescale as shown in Appendix Figures I.3, I.2 and I.4.

There was no precipitation recorded at the local weather station, Manchester Airport (EGCC), during this two-week period. Consequently, there would have been

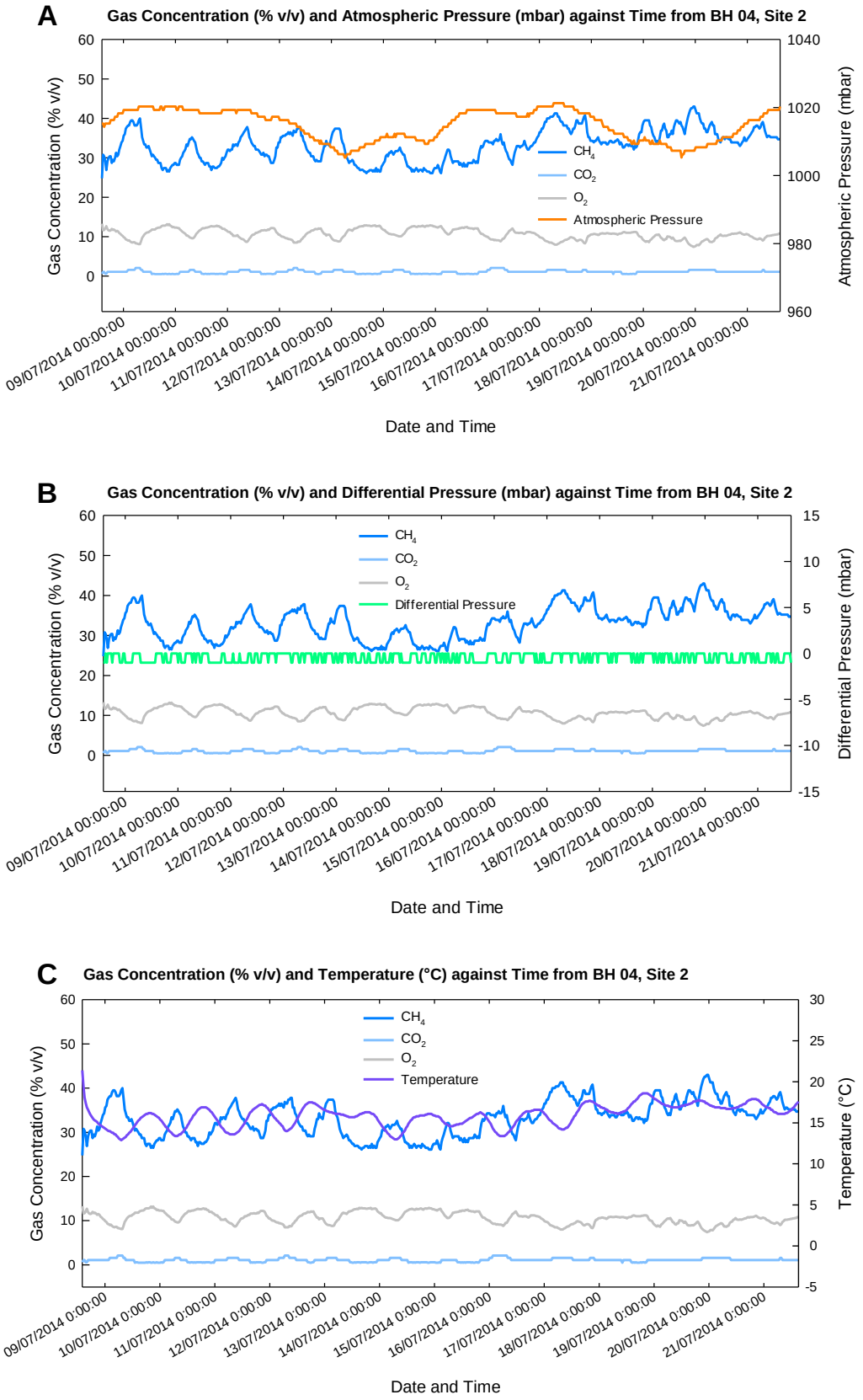

Figure 5.8: Site 2, BH 04 High Temporal Frequency Gas Data (08/07/2014 – 21/07/2014)

little to no variation in water table depth and the influence of hydrometric pumping was ruled out. It is possible that landfill gas was pumped for electricity generation during this monitoring period and this may have disrupted the periodicity.

BH 08 recorded no CH_4 as shown in Appendix Figure I.5. Fluctuations in CO_2 concentration between 0 and 6.3% appeared to be a diurnal variation as for BH 04. According to the historic gas monitoring data, BH 08 produced negligible or 0% CH_4 from September 2003 onwards (four years after this section of the landfill was capped). The high temporal frequency gas data is consistent with this.

The data captured in BHs 12 and 14 indicated persistent CH_4 ($\sim$ 10% and 30–65% respectively). However, at the end of the BH 12 time-series (7^{th} – 9^{th} November 2014), there appears to have been an error with the infrared sensor as CH_4 concentration increased to 15% without any displacement of CO_2 and O_2. The subsequent data capture from BH 14 between 10^{th} November 2014 and 5^{th} January 2015 showed flat-lining of both CH_4 and CO_2 channels (Figures I.8, I.9, I.10 and I.11). It was assumed that the infrared sensor was malfunctioning during the period 7^{th} November 2014 and 5^{th} January 2015 and that the data recorded were invalid.

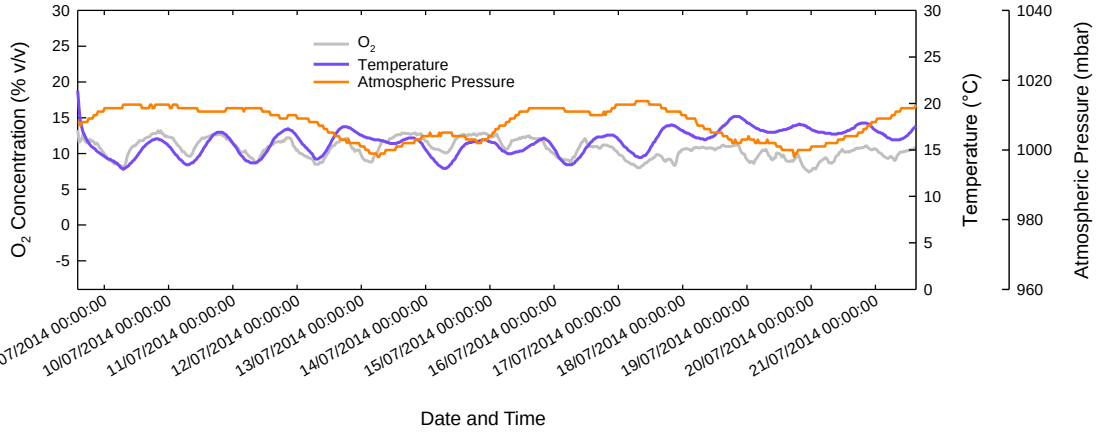

Figure 5.9: Site 2, BH 04 O_2 Concentration against Temperature and Atmospheric Pressure (08/07/2014 – 21/07/2014)

5.4.2 Comparison with Historic Gas Monitoring Data

As for Site 1, BH 03/4, the gas concentration data produced by the GasClam for Site 2, BH 04 was normalised to N_2 in order to produce a ternary plot of the relative proportions of CH_4/N_2, CO_2/N_2 and O_2/N_2. The historic gas monitoring data is shown in Figure 5.10a and the high temporal frequency gas data in Figure 5.10b.

Over the seventeen year gas monitoring period, a wide range of gas compositions was captured. Values approaching 100% CH_4/N_2 were previously identified as hav-

ing a geogenic gas contribution. Data points ranging along the CH_4/N_2 axis were also thought to represent a gas of geogenic origin. Values approaching 70%:30% CH_4/N_2:CO_2/N_2 perhaps represented a landfill gas mixing component.

By comparison, the high temporal frequency gas data recorded over a two-week period did not demonstrate a wide spread of different gas compositions. Data points ranged between 65% and 85% CH_4N_2 with little contribution from CO_2 (no more than 5%). The CH_4-rich gas captured by the GasClam corroborates some of the historic gas monitoring data and could be additional evidence that the gas monitored within BH 04 has a geogenic origin.

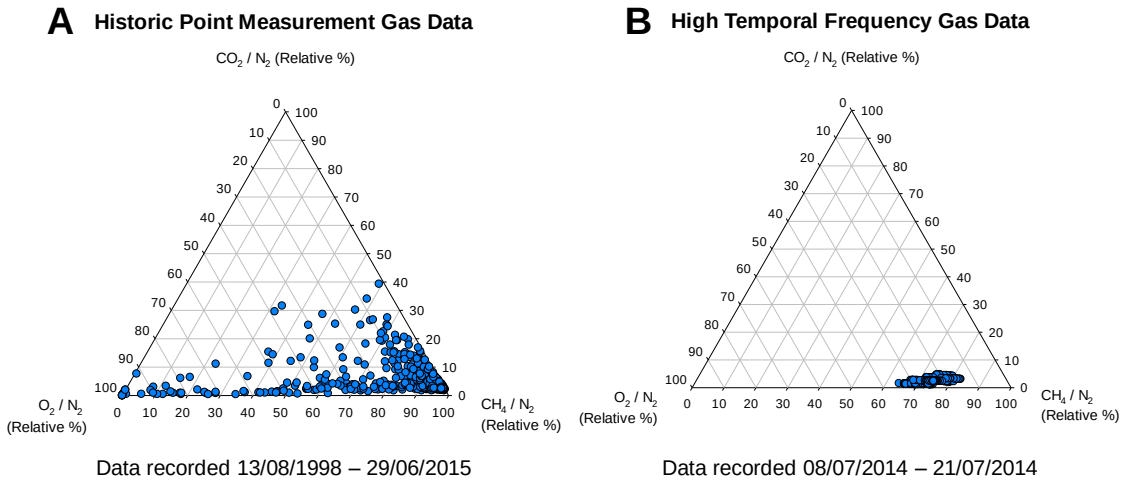

Figure 5.10: Site 2, BH 04 High Temporal Frequency Gas Data Comparison with Historic Gas Monitoring Data

At Site 1, BH 03/4, it was possible to replicate a distribution of gas compositions collected over ten years by point measurement on timescales as short as 24 hours by high temporal frequency measurement, but the same is not true for Site 2, BH 04. The data collected represent only a small cluster of the overall distribution. Further data capture over a much longer period such as a year may be more comprehensive. Alternatively, the data collected by high temporal frequency monitoring may indicate a change in the overall composition of the gas that collects in Site 2, BH 04. Further investigation would be required to resolve this issue.

5.5 Control Site

5.5.1 Data

A limitation arising from the time-series data derived from the control site is that there is no existing historic gas monitoring data. Therefore, it is not necessar-

ily practicable to make a direct comparison with the research sites. Furthermore, within the scope of this research only two weeks' of data are presented here. It would be necessary to monitor for a much more extensive period (such as a year) to absolutely determine the background conditions of the ground. An IonScience demonstration GasClam (*000041/12/09*) equipped with a 0-5% sensor was used to capture background CH_4 and CO_2 data. This choice reflected the need to measure small concentrations with increased accuracy and precision ($\sim$ 0.1% resolution (Klein, 2008)).

Figure 5.11 shows high temporal frequency time-series data obtained from GasClam for the two week period commencing 3rd February 2014. This was an acute period of unsettled weather conditions featuring four intense winter storms (depressions) crossing the UK on 4th/5th February 2014 (peak low pressure 968 mbar, 13:59, 5th February 2014), 7th/8th February 2014 (peak low pressure 965 mbar, 14:59, 8th February 2014), 12th February 2014 (peak low pressure 972 mbar, 14:53, 12th February 2014) and 14th February 2014 (peak low pressure 964 mbar, 22:53, 14th February 2014). Additionally, the average rate of fall in pressure during these four depressions were 1.06 mbar/hr, 1.17 mbar/hr, 2.40 mbar/hr and 2.00 mbar/hr respectively. Consequently, conditions were extremely favourable for measuring background concentrations of CH_4 and CO_2 in the ground gas environment.

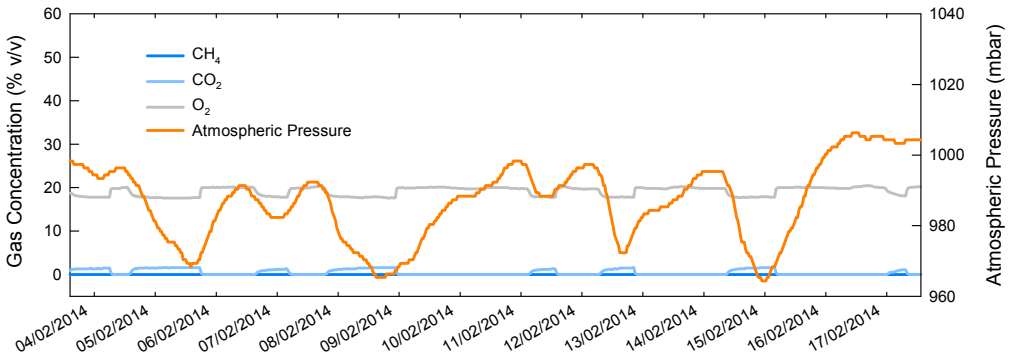

Figure 5.11: High Frequency Time-Series Data from Control Site (03/02/2014 – 17/02/2014)

During each of these depressions, the CO_2 rose from 0% v/v to a maximum of 1.6% v/v. Concurrently, O_2 decreased from atmospheric concentration $\sim$ 20% to an average of 17.8% v/v. As these are simultaneous processes, it is demonstrated that this is a direct response to changes in atmospheric pressure previously described. Displacement of O_2 is assumed to correspond with background CO_2 (1.6% v/v) entering the borehole from the sand formation as a result of rapid decrease in

atmospheric pressure.

Hooker and Bannon (1993) observed that typical contributions to CO_2 concentration from natural sources, such as weathering of bedrock, typically lie within the range 0-5% v/v. Peak CO_2 concentration lies comfortably within this range. Furthermore, no CH_4 was detected. Typically, surface ground gas CH_4 concentration varies between 0.2 and 1.6 ppm (mean concentration in air) (Hooker and Bannon, 1993). With no known external source of CH_4 at the Control Site, the concentration was no expected to exceed 0.1% v/v.

5.5.2 Comparison with Research Sites

Concentrations of CO_2 lying in the range 1.3% to 1.6% as a direct response to rapidly decreasing atmospheric pressure were thought to correspond to background CO_2 entering the borehole from the surrounding sand formation. No CH_4 was recorded. This was expected for background conditions.

The appearance of CO_2 in the control borehole followed the same pattern as Site 1, BH 03/4 when both CH_4 and CO_2 release was triggered by decreases in atmospheric pressure. Peak CH_4 concentration in Site 1 BH 03/4 tended to fall in the range 25–57%. Its complete omission in the control borehole is consistent with the absence of landfill microbial processes that produce CH_4. CH_4 gas is therefore interpreted as being absent from the background. Similarly, peak concentration of CO_2 recorded at Site 1, BH 03/4 was $\sim$ 10%. By comparison, the control borehole peak was only 1.6% CO_2. This concentration with background levels reported in the literature.

The control borehole data follow the same pattern as Site 1, BH 03/4 where atmospheric pressure dips resulted in the exchange of air with CH_4 and CO_2 gases. As only background CO_2 was present (1.6%) in the control borehole, a major difference with Site 1, BH 03/4 data is that O_2 is only slightly displaced. The O_2 concentration decreases from atmospheric (20.9%) to around 17% only. It is important that the change in atmospheric pressure appears to be the overriding variable that induces the change in gas composition for both the Control Site and for Site 1, BH 03/4. Therefore it is likely that atmospheric pressure is the most influential control on emission of gases from the sub-surface.

5.6 Refinement of Conceptual Model

Building on from the initial conceptual model design presented in Figure 4.13, it was demonstrated by the high temporal frequency gas monitoring data for both Site 1 and the Control Site that change in atmospheric pressure has an effect on gas emission. This was incorporated into the design as shown in Figure 5.12. As for Figure 4.13, no assumptions have been made about the mechanics of mass transfer of gases from the unsaturated zone to atmosphere or otherwise.

Unlike the initial design, there are now two clear scenarios to present. The first is during rising pressure where it was shown in the data that air displaced ground gases. The opposite is known to occur when atmospheric pressure is decreasing. During these conditions, ground gas concentration increased in the test boreholes at Site 1 (Figure 5.4) and the Control Site (Figure 5.11). This corresponded to a transfer of CH_4 and CO_2 from the sub-surface to the atmosphere.

The extent of the dilution that air has on ground gases is unquantified at this stage as it is not possible to measure the concentration of gases at depth. Therefore, the arrows showing the transfer of air to the ground only represent the top 1 m as that is the depth that the GasClam works at. Under falling atmospheric pressure conditions, CH_4 and CO_2 ground gases appear in the test boreholes, it is assumed that this is equivalent to expulsion of gases from the ground to the atmosphere. It would not have been possible to prove this mechanism using a point measurement strategy.

Site 2 boreholes' high temporal frequency data showed persistent CH_4 and CO_2 that appeared to vary slightly on a diurnal timescale. This was particularly apparent for Site 2, BH 04. However, further data capture over a longer period would be required to determine the extent of diurnal cycling of gases. A further dimension that could be added at this stage of the conceptual model design would be the diurnal variation shown in Site 2, BH 04 (Figure 5.8). The data showed that atmospheric pressure was the priority variable that effected gas composition. Therefore, the diurnal cycling shown in Figure 5.8 was not incorporated into the model design.

With a reasonable degree of confidence, it can be said that varying atmospheric pressure is a major control on release of CH_4 and CO_2 gases from the unsaturated zone. This intrinsic link has been clearly shown in the high temporal frequency gas data. However, there are some unknown variables which also play a roll in changing gas compositions and emissions from ground to atmosphere that lead to further research questions:

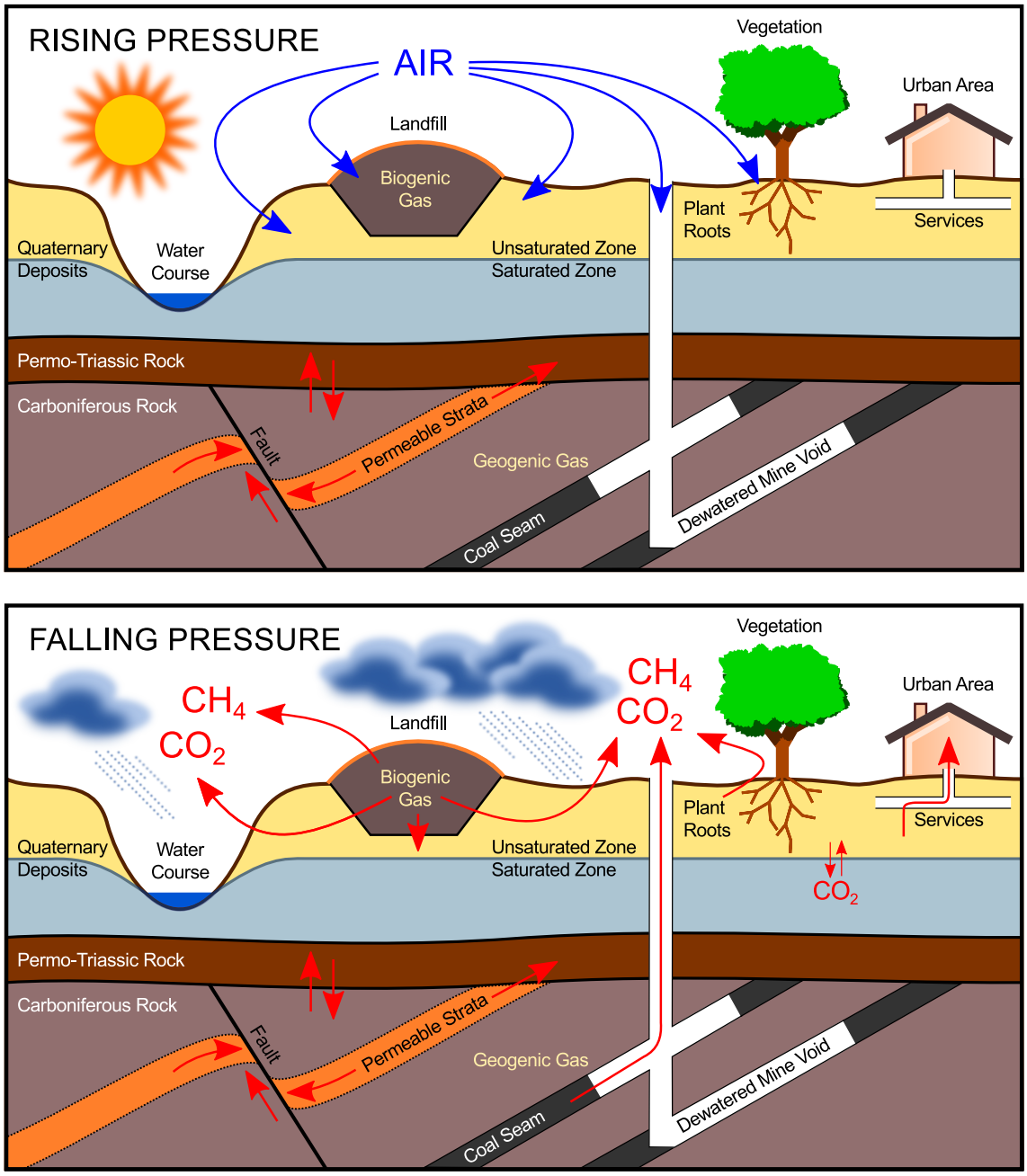

Figure 5.12: Refined Conceptual Model Design using High Temporal Frequency Data

- To what extent is there a change in gas composition occurring on diurnal timescales;
- Relating to diurnal variation, what is the effect of temperature on the composition of gas released from the sub-surface to the atmosphere;
- What is the effect of season on the frequency and composition of gas emissions; and,
- Can the high variance in gas composition observed here be replicated for other geologies.

In this context, the data that showed the high variance in gas composition may

be viewed as initial findings. In order to address the further research questions that have been identified, it is clear that multiple high temporal frequency data sets covering many years would be required. This would also require the use of multiple GasClam (or equivalent) units which is beyond the scope of the research presented here. Also, the sites selected for this research were deliberately chosen for their underlying geology which incorporated a thick, unconsolidated, unsaturated zone. Further studies would need to investigate different geologies.

Chapter 6

Determination of Gas Source

6.1 Introduction

This chapter introduces the concept of identification of ground gases by use of stable isotope analysis (^{13}C CH_4, ^{13}C CO_2 and ^{2}H (D) CH_4). A methodology that includes sampling technique, appropriate atmospheric conditions for sampling, measurement of absolute gas concentrations and measurement of stable isotopes by isotope-ratio mass spectrometry (IRMS) is outlined. Absolute concentrations of gases measured from landfill sites and coal mines by landfill gas analyser (GFM436) and gas chromatography mass spectrometry (GC-MS) are detailed along with the isotope ratios determined by IRMS.

A key concept in the use of stable isotopes to determine gas source is that CH_4 formed biochemically in landfills will be depleted in the heavier ^{13}C and ^{2}H (D) isotopes as microbes discriminate against these isotopes (i.e. lower, or more negative ^{13}C and ^{2}H) compared with thermogenic (e.g. geogenic) CH_4 (Kerfoot et al., 2013). Biogenic gas sources such as landfill tend to have more negative $^{13}\delta C_{CH_4}$ values and are isotopically depleted in the heavier ^{13}C isotope (values generally $< -60‰$ (Hitchman et al., 1989)). Correspondingly, CO_2 evolved from landfill gas is enriched in ^{13}C. Values of $^{13}\delta C_{CO_2}$ are higher than (more positive than) $^{13}\delta C_{CH_4}$. Hitchman et al. (1989) reported $^{13}\delta C_{CO_2}$ values from landfill in the range -12.8 to $+12.0‰$.

By comparison, thermogenic sources (e.g. geogenic) of CH_4 are relatively isotopically enriched in ^{13}C and have more positive $^{13}\delta C_{CH_4}$ values. For closed collieries in Nottinghamshire, UK, Zazzeri et al. (2015) observed $^{13}\delta C_{CH_4}$ values in the range $-33.3 \pm 1.8‰$ to $-30.9 \pm 1.4‰$.

Also used as a reference for gas source is D in CH_4. Like ^{13}C CH_4 from biogenic sources such as landfill, there is a depletion in D in CH_4. For example, Raco et al. (2014) reported δD_{CH_4} from biogenic sources in the range -329 to $-291‰$.

Thermogenic sources such as coal gas are relatively isotopically enriched in D in CH_4 and consequently have higher (or more positive) δD_{CH_4} values than biogenic sources. Kerfoot et al. (2013) observed δD_{CH_4} values in the range −197.4 to −193.7‰. Therefore, using the $^{13}\delta C_{CH_4}$, $^{13}\delta C_{CO_2}$ and δD_{CH_4} values, it is possible to differentiate biogenic gas source from geogenic gas source as both sources indicate distinct signatures.

Figure 6.1 is a schematic of carbon isotope fractionation in anoxic environments such as landfills in Phase 3 and 4 of gas production. In anaerobic environments of landfills the isotopic composition of CH_4 and CO_2 is predominantly controlled by acetoclastic methanogenesis, which results in CH_4 depleted in ^{13}C and CO_2 enriched ^{13}C as methanotrophic archaea preferentially degrade the ^{12}C-fraction of substrates (Clark, 2015).

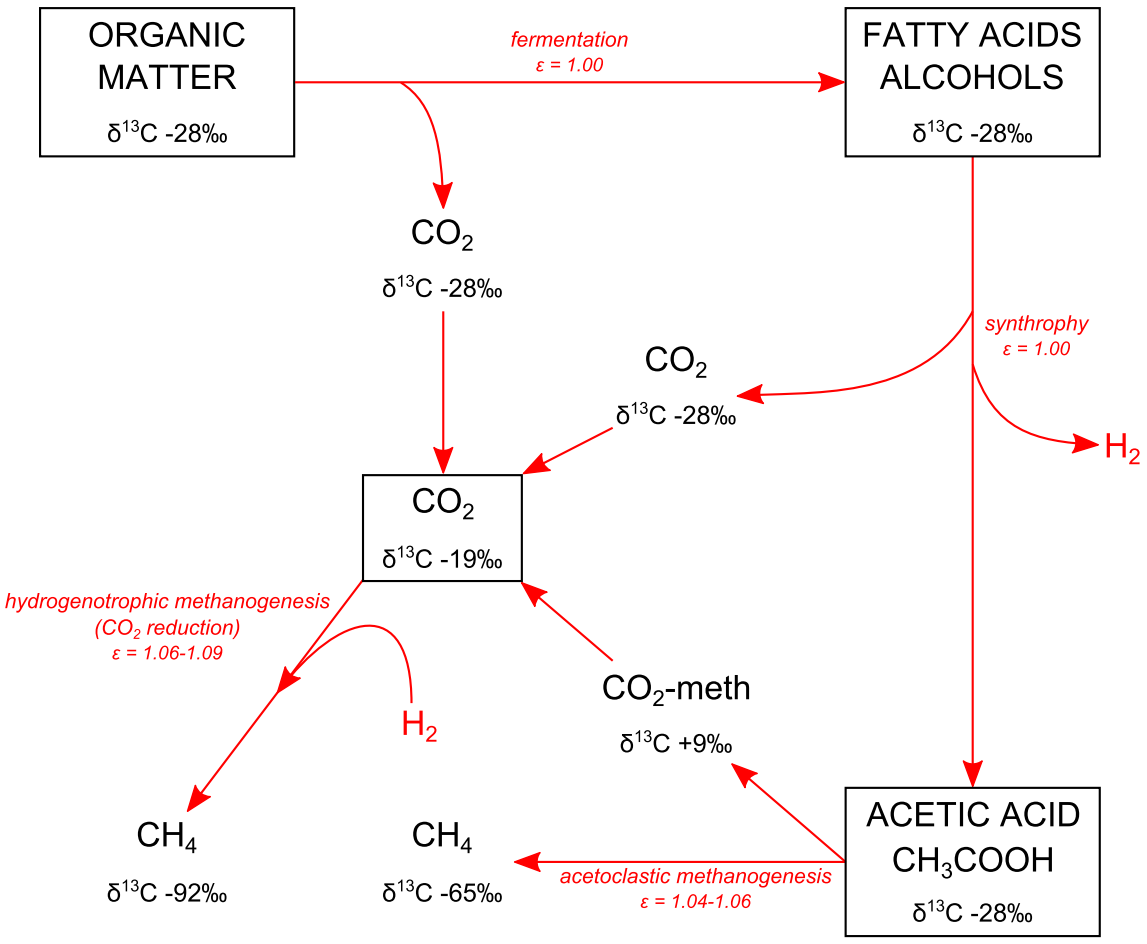

Figure 6.1: Schematic of Carbon Isotope Fractionation in Anoxic Environments (after Holmes et al. (2015)) Showing Processes (red italics), Fractionation Factors (ϵ), and Expected Isotopic Compositions ($\delta^{13}C$)

6.2 Methodology

6.2.1 Atmospheric and Meteorological Conditions

The landfill gas samples were collected from Sites 1 and 2 between 10:00 and 14:00 on 8th February 2016. The sampling was timed to coincide with rapidly falling atmospheric pressure to ensure that boreholes would be under pressure (i.e. positive borehole flow conditions) to allow easy collection of samples. On the day of the sample collection, the UK was impacted upon by 'Storm Imogen' as part of the 2015–16 UK and Ireland Windstorm Season. This was the first such season to have named storms by the Met Office and Storm Imogen was the ninth named storm of the season.

Storm Imogen recorded a maximum wind speed of 154.5 km/hr at Needles Old Battery, Isle of Wight and a peak low pressure of 962 mbar (Met Office, 2016). Local conditions at Sites 1 and 2 were windy and heavy rain. Peak wind gusts in the vicinity were recorded at 107.3 km/hr and low pressure at 973 mbar.

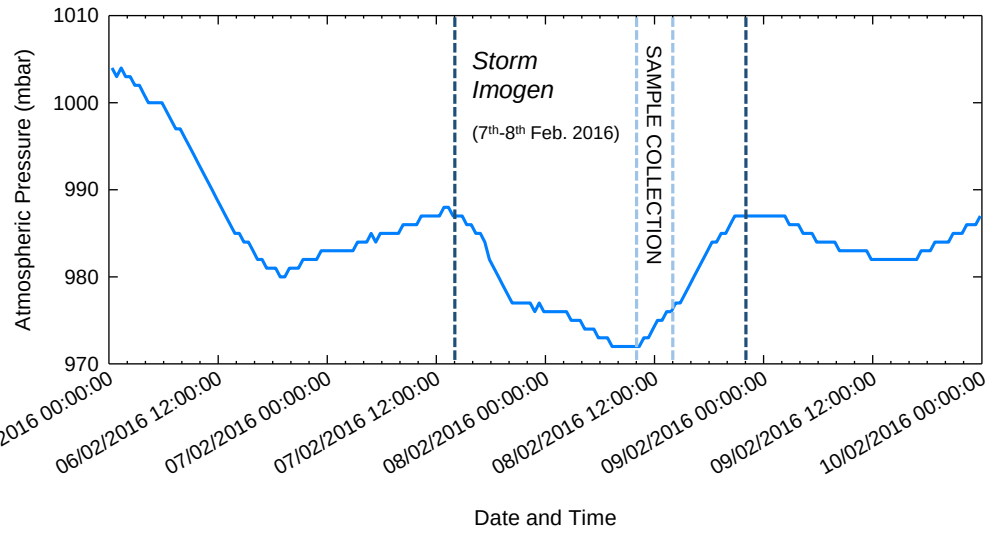

Figure 6.2: Atmospheric Pressure 06/02/2016 – 10/02/2016

Significantly, preceding the beginning of Storm Imogen on 7th February 2016, there was a steep decrease in atmospheric pressure on 6th February 2016. During the period 00:00 – 18:30 on 6th February, the pressure dropped from 1004 mbar to 980 mbar, this equated to an average rate of 1.3 mbar/hr. This deep atmospheric pressure decline coupled with a further drop of 16 mbar over 18 hours (average 0.89 mbar/hr) during Storm Imogen would have induced positive borehole pressure in the research boreholes.

6.2.2 Landfill Gas Sampling

The samples were collected in 1 *l* SKC FlexFoil sample bags with stainless steel fittings (Product Code 263–01). Prior to sample collection on 8th February 2016, the bags were cleaned three times with N_2.

At Sites 1 and 2, boreholes were targeted based upon historic composition of gas (see Chapter 4 and Appendices B and C). At Site 1, boreholes 03/4, 03/6 and 03/7 were selected and at Site 2, boreholes 04, 08 and 12 were selected. Additionally the flared gas and landfill waste were directly sampled at Site 2 as a reference for pure landfill gas.

Parameters were measured using a GFM436 hired from TerraConsult Ltd. These included CH_4 (%), CO_2 (%), O_2 (%), CO (ppm), H_2S (ppm), Atmospheric Pressure (mbar), Differential Pressure (mbar) and Flow (l/hr). Additionally a dip meter was used to measure the groundwater depth at Site 1. The recorded atmospheric pressure was corrected to sea level.

Following the measurement of gases using the GFM436, a sample bag was attached to the borehole valve via a hand pump. Gas was pumped into the sample bag using the hand pump over a period of 30 s (the large flows recorded aided the inflation of the sample bags). Once the sample was acquired, the flexifoil bag valve was securely closed. Using a 10 ml syringe, four 10 ml samples were aliquoted into 12 ml exetainers for analysis.

The atmospheric and ground conditions on 8th February 2016 are recorded in Table 6.1. The flared gas at Site 2 differential pressure was above the certified calibration range of the instrument. Groundwater depths are not routinely recorded at Site 2 as part of the gas monitoring regime and were not measured on the day of the sample collection.

6.2.3 Coal Gas Sampling

To reference the landfill gas samples, further samples from former colliery mineshaft vents were collected on 16th March 2016. The two former mineshaft vents were chosen as they were located in the South Lancashire Coalfield, UK, and were likely to contain CH_4-bearing rocks of a similar age to those that underlie Site 2. Furthermore, they exhibited persistent CH_4 from closure of the colliery in the mid-1990s. The two mineshaft vents were located in Merseyside, UK, at 53.447854 °N, -2.604223 °E and 53.447913 °N, -2.603292 °E. The sampling process was the same as for landfill gas sampling.

Sample ID	Atmospheric Pressure (mbar)	Differential Pressure (mbar)	Peak Flow (l/hr)	Steady Flow (l/hr)	Groundwater Depth (m)	Ambient Temp. (°C)
			Site 1 (08/02/2016)			
BH 03/4	973	13.58	72.6	72.6	Dry	7
BH 03/6	973	-0.31	0.2	-3.2	18.32	7
BH 03/7	976	1.42	14.8	14.7	Dry	7
			Site 2 (08/02/2016)			
BH 04	974	-0.17	0.8	-2.1	NM	7
BH 08	974	1.04	23.6	10.4	NM	7
BH 12	975	-0.05	-0.9	-0.9	NM	7
Flare	975	>>	110.3	110.3	NM	7
Landfill Cell	973	10.39	60.6	59.5	NM	7
			Mineshaft Vents (16/03/2016)			
Mineshaft 1	1027	0.0	0.0	0.0	NM	10
Mineshaft 2	1027	0.0	0.0	0.0	NM	10

Table 6.1: Atmospheric and Ground Conditions Measured by GFM436

6.2.4 GC-MS Analysis

To determine the concentration of gases contained in the 12 ml exetainers, the samples were analysed by GC-MS at Newcastle University. The analysis of biogenic gases was performed on a Fisons 8060 GC using split injection (150°C) linked to a Fisons MD800 MS (electron voltage 70 eV, filament current 4 A, source current 800 μA, source temperature 200°C, multiplier voltage 500 V, interface temperature 150°C). The acquisition was controlled by a Compaq Deskpro computer using Xcalibur software; in full scan mode (1-150 amu/scdwell 10 ms/amu) or in SIM mode 10 ions (dwell 100 ms/ion) for greater sensitivity. The headspace sample (100 μl) was injected in split mode and the GC programme and MS data acquisition commenced. Separation was performed on a HP-PLOT-Q capillary column (30 m $\times$ 0.32 mm i.d.) packed with 20 μm Q phase. The GC was held isothermally at 35°C with He as the carrier gas (flow 1 ml/min, pressure 65 kPa, split at 100 ml/min. The chromatograms of the separated gases (CH_4, CO_2, N_2O, SF_6 etc) were integrated and quantified. The acquired data was stored on DVD for any further data processing, integration and printing.

6.2.5 Stable Isotope Analysis

Newcastle University

Compound specific GC-IR-MS analysis of the gas samples was performed on a Thermo Trace Ultra GC using a splitless injector (150 °C) via a Combustion III Interface linked to a Thermo Delta V+ IR-MS (HT voltage 3-5 kV, Trap current 0.75 mA, Box current 0.7 mA). The acquisition was controlled by a Dell computer using Thermo Isodat software.

The Thermo Delta V+ GC-IR-MS instrument was initially set in Carbon mode monitoring the CO_2 $^{44/45}$ δC $^{12/13}$ ratio. The sample (1-100 μl) was injected manually with the split open at 500:1. The GC column was kept at 35 °C for the entire run with He as the carrier gas (flow 1 ml/min, at a pressure of 80 kPa, split at 500 ml/min). Chromatographic separation of the mixture of gases was performed on a fused silica capillary column (30 m × 0.32 mm i.d.) filled with 20 μm PLOT-Q powder phase. The Reference Gas was pulsed into the mass spectrometer and after 5 minutes the back flush valve directed the split sample from the end of the GC column via the Combustion Furnace (940 °C) and Reduction Furnace (650 °C) to CO_2 and into the mass spectrometer through a micro capillary isolation valve into the source where the gas is ionized and the resulting ions separated in a magnetic field to 3 cup detectors for masses 44, 45, 46 and so give an isotopic ratio value determined from a pulsed reference gas (CO_2) calibrated from a reference 15 Alkane (A4) or 8 Fame (F8) mixture with peak specific known isotopic values for Carbon. (Arndt Schimmelmann, Indiana University, USA)(Certificate of Analysis).

The Thermo Delta V+ GC-IR-MS instrument was then set in hydrogen mode monitoring the H_2 $^{2/3}$ δD $^{2/3}$ ratio. As before the hydrogen reference gas was pulsed into the mass spectrometer and after 5 minutes the back flush valve directed the split sample from the end of the GC column via the combustion furnace (1400 °C) only, to H_2 and into the mass spectrometer through a micro capillary isolation valve into the source where the gas is ionised and the resulting ions separated in a magnetic field to 2 cup detectors for masses 2, 3 and so gives an isotopic ratio value determined from a pulsed reference gas (H_2) calibrated from a reference 15 Alkane (A5) or 8 Fame (F83) mixture with peak specific known isotopic values for H_2. (Arndt Schimmelmann, Indiana University, USA)(Certificate of Analysis).

The resulting isotope ratios were measured by the Thermo Isodat dynamic background integration Workspace software to give the peak retention times and isotope ratios as δ3 H values. The data was also stored on DVD for any further data processing or integration or printing.

University of California Davis Stable Isotope Facility

Samples were analysed by Isotope-Ratio Mass Spectrometry (IRMS) according to the method prescribed by Yarnes (2013) and UC Davis Stable Isotope Facility (2016).

Stable isotope ratios of $^{13}\delta$C and δD in CH_4 were measured using a Thermo-Scientific PreCon concentration system interfaced to a ThermoScientific Delta V Plus IRMS (ThermoScientific, Bremen, DE). Gas samples were purged from vials through a double-needle sampler into a He carrier stream (20 ml/min), which was passed through a H_2O/CO_2 scrubber ($Mg(ClO_4)_2$, Ascarite) and a cold trap cooled by liquid N_2.

The CH_4 was separated from residual gases by a Rt-Q-BOND GC column (30 m $\times$ 0.32 mm $\times$ 10μm, 30°C, 1.5 ml/min). After the CH_4 was eluted from the separation column, CH_4 was either oxidised to CO_2 by reaction with nickel (II) oxide (NiO) at 1000°C ($^{13}\delta$C), or pyrolysed in an empty alumina tube heated to 1350°C (δD). Subsequently the sample was transferred to the Isotope Ratio Mass Spectrometer (IRMS).

A pure reference gas (CO_2 or H_2) was used to calculate provisional δ-values for the sample peak. Final δ-values were obtained after adjusting the provisional values for changes in linearity and instrumental drift so that correct δ-values for laboratory standards were obtained. Laboratory standards were commercially prepared CH_4 gas diluted in He or air and were calibrated against National Institute of Standards and Technology (NIST) reference materials (SRM) 8559 (Natural gas/coal origin), 8560 (Natural gas/petroleum origin), and 8561 (Natural gas/biogenic).

Stable isotope ratios of $^{13}\delta$C in CO_2 were measured using a ThermoScientific PreCon-GasBench system interfaced to a ThermoScientific Delta V Plus IRMS (ThermoScientific, Bremen, DE). CO_2 was sampled by a six-port rotary valve (Valco, Houston TX) with a 100 μl loop programmed to switch at the maximum CO_2 concentration in the He carrier gas. The CO_2 was subsequently separated from N_2O and other residual gases by a Poroplot Q GC column (25 m $\times$ 0.32 mm i.d., 45°C, 2.5 ml/min).

A pure reference gas (CO_2) was used to calculate provisional δ-values of the sample peak. Final $^{13}\delta$C values were obtained after adjusting the provisional values so that correct $^{13}\delta$C values for laboratory standards were obtained. Two laboratory standards were analysed with every 10 samples. NIST SRM 8545 (LSVEC/C, O, and Li isotopes in Li_2CO_3) was used to directly calibrate laboratory standards.

Limits of Quantification

The IRMS limits of quantification are summarised in Table 6.2.

Analysis	Limit of Quantification (nmol)	Long-term Standard Deviation (‰)
^{13}C CH_4	0.8	0.2
D CH_4	2.0	2.0
^{13}C CO_2	150	0.1

Table 6.2: IRMS Limits of Quantification (from UC Davis Stable Isotope Facility (2016))

6.3 Absolute Concentration of Samples

The gas concentrations measured by the GFM436 landfill gas analyser and by gas chromatography-mass spectrometry (GC-MS) are compared in this section.

6.3.1 GFM436 Data

The measured concentrations of CH_4 (%), CO_2 (%), O_2 (%), CO (ppm) and H_2S (ppm) on 8th February 2016 are recorded in Table 6.3.

As with the historic ground gas monitoring data reviewed in Chapter 4, the gas concentrations were normalised to N_2 (assuming N_2 to be the balance) as shown in Figure 6.3. Where the concentration of these gases was below the detection limit of the GFM436 ($< 0.1\%$), the concentration was assumed to be 0.0%. These ratios were then normalised to 100% thereby enabling the sample concentrations to be presented in a ternary plot (Figure 6.3).

The samples show an interesting range of CH_4 and CO_2 compositions. As would be expected, 'Site 2: Flare' and 'Site 2: Landfill Cell' samples show a ratio of 60:40 CH_4:CO_2 in accordance with the landfill gas ratio. Likewise, the proportion of CH_4 to CO_2 in 'Site 1: BH 03/4' is 60:40 which is also indicative of landfill gas. This differs slightly from the historic data and high temporal frequency data where the 60:40 ratio was observed on few occasions. The most likely explanation for this would be that scrubbing of CO_2 from the system did not occur when the monitoring well was sampled. 'Site 1 BH: 03/7' also shows a landfill gas signature but in a slightly richer CH_4 proportion to CO_2 (70:30). Of all the boreholes sampled, 'Site 2: BH 04' contained the greatest proportion of CH_4 at 80% compared with 20% CO_2. Importantly, the relative quantities of CH_4, CO_2 and O_2 measured in these samples

are consistent with those measured historically (Chapter 4) and the high temporal frequency data (Chapter 5).

Sample ID	**CH_4** (%)	**CO_2** (%)	**O_2** (%)	**CO** (ppm)	**H_2S** (ppm)
		Site 1 (08/02/2016)			
BH 03/4	15.8	9.0	< 0.1	< 1	< 1
BH 03/6	< 0.1	0.5	1.8	< 1	< 1
BH 03/7	19.2	7.1	< 0.1	< 1	< 1
		Site 2 (08/02/2016)			
BH 04	22.1	5.6	1.0	< 1	< 1
BH 08	< 0.1	5.2	10.5	< 1	< 1
BH 12	2.0	5.6	1.0	< 1	< 1
Flare	41.7	25.5	< 0.1	< 1	25
Landfill Cell	39.3	24.2	0.1	< 1	< 1
		Mineshaft Vents (16/03/2016)			
Mineshaft 1	98.8	0.8	0.3	< 1	< 1
Mineshaft 2	35.0	0.6	11.4	< 1	< 1

Table 6.3: Gas Concentrations Measured by GFM436

Borehole 12, Site 2 demonstrated a mixing of CH_4, CO_2 and O_2 in the relative proportions CH_4/N_2 23.3%, CO_2/N_2 65.1% and O_2/N_2 11.6%. The differential pressure and flow rate were both slightly negative (-0.05 mbar and -0.9 l/hr respectively) despite the large drop in atmospheric pressure that had induced very large flows elsewhere on Site 2 (23.6 l/hr peak flow BH 08 and 60.6 l/hr peak flow LFC). Similarly, BH 04 recorded a weak negative differential pressure (-0.17 mbar) and a weak peak flow of 0.8 l/hr. However, steady flow was weakly negative (-2.1 l/hr). Despite this CH_4 and CO_2 were present in the ratio CH_4/N_2:CO_2/N_2 80:20.

Likewise, at Site 1, BH 03/6 was the only borehole to record a negative differential pressure (-0.31 mbar) and flow rate (-3.2 l/hr steady). Considering BH 03/4 and BH 03/7 recorded differential pressures of 13.58 and 1.42 mbar respectively and steady flow rates of 72.6 l/hr and 14.7 l/hr respectively, BH 03/6 seems to be anomalous in the context of the Site and proximity to the landfill waste. It could be that this borehole does not have an air-tight seal thereby diluting the CH_4 and CO_2 concentrations. Additionally, the concentrations of CH_4, CO_2 and O_2 are such that the balance (i.e. N_2) is 97.7% which is an unlikely stable scenario. This could be attributed to instrument error. However, as will be seen with the GC-MS data, the concentration of CO_2 is in reasonable agreement with the GFM436.

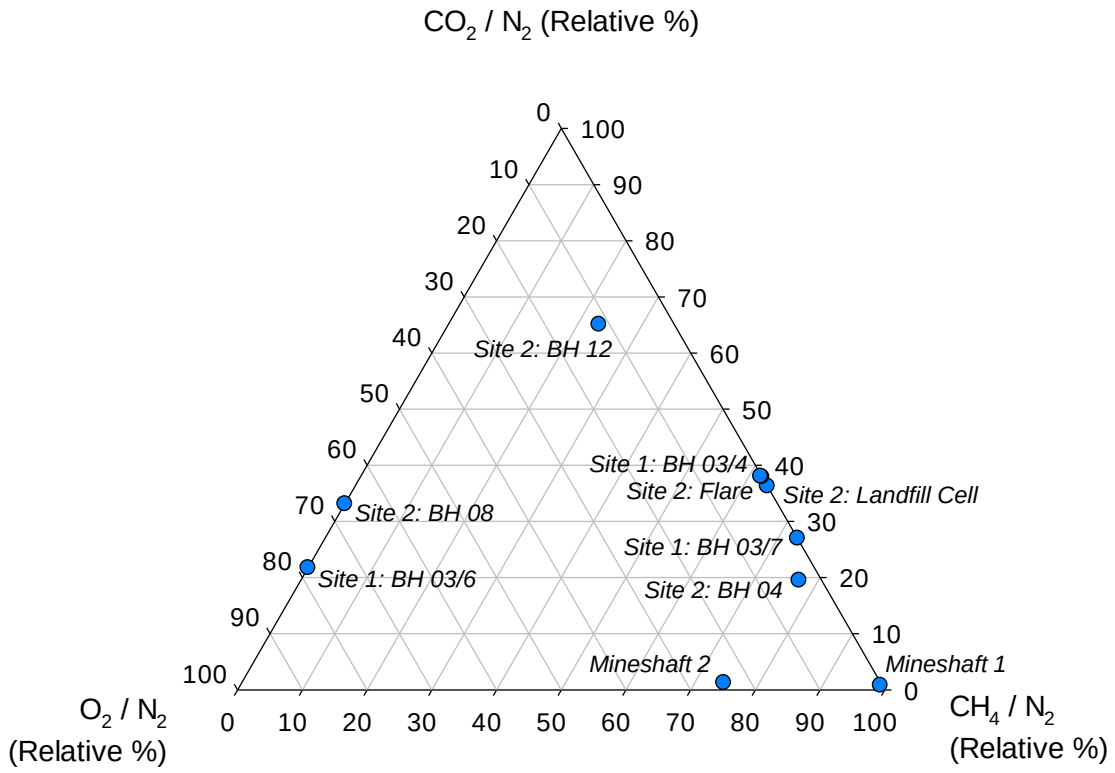

Figure 6.3: Measured Gas Compositions for Landfill and Mineshaft Vent Samples

By comparison, the mineshaft vents showed very different relative proportions of CH_4 and CO_2. Mineshaft 1 approached 100% CH_4/N_2 while Mineshaft 2 gas was in the ratio 75:25 CH_4/N_2:O_2/N_2. These gas compositions were consistent with CH_4-rich gas derived from underlying Carboniferous Coal Measures. It is interesting to note that on numerous occasions Site 2, BH 04 also approached 100% CH_4/N_2 during the historic monitoring period (1998–2015).

6.3.2 GC-MS Data

In most cases, the GC-MS data were in reasonable agreement with the GFM436 data measured on 8th February 2016. Measured concentrations of CH_4 by GC-MS were within ±11.4% and CO_2 were within ±7.8%. Notable exceptions included Site 1 BH 03/4 where the concentration of CH_4 and CO_2 was two orders of magnitude lower than that measured by the GFM436. It was assumed that a sampling error had occurred. Likewise, the concentration of CH_4 and CO_2 measured in the landfill cell by GC-MS was one order of magnitude lower than what was measured by the GFM436. A sampling error was also attributed to this lower concentration.

For the purposes of IR-MS analysis, all samples were above the limits of quantification (Table 6.2). Although an order of magnitude less than measured by the

GFM436, the concentration of CH_4 and CO_2 measured in the landfill cell by GC-MS approximately equated to the expected 60:40 CH_4:CO_2 landfill gas ratio. When calculating concentrations by peak area from the GC-MS chromatogram, there is a scaling error beyond the calibration curve limits. This would account for some of the deviations observed between concentration measured by GC-MS and GFM436.

The GC-MS data for landfill gas samples are compared against the GFM436 data in Table 6.4.

	GFM436 Data		*GC-MS Data*	
Sample ID	**CH_4** (%)	**CO_2** (%)	**CH_4** (%)	**CO_2** (%)
		Site 1		
BH 03/4	15.8	9.0	0.4	0.2
BH 03/6	< 0.1	0.5	0.0	0.2
BH 03/7	19.2	7.1	17.9	6.1
		Site 2		
BH 04	22.1	5.6	20.4	4.0
BH 08	< 0.1	5.2	NM	NM
BH 12	2.0	5.6	2.1	5.0
Flare	41.7	25.5	53.1	17.7
Landfill Cell	39.3	24.2	5.9	3.4
		Mineshaft Vents		
Mineshaft 1	98.8	0.8	NM	NM
Mineshaft 2	35.0	0.6	NM	NM

Table 6.4: Gas Concentrations Measured by GC-MS

6.4 Stable Isotope Data

6.4.1 Comparison of Data Sets

A summary of the data produced at Newcastle University and the data acquisition from the University of California Davis Stable Isotope Facility (UC Davis SIF) is provided in Table 6.5. This table provides a clear comparison between the two data sets used for the analysis of gas source. The difference between data sets is shown in Table 6.6.

On inspection of the two data sets, it is clear the $^{13}\delta C_{CH_4}$ and $^{13}\delta C_{CO_2}$ values are largely in good agreement. The average difference between data sets is 1.80‰ with a standard deviation of 1.23‰ for $^{13}\delta C_{CH_4}$ values. Similarly, the $^{13}\delta C_{CO_2}$ values show a low dispersion with an average difference of 1.06‰ between the two data sets. A slightly larger standard deviation of 3.33‰ was derived for $^{13}\delta C_{CO_2}$ values owing to

the large difference of 35.59‰ between Newcastle University and UC Davis SIF data for Site 1, BH 03/6. The data for Site 1, BH 03/6 represents the only significant deviation in ^{13}C values.

Owing to the fact that δD_{CH_4} values are an order of magnitude greater than $^{13}\delta C_{CH_4}$ and $^{13}\delta C_{CO_2}$ values, it is understandable that there is greater deviation between the two data sets. The average difference between values calculated at Newcastle University and UC Davis SIF was 9.81‰ with a standard deviation of 14.13‰. Similarly to ^{13}C values, the greatest difference between data sets was recorded at 35.67‰ for Site 2, BH 08 for δD_{CH_4}. This value is approximately the same maximum deviation as was recorded for $^{13}\delta C_{CO_2}$ values.

	Newcastle University			*UC Davis SIF*		
Sample ID	$^{13}\delta C_{CH_4}$ (‰)	δD_{CH_4} (‰)	$^{13}\delta C_{CO_2}$ (‰)	$^{13}\delta C_{CH_4}$ (‰)	δD_{CH_4} (‰)	$^{13}\delta C_{CO_2}$ (‰)
			Site 1			
BH 03/4	−58.2	−298	−55.6	−54.07	−307.1	−57.67
BH 03/6	N/A	N/A	−13.3	N/A	N/A	−48.92
BH 03/7	−61.0	−253	−51.0	−60.60	−238.1	−50.48
			Site 2			
BH 04	−55.6	−172	−47.0	−53.77	−158.2	−46.74
BH 08	−55.0	−173	−37.0	−53.80	−137.3	−28.10
BH 12	−48.0	+55	−32.8	−47.06	+74.0	−32.79
Flare	−65.0	−319	+5.0	−63.58	−309.8	+6.96
Landfill Cell	−64.5	−316	+5.5	−62.12	−326.3	+6.50
			Mineshaft Vents			
Mineshaft 1	−46.2	−214	−10.9	−43.05	−202.6	−9.21
Mineshaft 2	−50.5	−208	−46.1	−49.85	−204.2	−48.81

Table 6.5: Stable Isotope Ratios Measured at Newcastle University and UC Davis Stable Isotope Facility

As the variation between data sets for $^{13}\delta C_{CH_4}$ and $^{13}\delta C_{CO_2}$ values was so little, there is a good degree of confidence that the values reported are close to the true value for the samples. The only exception was the $^{13}\delta C_{CO_2}$ value for Site 1, BH 03/6 where the discrepancy was 35.59‰. Therefore it cannot be determined what the true value is with any certainty. The δD_{CH_4} values demonstrated a greater average difference between the two data sets. The standard deviation was only 14.13‰ and the maximum difference was 35.67‰ (Site 2, BH 08), a similar discrepancy to the maximum $^{13}\delta C_{CO_2}$ difference value that was recorded for Site 1, BH 03/6. Owing to the greater dispersal of the data, there is perhaps less confidence in the δD_{CH_4} values. However, it was thought that the discrepancies between the data sets was

not large enough to be a major concern.

Sample ID	$^{13}\delta C_{CH_4}$ (‰)	δD_{CH_4} (‰)	$^{13}\delta C_{CO_2}$ (‰)
Site 1 BH 03/4	−4.12	+9.12	+2.05
Site 1 BH 03/6	N/A	N/A	+35.59
Site 1 BH 03/7	−0.40	−14.89	−0.52
Site 2 BH 04	−1.80	−13.78	−0.26
Site 2 BH 08	−1.20	−35.67	−8.90
Site 2 BH 12	−0.94	−18.98	−0.03
Site 2 Flare	−1.42	−9.21	−1.96
Site 2 Landfill Cell	−2.43	+10.30	−0.95
Mineshaft 1	−3.16	−11.38	−1.72
Mineshaft 2	−0.70	−3.77	+2.71
Average	−1.80	−9.81	−1.06
Standard Deviation	1.23	14.13	3.33

Table 6.6: Difference between Stable Isotope Ratios Measured at Newcastle University and UC Davis Stable Isotope Facility

6.4.2 Determination of Gas Source

$^{13}\delta C_{CH_4}$ versus $^{13}\delta C_{CO_2}$

The $^{13}\delta C_{CH_4}$ versus $^{13}\delta C_{CO_2}$ data (Figure 6.4) show substantial variation in the landfill gas samples and mineshaft vent samples. It is useful to use Landfill Site 2 Flare and Landfill Cell samples as a reference point. According to Kerfoot et al. (2013), microbes discriminate against ^{13}C and ^{2}H. Consequently, residual CH_4 is isotopically depleted in the heavier stable carbon isotope (^{13}C) producing a more negative δC value, while residual CO_2 is relatively enriched in ^{13}C leading to a more positive δC value. The data for Site 2 Flare and Landfill Cell demonstrate this isotope signature ($^{13}\delta C_{CH_4}$ −65.0‰, $^{13}\delta C_{CO_2}$ +5.0‰ and $^{13}\delta C_{CH_4}$ −64.5‰, $^{13}\delta C_{CO_2}$ +5.5‰ recorded respectively for Site 2 Flare and Site 2 Landfill Cell at Newcastle University).

With reference to these values, the perimeter boreholes at Site 1 and Site 2, along with the mineshaft vents and North Sea Gas samples are all relatively depleted in $^{13}CO_2$. Values recorded for $^{13}\delta C_{CO_2}$ at Site 1 landfill were −55.6‰ and −51.0‰ for BH 03/4 and BH 03/7 respectively, while Site 2 landfill perimeter boreholes were slightly more enriched in $^{13}CO_2$ with more positive $^{13}\delta C_{CO_2}$ values −47.0‰, −37.0‰ and −32.8‰ measured for BH 04, BH 08 and BH 12 respectively. These data indicate that the perimeter boreholes at both sites are isotopically depleted in $^{12}CO_2$ with respect to Site 2 Landfill Flare and Landfill Cell gases. This observed

discrepancy could be due to several factors including the age of the waste and the composition of the waste material.

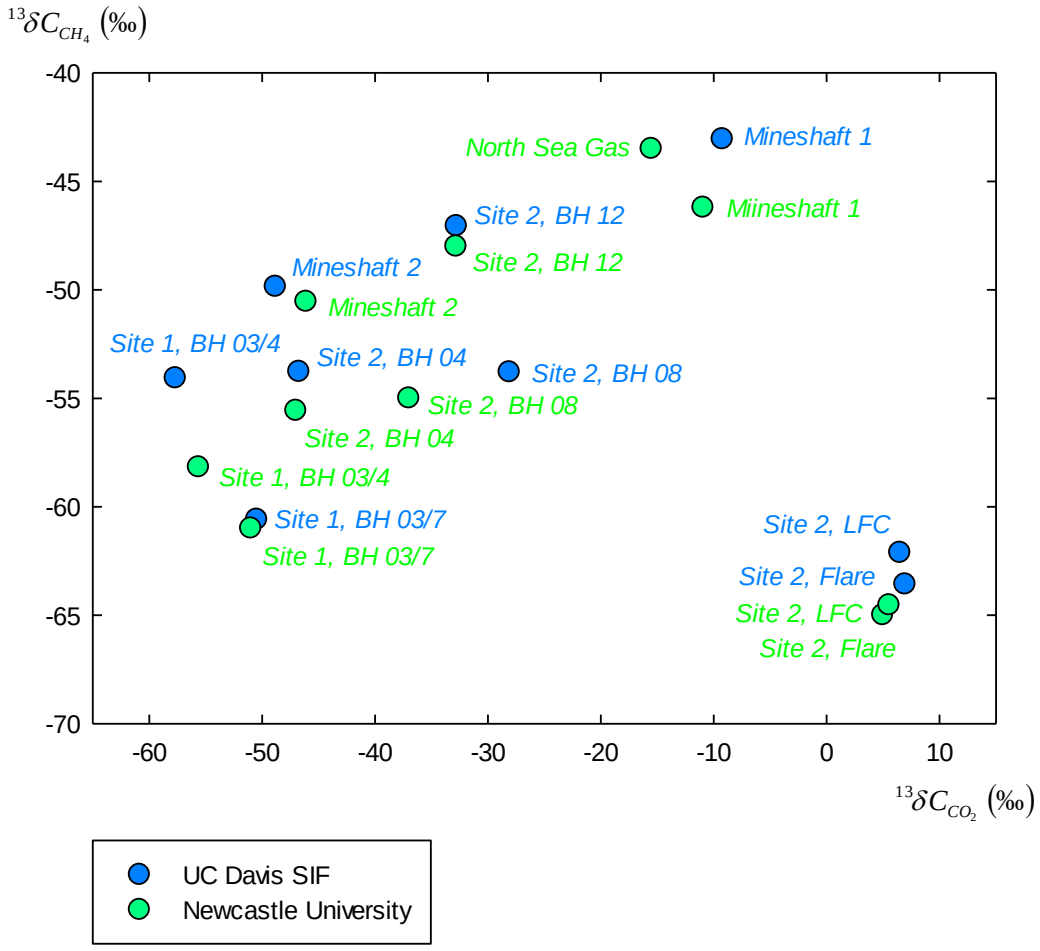

Figure 6.4: $^{13}\delta C_{CH_4}$ (‰) versus $^{13}\delta C_{CO_2}$ (‰) (Measured at UC Davis SIF and Newcastle University)

By comparison, Mineshaft Vent 1 and North Sea Gas samples show a slight enrichment in ^{13}C by comparison with the landfill perimeter borehole gas samples. The values recorded for $^{13}\delta C_{CH_4}$ and $^{13}\delta C_{CO_2}$ were -46.2‰ and -10.9‰ respectively for Mineshaft 1 and -43.5‰ and -15.5‰ respectively for North Sea Gas. This was consistent with older, geogenic gas sources being enriched in $^{13}CH_4$ and $^{12}CO_2$. However, Mineshaft Vent 2 showed an isotope signature that was similar to the landfill perimeter boreholes, particularly at Site 2. The values recorded for Mineshaft Vent 2 $^{13}\delta C_{CH_4}$ and $^{13}\delta C_{CO_2}$ were -50.5‰ and -46.1‰ respectively. This demonstrated an overlap with Site 2 landfill perimeter boreholes. This could be attributed to air leaking into this mineshaft vent (11.4% O_2).

$^{13}\delta C_{CH_4}$ versus δD_{CH_4}

Perhaps more useful for the determination of gas source is the $^{13}\delta C_{CH_4}$ ratio versus δD_{CH_4} ratio as shown in Figure 6.5.

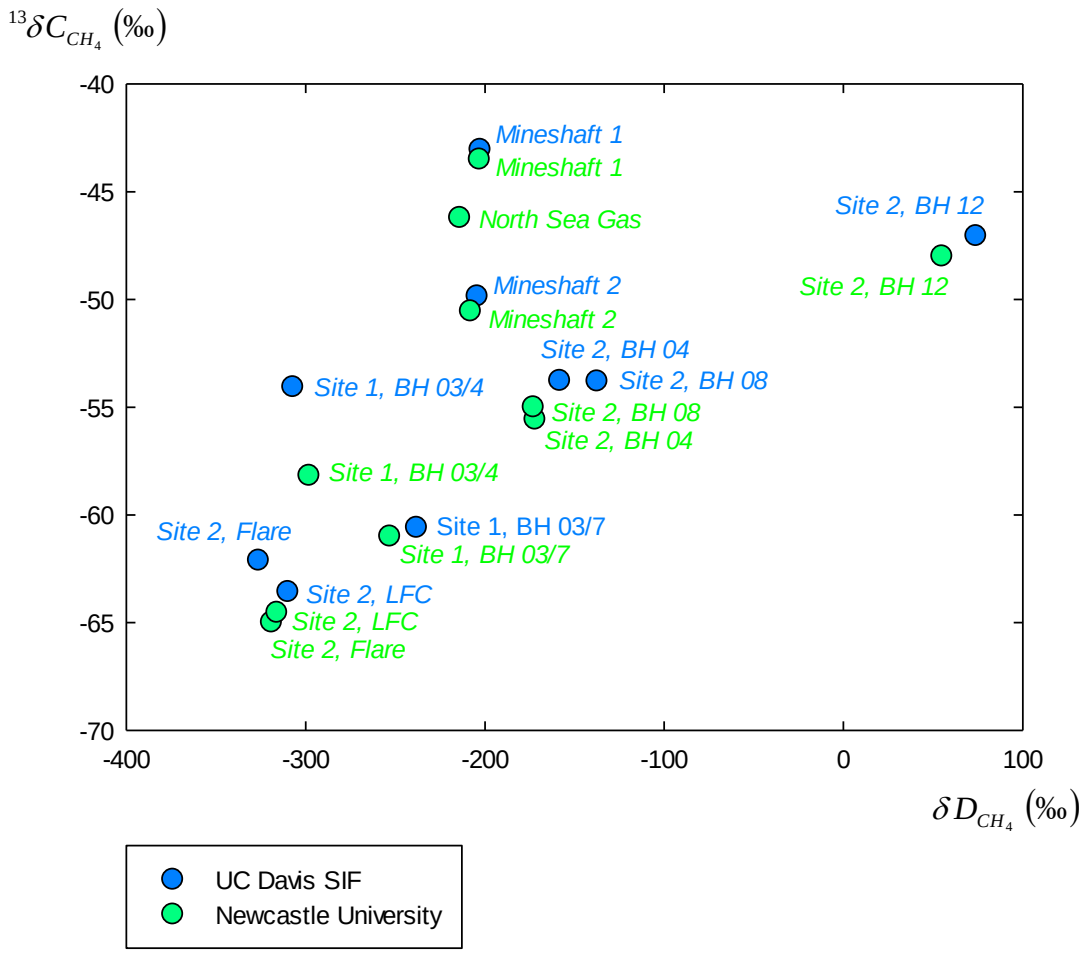

Figure 6.5: $^{13}\delta C_{CH_4}$ (‰) versus δD_{CH_4} (‰) (Measured at UC Davis SIF and Newcastle University)

Figure 6.5 clearly demonstrates a spectrum of stable isotope signatures ranging from biogenic gas source to geogenic gas source. Using Site 2 Landfill Flare and Landfill Cell gas samples as a reference, the $^{13}\delta C_{CH_4}$ values were measured at -65.0‰ and -64.5‰ respectively while δD_{CH_4} values were measured at -319‰ and -316‰ respectively. Site 2 Landfill Flare and Landfill Cell Gas samples demonstrated an isotopic depletion in ^{13}C and D in CH_4. All other samples were isotopically enriched in ^{13}C and D in CH_4 with respect to Site 2 Landfill Flare and Landfill Cell gases.

Site 1 landfill monitoring wells recorded $^{13}\delta C_{CH_4}$ values of $-58.2‰$ and $-61.0‰$ (BH 03/4 and BH 03/7 respectively) and δD_{CH_4} values of $-298‰$ and $-253‰$ (BH 03/4 and BH 03/7 respectively). The $^{13}\delta C_{CH_4}$ and δD_{CH_4} ratios for Site 1 BH 03/4 and BH 03/7 also indicate a biogenic gas source as the values were similar to the pure landfill gas samples from Site 2 and biogenic sources generally yield $^{13}\delta C_{CH_4}$ values $< -60‰$ (Hitchman et al., 1989).

Site 2 perimeter boreholes (BH 04, BH 08 and BH 12) diverge significantly from the Site 2 Flare and Landfill Cell gas stable isotope ratios. The stable isotope ratios acquired for $^{13}\delta C_{CH_4}$ and δD_{CH_4} demonstrated a enrichment in both ^{13}C and D in CH_4. This was inconsistent with a biogenic gas source and more consistent with a geogenic gas source. Owing to the complicated geology of Site 2 which includes underlying Carboniferous Coal Measures, this is perhaps not unexpected. The $^{13}\delta C_{CH_4}$ ratios measured for BH 04, BH 08 and BH 12 were -55.6, -55.0 and $-48.0‰$ respectively. Borehole 12 in particular shows a significant enrichment in $^{13}CO_2$ with respect to the Flare and Landfill Cell gases which were $\sim -65.0‰$. Using Hitchman et al. (1989) rule that thermogenic gas sources generally yield $^{13}\delta C_{CH_4}$ values $> -60‰$, this would suggest that the Site 2 perimeter monitoring wells indicate a geogenic gas source.

By comparison, the $^{13}\delta C_{CH_4}$ values for known geogenic gas sources were -46.2, -50.5 and $-43.5‰$ for Mineshaft Vent 1, Mineshaft Vent 2 gas samples and North Sea Gas (gas standard). The Site 2 perimeter borehole gas samples certainly overlap this range of $^{13}\delta C_{CH_4}$ ratios and provides further evidence that there is a geogenic gas source contribution present at Site 2.

Perhaps the most surprising results were the δD_{CH_4} ratios for the Site 2 perimeter boreholes which all yielded values greater than the mineshaft vents and North Sea Gas standard. The Site 2 boreholes produced δD_{CH_4} values of -172, -173 and $+55‰$ for BH 04, 08 and 12 respectively. These data indicate D enrichment compared with Mineshaft 1 and Mineshaft 2 which produced δD_{CH_4} values of -214 and $-208‰$ respectively. As Site 2 perimeter boreholes show $^{13}\delta C_{CH_4}$ ratios similar to the mineshaft vent samples and δD_{CH_4} ratios greater than the mineshaft vents, in this context, it provides evidence that Site 2 boreholes have a geogenic gas source contribution.

The δD_{CH_4} result for BH 12 stands out from all the other samples. The very positive value of $+55‰$, corroborated by the UC Davis SIF figure of $+74.0‰$ implies an enrichment of deuterium in CH_4. As residual CH_4 in landfills is expected to be depleted in the heavier isotopes of carbon (^{13}C) and hydrogen (D), the data strongly indicate that the origin of CH_4 in this particular borehole is different from BHs 04

and 08. Bacterial oxidation of CH_4 enriches residual CH_4 in both ^{13}C and D with changes in δD_{CH_4} values typically $\sim$ 8 to 14 times greater than $^{13}\delta C_{CH_4}$ (Aelion et al., 2009; Coleman et al., 1981). Given that the gas composition of BH 12 as per Figure 6.3 was (relatively) $\sim$ 23% CH_4, 65% CO_2 and 12% O_2, indicating a proportion of CH_4 oxidation to CO_2 in an oxic environment, this could be a likely scenario. However, it was not possible to obtain comparable δD_{CH_4} values from the literature. If this hypothesis is correct, the gas present in Site 2 BH 12 is of a biogenic origin. This would also agree with the historic gas monitoring data for this borehole (Chapter 4, Figure 4.4c) which predominantly showed a landfill gas composition between 1998 and 2015. However, this is an unsatisfactory explanation as O_2 should be absent from the landfill environment.

To put the data into context, they were plotted along with data from the literature as discussed in Chapter 2 Figure 2.5. Data from Bergamaschi and Harris (1995); Bergamaschi et al. (1998); Dai et al. (2012); Widory et al. (2012); Kerfoot et al. (2013); Hu et al. (2014); Ni et al. (2014); Raco et al. (2014) demonstrating stable isotope ratios for biogenic gas sources (landfill) and thermogenic sources (geologic gas originating from Sichuan and Turpan-Harmi Provinces, China and California, USA) are plotted along with data from Site 1 and Site 2 landfills, mineshaft vents and North Sea Gas in Figure 6.6. Site 2, BH 12 is not shown in Figure 6.6 owing to its high δD_{CH_4} value lying far outside the common range for stable isotopes.

Figure 6.6 provides a useful reference for the determination of gas sources at Site 1 and Site 2 landfills. Both Site 2 Flare and Landfill Cell gases, and Site 1 BH 03/4 and BH 03/7 gases are shown to be in the biogenic gas range. For landfill gas, Raco et al. (2014) reported $^{13}\delta C_{CH_4}$ values in the range -66.3 to -46.1‰ and δD_{CH_4} values in the range -329 to -291‰. Similarly, Kerfoot et al. (2013) reported $^{13}\delta C_{CH_4}$ values in the range -63.2 to -47.2‰ and δD_{CH_4} values in the range -299.6 to -253.7‰. Site 2 Flare and Landfill Cell gases are shown to be at the lower end of the ranges outlined by Raco et al. (2014) indicating the greatest amount of isotopic depletion in ^{13}C in CH_4.

At Site 1 where this no known input of CH_4 and CO_2 except from the landfill, the values recorded for the perimeter boreholes BH 03/4 and BH 03/7 were -58.2‰ $^{13}\delta C_{CH_4}$, -298‰ δD_{CH_4} and -61.0‰ $^{13}\delta C_{CH_4}$, -253‰ δD_{CH_4}. These values also agree with those reported by Raco et al. (2014); Kerfoot et al. (2013) and clearly plot in the biogenic range in Figure 6.6. The δD_{CH_4} value of -253‰ recorded for Site 1 BH 03/7 is perhaps on the cusp of the biogenic gas source range when compared with data from the literature.

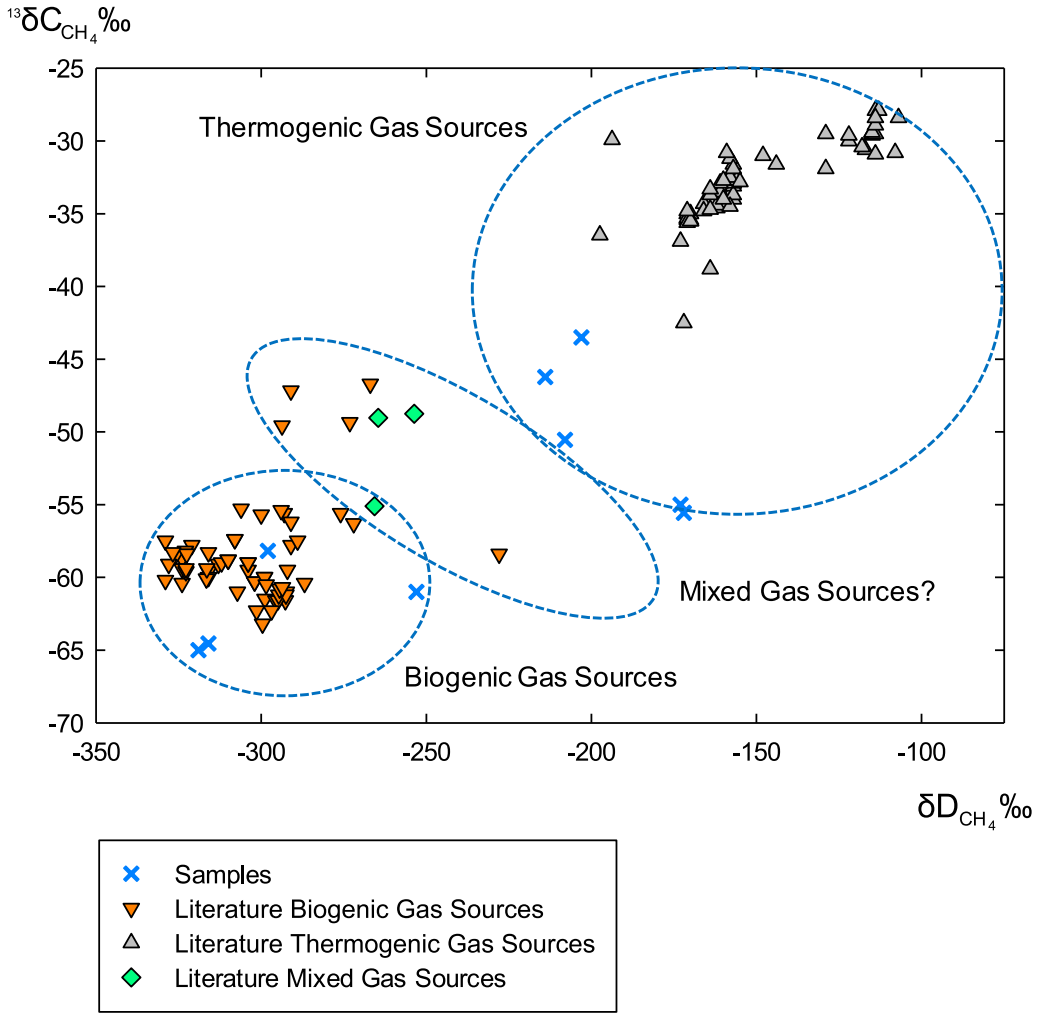

Figure 6.6: $^{13}\delta C_{CH_4}$ (‰) against δD_{CH_4} (‰) derived from Newcastle University compared with Literature Data. (Biogenic gas sources: landfill gas samples (Bergamaschi and Harris, 1995; Bergamaschi et al., 1998; Kerfoot et al., 2013; Raco et al., 2014; Widory et al., 2012); thermogenic gas sources: natural gas samples from Sichuan Basin, China (Dai et al., 2012; Hu et al., 2014), Turpan-Harmi Basin, China (Ni et al., 2014), and California, USA (Kerfoot et al., 2013))

Site 2 BH 04 and BH 08 indicate $^{13}\delta C_{CH_4}$ and δD_{CH_4} values outside the biogenic range despite being perimeter monitoring wells for the landfill. While the $^{13}\delta C_{CH_4}$ ratios recorded for BH 04 and 08 (-55.6 and -55.0‰ respectively) were not atypical of biogenic source according to Raco et al. (2014), the δD_{CH_4} ratios (-172 and -173‰ respectively) were outside the biogenic range. These boreholes showed an enrichment of $^{13}CH_4$ that is more typical of geogenic gas sources. These figures compared to Dai et al. (2012) who reported a δD_{CH_4} range of values between -173 and -155‰ for natural gases in the Xujiahe Formation, Sichuan Basin, China. As residual CH_4 in landfill gas is expected to be isotopically depleted in ^{13}C and D, the evidence suggests that the gas captured in Site 2 BH 04 and BH 08 is of geogenic origin or at the very least has a geogenic contribution.

In the context of the literature data, the mineshaft vent gas samples and North Sea Gas samples show a depletion in ^{13}C and D with respect to the natural gas samples reported by Kerfoot et al. (2013) and Dai et al. (2012). Mineshaft Vent 1 produced a $^{13}\delta C_{CH_4}$ of $-46.2‰$ and a δD_{CH_4} of $-214‰$ while Mineshaft Vent 2 produced a $^{13}\delta C_{CH_4}$ and a δD_{CH_4} of -50.5 and $-208‰$ respectively. This compares with North Sea Gas, which produced a stable isotope signature of $-43.5‰$ $^{13}\delta C_{CH_4}$ and $-203‰$ δD_{CH_4}.

However, for California, USA, Kerfoot et al. (2013) reported a range of stable isotope ratios between -36.46 and $-29.91‰$ $^{13}\delta C_{CH_4}$, and -197.4 and $-193.7‰$ δD_{CH_4}. Similarly, for natural gas samples originating from Sichuan Province, China, Dai et al. (2012) detailed a range of stable isotope ratios between -36.9 and $-30.8‰$ $^{13}\delta C_{CH_4}$, and -173 and $-155‰$ δD_{CH_4}. With respect to these data, the mineshaft vent samples and North Sea Gas are isotopically depleted in both ^{13}C and D. Some variation is anticipated in natural gas samples depending on the origin of the gas, the geology, and mixing from external sources. Using both the mineshaft vent gas samples, North Sea Gas and the literature data, the evidence strongly supports the conclusion that Site 2 landfill perimeter borehole gas has a geogenic component. It is interesting to note that Site 2 perimeter borehole gases are isotopically enriched in D with respect to the mineshaft vent gas samples and North Sea Gas.

Figure 6.7 shows the stable isotope data in the context of a review of stable isotope data for coal bed CH_4 published by Golding et al. (2013).

Slightly different from the literature review that was conducted for this research, all gas samples used by Golding et al. (2013) are derived from natural environments and none are from anthropogenic environments. Samples procured from the Powder River Basin, USA, by Bates et al. (2011) indicate a microbial influence on stable isotope ratios. The presence of active methanogenic communities in coal bed CH_4 coupled with fresh nutrient recharge from the Powder River Basin margins have been hypothesised to encourage microbial growth, specifically favouring CH_4 generation via acetate fermentation (Flores et al., 2008). That is the same process occurring in landfills that produces CH_4 and CO_2.

Confirming what was shown in Figure 6.6, Site 2 Landfill Flare and Landfill Cell gases along with Site 1 BH 03/4 plot in the 'acetoclastic reactions' range. Site 1 BH 03/7 plots on the boundary between 'mixing' gases and 'microbial CH_4'. As was previously shown, Site 2 BH 04 and BH 08 gases are totally different in nature from landfill gases as they plot in the 'mixing' region of Figure 6.7. Mineshaft Vent 1 gas and North Sea Gas plot in the 'thermogenic CH_4' region of the plot while Mineshaft Vent 2 gas lies on the boundary between thermogenic and mixing gases.

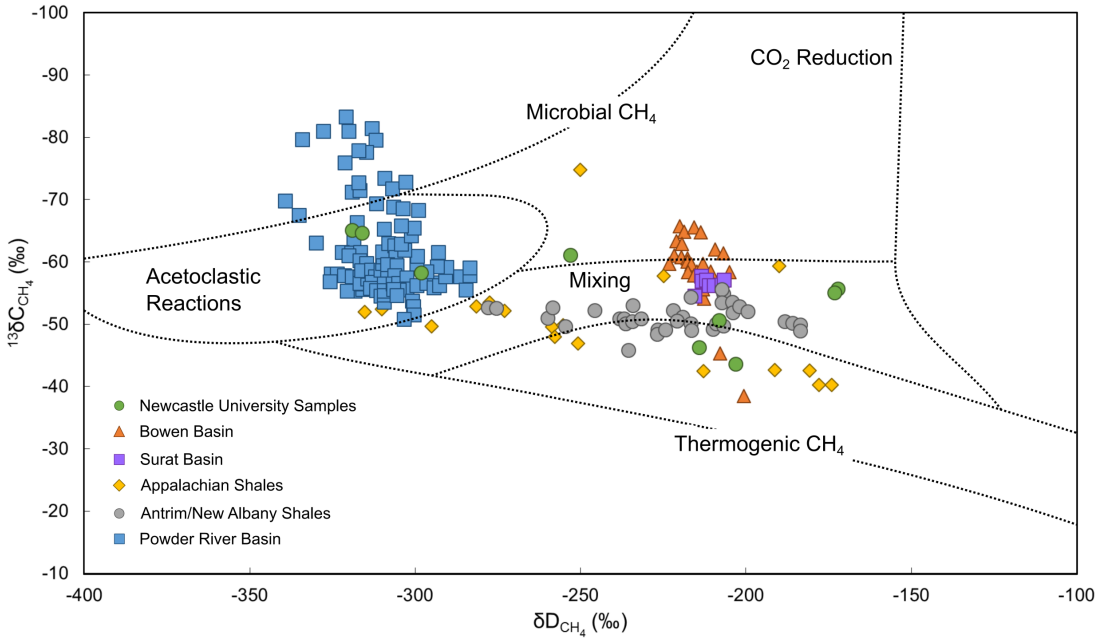

Figure 6.7: $^{13}\delta C_{CH_4}$ (‰) against δD_{CH_4} (‰) derived from Newcastle University compared with Golding et al. (2013). (Bowen and Surat Basins coal bed and coal mine CH_4 (Kinnon et al., 2010); gas samples from the Powder River Basin (Bates et al., 2011; Flores et al., 2008); gas samples from the Antrim and New Albany Shales (Martini et al., 1998; McIntosh et al., 2002); and gas samples from organic-rich shales of the northern Appalachian Basin (Osborn and McIntosh, 2010))

While stable isotope ratios go a long way to differentiating the source of ground gases, it is clearly not the whole picture as there is an overlap in the ratios shown here. Coupled with radiocarbon dating it would be possible to fully differentiate gas sources. Owing to the relatively short half-life of ^{14}C of 5,730 years, geological sources of gases are totally depleted in ^{14}C by virtue of their great age while modern biogenic sources contain ^{14}C that reflects contemporary atmospheric ^{14}C levels (Muir et al., 2015; Fellner and Rechberger, 2009). Williams and Aitkenhead (1991) were able to prove the biogenic source of the CH_4 and CO_2 from a nearby landfill that caused the Loscoe explosion in 1986 using radiocarbon dating in conjunction with stable isotope ratios. In the case of Site 2 landfill perimeter boreholes, this would provide conclusive evidence for the mixing of landfill gas with coal bed gas from the underlying strata that the stable isotope ratios indicate.

Another important conclusion to draw is the effective storage time of samples. Samples were collected in flexifoil sample bags and aliquoted into 12 ml vacutainers for storage. A period of one month elapsed before analysis at Newcastle University and a further month elapsed before analysis at UC Davis SIF. There was little variation between the two data sets despite the time lag between sampling and analysis. The vacutainers were, therefore, shown to store samples without degradation for at least two months. This gave further confidence to the accuracy of the data.

6.5 Refinement of Conceptual Model

Using the data from Chapter 6, it is possible to add a further layer of information to the Conceptual Model presented in Chapter 5 Figure 5.12. The refined conceptual model is presented in Figure 6.8.

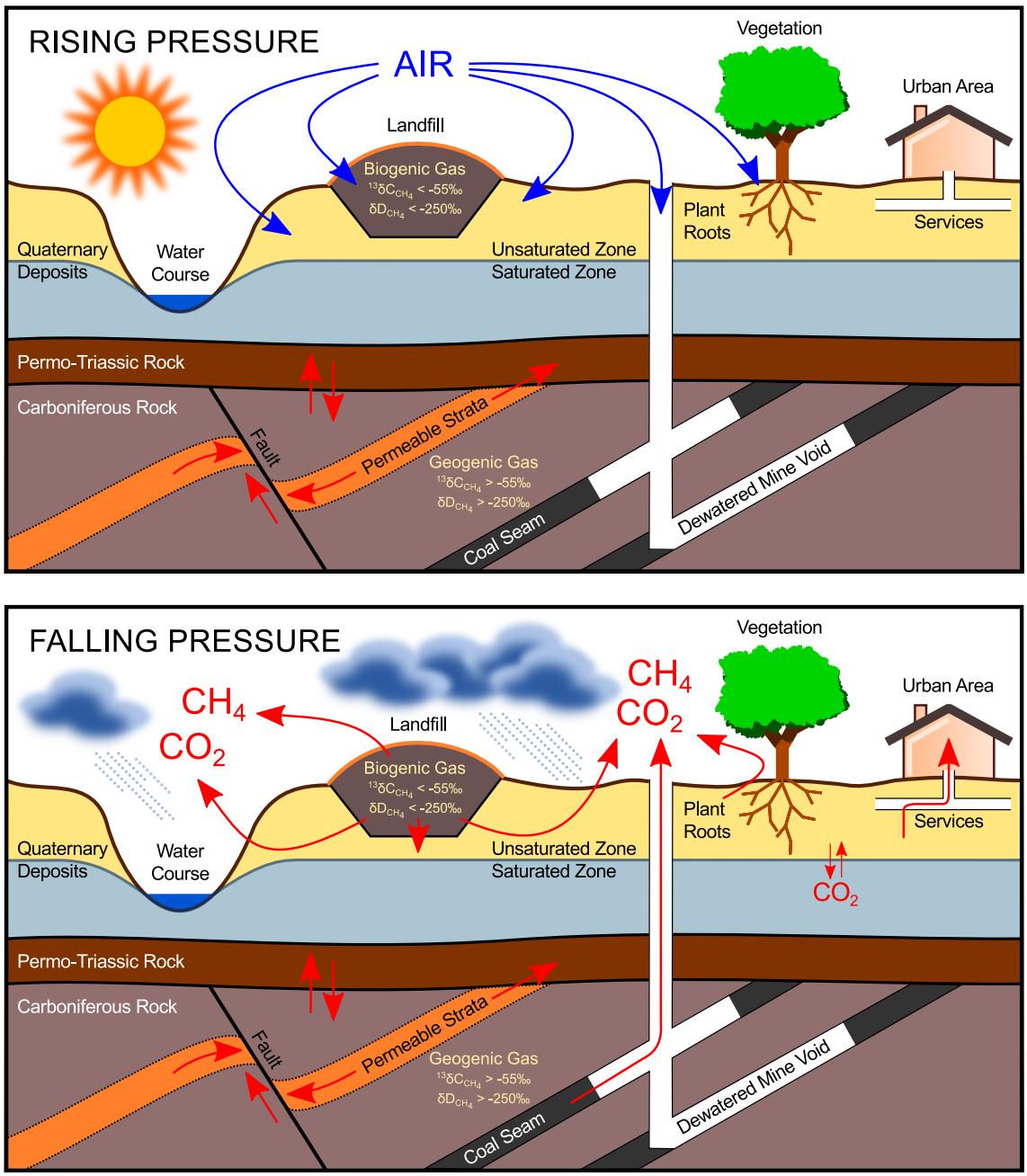

Figure 6.8: Refined Conceptual Model Design Incorporating Stable Isotope Data

As has been discussed in this chapter, stable isotope ratios do differentiate gas sources. Owing to the physiology of landfill microbe communities, ^{12}C is preferentially consumed in acetoclastic reactions. Consequently, residual CH_4 is isotopically depleted in the heavier stable isotope ^{13}C. Also, CH_4 is isotopically depleted in the

heavier hydrogen isotope, deuterium. Hitchman et al. (1989) proposed the following as a guideline for gas source:

$$^{13}\delta C_{CH_4} > -60‰ = \text{Thermogenic Source}$$
$$^{13}\delta C_{CH_4} < -60‰ = \text{Biogenic Source}$$

However, the data presented here from landfill and literature data from biogenic sources show that often the $^{13}\delta C_{CH_4}$ value can be $-50‰$. The maximum $^{13}\delta C_{CH_4}$ obtained in this research for geogenic gas source was $-50.5‰$. Likewise, data reported in the literature rarely show the $^{13}\delta C_{CH_4}$ ratio exceeding $-55‰$. As a slight adjustment to Hitchman et al. (1989), it is proposed that biogenic gas sources will yield a $^{13}\delta C_{CH_4} < -55‰$ while geogenic gas sources will produce a $^{13}\delta C_{CH_4} > -55‰$. The data reported here and data from the literature suggest a general trend for biogenic sources to be $< -250‰$ δD_{CH_4} and geogenic sources to be $> -250‰$ δD_{CH_4}. Caution should be exercised with these figures as the data also indicate overlap of stable isotope ratios between gas sources.

The Conceptual Model shown in Figure 6.8 has been adjusted to include the determination of gas source according to stable isotope ratios. This should be treated as a guide only. Generally speaking the more negative the $^{13}\delta C_{CH_4}$ and the δD_{CH_4}, the more isotopically depleted the CH_4 is in the heavier isotopes ^{13}C and D. CH_4 derived from biogenic sources such as municipal landfills is depleted in the heavier isotopes ^{13}C and D by comparison with geogenic gas sources.

However, where stable isotope ratios indicate a mixed gas source as for perimeter boreholes at Site 2, it may be necessary to perform radiocarbon dating on samples to conclusively determine gas source. Modern CH_4 reflects contemporary atmospheric concentrations of ^{14}C (currently $\sim$ 104 pMC) while older, geologic sources are completed depleted in ^{14}C owing to the relatively short half-life of ^{14}C (5,730 years). It is anticipated that in the case of Site 2 landfill perimeter boreholes (BH 04, BH 08 and BH 12), the CH_4 present in these boreholes would be $\sim$ 0 pMC if a geogenic gas input from the underlying Coal Measures is present as hypothesised in this chapter.

From a regulation perspective, stable isotopes in conjunction with radiocarbon dating could be used to determine gas source. While stable isotopes should be enough to differentiate gas sources in most cases, in the case of Site 2, it was unclear where the gas source had originated from. For examples such as Site 2, radiocarbon dating may be needed to fully clarify gas sources. This is particularly pertinent for regulation, especially in the case of Site 2, as the site owner/regulator would need to know if they were responsible in the event of a gas leak.

Chapter 7

Gas Transport Mechanics

7.1 Introduction

It is possible to compartmentalise gas transport processes in the environment into two types: *'advection'* and *'diffusion'*. Advection refers to transport with the mean fluid flow while diffusion encompasses transport resulting from random motions of particles down a concentration gradient. To illustrate these differences, advective flow can be visualised as dye being emptied into the centre of a river and the centre of the dye spot being transported by the river. By comparison, diffusion spreads out the concentrated dye spot to a larger, less concentrated area (Honrath, 1995). These mechanisms can equally be applied to gas transport in the environment. An important research question is to determine which, if any, is the dominant gas transport mechanism in the unsaturated zone.

An important tool for interpreting gas transport in the sub-surface is Fick's Law of Diffusion which is defined by Crank (1979) in Equation 7.1 as:

$$J = -D\frac{dC}{dx} \tag{7.1}$$

Where:
J = Flux density (rate of transfer per unit area of section, e.g. mol/cm^2/s)
D = Diffusion Coefficient (cm^2/s)
dC = Change in concentration (mol)
dx = Change in position (cm)

Commonly, Fick's Law is applied to the calculation of diffusion in liquids. It is equally as applicable to the calculation of diffusion in the gas phase. Using an effective diffusion coefficient for the medium through which gas is being transported, rearranging Fick's Law according to Crank (1979) for gases produces Equation 7.2:

$$E = A\,(C_{source} - C_{g^0})\,D^{eff}/L \tag{7.2}$$

Where:
E = Rate of mass transfer due to diffusion (g/s).
A = Cross-sectional area through which migration occurs (cm^2).
C_{source} = Concentration of gas being considered at source (g/cm^3).
C_{g^0} = Concentration of gas being considered at limit of migration (g/cm^3).
D^{eff} = Effective diffusion coefficient in the medium being considered (cm^2/s).
L = Distance over which migration occurs (cm).

This provides a useful basis on which to model CH_4 and CO_2 transport in the unsaturated zone. Using a controlled environment in the laboratory, it is possible to examine whether flow is caused by diffusion, advection or a combination of both.

However, there are some limitations associated with modelling gas transport in this manner. Gas diffusion coefficients vary according to the type of porous medium and the degree of saturation (Hooker and Bannon, 1993). Fick's Law assumes that isobaric conditions are prevalent (i.e. that there is a constant reservoir of gas), there is no pressure driven flow, relatively low concentration of gas and high soil permeability (Wilson et al., 2009). Additionally, it is assumed that diffusion only occurs in one direction, diffusion coefficient is constant (although it varies with concentration and temperature) and it excludes the effect of Knudsen diffusion (where the scale length of a system is comparable to or smaller than the mean free path, i.e. tortuosity) and non-equimolar diffusion.

This chapter presents the results of a pilot study of gas transport mechanics in the unsaturated zone through the application of Fick's Law. Diffusion was modelled using Fick's Law and is compared with data that was generated using an experimental set up. The apparatus used to test gas diffusion comprised a 3 m high 'artificial borehole' that was analogous to gas monitoring boreholes in the field. Tests were carried out with and without the presence of resistance in the form of Leighton Buzzard Sand.

7.2 Modelled Data

The diffusion of CH_4 and CO_2 was modelled in accordance with Fick's Law adjusted for a finite reservoir according to Crank (1979) in Equation 7.3:

$$\frac{C}{C_0} = \frac{1}{2}\left(erfc\frac{L}{2\sqrt{D^{eff}\cdot t}}\right) \tag{7.3}$$

Where:
C/C_0 = Concentration Change
L = Distance over which migration occurs (m)
D^{eff} = Effective diffusion coefficient in the medium being considered (cm^2/s)
t = time (s)
$erfc$ = complementary error function

The value yielded from the ratio in parentheses for a specific time was subjected to the complementary error function (erfc) to yield a value for C/C_0. The C/C_0 values were plotted against distance (m) using a logarithmic scale. In order to model CH_4 and CO_2 diffusion the effective diffusion coefficient (D^{eff}) in air was applied. The D^{eff} used were 0.1952 cm^2/s and 0.1381 cm^2/s for CH_4 and CO_2 respectively in accordance with modelled values reported by Massman (1998). The lighter and smaller CH_4 molecule yielded a larger D^{eff} and therefore a quicker diffusion rate.

Under sealed test conditions a maximum pressure of 50 mbar was attained in the apparatus. Gas was confined to a fixed volume assuming no leaks. Furthermore, Fick's Law assumes steady state conditions. Gas flux across a concentration gradient is from regions of high concentration to regions of low concentration. However, in an unconsolidated medium such as sand, no matter how homogenised, there is potential for preferential pathways to exist. This could mean that flow was not uniform across the apparatus.

Another assumption is the absence of interaction between species for gas mixtures. For a CH_4/CO_2 gas mixture, such as those emanating from landfill sites, it was assumed that the two gases do not interact with each other or with the air. Additionally, it must be assumed that gases do not separate and stratify in the gas column. If the medium through which gases were to be transported was saturated with water, there would be a 'scrubbing' of CO_2 from the system which would have to be taken into account. It was assumed that the sand used was dry and contained residual moisture only. Moisture testing revealed a residual mositure content of 0.6% (Appendix Table L.2). Saturation of the test medium was outside the scope of the experimentation presented here.

Gas diffusion was modelled using gas diffusion coefficients in air for CH_4 and CO_2. If gas transport was determined to be by diffusive flow it would be anticipated that once the apparatus was filled with sand, gas flow would be impeded. This would result in a slowing of the rate of diffusion through the gas column. In practice, this would be observed as a longer time taken for gas to appear at the top of the gas column.

7.2.1 Combined CO_2 and CH_4 Diffusion Model

The modelled data for CO_2 and CH_4 diffusion in air are presented in Figure 7.1 (where 'x' is distance from source).

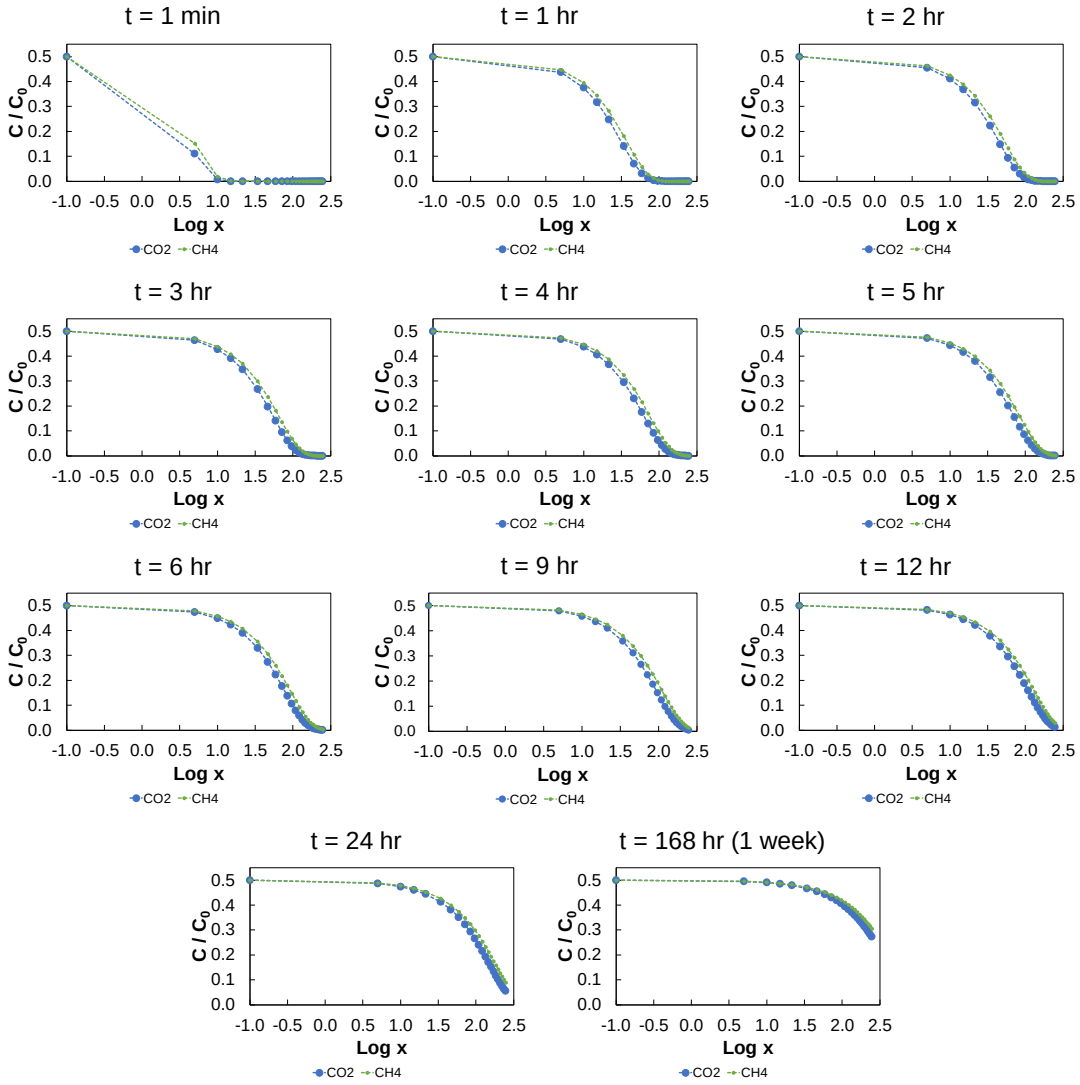

Figure 7.1: Modelled CO_2 and CH_4 Diffusion in Air

The modelled data between t = 72 hr (3 days) and t = 168 hr (1 week) show little change in the diffusion curve. Therefore, it was determined that one week would be sufficient time required for an individual experiment. For a given distance and time, a greater proportion of CH_4 than CO_2 will diffuse. This observation aligns with the larger diffusion coefficient of CH_4 compared with CO_2. The lower molecular mass (16.04 g/mol) and density (0.71 kg/m^3 at ATP) of CH_4 compared with CO_2 (molecular mass 44.01 g/mol and density 1.98 kg/m^3 at ATP), means that the CH_4 molecule is more buoyant than the CO_2 molecule.

7.3 Methodology

7.3.1 Apparatus

In order to simulate conditions in the field, a 'artificial borehole' was constructed to test gas transport mechanics. Figure 7.2 shows the apparatus structure. Full details of the borehole design and construction are included in Appendix H.

Figure 7.2: 'Artificial Borehole' Apparatus

The apparatus may be separated into three distinct components: the gas injection reservoir, the outer column (annulus), and inner column (core). The gas injection reservoir and outer column were constructed from polyvinyl chloride (PVC) while the inner column was a 50 mm external diameter slotted standpipe covered in a geotextile membrane. Three 1 m sections of standpipe were used to give a 3 m high pipe that determined the overall height of the experimental rig.

The PVC gas injection reservoir external dimensions were 665 × 425 × 335 mm while the internal dimensions were 605 × 370 × 280 mm to give a capacity of 62.7 l. It was equipped with two gas inlet valves (also made from PVC) and a gas bleed

valve (also PVC). Two lids were made in order to access the reservoir to add sand to the reservoir. While not in use these lids were sealed with silicone to produce an air-tight seal.

Mounted in the centre of the reservoir, the external PVC pipe had a total height of 3,000 mm with 12 mm thick walls. The external diameter of the pipe was 300 mm while the internal diameter was 276 mm. The lower-most 330 mm of the pipe sitting within the reservoir had 10 mm slots, 10 mm apart cut into it to allow the movement of gas from the reservoir into the annulus of the borehole. The outer pipe was fitted with a 276 mm diameter PVC lid with a 50 mm diameter hole in the centre to allow the top of the internal standpipe to pass through. This lid also had an air-tight silicone seal.

The external pipe was equipped with sample ports that extended 62.5 mm into the annulus of the apparatus. The sample ports were threaded and constructed from PVC. A geotextile membrane covered the internal end of the sample ports to prevent sand encroachment. The external ends were fitted with rubber septa and sealed onto the end of the spigots with brass swagelok nuts. Spaced 125 mm apart, there were 19 sample ports up one side of the external pipe. The total distance between Sample Port 1 (bottom) and Sample Port 19 (top) was 2,250 mm. Additionally, on the off-side of the external pipe there were three auxiliary sample ports (A, B and C) located at the bottom, mid-point and top of the external pipe.

Located in the centre of the external pipe was a 3 m length of 50 mm external diameter slotted standpipe covered in geotextile membrane as typically used in borehole construction. The top of the standpipe was fitted with a valved rubber bung. Initially it had been intended to use three piezometer tubes to measure the internal gas concentration of the standpipe at the bottom, mid-point and top using a GFM435 landfill gas monitor. However, a single-valved rubber bung was used instead. The purpose of this valve was to enable the experimental rig to be purged following the conclusion of an experiment.

Once the annulus and reservoir had been filled with sand, a preferential pathway existed through the core of the apparatus. To mitigate against this, an industrial blank inflatable pipe stopper (supplied by Allpipe Stoppers & Ground Equipment, Healey & Lord Ltd, Norwich) was deployed inside the standpipe as a lateral packer. This rendered the use of the piezometer tubes in the core of the apparatus an impossibility. The empty capacity of the entire rig was $\sim$ 214 l, 62.7 l in the reservoir and $\sim$ 151 l in the column (above the reservoir). The borehole core volume was 5.42 l while the borehole annulus volume was 166 l. Figure 7.3 shows a scale schematic of the apparatus.

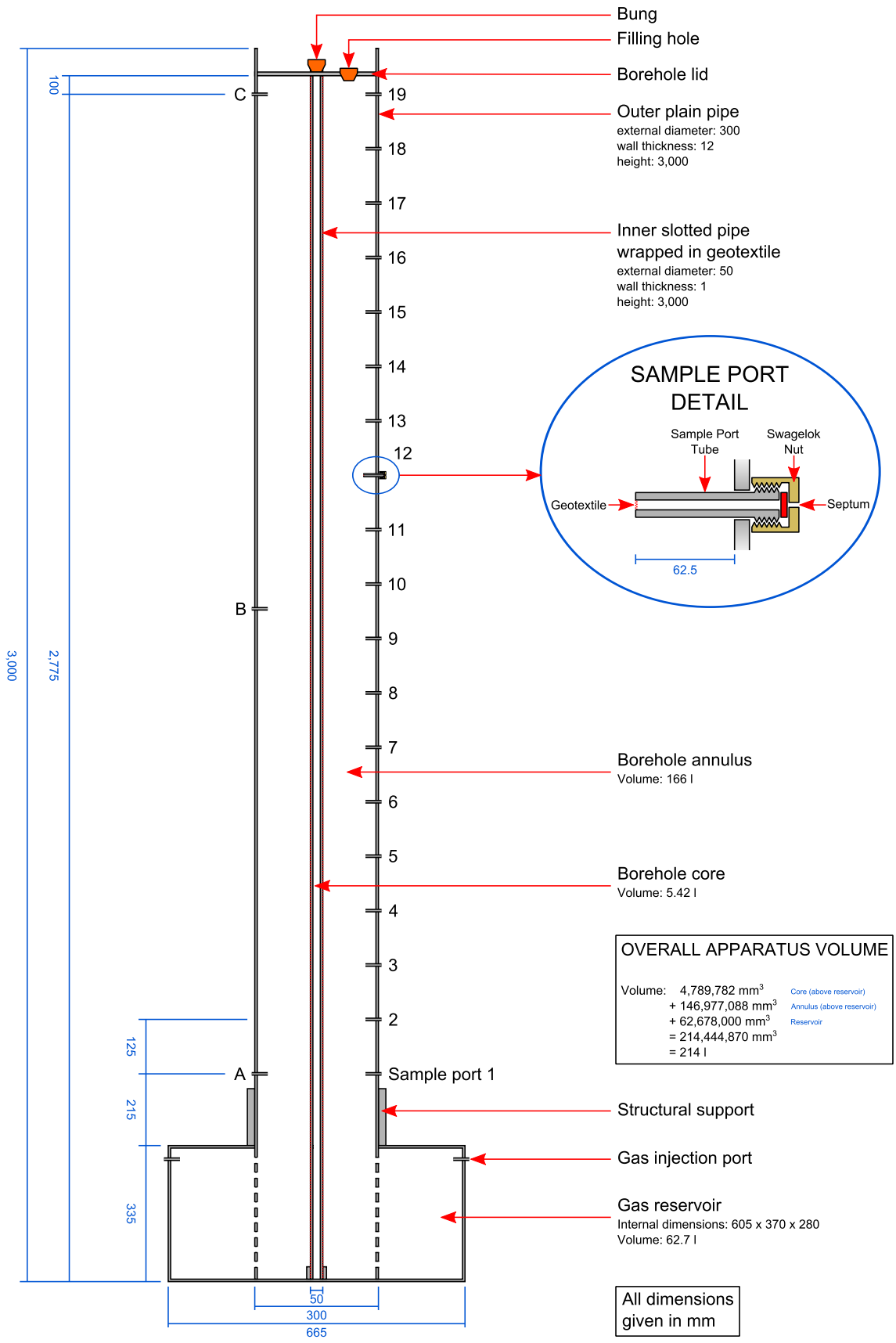

Figure 7.3: 'Artificial Borehole' Schematic Indicating Component Dimensions and Capacities

7.3.2 Gas Injection Process

Using a manometer, pressure testing of the rig determined that the maximum pressure that could be received by the apparatus without leaks was 50 mbar. This value far exceeded the differential pressures commonly encountered in the field (typically < 15 mbar during deep depression weather systems). Figure 7.4 shows the gas injection port.

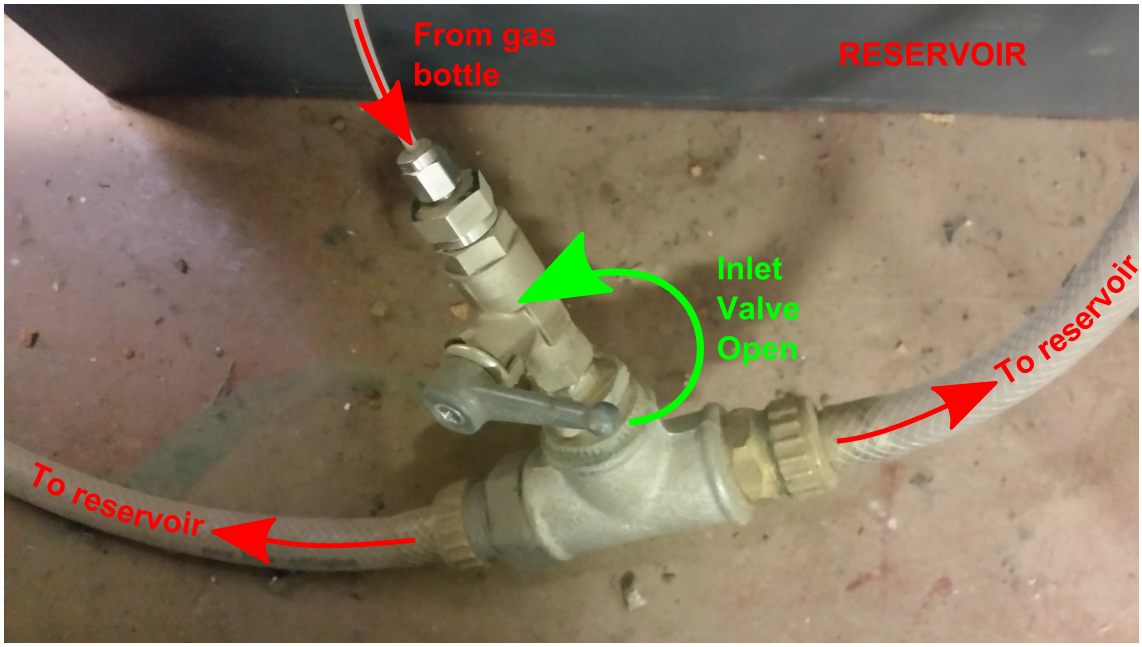

Figure 7.4: Experimental Borehole Injection Port Detail

A pressurised gas canister was attached to the tap via a tube. The injection port tap was opened and the gas canister valve opened. Gas entered the borehole reservoir via the large tubing in Figure 7.4 which was securely attached to the two reservoir inlets. This allowed a more even distribution of gas throughout the reservoir initially. Checking the apparatus using a manometer, the reservoir was allowed to charge with gas until the pressure had reached 50 mbar (approximately 20 minutes to full pressure). Once maximum pressure had been attained, the injection port tap was switched off and the pressurised gas canister valve was closed.

Following the conclusion of an experiment, the borehole was purged of the test gas(es) over a 3 to 4 hour period. This was achieved by attaching the gas injection port to a pressurised air line and opening the valve on the bung on the top of the 50 mm internal pipe. To determine that all gases had been removed from the apparatus, it was regularly tested with a GFM435 landfill gas monitor. Gas concentrations were tested at the top of the experimental rig and in the reservoir via the bleed port (to atmosphere). Once both locations recorded three consecutive readings of 0% CH_4 and CO_2, and 20.9% O_2, the apparatus purge was complete.

7.3.3 Sampling Regime

Preliminary experiments determined which sample ports needed to be targeted during each sampling session and an idealised sampling regime (assuming infinite consumables) is summarised in Table 7.1.

Sample	**Time** (hr)										
Port	0	1	2	3	4	5	6	9	12	24	168
1	•	•	•	•	•	•	•	•	•	•	•
2		•	•	•	•	•	•				
3		•	•	•	•	•	•				
4		•	•	•	•	•	•	•	•	•	•
5		•	•	•							
6					•	•	•	•			
7		•	•	•					•	•	•
8					•	•	•	•			
9											
10	•	•	•	•	•	•	•	•	•	•	•
11											
12								•	•		
13										•	•
14								•	•		
15											
16									•	•	•
17											
18											
19	•	•	•	•	•	•	•	•	•	•	•

Table 7.1: Artificial Borehole Idealised Sampling Regime

Samples were extracted from the experimental rig through the sample ports using a 10 ml syringe. Samples were subsequently transferred to 12 ml exetainers for storage prior to analysis by GC-MS. Sampling took place on an hourly basis from t = 0 – 6 hr and subsequently at t = 9 hr, t = 12 hr, t = 24 hr and t = 168 hr (1 week). During each sampling session a maximum of 8 sample ports were targeted to identify the gas interface up the gas column. This equated to a maximum of 10 min required to complete sampling. For reference, a complete sampling of all 19 ports and the 3 auxiliary ports took approximately 30 minutes.

Additional Measurements

At the point of sampling each sample port, the internal pressure of the experimental rig was measured using a manometer. It was vital to determine changes in pressure throughout each experiment as the apparatus would be subject to changes in atmospheric pressure, potential gas leaks, and gas extraction of samples. Assuming the experimental rig was completely air-tight, changes in atmospheric pressure would

potentially lower or increase the internal pressure of the apparatus (as observed in the field). Falling atmospheric pressure would equate to an increase in internal pressure. Indeed, when the apparatus was pressure tested during a fall in atmospheric pressure, a positive internal pressure in the experimental rig was induced. This was the same observation as for field conditions. In addition to external changes in atmospheric pressure, gas leaks and gas extractions would result in a lowering of the internal pressure of the apparatus.

In order to ensure that a temperature gradient was not affecting the transport of gas in the apparatus, the external temperature was measured at the gas injection reservoir, the bottom, mid-point and top of the column using pre-calibrated thermocouples. The thermocouples were calibrated at 75°C and 0°C, and were programmed to log temperature every 10 minutes for 1 week.

7.3.4 Sample Analysis

To determine the concentration of gases contained in the 12 ml exetainers, the samples were analysed by GC-MS. The analysis of CH_4 and CO_2 gases was performed on a Fisons 8060 GC using split injection (150°C) linked to a Fisons MD800 MS (electron voltage 70 eV, filament current 4 A, source current 800 μA, source temperature 200°C, multiplier voltage 500 V, interface temperature 150°C). The acquisition was controlled by a Compaq Deskpro computer using Xcalibur software; in full scan mode (1-150 amu/scdwell 10 ms/amu) or in SIM mode 10 ions (dwell 100 ms/ion) for greater sensitivity. The headspace sample (100 μl) was injected in split mode and the GC programme and MS data acquisition commenced. Separation was performed on a HP-PLOT-Q capillary column (30 m $\times$ 0.32 mm i.d.) packed with 20 μm Q phase. The GC was held isothermally at 35°C with He as the carrier gas (flow 1 ml/min, pressure 65 kPa, split at 100 ml/min. The chromatograms of the separated gases (CH_4, CO_2, N_2O etc) were integrated and quantified. The acquired data was stored on DVD for any further data processing, integration and printing.

7.4 Results

The concepts of diffusion and advection are demonstrated in Figure 7.5.

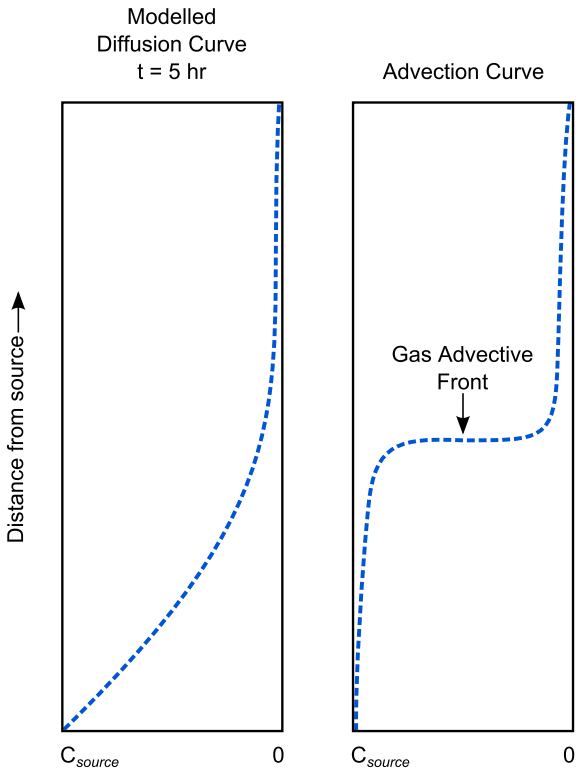

Figure 7.5: Conceptual Model of Diffusion and Advection Curves

Diffusion may be viewed as a gradual dispersal of gas concentration from source to terminal distance in the column. Overtime the curve moves away from source until the entire column achieves a uniform concentration less than that of the initial gas source. Conversely, advection may be viewed as a front gradually moving up the column away from the gas source. However, care must be taken as the experimental rig has a finite capacity. A small percentage of reflective diffusion may be observed once the gas has reached the top surface of the apparatus assuming there were no leaks.

A summary of the experimental results presented in this chapter is as follows:

- Empty Artificial Borehole
  - 100% CO_2
  - 20% CO_2 / 10% CH_4
  - 40% CO_2 / 60% CH_4
- Leighton Buzzard Sand-Filled Artificial Borehole
  - 100% CO_2
  - 40% CO_2 / 60% CH_4

7.4.1 Empty Artificial Borehole Data

100% CO_2 Experiment

Welding gas (100% CO_2 (see Appendix Figure L.22 for GC-MS output)) was slowly injected into the artificial borehole reservoir over a 20 minute period. Sampling of the borehole sample ports occurred at t = 0, 1 hr, 2 hr, 3 hr, 4 hr, 5 hr, 6 hr, 24 hr and 168 hr. Samples were analysed by GC-MS to produce concentration curves for the specific sampling times. The results of the GC-MS analysis are shown in Figure 7.6. All standard error calculations are shown in Appendix Tables L.3 and L.4.

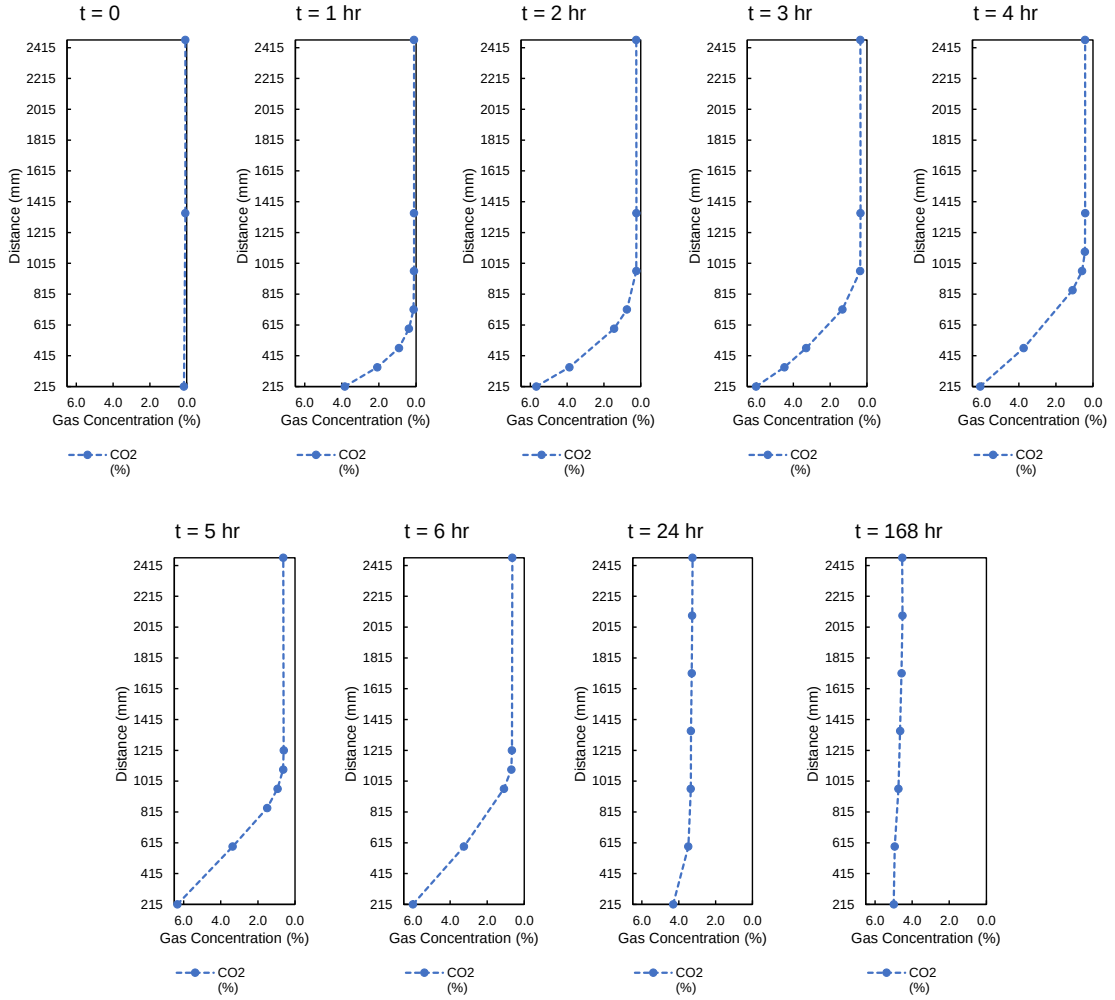

Figure 7.6: Concentration Curve for 100% CO_2 in Empty Artificial Borehole

The data produced for 100% CO_2 in the empty artificial borehole indicate diffusion of CO_2 in the apparatus. There was no evidence of advection as there was no frontal system observed in the data. This was not unexpected as the apparatus was empty and with no medium offering any resistance or impedance to gas flow. Uniform concentration $\sim$ 5.0% CO_2 was achieved after 1 week. This satisfied the mass balance calculation for initial CO_2 concentration injected at t = 0.

Little change was observed between t = 24 hr and t = 168 hr, indicating that diffusion primarily took place over a 24 hour period. At t = 0, negligible CO_2 was recorded at the bottom, mid-point and top of the column (0.154% – 0.0772% CO_2). Between t = 1 and 6 hr, the concentration of CO_2 peaked at ∼ 6% at the bottom of the artificial borehole (215 mm from the reservoir). At the mid-point of the artificial borehole (sample port 10, 1,340 m from source), CO_2 concentration ranged between 0.1% and 0.6%. Likewise, at the top of the artificial borehole (sample port 19, 2,465 mm from source), CO_2 concentration ranged from 0.1% to 0.6%. This suggests that although the rate of diffusion was slow, the bulk transport of gas occured between 6 and 24 hours in the empty apparatus.

The measured $C/C_{\max}$ was compared against the modelled C/C_0 for t = 2 hr, t = 4 hr and t = 24 hr as shown in Figure 7.7.

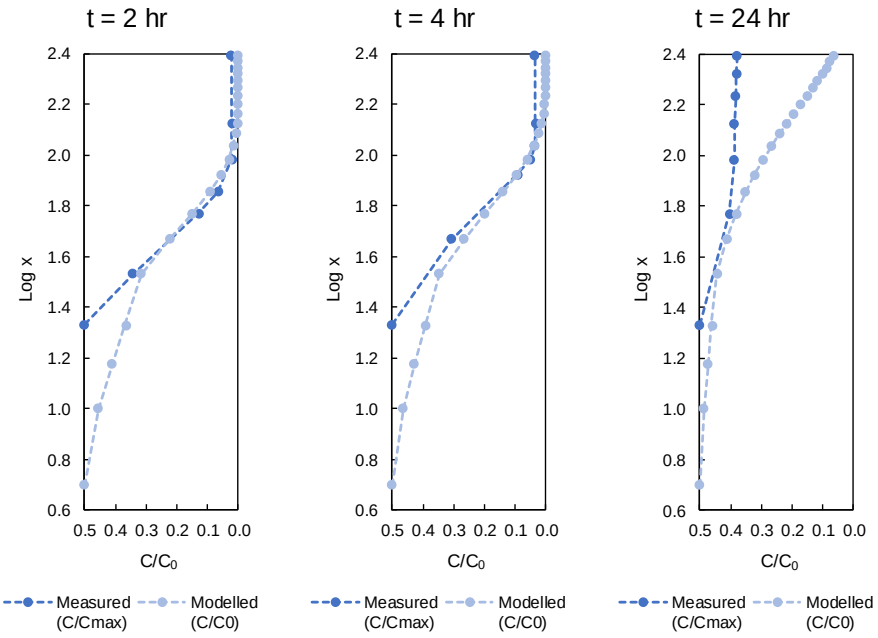

Figure 7.7: Measured $C/C_{\max}$ Comparison with Modelled C/C_0 for t = 2 hr, t = 4 hr and t = 24 hr during 100% CO_2 in Empty Artificial Borehole Experiment

For t = 2 hr and t = 4 hr, the measured $C/C_{\max}$ matched the modelled C/C_0 quite well. The slight deviation in the curves was an artefact of the lack of available sample port into the gas reservoir at the bottom of the apparatus. With increasing distance from source, the measured $C/C_{\max}$ mapped directly onto the modelled C/C_0. This indicated that the observed transport curves were driven by diffusion as predicted by the diffusion model. The concentration curve for t = 24 hr deviated significantly from the predicted C/C_0. A refinement to the model would need to be made to compensate for a confined region such as the artificial borehole apparatus.

20% CO_2 / 10% CH_4 Experiment

A calibration gas standard containing 20% CO_2 and 10% CH4 (balance N_2) was subsequently tested. The results from the GC-MS analysis are shown in Figure 7.8.

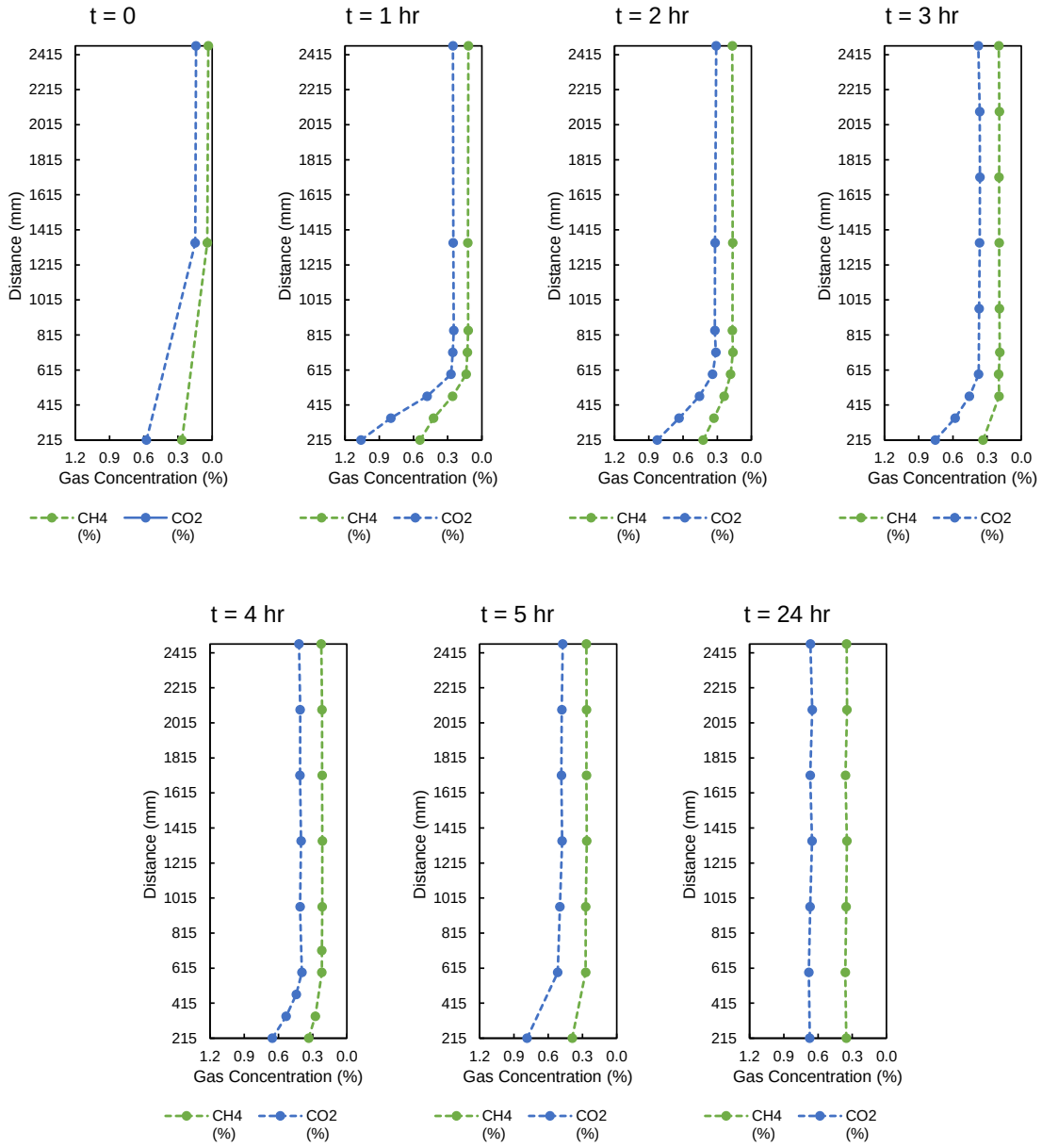

Figure 7.8: Concentration Curves for 20% CO_2 / 10% CH_4 Gas Mixture in Empty Artificial Borehole

As for 100% CO_2, concentration curves were yielded for a gas mixture comprising 20% CO_2 and 10% CH4. Owing to the weaker initial concentration of the gases, mixing with air had almost reached completion after 5 hours. This may indicate that the rate of transport is dependent on initial concentration of gas at source. The data also corroborated the initial statement that there was no interaction between the gases. In the absence of any catalyst to initiate oxidation of CH_4, this result was not unexpected. Furthermore the data also confirm that a mixture of CH_4 and

CO_2 does not stratify in the gas column as a consequence of the greater density of CO_2.

Figure 7.9 shows the measured $C/C_{\max}$ compared with the modelled C/C_0 for this experiment.

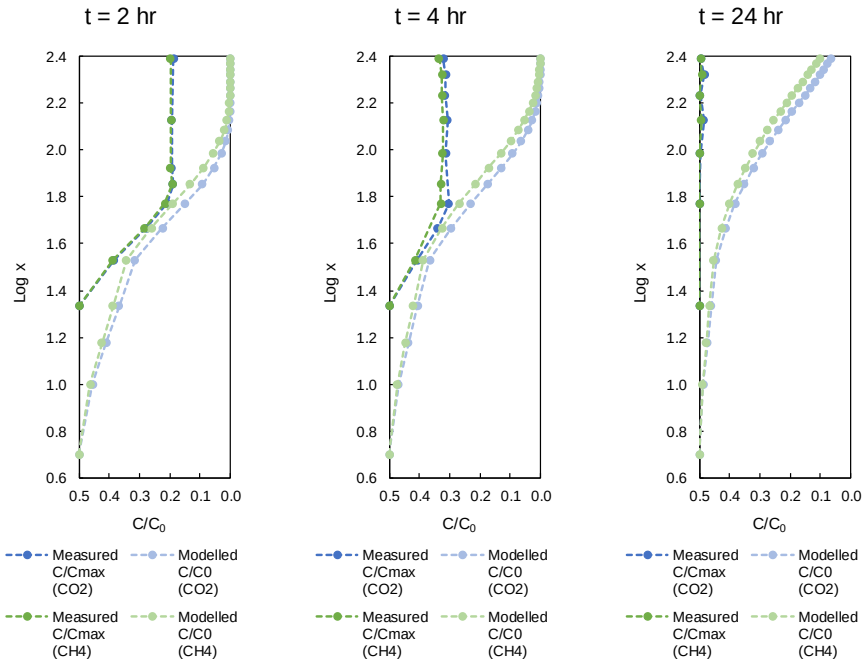

Figure 7.9: Measured $C/C_{\max}$ Comparison with Modelled C/C_0 for t = 2 hr, t = 4 hr and t = 24 hr during 20% CO_2 / 10% CH_4 in Empty Artificial Borehole Experiment

The data presented in Figure 7.9 indicate that initial concentration of gas is an important controlling factor when contrasted with the data presented in Figure 7.7. While the CO_2 and CH_4 $C/C_{\max}$ curves are the same general shape as the modelled C/C_0 curves, indicating that diffusion had occurred, the higher distances from source deviated from the modelled C/C_0 curves at t = 2 hr and t = 4 hr. The same observation was noted for 100% CO_2 at t = 24 hr as shown in Figure 7.7. The weaker initial concentration of CO_2 and CH_4 would account for this observation occurring in a shorter time period after t = 0. At t = 24 hr, both CO_2 and CH_4 measured C/C_0 are $\sim$ 0.5 indicating a uniform gas concentration of both gases throughout the column.

It may be noted that CH_4 attained a more uniform concentration throughout the column in a shorter time period than CO_2. At t = 5 hr, the concentration of CO_2 was 0.786%, 0.479% and 0.474% at a distance of 215 mm, 1,340 mm and 2,465 mm from the reservoir respectively. This compared with CH_4 which recorded concentrations of 0.390%, 0.262% and 0.266% at distances of 215 mm, 1,340 mm and 2,465 mm from the reservoir respectively. The difference in concentration of CH_4 and CO_2 at the bottom of the rig compared with the top of the rig at t = 5

hr was 0.124% and 0.312% respectively. Consequently, the starting ratio of 0.5 CH_4 / CO_2 increased to 0.56 at 2,465 mm from source at t = 5 hr. However, a more meaningful comparison of the rate of diffusion for a mixture of CH_4 and CO_2 would be acquired from a 1:1 gas mixture.

40% CO_2 / 60% CH_4 Experiment

For comparison the results from a gas mixture containing 60% CH_4 / 40% CO_2 are shown in Figure 7.10.

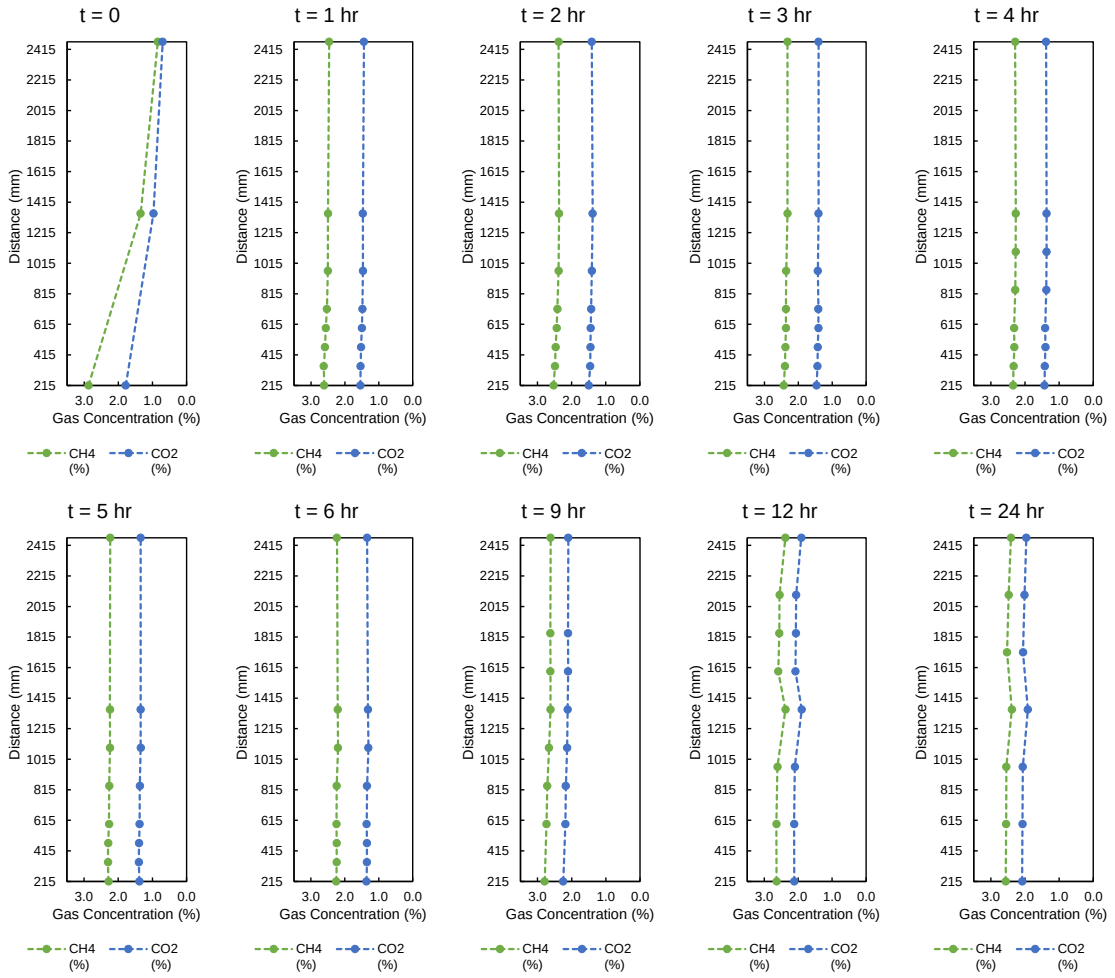

Figure 7.10: Concentration Curve for 40% CO_2 / 60% CH_4 Gas Mixture in Empty Artificial Borehole

From t = 1 hr both CH_4 and CO_2 reached their terminal concentrations of $\sim$ 2.5% and $\sim$ 1.5% respectively. Equilibrium conditions were achieved in a short space of time as a result of the rate of the initial gas injection. A slow injection building the internal pressure of the experimental rig gradually over 20 minutes was not achieved. The injection took place over 5 minutes. This likely induced a large pressure gradient that caused CH_4 and CO_2 to advect in less than an hour.

It should be noted that there was a slight problem with the GC-MS analysis of samples. Between t = 0 and t = 6 hr, the ratio of CH_4 / CO_2 was 1.67, which was greater than expected for a 60:40 mixture. For t = 9 hr to t = 24 hr (a separate GC-MS run) the ratio between the gases had reduced to 1.25. This was most likely due to a calibration error. A repeat analysis of these samples would be required to check the calibration of the GC-MS to ensure the reliability of the data.

In this experiment, a leak in the artificial borehole occurred at sample ports 10 and 19 (1,340 mm and 2,465 mm from source) which may have affected the differential pressure and may have induced a flow which could also account for the uniformity of the data. (See Appendix Figure L.6 for artificial borehole performance.) It is interesting to note that the diffusion curves obtained for t = 12 hr and t = 24 hr have a kink in them at 1,340 mm and 2,465 mm from source (i.e. where the experimental rig was leaking and losing pressure). This may represent an advective element of gas transport.

7.4.2 Artificial Borehole Filled with Leighton Buzzard Sand Data

100% CO_2 Experiment

For comparison, 100% CO_2 and the 60% CH_4 / 40% CO_2 gas mixture were individually tested in the artificial borehole filled with Leighton Buzzard Sand. The specification of the Leighton Buzzard Sand may be found in Appendix Figure L.18, and Tables L.1 and L.2. The particle size distribution showed that the sand was very well sorted while moisture testing revealed a residual moisture of 0.6%. For the purpose of the investigation presented here, the sand was assumed to be dry. The choice of Leighton Buzzard Sand was designed to mimic the unconsolidated Quaternary deposits in which the Research Site 1 municipal landfill was constructed and the sand lenses that serve as gas transport corridors at Research Site 2. The experimental rig was filled with 209 l of sand. Assuming the mass of 1 l of sand was 1.5 kg, the total mass of sand contained in the apparatus was 313.5 kg. A void of 61 l was assumed to be the unfilled reservoir at the bottom of the apparatus. It was not thought that this would affect the results of the experiment.

The results of 100% CO_2 in the sand-filled artificial borehole are illustrated and compared against 100% CO_2 in the empty artificial borehole data in Figure 7.11.

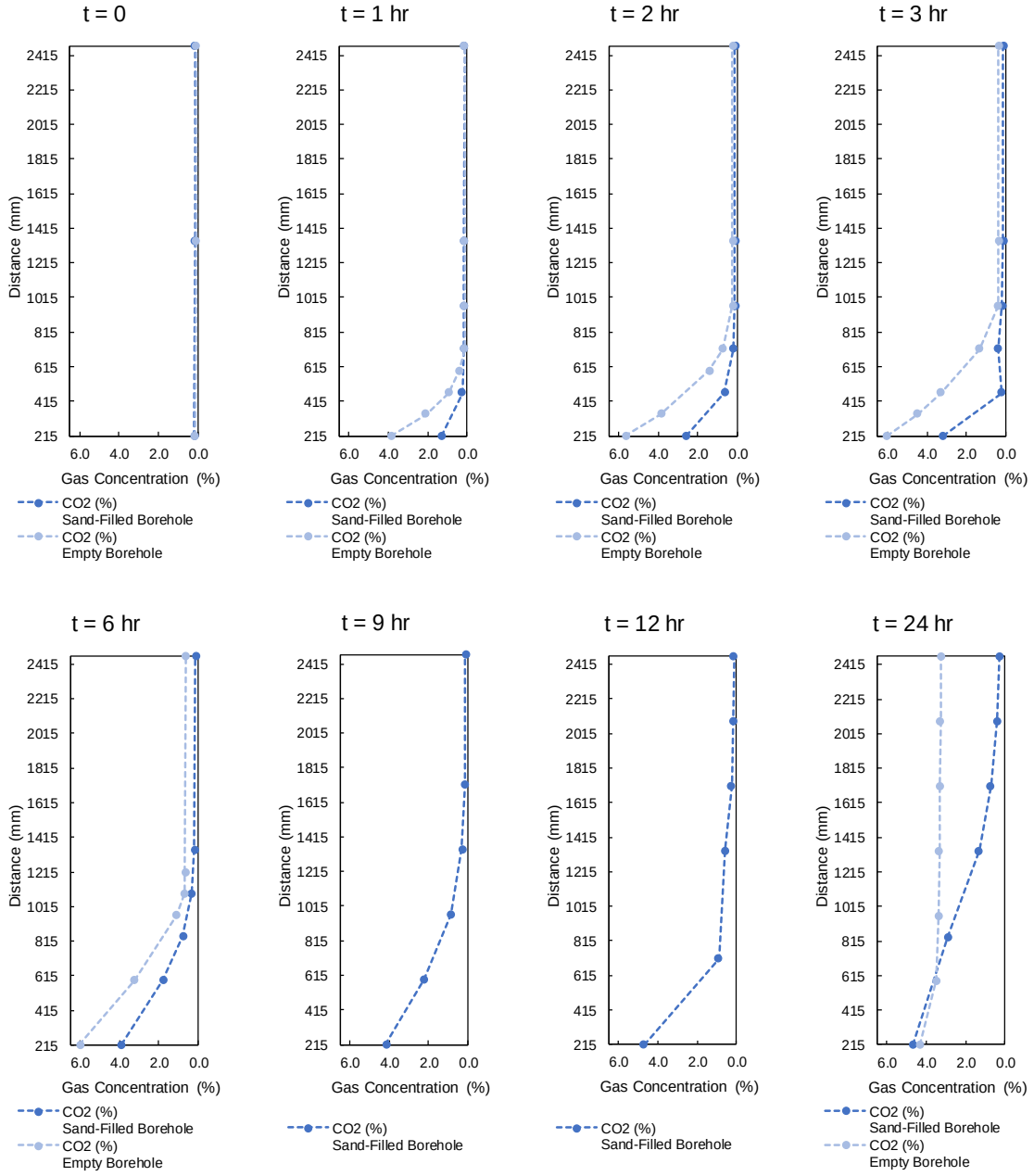

Figure 7.11: Diffusion Curve for 100% CO_2 in Artificial Borehole filled with Leighton Buzzard Sand

As for the 100% CO_2 experiment conducted in the empty artificial borehole, the repeated experiment in the sand-filled apparatus also produced diffusion curves. A greater concentration of CO_2 was yielded in the lower portion of the experimental rig when it was empty than when it was filled with Leighton Buzzard Sand. That is, a greater concentration of CO_2 diffused a given distance in a given time. For example, at t = 1 hr, the concentration of CO_2 at 465 mm from the reservoir was 0.245% in the sand-filled borehole while it was 0.920% in the empty borehole. The

concentration of CO_2 at 465 mm was 3.75 times stronger in the empty borehole than in the sand-filled borehole.

An outlier was yielded for t = 3 hr at a distance of 465 mm from the gas reservoir. This would most likely be attributed to a sampling error or a leaky exetainer. Therefore, no direct comparison may be made between the two data sets for this specific point of measurement. However, it is possible to compare t = 3 hr for 715 mm from the gas source. In the empty artificial borehole, a CO_2 concentration of 1.34% was recorded, while at the same moment in time for the sand-filled artificial borehole, a concentration of 0.392% CO_2 was produced. This amounted to a difference of 3.41% for the two data sets at this point. This amounted to a similar value as was mentioned for t = 1 hr at 465 mm from gas source.

A repeat sampling for t = 12 hr would be required for the lower distances from gas source as there is currently a 'kink' in the curve. A greater number of sample ports sampled lower down the column would fully resolve the transport curve for this moment in time.

Perhaps the most stark contrast in diffusion curves between the empty artificial borehole and the sand-filled artificial borehole was produced at t = 24 hr. Where the empty artificial borehole produced a near homogenised CO_2 concentration throughout the length of the column, the sand-filled artificial borehole showed a larger range of CO_2 concentration. In the empty artificial borehole at t = 24 hr, the maximum CO_2 concentration was 4.31% at 215 mm from gas source and decreased to 3.26% at 2,465 mm from gas source. This was a CO_2 range of 1.05%. By comparison, the sand-filled artificial borehole at t = 24 hr, produced a 4.68% CO_2 concentration at 215 mm from gas source and a 0.267% CO_2 concentration at 2,465 mm from gas source (a range of 4.41%). Undoubtedly further testing would be required to determine the exact resistance that Leighton Buzzard Sand causes to gas transport.

Figure 7.12 shows the measured $C/C_{\max}$ for the 100% CO_2 in sand-filled borehole experiment compared against the measured $C/C_{\max}$ for the 100% CO_2 in empty borehole experiment and modelled C/C_0. When compared against the $C/C_{\max}$ for the 100% CO_2 in empty borehole experiment and the modelled C/C_0, the $C/C_{\max}$ for the sand-filled borehole experiment consistently underestimated the modelled and empty borehole experimental data. The overall shape of the curve suggested that diffusion was still the driving transport mechanism. A slower diffusion profile was produced from the impedance presented by the sand. An increase in tortuosity in diffusion path of CO_2 molecules resulted from the sand grain matrix. This would have produced the underestimate compared with the modelled data. At t = 24 hr, a big deviation between the $C/C_{\max}$ empty borehole curve and $C/C_{\max}$ sand-filled

borehole curve was observed. Where the $C/C_{\max}$ empty borehole curve implied a near-uniform concentration of CO_2 throughout the borehole at t = 24 hr, the $C/C_{\max}$ sand-filled borehole curve demonstrated a much slower diffusion rate.

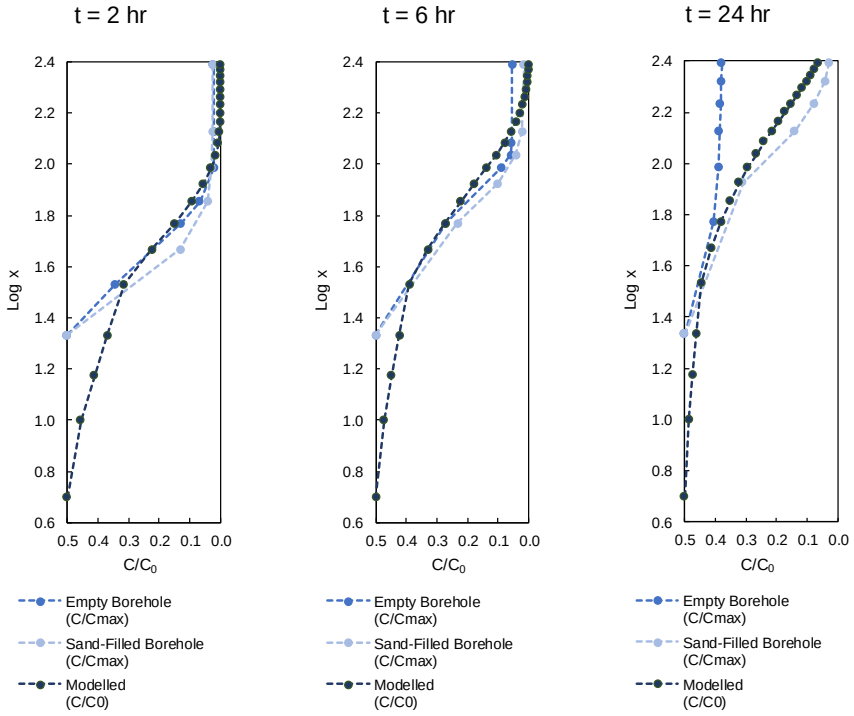

Figure 7.12: Measured $C/C_{\max}$ for 100% CO_2 in Sand-Filled and Empty Borehole Experiments Compared against Modelled C/C_0 for t = 2 hr, t = 6 hr and t = 24 hr

40% CO_2 / 60% CH_4 Experiment

Figure 7.13 shows the results of 40% CO_2 / 60% CH_4 diffusion in Leighton Buzzard Sand-filled artificial borehole. No direct comparison may be made with the diffusion profiles acquired from the empty apparatus for previously mentioned reasons. These data provide an interesting interpretation challenge.

Although in the lower half of the apparatus, CH_4 concentration exceeded CO_2 concentration, CO_2 was recorded at 2,465 mm from source ahead of CH_4. CH_4 was only first recorded at 2,465 mm at t = 9 hr. This contravened the expected modelled outcome according to Figure 7.1. Removal of CH_4 from the system may have been occurring. If, for example, the sand was not pristine, there would be potential for microbes to exist and consume CH_4. However, aerobic conditions existed in the apparatus, ruling out the possibility of anaerobic digestion of CH_4 by microbes. Further analysis of the Leighton Buzzard Sand to determine the presence of microbiological cultures may be required to rule out decomposition. An alternative to microbial degradation of CH_4 could be a reaction between CO_2 and iron(III) oxide

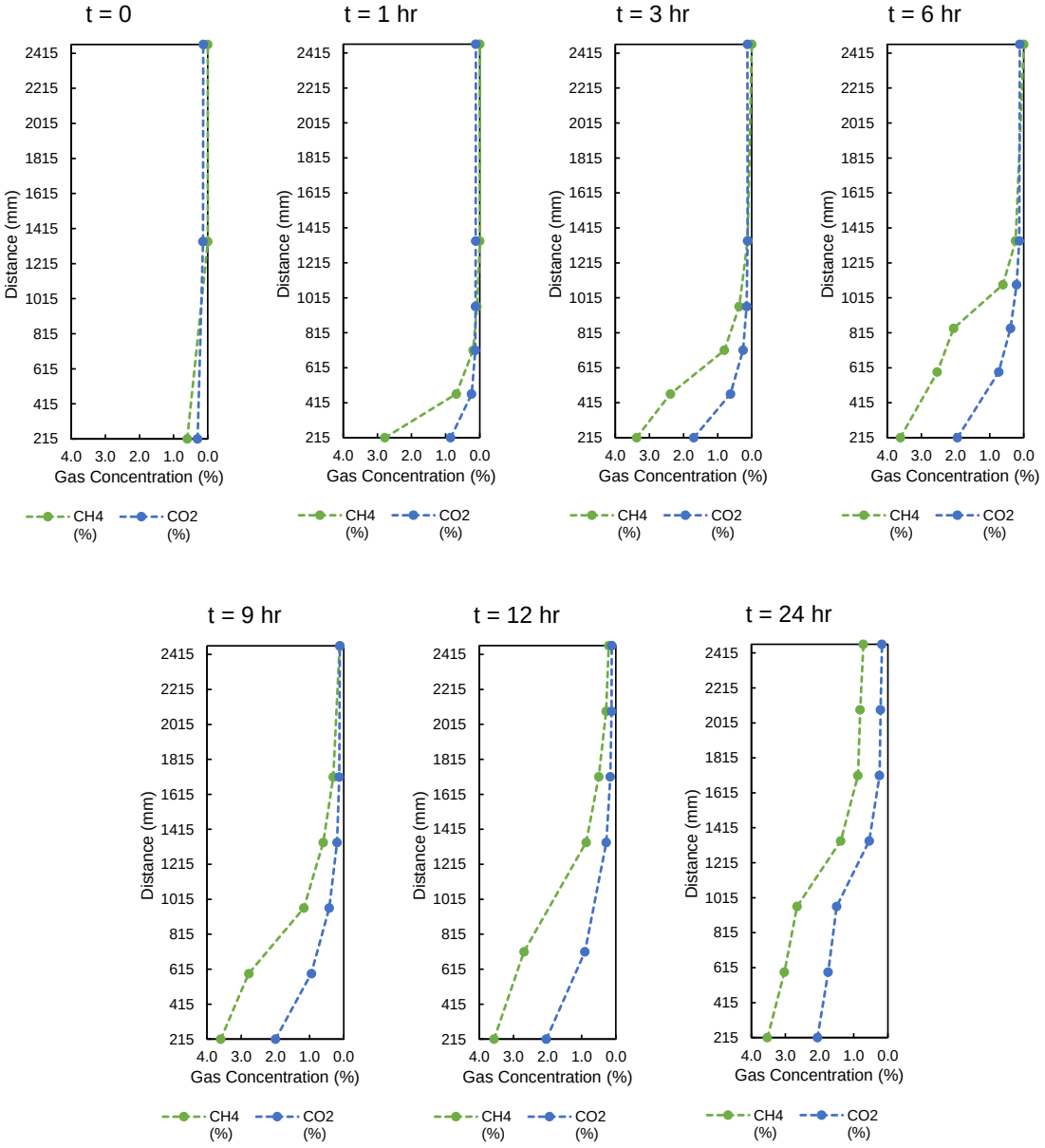

Figure 7.13: Diffusion Curve for 40% CO_2 / 60% CH_4 Gas Mixture in Artificial Borehole filled with Leighton Buzzard Sand

(Fe_2O_3) that coats the Leighton Buzzard Sand grains. It is the Fe_2O_3 that gives the sand its distinctive red colour. A simple experiment passing CO_2 at constant pressure through a sample of Leighton Buzzard Sand could determine if a reaction occurs by observing a colour change (i.e. Fe(III) (red) reduced to Fe(II) (green)).

Further evidence of this possibility is due to the fact the CH_4 transport curve is kinked from t = 3 hr onwards. This resulted in the ratio of CH_4:CO_2 deviating away from the initial 1.5 that was injected into the reservoir. For example, the ratio of CH_4 / CO_2 at t = 3 hr, at 465 mm distant from gas source was 3.8, while at t = 6 hr, 840 mm distant from gas source, the CH_4 / CO_2 ratio was 5.3. If the CH_4 was being degraded, a decrease in CH_4 concentration would be anticipated with a

corresponding reduction in CH_4 / CO_2 ratio. The reverse was observed. Therefore it was thought to be highly unlikely that this process was occurring.

Other reasons why the CH_4 diffusion curve may have been kinked were postulated. Firstly, the kink may be a result of compaction of sand in the lower apparatus resulting from the weight of material above. However, the position of the kink in the curve was not uniform and varied over time, so this may also be an unlikely explanation. Furthermore, if compaction were a factor, the CO_2 diffusion curve would be expected to exhibit the same behaviour. There was no evidence of the CO_2 diffusion curve kinking until t = 24 hr. A further and more likely reason could be the result of a calibration error in the GC-MS instrument or drift in ion response over the course of the analyses.

Perhaps the most viable explanation for the observed data pattern could be that a mixture of diffusion and advection had taken place. The kink in the concentration curve may represent an element of advection in the transport of CH_4. This would also account for the 9 hr time lag observed for the first occurrence of CH_4 at 2,465 mm relative to CO_2. If this theory is true then it could be argued that an element of a gas frontal system exists. However, if transport of gases was exclusively resulting from advective flow, the ratio of CH_4 / CO_2 would have remained consistent throughout the experiment. The fact that the ratio of CH_4 / CO_2 fluctuated over time more strongly supports the argument for diffusive flow of gases. It would be a useful exercise to repeat this particular experiment to see if the data are reproducible and test their robustness.

Figure 7.14 compares the measured $C/C_{\max}$ against C/C_0 for CO_2 and CH_4. The modelled C/C_0 poorly predicted the measured $C/C_{\max}$ throughout the experiment. The shape of the $C/C_{\max}$ curves consistently did not match the modelled diffusion curves. This implied that diffusion was not the dominant transport mechanism for this experiment.

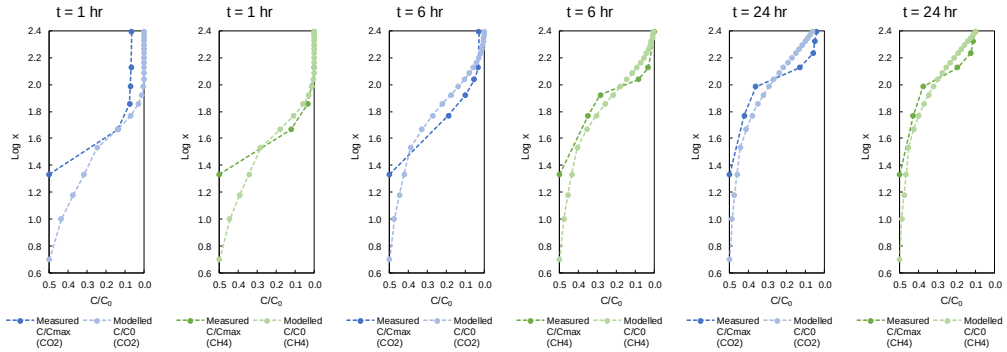

Figure 7.14: Measured $C/C_{\max}$ for CO_2 and CH_4 during 40% CO_2 / 60% CH_4 in Sand-Filled Borehole Experiment Compared against Modelled C/C_0 for t = 1 hr, t = 6 hr and t = 24 hr

7.5 Discussion and Development of Conceptual Model

Gas transport was tested in an experimental rig in air as a reference and in Leighton Buzzard Sand as an analogue for unconsolidated Quaternary Deposits such as those encountered at research Sites 1 and 2. The motivation for designing and constructing a large-scale experiment was to test the mechanism of gas transport in the near-surface unsaturated zone. It was important that the conceptual model design could predict lateral transport (and the rate of lateral transport). Field evidence of diffusive transport was observed at Site 3 for monitoring wells GM5 and GM14 as discussed in Chapter 4 and shown in Figure 4.10. The observed pattern was hypothesised to be as a result of diffusion of CO_2 up the gas column or stratification of CO_2 owing to its low buoyancy.

The data reported here suggest that in a closed system in air and in unconsolidated (sorted) material, the transport of CH_4 and CO_2 is primarily by diffusive transport. A refinement was made to the conceptual model by showing diffusion (dashed) arrows through the Quaternary Deposits. No conclusions could be drawn about the mechanism of gas transport in the Permo-Triassic bedrock or the Carboniferous bedrock and so these arrows remain unchanged in the conceptual model. However, these data must be treated as preliminary only and further testing would be required to confirm, dispel or refine the theories reported here.

The data appeared to support historic gas monitoring data from Research Site 3. Site 3, located in the London Basin, has a geology comprising 55.8 m of Upper Chalk and 69.2 m of Middle Chalk dating from the Cretaceous Period. Chalk has dual porosity derived from its own matrix and secondarily through fractures. It is a good aquifer and may transport gas as well as groundwater. Boreholes GM 5 and GM 14 (a closed system) at Site 3 showed an increase in CO_2 concentration with increasing depth from surface (Chapter 4 Figure 4.10).

Assuming no dissolution of CO_2 in groundwater, the historic gas monitoring data for these boreholes appear to show a gradient of CO_2 concentration from strong concentration at depth to weak concentration near the ground surface. It could be argued that this indicated a diffusion of CO_2 from the landfill through the Chalk. It would be a useful exercise to conduct a time-series analysis on these boreholes following a pumping of CO_2 into the ground gas regime (i.e. during falling atmospheric pressure) to produce a changing diffusion profile over time.

A refinement of the conceptual model design based on the findings of the gas transport mechanics data is shown in Figure 7.15.

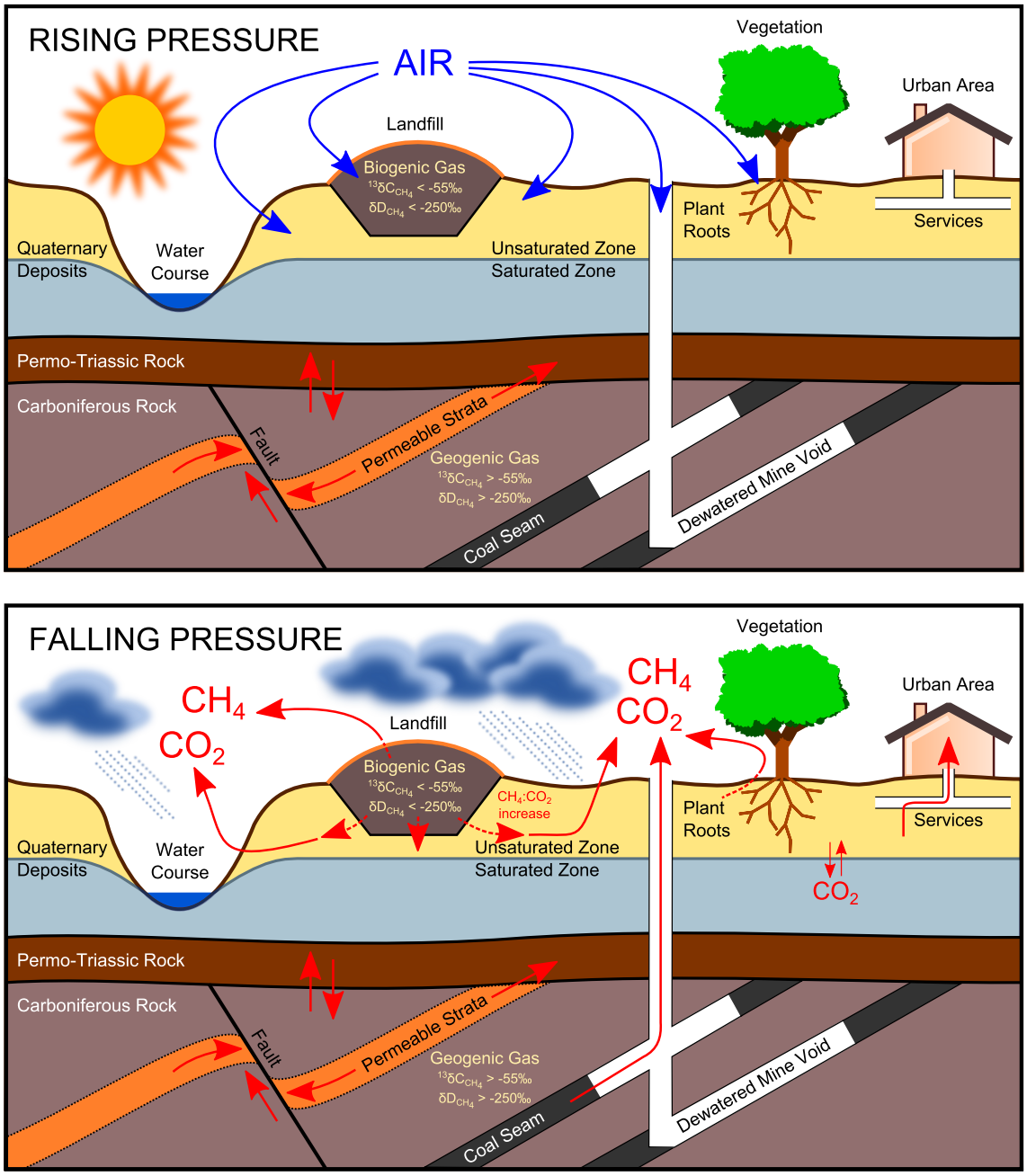

Figure 7.15: Refined Conceptual Model Design Incorporating Gas Transport Mechanics

Contrary to the data illustrated in this chapter, in an open system Gebert and Gröngröft (2006) asserted that gas transport was conveyed by advection in a study of the operation of methane-oxidising biofilters on German landfill sites and the influence of barometric pressure. Gebert and Gröngröft (2006) determined that diffusive flow of ground gas was a highly inefficient transport mechanism and that advection was more efficient in response to changes in atmospheric pressure. They also observed that gas emission was sensitive to atmospheric pressure changes as low as 1 mbar. This observation is not dissimilar to the findings of the high temporal frequency data discussed in Chapter 5 (e.g. Figure 5.4).

While the data reported in this chapter indicated that diffusion is a quick process, advective mixing may subsequently take over. In the exchange of ground gases from the geosphere to the atmosphere, diffusion may be less important than advection. Figure 7.16 shows a diffusion conceptual model for a closed system. The unconsolidated deposits provide a porous medium for gas transport. In this conceptual model, the unconsolidated layer is confined by an impermeable layer (e.g. clay) that isolates the system from atmospheric pressure change. Consequently, diffusion of ground gases is more likely to be the dominant transport mechanism. Diffusion is assumed to be random. Dashed arrows in Figure 7.16 indicate diffusive flow. The data from this chapter indicated that by this process, the ratio of CH_4 / CO_2 increases owing to the greater buoyancy of CH_4.

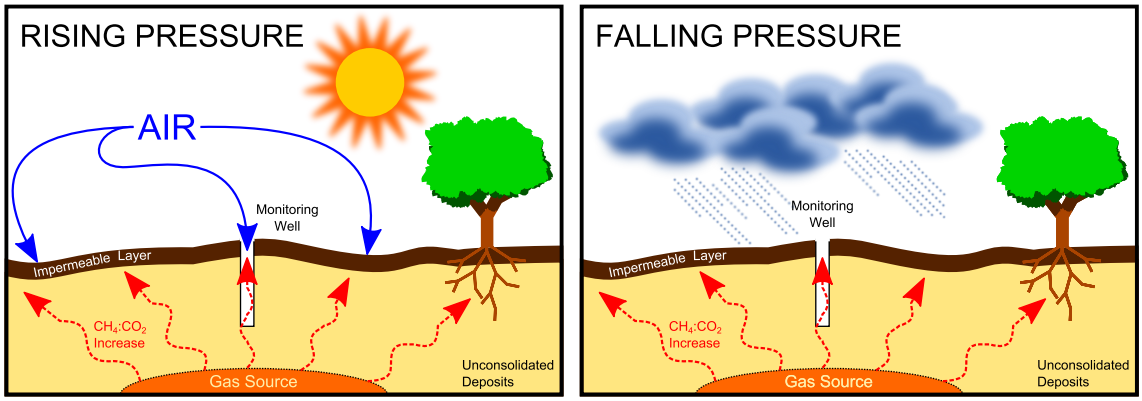

Figure 7.16: Diffusion Conceptual Model

Figure 7.17 presents an alternative conceptual model of ground gas dynamics. It indicates a gas concentration frontal system driven by advection which in turn is responsive to changes in atmospheric pressure.

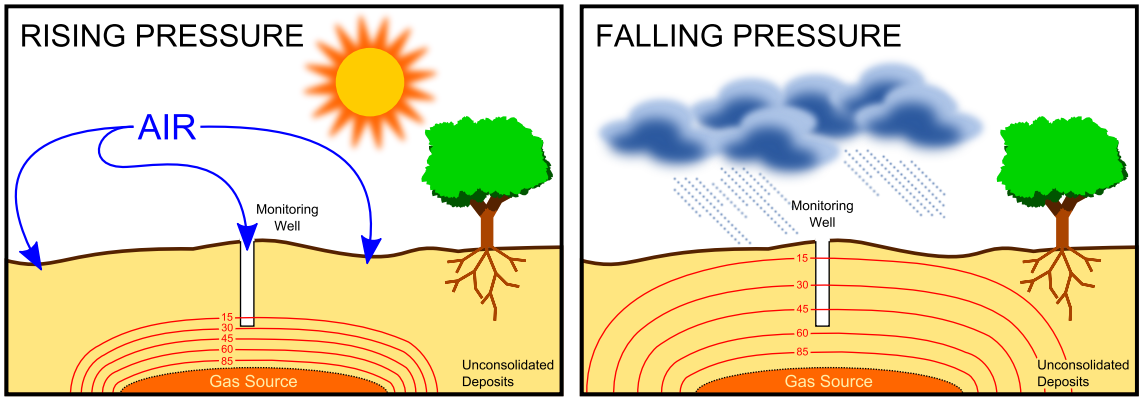

Figure 7.17: Advection Conceptual Model with Contours Indicating Relative Gas Concentration

A useful feature of a large-scale experiment such as this is that there is great potential for further work with increasing layers of complexity. Further research questions arising from this chapter and suggestions for future work are as follows:

- Add a sample port to the gas reservoir at the bottom of the artificial borehole. There was a need to measure C_0 in the experiments. If C_0 could be measured accurately, it would be possible to conduct a direct comparison of the experimental data with the modelled data;
- Refine the modelled data for diffusion of a substance initially confined in the region $-h < x < +h$. The integration is from $x - h$ to $x + h$ instead of from x to ∞ as demonstrated in this chapter. According to Crank (1979), this produces the solution shown in Equation 7.4:

$$C = \frac{1}{2}C_0\left\{erf\frac{h-x}{2\sqrt{D^{eff}\cdot t}} + erf\frac{h+x}{2\sqrt{D^{eff}\cdot t}}\right\} \tag{7.4}$$

- Model and measure gas transport by advective flow using Darcy's Law as shown in Equation 7.5 (McBean et al., 1995):

$$q = -K_g\frac{dh}{dx} \tag{7.5}$$

  Where:
  q = specific discharge of macroscopic velocity of gas (m/s).
  K_g = conductivity (m/s).
  h = piezometer height.
  x = length in the direction of flow (m).
- Model and measure gas transport using a combined advection/diffusion model. A likely scenario is that both transport processes occur simultaneously. A typical approach noted by McBean et al. (1995) is to combine Darcy's Law with a mass conservation equation as shown in Equation 7.6:

$$\frac{\partial C}{\partial t} = \frac{\partial^2 (DC)}{\partial x^2} - \nu\frac{\partial C}{\partial x} \pm S \tag{7.6}$$

  Where:
  C = gas concentration (mole fraction/m^3).
  t = time (s).
  D = dispersion coefficient m^2/s.
  x = length in the direction of flow (m).
  ν = macroscopic velocity of flow (m/s).
  S = source, sink, or decay constant.
- Determine the effect of the initial starting pressure on the rate of diffusion of CH_4 and CO_2 in the gas column;
- Determine the effect of the initial starting concentration of ground gases on the rate of diffusion;

- Determine the effect of different media on the rate of gas diffusion. For example, it would be useful to test CH_4 and CO_2 diffusion in finer-grained sands, less sorted sands and coarser-grained sands;
- Determine the effect of the rate of gas diffusion for multi-layered different media (i.e. increasingly complex unconsolidated strata layers);
- Determine the effect of the degree of saturation on the diffusion of gases in the near-surface environment. What is the critical saturation where the maximum concentration of CO_2 is 'scrubbed' from the system (dissolved in solution) is achieved;
- Determine the effect of a temperature gradient have on the rate of CH_4 and CO_2 diffusion in the gas column;
- Determine the effect of natural microbial colonies on CH_4 and CO_2 diffusion in the gas column, and;
- For a given strata, is it possible to predict the rate of lateral transport of ground gases away from source (such as a municipal landfill), the maximum distance of transport and the likely terminal concentration by diffusion models.

In this context, the experimental apparatus and methodology present a promising tool for investigating gas transport mechanics in the near-surface environment. The data provide a useful pilot study and show that the experimental apparatus and general methodology perform as anticipated. A preliminary conceptualisation of gas transport has been started. Modelling of CO_2 diffusion in air was successful. On addition of an impedance to gas flow, the rate of mass transport was reduced due to an increase in tortuosity in molecule transport path. Consequently, on a larger scale, advection may be more important than diffusive flow. Further research as noted above may be conducted to build on the initial findings and concepts demonstrated in the data.

Chapter 8

Discussion and Conceptual Model

8.1 Context of the Research in the Literature

Gas Monitoring Data

The high temporal frequency gas monitoring data identified the same groupings of gas compositions demonstrated by the ternary diagrams produced from the historic gas monitoring data (Chapter 5, Figures 5.6, 5.7 and 5.10). Historic gas monitoring data for Site 1 BH 03/4 indicated that landfill gas emission was linked to changes in atmospheric pressure (Chapter 4, Figure 4.2 and Table 4.1). The high temporal frequency gas monitoring data captured from this borehole corroborated this observation (Chapter 5, Figures 5.4 and 5.5). For example, when the ambient pressure decreased 4 mbar over 16 hours (average 0.25 mbar/hr) on 8th November 2013, it induced a positive borehole flow in Site 1, BH 03/4, and introduced CO_2 and CH_4 gases into the borehole. Peak CH_4 and CO_2 during this emission event was recorded at 29.0% and 7.9% respectively (Chapter 5, Figure 5.4 and Table 5.2). When ambient pressure increased, negative borehole flow conditions resumed and the borehole gas composition was air.

The change in gas composition in Site 1 BH 03/4 (Chapter 5, Figures 5.4 and 5.5) occurred as a result of small atmospheric pressure changes (typically 6 mbar or less) over short periods of time (typically less than 12 hours, but in some examples, the time-frame was under 4 hours), equating to pressure gradients that were generally less than 1 mbar/hr and in some instances, pressure gradients less than 0.25 mbar/hr were encountered. The highest pressure gradient recorded was 1.55 mbar/hr and occurred on 2nd November 2013. These observations tended to agree with Gebert and Gröngröft (2006) who recorded the same phenomenon as a result of atmospheric changes as low as 1 mbar on a passively vented landfill site. Gebert and Gröngröft (2006) noted that changes are immediate and highly sensitive, resulting in a highly

variable flow rate (in both directions) and concentration of CH_4 and CO_2 gases.

Although flow rate was not measured in this study, the difference between internal borehole pressure and ambient atmospheric pressure was calculated. This varied between −15 and +10 mbar in response to changes in atmospheric pressure. This served as a useful analogue for borehole flow. A positive pressure difference occurred when atmospheric pressure decreased and internal borehole pressure was greater than atmospheric pressure. The changes in pressure difference generally inversely mapped onto variations in atmospheric pressure (Chapter 5, Figure 5.4 and 5.5).

Other authors who have previously noted a strong positive correlation between negative atmosperic pressure gradient and gas emission from the near-surface include: Czepiel et al. (2003), Scheutz et al. (2009), Gebert et al. (2011) and Rachor et al. (2013). However, Christophersen et al. (2001) did not consider atmospheric pressure to be an important factor. It could be that ground conditions for the site studied by Christophersen et al. (2001) were not in good connectivity with atmospheric pressure (e.g. impermeable, consolidated media).

Alternative techniques for measuring landfill gas emissions include the mobile tracer dispersion method. This method combines a controlled release of a tracer gas with downwind landfill gas concentration measurement conducted using a mobile high resolution analytical instrument such as a cavity ring-down spectrometer (Mønster et al., 2015). In a study of 15 Danish landfills of varying age, Mønster et al. (2015) demonstrated that CH_4 emissions ranged from 2.6 to 60.8 kg/hr, with the lowest emissions from the older and smaller landfill facilities and the highest emissions from the newer and larger landfill facilities. These emissions were recorded during stable atmospheric pressure conditions (i.e. little variance in wind speed and direction, and small changes in atmospheric pressure) and perhaps it would be useful to replicate this experiment on the study sites explored in this research. It would be particularly interesting to examine the research sites using this method (or equivalent) in changing atmospheric pressure conditions to compare with the GasClam instrument data.

Similarly to Mønster et al. (2015), Delkash et al. (2016) measured landfill CH_4 emissions coupling an atmospheric infra-red sounder with the tracer dilution method. While the positive correlation between CH_4 emission and negative atmospheric pressure gradient was observed, the AIRS data had some deviations from the field measured TDM data. However, due to the uncertainties in the TDM, the AIRS data could not be accurately calibrated (Delkash et al., 2016). Despite the uncertainties in the data, Delkash et al. (2016) reported correlations ranging from $r^2 = 0.54$

to 0.67 between barometric pressure and CH_4 landfill emissions using the AIRS method. In the context of the results in the literature, it is clear that different analytical techniques corroborate the correlation between atmospheric pressure and ground gas emission from the near-surface environment. There is some variance in the correlations reported, but this could be an artefact of the difference in specific local conditions.

Determination of Gas Source

Gas samples were collected from research Sites 1 and 2 and were referenced against mineshaft vent gas samples and North Sea Gas. Referencing the research samples against published data from Golding et al. (2013), it was possible to ascertain gas sources. Landfill gas samples from Site 1 along with Site 2 cell gas and flare gas showed depleted $^{13}\delta C_{CH_4}$ and δD_{CH_4} ratios ($< -60‰$ and $< -250‰$ respectively) consistent with acetoclastic reactions (Flores et al., 2008).

Relative to the landfill gas samples, Site 2 perimeter monitoring well gas samples showed an enrichment in both ^{13}C and D that was not consistent with a biogenic gas origin. Site 2 borehole gas samples ranged from -55.6 to -48.0‰ $^{13}\delta C_{CH_4}$ and -173 to $+55.0‰$ δD_{CH_4}. Further research would be required to ascertain the microbial and/or thermogenic processes that could lead to a heavy enrichment in D. The range of ^{13}C ratios was consistent with thermogenic sources reported by Martini et al. (1998) and McIntosh et al. (2002) for Antrim and New Albany Shales, USA; and Osborn and McIntosh (2010) for northern Appalachian Basin Shales, USA.

Typically, thermogenic CH_4 is relatively enriched in ^{13}C and D as the stable isotope ratios produced in this research have shown. However, biogenic CH_4 may also have $^{13}\delta C_{CH_4}$ that lie within the established thermogenic range (Owen et al., 2016). Processes that may produce CH_4 enriched in ^{13}C and D include acetoclastic methanogenesis (Golding et al., 2013), shifts in seasonal availability of substrate (Moura et al., 2008), enrichment of the CO_2 pool as a result of on-going methanogenesis (Whiticar, 1999), and anaerobic or aerobic oxidation of CH_4 (Tsunogai et al., 2002).

For example, in a recent study, Owen et al. (2016) reported CH_4 stable isotope ratio for deep coal seam gas (200–500 m) of -58 to $-49‰$ for the Walloon Coal Measures, Australia. The shallower coal gas CH_4 underlying the Condamine River alluvium produced $^{13}\delta C_{CH_4}$ values -80 to $-65‰$ (Owen et al., 2016). Consequently, Owen et al. (2016) concluded that there was no CH_4 migration from the deep coal gas reservoir to the shallower formations due to the depleted $^{13}\delta C_{CH_4}$ values obtained. An important conclusion to be drawn from this study is that thermogenic $^{13}\delta C_{CH_4}$

end member may not be the most appropriate ratio to use. Owen et al. (2016) reported variable ratios within the same formation as a consequence of differing hydrogeological and microbial conditions. Therefore, alternative and/or additional isotope measurements may be required to substantiate gas origins.

This issue was particularly pertinent to the Abbeystead disaster in 1984 as the source of the CH_4 was largely thought to be geogenic in origin due to absence of ^{14}C in gas samples (HSE, 1985). However, the contribution of newer biogenic gas could not be ruled out as sludge and slime deposits within the tunnel complex at Abbeystead were found to have methanogenic organisms through culture testing. However, the CH_4 generating potential of these deposits was thought to be substantially lower than the Bowland Shales (HSE, 1985). The analysis of trace gas components contained in gas samples may be used to further differentiate the source of gases between biogenic and geogenic.

From a regulation perspective, stable isotopes in conjunction with radiocarbon dating could be used to determine gas source. While stable isotopes should be sufficient to differentiate gas sources in most cases, in the case of Site 2, it was unclear where the gas source had originated from. For examples such as Site 2, radiocarbon dating may be needed to fully clarify gas sources.

This is particularly pertinent for regulation, especially in the case of Site 2, as the site owner/regulator would need to know if they were responsible in the event of a gas leak. Following the Loscoe Landfill Gas explosion in Derbyshire, UK, 1986, radiocarbon dating determined that the gas that had caused the explosion had originated from the landfill 70 m distant from the houses (Williams and Aitkenhead, 1991). However, the cost of radiocarbon dating is far greater than stable isotope analysis and may not be economically viable in some instances (Hitchman et al., 1989).

According to Boltze and de Freitas (1997), in the preceding 7 hours before the Loscoe Explosion in 1986, the atmospheric pressure dropped 29 mbar (∼4 mbar/hr). Williams and Aitkenhead (1991) noted that such extreme pressure drops occur once every 6 years. By comparison, Massmann and Farrier (1992), observed that more than 50% of observations over a 6 hour period were the result of pressure changes of no more than 5 mbar (0.83 mbar/hr). The much smaller rate of change reported by Massmann and Farrier (1992), was more in line with data reported in Chapter 5 by high temporal frequency gas monitoring. For example an inverse pressure gradient of 0.81 mbar/hr on 5th November 2013 resulted in peak concentrations of 40.1% CH_4 and 7.9% CO_2 in BH 03/4, Site 1.

However, Site 1 BH 03/4 demonstrated much greater sensitivity to atmospheric pressure than either Boltze and de Freitas (1997) or Massmann and Farrier (1992) reported. For example, peak CH_4 and CO_2 40.6% and 4.5% respectively were recorded on 7th August 2013 resulting from an inverse 0.17 mbar/hr pressure gradient. Over an 18-hour-period, the atmospheric pressure dropped 3 mbar. Similarly on 10–12th August 2013, an inverse pressure gradient of 0.20 mbar/hr induced peak CH_4 and CO_2 concentrations of 54.4% and 7.4% respectively. During this sustained emission event, the atmospheric pressure decreased by 7 mbar over a 35-hour-period. Similar observations were made in the autumn when peak CH_4 and CO_2 concentrations of 35.3% and 8.5% respectively resulted from an atmospheric pressure gradient of -0.25 mbar/hr on 9th November 2013. During this gas emission event, the atmospheric pressure decreased by 3 mbar over 12 hours.

These data imply that this particular system is so sensitive to pressure gradient and length of time over which atmospheric pressure decreases, that the magnitude of both these variables is almost irrelevant. This is likely to be a consequence of the unsaturated zone of Site 1 being comprised of a thick layer (*sim* 30 m) of Middle Sands (Quaternary) that is highly porous and permeable, thus permitting the easy transport of gas. Consequently, for sites of similar geological setting as Site 1, the data indicate that the transport and emission of ground gases may be more sensitive to changes in atmospheric pressure than both Boltze and de Freitas (1997), and Massmann and Farrier (1992) considered.

Gas Transport Mechanics

Gas transport mechanisms for CO_2 and CH_4 in the unsaturated zone was modelled by diffusion using Fick's Law (Equation 8.1).

$$\frac{C}{C_0} = \frac{1}{2}\left(erfc\frac{L}{2\sqrt{D^{eff}\cdot t}}\right) \tag{8.1}$$

An experimental rig called an 'artificial borehole' was used to test gas diffusion. A sealed apparatus, the artificial borehole could be viewed as a closed-system and not influenced by changes in ambient conditions. Gases injected into the artificial borehole reservoir located at the base of the apparatus were continually measured through sample ports up the side of the column in order to ascertain the gas/air interface change over time.

The data shown in Chapter 7 Figures 7.6, 7.7, 7.8 and 7.9 demonstrated that when the borehole was empty, gas transport for both CH_4 and CO_2 was governed by diffusive flow as the measured data closely agreed with the modelled data. How-

ever, when sand was added to the borehole apparatus, the rate of diffusion was significantly reduced owing to an increase in tortuosity of CH_4 and CO_2 paths. Furthermore, in an experiment conducted using a 60% / 40% gas mixture of CH_4 and CO_2, the ratio of CH_4 / CO_2 increased from 1.5 to 3.0 suggesting that CH_4 diffusion was less impeded by the sand. The measured transport curve differed significantly for the modelled diffusion curves in air (Chapter 7, Figure 7.14).

The concentration curves yielded in Chapter 7, Figures 7.6, 7.7, 7.11 and 7.12 could be used to interpret the gas compositions for Site 3 BHs GM5 and GM14 which show increasing CO_2 concentration with increasing depth (Chapter 4, Figure 4.10). The increasing CO_2 concentration with depth is resultant from advective transport of CO_2 gas from source towards the surface, slowly over time through the Quaternary deposits, as shown in the advection transport conceptual model (Chapter 7, 7.17).

Diffusive transport of CH_4 and CO_2 was shown to be efficient initially (up to 6 hours). However, after 1 day, CO_2 transport was slower and uniform concentration was achieved throughout the apparatus after 1 week. Gebert and Gröngröft (2006) noted that diffusive transport was an inefficient process and that advection was the principle transport mechanism on a passively vented landfill. Gebert and Gröngröft (2006) noted that a drop in atmospheric pressure as little as 1 mbar was enough to induce landfill gas emissions. The observation that pressure changes induced changes in landfill gas flow strongly suggest that advection is a principal transport driver. When Site 1 BH 03/4 was monitored at high temporal frequency in 2013, a similar observation was noted. Pressure gradients as small as -0.7 mbar/hr (over 3 hours) were enough to induce a landfill gas emission comprised of 40% CH_4 and 9% CO_2 (Chapter 5, Figure 5.4).

However, when monitoring wells on Site 2 were monitored at high temporal frequency, none showed any relationship between atmospheric pressure, flow and gas composition. Diurnal cycling of CH_4 and CO_2 was demonstrated in response to changing temperature (Chapter 5, Figure 5.8). A key difference between Sites 1 and 2 is the composition of the unsaturated zone. Site 1 comprises $\sim$30 m of unconsolidated Middle Sands while Site 2 is predominantly Glacial Till with occasional sand lenses. Gebert et al. (2011) noted that for sites dominated by diffusive transport, soil temperature and moisture were important factors. The high temporal frequency data for Site 2 are indicative of diffusive transport as gas compositions varied in response to temperature changes. Gebert et al. (2011) also commented that the opposite is true for sites dominated by advective gas transport and that changes in gas composition are shown on all time-scales when transport is predominantly

advective. Therefore, site geology is an important factor in whether gas transport is likely to be diffusive or advective and this should be a key consideration in the conceptual model design.

Although the methodology described in this thesis can predict gas transport by diffusion as shown in Chapter 7, Figures 7.7, 7.9 and 7.12 , there is still much work to be done particularly simulating and measuring advective transport. Further testing under different conditions using the apparatus will be required. Importantly, different media with different porosities would need to be investigated in order to establish a larger data resource that can be used to refine the conceptual model. As a methodology, the artificial borehole is a useful research tool in the investigation of gas transport.

8.2 Conceptual Model Design

Figure 8.1 illustrates the final conceptual model design derived from the evidence compiled during the research. The conceptual model characterises sources of CO_2 and CH_4 contamination in the sub-surface and demonstrates migration pathways that may pose hazards to property and life.

Encapsulating two common sources of ground gases, the conceptual model demonstrates the source of CH_4 and CO_2 from landfill and dewatered mine voids. Although mine void gas was not examined in this research, Hall (2007) demonstrated that mine gas emissions were subject to rises and falls in atmospheric pressure. Furthermore, there have been historic incidents relating to mine gas such as the Arkwright Town disaster, Derbyshire, UK, 1988 and the death of Donald Tollett, Widdrington, Northumberland, UK, 1995. Therefore, it was pertinent to include mine gas hazard in the conceptual model. Other sources of ground gases not considered in this research and not incorporated into the conceptual model design include: made ground, foundry sands, sewage sludge, shale gas, natural gas plants and pipelines (leaks), wetlands, and chalk and limestone (reaction of $CaCO_3$ with acidic rainwater to evolve CO_2).

Sources of ground gases can be categorised into two broad bands: 'biogenic' (anaerobic digestion by methanogenic bacteria) and 'thermogenic' (anaerobic decomposition of ancient vegetation trapped within rock such as Coal Measures, also known as 'geogenic' gas). It is possible to differentiate biogenic and geogenic gas sources through stable isotope analysis. Biogenic gases tend to be depleted in the heavier stable isotopes of C and H (^{13}C and ^{2}H (or D)) and consequently yield lower (more negative) $^{13}\delta C$ and δD values relative to geogenic sources.

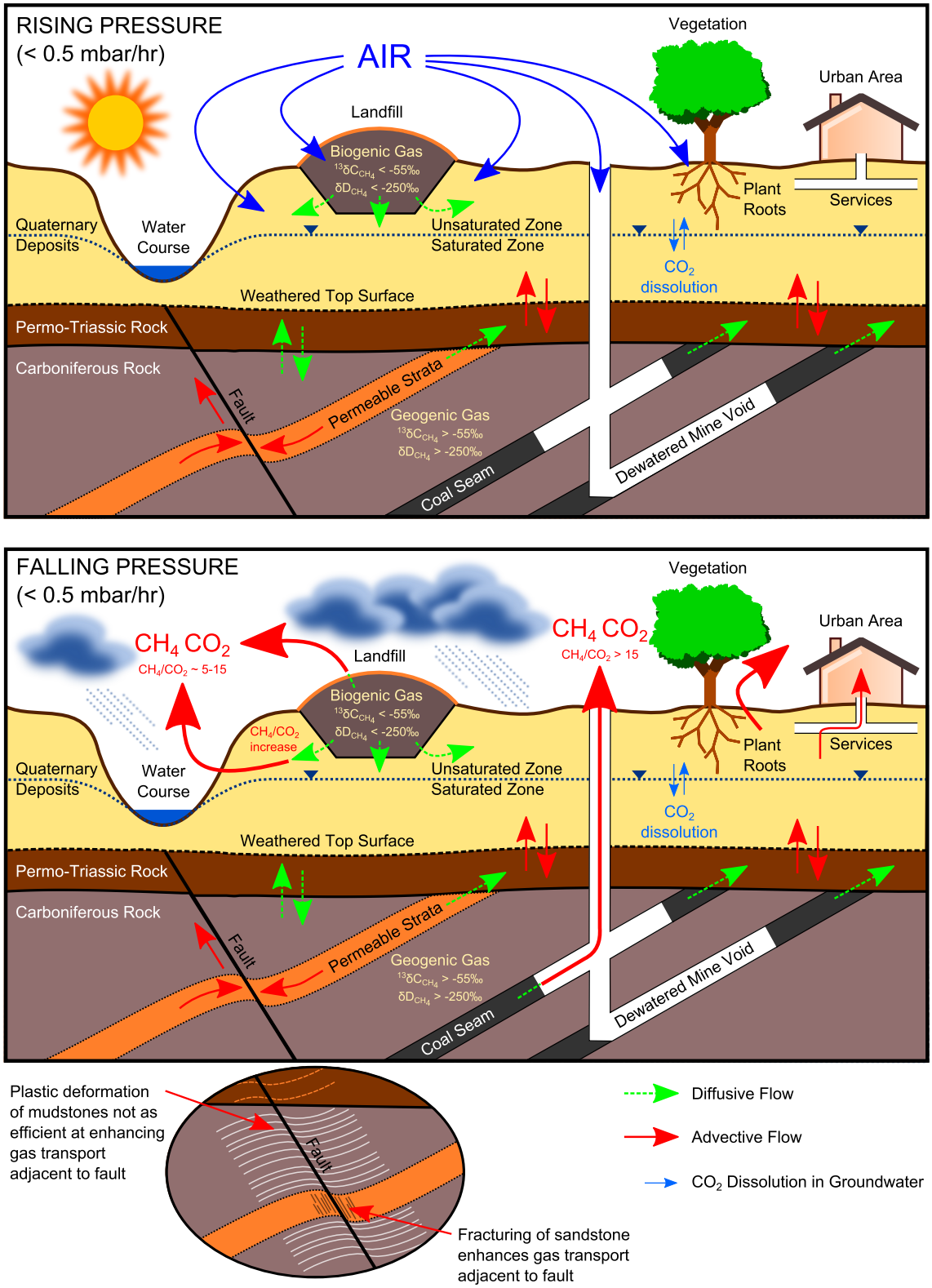

Figure 8.1: Conceptual Model Design

As a general guide, Hitchman et al. (1989) proposed that biogenic gas sources produce $^{13}\delta C_{CH_4}$ values less than $-60‰$ while thermogenic gas sources produce $^{13}\delta C_{CH_4}$ greater than $-60‰$. The data reported in Chapter 6 corroborate this

general guide to an extent. However, there were some cross-over values observed. For example, Site 1 landfill BH 03/4 yielded a $^{13}\delta C_{CH_4}$ value of −58.2‰. As a slight amendment to Hitchman et al. (1989), it was proposed that biogenic sources generally produce a $^{13}C_{CH_4} < -55$‰ while thermogenic sources generally produce a $^{13}C_{CH_4} > -55$‰. This general guide is incorporated into the conceptual model design for landfill gas (biogenic source) and coal gas (thermogenic source).

As for C stable isotopes, biogenic sources are generally depleted in the heavier H isotope (D) while thermogenic sources are relatively enriched in the heavier H isotope. All thermogenic gas sources yielded δD_{CH_4} values greater than −250‰ while all biogenic gas sources produced δD_{CH_4} values less than −250‰. For example, Site 2 landfill cell gas produced a δD_{CH_4} value −316‰ while −214‰ δD_{CH_4} was recorded for an abandoned mine shaft vent. These figures were also incorporated into the design of the conceptual model.

The prediction and measurement of CO_2 and CH_4 lateral migration in the unsaturated zone was a prerequisite of the conceptual model design. Experiments conducted in an 'artificial borehole' (a closed system) showed that gas migration was facilitated by diffusive transport when compared against modelled data. Furthermore, when diffusion was measured through Leighton Buzzard Sand (a very well sorted coarse-grained sand), CH_4 was shown to be transported at a faster rate than CO_2. A consequence of this observation is that the ratio of CH_4 / CO_2 increases as indicated in the conceptual model. In the example of landfill gas which is typically comprised of 60% CH_4 and 40% CO_2 (Kjeldsen et al., 2002), it is possible that a larger proportion of CH_4 may be measured relative to CO_2 (e.g. 70% CH_4 / 30% CO_2) when monitoring gas at distance from source. In the case of Site 1, BH 03/4, the ratio CH_4/CO_2 increased from 1.5 (i.e. 60% CH_4, 40% CO_2) to 5 and in some instances, increased to 15 (Chapter 5, Figures 5.4 and 5.5). This may indicate that CH_4 lateral transport is more efficient than CO_2 lateral transport by advection in the unsaturated zone. By comparison, the CH_4/CO_2 ratio increased to an excess of 15 for Site 2, BH 04 (Chapter 5, Figure 5.8). And on some occasions, the CH_4/CO_2 ratio approached 80. Coupled with the stable isotope analysis of ground gases, the ratio of the proportions of CH_4 and CO_2 may also be used as an indicator as to the source of the gases.

A caveat on the experimental apparatus is that it constituted a closed system. In the field, a closed system may be described as one that is bounded by the top surface of the groundwater at its base and by an impermeable layer (such as clay) at its top. Under these circumstances it is proposed by the conceptual model that the dominant transport mechanism is diffusion and that gas is transported laterally from

source. An example of a closed system would be transport of gases through the basal lining of a containment-type landfill. In these types of landfill, the base lining is designed to be as impermeable to leachate and gas as possible. This is often achieved through multiple layers of clays and geosynthetic materials that are impermeable and compact to provide a protective barrier. For older natural attenuation facilities, advective transport may be more effective than diffusive transport.

However, great care must be taken to understand the site specific geology when predicting lateral migration of CO_2 and CH_4 ground gases. If an open system exists it will be subject to changes in atmospheric pressure. When these conditions prevail gas transport is principally conducted by advection (as transport will be driven by pressure gradients). Advective transport of CO_2 and CH_4 is indicated by thick, solid, red arrows while diffusive transport is indicated by thinner, dashed, green arrows. This distinction is made to show that advection is a more efficient mass transport mechanism than diffusion. The conceptual model illustrates these conditions assuming gas transport to be diffusive through basal lining of landfills (in agreement with Quigley et al. (1988)). Applying the same assumption, gas transport through landfill caps is also diffusive. Labelling systems as open or closed is not a true reflection of ground conditions and is a simplification used in the conceptual model. When gases encounter impermeable barriers such as clay, they are forced to migrate laterally.

Under falling atmospheric pressure conditions, a positive pressure gradient between the geosphere and atmosphere is established. Mass flow of CO_2 and CH_4 is from the ground to the atmosphere as indicated in the conceptual model. Gas moving away from landfill sites may readily be transported through unconsolidated Quaternary Deposits (in the unsaturated zone). Gas may reach the atmosphere through cracks and defects in landfill caps, valley sides, cracks and fissures in the soil, or via plant roots by advective transport. In terms of risk posed to property and life, these conditions present a significant hazard. An important concern is if ground gases were to break into underground services and enter buildings as indicated on the conceptual model. A source of ignition would result in damage or destruction of property if CH_4 were present in the explosive range (5–15% v/v). If CO_2 were to displace enough O_2 in air, an asphyxiation hazard would endanger human life.

When atmospheric conditions are reversed (i.e. rising pressure), the pressure gradient between the geosphere and atmosphere is reversed. Under these conditions, air enters the ground and has a diluting effect on the concentration of CH_4 and CO_2 as indicated in the conceptual model. The research presented here cannot ascertain how deep into the sub-surface this effect is observed. The impact of atmospheric

pressure on the ground gas regime is particularly dynamic. For Site 1 BH 03/4, a pressure drop of less than 2 millibar over as little as three hours was enough to induce an emission of CH_4 and CO_2 gases from the sub-surface. Gas emission events were recorded when the pressure gradient was less than 0.2 mbar/hr, but generally less than 1 mbar/hr. When atmospheric conditions were reversed, the 'switch' to ingress of air into the ground, the atmospheric pressure gradient required was similar in magnitude. Data collected from Site 1 BH 03/4 showed that gradients were generally less than 1 mbar/hr, but mainly less than 0.5 mbar/hr.

However, there are a number of assumptions associated with the conceptual model design. Firstly, gas transport in the unsaturated zone through unconsolidated media is assumed to be uniform and ignores the potential for preferential pathways to exist. Additionally, it was assumed that there were no changes to CO_2 and CH_4 concentration between source and atmosphere. This is not a true reflection of the sub-surface as there are multiple mechanisms by which CH_4 and CO_2 may be retarded or removed from the system. These could include adsorption onto clay minerals, degradation by microbes and dissolution of CO_2 (58 times more soluble in water than CH_4) in groundwater. Consequently, there is potential for additional layers to be made to the conceptual model in future research.

8.3 Wider Applications in Industry

Design of Gas Monitoring Programmes

The data collected from continuous monitoring show considerable variation with time, and are consistent with the overall CH_4 and CO_2 compositional data collected by hand-held meters. Using these, measurements are made at specific times/dates. If the periodicity of the sampling points is superimposed on the high frequency data series, gas composition is measured as a snapshot view of a highly variable system, and measured concentrations will vary considerably (as shown in Chapter 5, Figures 5.4 and 5.7 in particular).

From a regulatory perspective, high temporal resolution allows a clearer understanding of the processes that are occurring in the near-surface ground gas regime. As has been noted, air pressure and depth of water table are key factors. Current UK practice is to take point measurements from all monitoring wells on a site for a minimum investigation period of six weeks. It is required that at least one of the point measurements needs to be taken during falling atmospheric pressure. This process may be conducted irregularly at different times of year as required.

The data presented here show high temporal variability. The periodicity of the cycling of gases can be as short as a few hours to as long as a few days. Under current regulatory practice, two point measurements would have been made during the selected two week period shown in Chapter 5, Figure 5.4. For 70% of that monitoring period, only air (N_2 + O_2) was present in the test borehole. Thus there is a high likelihood of missing an emission event. To be certain of the ground gas regime for a site where CH_4 and CO_2 are likely to pose a hazard, a high temporal resolution data set may be required. Furthermore, a longer statutory monitoring period could be necessary to identify any longer-term seasonal variations in the ground gas regime.

Stable isotopes may indicate the origin of CH_4 and CO_2 in the sub-surface where multiple sources exist. However, there are instances in the literature and some uncertainty reported in Chapter 6 where biogenic CH_4 stable isotope ratios may trespass thermogenic $^{13}\delta C_{CH_4}$ end-members (Owen et al., 2016). Where uncertainty exists, radiocarbon dating to distinguish between biogenic (new sources) and thermogenic (old sources) of CH_4 may be required for regulation (Williams and Aitkenhead, 1991).

Carbon Capture and Storage (CCS), Hydraulic Fracturing ('Fracking') and other Industries

The monitoring data reported here demonstrate the complex behaviour of gases within the unsaturated zone, emphasising the highly variable nature with time of exchanges of CO_2 and CH_4 between the soil and the atmosphere. Great care needs to be taken in the interpretation of ground gas data to distinguish variation arising from meteorological controls from those arising from changes in geogenic or anthropogenic inputs, which need to be recognised in any attempt to attribute an artificial cause for an emission.

It is essential that the time period for monitoring is sufficient to capture meteorological events such as a rapid reduction in atmospheric pressure, and that the frequency of sampling is small enough to determine changes arising from these. Furthermore, other practices of continuous ground gas monitoring in relation to CCS have been discussed by Schlömer et al. (2013) and Schlömer et al. (2014) and outline the importance of establishing baseline conditions in the unsaturated zone before and during operations to determine any leakages of CO_2 from geologic formations.

Recently, Dixon and Romanak (2015) advocated adding attribution monitoring to CCS monitoring protocols. In addition to knowledge of background conditions and assess performance of CO_2 storage reservoir performance, Dixon and Romanak

(2015) argued that attribution is required because of the challenge of discerning a leakage from natural CO_2 variation in the near-surface. Teasdale et al. (2014) commented that there was a need to establish baseline conditions using high temporal frequency monitoring before engineering works commence. As the near-surface is the last geologic receptor before release to the atmosphere and non-storage related phenomena can mimic shallow leakage, Dixon and Romanak (2015) argued that it is important to attribute anomalous CO_2 occurrences to source in order to avoid any unnecessary heightened quantification monitoring. The stable isotope data shown in Chapter 6 corroborate the view that there is a regulatory requirement to determine gas source where multiple gas sources are possible.

It is clear that from the development of a conceptual model of the ground gas regime, the principles that are applied to landfill sites are equally applicable to gas emissions from other subsurface activities including CCS and hydraulic fracturing. It is possible that leakages occur along undetected faults and fractures coupled with changes in atmospheric pressure.

Without rigorous monitoring, there is potential for low intensity leakages to go undetected for prolonged periods of time (Harvey et al., 2012). For example, Klusman (2003) estimated that approximately 170 tons of CO_2 was lost per annum through leakage from deep storage to the atmosphere at an enhanced oil recovery/CO_2 sequestration site at Rangely, Colorado, USA. In order to establish baseline levels of CO_2, monitoring programmes are required, before injection (with respect to CCS) and continuing through operations for safety, public acceptance and model calibration (Korre et al., 2011).

In a recent case study of CO_2 surface leaks in Qinghai, China, Schroder et al. (2016) noted a significant 20–50 m CO_2 migration away from the source of a leak. Schroder et al. (2016) argued that soil flux surveys cannot simply focus on the area immediately surrounding the leak as it would limit the effectiveness of long-term continuous soil flux survey installations as a primary detection method. Therefore, a systematic regular pattern may be better for detecting leaks while an irregular sampling regime with high sampling density in known high-flux zones may be more suited for CO_2 leak quantification (Schroder et al., 2016). The high temporal frequency capabilities of the GasClam demonstrated in Chapter 5 could be used to meet this brief.

Chapter 9

Conclusion

9.1 Summary and Key Findings of the Research

In order to meet the research aim of developing a widely-applicable conceptual model of ground gas dynamics, the following were conducted: a review of historic gas monitoring data, field work using a high temporal frequency gas monitor, stable isotope analysis of gas samples, and laboratory-based experiments designed to test gas transport mechanics.

A literature review establishing the principles of ground gas dynamics was undertaken to meet the research objective set at the beginning of this investigation. It encompassed the chemical, physical and hazardous properties of common ground gases, reviewed the sources of ground gases including historic investigations that quantified sources, appraised previous studies that explored gas migration and emissions, and detailed historic incidents of uncontrolled gas migrations.

Historic data sets from municipal landfill monitoring wells based in similar geological settingd in NW England were analysed and reviewed. These data sets were extended to 30th June 2015. Gas compositions were presented in ternary plots to allow easy comparison between boreholes and sites. This met the research objective to establish baseline CO_2 and CH_4 concentration and determine natural variations in the near-surface ground gas environment. It also met the research objective to update data sets for these municipal landfill sites (that overlie the Bowland-Hodder Shales).

Historic gas monitoring data for Site 1 showed changes in gas composition with changes in atmospheric pressure (Chapter 4, Figures 4.1 and 4.2). When atmospheric pressure decreased, landfill gas (70:30 CH_4:CO_2) was present in the nearest borehole to the landfill boundary. On some occasions, landfill gas was observed at a distance 25 m away from the landfill. On no occasions was landfill gas present

100 m away from the landfill. These data suggested that landfill gas migrated at least 25 m through unconsolidated Quaternary Deposits during negative atmospheric pressure gradients. When opposing atmospheric pressure conditions prevailed (i.e. rising pressure), no landfill gas was observed in the monitoring wells. The internal pressure of the landfill was not measured, but the internal borehole pressure was measured and the difference between borehole pressure and atmospheric pressure was calculated. This typically varied between −15 mbar (negative borehole pressure, increasing atmospheric pressure) and 15 mbar (positive borehole pressure, decreasing atmospheric pressure, which equated to movement of ground gas from the sub-surface to atmosphere).

Conversely, some monitoring wells on a second municipal landfill (Site 2) demonstrated gas compositions that were not indicative of landfill gas (Chapter 4, Figure 4.4). Borehole 4 gas composition at this site frequently approached 100% CH_4/N_2 end member. This occurred frequently over a 17 year monitoring period from site inception. BH 12 and BH 14 frequently recorded gas composition in excess of 80% CH_4. This site overlies Carboniferous rock with inter-bedded coal seams. Consequently, the higher ratio of CH_4/CO_2 demonstrated in monitoring wells at this site may have represented a geogenic gas contribution.

A third municipal landfill site, located within the London Basin (Chalk), demonstrated different behaviour from Sites 1 and 2. Monitoring wells at Site 3 were separated into isolated monitoring zones. Some boreholes on this site showed changing gas composition with increasing depth from surface. For example, boreholes GM 5 and GM 14 (Chapter 4, Figure 4.10) showed an increasing CO_2 concentration gradient with increasing depth from surface.

In order to fulfil the research objective to capture and interpret high temporal frequency data for the aforementioned research sites, a GasClam® (IonScience Ltd) was deployed on Sites 1 and 2 between April 2013 and January 2015. Data from Site 1 BH 03/4 showed a close relationship with atmospheric pressure (Chapter 5, Figure 5.4) and showed that changes in gas composition were extremely sensitive to changes in atmospheric pressure as a pressure drop as little as 3 mbar over 2 to 4 hours was sufficient to induce an emission of landfill gas (70% CH_4 / 30% CO_2). Crucially, the high temporal frequency gas data showed that the array of gas compositions compiled over 10 years occurred over time-scales as short as 24 hours (Chapter 5, Figures 5.6 and 5.7).

Contrastingly, Site 2 boreholes did not show a change in gas composition that was related to changes in atmospheric pressure (Chapter 5, Figures 5.8 and 5.9). The pressure difference induced by atmospheric pressure was never greater than 1 mbar

on Site 2, in contrast to Site 1 BH 03/4 where a pressure difference of 10 mbar was measured as a result of negative atmospheric pressure gradients. Concentrations of CH_4 and CO_2 cycled diurnally with respect to O_2. At the time of data capture this was hypothesised to be due to a poor borehole seal. However, as Site 2 landfill is set in a thick layer of glacial till, it is possible that the ground gas regime was isolated from changes in atmospheric pressure. The diurnal cycling may be a consequence of diffusive gas transport which will be subject to changes in ground conditions such as temperature and saturation (Chapter 5, Figure 5.8). The different trends noted at Site 1 and 2 landfills from the high temporal frequency gas data consequently helped to add to the understanding of the ground gas regime.

In addition, a control borehole at a site distant from landfill and coal-bearing rocks was monitored to establish background conditions. The data produced from this borehole also contributed to the research objective to establish baseline CO_2 and CH_4 concentration in the near-surface. A two-week monitoring period commencing 3rd February 2014 (at 14:30) yielded a peak CO_2 concentration 1.3% in response to steep atmospheric pressure falls (Chapter 5, Figure 5.11). No CH_4 was recorded. It was supposed that the small CO_2 concentration constituted background CO_2 in the Middle Sands formation.

The GasClam was deployed on closed vent mode on all the research sites. It was programmed to sample ground gases every 30 minutes. On this sampling regime, a maximum battery life of two weeks was achieved. As a recommendation for high temporal frequency gas monitoring methodology for the GasClam, it was determined that: the vent should be closed (to prevent disruption to internal borehole conditions), sampling should be every hour or less (to capture all changes in gas composition whilst maximising battery life), a filter should be applied to the external vent to prevent water ingress (e.g. condensation) that may affect accuracy of measurements, and multiple GasClams should be deployed simultaneously to ensure data sets are directly comparable.

Gas samples were collected from Sites 1 and 2 for analysis to determine their origin. This was undertaken to meet the research objective to sample landfill gases from landfill sites (Site 2) with suspected multiple gas sources and to use stable isotope ratios to ascertain the source. Using flared landfill gas from Site 2 as a reference, stable isotope ratios were determined as $^{13}\delta C_{CH_4}$ −65.0‰ and δD_{CH_4} −319‰. Relative to these values, Site 1 BH 03/7 produced a $^{13}\delta C_{CH_4}$ −61.0‰ and δD_{CH_4} −253‰ while Site 2 BH 04 yielded a $^{13}\delta C_{CH_4}$ −55.6‰ and δD_{CH_4} −172‰ (the full complement of stable isotope results is given in Chapter 6, Table 6.5). Site 2 perimeter monitoring wells gases indicated an enrichment in the heavier stable

isotopes (^{13}C and D) which suggested a possible geogenic origin. When compared against published data (Chapter 6, Figures 6.6 and 6.7), the Site 2 perimeter boreholes appeared to agree with previous isotope ratios quoted in the literature for geogenic gas sources.

It was also determined in Table 6.6, that the two methods of isotope ratio mass spectrometry employed at Newcastle University and UC Davis Stable Isotope Facility, California, US (UCDSIF), produced results that agreed with each other to within a small margin of error. The average differences between data sets were 1.80‰, 9.81‰, and 1.06‰ for $^{13}\delta C_{CH_4}$, δD_{CH_4}, and $^{13}\delta C_{CO_2}$ respectively, while the standard deviations were 1.23‰, 14.1‰, and 3.33‰ for $^{13}\delta C_{CH_4}$, δD_{CH_4}, and $^{13}\delta C_{CO_2}$ respectively. Thus, this fulfilled the research objective to compare stable isotope analysis methodologies. Additionally, it was determined that samples stored in evacuated containers had at least an effective storage time of two months and had survived air transit. One month elapsed before analysis at Newcastle University and a further month passed before analysis at UCDSIF. Despite this time-lag, the two data sets were in close agreement with one another.

An 'artificial borehole' 3 m in height was designed and constructed to test gas transport mechanics in the unsaturated zone. Experiments conducted using the artificial borehole were in fulfilment of the research objective to investigate gas transport mechanisms that synthesise research municipal landfill site conditions. Data generated from these experiments yielded concentration curves that, when compared against modelled diffusion data, provided evidence that for a closed system, diffusive transport was the dominant mechanism (Chapter 7, Figures 7.7 and 7.12).

The collated evidence from the historic gas monitoring data review, the high temporal frequency data capture, stable isotope analysis of gas samples, and modelling and experimental data of gas transport mechanisms fed back into the overall design of a conceptual model (Chapter 8, Figure 8.1). The model had three main elements: source, migration and hazard. Gas sources are identifiable by stable isotope 'signatures'. For closed systems gas transport is diffusive while for open systems gas transport is advective and subject to changes in atmospheric pressure. Risks are posed to property and life when ground gases CH_4 and CO_2 accumulate at specific concentrations to present an explosion hazard in absence of O_2. If O_2 is displaced or reduced, CO_2 poses an asphyxiation hazard. The development of the conceptual model presented in Chapter 8 met the overall research aim of this project. Based on the findings of this research, it was designed to be widely-applicable for future use and meet the research objective set out in the introduction of this thesis.

9.2 Implications for Industry, Policy Making and Regulation

Design of Gas Monitoring Programmes

The data collected from continuous monitoring show considerable variation with time, and are consistent with the CH_4 and CO_2 data collected by hand-held meters. Using these, measurements are made at specific times/dates. If the periodicity of the sampling points is superimposed on the high frequency data series, gas composition is measured as a snapshot view of a highly variable system, and measured concentrations will vary considerably (as shown in Chapter 5, Figures 5.6 and 5.7 in particular).

From a regulatory perspective, high temporal resolution allows a clearer understanding of the processes that are occurring in the near-surface ground gas regime. As has been noted, air pressure gradients and depth of water table are key factors. The data presented here show high temporal variability. The periodicity of the cycling of gases can be as short as a few hours to as long as a few days. If two point measurements had been made in the test borehole during the two week period 29/10/2013 – 12/11/2013 shown in Chapter 5, Figure 5.4 there would have been a high probability of missing an emission event as only air was present for 70% of that monitoring period.

To be certain of the ground gas regime for a site where CH_4 and CO_2 are likely to pose a hazard, a high temporal resolution data set may be required. Furthermore, a longer statutory monitoring period could be necessary to identify any longer-term seasonal variations in the ground gas regime. Chapter 5, Figure 5.7 clearly demonstrates how gas compositions for Site 1 BH 03/4 were observed on a range of time-scales from one day to a decade.

Carbon Capture and Storage (CCS) and Hydraulic Fracturing 'Fracking' Industries

The gas monitoring data reported in Chapters 4 and 5 demonstrate the complex behaviour of gases within the unsaturated zone. The highly variable nature of CO_2 and CH_4 exchange between the sub-surface and the atmosphere with time is emphasised in the data. Care needs to be taken in the interpretation of ground gas data to distinguish variation arising from meteorological controls and variation arising from changes in geogenic or anthropogenic inputs, which need to be recognised in any attempt to attribute an artificial cause for an emission. It is essential that the

time period for monitoring is sufficient to capture meteorological events such as a rapid reduction in atmospheric pressure, and that the frequency of sampling is small enough to determine changes arising from these. It is important to establish baseline conditions in the unsaturated zone before and during operations to determine any leakages of CO_2 from geologic formations.

From the development of a conceptual model of the ground gas regime, the principles that are applied to municipal landfill sites are also applicable to gas emissions from other subsurface activities including CCS and hydraulic fracturing. Leakages could occur along undetected faults and fractures coupled with falls in atmospheric pressure. Without rigorous monitoring, there is potential for low intensity leakages to go undetected for prolonged periods of time. In order to establish baseline levels of CO_2, monitoring programmes are required, before injection (with respect to CCS) and continuing through operations for safety, public acceptance and model calibration.

Importantly, the data presented in this thesis demonstrate that ground gas compositions vary greatly with time. Conventional monitoring protocols are likely to fail to detect some emission events. It is important that high frequency measurements are made as part of a monitoring regime that is underpinned by a sound conceptual model of the geological characteristics of the location of interest. As a recommendation, a sampling frequency of at least once every half hour would be sufficient to capture changes in ground gas composition in response to changes in atmospheric pressure. Data collated in Chapter 5, Figures 5.4 and 5.5 demonstrated that atmospheric pressure gradients less than 0.5 mbar/hr over 2 to 3 hours could induce emissions of up to 55% CH_4 and 10% CO_2 in Site 1, BH 03/4 adjacent to the municipal landfill. The proposed high temporal frequency gas monitoring regime of half-hourly sampling would be sufficient to capture these changes in ground gas composition.

9.3 Recommendations for Future Work

This research presents several areas of future work that are grouped according to separate research threads:

Ground Gas Monitoring

- Deploy GasClam (or equivalent high temporal frequency gas monitors) over longer time periods to establish trends on different time-scales. For sites where diffusive transport is more important than advective flow, a range of trends on

different time-scales ranging from hours to months could be observed. For sites where advective transport is more important than diffusive transport, time-scales are typically very short ranging from minutes to hours. Consequently, monitoring the ground gas regime using high temporal frequency data capture instruments is important to resolve trends on differing time-scales. It is important to determine how these trends interact with each other and are superimposed upon each other;

- By extension, it is proposed that multiple high temporal frequency gas monitors should be deployed on one site and at other sites simultaneously so that data sets are directly comparable. However, this is financially constrained and may not be feasible;
- Monitor other engineered environments at high temporal frequency where CO_2 and CH_4 are generated and/or accumulate such as hydraulic fracturing works and carbon dioxide containment (CCS), and;
- For a virgin site (preferably in an area of future engineering work) design an array of monitoring wells for detection and measurement of ground gases. Predict expected ground gas composition and migration based on known gas sources and ground conditions. Establish a baseline reading over a period of months to years before engineering works and examine the changes induced by engineering to the ground gas regime.

Carbon, Hydrogen and Oxygen Isotope Fingerprinting

- Determine gas origin by radiocarbon dating (^{14}C). Collect gas samples from municipal landfills, abandoned mine shaft vents, shale gas and other engineered environments where CO_2 and CH_4 are generated and accumulate. When complemented with stable isotope analysis ($^{13}C/^{12}C$ in CO_2 and CH_4, D/H in CH_4, and $^{18}O/^{16}O$ in CO_2) gas sources should be fully differentiated. Already, the research presented in this thesis has postulated the origin of gas on a municipal landfill site exhibiting multiple gas sources. Radiocarbon dating of samples would fully differentiate biogenic (new) and geogenic/thermogenic (old) sources of CO_2 and CH_4 ground gases. This is important for regulation and ascertaining responsibilities of site owners/contractors, especially in the event of an uncontrolled ground gas migration.

Gas Transport Modelling and Measurement

Gas Transport modelling was modelled according to Fick's Law of Diffusion and measured using an experimental 'artificial borehole' apparatus. Refinements to the

apparatus and model, and recommendations for further work using the apparatus are given in this section.

Refinements to experimental apparatus, model refinements and further modelling strategies:

- Add a sample port(s) to the gas reservoir at the bottom of the artificial borehole. There was a need to measure C_0 in the experiments. If C_0 could be measured accurately, it would be possible to conduct a direct comparison of the experimental data with the modelled data;
- Refine the modelled data for diffusion of a substance initially confined in the region $-h < x < +h$. The integration is then from $x - h$ to $x + h$ instead of from x to ∞ as used in this research, and;
- Model and measure gas transport by advection (Darcy's Law), or combined diffusion/advection model (Darcy's Law combined with mass conservation equation). Additionally, it is suggested that these models should be expanded to incorporate three dimensions.

Further experimentation relating to gas transport mechanics and dynamics in the ground gas environment using the artificial borehole apparatus are proposed as follows:

- Determine the effect of the initial starting pressure on the rate of transport of CH_4 and CO_2 in the gas column;
- Determine the effect of the initial starting concentration of ground gases on the rate of diffusion;
- Determine the effect of different media on the rate of gas diffusion. For example, it would be useful to test CH_4 and CO_2 diffusion in finer-grained sands, less sorted sands and coarser-grained sands;
- Determine the effect of the rate of gas diffusion for multi-layered different media (i.e. increasingly complex unconsolidated strata layers);
- Determine the effect of the degree of saturation on the diffusion of gases in the near-surface environment. Establish the critical saturation where the maximum concentration of CO_2 is 'scrubbed' from the system (dissolved in solution) is achieved;
- Determine the effect of a temperature gradient on the rate of CH_4 and CO_2 diffusion in the gas column;
- Determine the effect of natural microbial colonies on CH_4 and CO_2 diffusion in the gas column;

- Using the principles of diffusive and/or advective transport, undertake field measurements to determine which model(s) works best for a given site, and;
- For a given strata, predict the rate of lateral transport of ground gases away from source (such as a municipal landfill), the maximum distance of transport and the likely terminal concentration by diffusion models.

References

Abu-Khader, M. M. (2006). Recent Progress in CO_2 Capture/Sequestration: A Review. *Energy Sources, Part A*, 28(14):1261–1279.

Aelion, C. M., Höhener, P., Hunkeler, D., and Aravena, R. (2009). *Environmental Isotopes in Biodegradation and Bioremediation*. CRC Press.

Aitkenhead, N. and Williams, G. M. (1986). *Geological Evidence to the Public Inquiry into the Gas Explosion at Loscoe*. Technical report, British Geological Survey Report No FP/87/8/83AS.

Allen, D. J., Brewerton, L. J., Coleby, L. M., Gibbs, B. R., Lewis, M. A., MacDonald, A. M., Wagstaff, S. J., and Williams, A. T. (1997a). *The Physical Properties of Major Aquifers in England and Wales*. Technical Report WD/97/34 and EA R&D Publication 8, British Geological Survey and Environment Agency, Keyworth, Nottingham.

Allen, M. R., Braithwaite, A., and Hills, C. C. (1997b). Trace Organic Compounds in Landfill Gas at Seven UK Waste Disposal Sites. *Environmental Science & Technology*, 31(4):1054–1061.

Amyx, J. W., Bass, D. M., and Whiting, R. L. (1960). *Petroleum Reservoir Engineering: Physical Properties*, volume 1. McGraw-Hill College.

Andrews, I. J. (2013). The Carboniferous Bowland Shale Gas Study: Geology and Resource Estimation.

Appels, L., Baeyens, J., Degrève, J., and Dewil, R. (2008). Principles and Potential of the Anaerobic Digestion of Waste-Activated Sludge. *Progress in energy and combustion science*, 34(6):755–781.

Archer, D. (2005). The Fate of CO_2 in Geologic Time. *Journal of Geophysical Research*, 110.

Bachu, S. (2003). Screening and Ranking of Sedimentary Basins for Sequestration of CO_2 in Geological Media in Response to Climate Change. *Environmental Geology*, 44(3):277–289.

Bachu, S., Bonijoly, D., Bradshaw, J., Burruss, R., Holloway, S., Christensen, N. P., and Mathiassen, O. M. (2007). CO_2 Storage Capacity Estimation: Methodology and Gaps. *International Journal of Greenhouse Gas Control*, 1(4):430–443.

Bagchi, A. (2004). *Design of Landfills and Integrated Solid Waste Management*. John Wiley & Sons, 3rd edition.

Bareither, C. A., Wolfe, G. L., McMahon, K. D., and Benson, C. H. (2013). Microbial Diversity and Dynamics during Methane Production from Municipal Solid Waste. *Waste Management*, 33(10):1982–1992.

Barlaz, M. A., Schaefer, D. M., and Ham, R. K. (1989). Bacterial Population Development and Chemical Characteristics of Refuse Decomposition in a Simulated Sanitary Landfill. *Applied and Environmental Microbiology*, 55(1):55–65.

Barlow, S. G. (1996). *The Mineralogical, Geochemical and Experimental Evaluation of Boulder Clay from Adswood, Stockport, as a Model Brickclay Raw Material*. PhD thesis, Department of Earth Sciences in the Faculty of Science, University of Manchester, Manchester, UK.

Barry, D. L. (1986). Hazards from Methane on Contaminated Sites. In *International Conference on Building on Marignal and Derelict Land*, Glasgow.

Bates, B. L., McIntosh, J. C., Lohse, K. A., and Brooks, P. D. (2011). Influence of Groundwater Flowpaths, Residence Times and Nutrients on the Extent of Microbial Methanogenesis in Coal Beds: Powder River Basin, USA. *Chemical Geology*, 284(1):45–61.

Batjes, N. H. (1996). Total Carbon and Nitrogen in the Soils of the World. *European Journal of Soil Science*, 47(2):151–163.

Beauchamp, R. O., Bus, J. S., Popp, J. A., Boreiko, C. J., Andjelkovich, D. A., and Leber, P. (1984). A Critical Review of the Literature on Hydrogen Sulfide Toxicity. *CRC Critical Reviews in Toxicology*, 13(1):25–97.

Beluche, R. (1968). *Degradation of Solid Substrate in a Sanitary Landfill*. PhD thesis, University of Southern California, Los Angeles, CA.

Beresford, J. J. (1989). Paper 4.2. In *Methane: Facing the Problems Symposium*, Nottingham.

Bergamaschi, P. and Harris, G. W. (1995). Measurements of Stable Isotope Ratios ($^{13}CH_4/^{12}CH_4$; $^{12}CH_3D/^{12}CH_4$) in Landfill Methane using a Tunable Diode Laser Absorption Spectrometer. *Global Biogeochemical Cycles*, 9(4):439–447.

Bergamaschi, P., Lubina, C., Königstedt, R., Fischer, H., Veltkamp, A. C., and Zwaagstra, O. (1998). Stable Isotopic Signatures ($\delta^{13}C$, δD) of Methane from European Landfill Sites. *Journal of Geophysical Research: Atmospheres (1984–2012)*, 103(D7):8251–8265.

Boltze, U. and de Freitas, M. H. (1997). Monitoring Gas Emissions from Landfill Sites. *Waste Management & Research*, 15(5):463–476.

Boru, G., Vantoai, T., Alves, J., Hua, D., and Knee, M. (2003). Responses of Soybean to Oxygen Deficiency and Elevated Root-Zone Carbon Dioxide Concentration. *Annals of Botany*, 91(4):447–453.

Bozkurt, S., Moreno, L., and Neretnieks, I. (1999). Long-Term Fate of Organics in Waste Deposits and its Effect on Metal Release. *Science of the Total Environment*, 228(2):135–152.

Bozkurt, S., Moreno, L., and Neretnieks, I. (2000). Long-Term Processes in Waste Deposits. *Science of the Total Environment*, 250(1):101–121.

British Geological Survey (2010). *Mineral Planning Factsheet: Coal*. URL: `https://www.bgs.ac.uk/mineralsuk/planning/mineralPlanningFactsheets.html`. [Accessed 29th September 2015].

British Geological Survey (2015). *Macclesfield: Solid and Drift Geology Map, Sheet 110 (England and Wales) (1:50,000 Series Geological Maps (England and Wales))*. URL: `http://digimap.edina.ac.uk/geologyroam/geology`. [Accessed: 17th August 2015].

Buryakovsky, L., Eremenko, N. A., Gorfunkel, M. V., and Chilingarian, G. V. (2005). *Geology and Geochemistry of Oil and Gas*, volume 52. Elsevier.

Calli, B., Durmaz, S., and Mertoglu, B. (2006). Identification of Prevalent Microbial Communities in a Municipal Solid Waste Landfill. *Water Science and Technology*, 53(8):139–148.

Calmano, W., Hong, J., and Förstner, U. (1993). *Binding and Mobilization of Heavy Metals in Contaminated Sediments Affected by pH and Redox Potential.*

Card, G. B. (1995). *Protecting Development from Methane.* Construction Industry Research and Information Association (CIRIA), London.

Carson, P. and Mumford, C. (2007). The Abbeystead Explosion. *Loss Prevention Bulletin*, 195(1).

Cashdollar, K. L., Zlochower, I. A., Green, G. M., Thomas, R. A., and Hertzberg, M. (2000). Flammability of Methane, Propane, and Hydrogen Gases. *Journal of Loss Prevention in the Process Industries*, 13(3):327–340.

Christensen, A. G., Fischer, E. V., Nielsen, H. H., Nygaard, T., Østergaard, H., Lenschow, S. R., Sïrensen, H., Fuglsang, I. A., and Larsen, T. H. (2000). Passive Soil Vapor Extraction of Chlorinated Solvents using Boreholes. *Groundwater*, 2000:409–410.

Christensen, T. H., Cossu, R., and Stegmann, R. (1992). *Landfilling of Waste: Leachate*, volume 1. CRC Press.

Christophersen, M. and Kjeldsen, P. (2001). Lateral Gas Transport in Soil adjacent to an Old Landfill: Factors Governing Gas Migration. *Waste Management & Research*, 19(6):579–594.

Christophersen, M., Kjeldsen, P., Holst, H., and Chanton, J. (2001). Lateral Gas Transport in Soil adjacent to an Old Landfill: Factors Governing Emissions and Methane Oxidation. *Waste Management & Research*, 19(6):595–612.

Clark, I. (2015). *Groundwater Geochemistry and Isotopes.* CRC Press, Taylor & Francis Group, Florida, United States.

Coleman, D. D., Risatti, J. B., and Schoell, M. (1981). Fractionation of Carbon and Hydrogen Isotopes by Methane-oxidizing Bacteria. *Geochimica et Cosmochimica Acta*, 45(7):1033–1037.

Cradock-Hartopp, M. A., Moseley, R., Bruce, B., and Day, J. B. W. (1984). *Hydrogeological Map of the Area between Cambridge and Maidenhead Including Parts of Hyrdometric Areas 33, 38 and 39 (Sheet 14).* Map 1:100,000.

Crank, J. (1979). *The Mathematics of Diffusion.* Oxford University Press.

Czech, E. and Troczynski, T. (2010). Hydrogen Generation through Massive Corrosion of Deformed Aluminum in Water. *International Journal of Hydrogen Energy*, 35(3):1029–1037.

Czepiel, P. M., Shorter, J. H., Mosher, B., Allwine, E., McManus, J. B., Harriss, R. C., Kolb, C. E., and Lamb, B. K. (2003). The Influence of Atmospheric Pressure on Landfill Methane Emissions. *Waste Management*, 23(7):593–598.

d-maps.com (2015). *United Kingdom of Great Britain and Northern Ireland Boundaries (White)*. URL: `http://www.d-maps.com/m/europa/uk/royaumeuni/royaumeuni10.svg`. [Accessed 14th August 2015].

Dai, J., Li, J., Ding, W., Hu, G., Luo, X., Hou, L., Tao, S., Zhang, W., and Zhu, G. (2007). Geochemical Characteristics of Natural Gas at Giant Accumulations in China. *Journal of Petroleum Geology*, 30(3):275–288.

Dai, J., Ni, Y., and Zou, C. (2012). Stable Carbon and Hydrogen Isotopes of Natural Gases Sourced from the Xujiahe Formation in the Sichuan Basin, China. *Organic Geochemistry*, 43:103–111.

Dai, J., Ni, Y., Zou, C., Tao, S., Hu, G., Hu, A., Yang, C., and Tao, X. (2009). Stable Carbon Isotopes of Alkane Gases from the Xujiahe Coal Measures and Implication for Gas-Source Correlation in the Sichuan Basin, SW China. *Organic Geochemistry*, 40(5):638–646.

D'Alessandro, D. M., Smit, B., and Long, J. R. (2010). Carbon Dioxide Capture: Prospects for New Materials. *Angewandte Chemie International Edition*, 49(35):6058–6082.

Davidson, E., Belk, E., and Boone, R. D. (1998). Soil Water Content and Temperature as Independent or Confounded Factors Controlling Soil Respiration in a Temperate Mixed Hardwood Forest. *Global Change Biology*, 4(2):217–227.

Davies, R. J. (2011). Methane Contamination of Drinking Water Caused by Hydraulic Fracturing Remains Unproven. *Proceedings of the National Academy of Sciences*, 108(43):E871–E871.

Davies, R. J., Mathias, S. A., Moss, J., Hustoft, S., and Newport, L. (2012). Hydraulic Fractures: How Far Can They Go? *Marine and Petroleum Geology*, 37(1):1–6.

Delkash, M., Zhou, B., and Singh, R. (2016). Measuring Landfill Methane Emissions Using Satellite and Ground Data. *Remote Sensing Applications: Society and Environment*, 4:18–29.

Dixon, N. and Murray, E. J., editors (1998). *Geotechnical Engineering of Landfills: Proceedings of the Symposium Held at Nottingham Trent University Department of Civil and Structural Engineering on 24th September 1998*. Thomas Telford.

Dixon, T. and Romanak, K. D. (2015). Improving Monitoring Protocols for CO_2 Geological Storage with Technical Advances in CO_2 Attribution Monitoring. *International Journal of Greenhouse Gas Control*, 41:29–40.

Drever, J. I. (1997). *The Geochemistry of Natural Waters: Surface and Groundwater Environments*. Prentice Hall, 3rd edition.

Drummond, S. E. (1981). *Boiling and Mixing of Hydrothermal Fluids: Chemical Effects on Mineral Precipitation*. PhD thesis, Pennsylvania State University.

Eccles, J. K., Pratson, L., Newell, R. G., and Jackson, R. B. (2012). The Impact of Geologic Variability on Capacity and Cost Estimates for Storing CO_2 in Deep-Saline Aquifers. *Energy Economics*, 34(5):1569–1579.

Edwards, J. S. (1989). Paper 1.3: Gases – Their Basic Properties. In *Methane: Facing the Problems Symposium*, Nottingham.

Environment Agency (2010a). *Groundwater Source Protection Zones*. URL: `http://apps.environment-agency.gov.uk/wiyby/37833.aspx`. [Accessed: 31st October 2014].

Environment Agency (2010b). *Waste Acceptance at Landfills: Guidance on Waste Acceptance Procedures and Criteria*. URL: `https://www.gov.uk/government/uploads/system/uploads/attachment_data/file/296422/geho1110btew-e-e.pdf`. [Accessed: 8th February 2017].

European Commission (2016). *Paris Agreement*. URL: `http://ec.europa.eu/clima/policies/international/negotiations/paris/index_en.htm`. [Accessed: 11th October 2016].

Evans, W. B. (1968). *The Geology of the Country around Macclesfield, Congleton, Crewe and Middlewich*, volume 110. HM Stationery Office, London, 2nd edition.

Fang, J.-J., Yang, N., Cen, D.-Y., Shao, L.-M., and He, P.-J. (2012). Odor Compounds from Different Sources of Landfill: Characterization and Source Identification. *Waste Management*, 32(7):1401–1410.

Farquhar, G. J. and Rovers, F. (1973). Gas Production during Refuse Decomposition. *Water, Air, and Soil Pollution*, 2(4):483–495.

Fellner, J. and Rechberger, H. (2009). Abundance of ^{14}C in Biomass Fractions of Wastes and Solid Recovered Fuels. *Waste Management*, 29(5):1495–1503.

Flores, R. M., Rice, C. A., Stricker, G. D., Warden, A., and Ellis, M. S. (2008). Methanogenic Pathways of Coal-Bed Gas in the Powder River Basin, United States: The Geologic Factor. *International Journal of Coal Geology*, 76(1):52–75.

Friedman, M. A. (1988). *Volatile Organic Compounds in Groundwater and Leachate at Wisconsin Landfills*. Technical Report PUBL-WR-192-88, Wisconsin Department of Natural Resources, Madison, Wisconsin, USA.

Gas Data UK Ltd (2012). *GFM4XX Series Gas Analyser User Manual*. Gas Data UK Ltd, Pegasus House, Wheler Road, Seven Stars Estate, Coventry, UK, CV3, 4LB, issue: b, revision: 3 edition.

Gebert, J. and Gröngröft, A. (2006). Passive Landfill Gas Emission:Influence of Atmospheric Pressure and Implications for the Operation of Methane-Oxidising Biofilters. *Waste Management*, 26(3):245–251.

Gebert, J., Rachor, I., Gröngröft, A., and Pfeiffer, E.-M. (2011). Temporal Variability of Soil Gas Composition in Landfill Covers. *Waste Management*, 31(5):935–945.

Golding, S. D., Boreham, C. J., and Esterle, J. S. (2013). Stable Isotope Geochemistry of Coal Bed and Shale Gas and Related Production Waters: A Review. *International Journal of Coal Geology*, 120:24–40.

Gooddy, D. C., Mathias, S. A., Harrison, I., Lapworth, D. J., and Kim, A. W. (2007). The Significance of Colloids in the Transport of Pesticides through Chalk. *Science of the Total Environment*, 385(1):262–271.

Gordon, M. E., Huebner, P. M., and Miazaga, T. J. (1989). Hydraulic Conductivity if Three Landfill Clay Liners. *Journal of Geotechnical Engineering*, 115:1148–1160.

Hall, J. A. (2007). *Sources and Pathways of Hazardous Gases in Disused Mine Workings*. PhD thesis, School of Civil Engineering and Geosciences, Newcastle University, Newcastle upon Tyne, UK.

Hall, J. A., Glendinning, S., and Younger, P. (2005). Is Mine Water a Source of Hazardous Gas? In Kleinmann, R., editor, *9th International Mine Water Association Congress*, Oviedo, Spain.

Hansen, J., Sato, M., Hearty, P., Ruedy, R., Kelley, M., Masson-Delmotte, V., Russell, G., Tselioudis, G., Cao, J., Rignot, E., et al. (2016). Ice Melt, Sea Level Rise and Superstorms: Evidence from Paleoclimate Data, Climate Modeling, and Modern Observations that 2°C Global Warming could be Dangerous. *Atmospheric Chemistry and Physics*, 16(6):3761–3812.

Harvey, O. R., Qafoku, N. P., Cantrell, K. J., Lee, G., Amonette, J. E., and Brown, C. F. (2012). Geochemical Implications of Gas Leakage Associated with Geologic CO_2 Storage – A Qualitative Review. *Environmental Science & Technology*, 47(1):23–36.

Hitchman, S. P., Darling, W. G., and Williams, G. M. (1989). *Stable Isotope Ratios in Methane Containing Gases in the United Kingdom*. Technical Report WE/89/30, British Geological Survey, Keyworth, Nottinghamshire, UK.

Holmes, M. E., Chanton, J. P., Tfaily, M. M., and Ogram, A. (2015). CO_2 and CH_4 Isotope Compositions and Production Pathways in a Tropical Peatland. *Global Biogeochemical Cycles*, 29(1):1–18.

Honrath, R. E. (1995). *Mass Transport Processes*. URL: `http://www.cee.mtu.edu/~reh/courses/ce251/251_notes_dir/node5.html`. [Accessed: 1st September 2016].

Hooker, P. J. and Bannon, M. P. (1993). *Methane: Its Occurrence and Hazards in Construction*. Construction Industry Research and Information Association (CIRIA), London.

Howarth, R. W., Santoro, R., and Ingraffea, A. (2011). Methane and the Greenhouse-Gas Footprint of Natural Gas from Shale Formations. *Climatic Change*, 106(4):679–690.

HSE (1985). *The Abbeystead Explosion: A Report of the Investigation by the Health and Safety Executive into the Explosion on 23 May 1984 at the Valve House of*

the Lune/Wyre Water Transfer Scheme at Abbeystead. Technical Report ISBN: 0118837958, Health and Safety Executive, London.

Hu, G., Yu, C., Gong, D., Tian, X., and Wu, W. (2014). The Origin of Natural Gas and Influence on Hydrogen Isotope of Methane by TSR in the Upper Permian Changxing and the Lower Triassic Feixianguan Formations in Northern Sichuan Basin, SW China. *Energy, Exploration & Exploitation*, 32(1):139–158.

Hua, Q., Barbetti, M., and Rakowski, A. Z. (2013). Atmospheric Radiocarbon for the Period 1950–2010. *Radiocarbon*, 55(4):2059–2072.

Huang, L.-N., Zhou, H., Chen, Y.-Q., Luo, S., Lan, C.-Y., and Qu, L.-H. (2002). Diversity and Structure of the Archaeal Community in the Leachate of a Full-Scale Recirculating Landfill as Examined by Direct 16S rRNA Gene Sequence Retrieval. *FEMS Microbiology Letters*, 214(2):235–240.

Humphries, P. (2001). Deep Concern: The Risk of Gas Leaks from Disused Mines. *The Guardian*. Accessed 2nd September 2015.

Jensen, F. B. (2004). Red Blood Cell pH, the Bohr Effect, and Other Oxygenation-Linked Phenomena in Blood O_2 and CO_2 Transport. *Acta physiologica Scandinavica*, 182(3):215–227.

Jones, E. (2008). *What's the Cost of Global Warming?* URL: `http://www.theregister.co.uk/2008/09/22/global_warming_mitigation_vs_adaptation/`. [Accessed 24th February 2012].

Jones, N. (2013). Troubling Milestone for CO_2. *Nature Geoscience*, 6(8):589–589.

Jowett, D. (2011). *Westmill Landfill Site, Ware, Hertfordshire: Gas Origin Assessment & Risk Appraisal*. Technical Report 915/R/001/4, TerraConsult Ltd, Bold Business Centre, Bold Lane, Sutton, St Helens, UK, WA9 4TX.

Jowett, D. and Martin, J. P. (2006). *Tenement Lane Landfill Site Cheadle Hulme, Cheshire Landfill Gas Risk Assessment*. Technical Report 0610/1, TerraConsult Ltd, Bold Business Centre, Bold Lane, Sutton, St Helens, UK, WA9 4TX.

Jowett, D. and Martin, J. P. (2008). *Tenement Lane Landfill Site Cheadle Hulme, Cheshire Landfill Gas Risk Assessment Addendum Report & Gas Management Plan*. Technical Report 0610/2, TerraConsult Ltd, Bold Business Centre, Bold Lane, Sutton, St Helens, UK, WA9 4TX.

Kanol, D. W. and Zetther, G. H. (1990). Abwassertechnische Vereinigung Ev. In *5th Sewage and Refuse Symposium*, Munich, Germany.

Karthikeyan, O. P. and Joseph, K. (2006). *Bioreactor Landfills for Sustainable Solid Waste Management*.

Kendon, M. and McCarthy, M. (2015). The UK's Wet and Stormy Winter of 2013/2014. *Weather*, 70(2):40–47.

Kerfoot, H. B., Hagedorn, B., and Verwiel, M. (2013). Evaluation of the Age of Landfill Gas Methane in Landfill Gas–Natural Gas Mixtures using Co-occurring Constituents. *Environmental Science: Processes & Impacts*, 15(6):1153–1161.

King, H. (2015). *Coal: What is it and how does it form?* URL: `http://geology.com/rocks/coal.shtml`. [Accessed 29th September 2015].

Kinnon, E. C. P., Golding, S. D., Boreham, C. J., Baublys, K. A., and Esterle, J. S. (2010). Stable Isotope and Water Quality Analysis of Coal Bed Methane Production Waters and Gases from the Bowen Basin, Australia. *International Journal of Coal Geology*, 82(3):219–231.

Kırmızı, S. and Bell, R. W. (2012). Responses of Barley to Hypoxia and Salinity during Seed Germination, Nutrient Uptake, and Early Plant Growth in Solution Cculture. *Journal of Plant Nutrition and Soil Science*, 175(4):630–640.

Kjeldsen, P., Barlaz, M. A., Rooker, A. P., Baun, A., Ledin, A., and Christensen, T. H. (2002). Present and Long-Term Composition of MSW Landfill Leachate: A Review. *Critical Reviews in Environmental Science and Technology*, 32(4):297–336.

Klein, J. (2008). *GasClam® Instrument User Manual*. IonScience Ltd, The Way, Fowlmere, Cambridge, SG8 7UJ, UK, 2.3 edition.

Klusman, R. W. (2003). Rate Measurements and Detection of Gas Microseepage to the Atmosphere from an Enhanced Oil Recovery/Sequestration Project, Rangely, Colorado, USA. *Applied Geochemistry*, 18(12):1825–1838.

Korre, A., Imrie, C. E., May, F., Beaubien, S. E., Vandermeijer, V., Persoglia, S., Golmen, L., Fabriol, H., and Dixon, T. (2011). Quantification Techniques for Potential CO_2 Leakage from Geological Storage Sites. *Energy Procedia*, 4:3413–3420.

Kotze, J. P., Thiel, P. G., and Hattingh, W. H. J. (1969). Anaerobic Digestion II. the Characterization and Control of Anaerobic Digestion. *Water Research*, 3(7):459–494.

Le Quéré, C., Moriarty, R., Andrew, R. M., Canadell, J. G., Sitch, S., Korsbakken, J. I., Friedlingstein, P., Peters, G. P., Andres, R. J., Boden, T., et al. (2015). Global Carbon Budget 2015. *Earth System Science Data*, 7(2):349–396.

Lewis, H., Mittermaier, M., Mylne, K., Norman, K., Scaife, A., Neal, R., Pierce, C., Harrison, D., Jewell, S., Kendon, M., et al. (2015). From Months to Minutes–Exploring the Value of High-Resolution Rainfall Observation and Prediction during the UK Winter Storms of 2013/2014. *Meteorological Applications*, 22(1):90–104.

Martin, J. P. (2005). *Sandy Lane Landfill Site Risk Based Environmental Monitoring Plan*. Technical Report 02/260-03, TerraConsult Ltd, Bold Business Centre, Bold Lane, Sutton, St Helens, UK, WA9 4TX.

Martini, A. M., Walter, L. M., Budai, J. M., Ku, T. C. W., Kaiser, C. J., and Schoell, M. (1998). Genetic and Temporal Relations between Formation Waters and Biogenic Methane: Upper Devonian Antrim Shale, Michigan Basin, USA. *Geochimica et Cosmochimica Acta*, 62(10):1699–1720.

Massman, W. J. (1998). A Review of the Molecular Diffusivities of H_2O, CO_2, CH_4, CO, O_3, SO_2, NH_3, N_2O, NO, and NO_2 in air, O_2 and N_2 near stp. *Atmospheric Environment*, 32(6):1111–1127.

Massmann, J. and Farrier, D. F. (1992). Effects of Atmospheric Pressures on Gas Transport in the Vadose Zone. *Water Resources Research*, 28(3):777–791.

McBean, E. A., Rovers, F. A., and Farquahar, G. J. (1995). *Solid Waste Landfill Engineering and Design*. Prentice Hall.

McGlade, C., Speirs, J., and Sorrell, S. (2013). Unconventional Gas – A Review of Regional and Global Resource Estimates. *Energy*, 55:571–584.

McIntosh, J. C., Walter, L. M., and Martini, A. M. (2002). Pleistocene Recharge to Midcontinent Basins: Effects on Salinity Structure and Microbial Gas Generation. *Geochimica et Cosmochimica Acta*, 66(10):1681–1700.

Met Office (2016). *Storm Imogen*. URL: `http://www.metoffice.gov.uk/uk-storm-centre/storm-imogen`. [Accessed 10th February 2016].

Mønster, J., Samuelsson, J., Kjeldsen, P., and Scheutz, C. (2015). Quantification of Methane Emissions from 15 Danish Landfills using the Mobile Tracer Dispersion Method. *Waste Management*, 35:177–186.

Moura, J., Sousa, M., Martens, C. S., Moreira, M. Z., Lima, R. L., Sampaio, I. C. G., Mendlovitz, H. P., and Menton, M. C. (2008). Spatial and Seasonal Variations in the Stable Carbon Isotopic Composition of Methane in Stream Sediments of Eastern Amazonia. *Tellus B*, 60(1):21–31.

Muir, G. K. P., Hayward, S., Tripney, B. G., Cook, G. T., Naysmith, P., Herbert, B. M. J., Garnett, M. H., and Wilkinson, M. (2015). Determining the Biomass Fraction of Mixed Waste Fuels: A Comparison of Existing Industry and ^{14}C-Based Methodologies. *Waste Management*, 35:293–300.

Nagata, Y. and Takeuchi, N. (2003). Measurement of Odor Threshold by Triangle Odor Bag Method. *Odor Measurement Review, Office of Odor, Noise and Vibration Environmental Management Bureau, Ministry of the Environment, Government of Japan, Tokyo, Japan*, pages 118–127.

Ni, Y., Dai, J., Gong, D., and Zhang, D. (2014). Geochemical Characteristics of Stable Carbon and Hydrogen Isotopes of Gases from the Hongtai Gas Field, Turpan-Harmi Basin, China.

Norton, G. E., Bloodworth, A. J., Cameron, D. G., Evans, D. J., Lott, G. K., Hobbs, S. F., Spencer, N. A., and Highley, D. E. (2006). *Mineral Resource Information in Support of National, Regional and Local Planning: Cheshire (comprising Cheshire, Boroughs of Halton and Warrington.* Technical Report CR/05/090N, British Geological Survey, Keyworth, Nottingham, UK.

Nosalewicz, M., Brzezinska, M., Pasztelan, M., and Supryn, G. (2011). Methane in the Environment (A Review). *Acta Agrophysica*, 18(2 [193]):355–373.

Omaye, S. T. (2002). Metabolic Modulation of Carbon Monoxide Toxicity. *Toxicology*, 180(2):139–150.

Ordnance Survey (1882). *Ordnance Survey County Series: Cheshire Sheet XXXVI 1th Edition (6 Miles to 1 Inch).* URL: `http://digimap.edina.ac.uk/ancientroam/historic`. [Accessed 19$^{\text{th}}$ August 2015].

Ordnance Survey (1884). *Ordnance Survey County Series: Hertfordshire Sheet XXIX 1th Edition (6 Miles to 1 Inch).* URL: `http://digimap.edina.ac.uk/ancientroam/historic`. [Accessed 19$^{\text{th}}$ August 2015].

Ordnance Survey (1899a). *Ordnance Survey County Series: Cheshire Sheet LI NW 2nd Edition (6 Inches to 1 Mile)*. URL: http://digimap.edina.ac.uk/ancientroam/historic. [Accessed 20th August 2015].

Ordnance Survey (1899b). *Ordnance Survey County Series: Cheshire Sheet XIX NE 2nd Edition (6 Inches to 1 Mile)*. URL: http://digimap.edina.ac.uk/ancientroam/historic. [Accessed 19th August 2015].

Ordnance Survey (1899c). *Ordnance Survey County Series: Cheshire Sheet XXXVI NE 2nd Edition (6 Inches to 1 Mile)*. URL: http://digimap.edina.ac.uk/ancientroam/historic. [Accessed 19th August 2015].

Ordnance Survey (1899d). *Ordnance Survey County Series: Hertfordshire Sheet XXIX NE 2nd Edition (6 Inches to 1 Mile)*. URL: http://digimap.edina.ac.uk/ancientroam/historic. [Accessed 19th August 2015].

Ordnance Survey (1911a). *Ordnance Survey County Series: Cheshire Sheet LI NW 3rd Edition (6 Inches to 1 Mile)*. URL: http://digimap.edina.ac.uk/ancientroam/historic. [Accessed 20th August 2015].

Ordnance Survey (1911b). *Ordnance Survey County Series: Cheshire Sheet XIX NE 3rd Edition (6 Inches to 1 Mile)*. URL: http://digimap.edina.ac.uk/ancientroam/historic. [Accessed 19th August 2015].

Ordnance Survey (1911c). *Ordnance Survey County Series: Cheshire Sheet XXXVI NE 3rd Edition (6 Inches to 1 Mile)*. URL: http://digimap.edina.ac.uk/ancientroam/historic. [Accessed 19th August 2015].

Ordnance Survey (1925). *Ordnance Survey County Series: Hertfordshire Sheet XXIX NE 3rd Edition (6 Inches to 1 Mile)*. URL: http://digimap.edina.ac.uk/ancientroam/historic. [Accessed 19th August 2015].

Ordnance Survey (1934). *Ordnance Survey County Series: Lancashire Sheet CXI NE and part of Cheshire Sheet XIX NE 4th Edition (6 Inches to 1 Mile)*. URL: http://digimap.edina.ac.uk/ancientroam/historic. [Accessed 19th August 2015].

Ordnance Survey (1938). *Ordnance Survey County Series: Cheshire Sheet LI NW 4th Edition (6 Inches to 1 Mile)*. URL: http://digimap.edina.ac.uk/ancientroam/historic. [Accessed 20th August 2015].

Ordnance Survey (1954a). *Ordnance Survey National Grid Series 1954 Revision (6 Inches to 1 Mile)*. URL: `http://digimap.edina.ac.uk/ancientroam/historic`. [Accessed 19th August 2015].

Ordnance Survey (1954b). *Ordnance Survey National Grid Series 1954 Revision (6 Inches to 1 Mile)*. URL: `http://digimap.edina.ac.uk/ancientroam/historic`. [Accessed 20th August 2015].

Ordnance Survey (1960). *Ordnance Survey National Grid Series 1960 Revision (6 Inches to 1 Mile)*. URL: `http://digimap.edina.ac.uk/ancientroam/historic`. [Accessed 19th August 2015].

Ordnance Survey (1966). *Ordnance Survey National Grid Series 1966 Revision (6 Inches to 1 Mile)*. URL: `http://digimap.edina.ac.uk/ancientroam/historic`. [Accessed 19th August 2015].

Ordnance Survey (1970). *Ordnance Survey National Grid Series 1970 Revision (1:25,000)*. URL: `http://digimap.edina.ac.uk/ancientroam/historic`. [Accessed 19th August 2015].

Ordnance Survey (1976). *Ordnance Survey National Grid Series 1976 Revision (1:10,000)*. URL: `http://digimap.edina.ac.uk/ancientroam/historic`. [Accessed 19th August 2015].

Ordnance Survey (1977). *Ordnance Survey National Grid Series 1977 Revision (1:10,000)*. URL: `http://digimap.edina.ac.uk/ancientroam/historic`. [Accessed 19th August 2015].

Ordnance Survey (1984). *Ordnance Survey National Grid Series 1984 Revision (1:10,000)*. URL: `http://digimap.edina.ac.uk/ancientroam/historic`. [Accessed 19th August 2015].

Ordnance Survey (1986). *Ordnance Survey National Grid Series 1986 Revision (1:10,000)*. URL: `http://digimap.edina.ac.uk/ancientroam/historic`. [Accessed 20th August 2015].

Ordnance Survey (2015a). *Cheadle 1:20,000 Ordnance Survey Map (from Ordnance Survey Landranger Map Series, 109: Manchester)*. URL: `http://digimap.edina.ac.uk/roam/os`. [Accessed 17th August 2015].

Ordnance Survey (2015b). *Macclesfied 1:20,000 Map (from Ordnance Survey Landranger Map Series, 118: Stoke-on-Trent & Macclesfield)*. URL: `http://digimap.edina.ac.uk/roam/os`. [Accessed 17th August 2015].

Ordnance Survey (2015c). *Ware 1:20,000 Ordnance Survey Map (from Ordnance Survey Landranger Map Series, 166: Luton & Hertford)*. URL: `http://digimap.edina.ac.uk/roam/os`. [Accessed 17th August 2015].

Orr, W. E., Wood, A. M., Beaver, J. L., Ireland, R. J., and Beagley, D. P. (1991). Abbeystead Outfall Works: Background to Repairs and Modifications and Lessons Learned. *Water and Environment Journal*, 5(1):7–18.

Osborn, S. G. and McIntosh, J. C. (2010). Chemical and Isotopic Tracers of the Contribution of Microbial Gas in Devonian Organic-Rich Shales and Reservoir Sandstones, Northern Appalachian Basin. *Applied Geochemistry*, 25(3):456–471.

Owen, D. D. R., Shouakar-Stash, O., Morgenstern, U., and Aravena, R. (2016). Thermodynamic and Hydrochemical Controls on CH_4 in a Coal Seam Gas and Overlying Alluvial Aquifer: New Insights into CH_4 Origins. *Scientific Reports*, 6.

Palstra, S. W. L. and Meijer, H. A. J. (2014). Biogenic Carbon Fraction of Biogas and Natural Gas Fuel Mixtures Determined with ^{14}C. *Radiocarbon*, 56(1):7–28.

Pedersen, G. B. (2010). Processes in a Compost Based Landfill Biocover; Methane Emission, Transport and Oxidation. *Department of Environmental Engineering, Technical University of Denmark*.

Poulsen, T. G., Christophersen, M., Moldrup, P., and Kjeldsen, P. (2003). Relating Landfill Gas Emissions to Atmospheric Pressure Using Numerical Modelling and State-Space Analysis. *Waste Management & Research*, 21(4):356–366.

Pullen, J. (2007). *Review of Odour Character and Thresholds*. Technical Report SC030170/SR2, Environment Agency, Rio House, Waterside Drive, Aztec West, Almondsbury, Bristol, BS32 4UD.

Quigley, R. M., Fernandez, F., and Rowe, R. K. (1988). Clayey Barrier Assessment of Impoundment of Domestic Waste Leachate (Southern Ontario) Including Clay-Leachate Compatability by Hydraulic Conductivity Testing. *Canadian Geotechnical Journal*, 25(3):574–581.

Rachor, I. M., Gebert, J., Gröngröft, A., and Pfeiffer, E.-M. (2013). Variability of Methane Emissions from an Old Landfill over Different Time-Scales. *European Journal of Soil Science*, 64(1):16–26.

Raco, B., Battaglini, R., and Dotsika, E. (2014). New Isotopic ($\delta^{13}C_{CO_2}$–$\delta^{13}C_{CH_4}$) Fractionation Factor Limits and Chemical Characterization of Landfill Gas. *Journal of Geochemical Exploration*, 145:40–50.

Raich, J. W. and Schlesinger, W. H. (1992). The Global Carbon Dioxide Flux in Soil Respiration and its Relationship to Vegetation and Climate. *Tellus B*, 44(2):81–89.

Ramaswamy, J. N. (1970). *Effects on Acid and Gas Production in Sanitary Landfills*. PhD thesis, University of West Virginia, Morgantown, WV.

Reiffenstein, R. J., Hulbert, W. C., and Roth, S. H. (1992). Toxicology of Hydrogen Sulfide. *Annual Review of Pharmacology and Toxicology*, 32(1):109–134.

Revans, A., Ross, D., Gregory, B., Meadows, M., Harries, C., and Gronow, J. (1999). Long Term Fate of Metals in Landfill. In Christensen, T. H., Cossu, R., and Stegmann, R., editors, *7th International Waste Management and Landfill Symposium, Volume I*, Cagliari, Sardinia, Italy.

Riley, R. (2009). *GA2000 Range Gas Analysers Operating Manual*. Geotechnical Instruments (UK) Ltd, Sovereign House, Queensway, Leamingto Spa, Warwickshire, CV31 3JR, OMGAUK 1.37 edition.

Rovers, F. A. and Farquhar, G. J. (1972). Sanitary Landfill Study Final Report, Volume II. Effect of Season on Landfill Leachate and Gas Production. *Waterloo Research Institute, Waterloo, Ontario. Project*, 8083.

Scheutz, C., Bogner, J., De Visscher, A., Gebert, J., Hilger, H., Huber-Humer, M., Kjeldsen, P., and Spokas, K. (2009). Microbial Methane Oxidation Processes and Technologies for Mitigation of Landfill Gas Emissions. *Waste Management & Research*.

Schlesinger, W. H. and Andrews, J. A. (2000). Soil Respiration and the Global Carbon Cycle. *Biogeochemistry*, 48(1):7–20.

Schlömer, S., Furche, M., Dumke, I., Poggenburg, J., Bahr, A., Seeger, C., Vidal, A., and Faber, E. (2013). A Review of Continuous Soil Gas Mmonitoring Related to CCS – Technical Advances and Lessons Learned. *Applied Geochemistry*, 30:148–160.

Schlömer, S., Möller, I., and Furche, M. (2014). Baseline Soil Gas Measurements as Part of a Monitoring Concept above a Projected CO_2 Injection Formation – A

Case Study from Northern Germany. *International Journal of Greenhouse Gas Control*, 20:57–72.

Schroder, I. F., Zhang, H., Zhang, C., and Feitz, A. J. (2016). The Role of Soil Flux and Soil Gas Monitoring in the Characterisation of a CO_2 Surface Leak: A Case Study in Qinghai, China. *International Journal of Greenhouse Gas Control*, 54:84–95.

Semrau, J. D. (2011). Current Knowledge of Microbial Community Structures in Landfills and its Cover Soils. *Applied Microbiology and Biotechnology*, 89(4):961–969.

Setschenow, J. (1889). Uber die konstitution der salzlosungenauf grund ihres verhaltens zu kohlensaure. *Zeitschrift fur Physikalische Chemie*, 4:117–125.

Sherlock, R. L., Pocock, R. W., Pringle, J., and Chatwin, C. P. (1924). *The Geology of the Country around Hertford*, volume 239. HM Stationery Office, London.

Skinner, F. A. (1968). The Anaerobic Bacteria of Soil. *The Ecology of Soil Bacteria. Liverpool University Press, England*, 573:592.

Smith, K. A., Ball, T., Conen, F., Dobbie, K. E., Massheder, J., and Rey, A. (2003). Exchange of Greenhouses Gases between Soil and Atmosphere: Iinteractions of Soil Phsyical Factors and Biological Processes. *European Journal of Soil Science*, 54(4):779–791.

Smith, P. (2004). Carbon Sequestration in Croplands: The Potential in Europe and the Global Context. *European journal of agronomy*, 20(3):229–236.

Solomon, S., Qin, D., Manning, M., Chen, Z., Marquis, M., Averyt, K. B., Tignor, M., and L., M. H. (2007). Contribution of Working Group I to the Fourth Assessment Report of the IPCC. *IPCC Fourth Assessment Report: Climate Change 2007 (AR4)*.

Taylor, B. J. (1963). *The Geology of the Country around Stockport and Knutsford*, volume 98. HM Stationery Office, London.

Teasdale, C. J., Hall, J. A., Martin, J. P., and Manning, D. A. C. (2014). Ground Gas Monitoring: Implications for Hydraulic Fracturing and CO_2 Storage. *Environmental Science & Technology*, 48(23):13610–13616.

Toerien, D. F. and Hattingh, W. H. J. (1969). Anaerobic Digestion i. the Microbiology of Anaerobic Digestion. *Water Research*, 3(6):385–416.

Tsunogai, U., Yoshida, N., and Gamo, T. (2002). Carbon Isotopic Evidence of Methane Oxidation through Sulfate Reduction in Sediment beneath Cold Seep Vents on the Seafloor at Nankai Trough. *Marine Geology*, 187(1):145–160.

Turton, F. B. (1981). Colliery Explosions and Fires: Their Influence upon Legislation and Mining Practice. *The Mining Engineer*, 141:157–64.

UC Davis Stable Isotope Facility (2016). *Methane (CH_4) Analysis by Trace Gas-IRMS*. URL: `http://stableisotopefacility.ucdavis.edu/ch4.html`. [Accessed 15th February 2016].

UNFCCC (2015). *United Nations Framework Convention on Climate Change Global Warming Potentials*. URL: `http://unfccc.int`. [Accessed 25th August 2015].

Wadey-Leblond, A. (2012). *Twenty One GasClam's Installed to Monitor Gas Concentrations during Fracking Operations*. URL: `http://www.ionscience.com/blog/2012/01/monitoring-fracking-a-local-solution-to-global-energy-problems/`. [Accessed: 25th February 2015].

WBB Minerals Ltd (2008). *The Proposed Extension to Silica Sand Extraction Operations at Bent Farm Quarry with Progressive Restoration*. Technical Report Non-Technical Summary, WBB Minerals Ltd, Sibelco UK Ltd, Brookside Hall, Sandbach, Cheshire, CW11 4TF.

White, C. M., Strazisar, B. R., Granite, E. J., Hoffman, J. S., and Pennline, H. W. (2003). Separation and Capture of CO_2 from Large Stationary Sources and Sequestration in Geological Formations – Coalbeds and Deep Saline Aquifers. *Journal of the Air & Waste Management Association*, 53(6):645–715.

Whiticar, M. J. (1999). Carbon and Hydrogen Isotope Systematics of Bacterial Formation and Oxidation of Methane. *Chemical Geology*, 161(1):291–314.

Widory, D., Proust, E., Bellenfant, G., and Bour, O. (2012). Assessing Methane Oxidation under Landfill Covers and its Contribution to the above Atmospheric CO_2 Levels: The Added Value of the Isotope (δ^{13}C and δ^{18}O CO_2; δ^{13}C and δD CH_4) Approach. *Waste Mmanagement*, 32(9):1685–1692.

Williams, G. M. and Aitkenhead, N. (1991). Lessons from Loscoe: The Uncontrolled Migration of Landfill Gas. *Quarterly Journal of Engineering Geology and Hydrogeology*, 24(2):191–207.

Wilson, E. J., Johnson, T. L., and Keith, D. W. (2003). Regulating the Ultimate Sink: Managing the Risks of Geologic CO_2 Storage. *Environmental Science & Technology*, 37(16):3476–3483.

Wilson, S., Card, G., and Haines, S. (2009). *Ground Gas Handbook*. Whittles; Distributed in North America by CRC Press.

Wilson, S. A., Oliver, S., Mallett, H., Hutchings, H., and Card, G. (2006). *Assessing Risks Posed by Hazardous Ground Gases to Buildings*. Construction Industry Research and Information Association (CIRIA), London.

Woese, C. R. and Fox, G. E. (1977). Phylogenetic Structure of the Prpkaryotic Domain: The Primary Kingdoms. *Proceedings of the National Academy of Sciences*, 74(11):5088–5090.

Xu, L., Lin, X., Amen, J., Welding, K., and McDermitt, D. (2014). Impact of Changes in Barometric Pressure on Landfill Methane Emission. *Global Biogeochemical Cycles*, 28(7):679–695.

Xu, M. and Qi, Y. (2001). Soil-Surface CO_2 Efflux and its Spatial and Temporal Variations in a Young Ponderosa Pine Plantation in Northern California. *Global Change Biology*, 7(6):667–677.

Yarnes, C. (2013). δ^{13}C and δ^{2}H Measurement of Methane from Ecological and Geological Sources by Gas Chromatography/Combustion/Pyrolysis Isotope-Ratio Mass Spectrometry. *Rapid Communications in Mass Spectrometry*, 27(9):1036–1044.

Zazzeri, G., Lowry, D., Fisher, R., France, J., Lanoisellé, M., and Nisbet, E. (2015). Plume Mapping and Isotopic Characterisation of Anthropogenic Methane Sources. *Atmospheric Environment*, 110:151–162.

Zehnder, A. J. B. (1978). Ecology of Methane Formation. *Water Pollution Microbiology*, 2:349–376.

Zinder, S. H. (1993). Physiological Ecology of Methanogens. In *Methanogenesis*, pages 128–206. Springer.

Appendices

Appendix A

Historic Site Maps

Site 1

From the time of 1st Edition Ordnance Survey County Series Map (1882) until the mid 1950s, the site was agricultural land used for pastoral and arable farming.

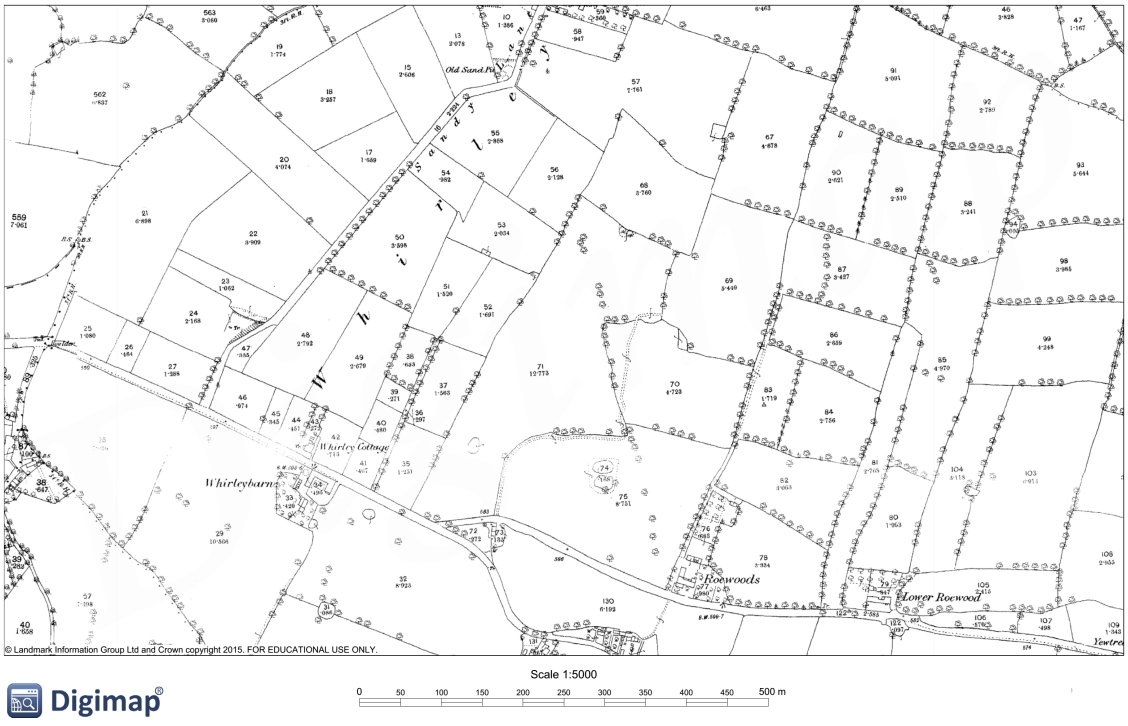

Figure A.1: Ordnance Survey County Series 1st Edition (1882) for Site 1 (from Ordnance Survey (1882))

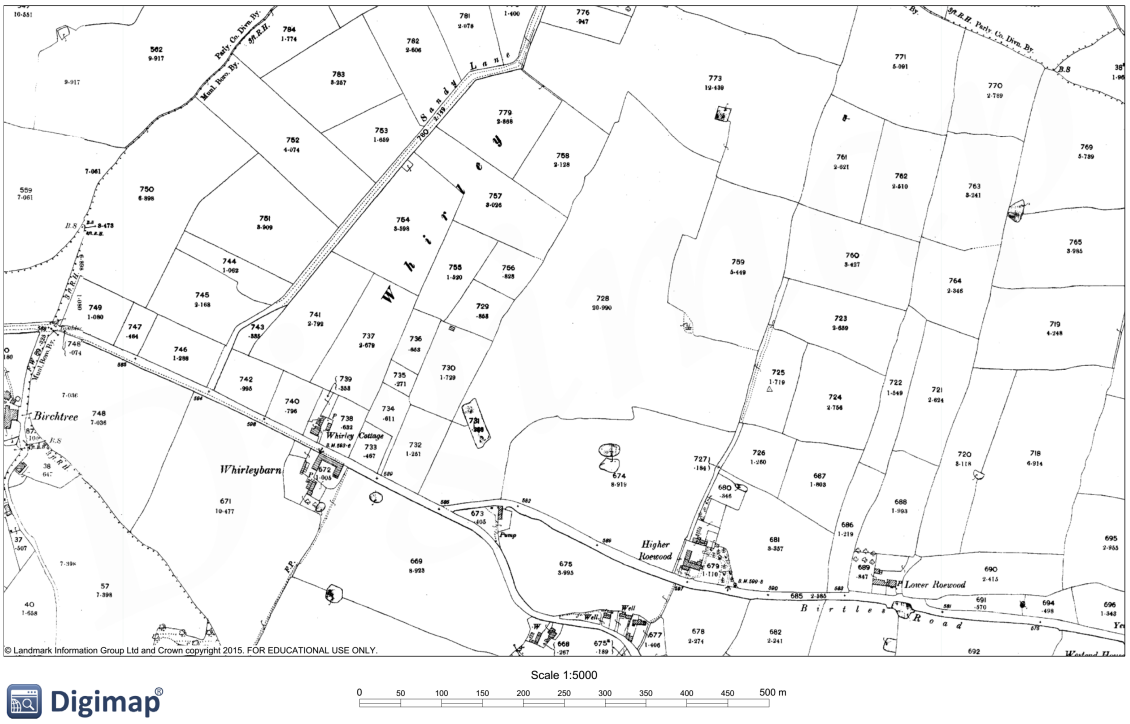

Figure A.2: Ordnance Survey County Series 2nd Edition (1899) for Site 1 (from Ordnance Survey (1899c))

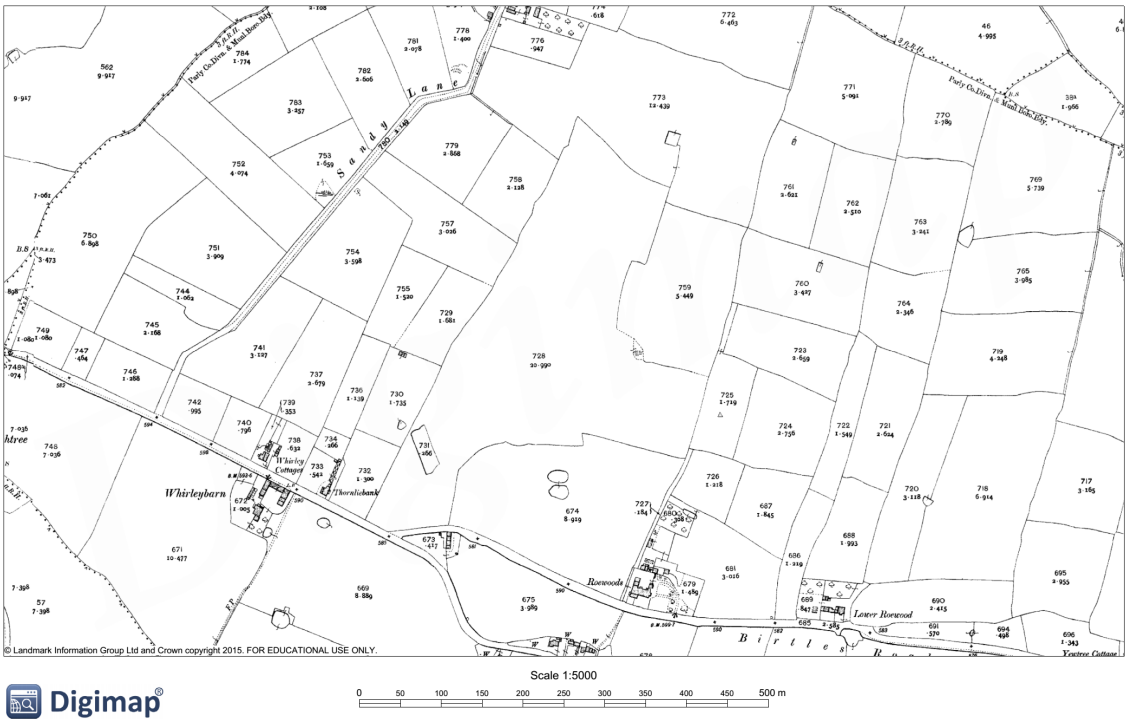

Figure A.3: Ordnance Survey County Series 3rd Edition (1911) for Site 1 (from Ordnance Survey (1911c))

By 1954, sand was beginning to be excavated from the north of the site on a small scale (Sand Pit) (Figure A.4).

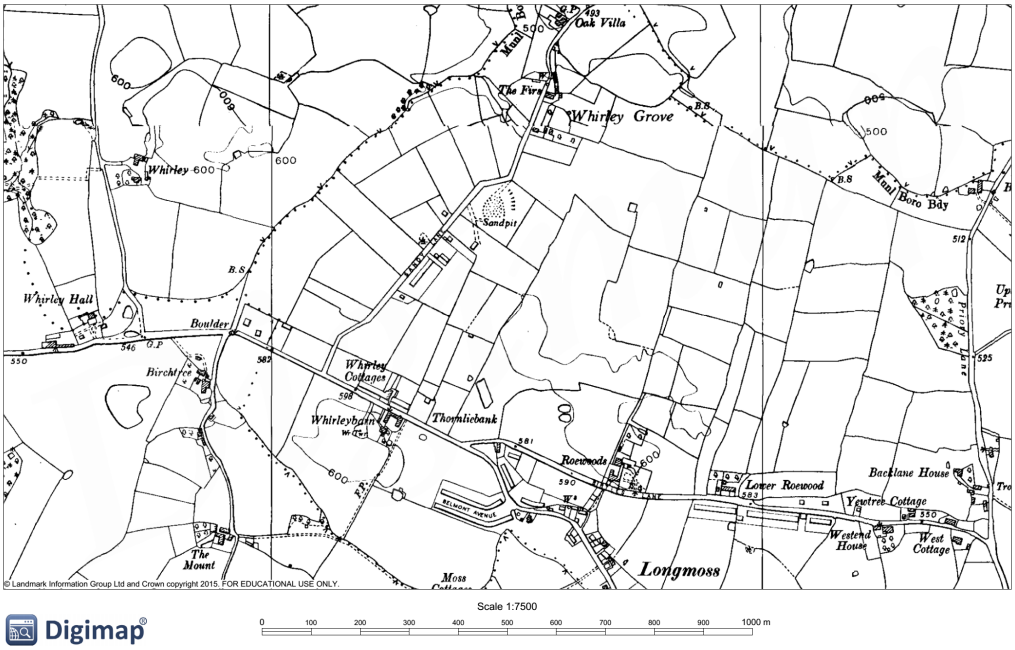

Figure A.4: Ordnance Survey National Grid Series 1954 Revision for Site 1 (from Ordnance Survey (1954a))

By 1970 the sand pit excavations had extended. A second sand pit was operational to the north of Sandy Lane. Overhead electricity cables running NE–SW with supporting pylons to the S and NE of the site were installed after 1954.

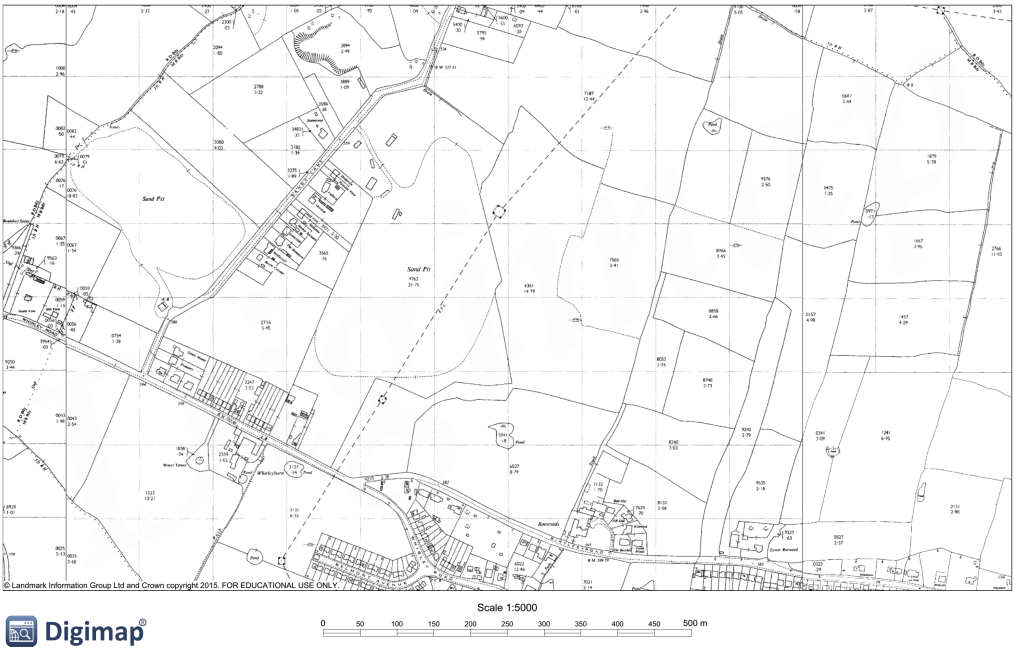

Figure A.5: Ordnance Survey National Grid Series 1970 Revision for Site 1 (from Ordnance Survey (1970))

By 1976, the sand pit operations had ceased and the filling of Site 1 had commenced. This agrees with the Site report by Martin (2005). The sand pit to the north of Sandy Lane would eventually be restored as a lake, known as Whirley Mere.

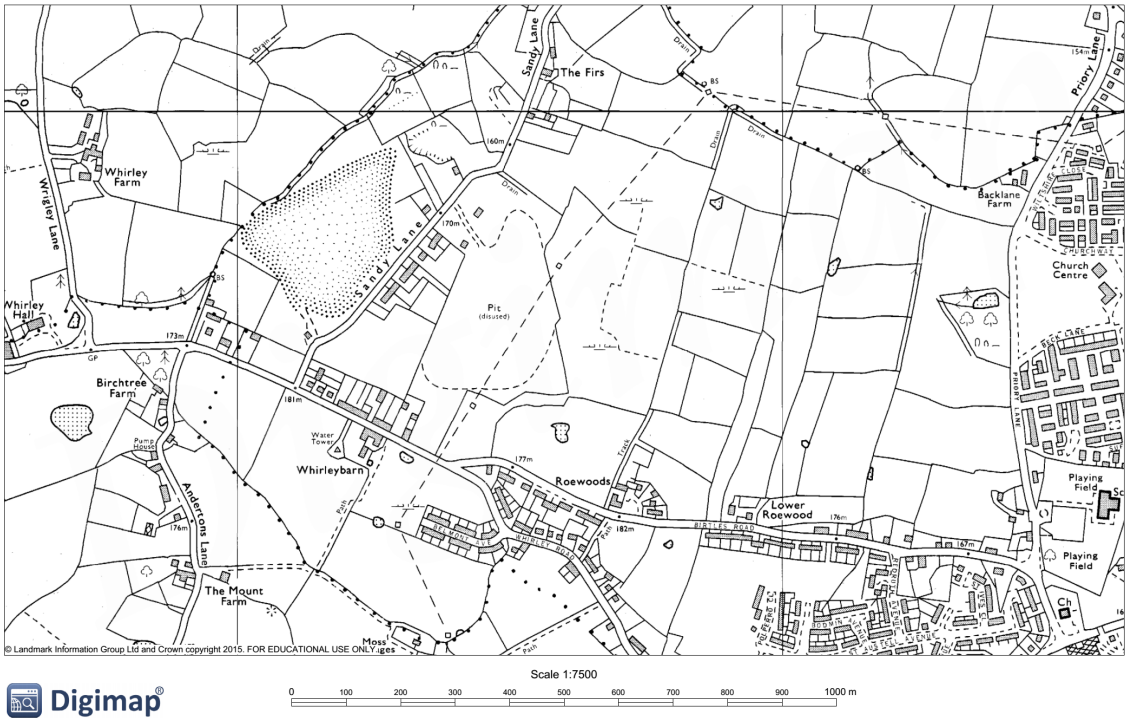

Figure A.6: Ordnance Survey National Grid Series 1976 Revision for Site 1 (from Ordnance Survey (1976))

There is no evidence of any other historic industry on or in close proximity to the site. Therefore any CH_4, CO_2 and other contaminants are assumed to originate from landfilling operations between 1968 and 2003.

Site 2

The historic Ordnance Survey maps document the urbanisation which took place around Site 2 mostly during the 20th Century. At the time of the 2nd Ed. Ordnance Survey map (1899), the Crewe and Manchester Branch Line that bounds the NW of the site had been operational for about 50 years as construction took place between 1841 and 1846. Many small brick works were also present to the north of the site at this time.

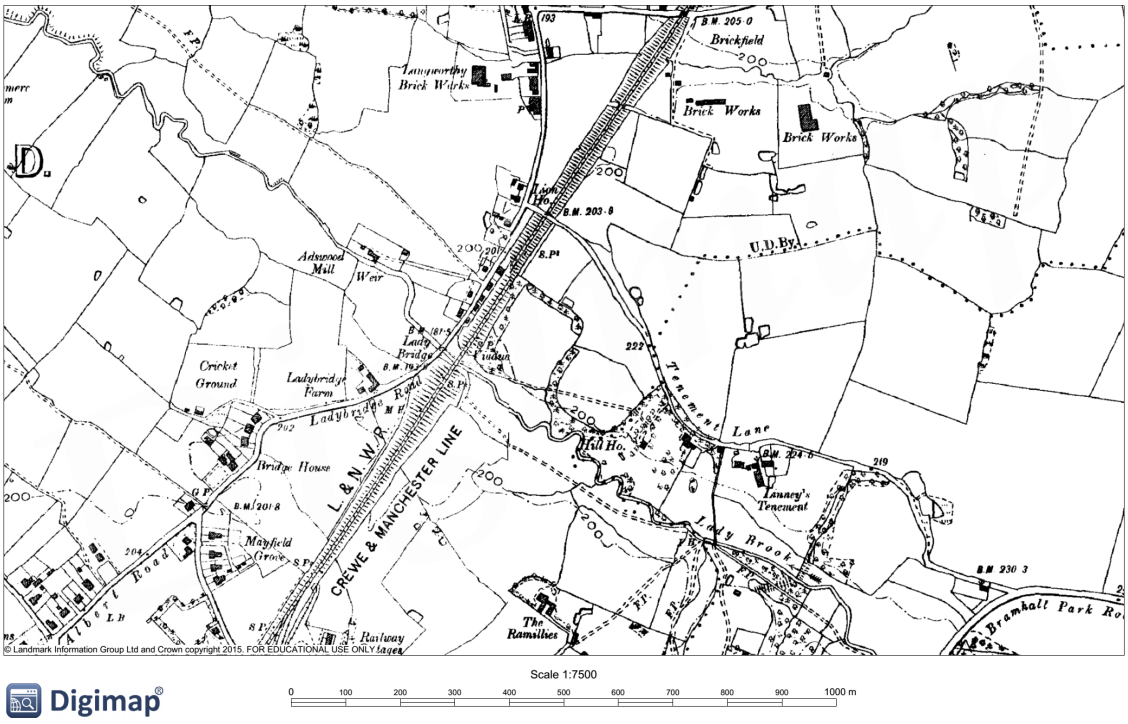

Figure A.7: Ordnance Survey County Series 2nd Edition (1899) for Site 2 (from Ordnance Survey (1899b))

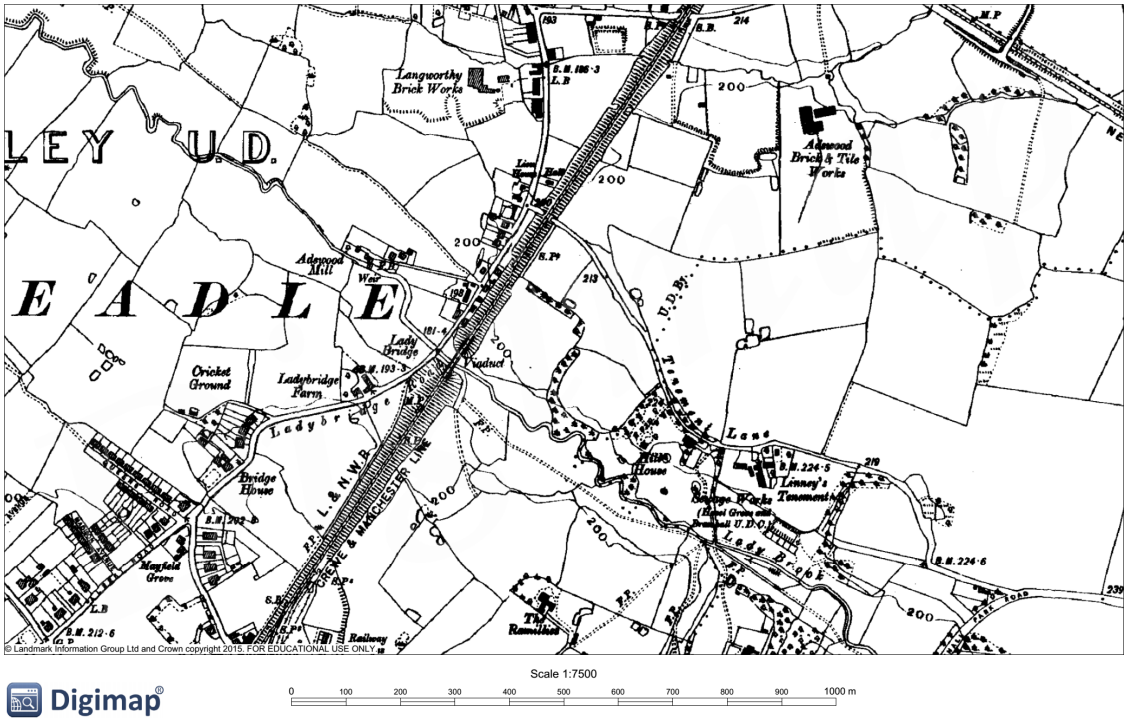

Figure A.8: Ordnance Survey County Series 3rd Edition (1911) for Site 2 (from Ordnance Survey (1911b))

By 1934, multiple housing estates to the south and west of the site had been completed while the brick works had been consolidated into one clay pit to the north of the site. This would later become the footprint of the first landfill site.

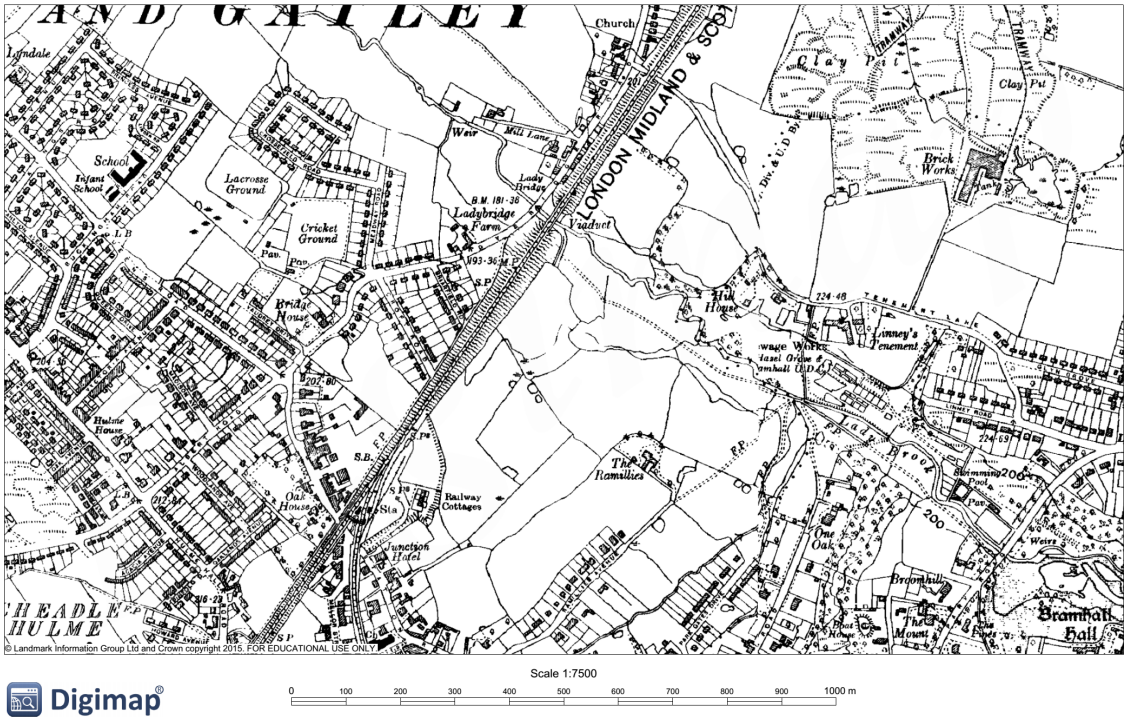

Figure A.9: Ordnance Survey County Series 4th Edition (1934) for Site 2 (from Ordnance Survey (1934))

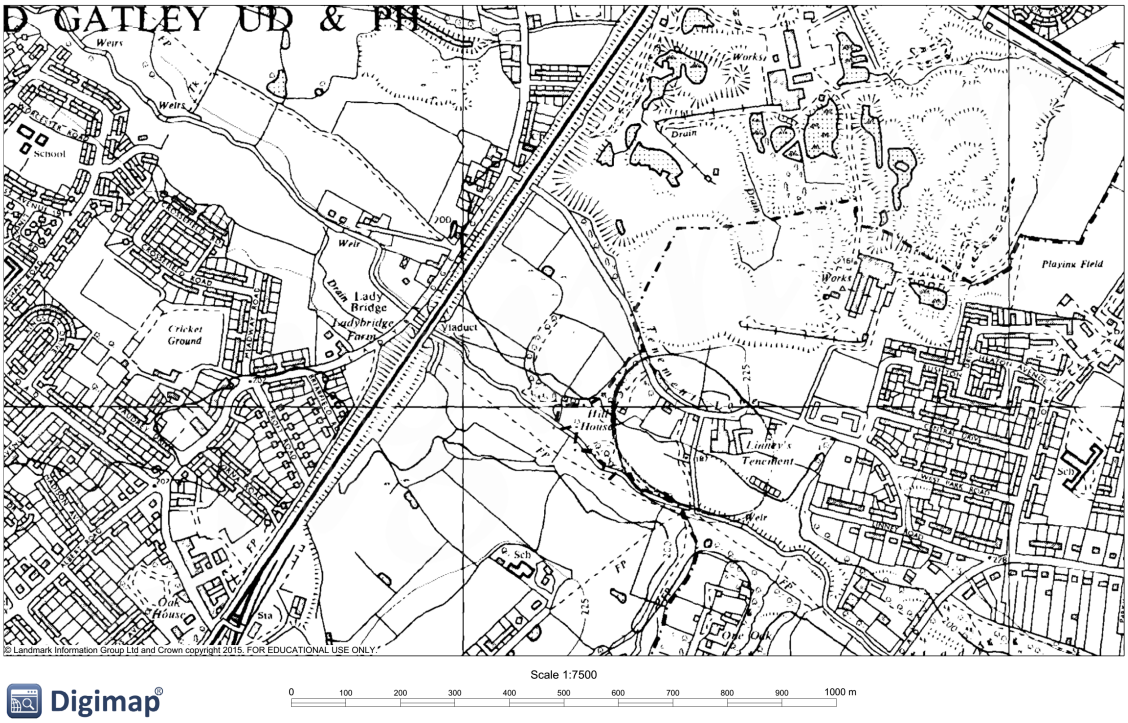

Figure A.10: Ordnance Survey National Grid Series 1966 Revision for Site 2 (from Ordnance Survey (1966))

A modern housing estate to the NW of the railway viaduct was constructed between 1978 and 1984. The clay pit to the north of the site was closed 1978/79 after more than 100 years of brick production in the locality.

Figure A.11: Ordnance Survey National Grid Series 1984 Revision for Site 2 (from Ordnance Survey (1984))

Site 3

Like Site 1, Site 3 has a largely unchanged past. For most of its history it has been used for agricultural land with later developments in infrastructure and excavation of local resources in the 20th Century.

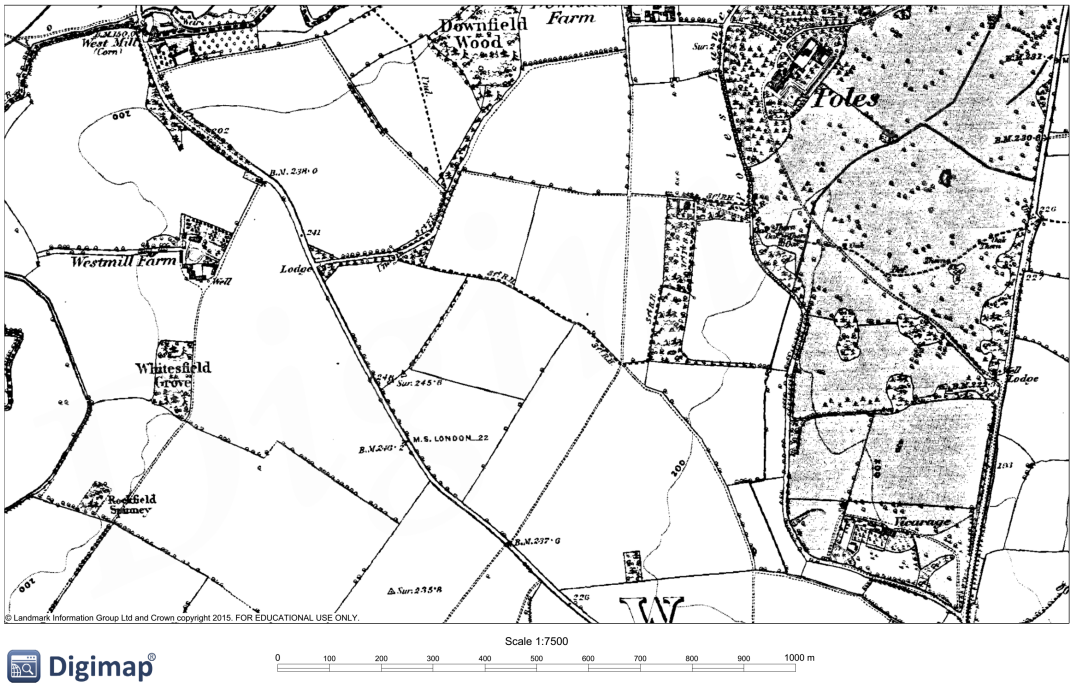

Figure A.12: Ordnance Survey County Series 1th Edition (1884) for Site 3 (from Ordnance Survey (1884))

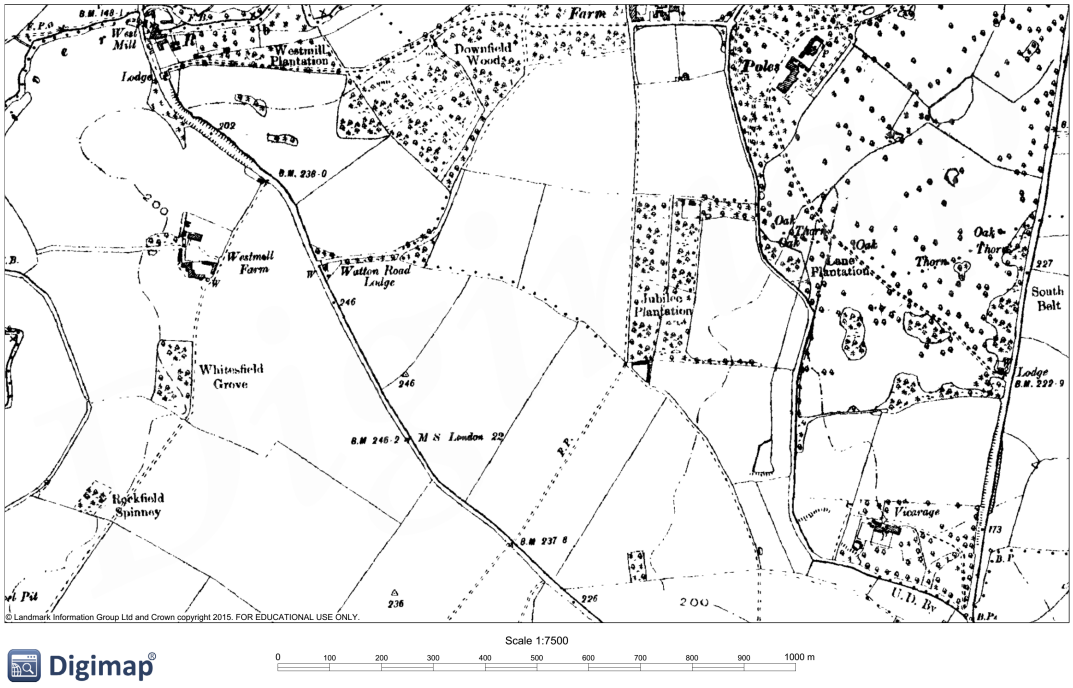

Figure A.13: Ordnance Survey County Series 2nd Edition (1899) for Site 3 (from Ordnance Survey (1899d))

Between the 1st and 2nd Edition Ordnance Survey Maps a Plantation ('Westmill Plantation') was planted to the north of the site and east of Westmill Road.

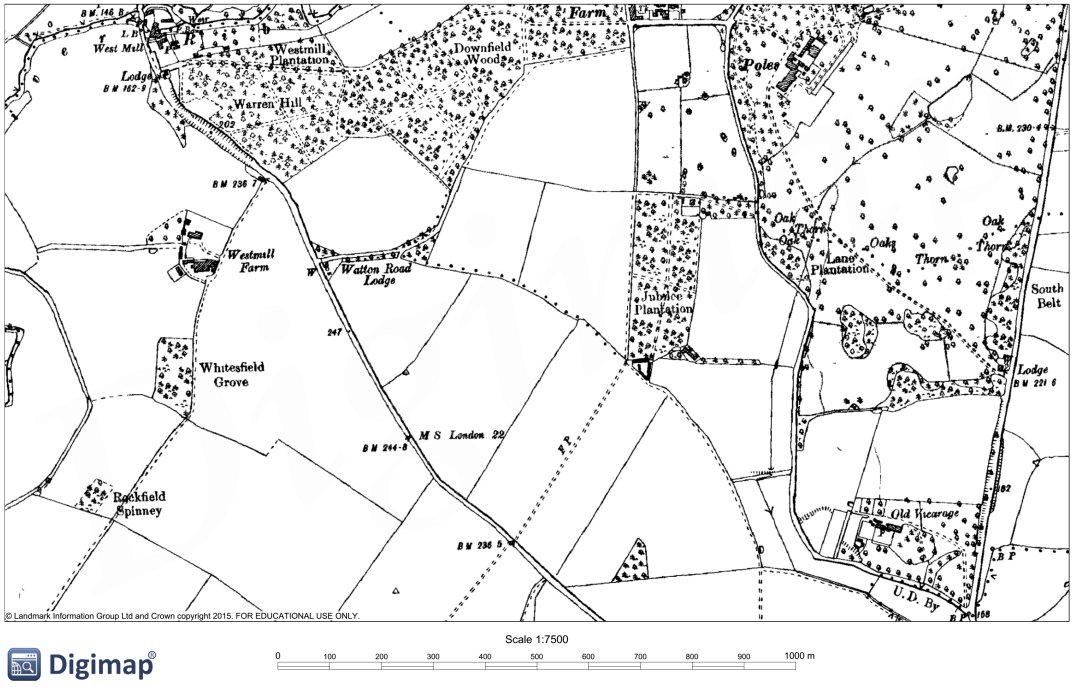

Figure A.14: Ordnance Survey County Series 3rd Edition (1925) for Site 3 (from Ordnance Survey (1925))

Over the decades the plantation was expanded and by 1960, gravel excavation to the south of the plantation and on both sides of Westmill Road had begun.

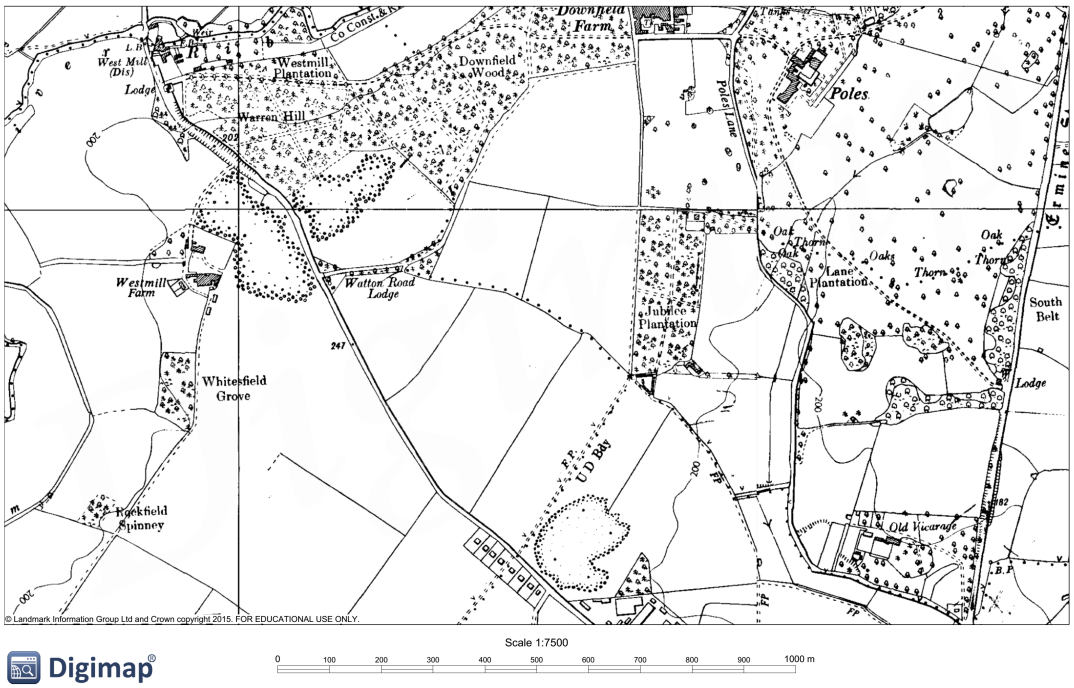

Figure A.15: Ordnance Survey National Grid Series 1960 Revision for Site 3 (from Ordnance Survey (1960))

A bypass around a nearby urban area was opened in the late 1970s. Expansion of the urban area advanced towards the new road during this decade. Additional gravel excavations were taking place on former agricultural land at this time. By 1977, the first two gravel pits had been exhausted. The larger disused pit to the east of Westmill Road would form the footprint of a landfill (licence granted in 1977).

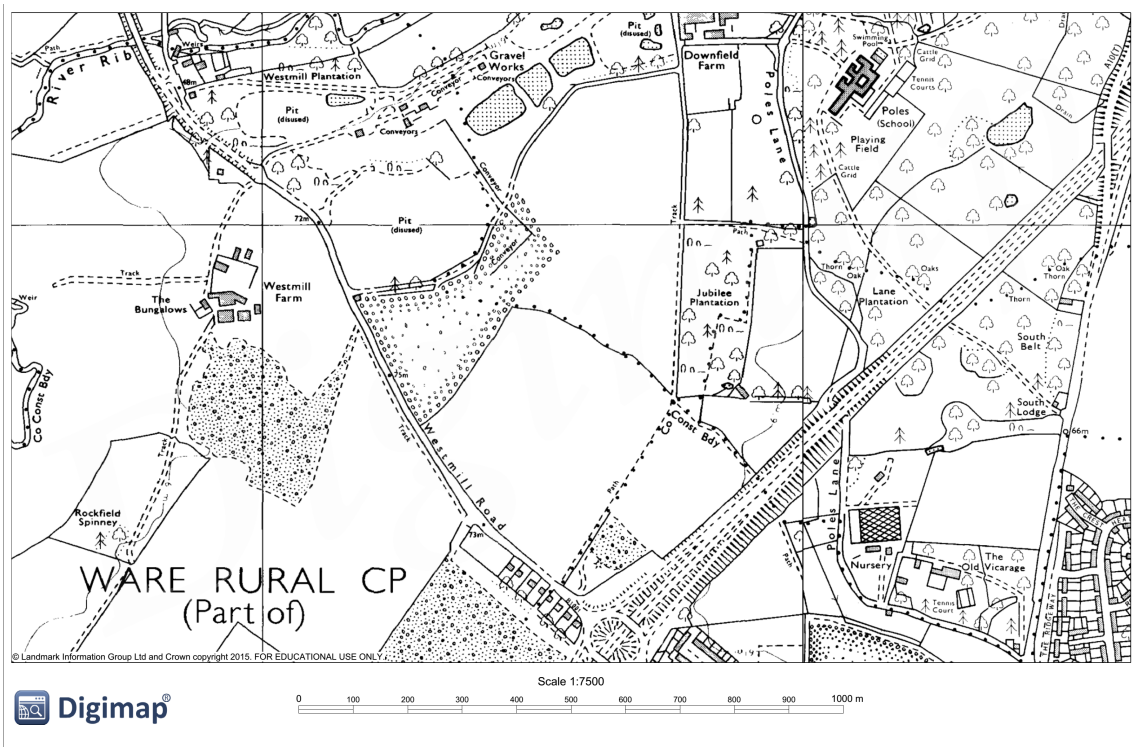

Figure A.16: Ordnance Survey National Grid Series 1977 Revision for Site 3 (from Ordnance Survey (1977))

Later in 1984, the former gravel pit to the west of Westmill Road (south of Westmill Farm) would be granted a landfill licence. The combined area of Site 3 includes the footprint of the former gravel pit to the east of Westmill Road and the 'Jubilee Plantation' lying to the east of the gravel pit. The modern dual carriageway bypass that opened in the late 1970s is the southern boundary of the site, while Poles Lane represents the eastern boundary and Westmill Road forms the western boundary.

Control Site

Likewise, with Sites 1 and 3, the control site has had a broadly unchanged history owing to its rural setting. Throughout the site's history there has been agricultural fields with many intermittent small woodlands, surface water features and small-scale sand excavations. Today, the control borehole is located to the west of Brownlow Farm, near to the small surface water feature.

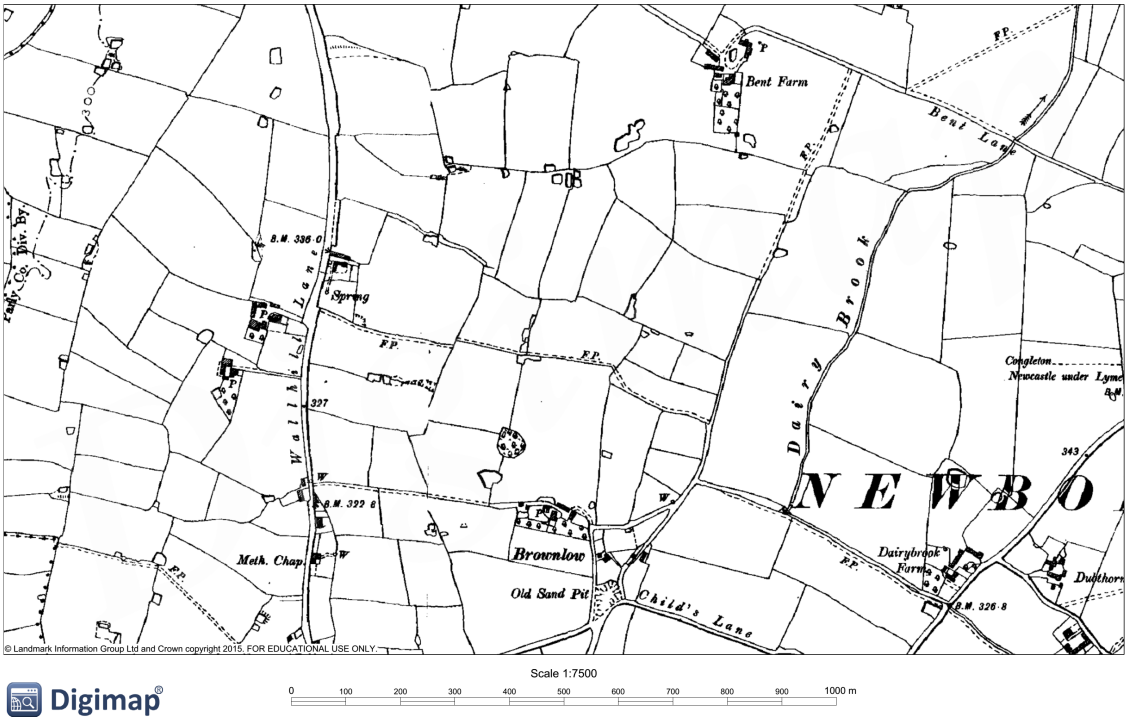

Figure A.17: Ordnance Survey County Series 2nd Edition (1899) for the Control Site (from Ordnance Survey (1899a))

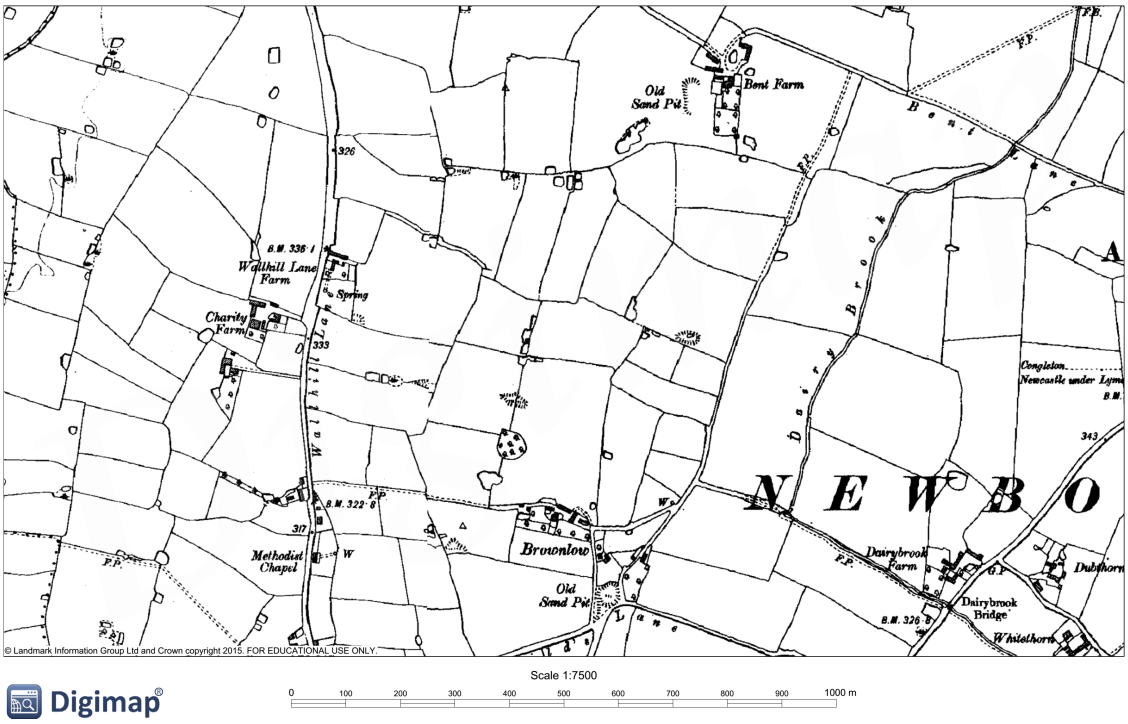

Figure A.18: Ordnance Survey County Series 3rd Edition (1911) for the Control Site (from Ordnance Survey (1911a))

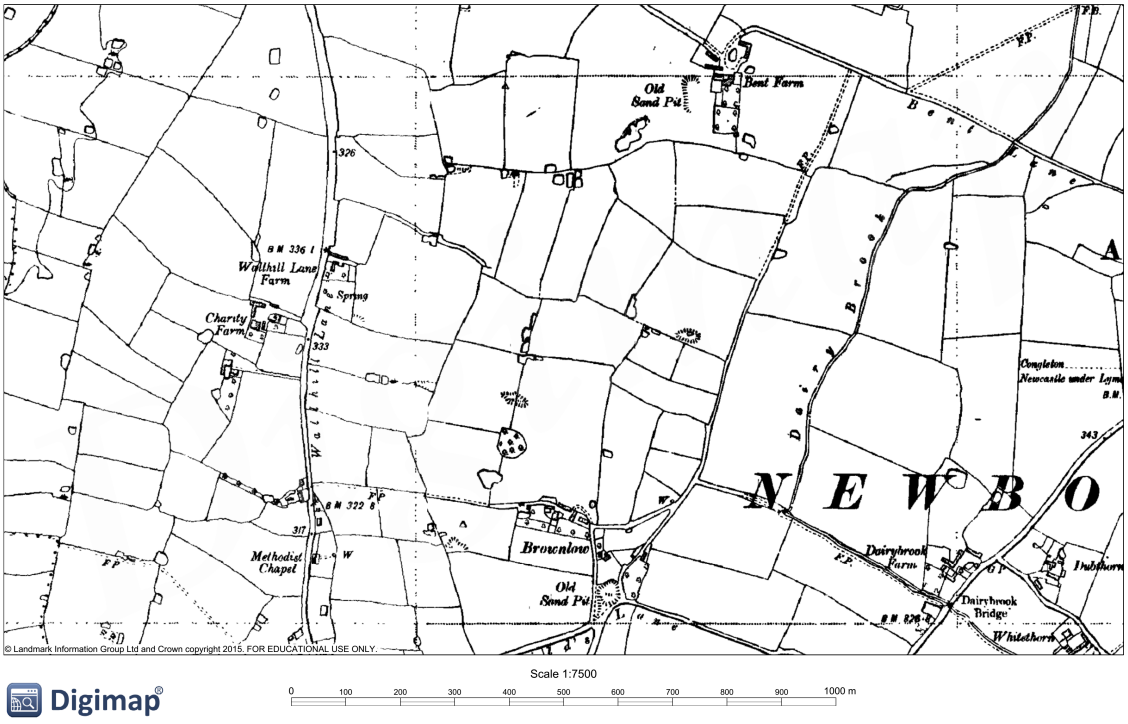

Figure A.19: Ordnance Survey County Series 4th Edition (1938) for the Control Site (from Ordnance Survey (1938))

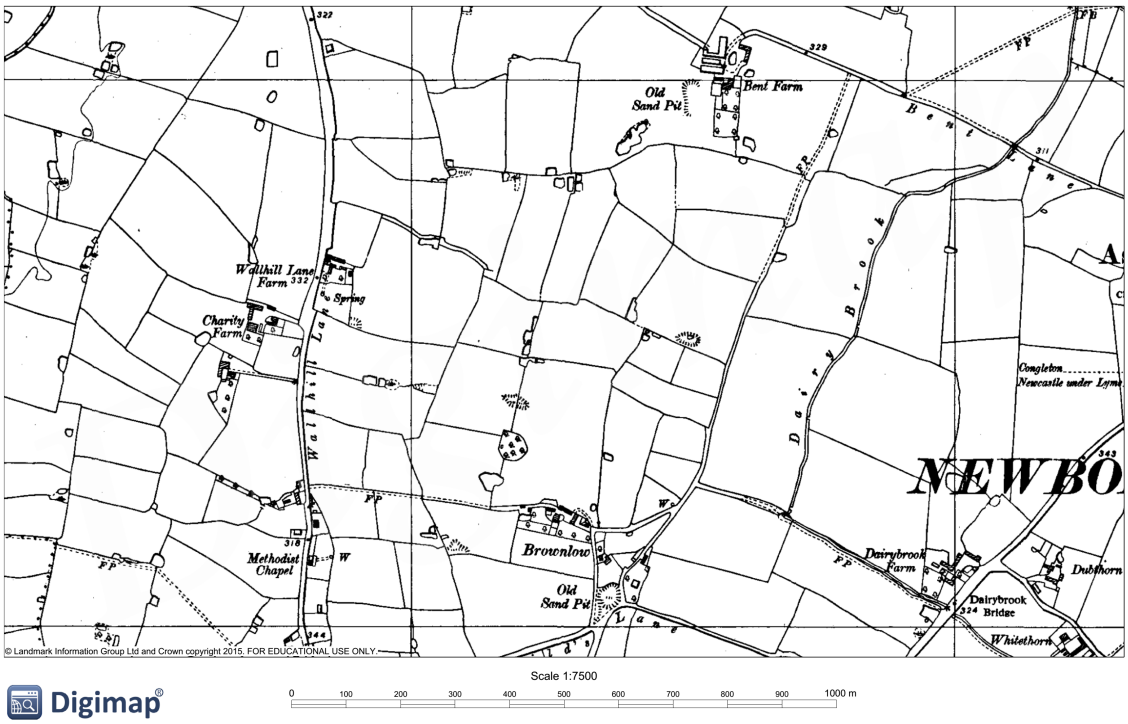

Figure A.20: Ordnance Survey National Grid Series 1954 Revision for the Control Site (from Ordnance Survey (1954b))

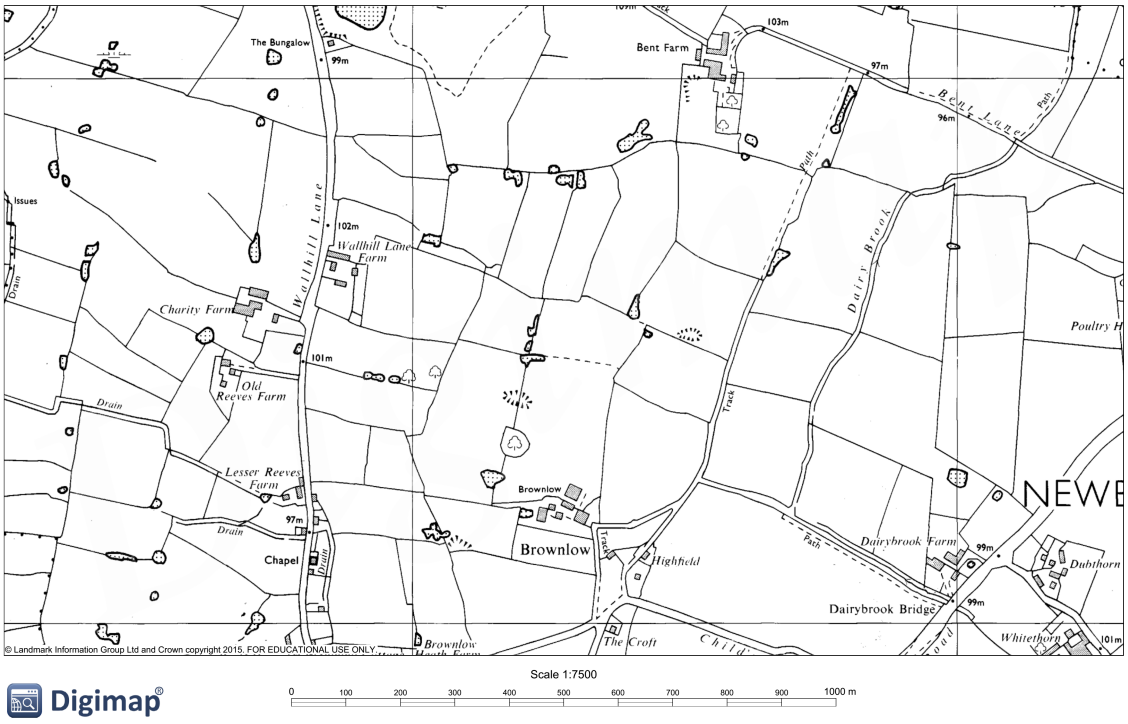

Figure A.21: Ordnance Survey National Grid Series 1986 Revision for the Control Site (from Ordnance Survey (1986))

Appendix B

Site 1 Borehole Logs

Summary

- Scale 1:50 at original A4 size.
- All installations have a 51 mm internal diameter pipe.
- BH 03/4
  - 5.5 m plain pipe. 0.5 m bentonite seal (0.5–1.0 m depth) and 1.0 m bentonite seal (4.5–5.5 m depth).
  - 22.0 m slotted pipe (5.5–27.5 m depth). Borehole terminates at 27.5 m. Response zone 5.5–27.5 m depth.
  - Response zone largely consists of unconsolidated material. Sand is light brown to brown and fine to medium grain-sized with some slightly clayey material below 11 m. Sand becomes damp below 15 m. This has implications for scrubbing of CO_2. Below 19 m, there is a little fine angular gravel and some fine coal fragments.
- BH 03/6
  - 5.0 m plain pipe, 0.5 m bentonite seal (05–1.0 m depth) and 1.0 m bentonite seal (4.0–5.0 m depth).
  - 24.0 m slotted pipe (5.0–27.0 m depth). Borehole terminates at 29.0 m depth (final 2.0 m plain pipe). Response zone 22.0 m (5.0–79.0 m depth).
  - Response zone comprises a thick (22.0 m) layer of sand. The sand is dark brown in colour and medium to coarse. It gradually becoming finer and lighter in colour with increasing depth. The sand is wet below 7.0 m and fine coal fragments are present below 12.0 m.
- BH 03/7
  - 1.0 m of plain pipe with a 0.75 m bentonite seal (0.25–1.0 m depth).
  - Slotted pipe 8.0 m (1.0–9.0 m depth). Response zone 8.0 m.
  - Borehole terminates at 11.0 m below ground level.

  - Upper most 3.0 m of the response zone comprises firm to stiff red-brown sandy clay with a little fine to medium sub-angular gravel. This material is not very permeable. Below 4.0 m to the end of the borehole, the response zone comprises sand. The sand is initially light brown and fine, and becomes increasingly darker and coarser with increasing depth. At 8.0 m, the sand becomes silty. The lower most 5.0 m of material is a porous medium that enables gas transport.

- BH 06/13
  - 3.5 m plain pipe (0–3.5 m depth) with 3.5 m bentonite seal.
  - Slotted pipe 3.5–34.5 m depth from surface. Borehole terminates at 34.5 m depth.
  - Response zone 31.0 m thick.
  - Response zone is comprised of medium dense brown fine to medium coarse sand. From 14. 0 m depth, occasional fine coal fragments are present. From 18.0 m depth, thin clay bands are present in the sand layer. From 27.0 m depth to the end of the borehole, the sand is dense brown fine silty sand. This thick response area (31.0 m) consists of permeable and porous material that allows the movement of gas.
- BH 06/14
  - 3.5 m plain pipe (0–3.5 m depth from surface) with 3.5 m bentonite seal.
  - Slotted pipe 3.5–30.0 m depth (26.5 m). Response zone 26.5 m thick. Borehole terminates at 30.0 m depth from ground level.
  - Response zone comprises 3.7 m (3.5–7.2 m depth) soft brown clayey silty sand. 7.2–15.0 m depth contains fine brown sand. Below 15.5 m the sand is fine to coarse with occasional thin clay binder.
- BH 06/19
  - Plain pipe 0–4.5 m depth with bentonite seal. This plain section of pipe runs through made ground.
  - Slotted pipe 4.5–15.3 mm depth (10.8 m). Borehole terminates at 15.3 m depth.
  - Response zone comprises 4.5 m of soft brown clayey silty sand (4.5–9.0 m depth), a thin (0.5 m) layer of firm brown silty clay. Below 9.5 m, the response zone is fine brown sand. The zone from 9.0 m to 14.5 m is particularly permeable and porous for gas transport. The last 0.8 m of the borehole is firm brown silty clay which acts as a barrier to gas movement.

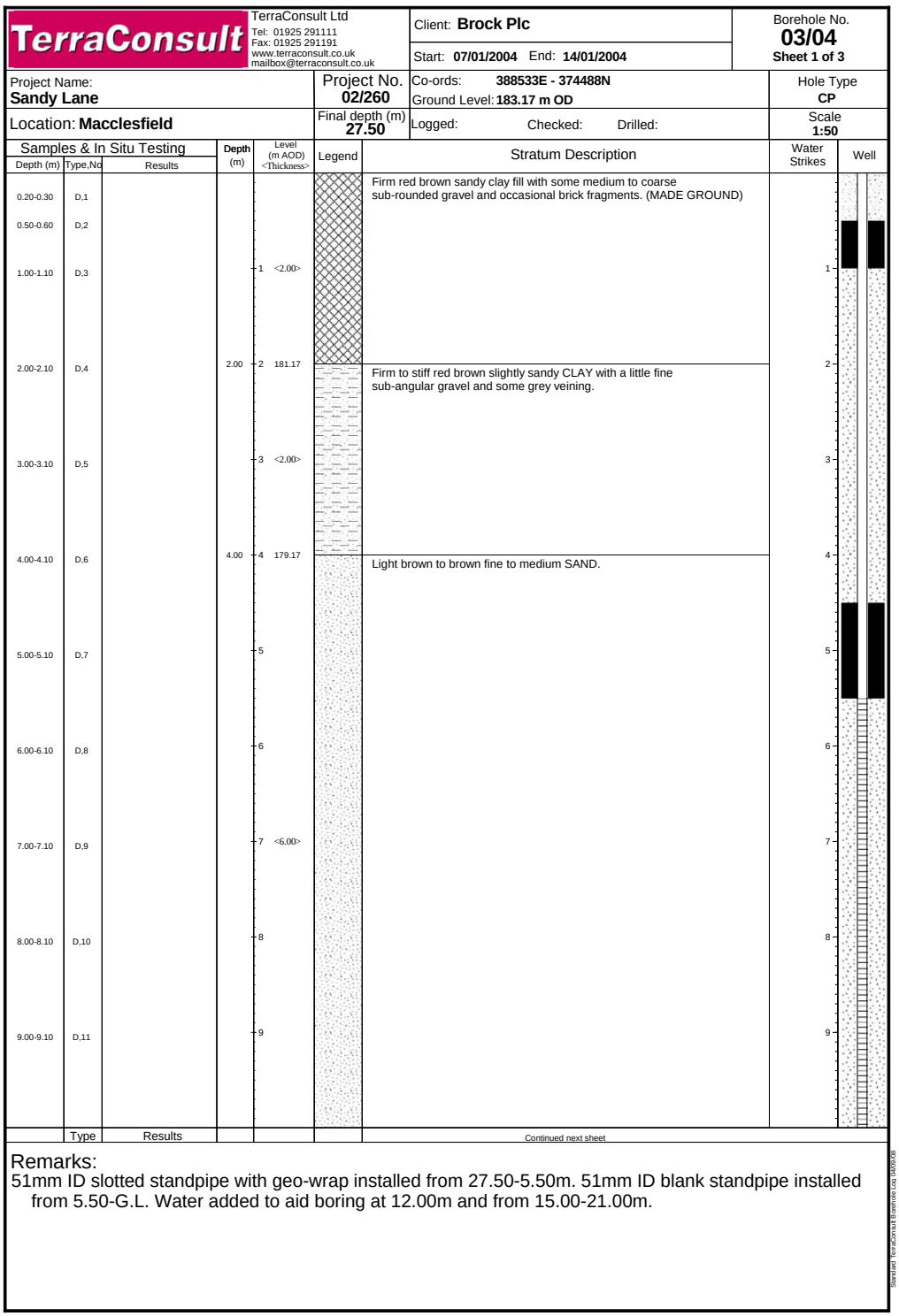

Figure B.1: Site 1 BH 03/4 Borehole Log (Part 1)

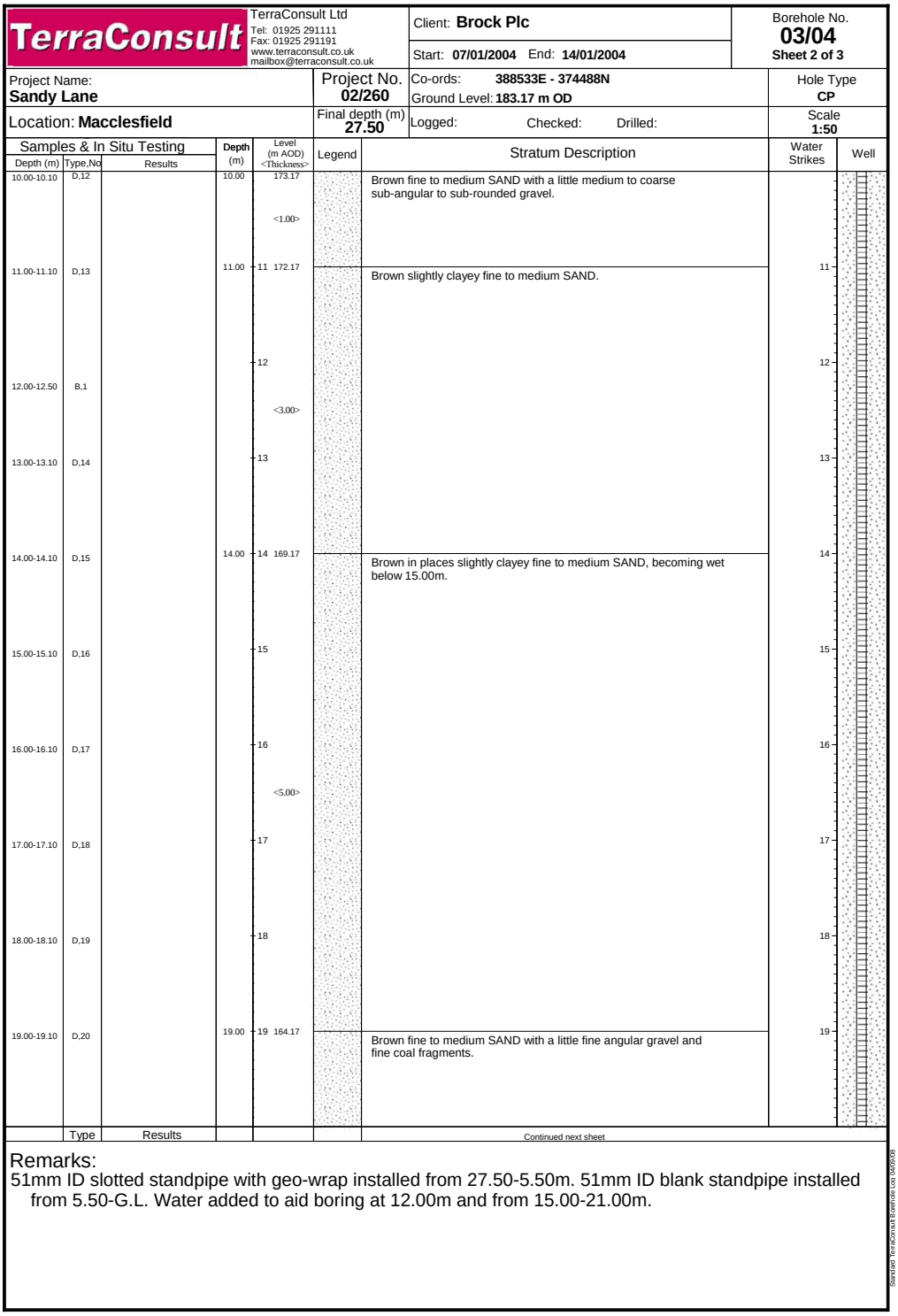

TerraConsult

TerraConsult Ltd
Tel: 01925 291111
Fax: 01925 291191
www.terraconsult.co.uk
mailbox@terraconsult.co.uk

Client: **Brock Plc**

Start: **07/01/2004** End: **14/01/2004**

Borehole No. **03/04** **Sheet 2 of 3**

Project Name: **Sandy Lane**

Project No. **02/260**

Co-ords: **388533E - 374488N**

Ground Level: **183.17 m OD**

Hole Type **CP**

Location: **Macclesfield**

Final depth (m) **27.50**

Logged: Checked: Drilled:

Scale **1:50**

Samples & In Situ Testing			Depth (m)	Level (m AOD) <Thickness>	Legend	Stratum Description	Water Strikes	Well
Depth (m)	Type,No	Results						
10.00-10.10	D,12		10.00	173.17 <1.00>		Brown fine to medium SAND with a little medium to coarse sub-angular to sub-rounded gravel.		
11.00-11.10	D,13		11.00	11 172.17		Brown slightly clayey fine to medium SAND.	11	
12.00-12.50	B,1			12 <3.00>			12	
13.00-13.10	D,14			13			13	
14.00-14.10	D,15		14.00	14 169.17		Brown in places slightly clayey fine to medium SAND, becoming wet below 15.00m.	14	
15.00-15.10	D,16			15			15	
16.00-16.10	D,17			16 <5.00>			16	
17.00-17.10	D,18			17			17	
18.00-18.10	D,19			18			18	
19.00-19.10	D,20		19.00	19 164.17		Brown fine to medium SAND with a little fine angular gravel and fine coal fragments.	19	
	Type	Results				Continued next sheet		

Remarks:
51mm ID slotted standpipe with geo-wrap installed from 27.50-5.50m. 51mm ID blank standpipe installed from 5.50-G.L. Water added to aid boring at 12.00m and from 15.00-21.00m.

Standard TerraConsult Borehole Log 04/00/08

Figure B.2: Site 1 BH 03/4 Borehole Log (Part 2)

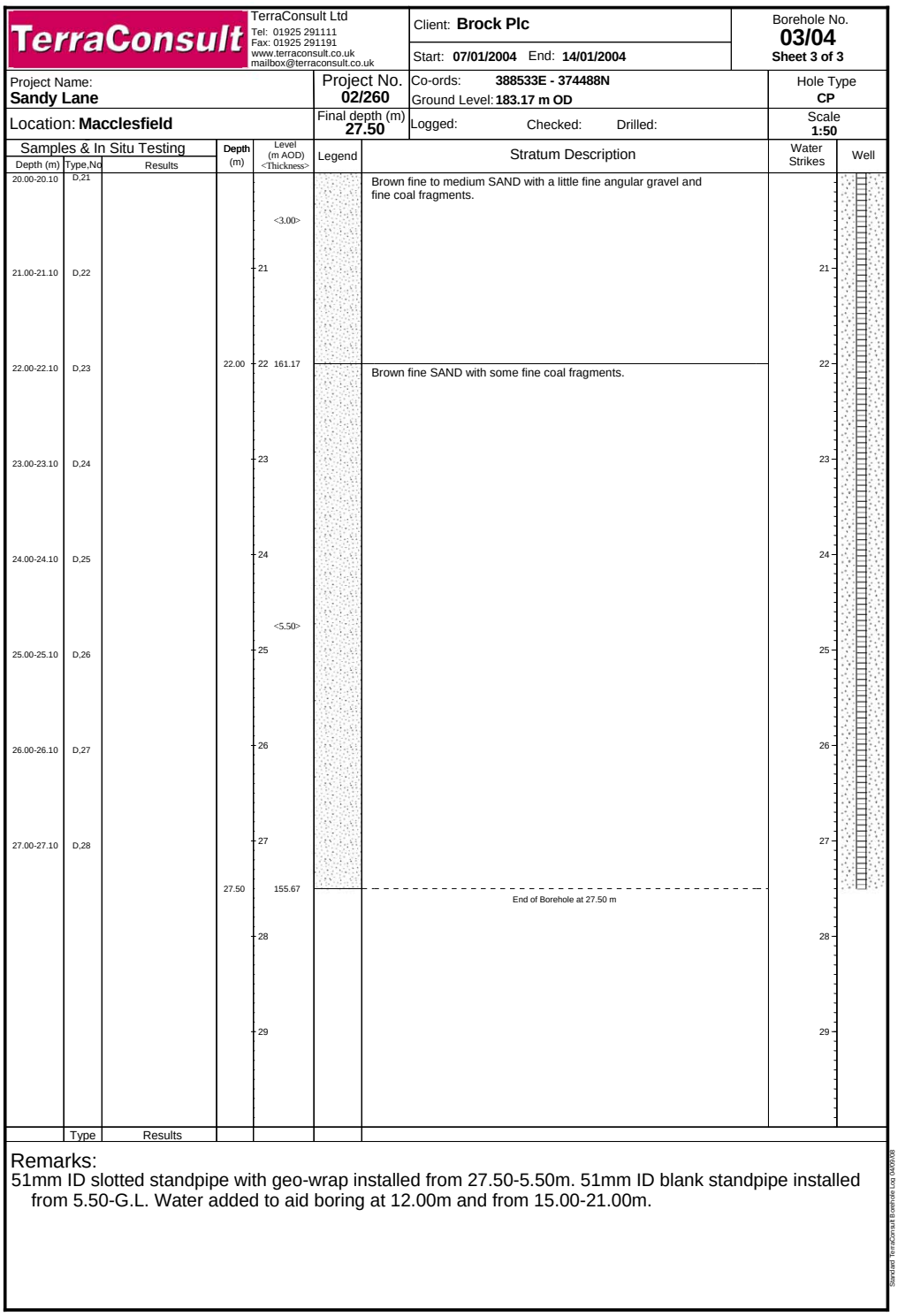

Figure B.3: Site 1 BH 03/4 Borehole Log (Part 3)

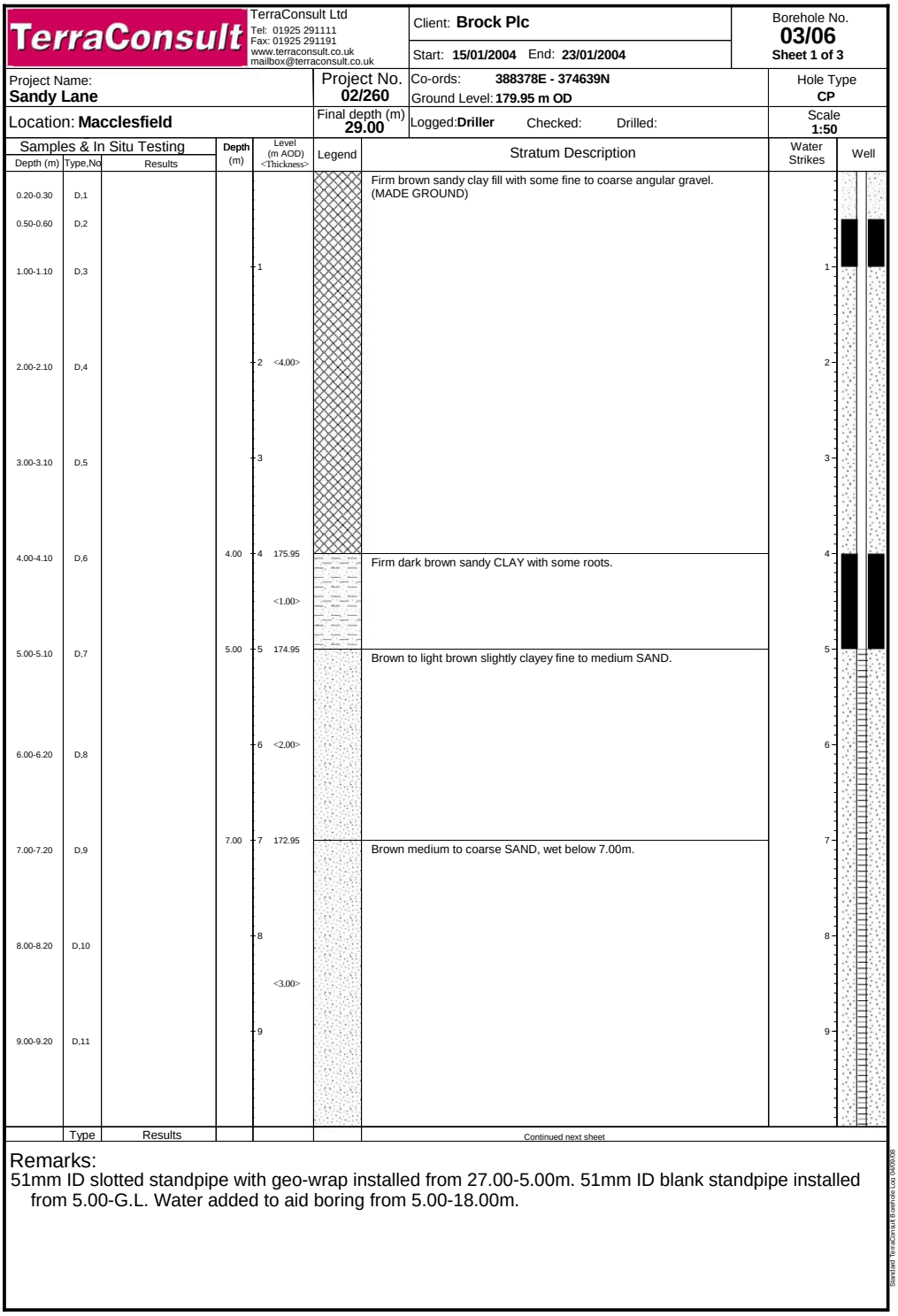

Figure B.4: Site 1 BH 03/6 Borehole Log (Part 1)

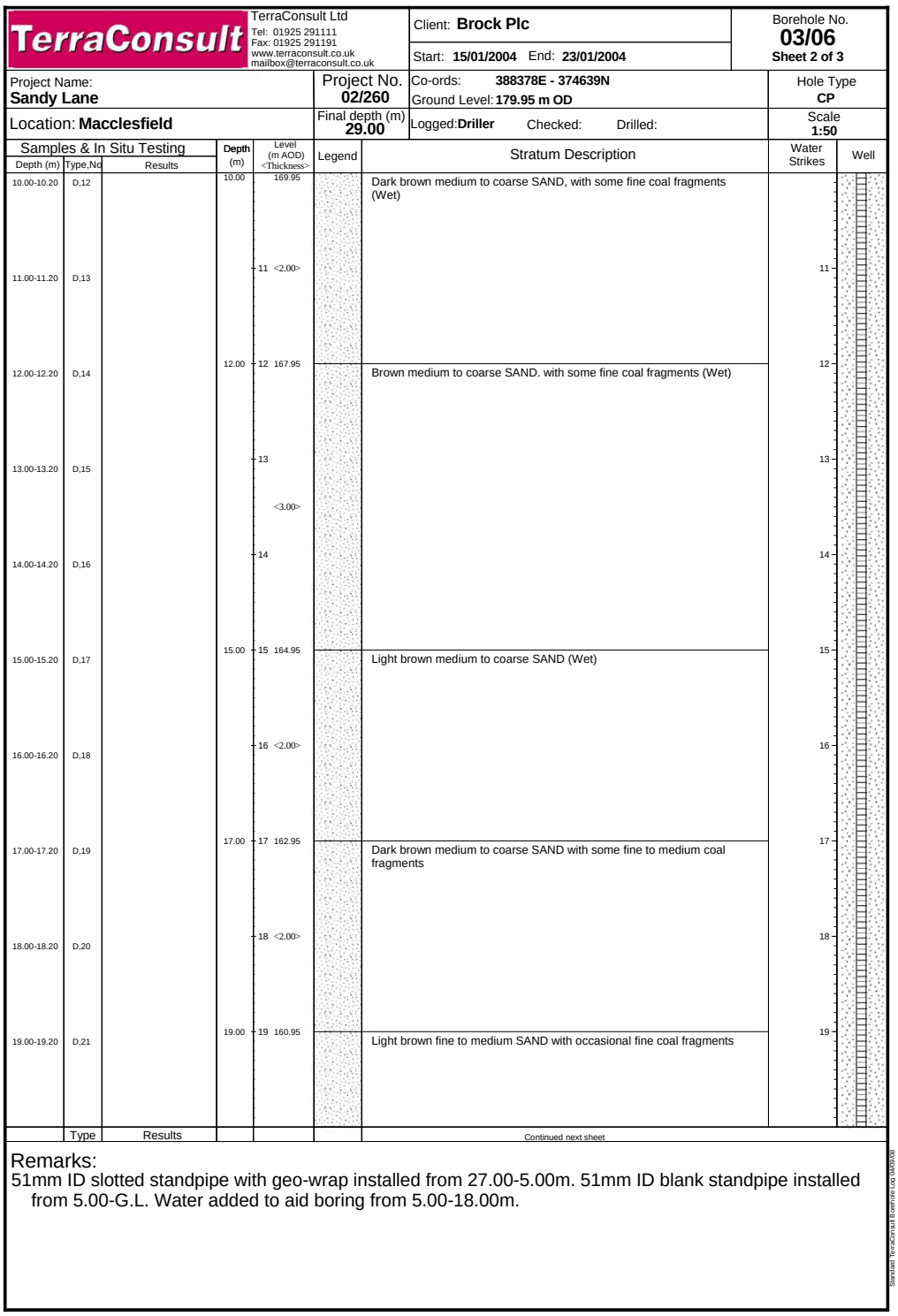

TerraConsult

TerraConsult Ltd
Tel: 01925 291111
Fax: 01925 291191
www.terraconsult.co.uk
mailbox@terraconsult.co.uk

Client: **Brock Plc**

Borehole No. **03/06** **Sheet 2 of 3**

Start: **15/01/2004** End: **23/01/2004**

Project Name: **Sandy Lane**

Project No. **02/260**

Co-ords: **388378E - 374639N**

Ground Level: **179.95 m OD**

Hole Type **CP**

Location: **Macclesfield**

Final depth (m) **29.00**

Logged: **Driller** Checked: Drilled:

Scale **1:50**

Samples & In Situ Testing			Depth (m)	Level (m AOD) <Thickness>	Legend	Stratum Description	Water Strikes	Well
Depth (m)	Type,No	Results						
10.00-10.20	D,12		10.00	169.95		Dark brown medium to coarse SAND, with some fine coal fragments (Wet)		
11.00-11.20	D,13			11 <2.00>			11	
12.00-12.20	D,14		12.00	12 167.95		Brown medium to coarse SAND. with some fine coal fragments (Wet)	12	
13.00-13.20	D,15			13 <3.00>			13	
14.00-14.20	D,16			14			14	
15.00-15.20	D,17		15.00	15 164.95		Light brown medium to coarse SAND (Wet)	15	
16.00-16.20	D,18			16 <2.00>			16	
17.00-17.20	D,19		17.00	17 162.95		Dark brown medium to coarse SAND with some fine to medium coal fragments	17	
18.00-18.20	D,20			18 <2.00>			18	
19.00-19.20	D,21		19.00	19 160.95		Light brown fine to medium SAND with occasional fine coal fragments	19	
	Type	Results				Continued next sheet		

Remarks:
51mm ID slotted standpipe with geo-wrap installed from 27.00-5.00m. 51mm ID blank standpipe installed from 5.00-G.L. Water added to aid boring from 5.00-18.00m.

Standard TerraConsult Borehole Log 04/09/08

Figure B.5: Site 1 BH 03/6 Borehole Log (Part 2)

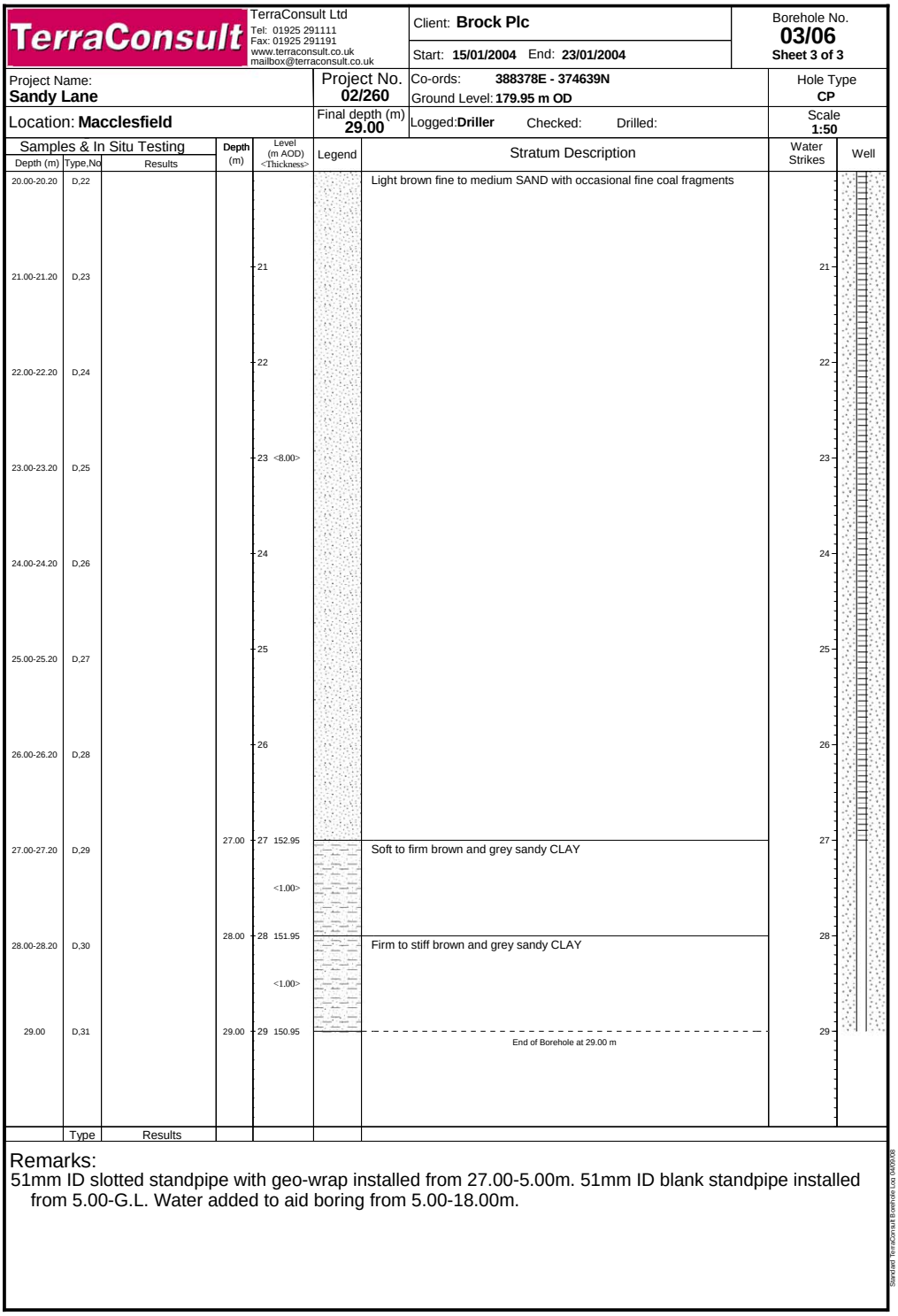

Figure B.6: Site 1 BH 03/6 Borehole Log (Part 3)

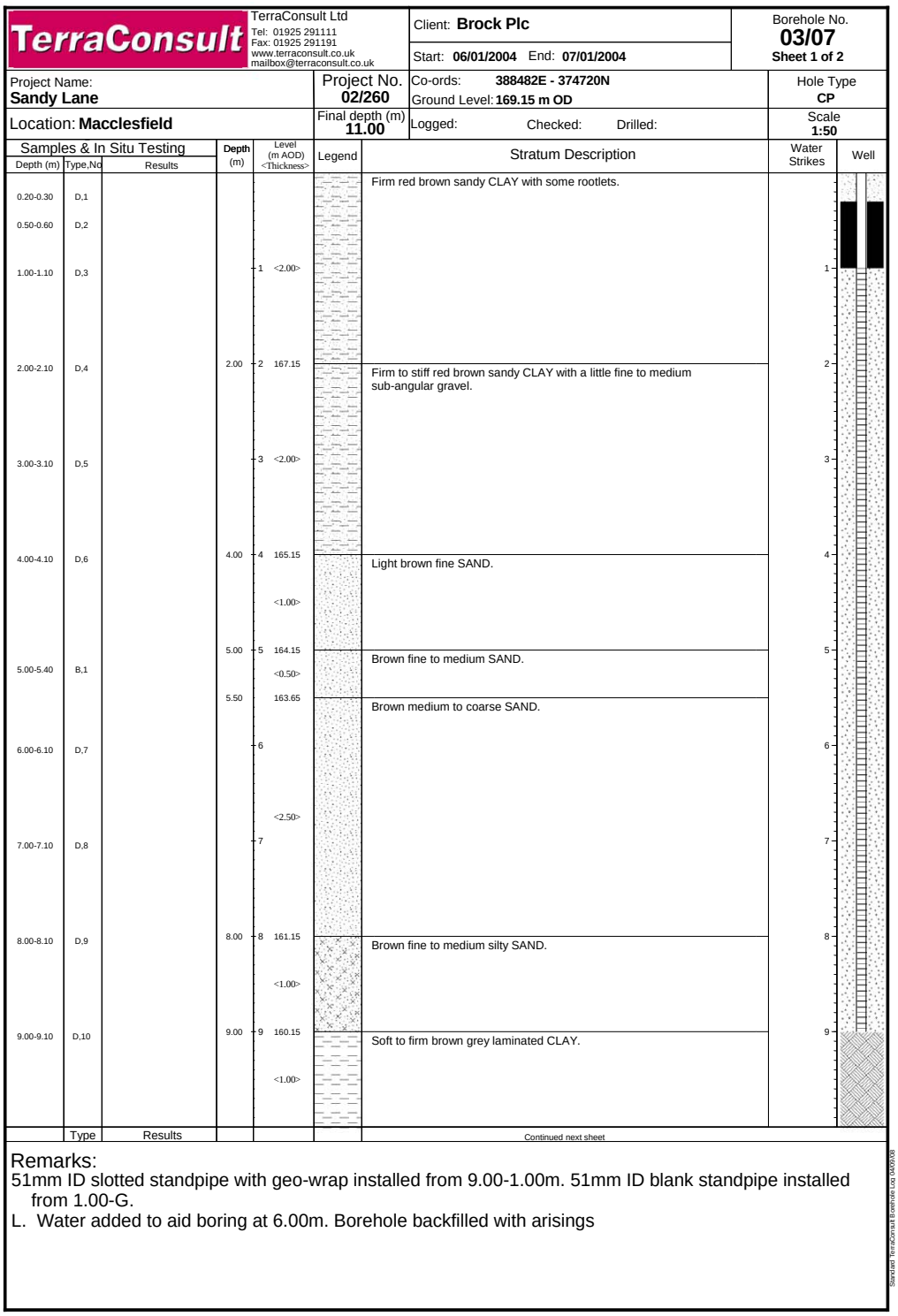

Figure B.7: Site 1 BH 03/7 Borehole Log (Part 1)

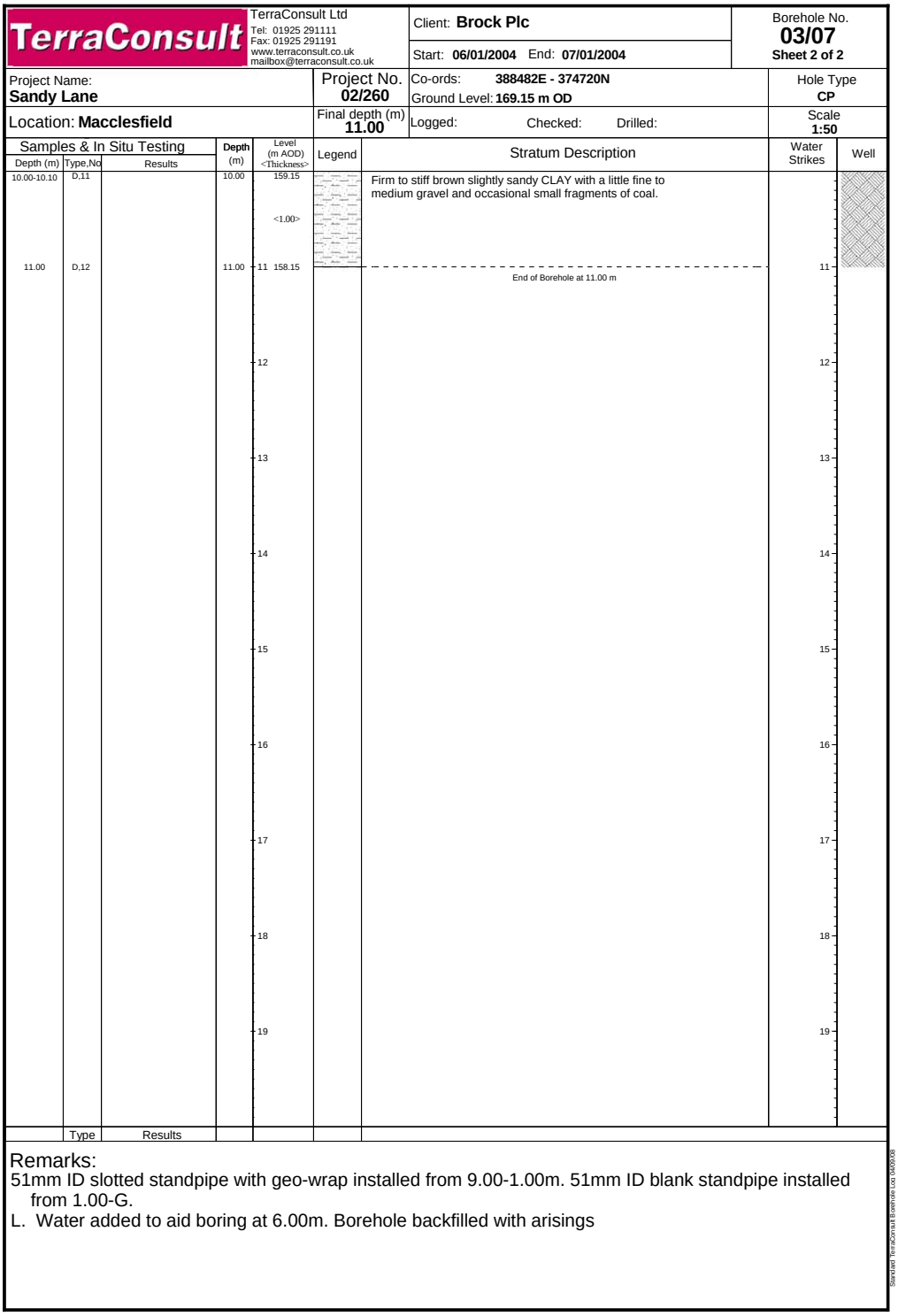

Figure B.8: Site 1 BH 03/7 Borehole Log (Part 2)

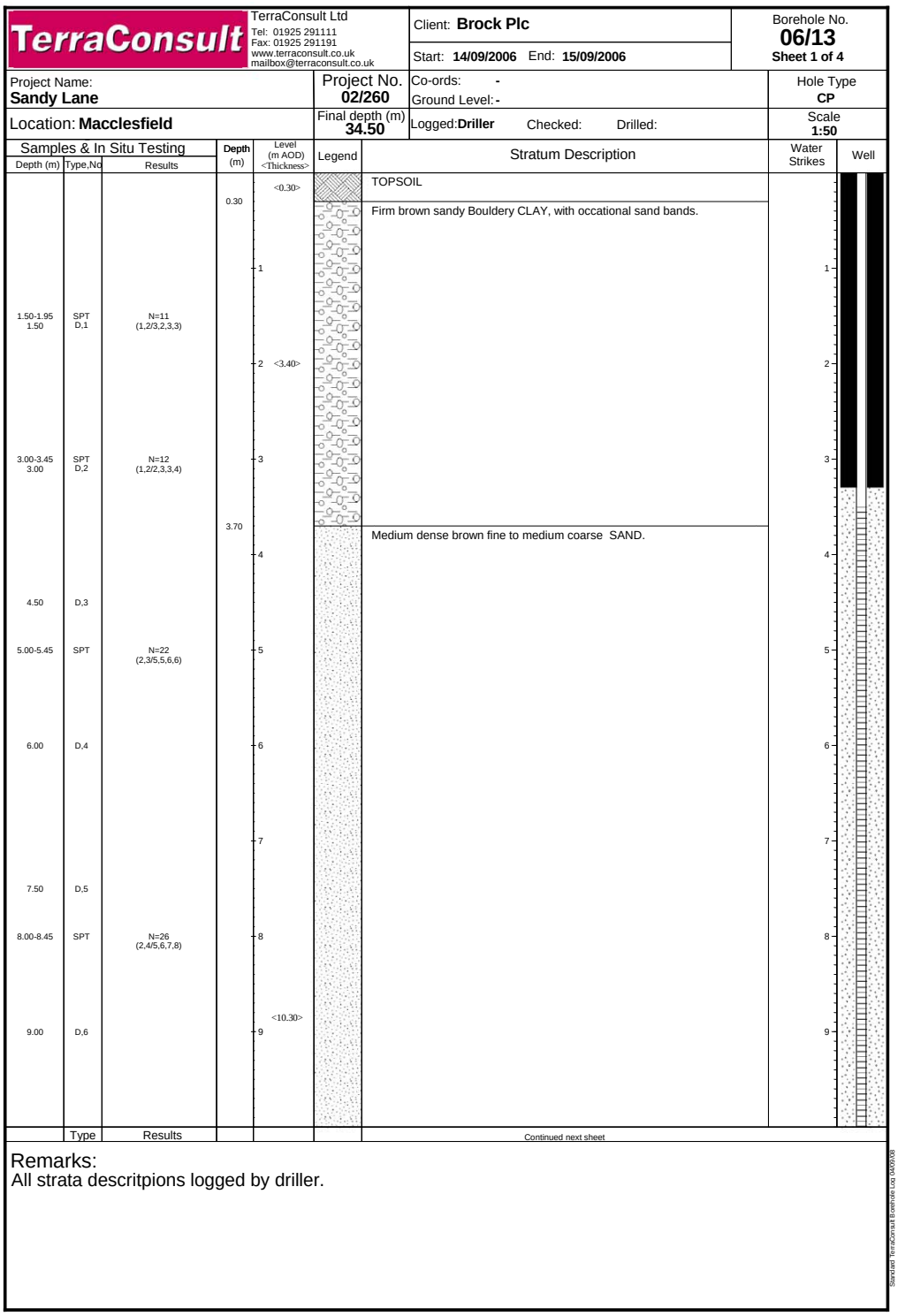

Figure B.9: Site 1 BH 06/13 Borehole Log (Part 1)

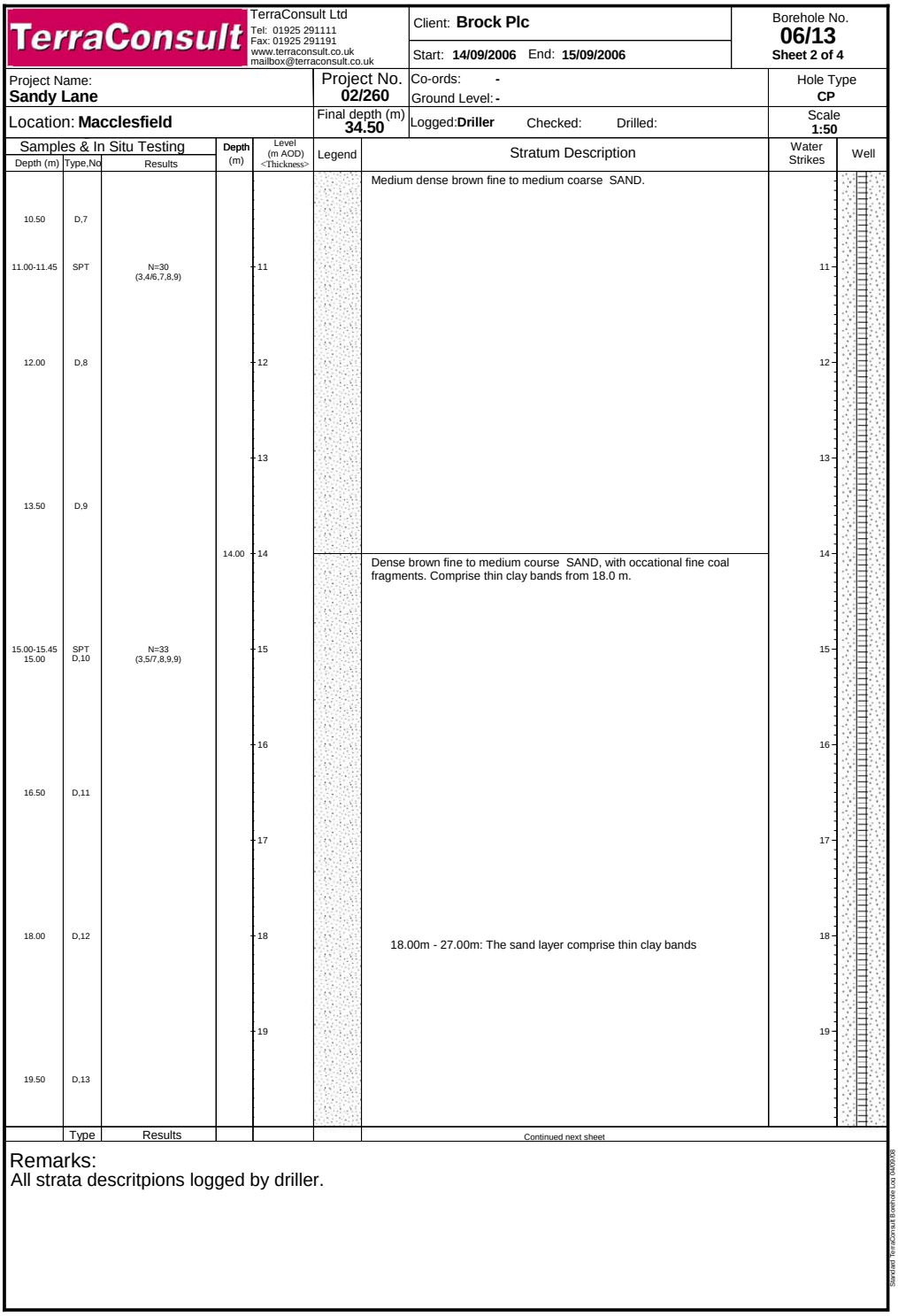

Figure B.10: Site 1 BH 03/7 Borehole Log (Part 2)

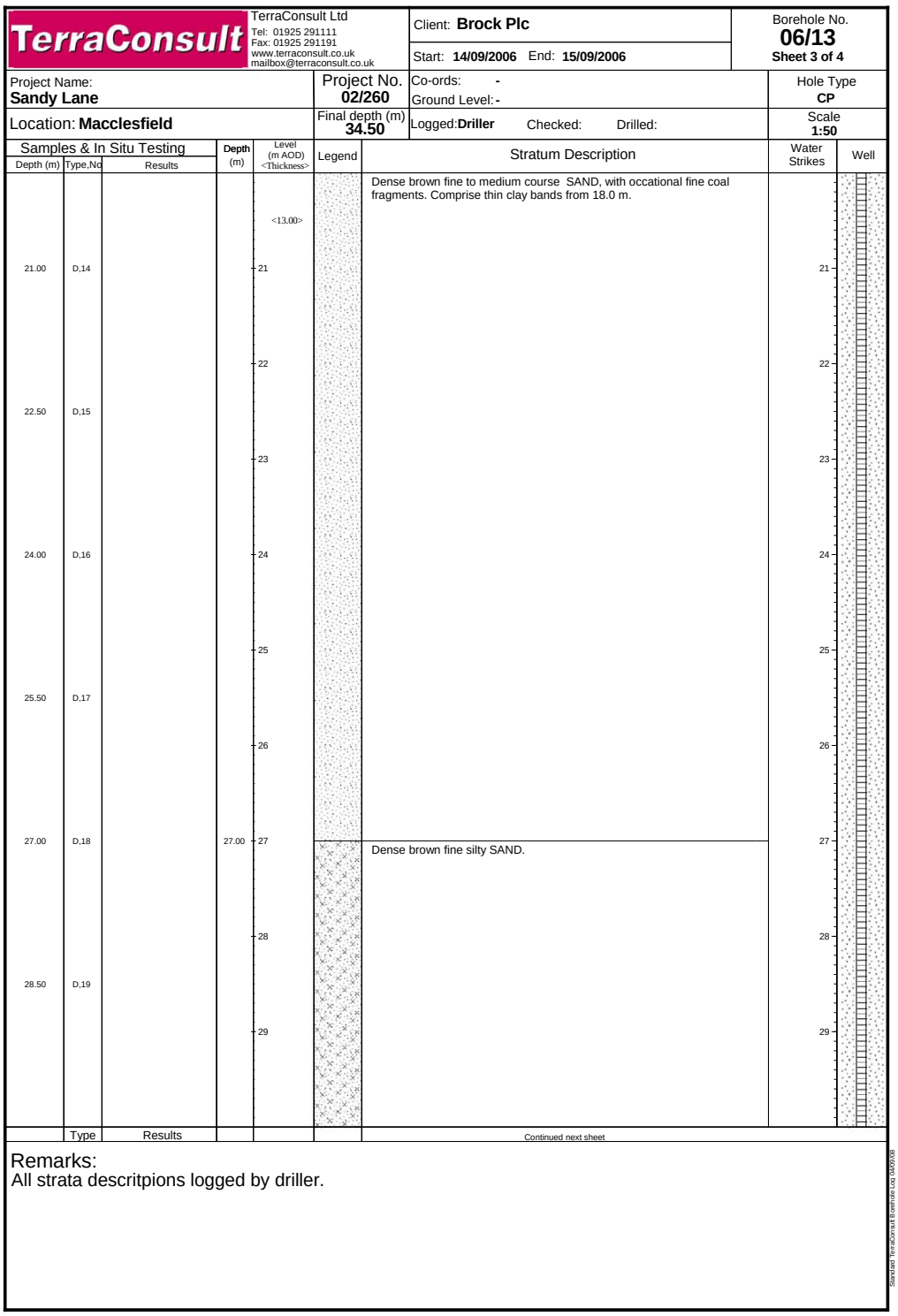

Figure B.11: Site 1 BH 06/13 Borehole Log (Part 3)

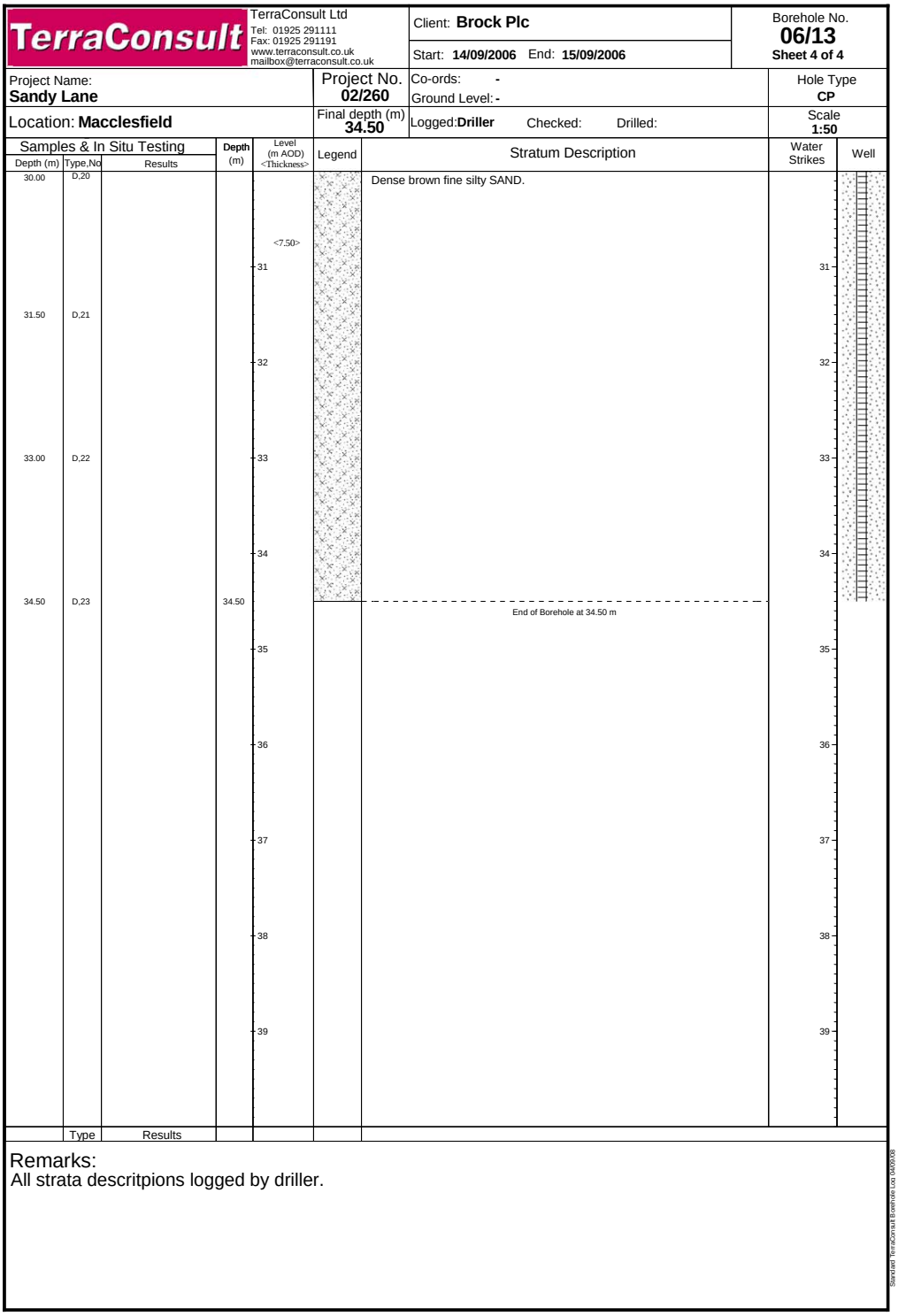

Figure B.12: Site 1 BH 06/13 Borehole Log (Part 4)

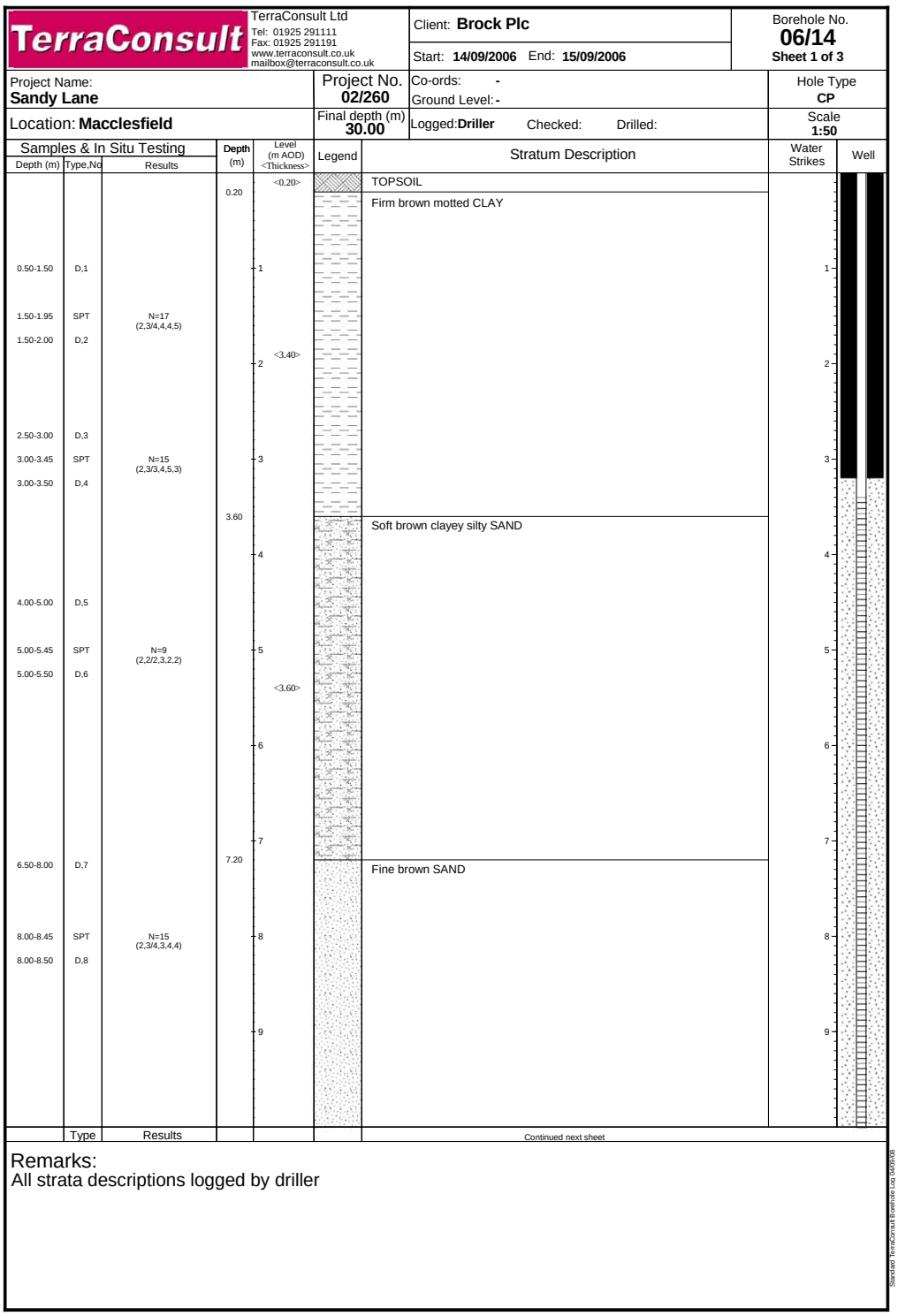

Figure B.13: Site 1 BH 06/14 Borehole Log (Part 1)

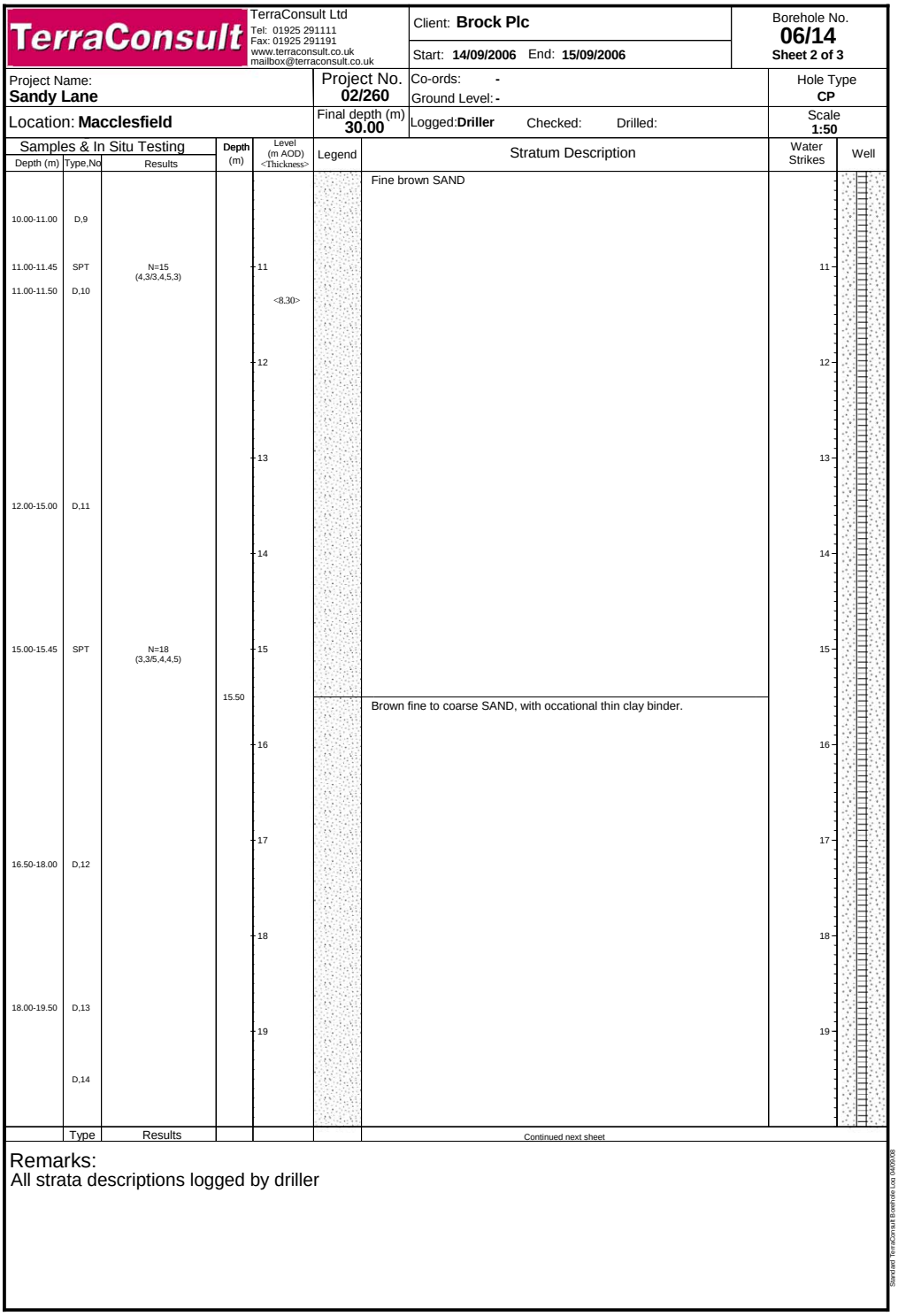

Figure B.14: Site 1 BH 06/14 Borehole Log (Part 2)

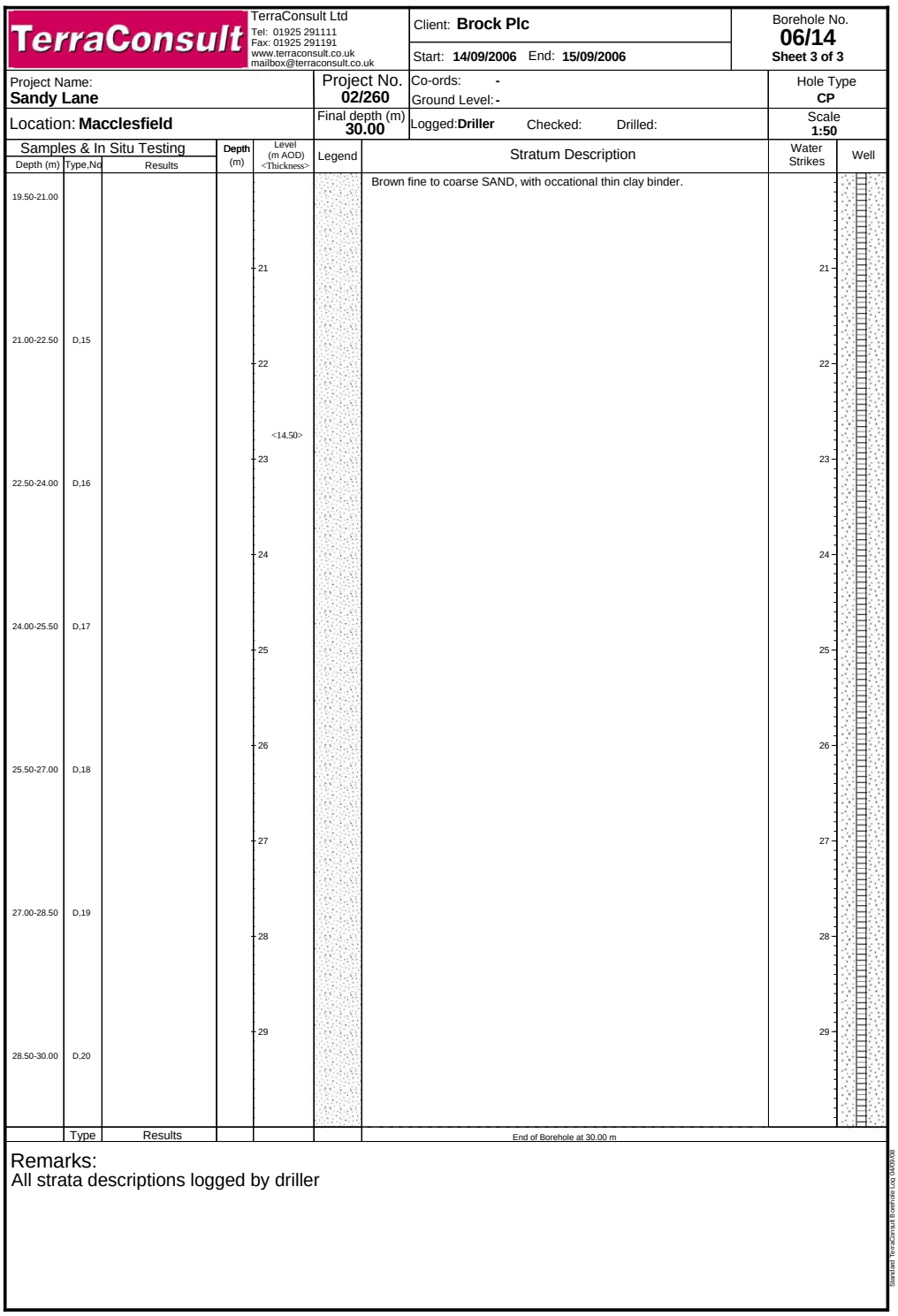

Figure B.15: Site 1 BH 06/14 Borehole Log (Part 3)

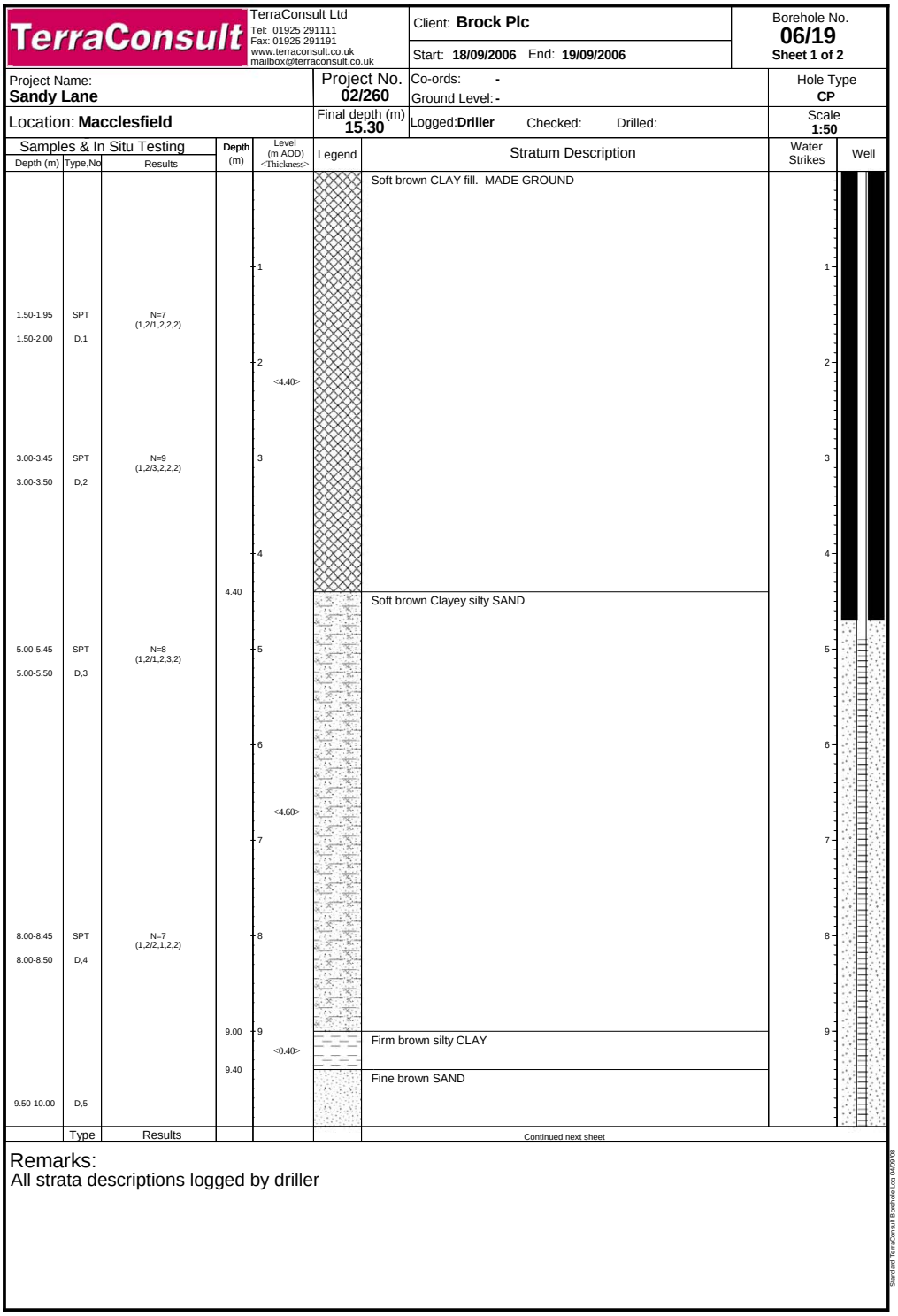

Figure B.16: Site 1 BH 06/19 Borehole Log (Part 1)

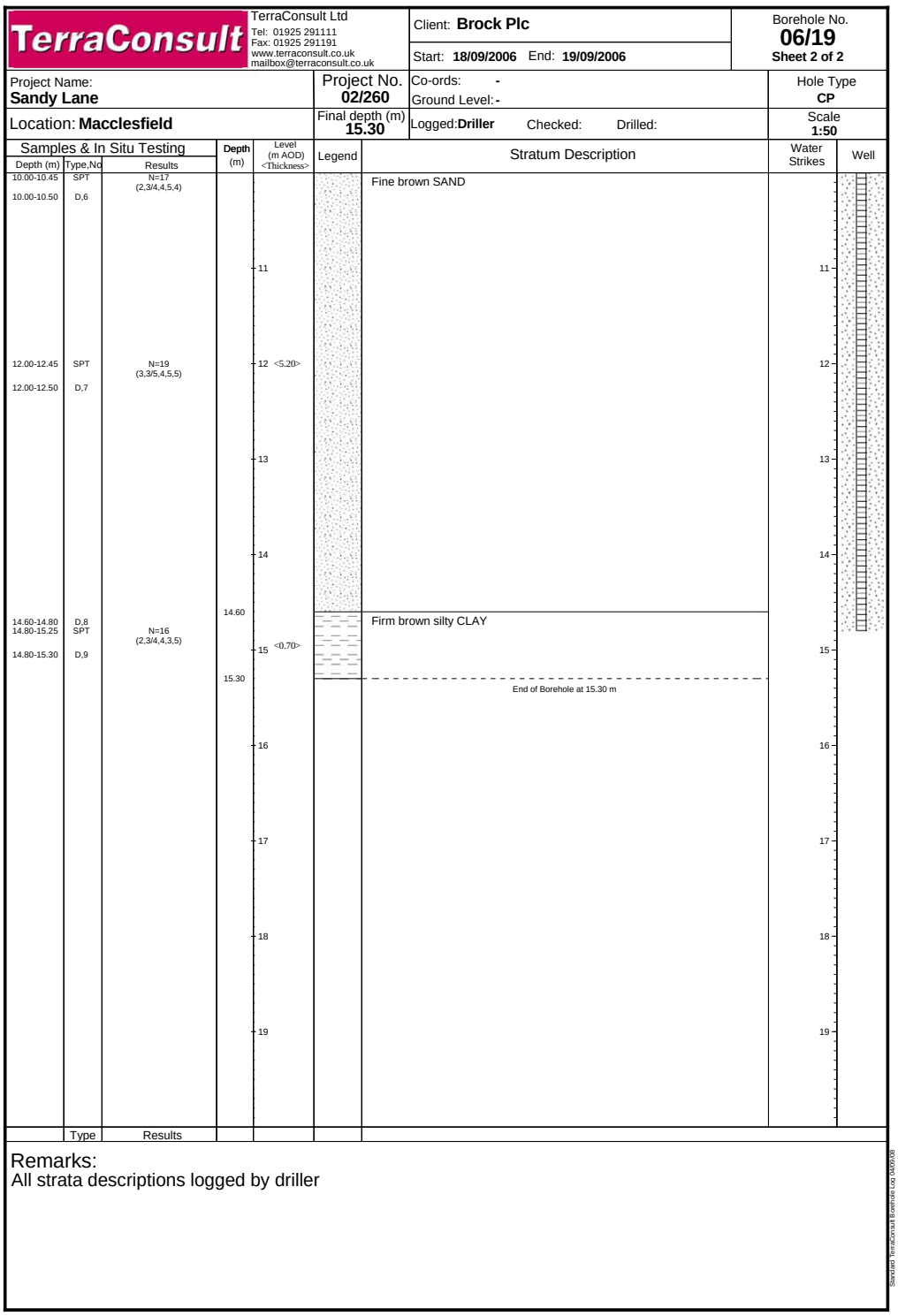

Figure B.17: Site 1 BH 06/19 Borehole Log (Part 2)

Appendix C

Site 2 Borehole Logs

Summary

- Scale 1:50 at original A4 size.
- Perimeter boreholes were not logged by original contractor in 1998.
- Boreholes drilled later (2007) by TerraConsult Ltd. These later logs were used for reference.
- Boreholes typically around 25.0 m deep.
- Boreholes are situated in glacial deposits. The glacial deposits are comprised mainly of glacial clay with occasional sand lenses. The response zones (slotted pipe sealed with bentonite at either end) are designed to capture gas from these regions in the sub-surface profile.
- The sand lenses tend to be 0.5–1.5 m thick and contain fine to coarse sand along with fine to coarse gravel that is sub-angular to sub-rounded originating from sandstone and mudstone. These sand lenses should provide channels for gas transport.

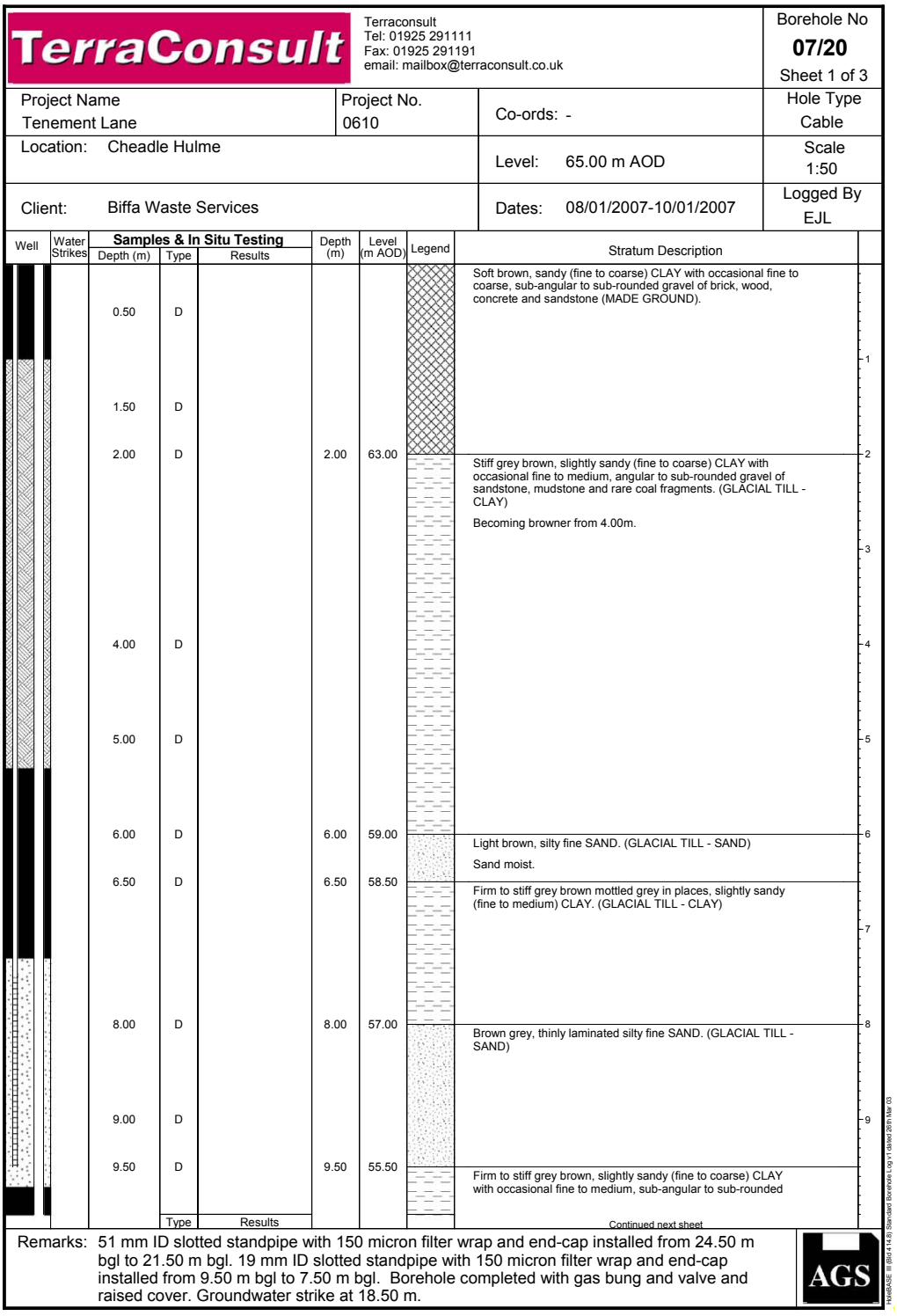

TerraConsult

Terraconsult
Tel: 01925 291111
Fax: 01925 291191
email: mailbox@terraconsult.co.uk

Borehole No **07/20** Sheet 1 of 3

Project Name	Project No.	Co-ords: -	Hole Type
Tenement Lane	0610		Cable
Location: Cheadle Hulme		Level: 65.00 m AOD	Scale 1:50
Client: Biffa Waste Services		Dates: 08/01/2007-10/01/2007	Logged By EJL

Well	Water Strikes	Samples & In Situ Testing Depth (m)	Type	Results	Depth (m)	Level (m AOD)	Legend	Stratum Description
		0.50	D					Soft brown, sandy (fine to coarse) CLAY with occasional fine to coarse, sub-angular to sub-rounded gravel of brick, wood, concrete and sandstone (MADE GROUND).
		1.50	D					
		2.00	D		2.00	63.00		Stiff grey brown, slightly sandy (fine to coarse) CLAY with occasional fine to medium, angular to sub-rounded gravel of sandstone, mudstone and rare coal fragments. (GLACIAL TILL - CLAY)
								Becoming browner from 4.00m.
		4.00	D					
		5.00	D					
		6.00	D		6.00	59.00		Light brown, silty fine SAND. (GLACIAL TILL - SAND)
		6.50	D		6.50	58.50		Sand moist. Firm to stiff grey brown mottled grey in places, slightly sandy (fine to medium) CLAY. (GLACIAL TILL - CLAY)
		8.00	D		8.00	57.00		Brown grey, thinly laminated silty fine SAND. (GLACIAL TILL - SAND)
		9.00	D					
		9.50	D		9.50	55.50		Firm to stiff grey brown, slightly sandy (fine to coarse) CLAY with occasional fine to medium, sub-angular to sub-rounded
			Type	Results				Continued next sheet

Remarks: 51 mm ID slotted standpipe with 150 micron filter wrap and end-cap installed from 24.50 m bgl to 21.50 m bgl. 19 mm ID slotted standpipe with 150 micron filter wrap and end-cap installed from 9.50 m bgl to 7.50 m bgl. Borehole completed with gas bung and valve and raised cover. Groundwater strike at 18.50 m.

AGS

HoleBASE B (Bid 14.8) Standard Borehole Log v1 dated 28th Mar 03

Figure C.1: Site 2 BH 07/20 Borehole Log (Part 1)

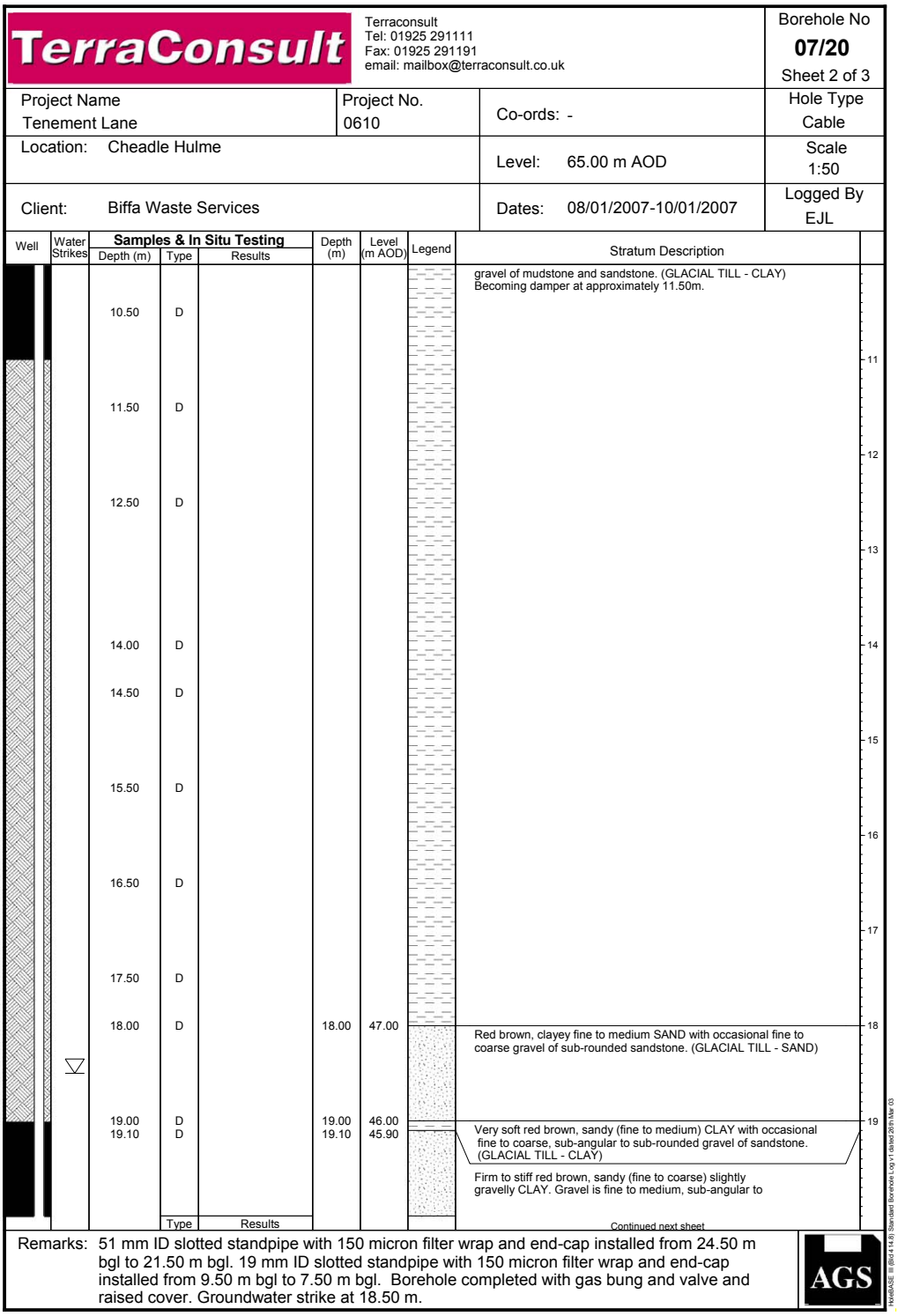

Figure C.2: Site 2 BH 07/20 Borehole Log (Part 2)

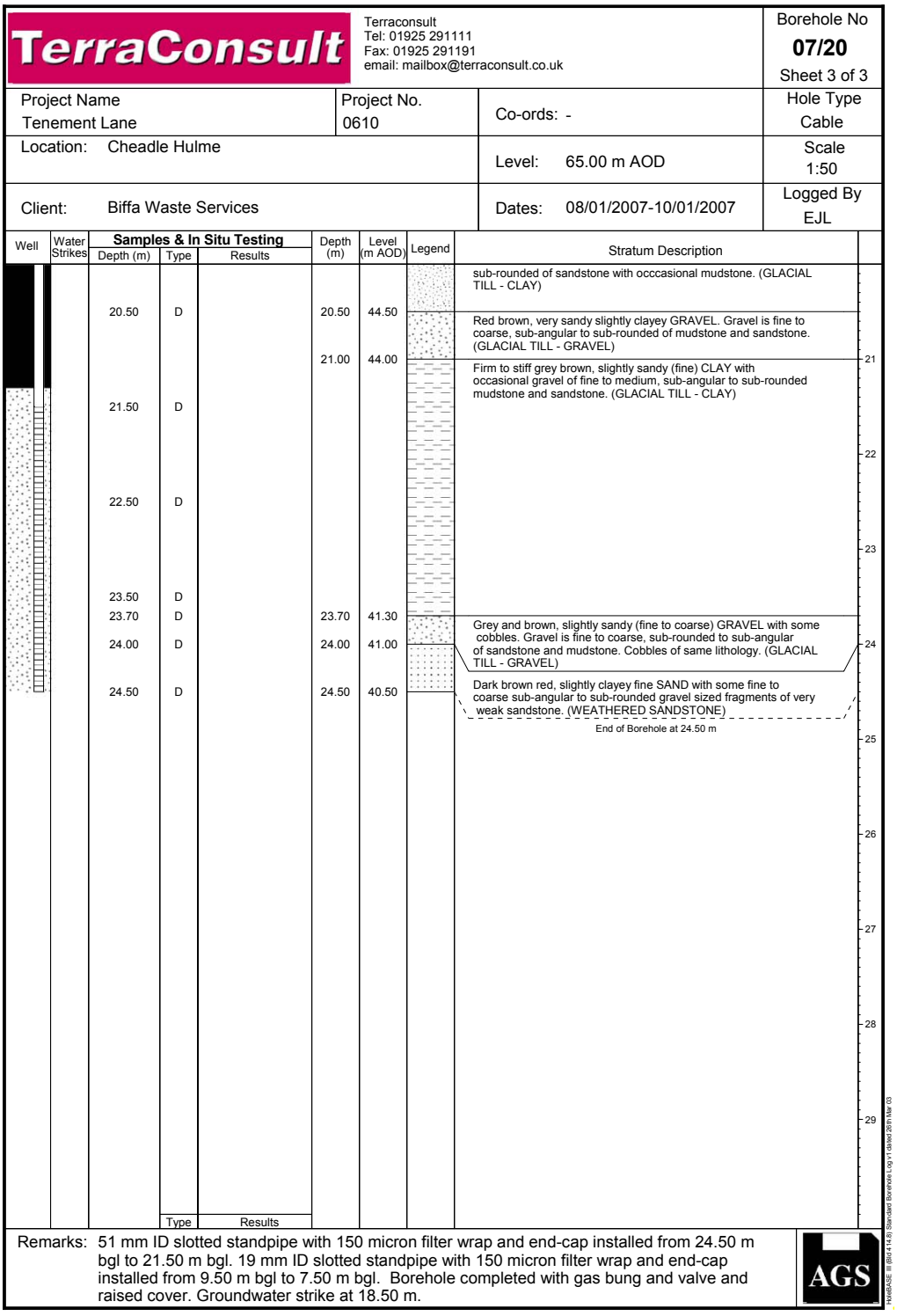

Figure C.3: Site 2 BH 07/20 Borehole Log (Part 3)

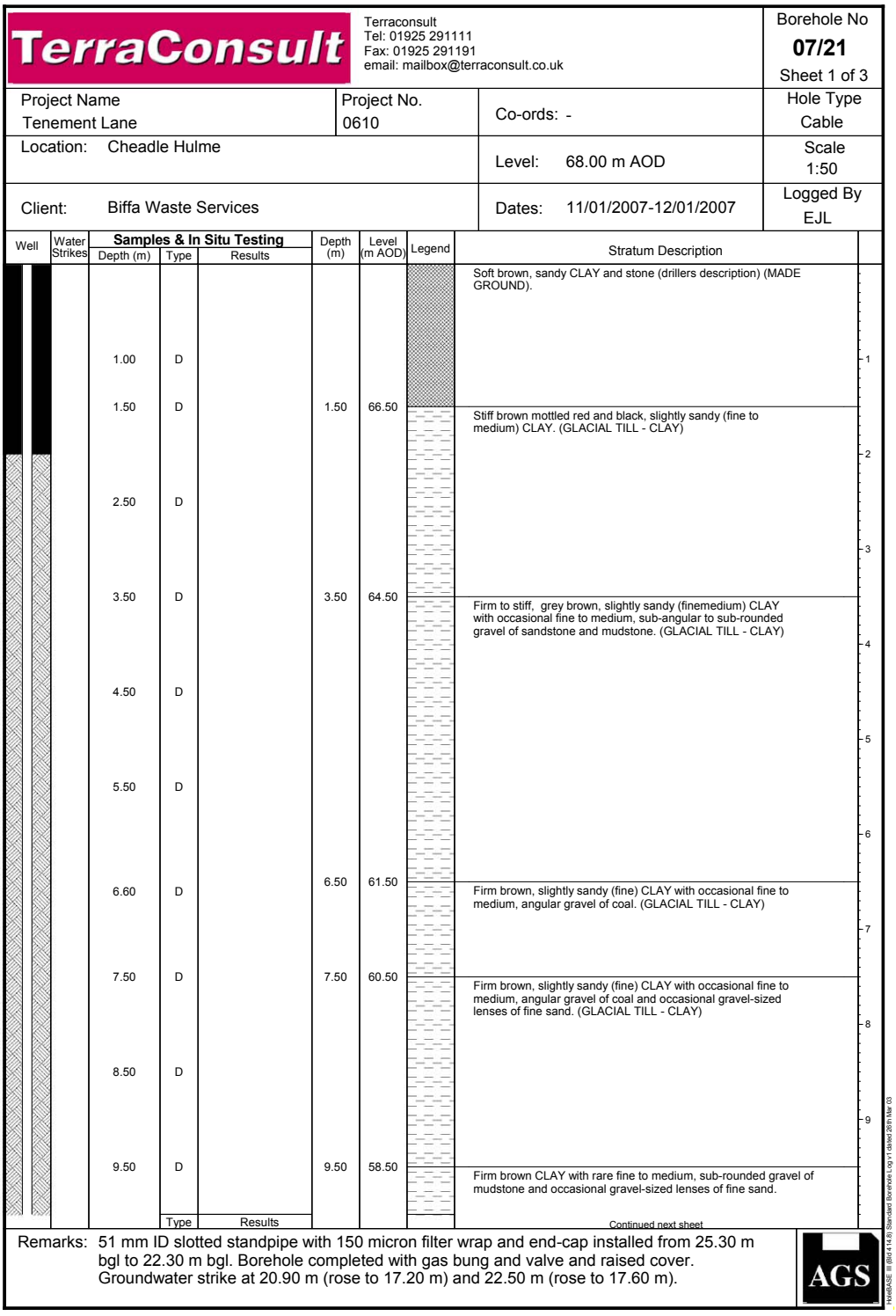

Figure C.4: Site 2 BH 07/21 Borehole Log (Part 1)

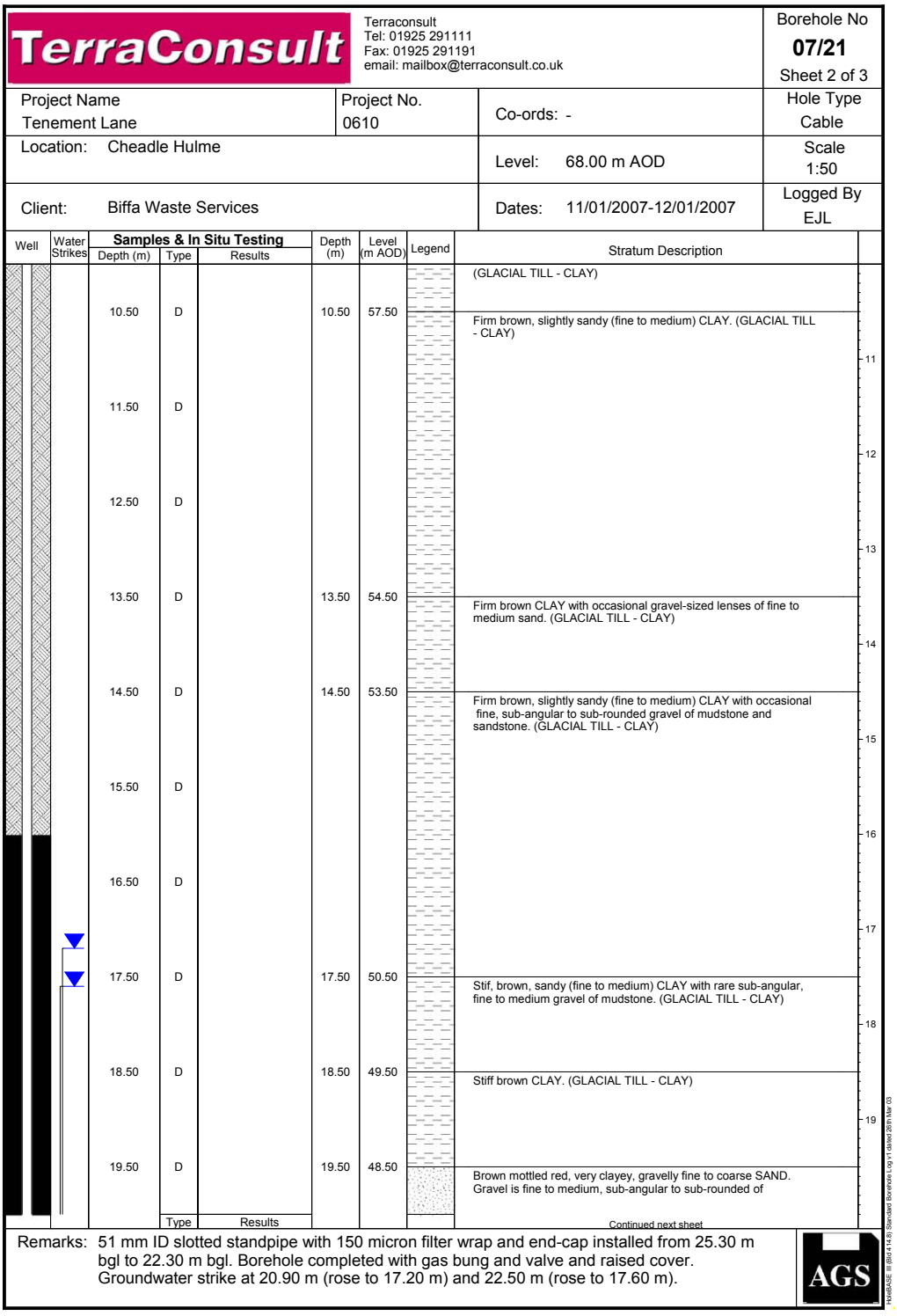

Figure C.5: Site 2 BH 07/21 Borehole Log (Part 2)

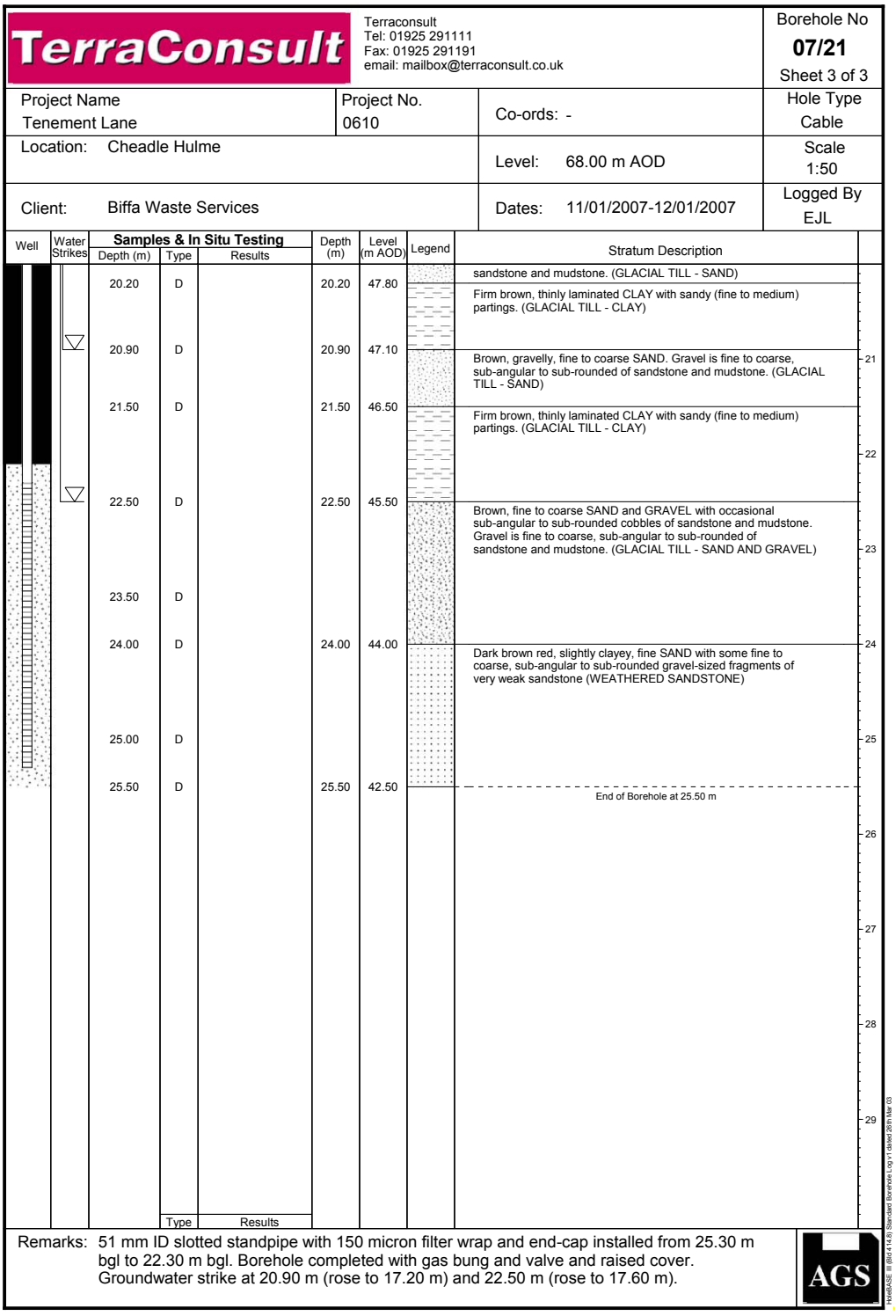

Figure C.6: Site 2 BH 07/21 Borehole Log (Part 3)

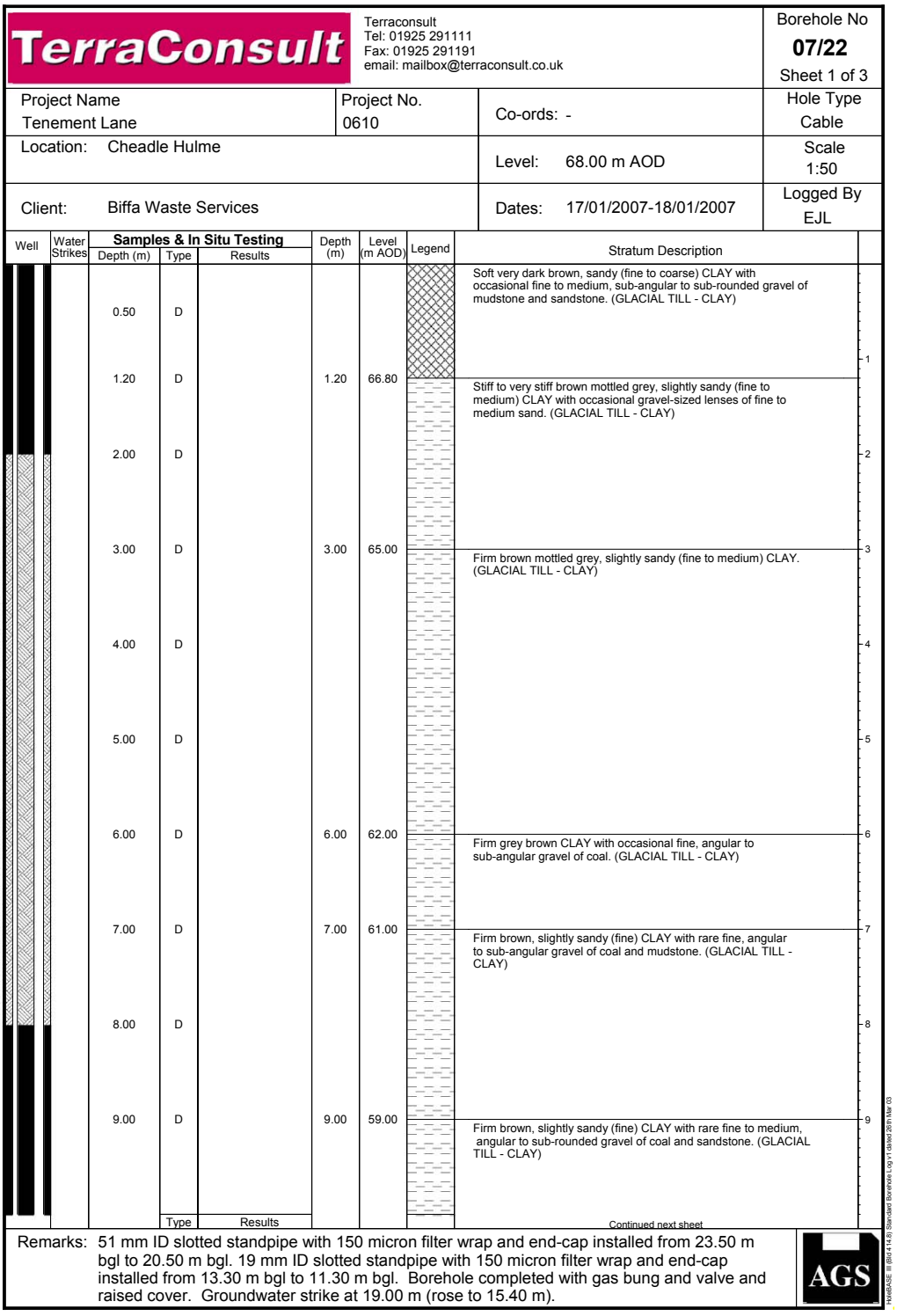

TerraConsult

Terraconsult
Tel: 01925 291111
Fax: 01925 291191
email: mailbox@terraconsult.co.uk

Borehole No **07/22** Sheet 1 of 3

Project Name	Project No.	Co-ords: -	Hole Type
Tenement Lane	0610		Cable
Location: Cheadle Hulme		Level: 68.00 m AOD	Scale 1:50
Client: Biffa Waste Services		Dates: 17/01/2007-18/01/2007	Logged By EJL

Well	Water Strikes	Samples & In Situ Testing Depth (m)	Type	Results	Depth (m)	Level (m AOD)	Legend	Stratum Description
		0.50	D					Soft very dark brown, sandy (fine to coarse) CLAY with occasional fine to medium, sub-angular to sub-rounded gravel of mudstone and sandstone. (GLACIAL TILL - CLAY)
		1.20	D		1.20	66.80		Stiff to very stiff brown mottled grey, slightly sandy (fine to medium) CLAY with occasional gravel-sized lenses of fine to medium sand. (GLACIAL TILL - CLAY)
		2.00	D					
		3.00	D		3.00	65.00		Firm brown mottled grey, slightly sandy (fine to medium) CLAY. (GLACIAL TILL - CLAY)
		4.00	D					
		5.00	D					
		6.00	D		6.00	62.00		Firm grey brown CLAY with occasional fine, angular to sub-angular gravel of coal. (GLACIAL TILL - CLAY)
		7.00	D		7.00	61.00		Firm brown, slightly sandy (fine) CLAY with rare fine, angular to sub-angular gravel of coal and mudstone. (GLACIAL TILL - CLAY)
		8.00	D					
		9.00	D		9.00	59.00		Firm brown, slightly sandy (fine) CLAY with rare fine to medium, angular to sub-rounded gravel of coal and sandstone. (GLACIAL TILL - CLAY)
			Type	Results				Continued next sheet

Remarks: 51 mm ID slotted standpipe with 150 micron filter wrap and end-cap installed from 23.50 m bgl to 20.50 m bgl. 19 mm ID slotted standpipe with 150 micron filter wrap and end-cap installed from 13.30 m bgl to 11.30 m bgl. Borehole completed with gas bung and valve and raised cover. Groundwater strike at 19.00 m (rose to 15.40 m).

AGS

HoleBASE B (Bd 4.14.8) Standard Borehole Log v1 dated 28th Mar 03

Figure C.7: Site 2 BH 07/22 Borehole Log (Part 1)

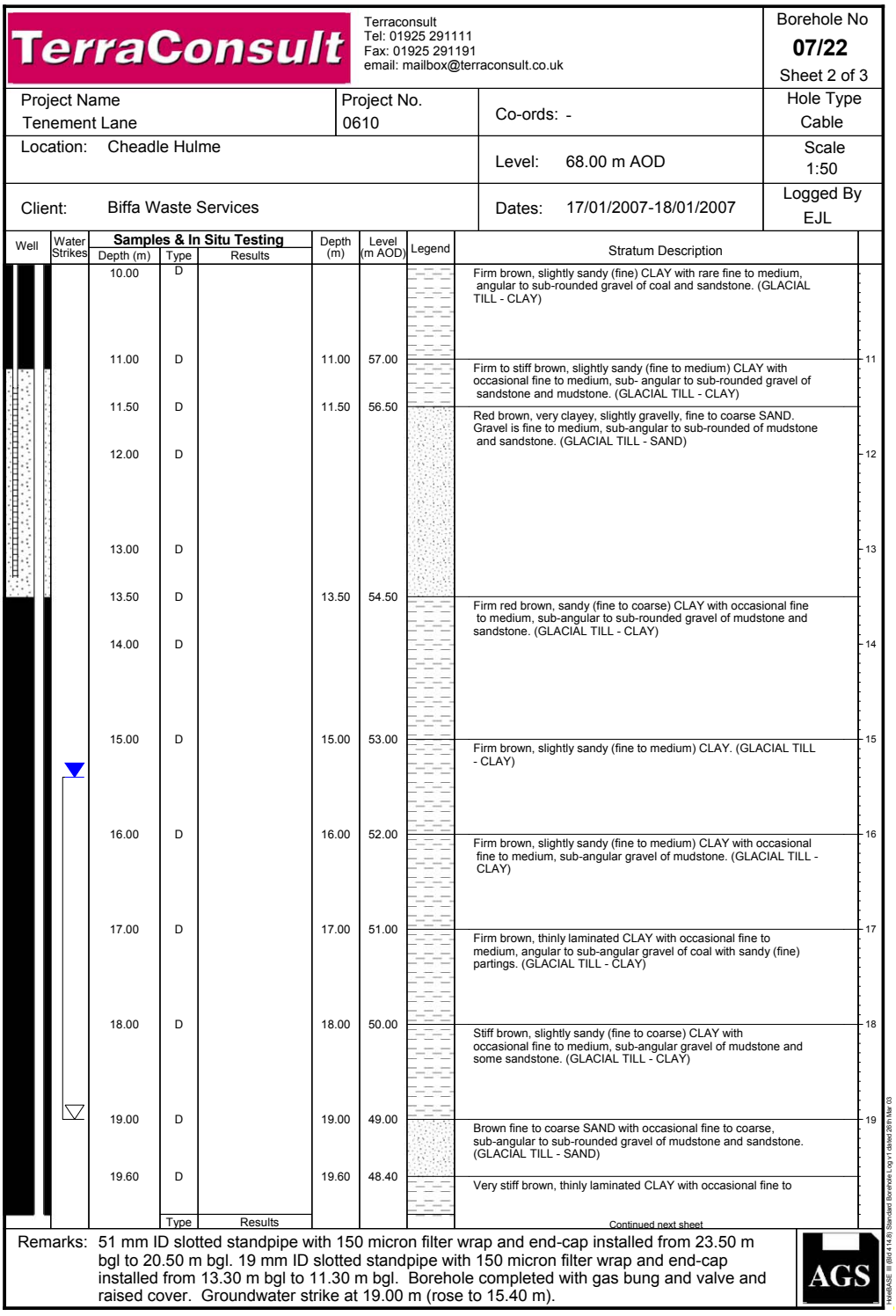

Figure C.8: Site 2 BH 07/22 Borehole Log (Part 2)

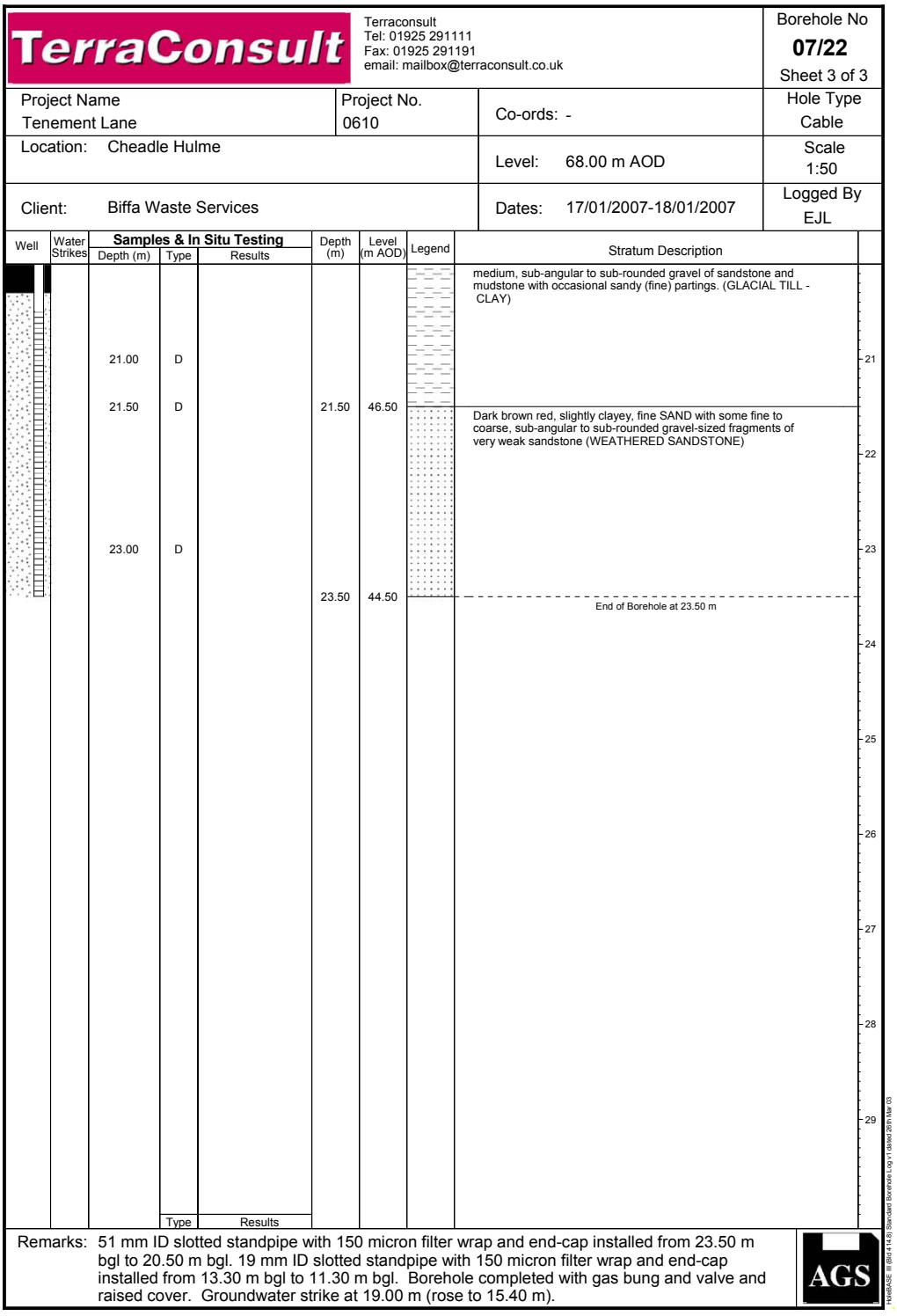

Figure C.9: Site 2 BH 07/22 Borehole Log (Part 3)

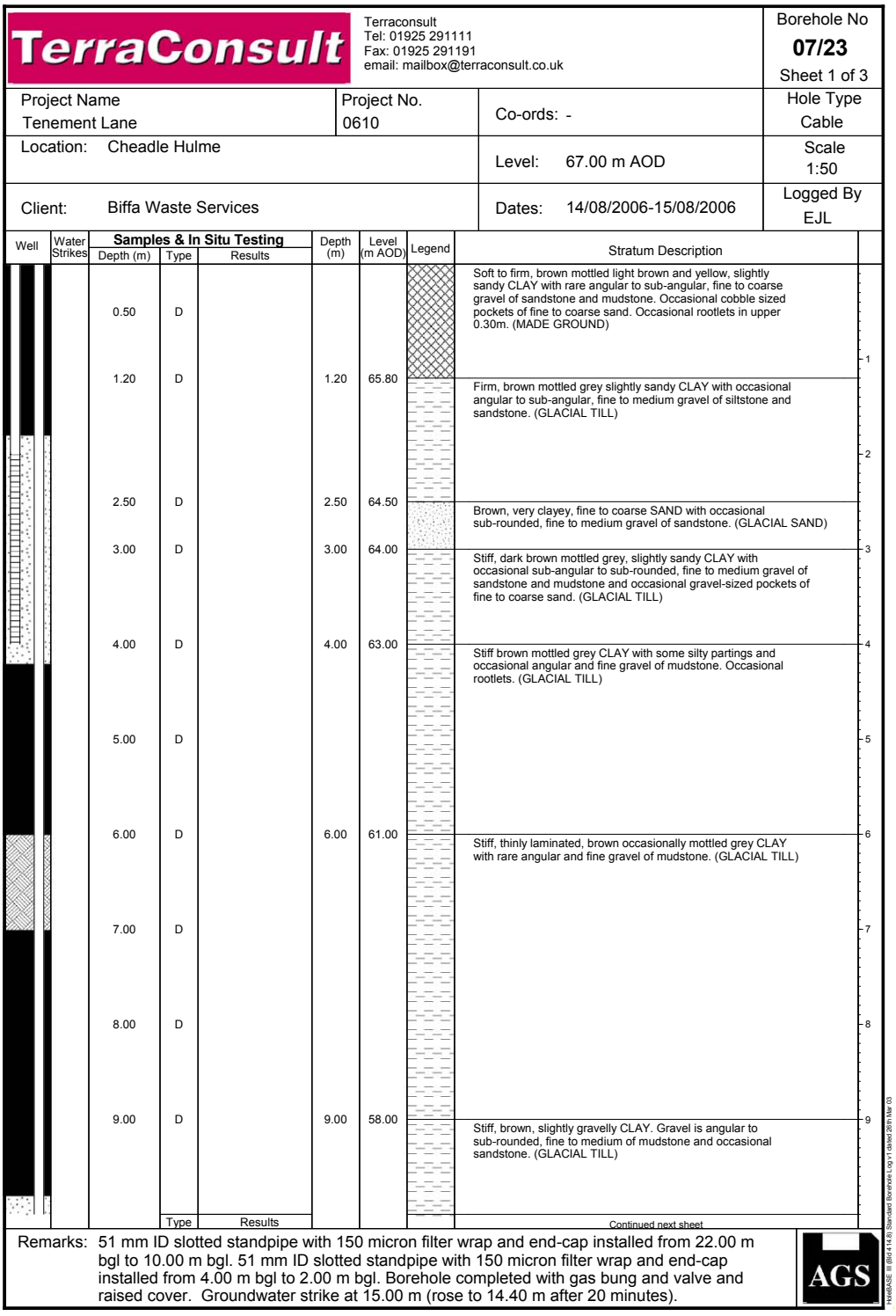

Figure C.10: Site 2 BH 07/23 Borehole Log (Part 1)

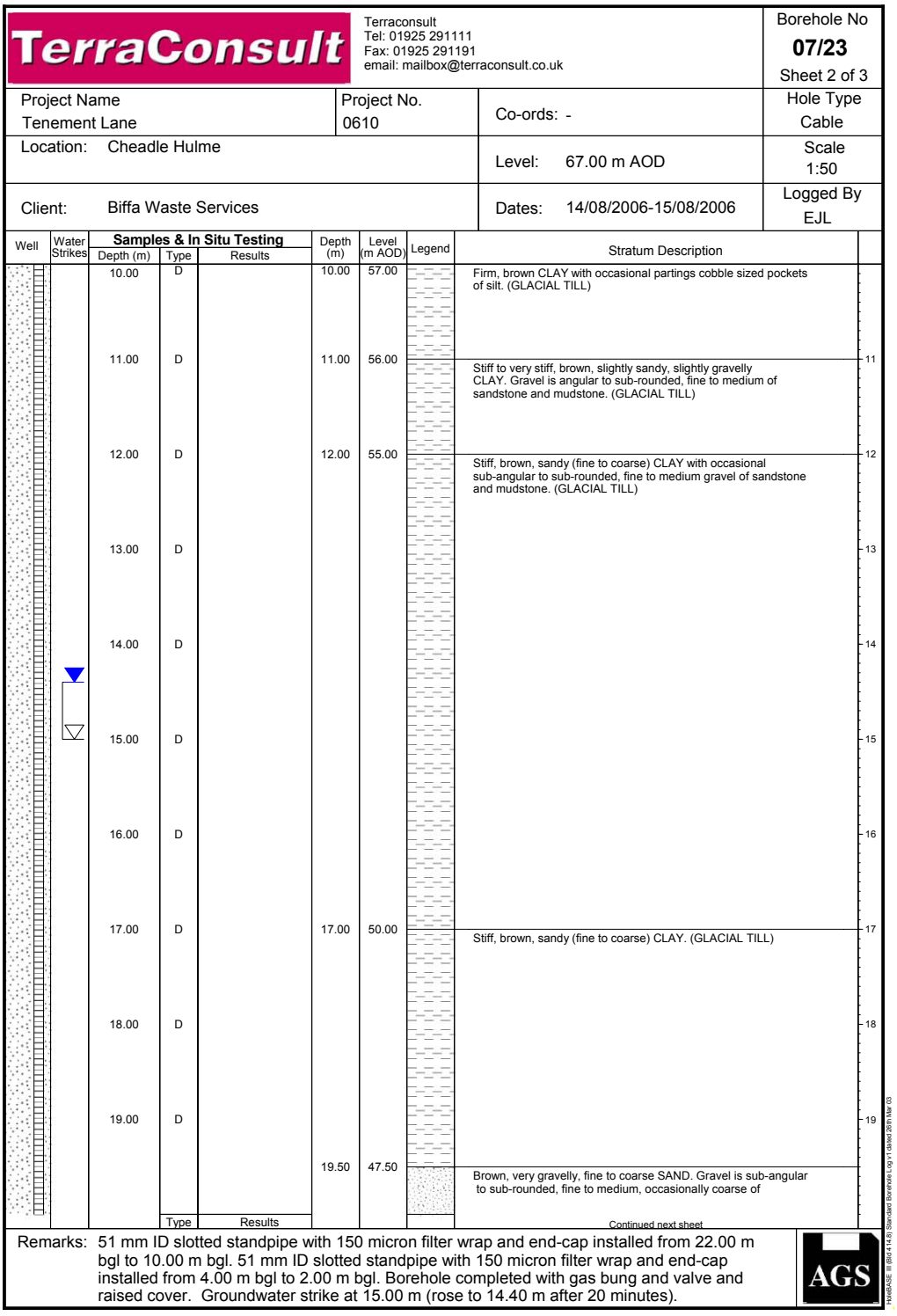

Figure C.11: Site 2 BH 07/23 Borehole Log (Part 2)

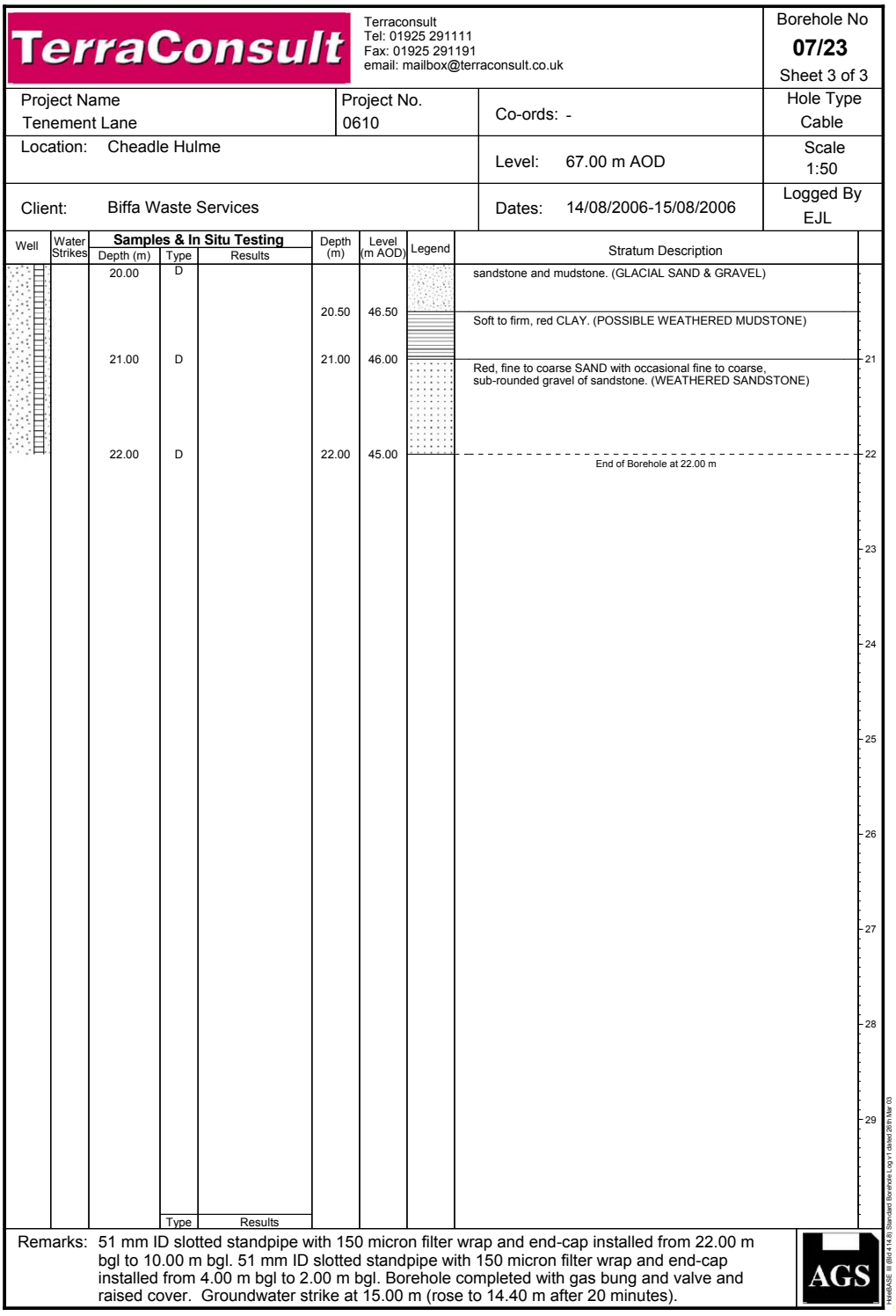

Figure C.12: Site 2 BH 07/23 Borehole Log (Part 3)

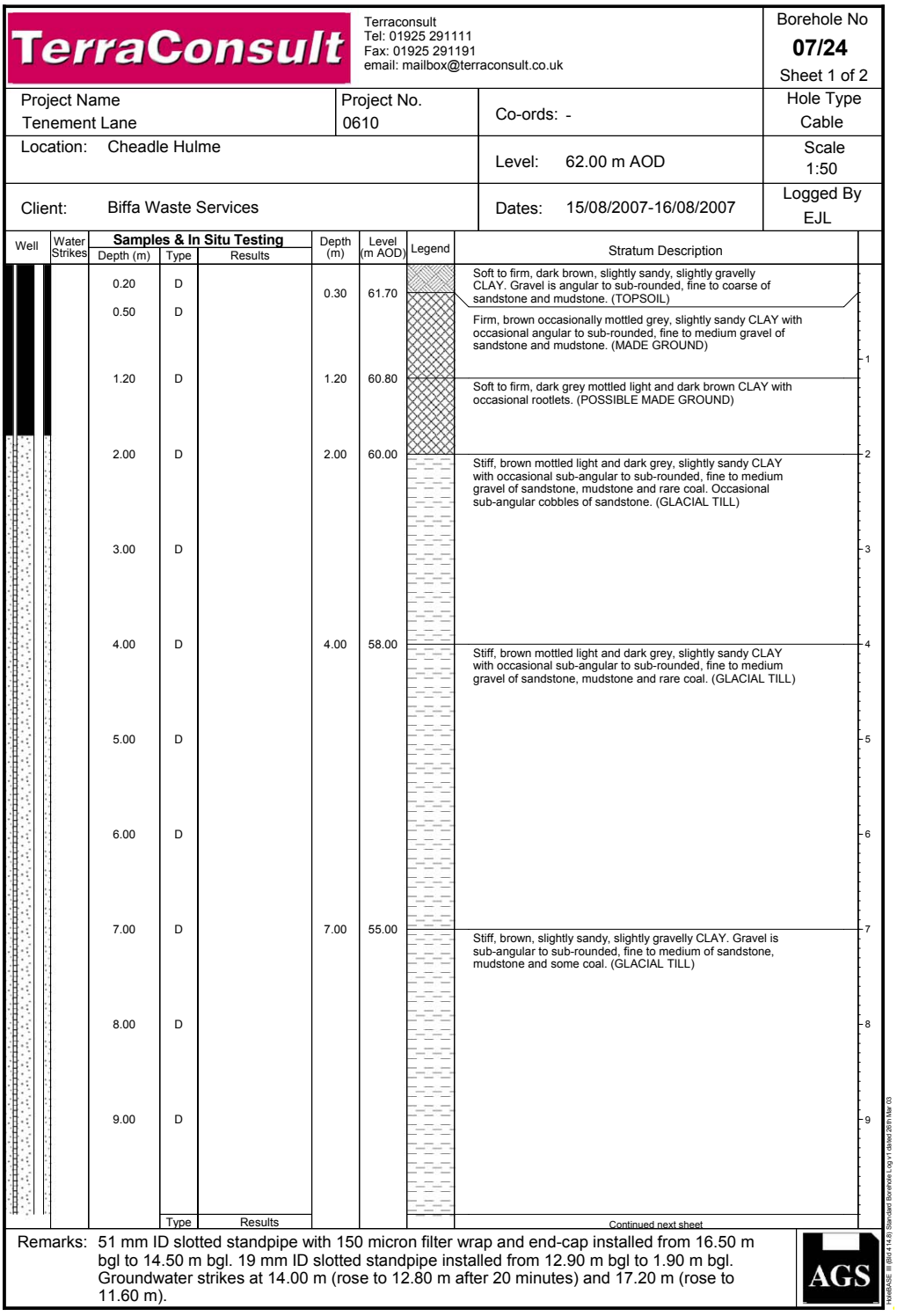

TerraConsult

Terraconsult
Tel: 01925 291111
Fax: 01925 291191
email: mailbox@terraconsult.co.uk

Borehole No **07/24** Sheet 1 of 2

Project Name	Project No.	Co-ords: -	Hole Type
Tenement Lane	0610		Cable
Location: Cheadle Hulme		Level: 62.00 m AOD	Scale 1:50
Client: Biffa Waste Services		Dates: 15/08/2007-16/08/2007	Logged By EJL

Well	Water Strikes	Samples & In Situ Testing Depth (m)	Type	Results	Depth (m)	Level (m AOD)	Legend	Stratum Description
		0.20	D		0.30	61.70		Soft to firm, dark brown, slightly sandy, slightly gravelly CLAY. Gravel is angular to sub-rounded, fine to coarse of sandstone and mudstone. (TOPSOIL)
		0.50	D					Firm, brown occasionally mottled grey, slightly sandy CLAY with occasional angular to sub-rounded, fine to medium gravel of sandstone and mudstone. (MADE GROUND)
		1.20	D		1.20	60.80		Soft to firm, dark grey mottled light and dark brown CLAY with occasional rootlets. (POSSIBLE MADE GROUND)
		2.00	D		2.00	60.00		Stiff, brown mottled light and dark grey, slightly sandy CLAY with occasional sub-angular to sub-rounded, fine to medium gravel of sandstone, mudstone and rare coal. Occasional sub-angular cobbles of sandstone. (GLACIAL TILL)
		3.00	D					
		4.00	D		4.00	58.00		Stiff, brown mottled light and dark grey, slightly sandy CLAY with occasional sub-angular to sub-rounded, fine to medium gravel of sandstone, mudstone and rare coal. (GLACIAL TILL)
		5.00	D					
		6.00	D					
		7.00	D		7.00	55.00		Stiff, brown, slightly sandy, slightly gravelly CLAY. Gravel is sub-angular to sub-rounded, fine to medium of sandstone, mudstone and some coal. (GLACIAL TILL)
		8.00	D					
		9.00	D					
			Type	Results				Continued next sheet

Remarks: 51 mm ID slotted standpipe with 150 micron filter wrap and end-cap installed from 16.50 m bgl to 14.50 m bgl. 19 mm ID slotted standpipe installed from 12.90 m bgl to 1.90 m bgl. Groundwater strikes at 14.00 m (rose to 12.80 m after 20 minutes) and 17.20 m (rose to 11.60 m).

AGS

HoleBASE B (Bd 14.8) Standard Borehole Log v1 dated 28th Mar 03

Figure C.13: Site 2 BH 07/24 Borehole Log (Part 1)

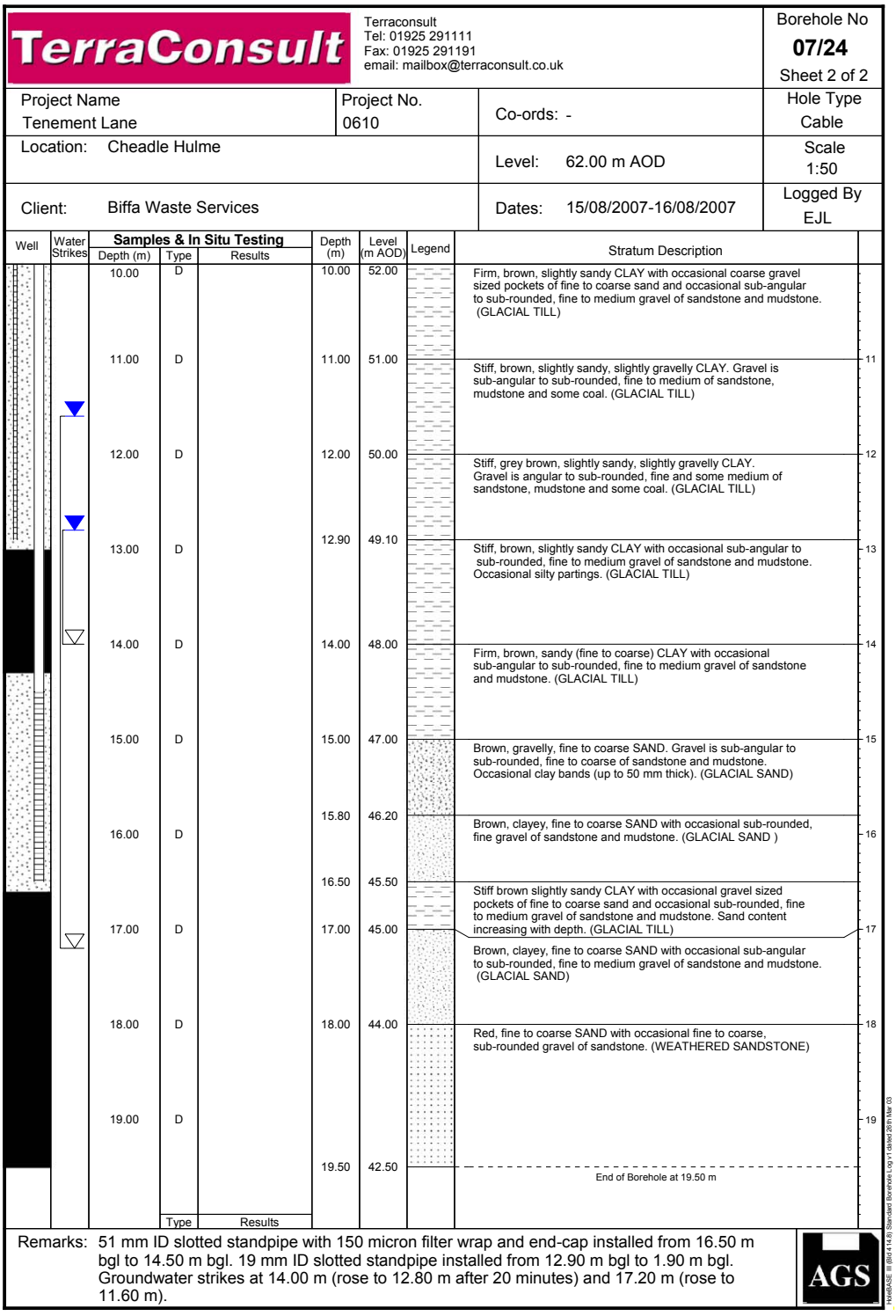

Figure C.14: Site 2 BH 07/24 Borehole Log (Part 2)

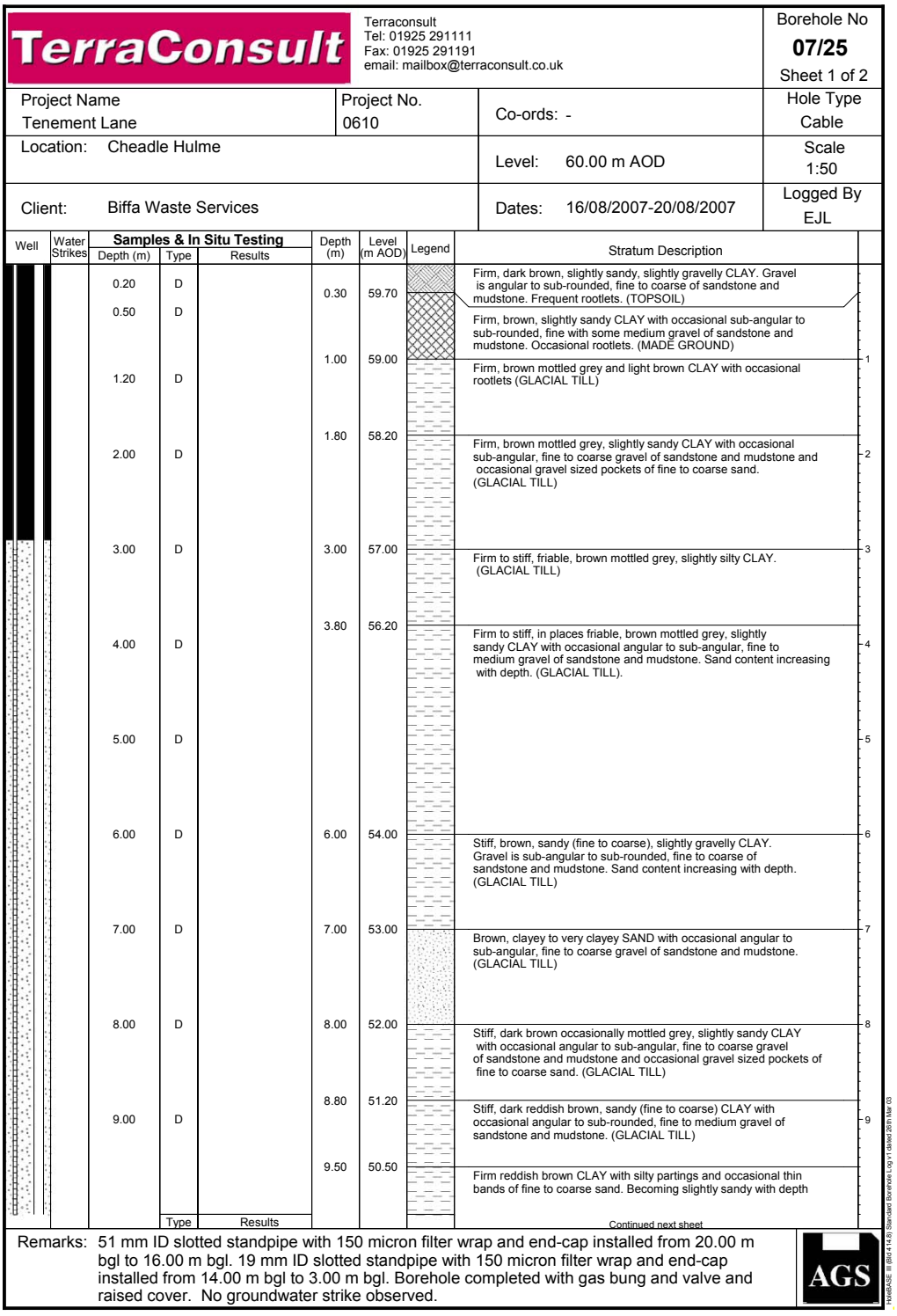

Figure C.15: Site 2 BH 07/25 Borehole Log (Part 1)

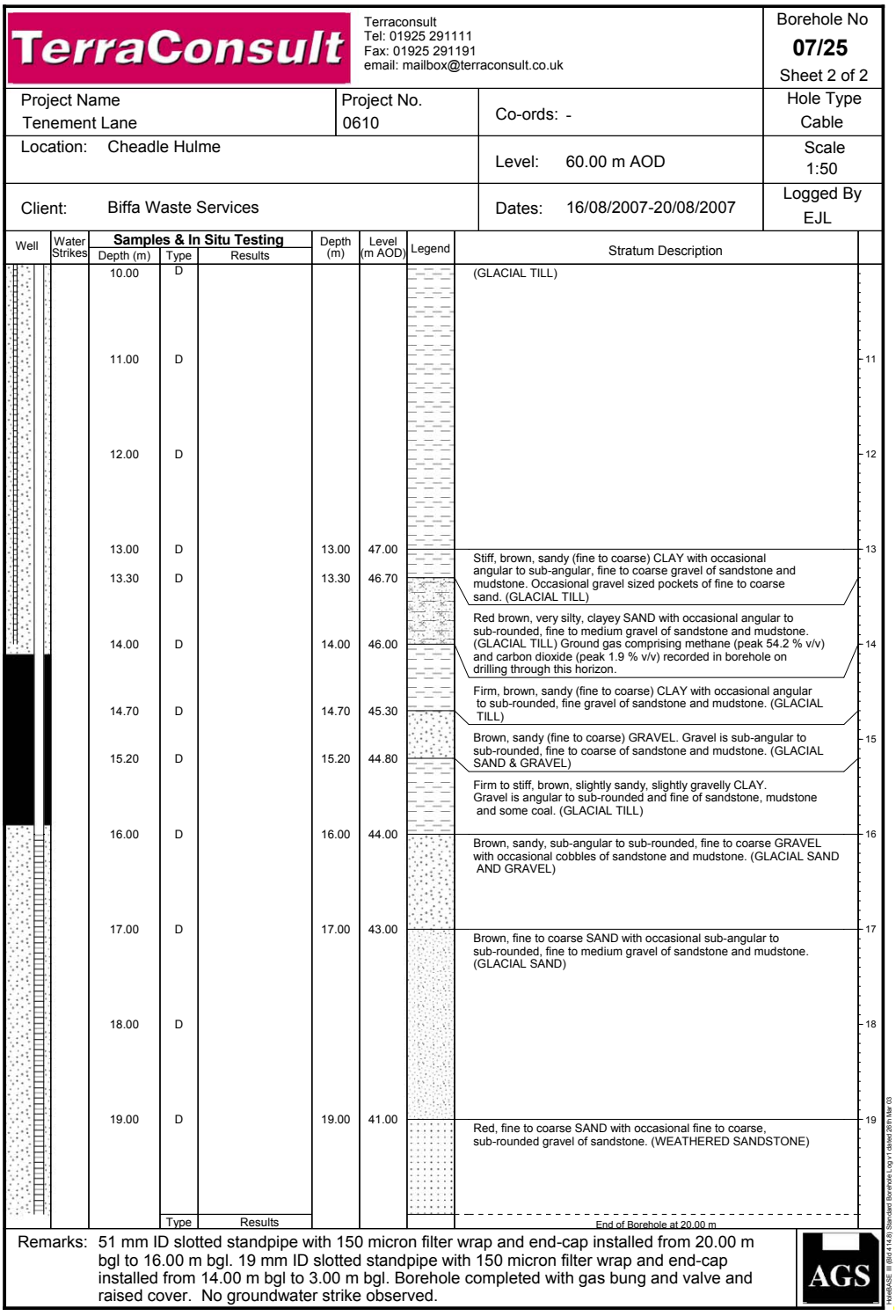

Figure C.16: Site 2 BH 07/25 Borehole Log (Part 2)

Appendix D

Site 3 Borehole Logs

Summary

- Boreholes are separated into distinct and isolated response zones using 0.5–1.0 m bentonite seals. S1 is the first response zone (nearest to the surface) for all boreholes.
- The boreholes are situated in glacial deposits that overlie the chalk bedrock. The chalk is typically encountered at 21.0–23.0 m depth at which point the boreholes terminate.
- The glacial deposits are largely comprised of sand and gravel (that is cobble-sized in places). In some boreholes the gravel is flinty. There are occasional thin layers of clay that are typically 0.5 m thick. The nature of the sand and gravel will give rise to large pore spaces which will allow the internal movement of gases through these media. The sand and gravel will also be highly permeable.
- Few water strikes were encountered. Water strikes occurred in Boreholes GM 14 and 17 at 1.5 and 11.2 m, and 10.3 m respectively.

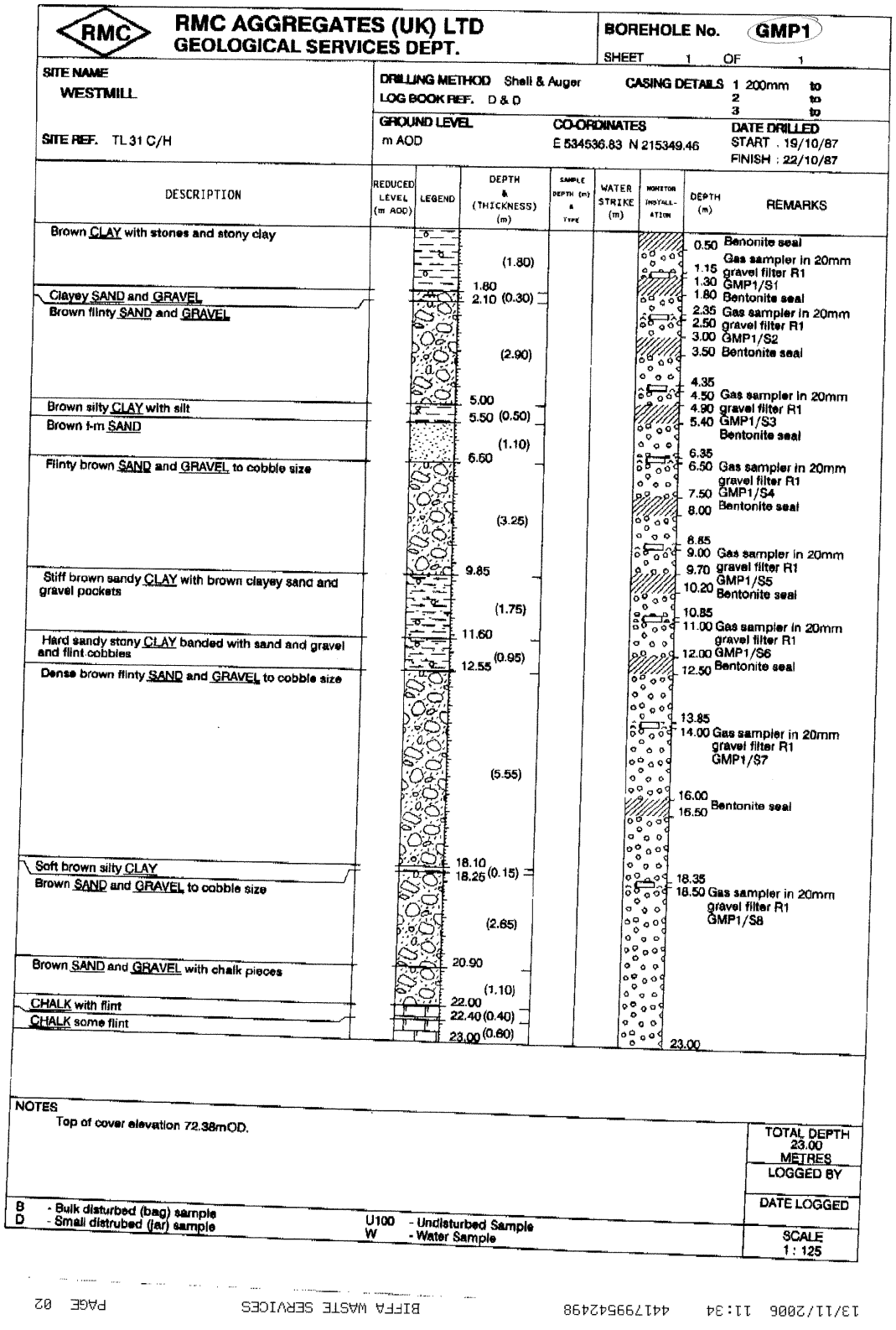

Figure D.1: Site 3 GM 01 Borehole Log

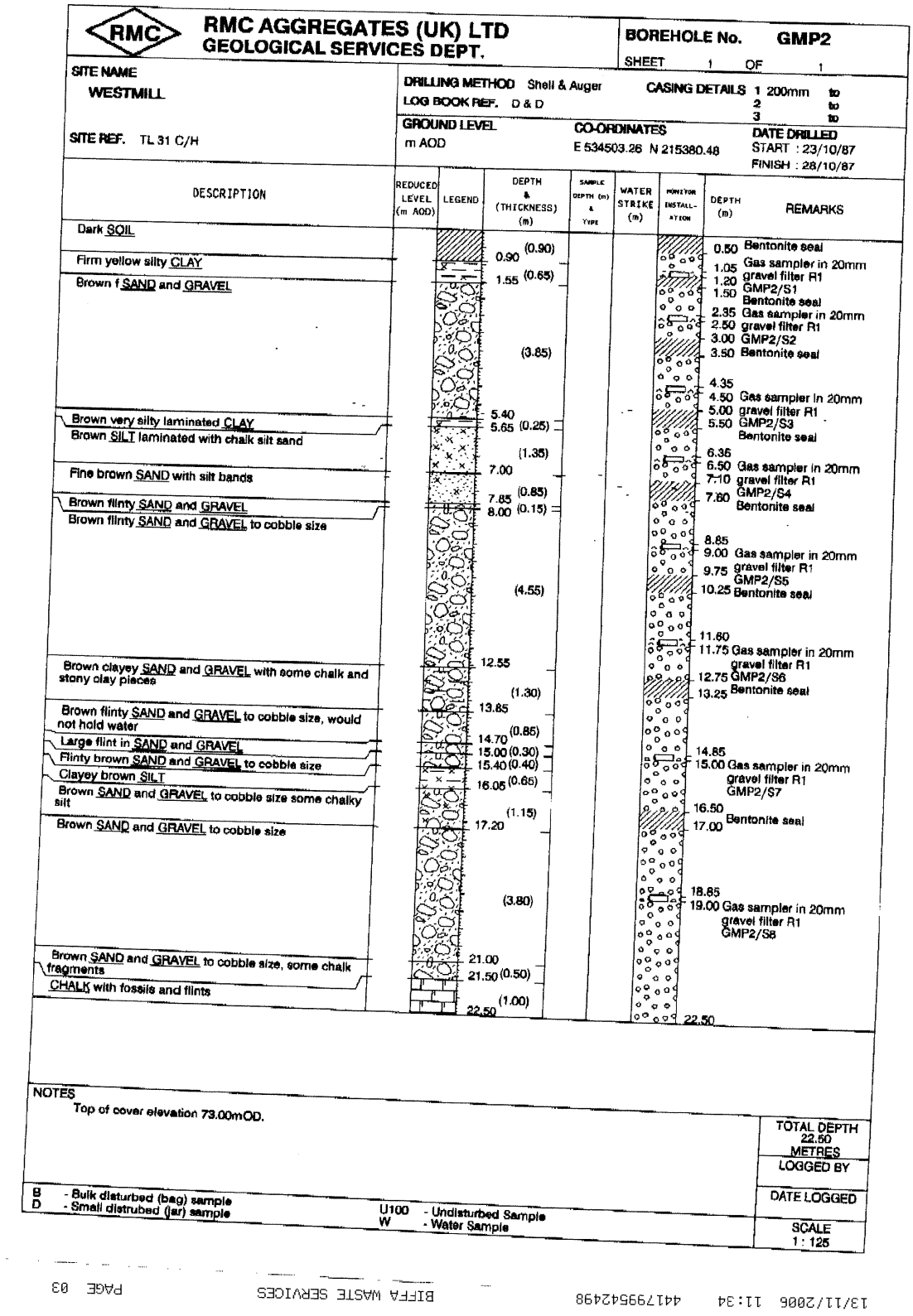

RMC AGGREGATES (UK) LTD
GEOLOGICAL SERVICES DEPT.

BOREHOLE No. GMP2
SHEET 1 OF 1

SITE NAME: WESTMILL
SITE REF. TL 31 C/H

DRILLING METHOD Shell & Auger
LOG BOOK REF. D & D
CASING DETAILS 1 200mm to
2 to
3 to

GROUND LEVEL m AOD
CO-ORDINATES E 534503.26 N 215380.48
DATE DRILLED START : 23/10/87
FINISH : 28/10/87

DESCRIPTION	REDUCED LEVEL (m AOD)	LEGEND	DEPTH & (THICKNESS) (m)	SAMPLE DEPTH (m) & TYPE	WATER STRIKE (m)	MONITOR INSTALL-ATION	DEPTH (m)	REMARKS
Dark SOIL			0.90 (0.90)				0.50	Bentonite seal
Firm yellow silty CLAY			1.55 (0.65)				1.05	Gas sampler in 20mm gravel filter R1
Brown f SAND and GRAVEL			(3.85)				1.20	GMP2/S1
							1.50	Bentonite seal
							2.35	Gas sampler in 20mm gravel filter R1
							2.50	GMP2/S2
							3.00	Bentonite seal
							3.50	
							4.35	
							4.50	Gas sampler in 20mm gravel filter R1
							5.00	GMP2/S3
							5.50	Bentonite seal
Brown very silty laminated CLAY			5.40				6.35	
Brown SILT laminated with chalk silt sand			5.65 (0.25)				6.50	Gas sampler in 20mm gravel filter R1
			(1.35)				7.10	GMP2/S4
Fine brown SAND with silt bands			7.00				7.60	Bentonite seal
			(0.85)					
Brown flinty SAND and GRAVEL			7.85 (0.15)				8.85	
Brown flinty SAND and GRAVEL to cobble size			8.00				9.00	Gas sampler in 20mm gravel filter R1
			(4.55)				9.75	GMP2/S5
							10.25	Bentonite seal
							11.60	
							11.75	Gas sampler in 20mm gravel filter R1
Brown clayey SAND and GRAVEL with some chalk and stony clay places			12.55				12.75	GMP2/S6
			(1.30)				13.25	Bentonite seal
Brown flinty SAND and GRAVEL to cobble size, would not hold water			13.85					
Large flint in SAND and GRAVEL			14.70 (0.85)				14.85	
Flinty brown SAND and GRAVEL to cobble size			15.00 (0.30)				15.00	Gas sampler in 20mm gravel filter R1
Clayey brown SILT			15.40 (0.40)					GMP2/S7
Brown SAND and GRAVEL to cobble size some chalky silt			16.05 (0.65)				16.50	
			(1.15)				17.00	Bentonite seal
Brown SAND and GRAVEL to cobble size			17.20					
			(3.80)				18.85	
							19.00	Gas sampler in 20mm gravel filter R1
								GMP2/S8
Brown SAND and GRAVEL to cobble size, some chalk fragments			21.00					
CHALK with fossils and flints			21.50 (0.50)					
			(1.00)					
			22.50				22.50	

NOTES
Top of cover elevation 73.00mOD.

TOTAL DEPTH 22.50 METRES
LOGGED BY
DATE LOGGED
SCALE 1 : 125

B - Bulk disturbed (bag) sample
D - Small distrubed (jar) sample
U100 - Undisturbed Sample
W - Water Sample

Figure D.2: Site 3 GM 02 Borehole Log

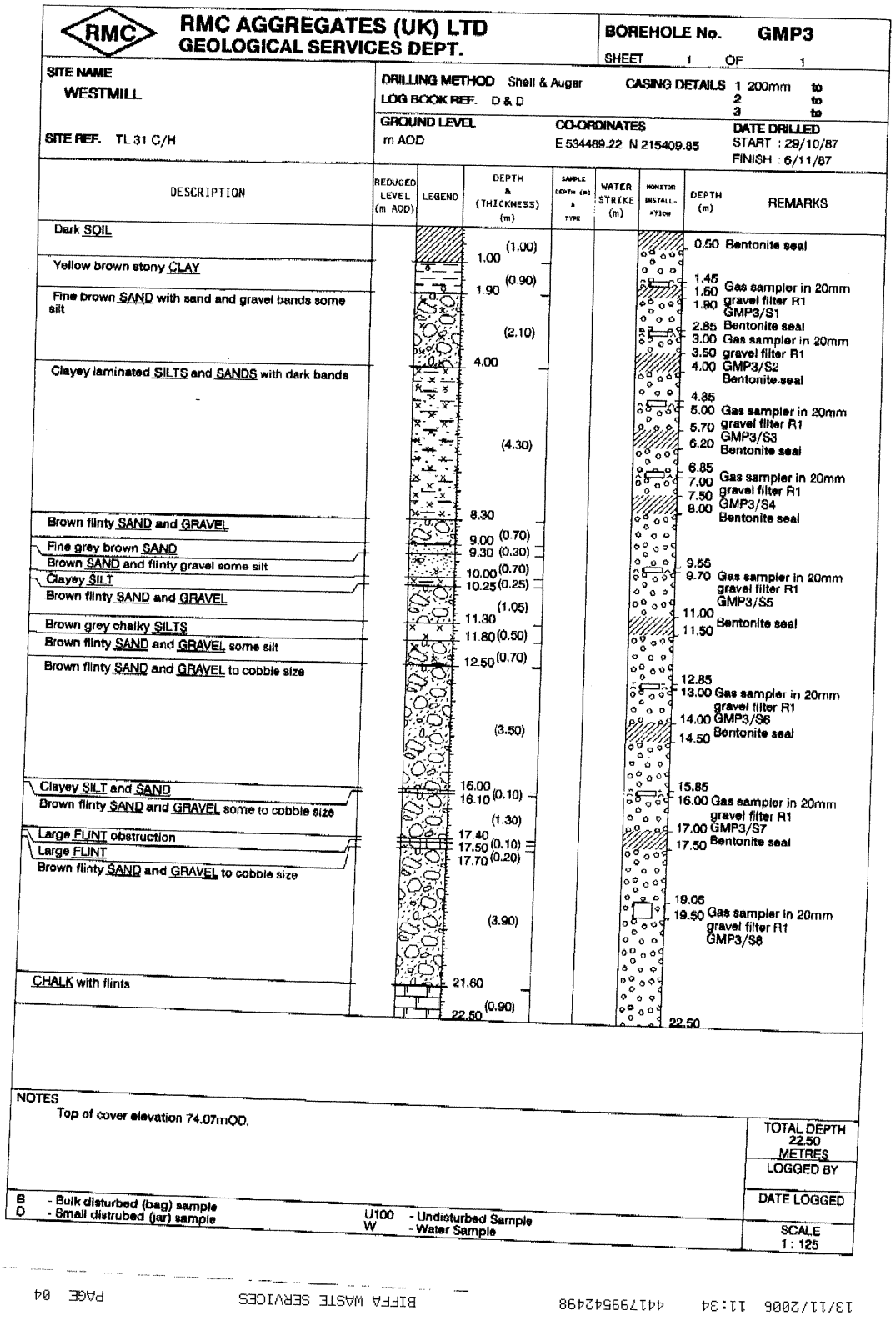

Figure D.3: Site 3 GM 03 Borehole Log

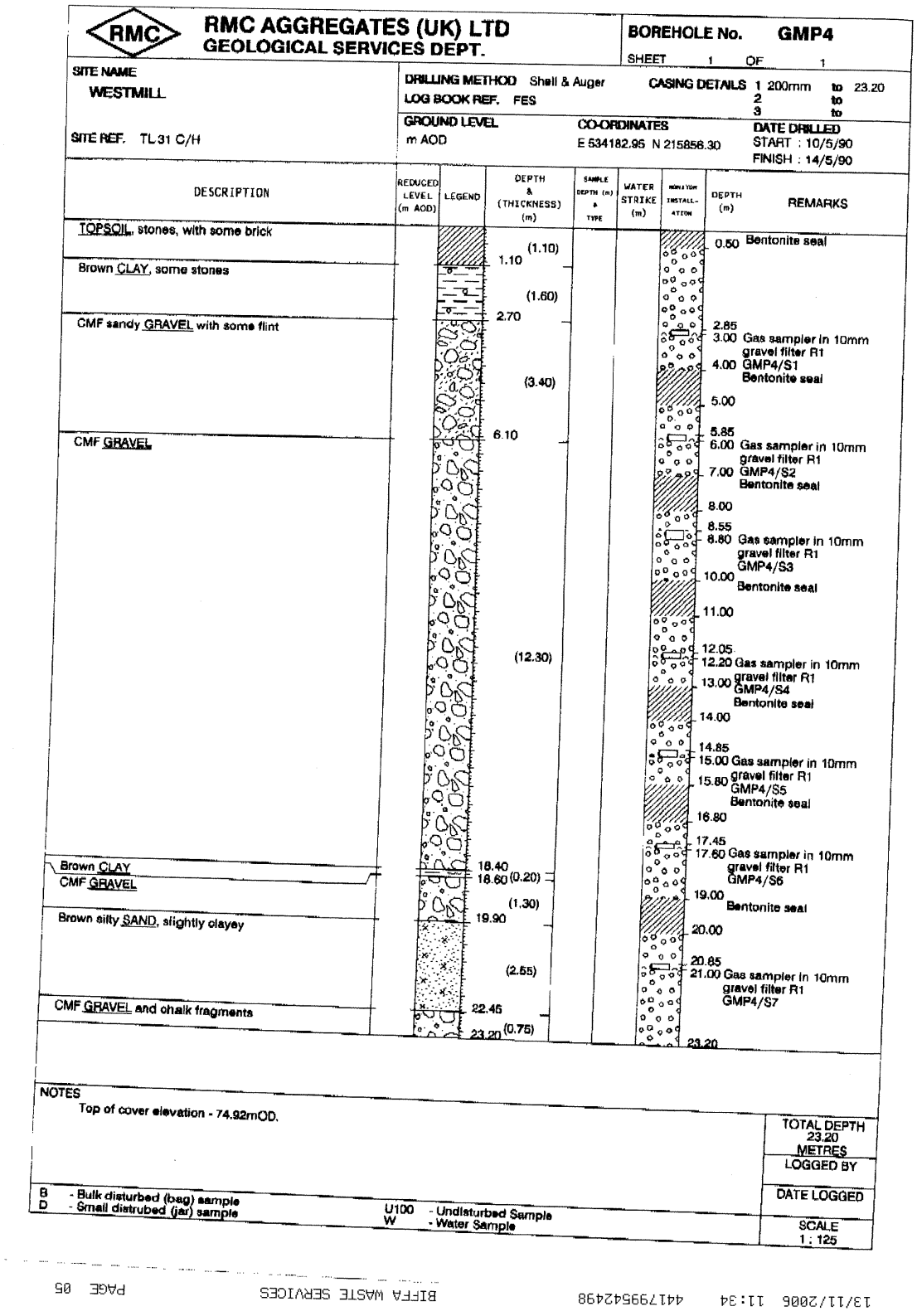

Figure D.4: Site 3 GM 04 Borehole Log

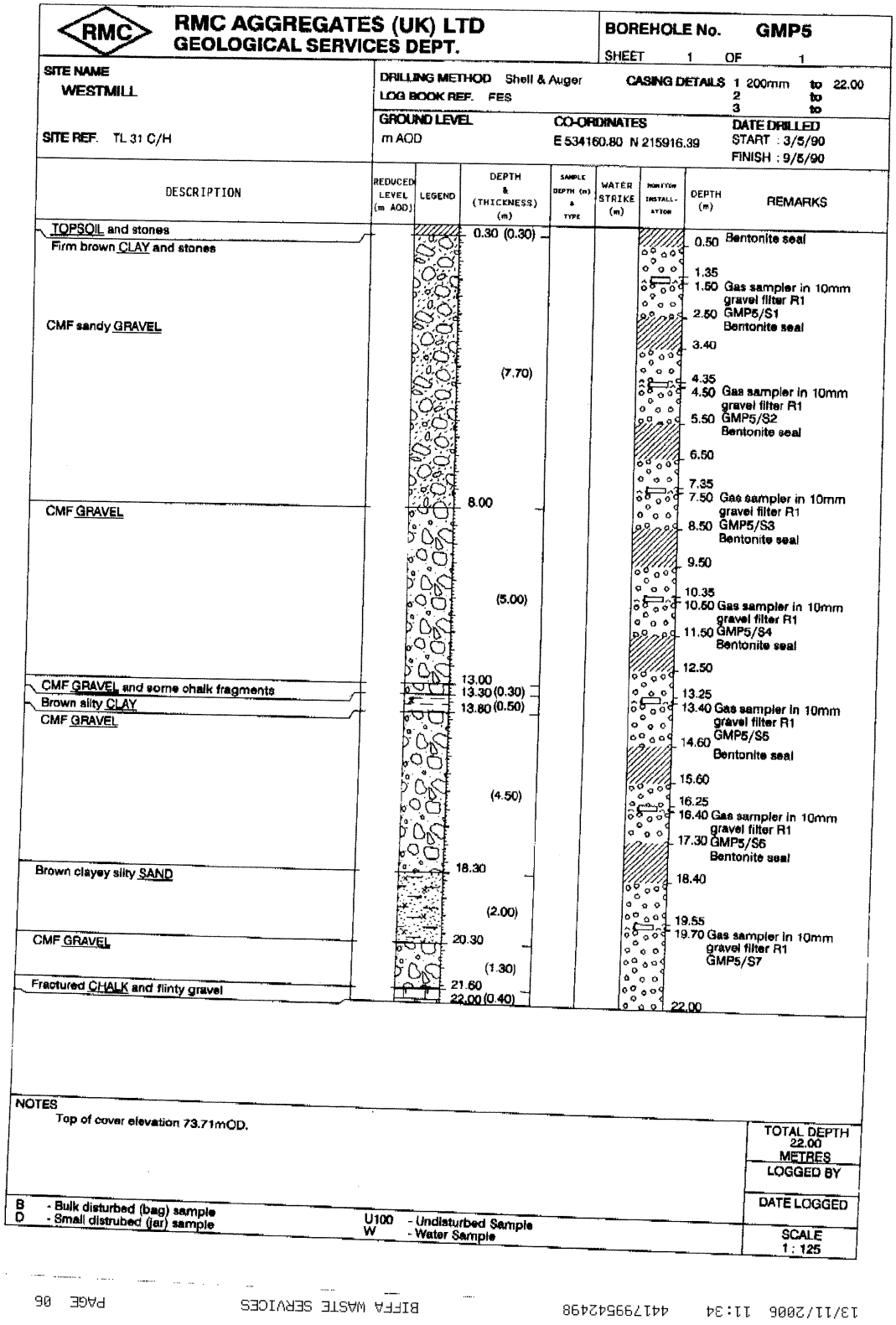

Figure D.5: Site 3 GM 05 Borehole Log

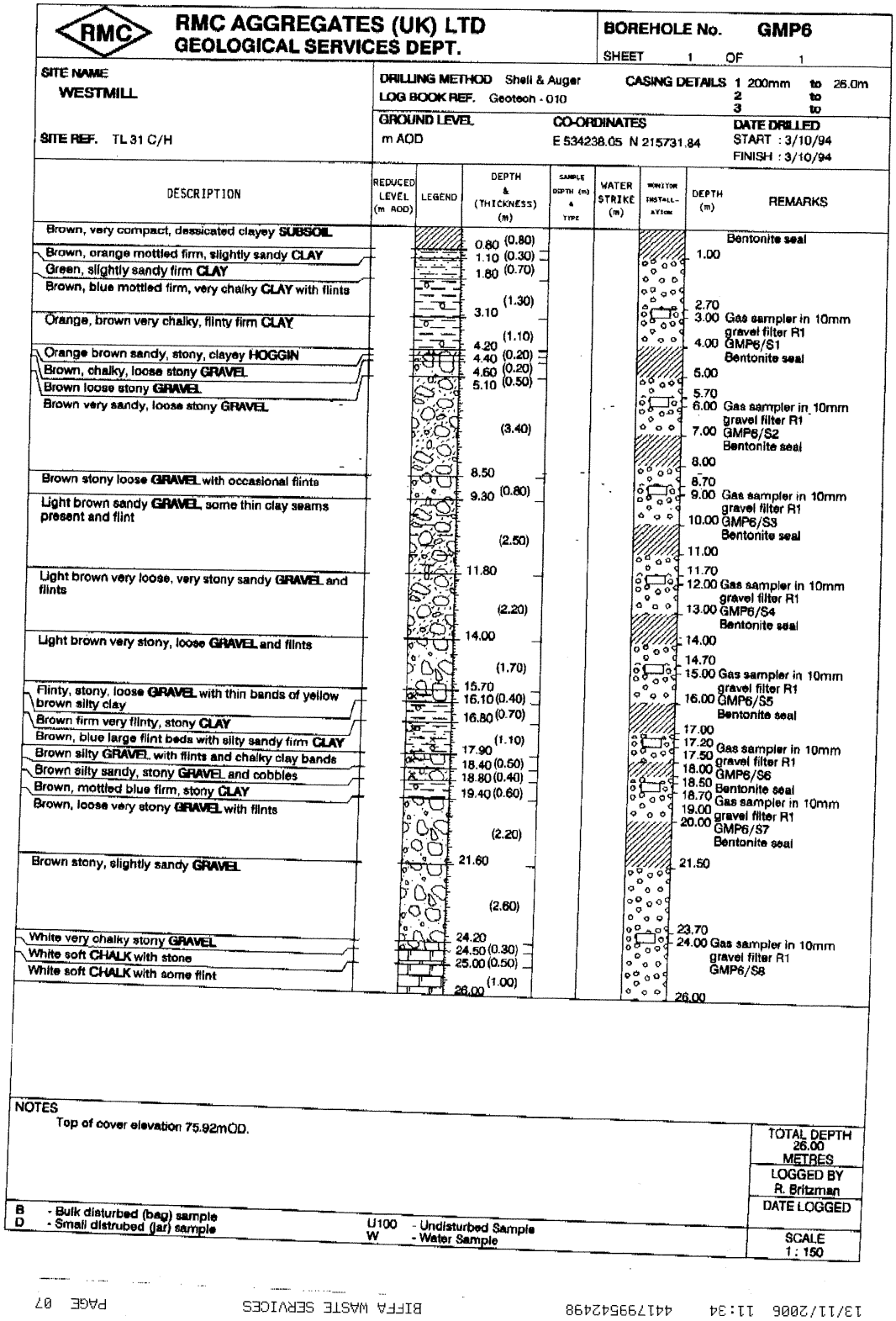

Figure D.6: Site 3 GM 06 Borehole Log

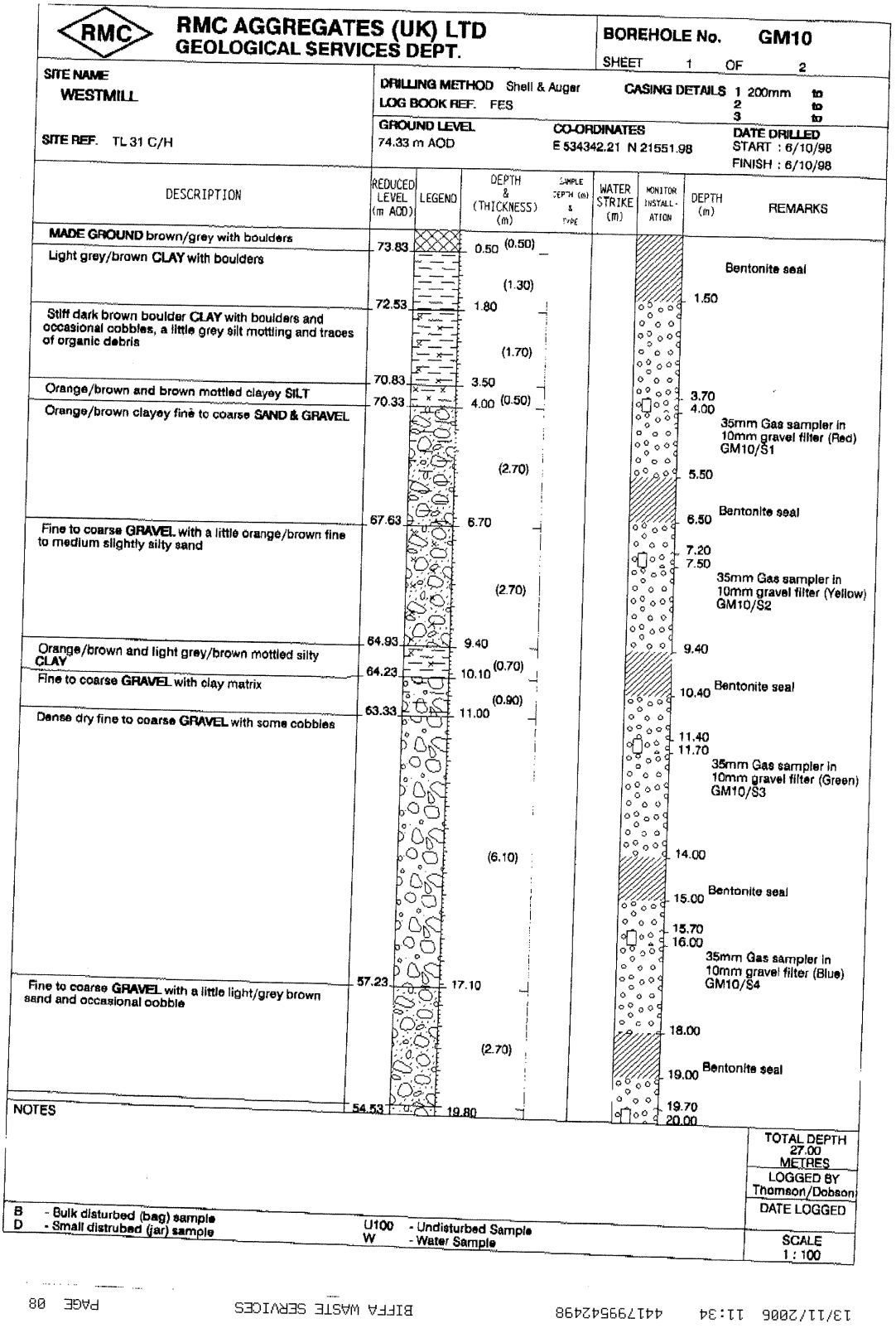

Figure D.7: Site 3 GM 10 Borehole Log (Part 1)

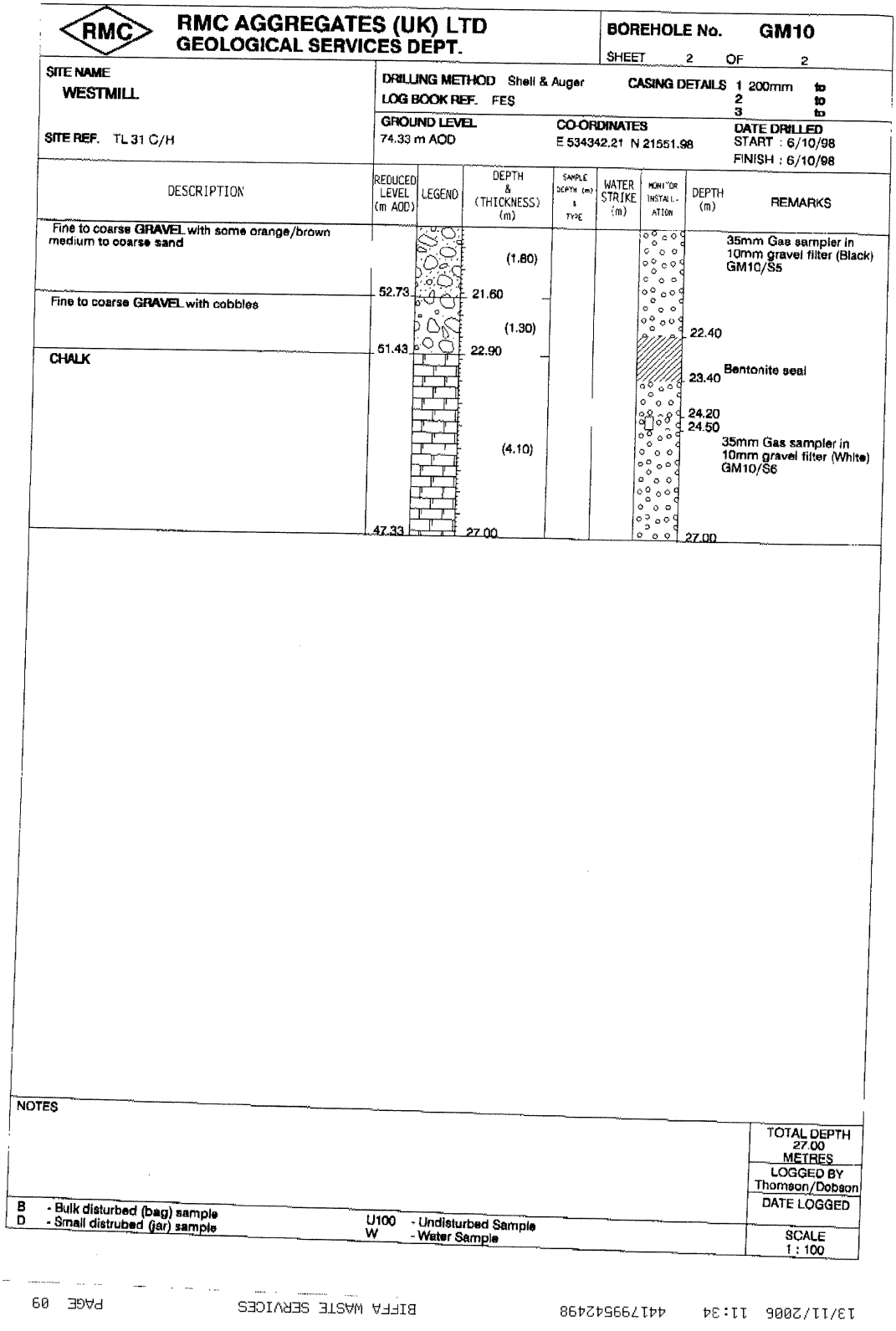

RMC AGGREGATES (UK) LTD
GEOLOGICAL SERVICES DEPT.

BOREHOLE No. GM10
SHEET 2 OF 2

SITE NAME: WESTMILL
SITE REF. TL 31 C/H

DRILLING METHOD Shell & Auger
LOG BOOK REF. FES

CASING DETAILS 1 200mm to
2 to
3 to

GROUND LEVEL 74.33 m AOD

CO-ORDINATES E 534342.21 N 21551.98

DATE DRILLED START : 6/10/98
FINISH : 6/10/98

DESCRIPTION	REDUCED LEVEL (m AOD)	LEGEND	DEPTH & (THICKNESS) (m)	SAMPLE DEPTH (m) & TYPE	WATER STRIKE (m)	MONITOR INSTALL-ATION	DEPTH (m)	REMARKS
Fine to coarse GRAVEL with some orange/brown medium to coarse sand			(1.60)					35mm Gas sampler in 10mm gravel filter (Black) GM10/S5
	52.73		21.60					
Fine to coarse GRAVEL with cobbles			(1.30)				22.40	
	51.43		22.90					
CHALK							23.40	Bentonite seal
							24.20	
							24.50	35mm Gas sampler in 10mm gravel filter (White) GM10/S6
			(4.10)					
	47.33		27.00				27.00	

NOTES

TOTAL DEPTH 27.00 METRES
LOGGED BY Thomson/Dobson
DATE LOGGED
SCALE 1 : 100

B - Bulk disturbed (bag) sample
D - Small distrubed (jar) sample
U100 - Undisturbed Sample
W - Water Sample

PAGE 09 BIFFA WASTE SERVICES 441799542498 13/11/2006 11:34

Figure D.8: Site 3 GM 10 Borehole Log (Part 2)

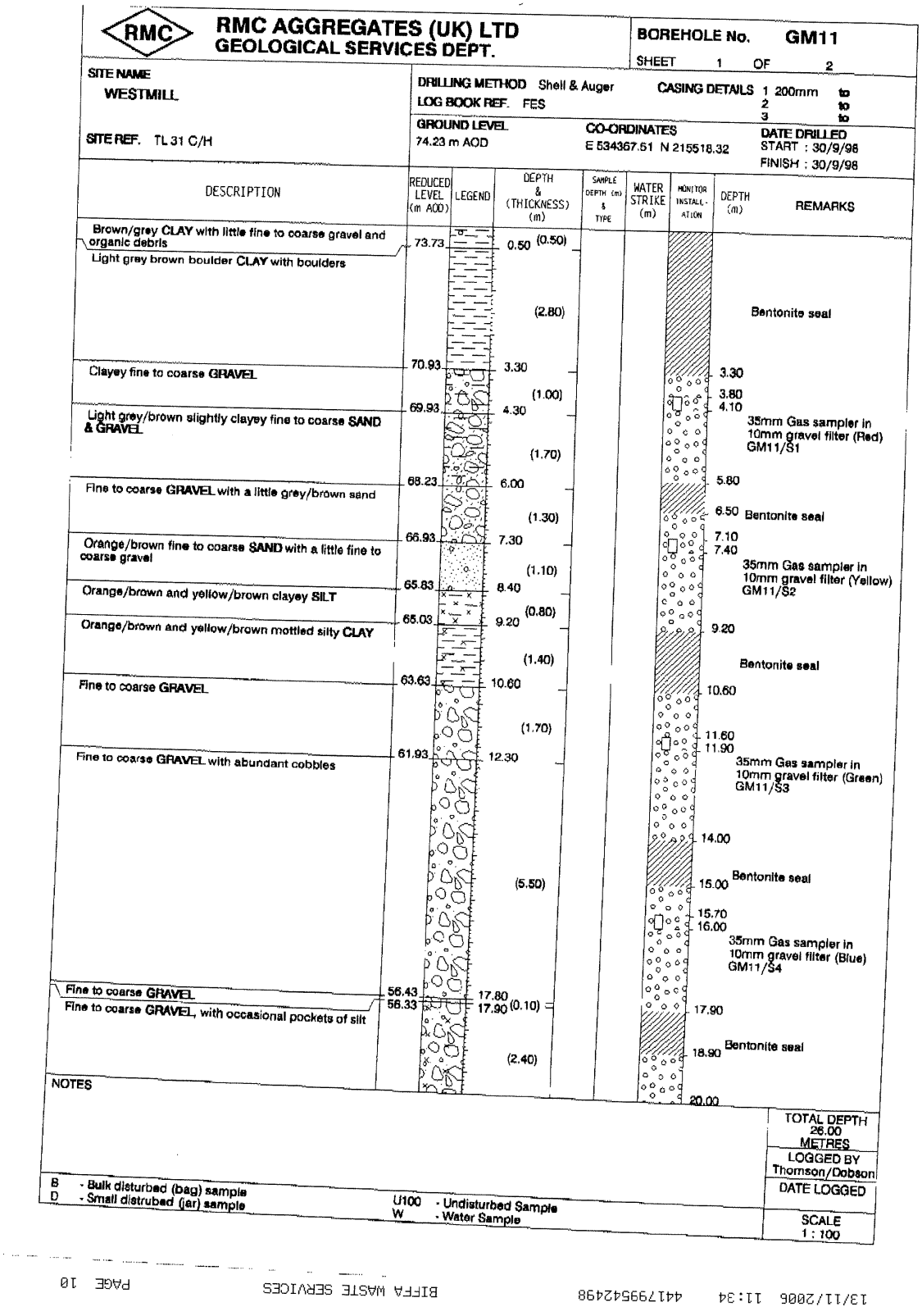

Figure D.9: Site 3 GM 11 Borehole Log (Part 1)

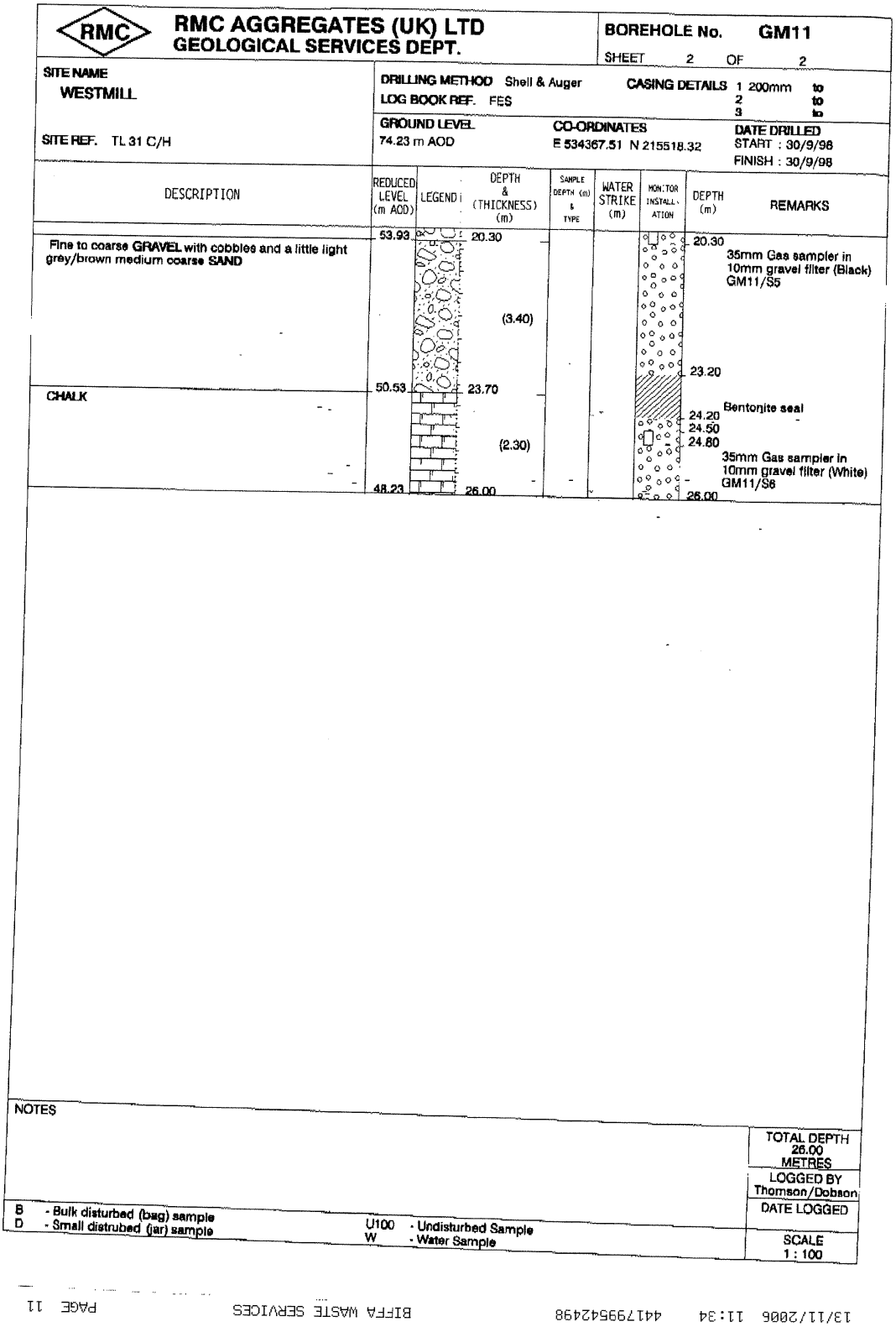

RMC AGGREGATES (UK) LTD
GEOLOGICAL SERVICES DEPT.

BOREHOLE No. GM11
SHEET 2 OF 2

SITE NAME: WESTMILL
SITE REF. TL 31 C/H

DRILLING METHOD Shell & Auger
LOG BOOK REF. FES
CASING DETAILS 1 200mm to
2 to
3 to

GROUND LEVEL 74.23 m AOD
CO-ORDINATES E 534367.51 N 215518.32
DATE DRILLED START : 30/9/98
FINISH : 30/9/98

DESCRIPTION	REDUCED LEVEL (m AOD)	LEGEND	DEPTH & (THICKNESS) (m)	SAMPLE DEPTH (m) & TYPE	WATER STRIKE (m)	MONITOR INSTALLATION	DEPTH (m)	REMARKS
Fine to coarse GRAVEL with cobbles and a little light grey/brown medium coarse SAND	53.93		20.30				20.30	35mm Gas sampler in 10mm gravel filter (Black) GM11/S5
			(3.40)				23.20	
CHALK	50.53		23.70				24.20	Bentonite seal
			(2.30)				24.50	
	48.23		26.00				24.80	35mm Gas sampler in 10mm gravel filter (White) GM11/S6
							26.00	

NOTES

TOTAL DEPTH 26.00 METRES
LOGGED BY Thomson/Dobson
DATE LOGGED
SCALE 1 : 100

B - Bulk disturbed (bag) sample
D - Small distrubed (jar) sample
U100 - Undisturbed Sample
W - Water Sample

13/11/2006 11:34 441799542498 BIFFA WASTE SERVICES PAGE 11

Figure D.10: Site 3 GM 11 Borehole Log (Part 2)

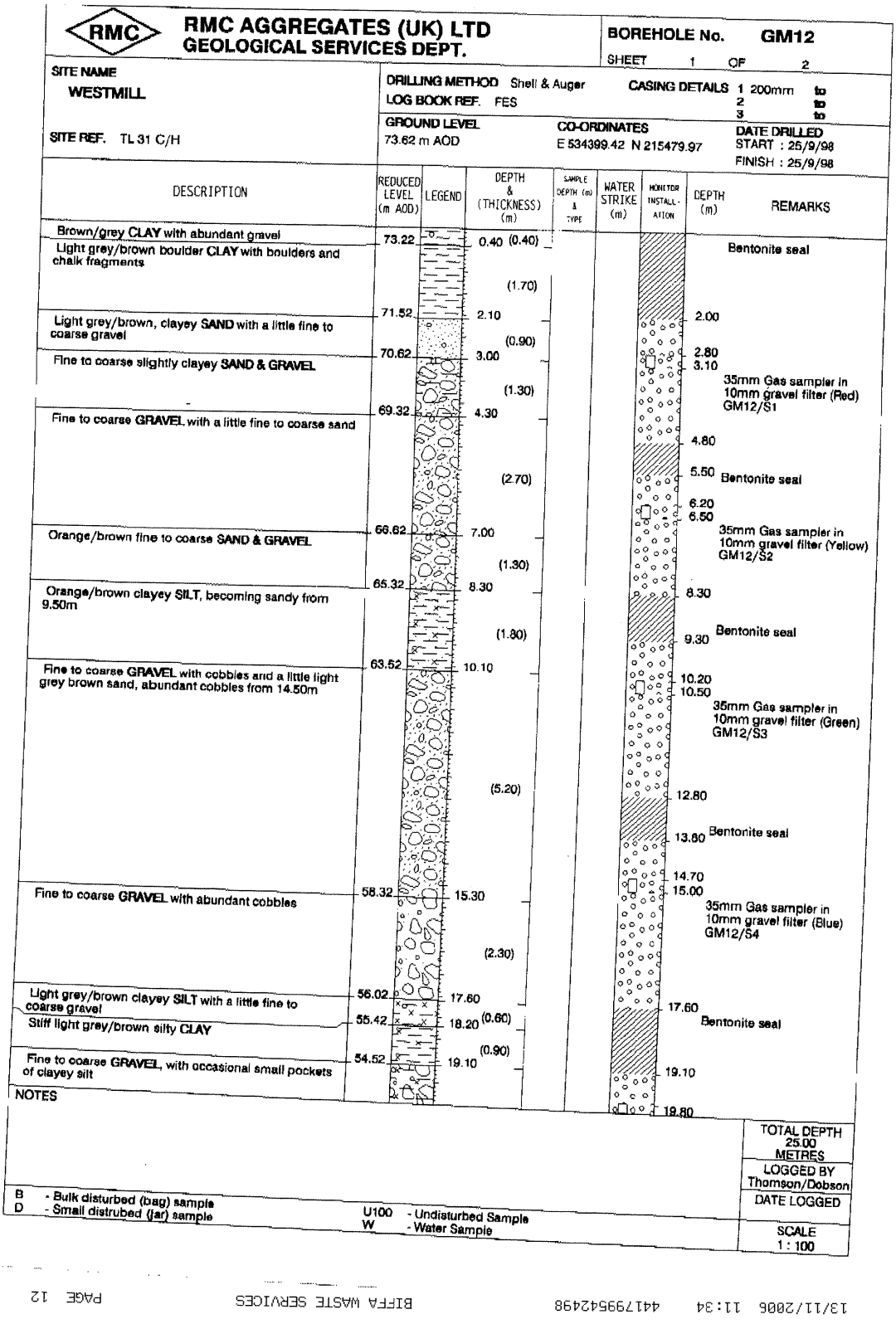

RMC AGGREGATES (UK) LTD
GEOLOGICAL SERVICES DEPT.

BOREHOLE No. GM12
SHEET 1 OF 2

SITE NAME: WESTMILL
SITE REF. TL 31 C/H

DRILLING METHOD Shell & Auger
LOG BOOK REF. FES
CASING DETAILS 1 200mm to
2 to
3 to

GROUND LEVEL 73.62 m AOD
CO-ORDINATES E 534399.42 N 215479.97
DATE DRILLED START : 25/9/98
FINISH : 25/9/98

DESCRIPTION	REDUCED LEVEL (m AOD)	DEPTH & (THICKNESS) (m)	WATER STRIKE (m)	DEPTH (m)	REMARKS
Brown/grey CLAY with abundant gravel	73.22	0.40 (0.40)			
Light grey/brown boulder CLAY with boulders and chalk fragments		(1.70)			Bentonite seal
Light grey/brown, clayey SAND with a little fine to coarse gravel	71.52	2.10 (0.90)		2.00	
Fine to coarse slightly clayey SAND & GRAVEL	70.62	3.00 (1.30)		2.80 3.10	35mm Gas sampler in 10mm gravel filter (Red) GM12/S1
Fine to coarse GRAVEL with a little fine to coarse sand	69.32	4.30 (2.70)		4.80 5.50	Bentonite seal
Orange/brown fine to coarse SAND & GRAVEL	66.62	7.00 (1.30)		6.20 6.50	35mm Gas sampler in 10mm gravel filter (Yellow) GM12/S2
Orange/brown clayey SILT, becoming sandy from 9.50m	65.32	8.30 (1.80)		8.30 9.30	Bentonite seal
Fine to coarse GRAVEL with cobbles and a little light grey brown sand, abundant cobbles from 14.50m	63.52	10.10 (5.20)		10.20 10.50	35mm Gas sampler in 10mm gravel filter (Green) GM12/S3
Fine to coarse GRAVEL with abundant cobbles	58.32	15.30 (2.30)		12.80 13.80 14.70 15.00	Bentonite seal 35mm Gas sampler in 10mm gravel filter (Blue) GM12/S4
Light grey/brown clayey SILT with a little fine to coarse gravel	56.02	17.60		17.60	Bentonite seal
Stiff light grey/brown silty CLAY	55.42	18.20 (0.60)			
Fine to coarse GRAVEL, with occasional small pockets of clayey silt	54.52	19.10 (0.90)		19.10 19.80	

NOTES

TOTAL DEPTH 25.00 METRES
LOGGED BY Thomson/Dobson
DATE LOGGED
SCALE 1 : 100

B - Bulk disturbed (bag) sample
D - Small distrubed (jar) sample
U100 - Undisturbed Sample
W - Water Sample

Figure D.11: Site 3 GM 12 Borehole Log (Part 1)

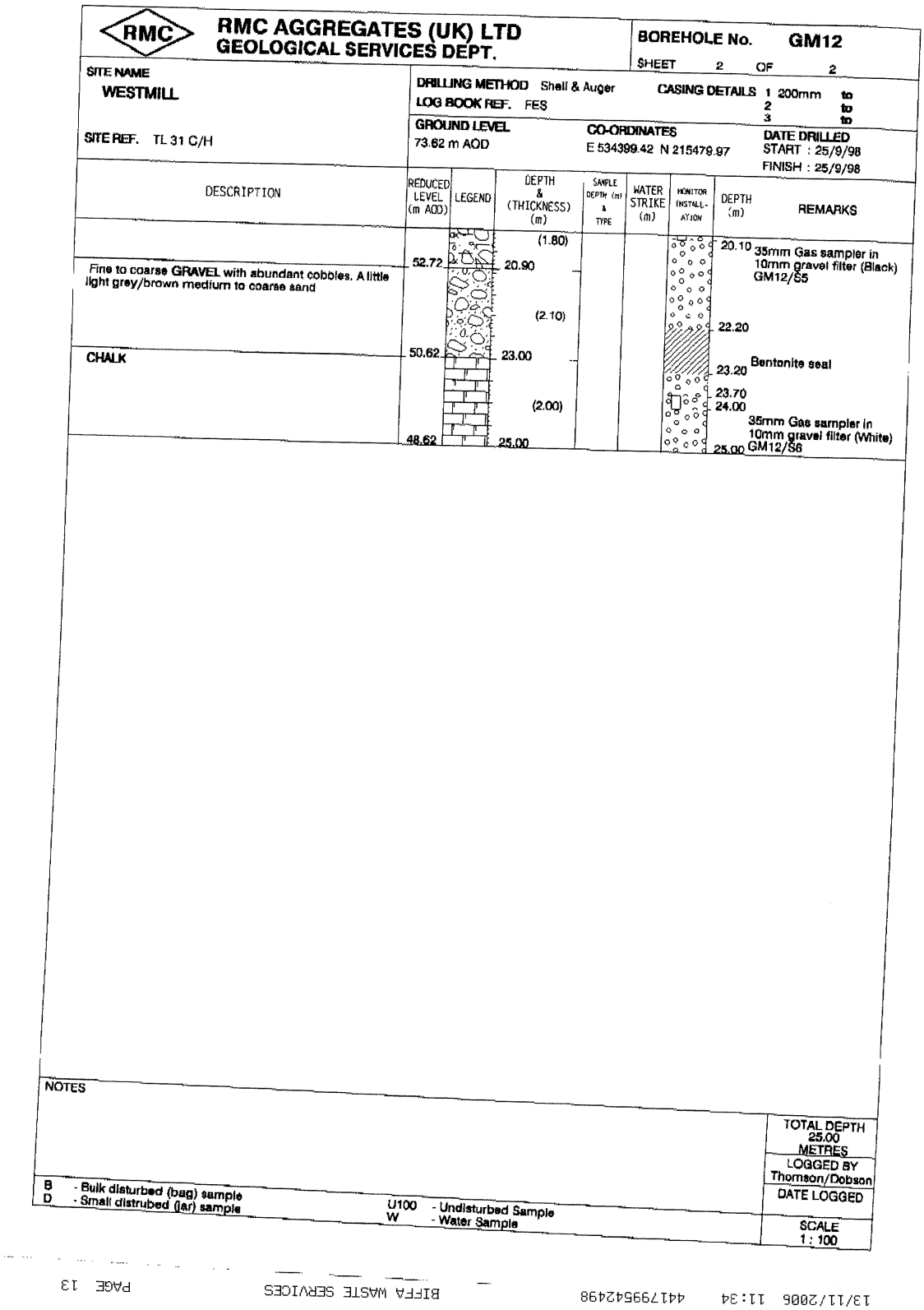

RMC AGGREGATES (UK) LTD
GEOLOGICAL SERVICES DEPT.

BOREHOLE No. GM12
SHEET 2 OF 2

SITE NAME: WESTMILL
SITE REF. TL 31 C/H

DRILLING METHOD Shell & Auger
LOG BOOK REF. FES
CASING DETAILS 1 200mm to
2 to
3 to

GROUND LEVEL 73.62 m AOD
CO-ORDINATES E 534399.42 N 215479.97
DATE DRILLED START : 25/9/98
FINISH : 25/9/98

DESCRIPTION	REDUCED LEVEL (m AOD)	LEGEND	DEPTH & (THICKNESS) (m)	SAMPLE DEPTH (m) & TYPE	WATER STRIKE (m)	MONITOR INSTALL-ATION	DEPTH (m)	REMARKS
			(1.80)				20.10	35mm Gas sampler in 10mm gravel filter (Black) GM12/S5
Fine to coarse GRAVEL with abundant cobbles. A little light grey/brown medium to coarse sand	52.72		20.90					
			(2.10)				22.20	
CHALK	50.62		23.00				23.20	Bentonite seal
			(2.00)				23.70 / 24.00	
	48.62		25.00				25.00	35mm Gas sampler in 10mm gravel filter (White) GM12/S6

NOTES

TOTAL DEPTH 25.00 METRES
LOGGED BY Thomson/Dobson
DATE LOGGED
SCALE 1 : 100

B - Bulk disturbed (bag) sample
D - Small distrubed (jar) sample
U100 - Undisturbed Sample
W - Water Sample

13/11/2006 11:34 441799542498 BIFFA WASTE SERVICES PAGE 13

Figure D.12: Site 3 GM 12 Borehole Log (Part 2)

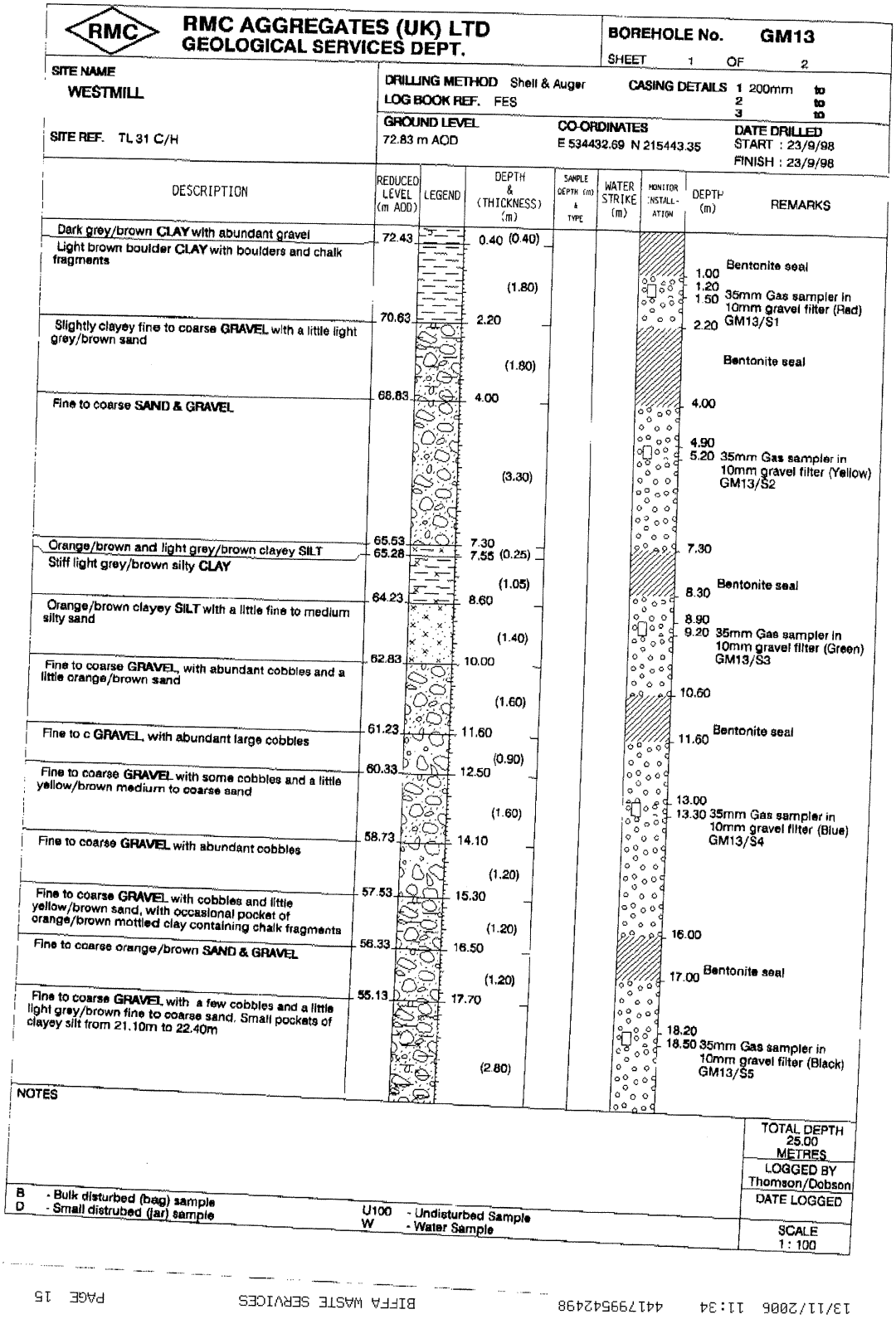

RMC AGGREGATES (UK) LTD
GEOLOGICAL SERVICES DEPT.

BOREHOLE No. GM13
SHEET 1 OF 2

SITE NAME: WESTMILL
SITE REF. TL 31 C/H

DRILLING METHOD Shell & Auger
LOG BOOK REF. FES
CASING DETAILS 1 200mm to
2 to
3 to

GROUND LEVEL 72.83 m AOD
CO-ORDINATES E 534432.69 N 215443.35
DATE DRILLED START : 23/9/98
FINISH : 23/9/98

DESCRIPTION	REDUCED LEVEL (m AOD)	LEGEND	DEPTH & (THICKNESS) (m)	SAMPLE DEPTH (m) & TYPE	WATER STRIKE (m)	MONITOR INSTALL-ATION	DEPTH (m)	REMARKS
Dark grey/brown **CLAY** with abundant gravel	72.43		0.40 (0.40)					
Light brown boulder **CLAY** with boulders and chalk fragments			(1.80)				1.00 1.20 1.50	Bentonite seal 35mm Gas sampler in 10mm gravel filter (Red)
Slightly clayey fine to coarse **GRAVEL** with a little light grey/brown sand	70.63		2.20				2.20	GM13/S1
			(1.80)					Bentonite seal
Fine to coarse **SAND & GRAVEL**	68.83		4.00				4.00	
			(3.30)				4.90 5.20	35mm Gas sampler in 10mm gravel filter (Yellow) GM13/S2
Orange/brown and light grey/brown clayey **SILT**	65.53		7.30				7.30	
Stiff light grey/brown silty **CLAY**	65.28		7.55 (0.25)					
Orange/brown clayey **SILT** with a little fine to medium silty sand	64.23		(1.05) 8.60				8.30	Bentonite seal
			(1.40)				8.90 9.20	35mm Gas sampler in 10mm gravel filter (Green) GM13/S3
Fine to coarse **GRAVEL**, with abundant cobbles and a little orange/brown sand	62.83		10.00				10.60	
			(1.60)					
Fine to c **GRAVEL**, with abundant large cobbles	61.23		11.60				11.60	Bentonite seal
			(0.90)					
Fine to coarse **GRAVEL** with some cobbles and a little yellow/brown medium to coarse sand	60.33		12.50				13.00	
			(1.60)				13.30	35mm Gas sampler in 10mm gravel filter (Blue) GM13/S4
Fine to coarse **GRAVEL** with abundant cobbles	58.73		14.10					
			(1.20)					
Fine to coarse **GRAVEL** with cobbles and little yellow/brown sand, with occasional pocket of orange/brown mottled clay containing chalk fragments	57.53		15.30					
			(1.20)				16.00	
Fine to coarse orange/brown **SAND & GRAVEL**	56.33		16.50					
			(1.20)				17.00	Bentonite seal
Fine to coarse **GRAVEL** with a few cobbles and a little light grey/brown fine to coarse sand. Small pockets of clayey silt from 21.10m to 22.40m	55.13		17.70				18.20 18.50	35mm Gas sampler in 10mm gravel filter (Black) GM13/S5
			(2.80)					

NOTES

TOTAL DEPTH 25.00 METRES
LOGGED BY Thomson/Dobson
DATE LOGGED
SCALE 1 : 100

B - Bulk disturbed (bag) sample
D - Small distrubed (jar) sample
U100 - Undisturbed Sample
W - Water Sample

Figure D.13: Site 3 GM 13 Borehole Log (Part 1)

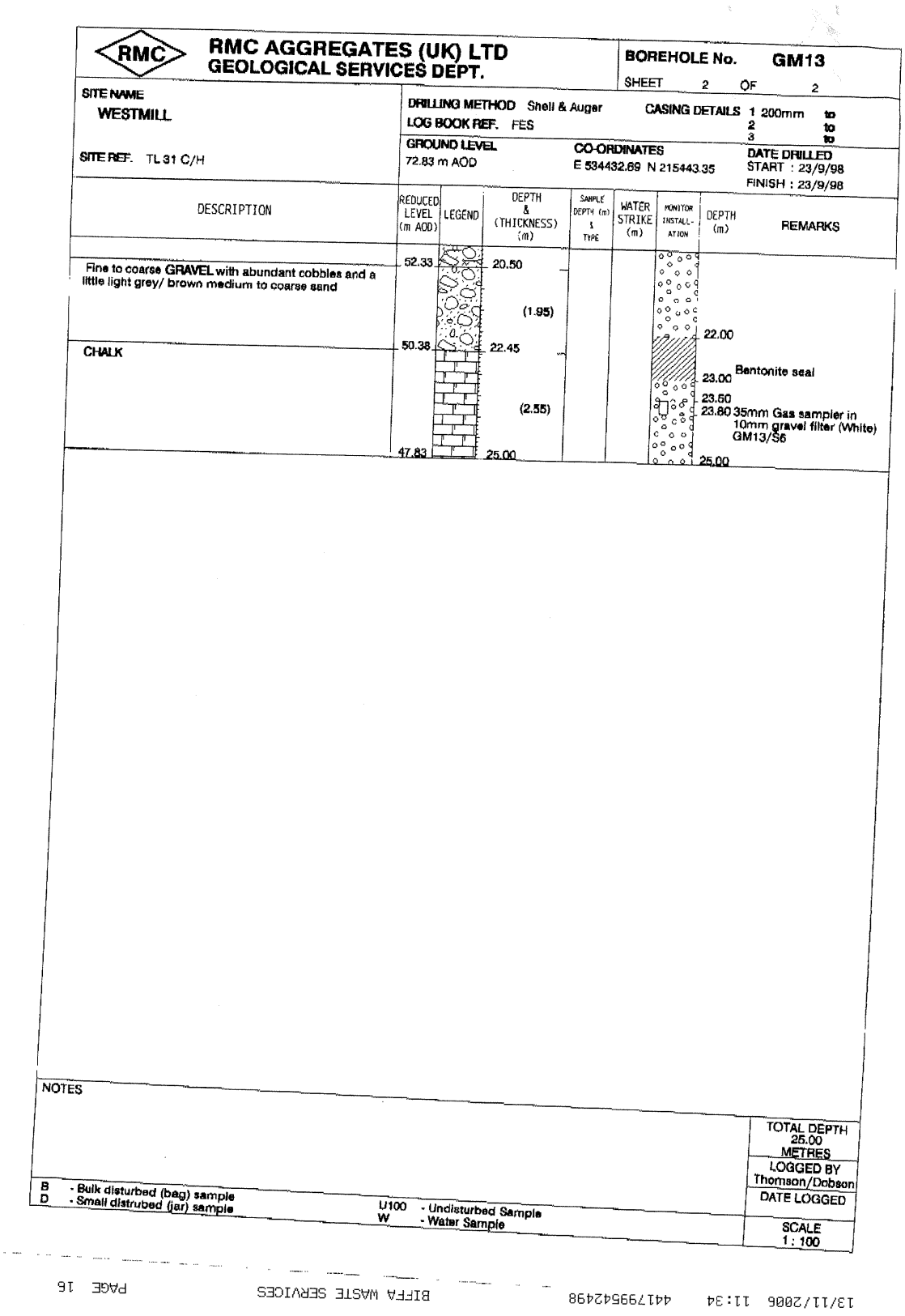

RMC AGGREGATES (UK) LTD
GEOLOGICAL SERVICES DEPT.

BOREHOLE No. GM13
SHEET 2 OF 2

SITE NAME: WESTMILL
SITE REF: TL 31 C/H

DRILLING METHOD: Shell & Auger
LOG BOOK REF.: FES
CASING DETAILS: 1 200mm to
2 to
3 to

GROUND LEVEL: 72.83 m AOD
CO-ORDINATES: E 534432.69 N 215443.35
DATE DRILLED: START : 23/9/98
FINISH : 23/9/98

DESCRIPTION	REDUCED LEVEL (m AOD)	LEGEND	DEPTH & (THICKNESS) (m)	SAMPLE DEPTH (m) & TYPE	WATER STRIKE (m)	MONITOR INSTALL-ATION	DEPTH (m)	REMARKS
Fine to coarse GRAVEL with abundant cobbles and a little light grey/ brown medium to coarse sand	52.33		20.50					
			(1.95)				22.00	
CHALK	50.38		22.45				23.00	Bentonite seal
			(2.55)				23.50	
	47.83		25.00				23.80 25.00	35mm Gas sampler in 10mm gravel filter (White) GM13/S6

NOTES

TOTAL DEPTH 25.00 METRES
LOGGED BY Thomson/Dobson
DATE LOGGED
SCALE 1 : 100

B - Bulk disturbed (bag) sample
D - Small distrubed (jar) sample
U100 - Undisturbed Sample
W - Water Sample

PAGE 16 BIFFA WASTE SERVICES 441799542498 13/11/2006 11:34

Figure D.14: Site 3 GM 13 Borehole Log (Part 2)

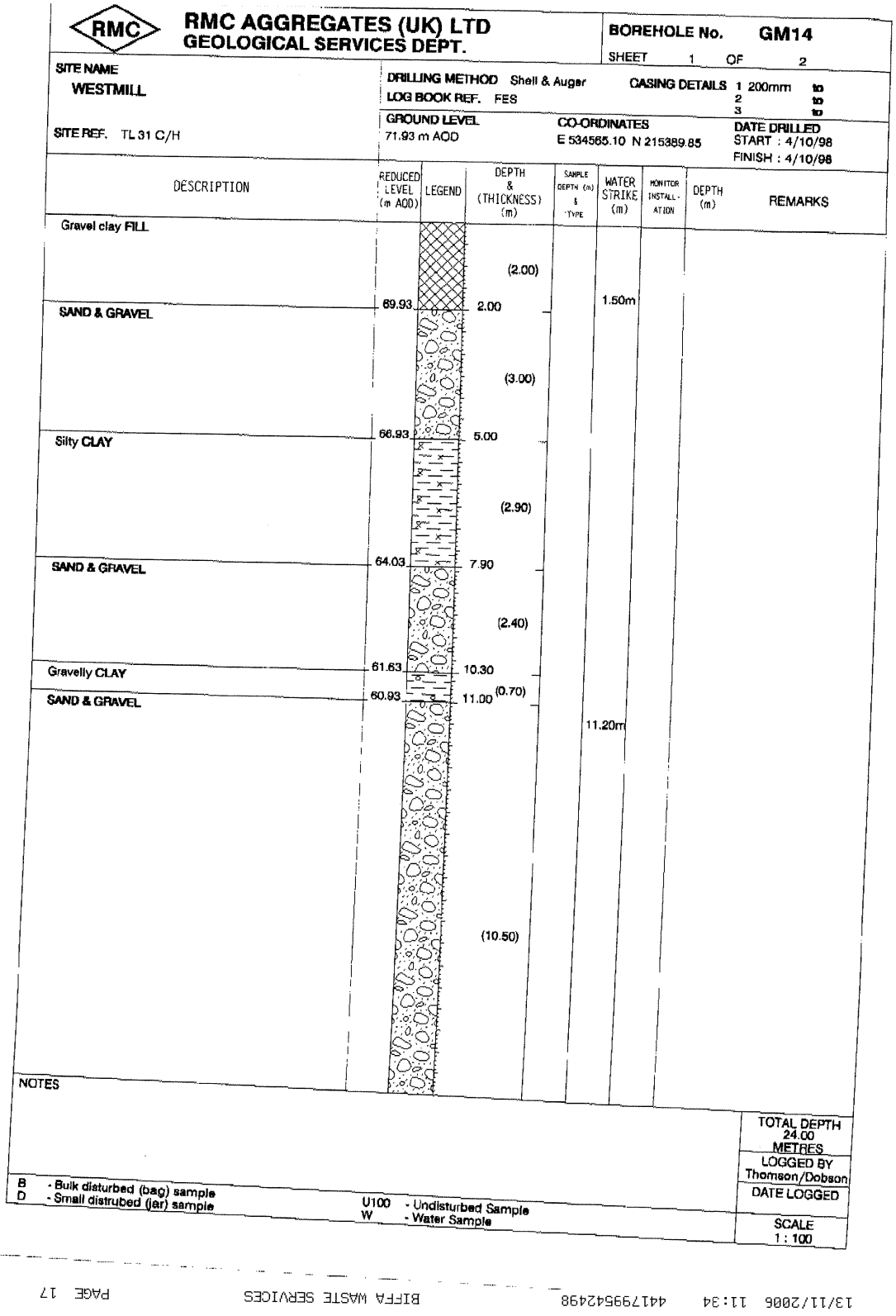

Figure D.15: Site 3 GM 14 Borehole Log (Part 1)

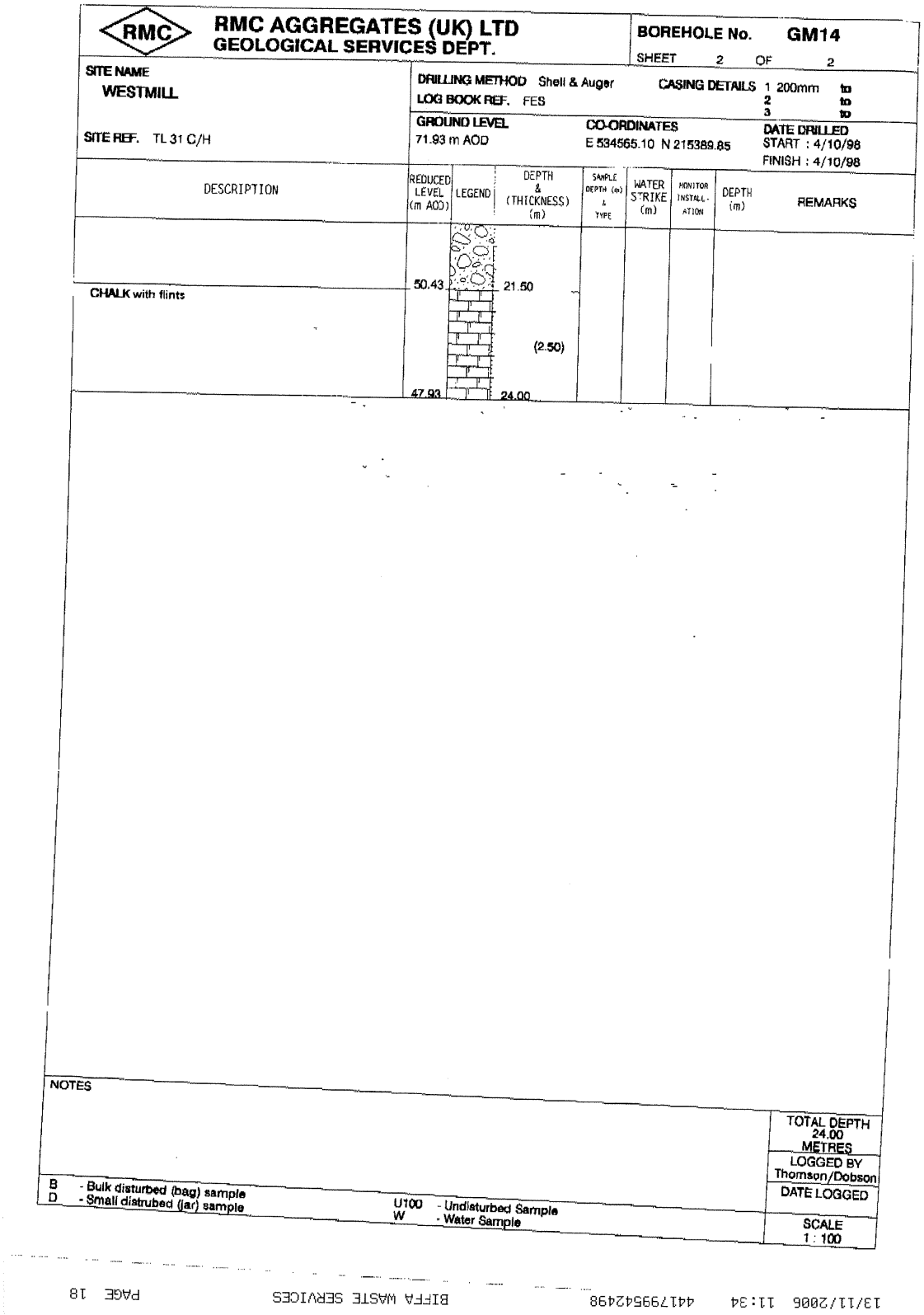

RMC AGGREGATES (UK) LTD
GEOLOGICAL SERVICES DEPT.

BOREHOLE No. GM14
SHEET 2 OF 2

SITE NAME: WESTMILL
SITE REF. TL 31 C/H

DRILLING METHOD Shell & Auger
LOG BOOK REF. FES
CASING DETAILS 1 200mm to
2 to
3 to

GROUND LEVEL 71.93 m AOD
CO-ORDINATES E 534565.10 N 215389.85
DATE DRILLED START : 4/10/98
FINISH : 4/10/98

DESCRIPTION	REDUCED LEVEL (m AOD)	LEGEND	DEPTH & (THICKNESS) (m)	SAMPLE DEPTH (m) & TYPE	WATER STRIKE (m)	MONITOR INSTALL-ATION	DEPTH (m)	REMARKS
CHALK with flints	50.43		21.50					
			(2.50)					
	47.93		24.00					

NOTES

TOTAL DEPTH 24.00 METRES
LOGGED BY Thomson/Dobson
DATE LOGGED
SCALE 1 : 100

B - Bulk disturbed (bag) sample
D - Small distrubed (jar) sample
U100 - Undisturbed Sample
W - Water Sample

Figure D.16: Site 3 GM 14 Borehole Log (Part 2)

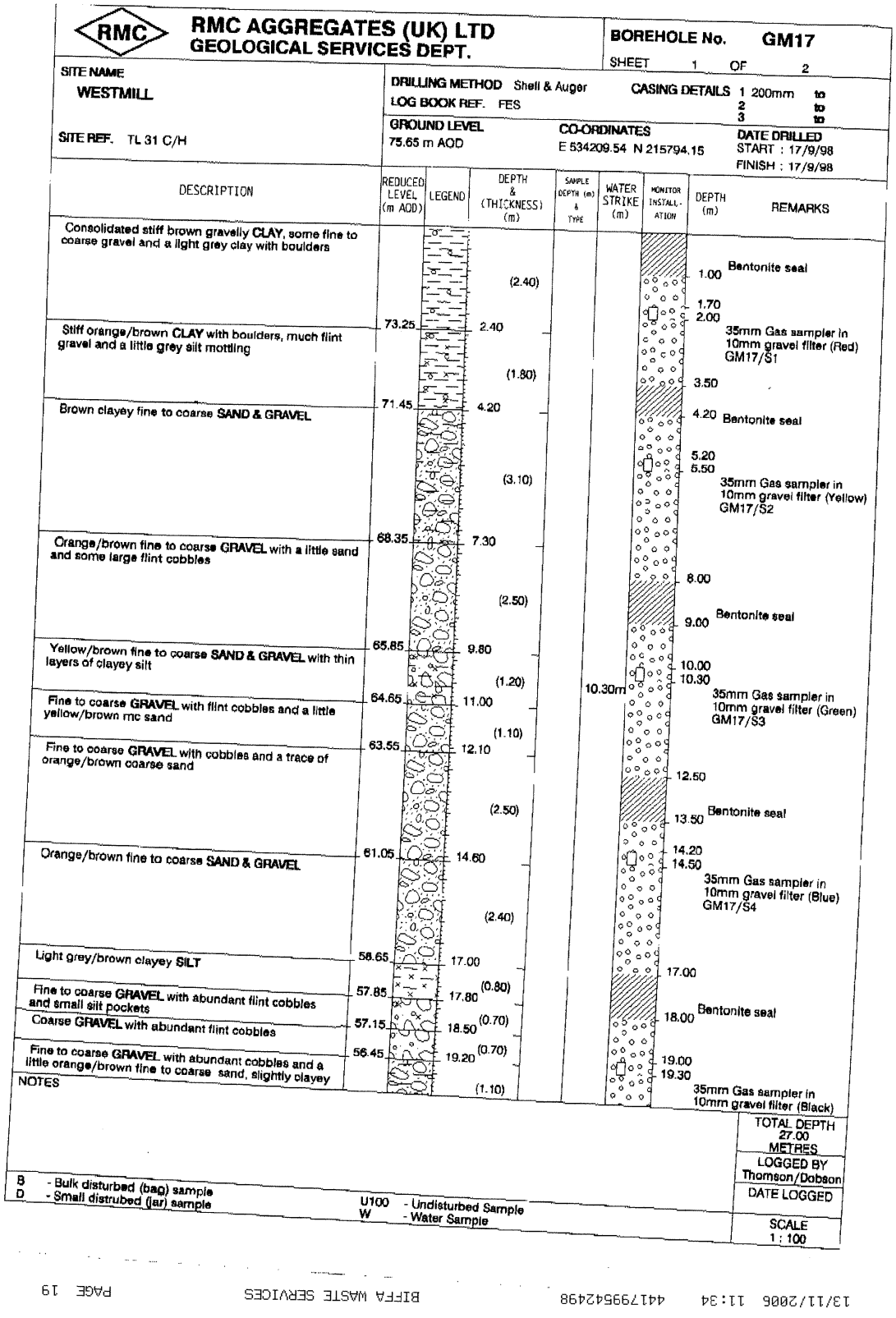

Figure D.17: Site 3 GM 17 Borehole Log (Part 1)

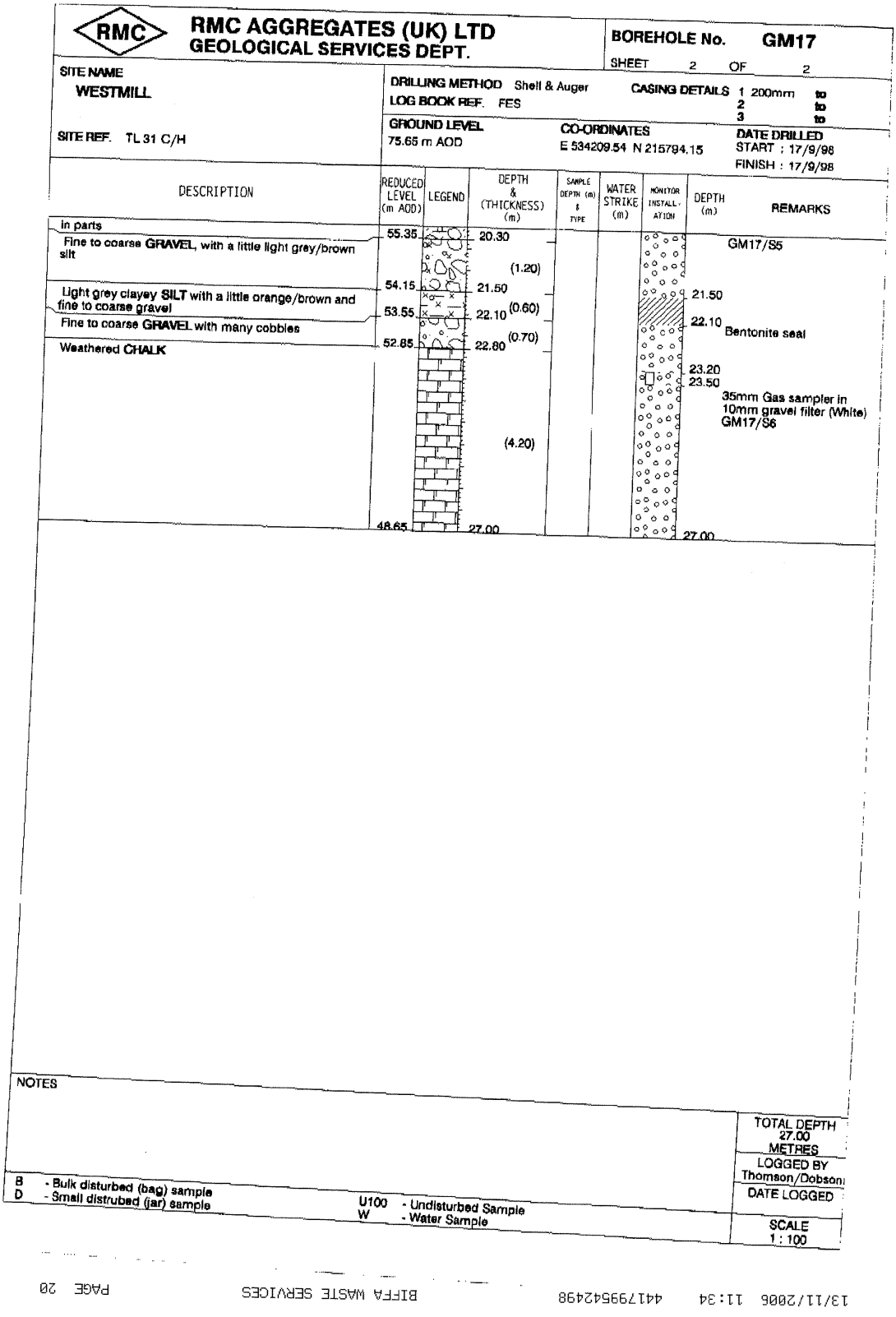

Figure D.18: Site 3 GM 17 Borehole Log (Part 2)

Appendix E

Site 1 Historic Gas Monitoring Data

Ternary diagrams illustrating gas compositions for boreholes not primarily discussed in relation to Site 1 in Chapter 4 are presented in this section.

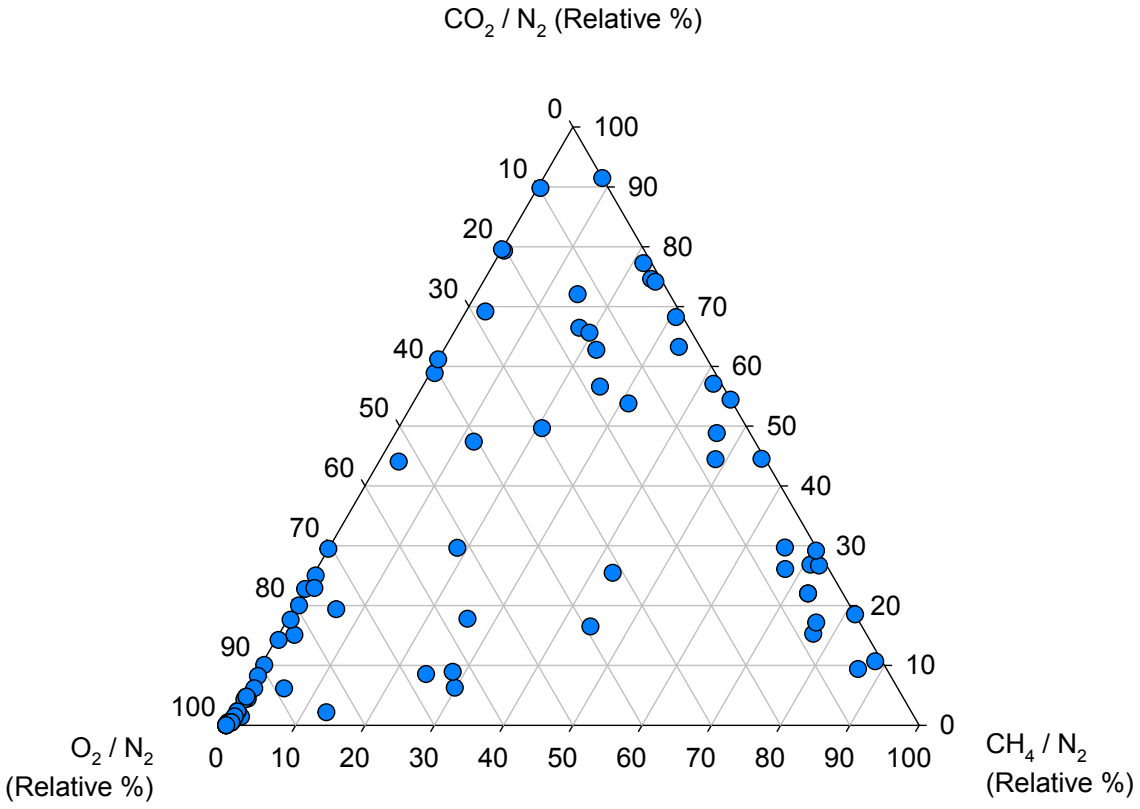

Figure E.1: Gas Compositions for BH 03, Site 1 (25/03/2003 – 08/05/2015)

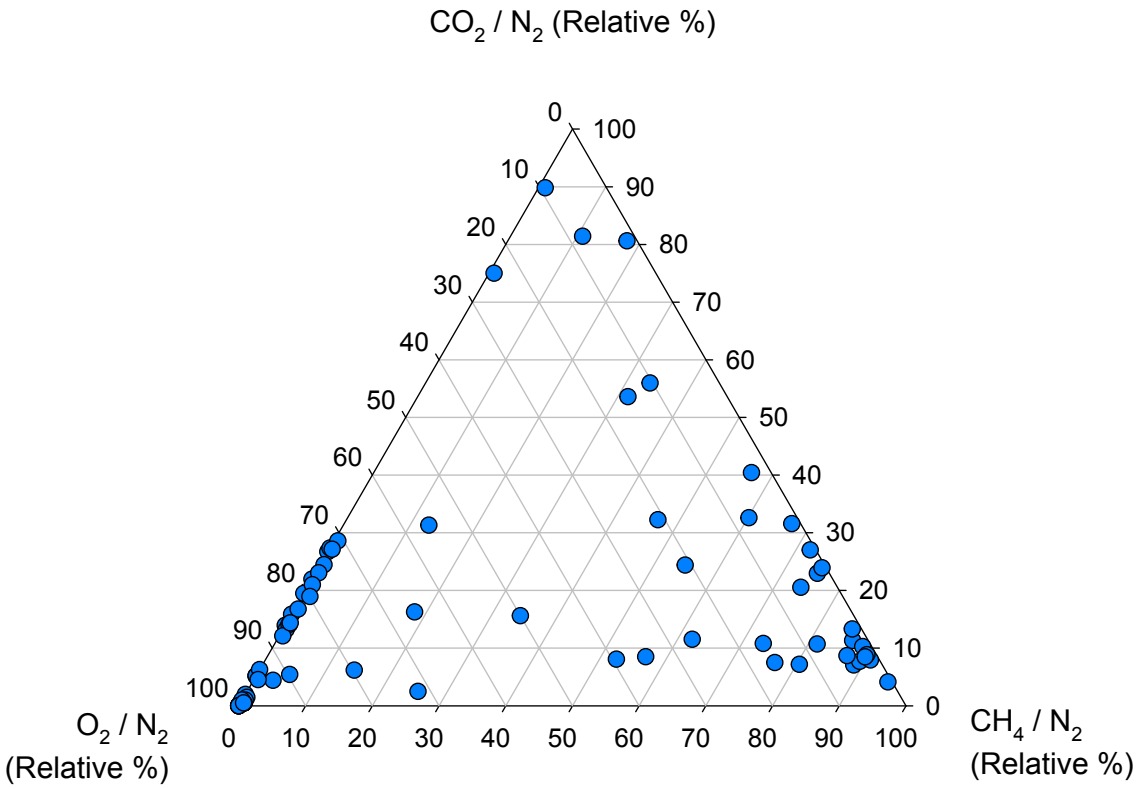

Figure E.2: Gas Compositions for BH 03/6, Site 1 (29/01/2004 – 08/05/2015)

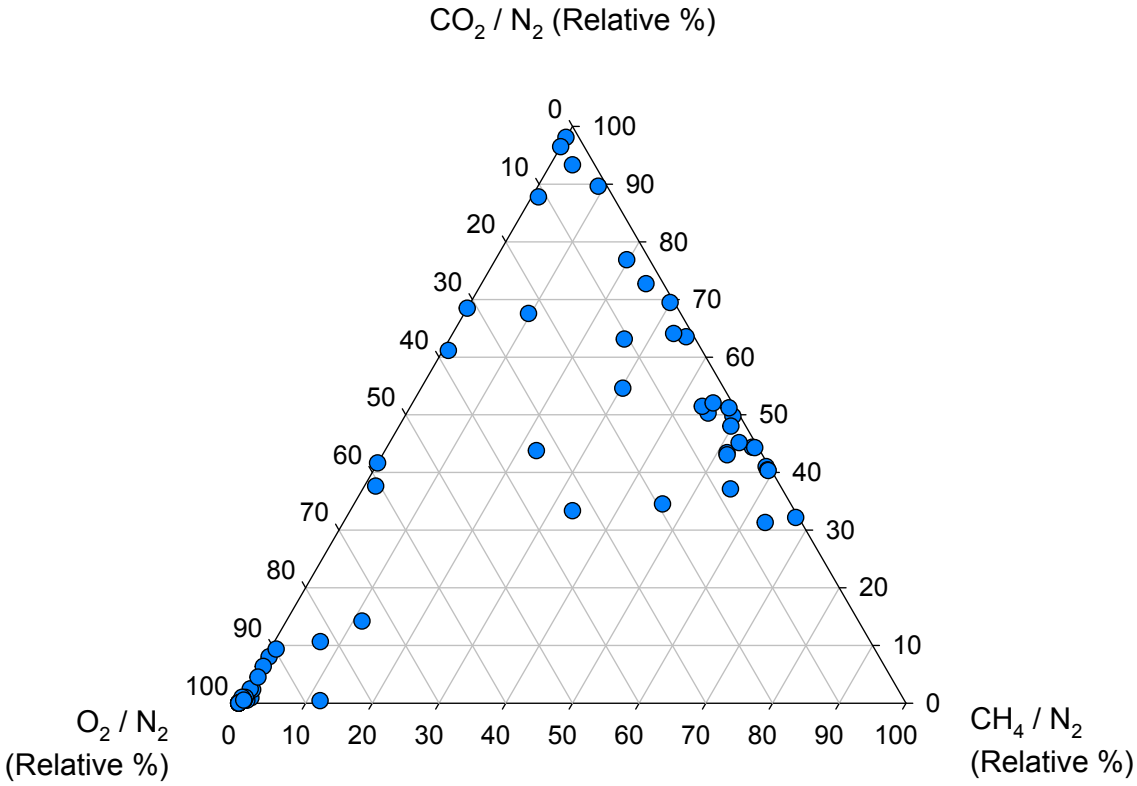

Figure E.3: Gas Compositions for BH 03/7, Site 1 (29/01/2004 – 08/05/2015)

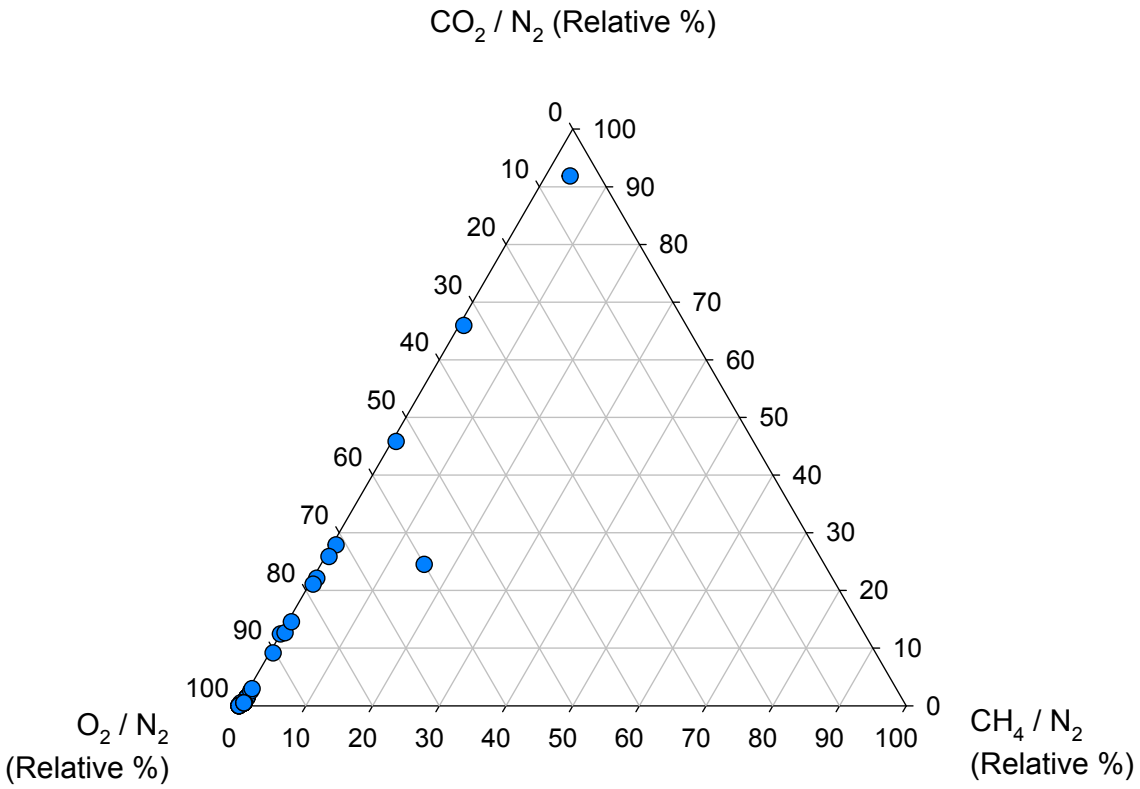

Figure E.4: Gas Compositions for BH 06/13, Site 1 (04/10/2006 – 08/05/2015)

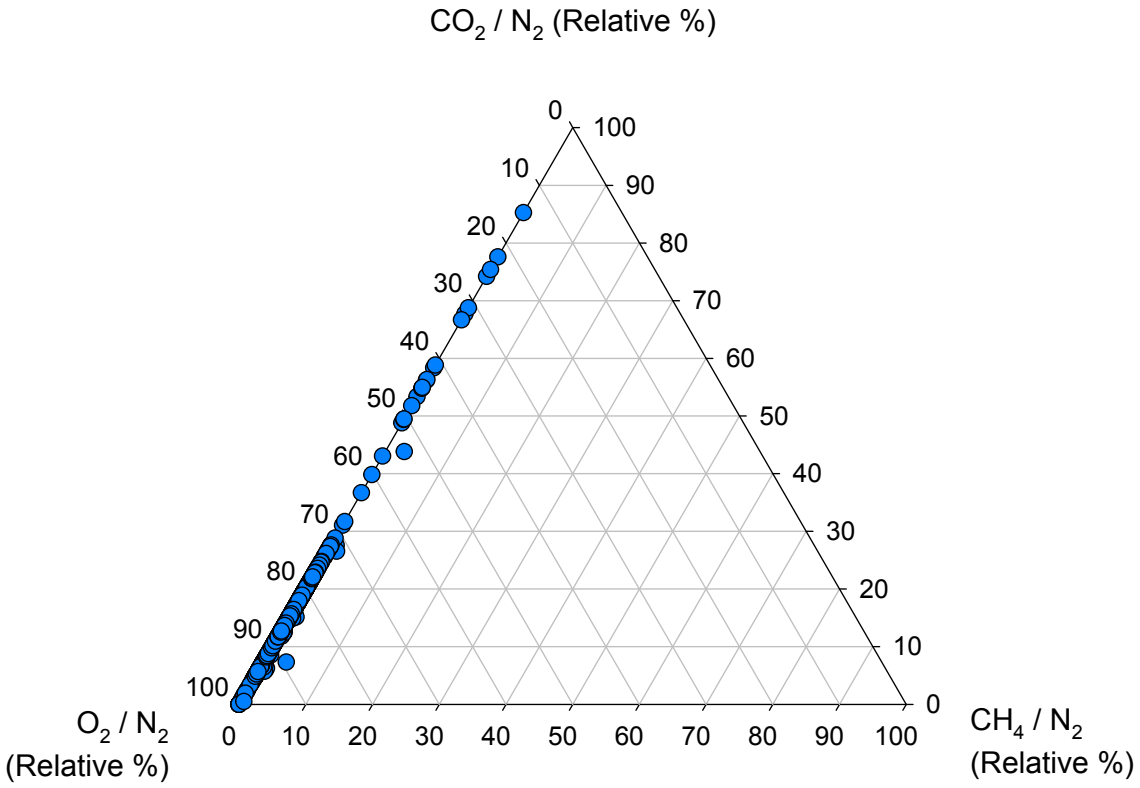

Figure E.5: Gas Compositions for BH 06/15, Site 1 (04/10/2006 – 08/05/2015)

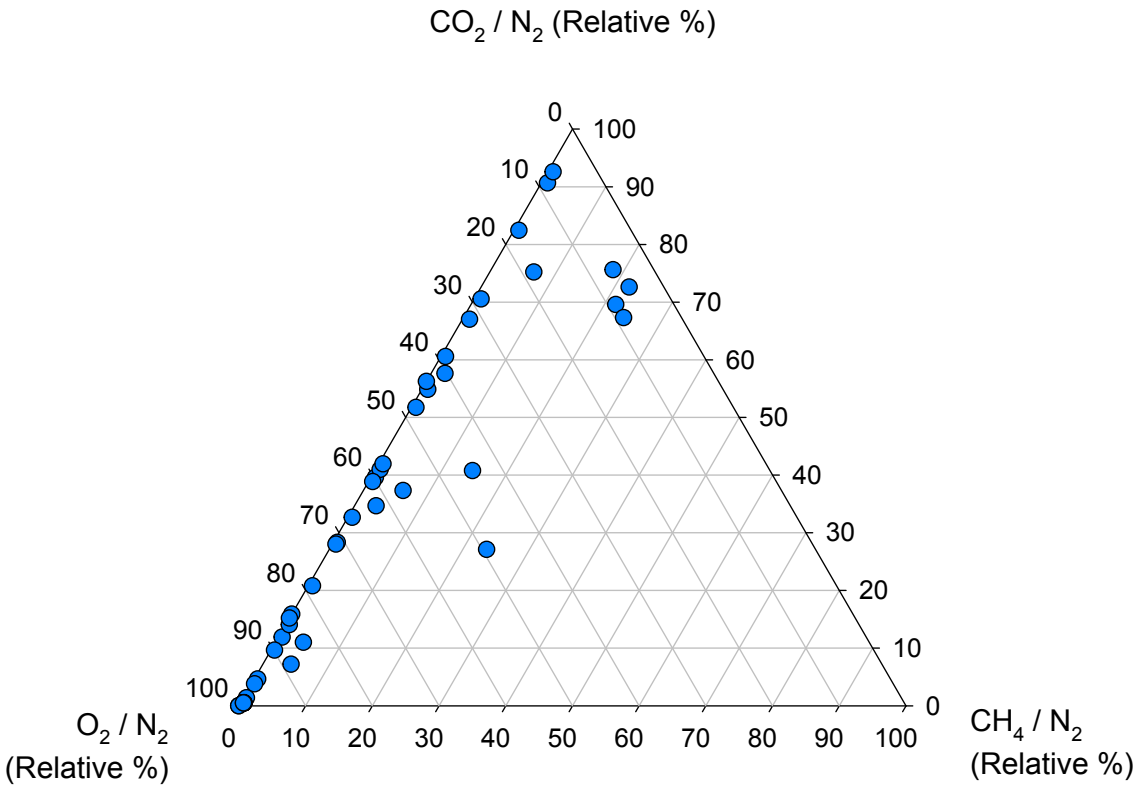

Figure E.6: Gas Compositions for BH 06/16, Site 1 (04/10/2006 – 08/05/2015)

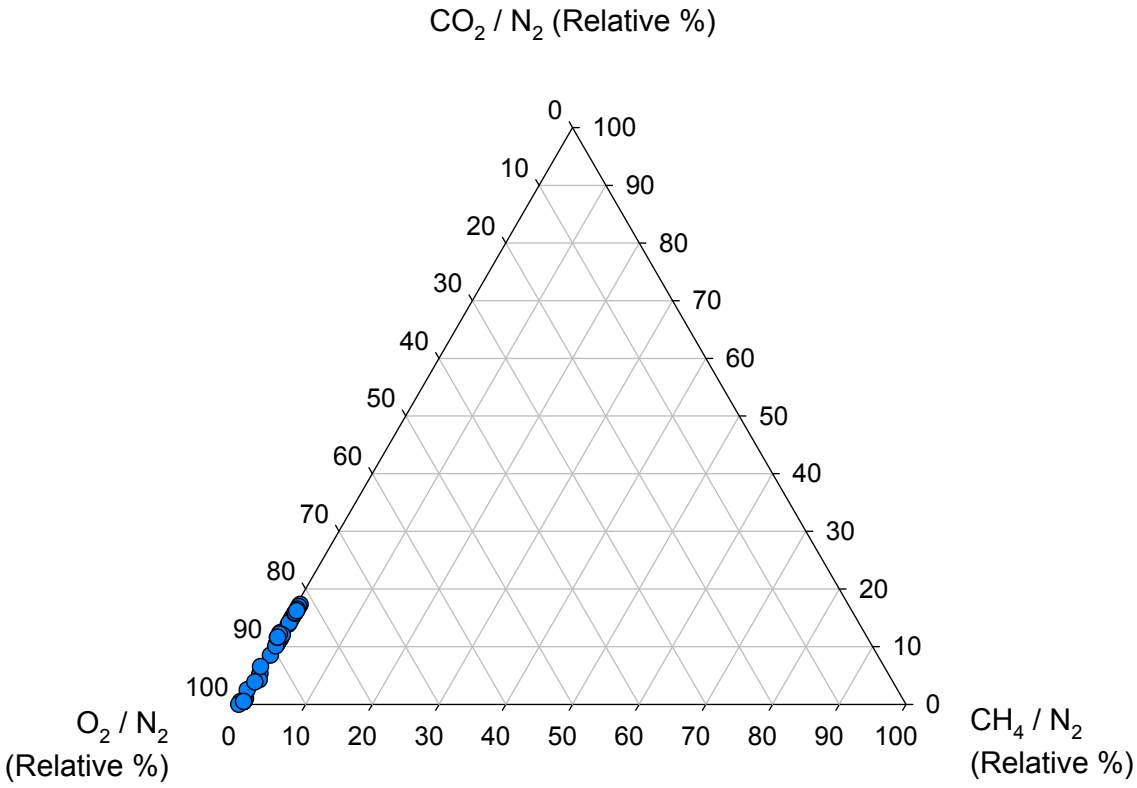

Figure E.7: Gas Compositions for BH 06/18, Site 1 (20/10/2006 – 08/05/2015)

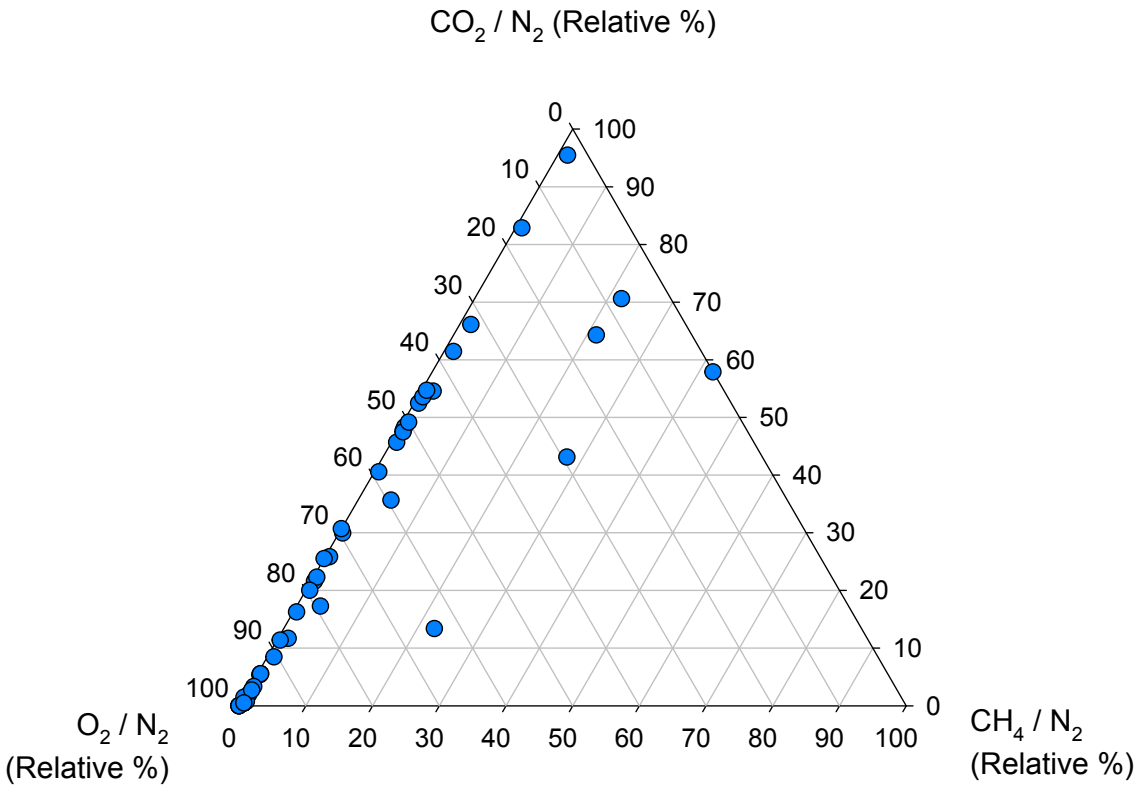

Figure E.8: Gas Compositions for BH 06/19, Site 1 (04/10/2006 – 08/05/2015)

Appendix F

Site 2 Historic Gas Monitoring Data

Ternary diagrams illustrating gas compositions for boreholes not primarily discussed in relation to Site 2 in Chapter 4 are presented in this section.

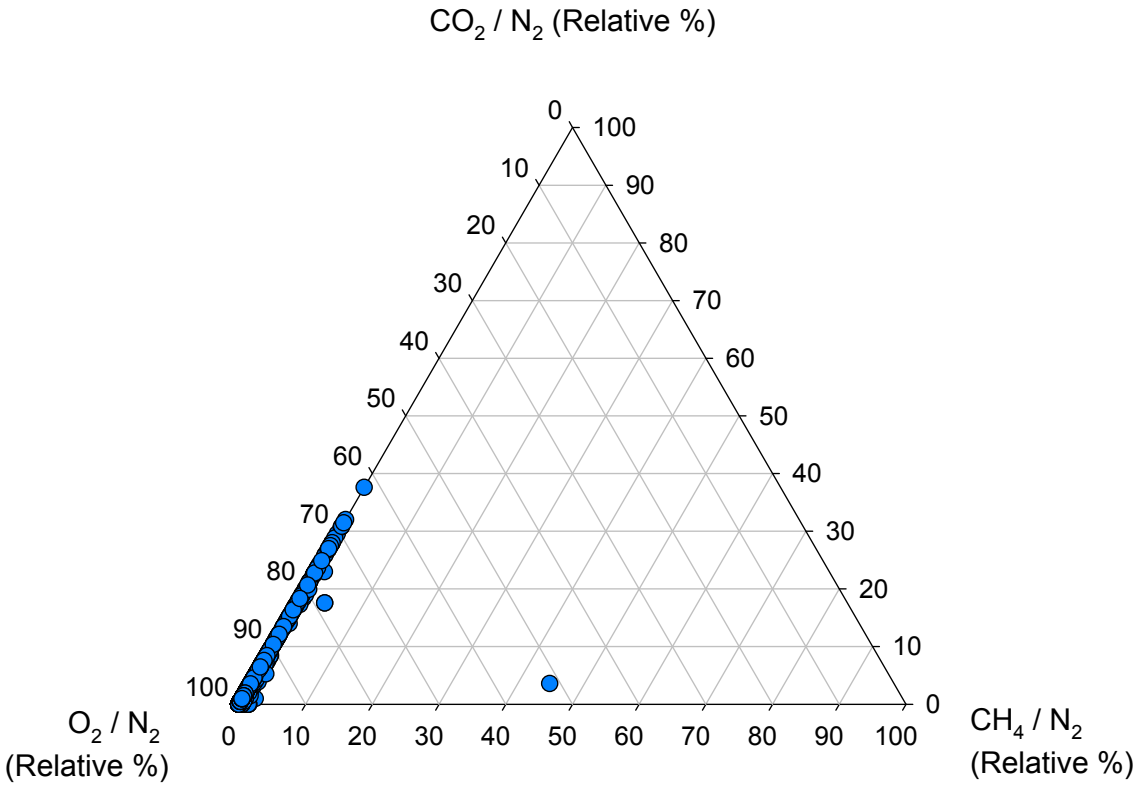

Figure F.1: Gas Compositions for BH 01, Site 2 (27/03/1998 – 29/06/2015)

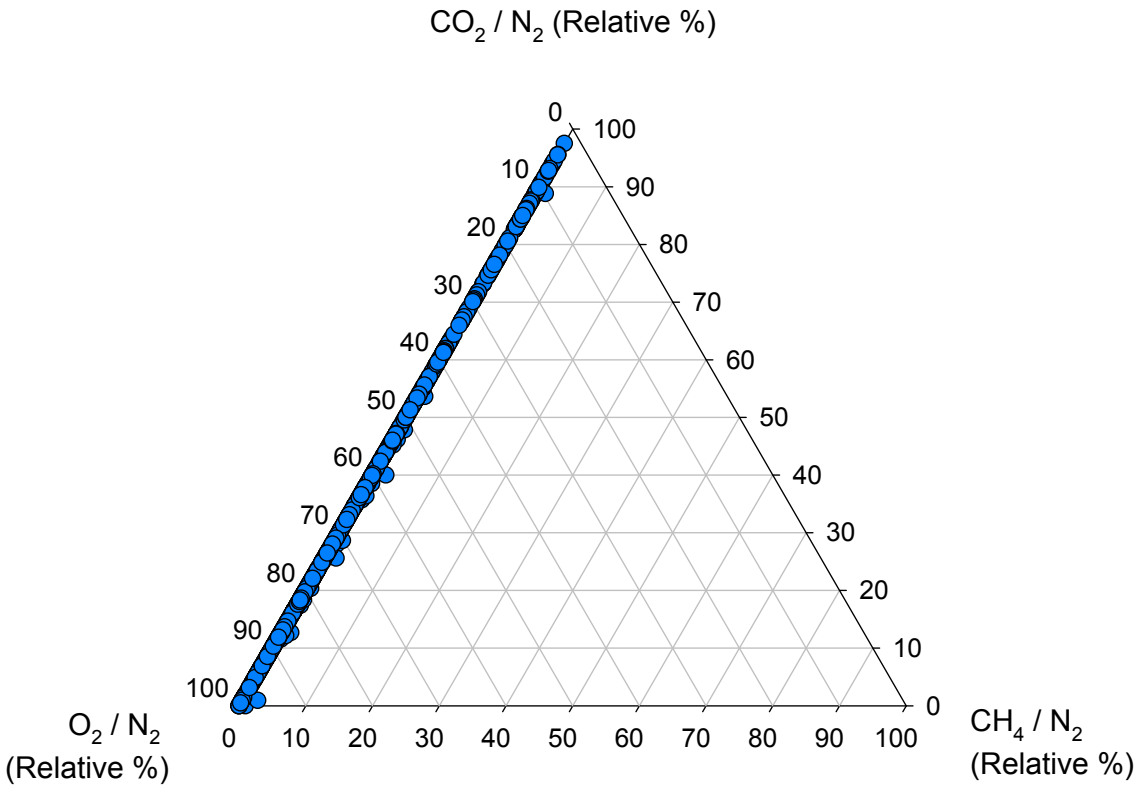

Figure F.2: Gas Compositions for BH 02, Site 2 (19/10/1998 – 29/06/2015)

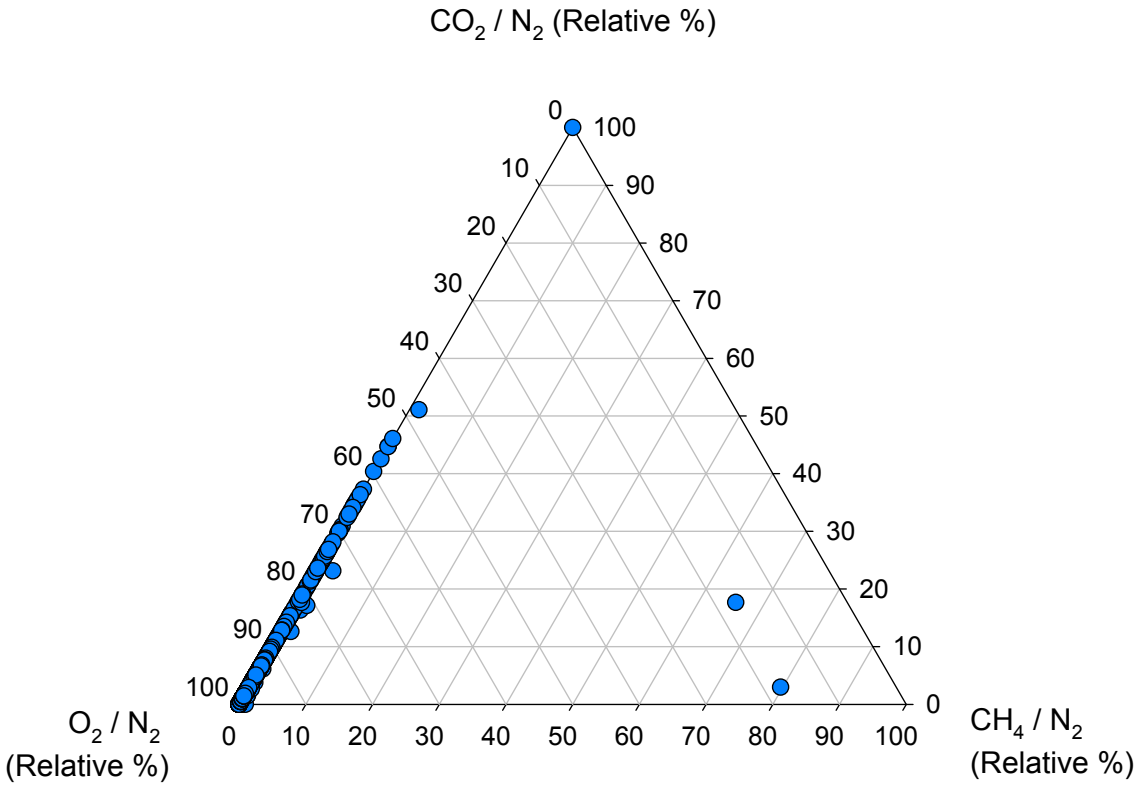

Figure F.3: Gas Compositions for BH 03, Site 2 (13/08/1998 – 29/06/2015)

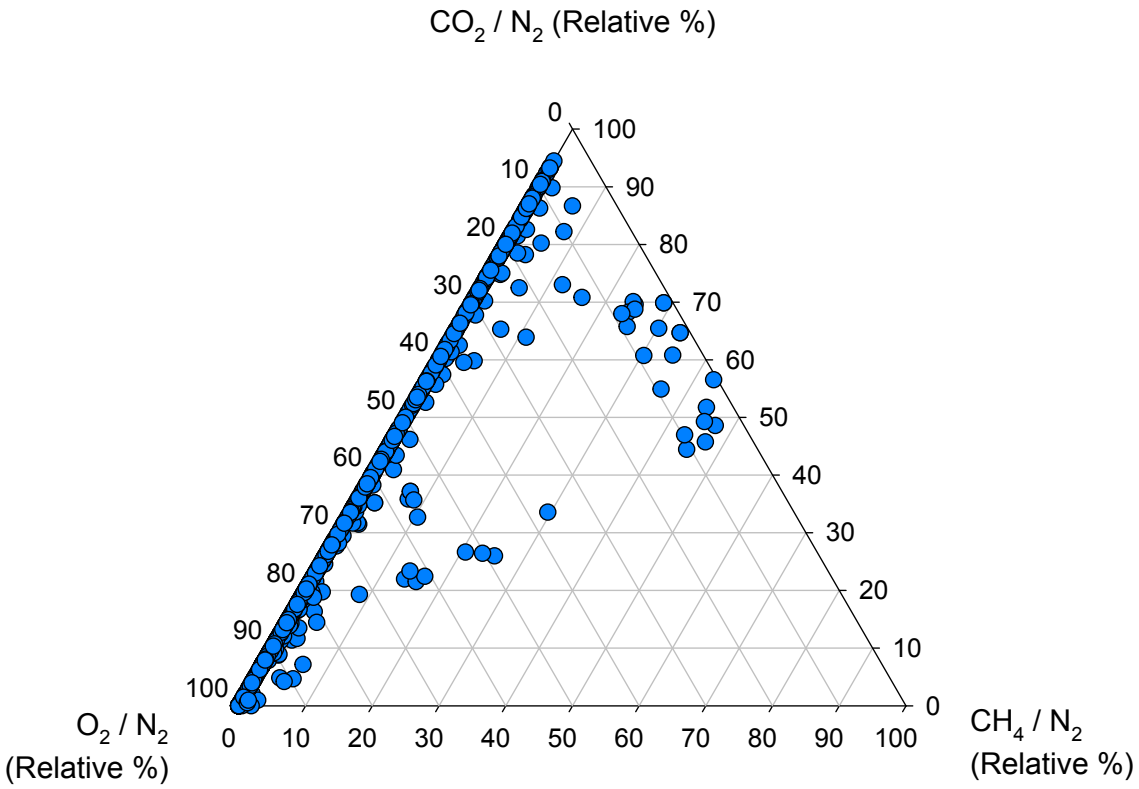

Figure F.4: Gas Compositions for BH 05, Site 2 (13/08/1998 – 29/06/2015)

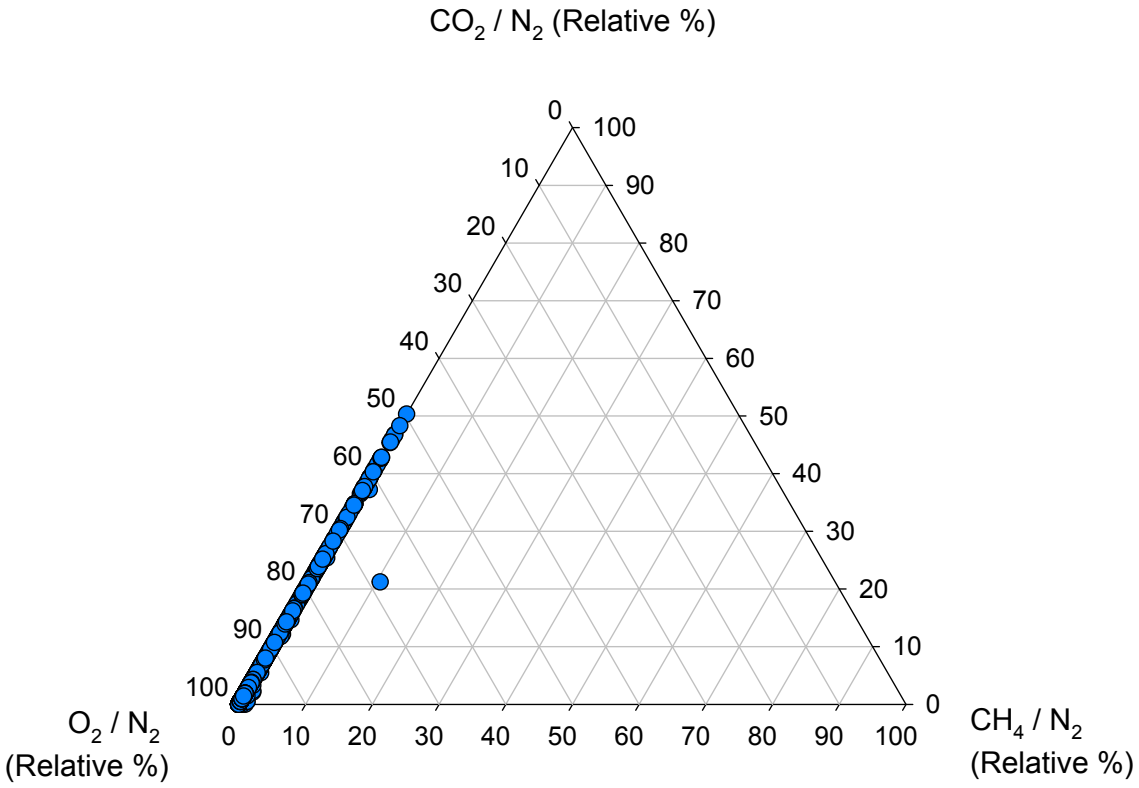

Figure F.5: Gas Compositions for BH 06, Site 2 (13/08/1998 – 29/06/2015)

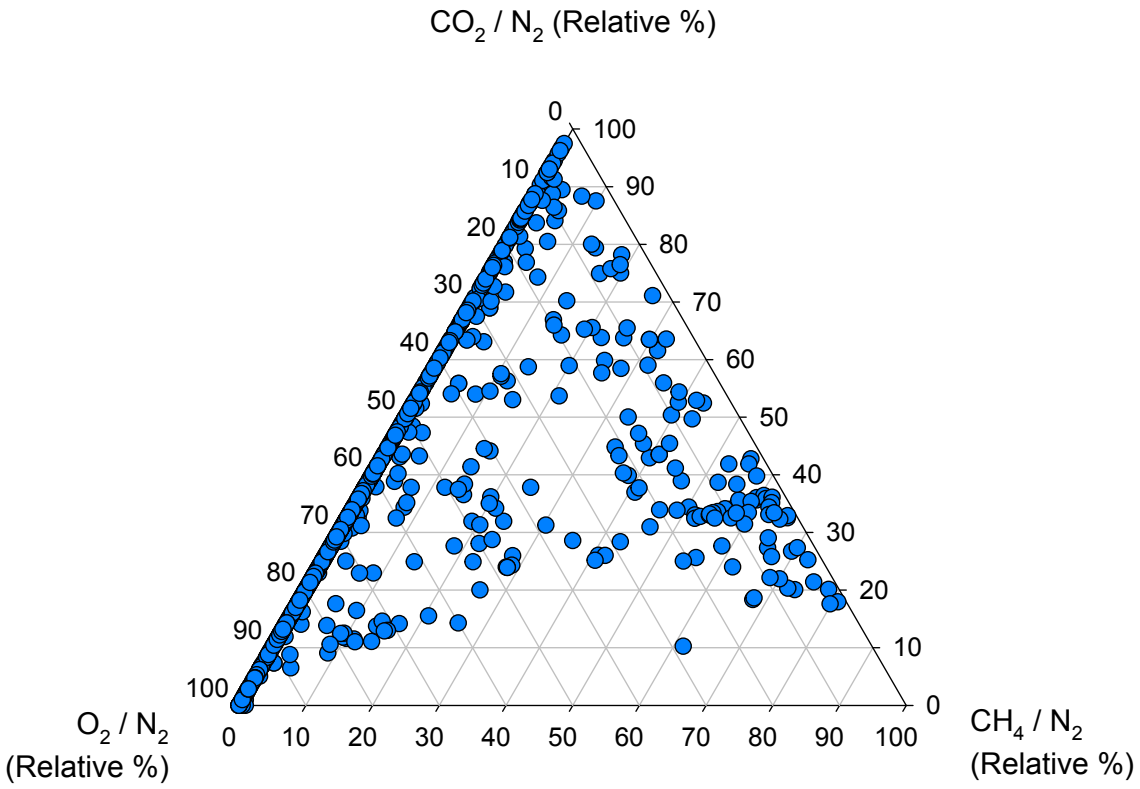

Figure F.6: Gas Compositions for BH 08, Site 2 (13/08/1998 – 29/06/2015)

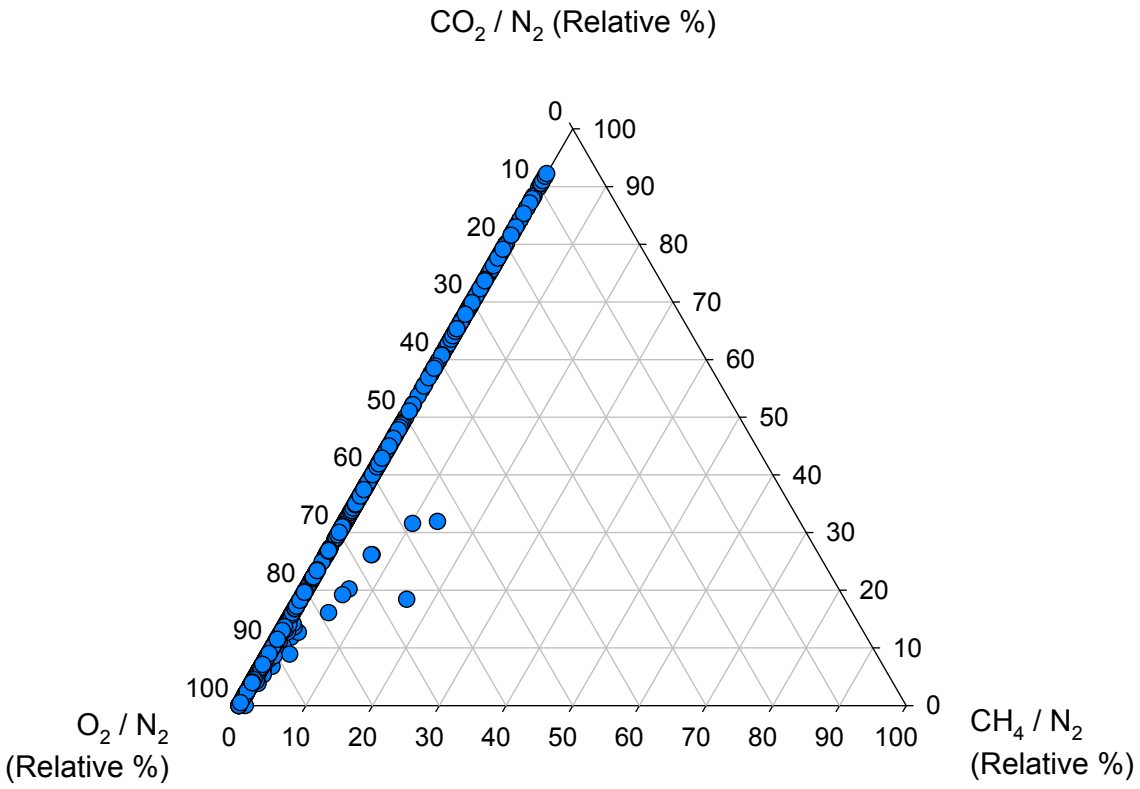

Figure F.7: Gas Compositions for BH 09, Site 2 (13/08/1998 – 29/06/2015)

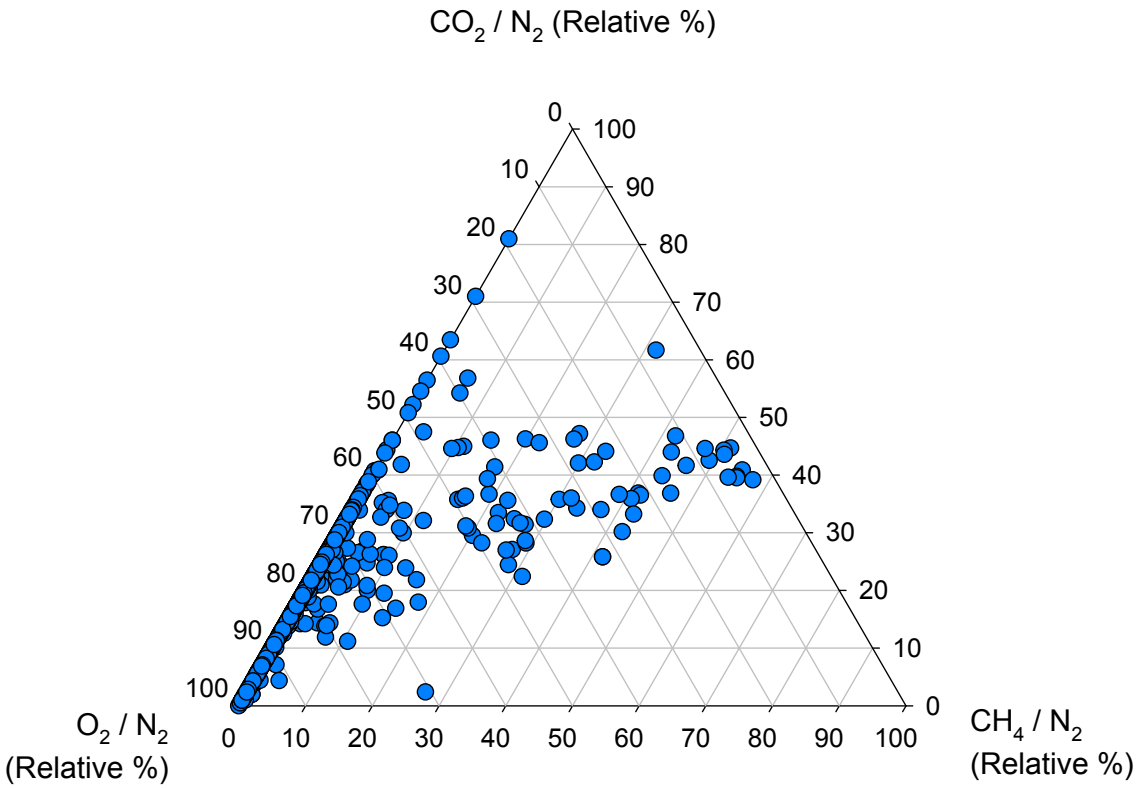

Figure F.8: Gas Compositions for BH 10, Site 2 (13/08/1998 – 29/06/2015)

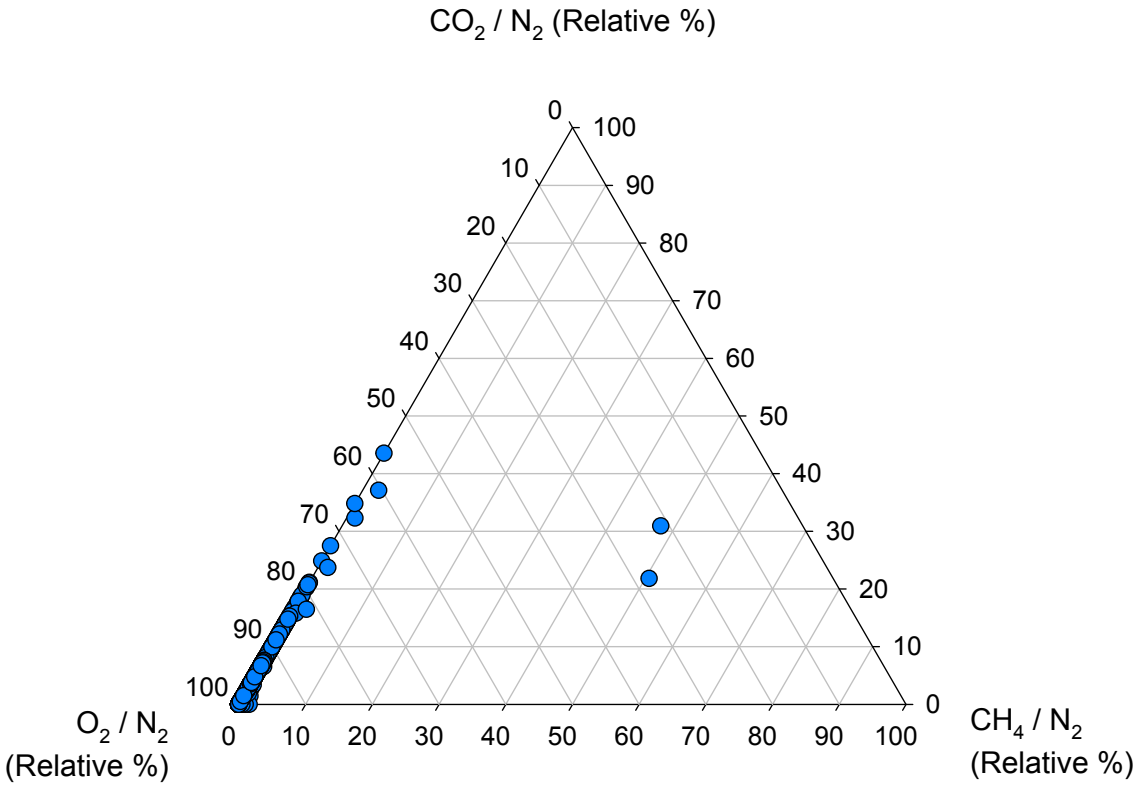

Figure F.9: Gas Compositions for BH 11, Site 2 (08/07/1997 – 29/06/2015)

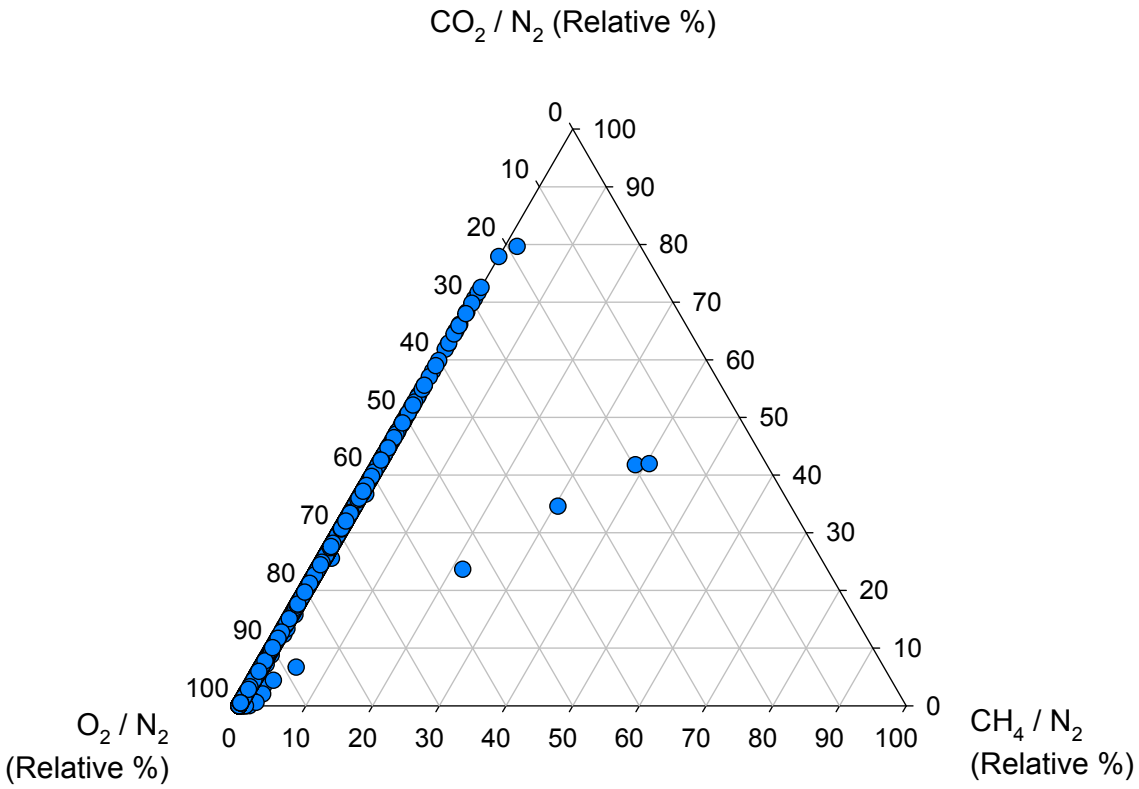

Figure F.10: Gas Compositions for BH 13, Site 2 (13/08/1998 – 29/06/2015)

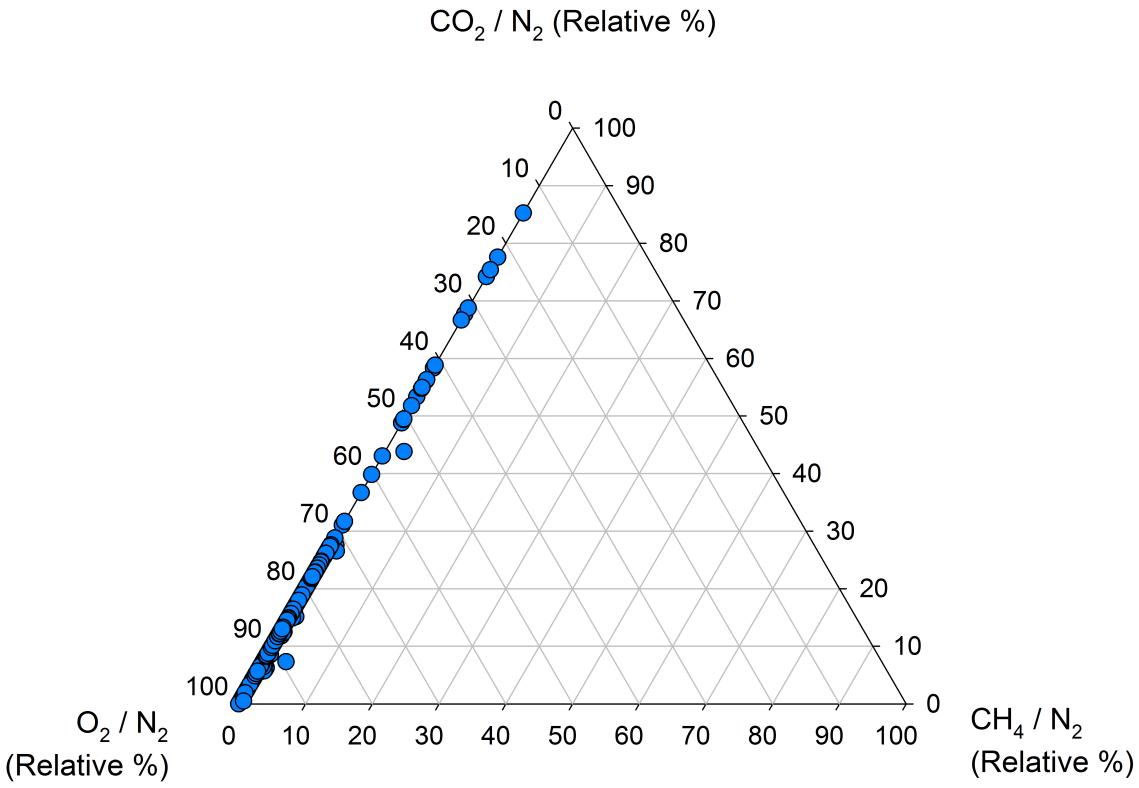

Figure F.11: Gas Compositions for BH 15, Site 2 (02/11/2001 – 29/06/2015)

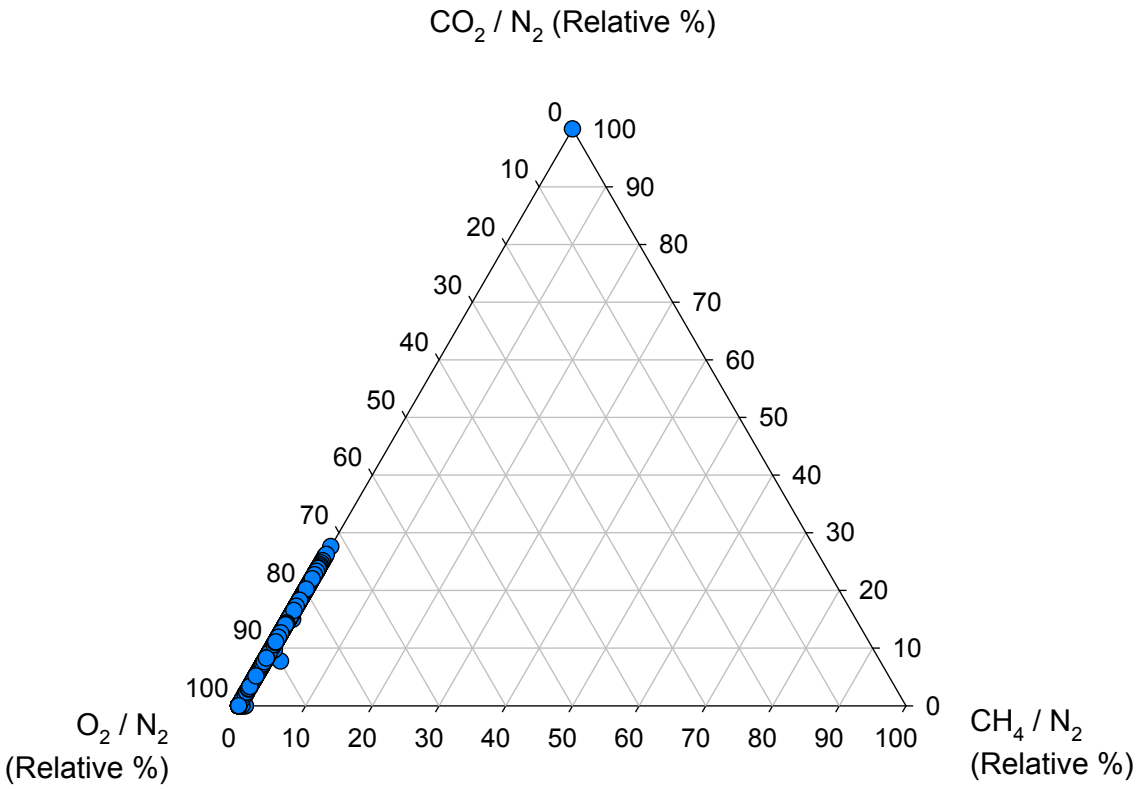

Figure F.12: Gas Compositions for BH 16, Site 2 (28/02/1997 – 29/06/2015)

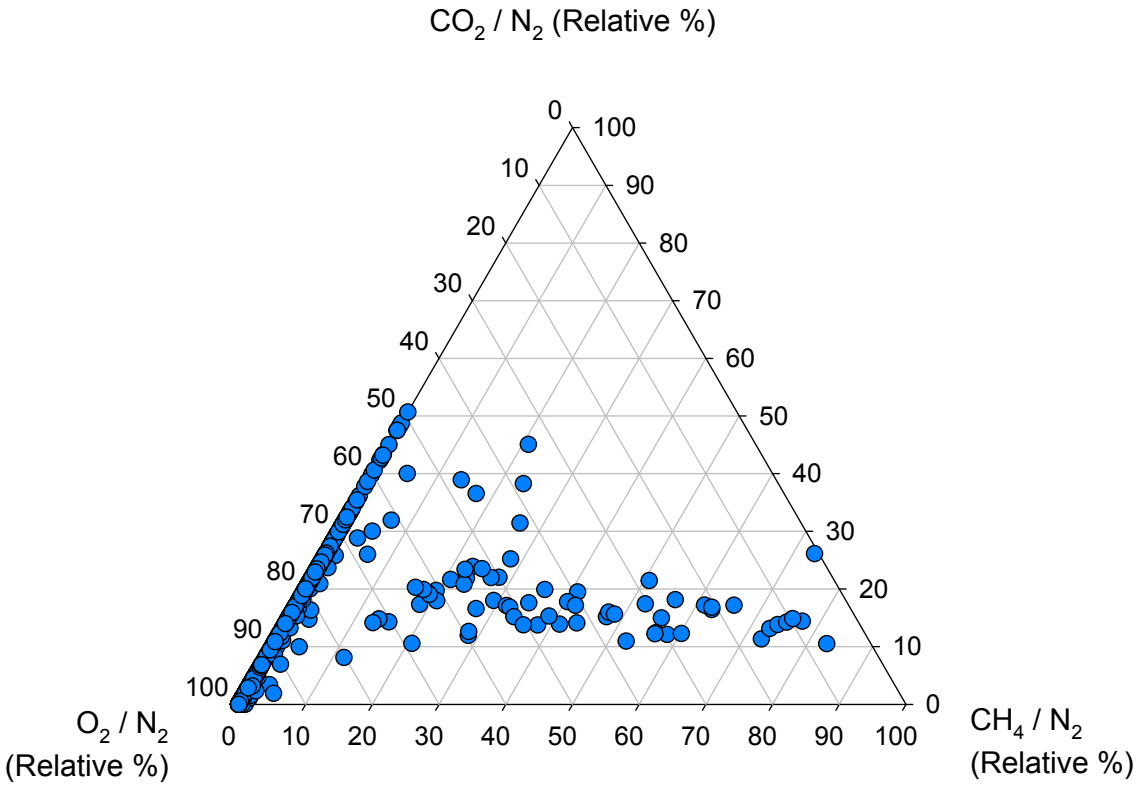

Figure F.13: Gas Compositions for BH 17, Site 2 (26/07/2001 – 29/06/2015)

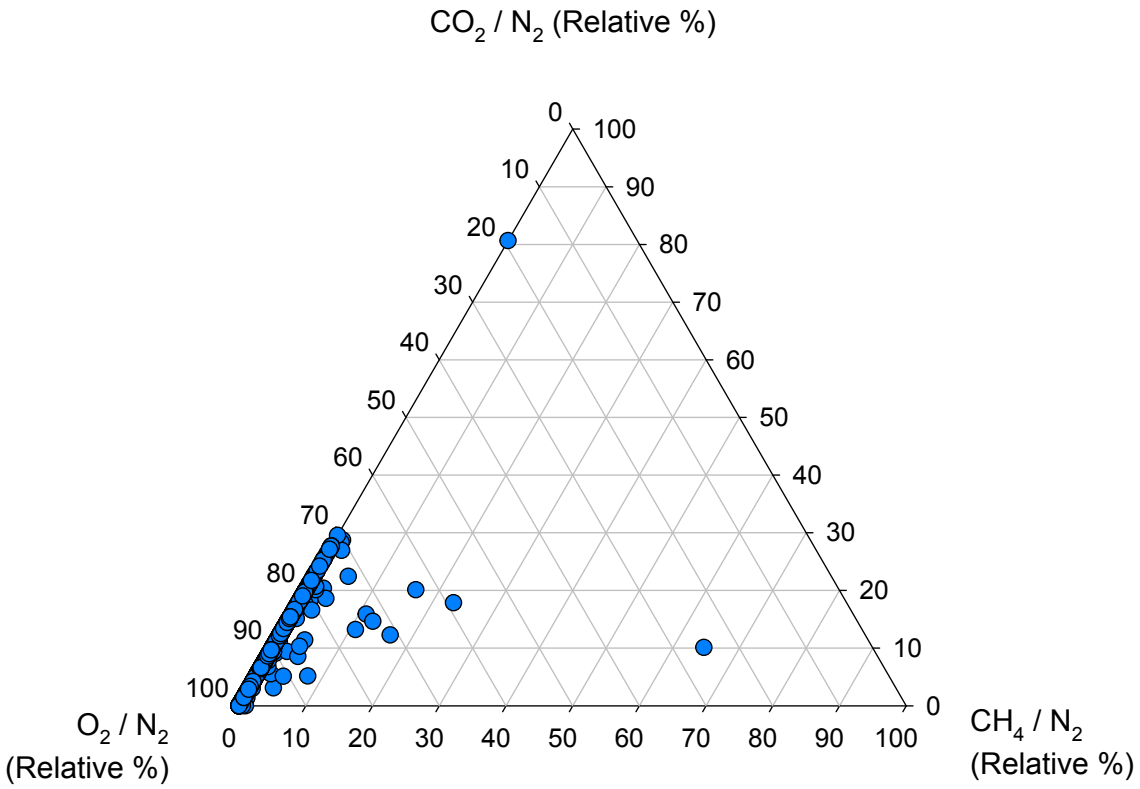

Figure F.14: Gas Compositions for BH 18, Site 2 (15/09/2000 – 29/06/2015)

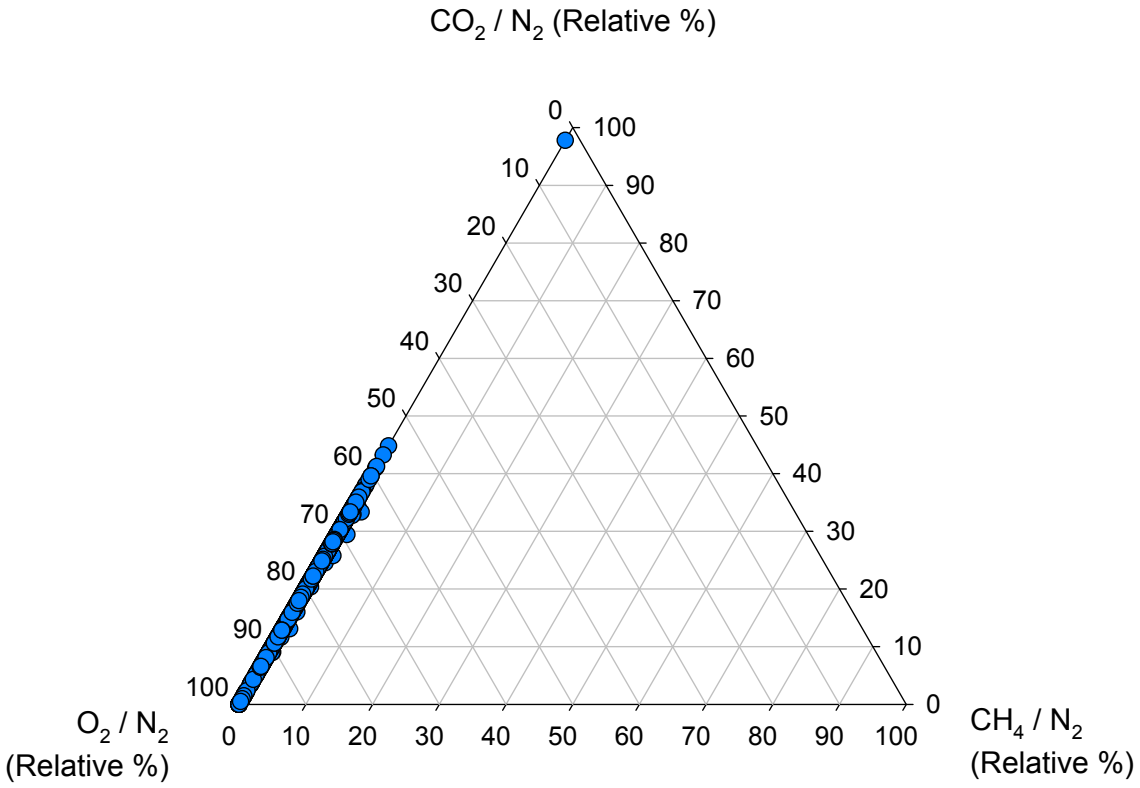

Figure F.15: Gas Compositions for BH 19, Site 2 (15/09/2000 – 29/06/2015)

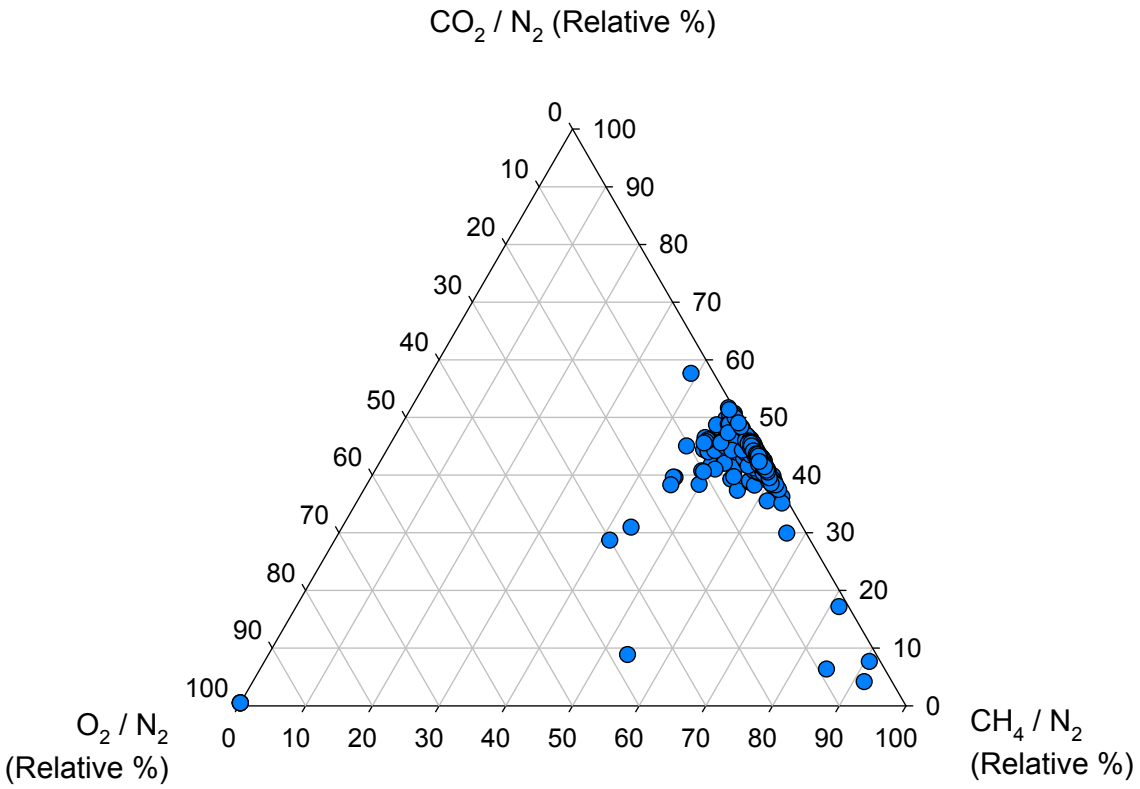

Figure F.16: Gas Compositions for Flare, Site 2 (05/01/2006 – 29/06/2015)

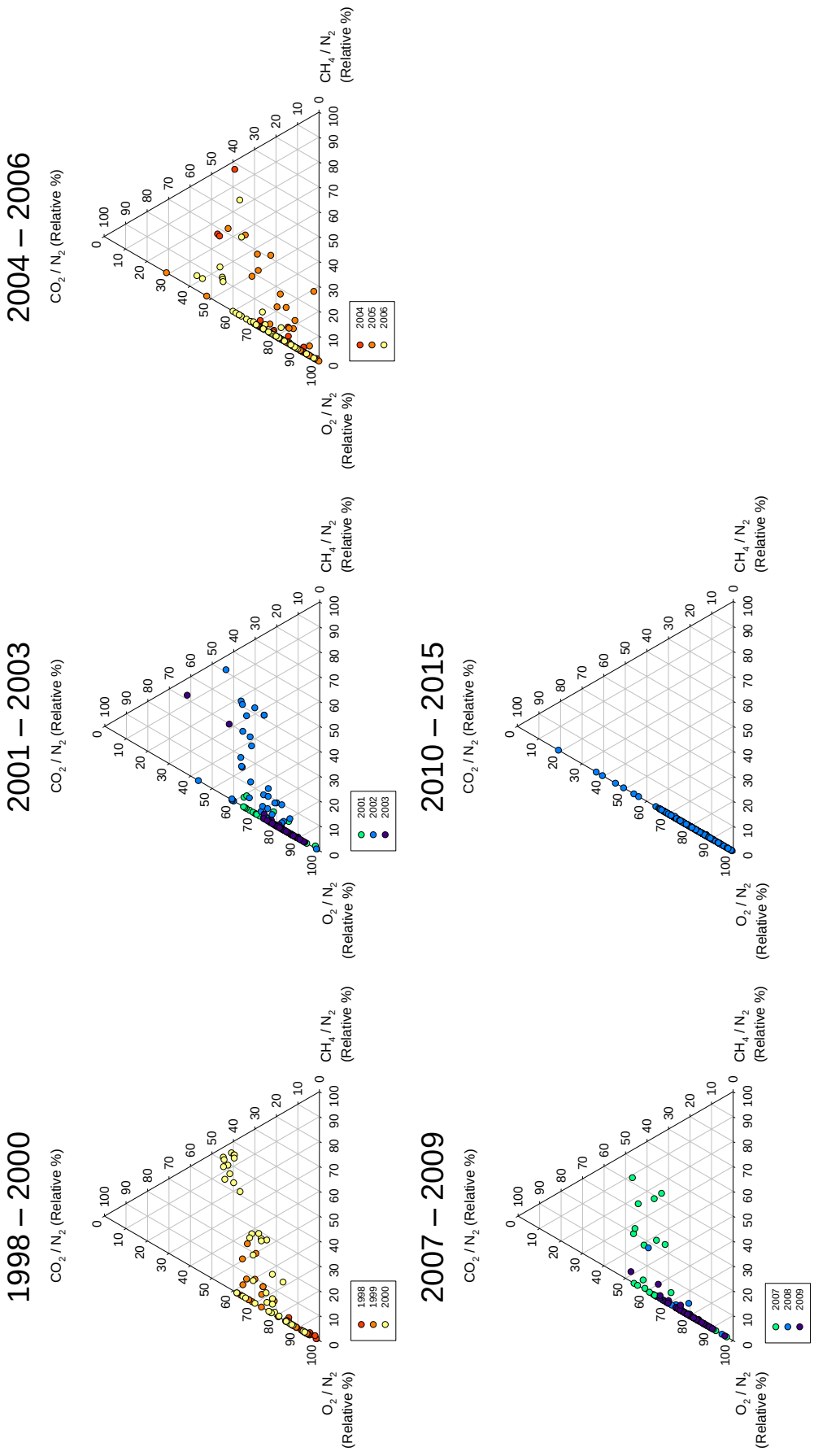

Figure F.17: Gas Composition for BH 10, Site 2 (13/08/1998 – 29/06/2015)

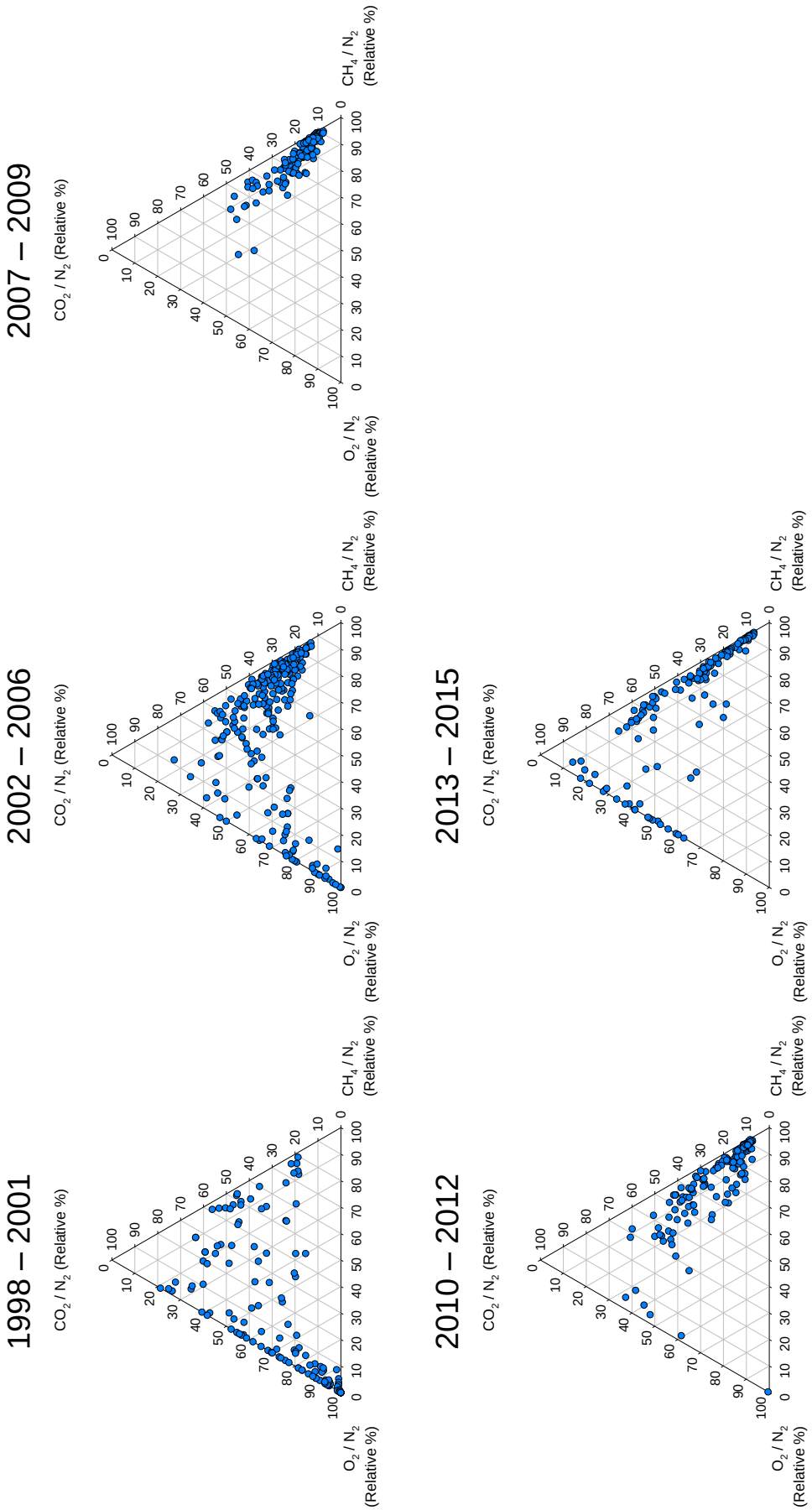

Figure F.18: Gas Composition for BH 12, Site 2 (13/08/1998 – 29/06/2015)

Appendix G

Site 3 Historic Gas Monitoring Data

Ternary diagrams illustrating gas compositions for boreholes not primarily discussed in relation to Site 3 in Chapter 4 are presented in this section.

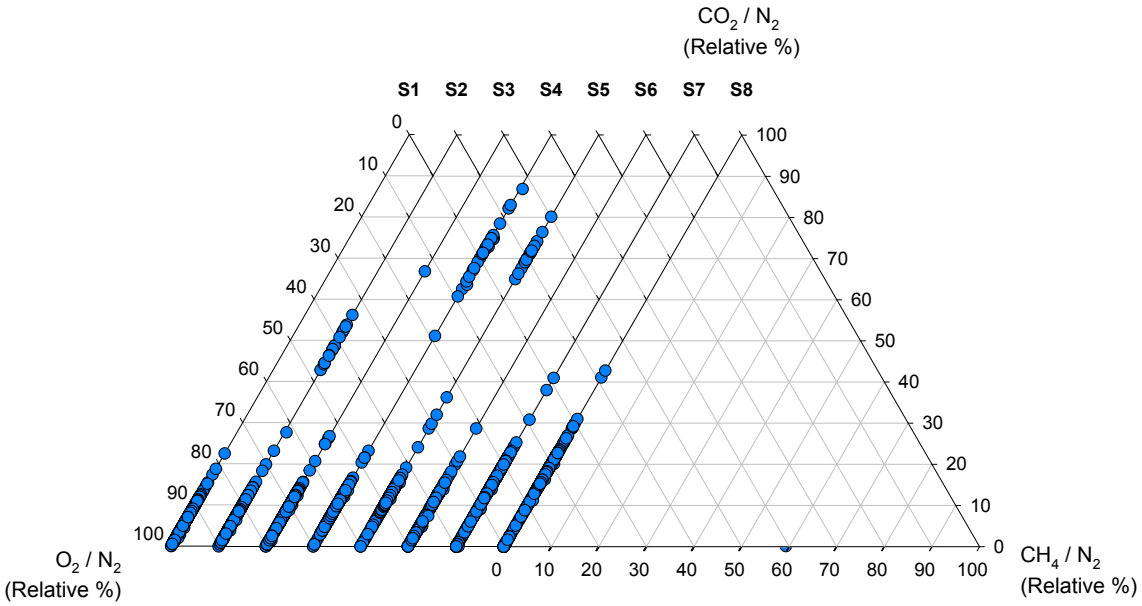

Figure G.1: Gas Composition for GM 1, Site 3 (21/02/1995 – 18/05/2015)

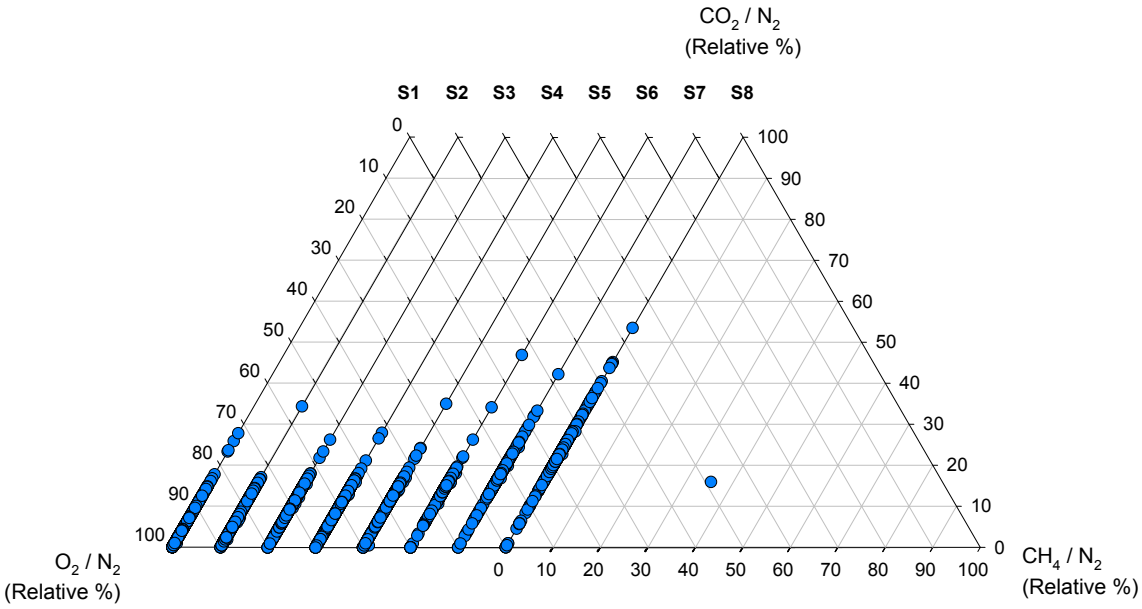

Figure G.2: Gas Composition for GM 2, Site 3 (21/02/1995 – 18/05/2015)

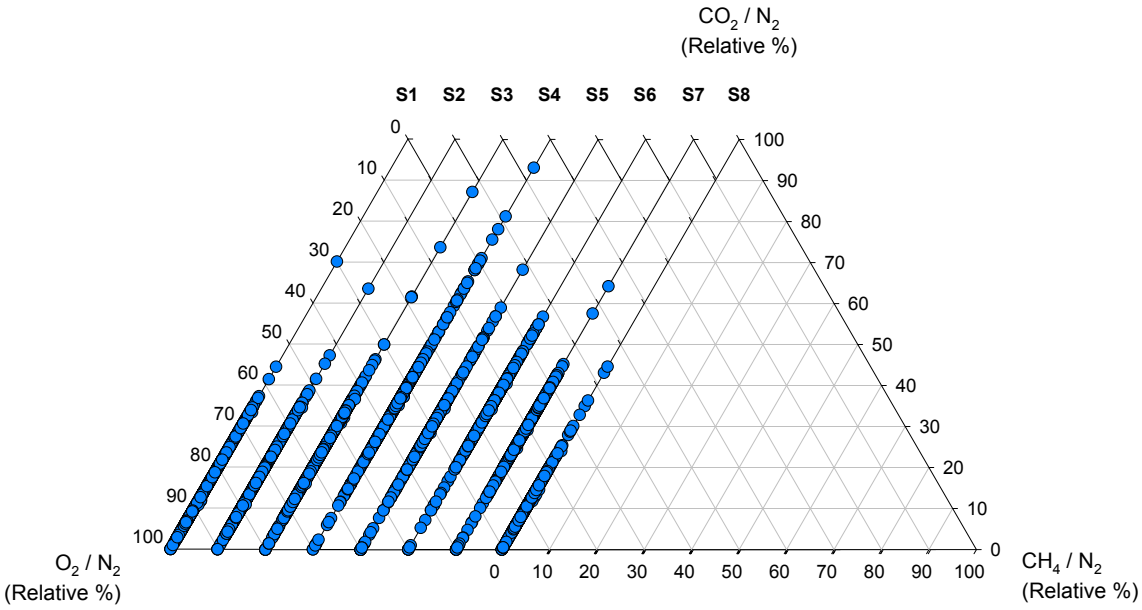

Figure G.3: Gas Composition for GM 3, Site 3 (21/02/1995 – 18/05/2015)

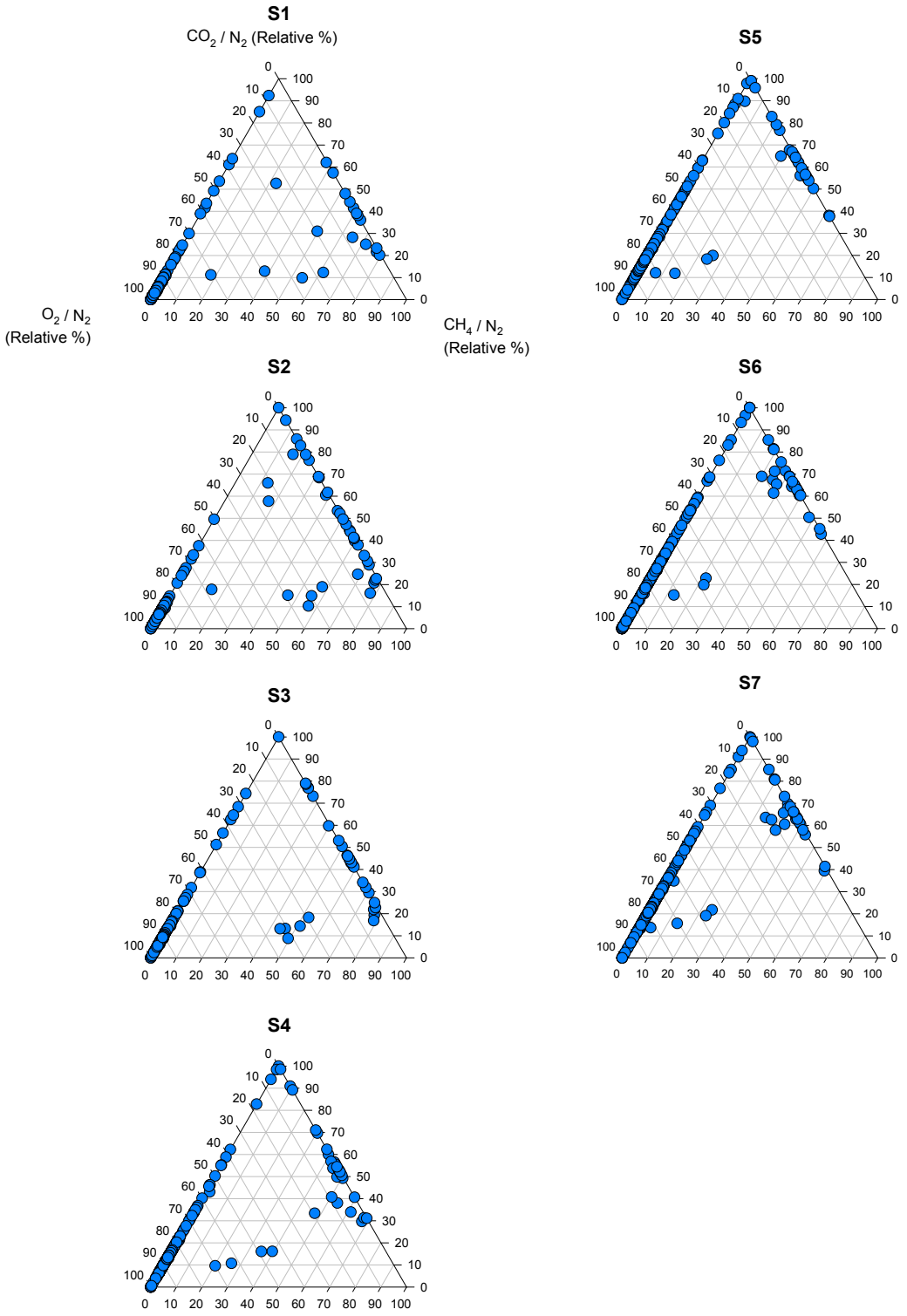

Figure G.4: Gas Composition for GM 4, Site 3 (21/02/1995 – 18/05/2015)

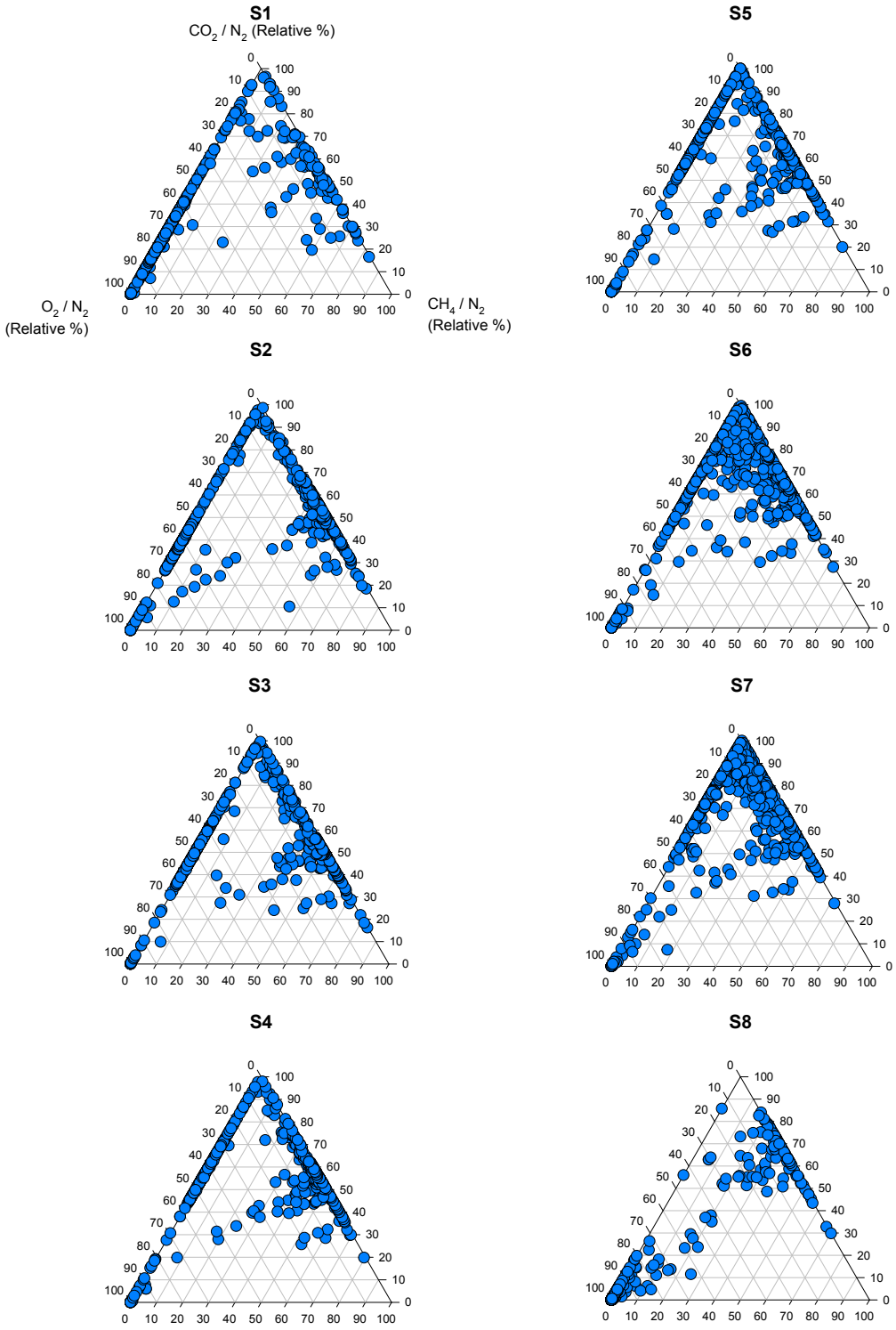

Figure G.5: Gas Composition for GM 6, Site 3 (21/02/1995 – 18/05/2015)

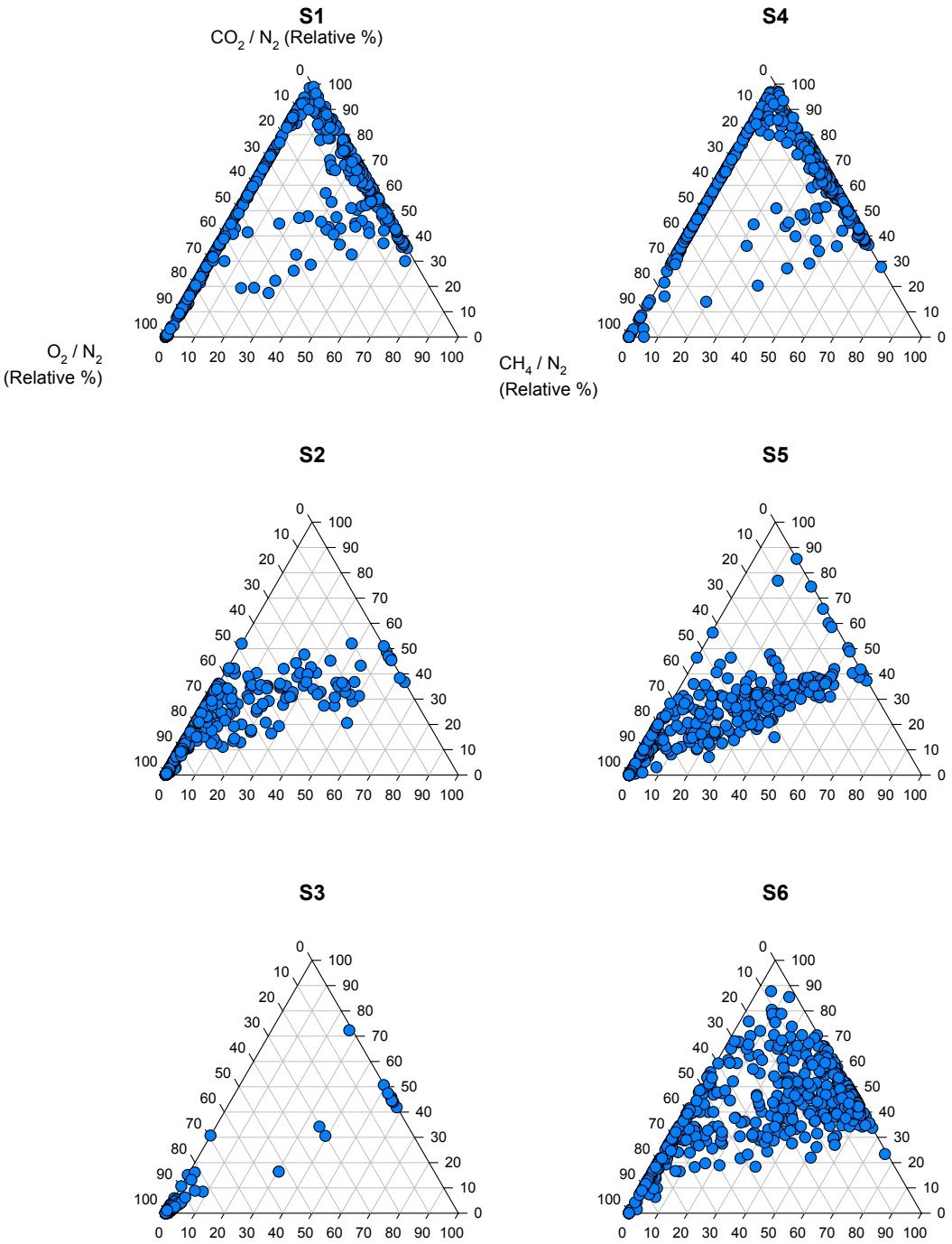

Figure G.6: Gas Composition for GM 11, Site 3 (29/10/1998 – 18/05/2015)

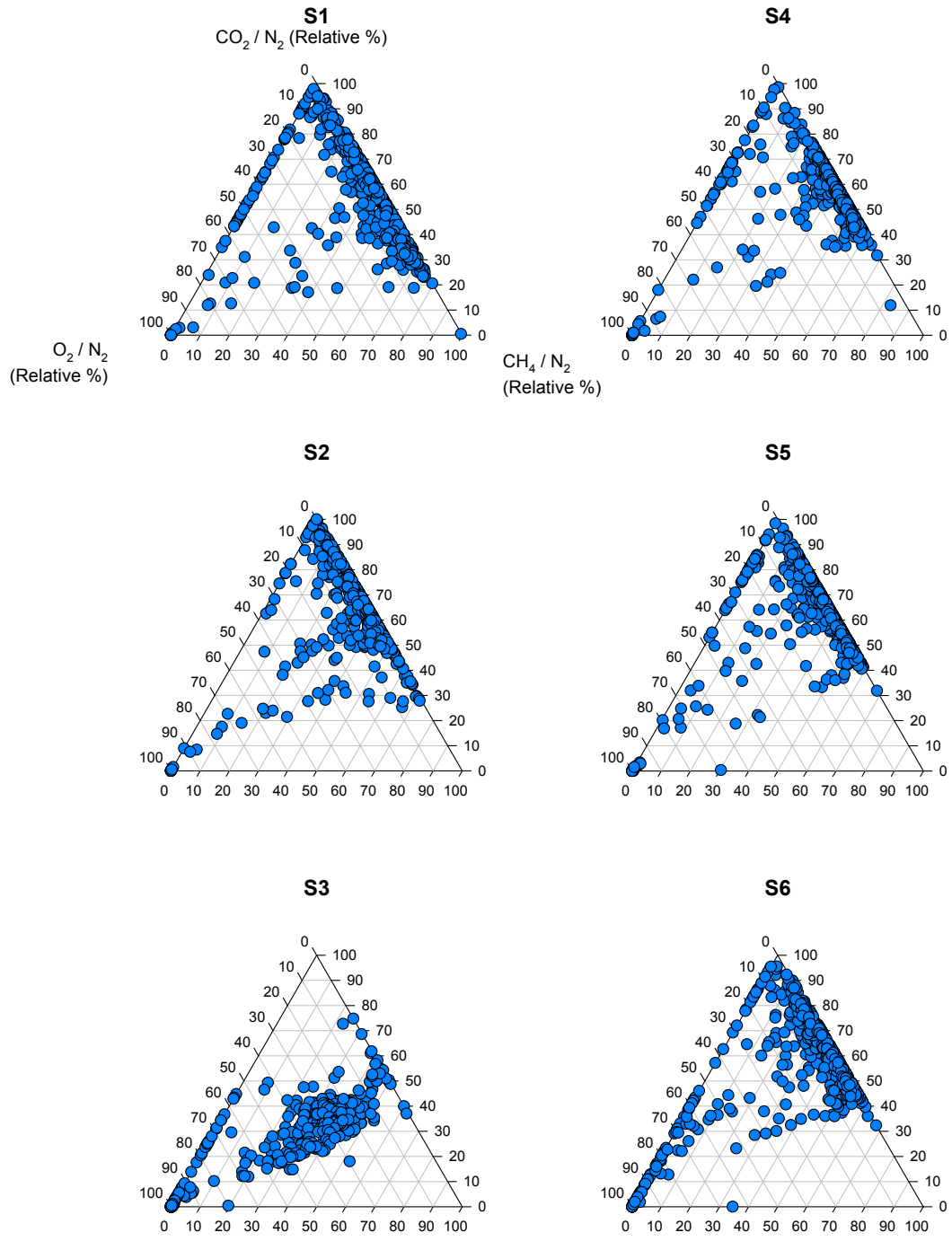

Figure G.7: Gas Composition for GM 12, Site 3 (29/10/1998 – 18/05/2015)

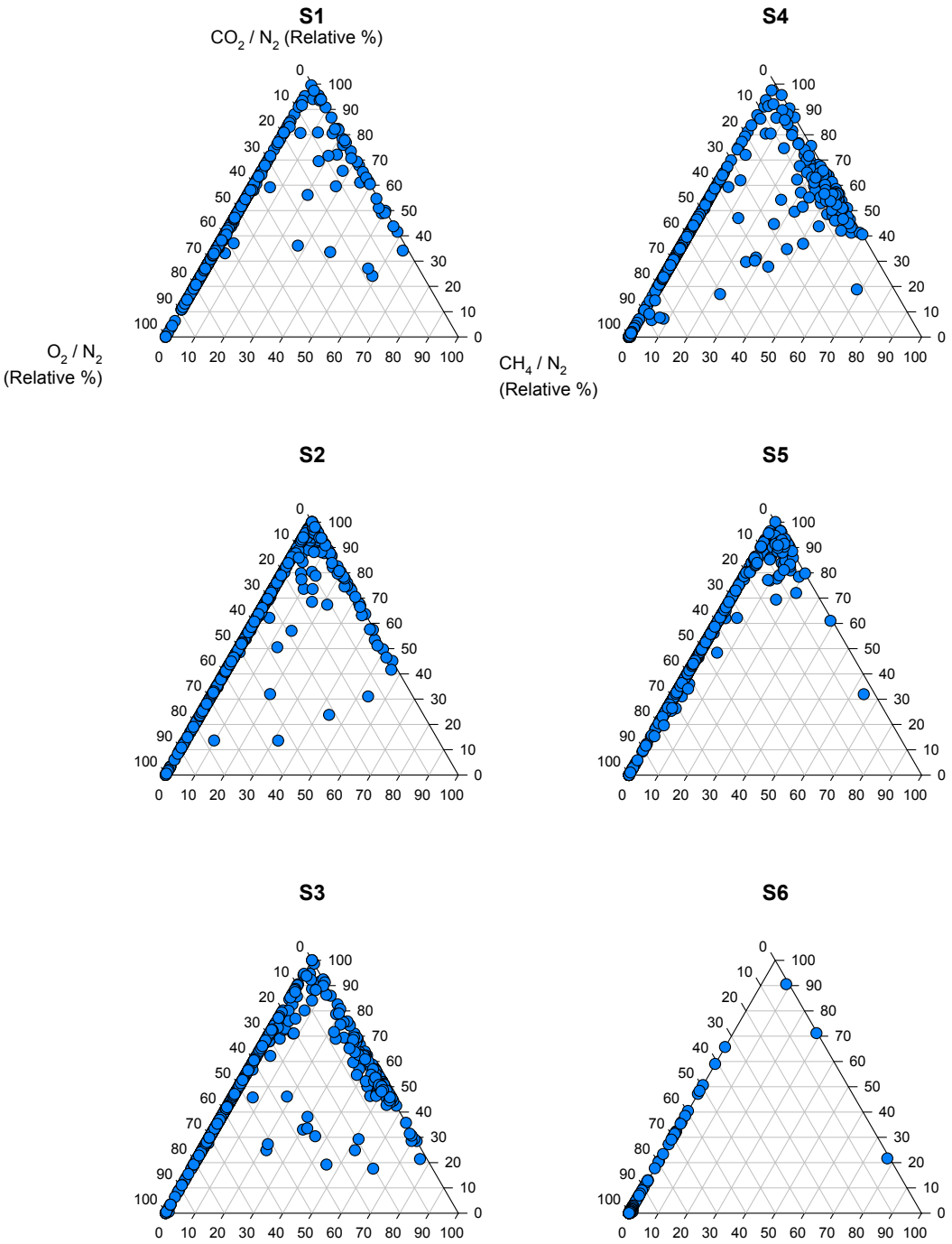

Figure G.8: Gas Composition for GM 13, Site 3 (29/10/1998 – 18/05/2015)

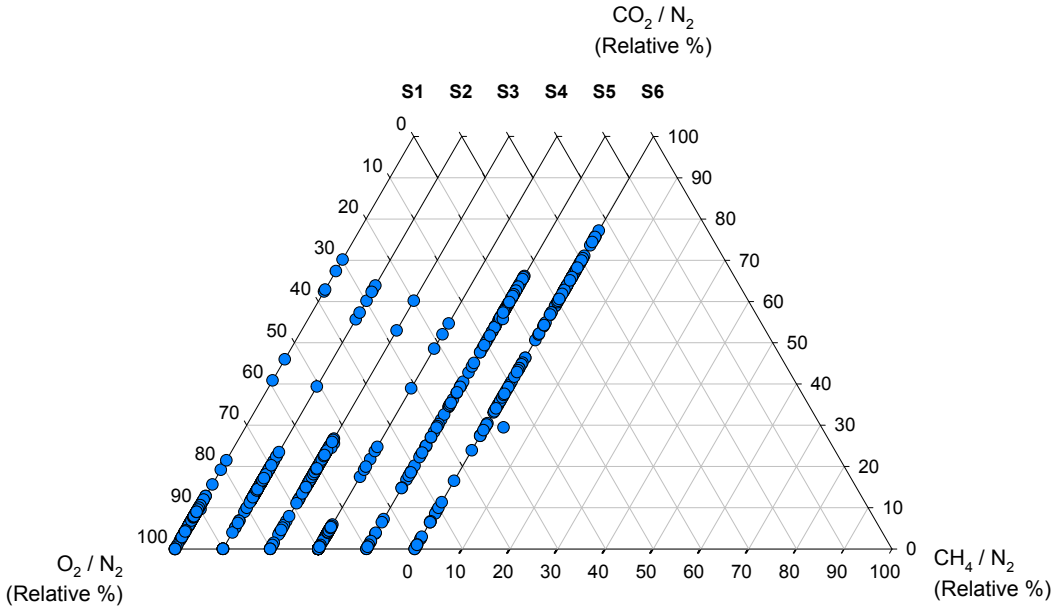

Figure G.9: Gas Composition for GM 15, Site 3 (20/04/1998 – 18/05/2015)

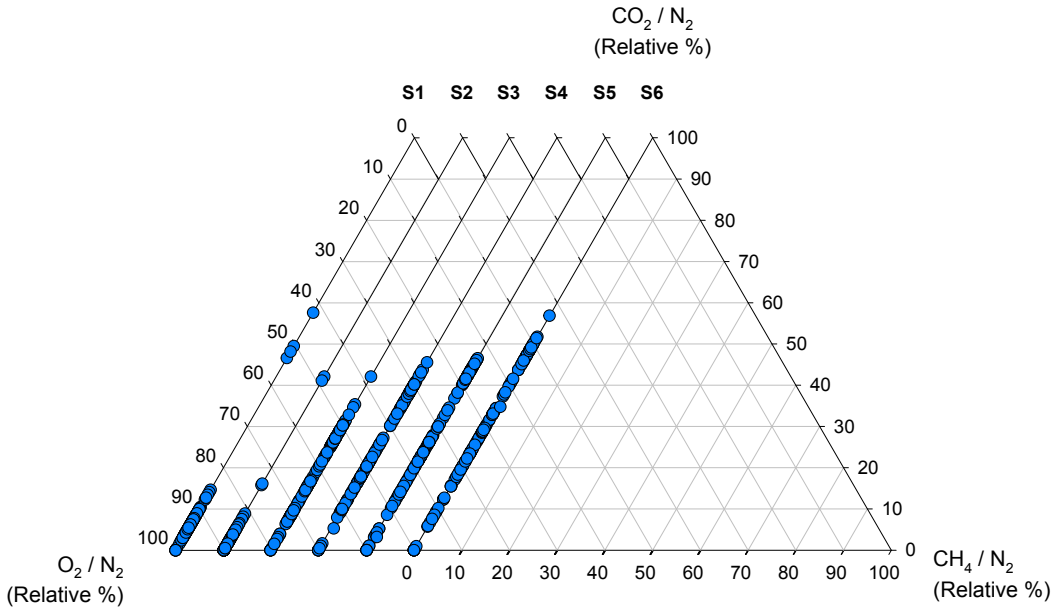

Figure G.10: Gas Composition for GM 16, Site 3 (20/04/1998 – 18/05/2015)

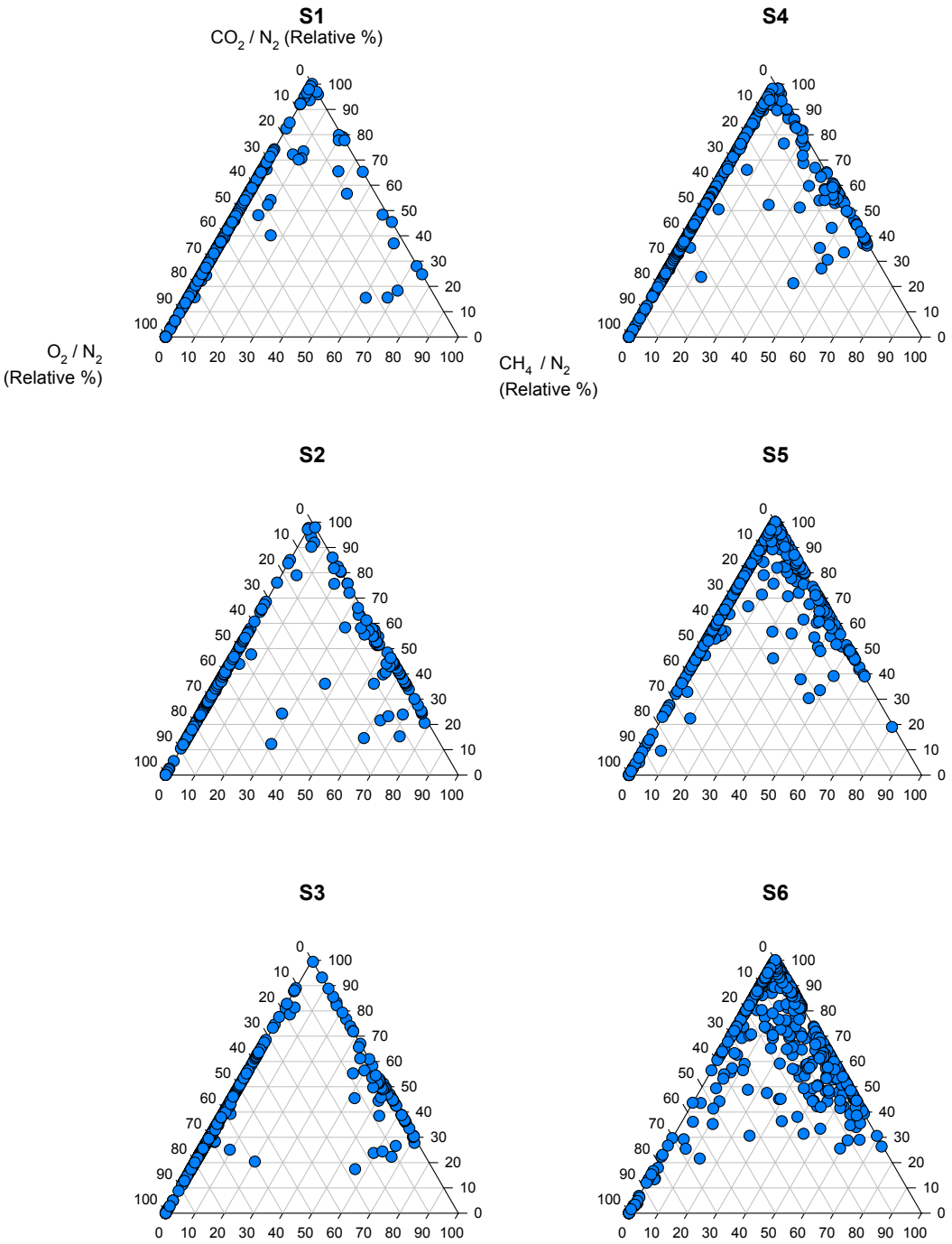

Figure G.11: Gas Composition for GM 17, Site 3 (20/04/1998 – 18/05/2015)

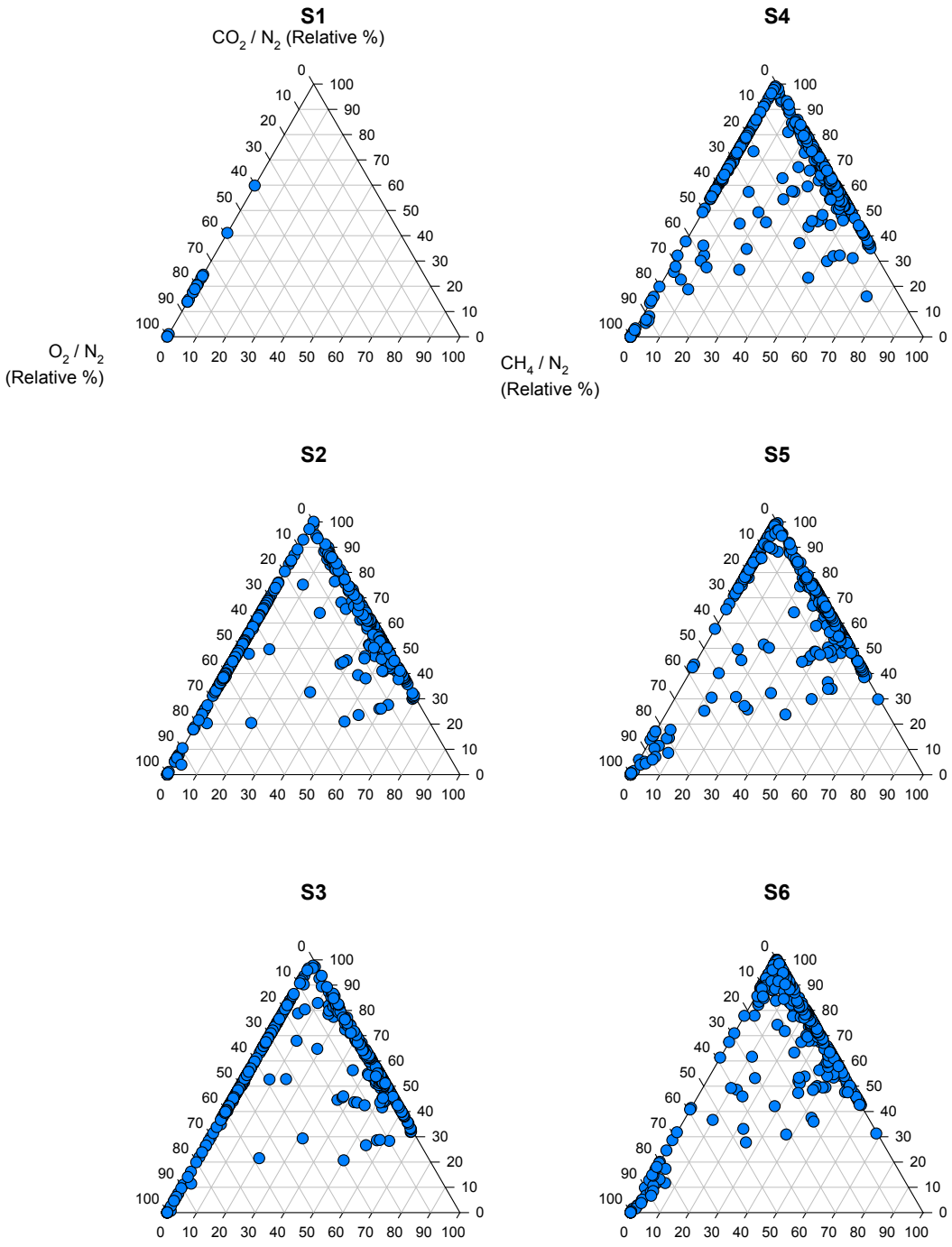

Figure G.12: Gas Composition for GM 18, Site 3 (20/04/1998 – 18/05/2015)

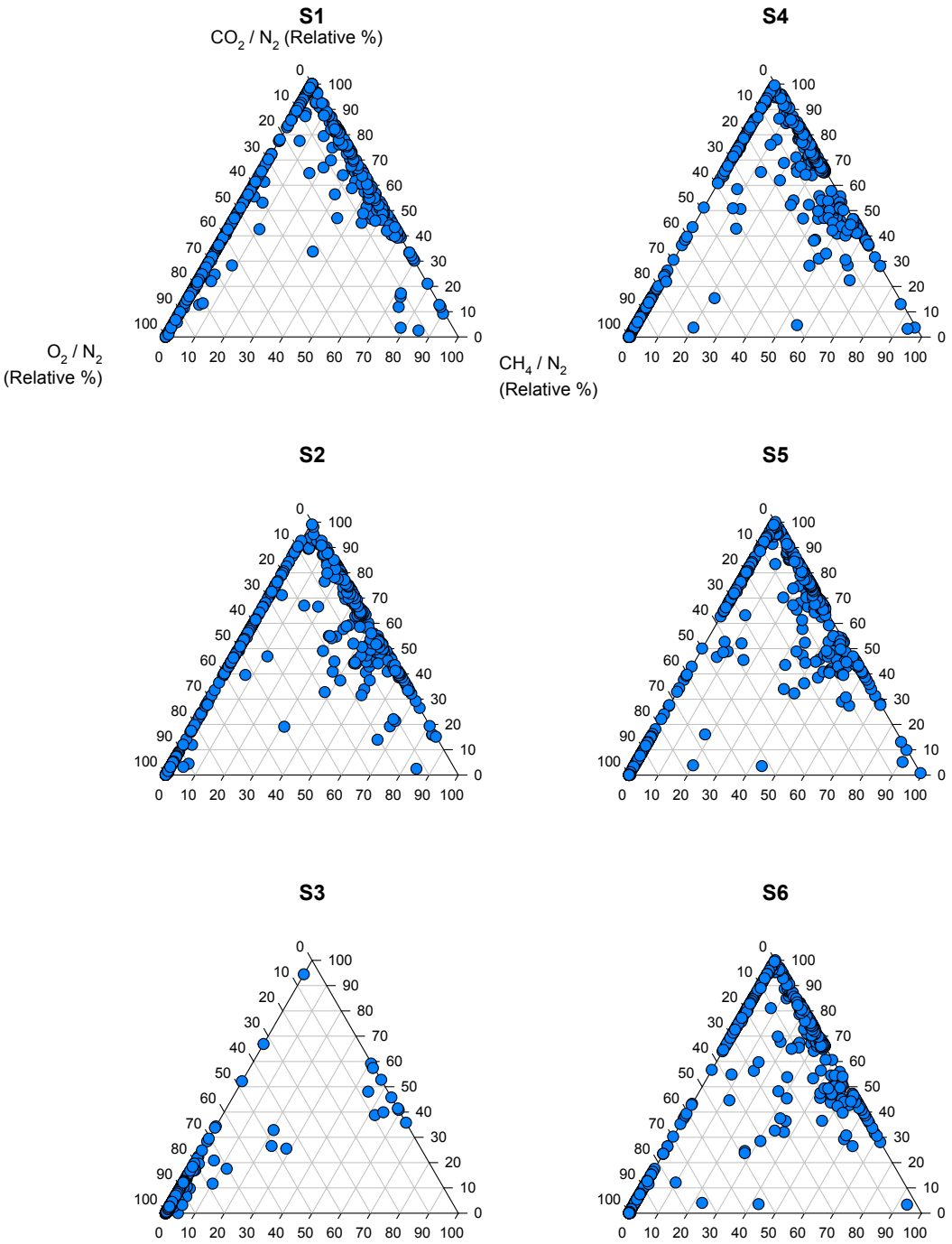

Figure G.13: Gas Composition for GM 19, Site 3 (20/04/1998 – 18/05/2015)

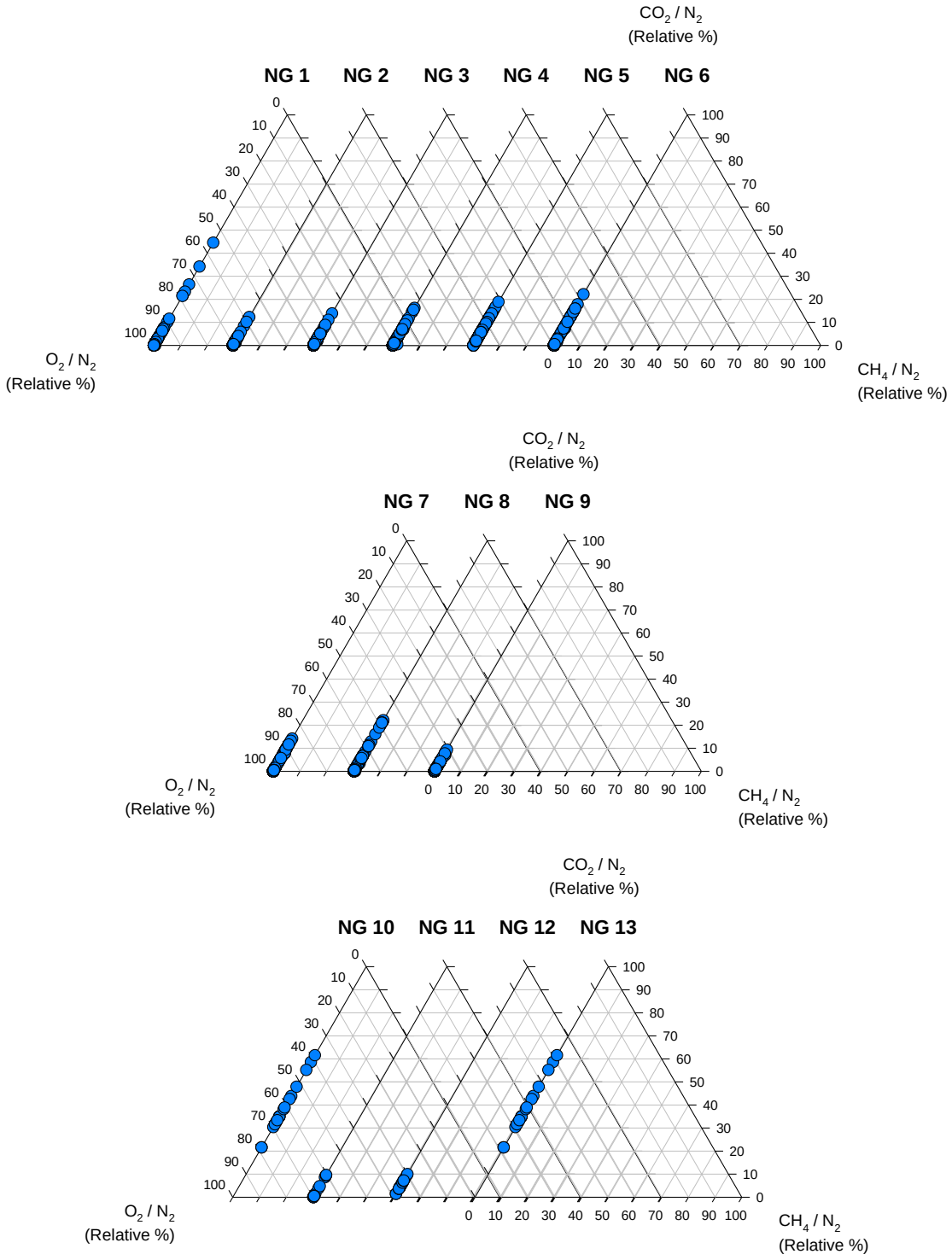

Figure G.14: Gas Compositions for NG Series, Site 3 (26/08/2003 – 18/05/2015)

Appendix H

Site 1 High Temporal Frequency Gas Data

Time-series diagrams illustrating gas compositions for BH 03/4, Site 1, recorded by GasClams *000237/05/12* and *000049/09/09* not primarily discussed in Chapter 5 are presented in this appendix.

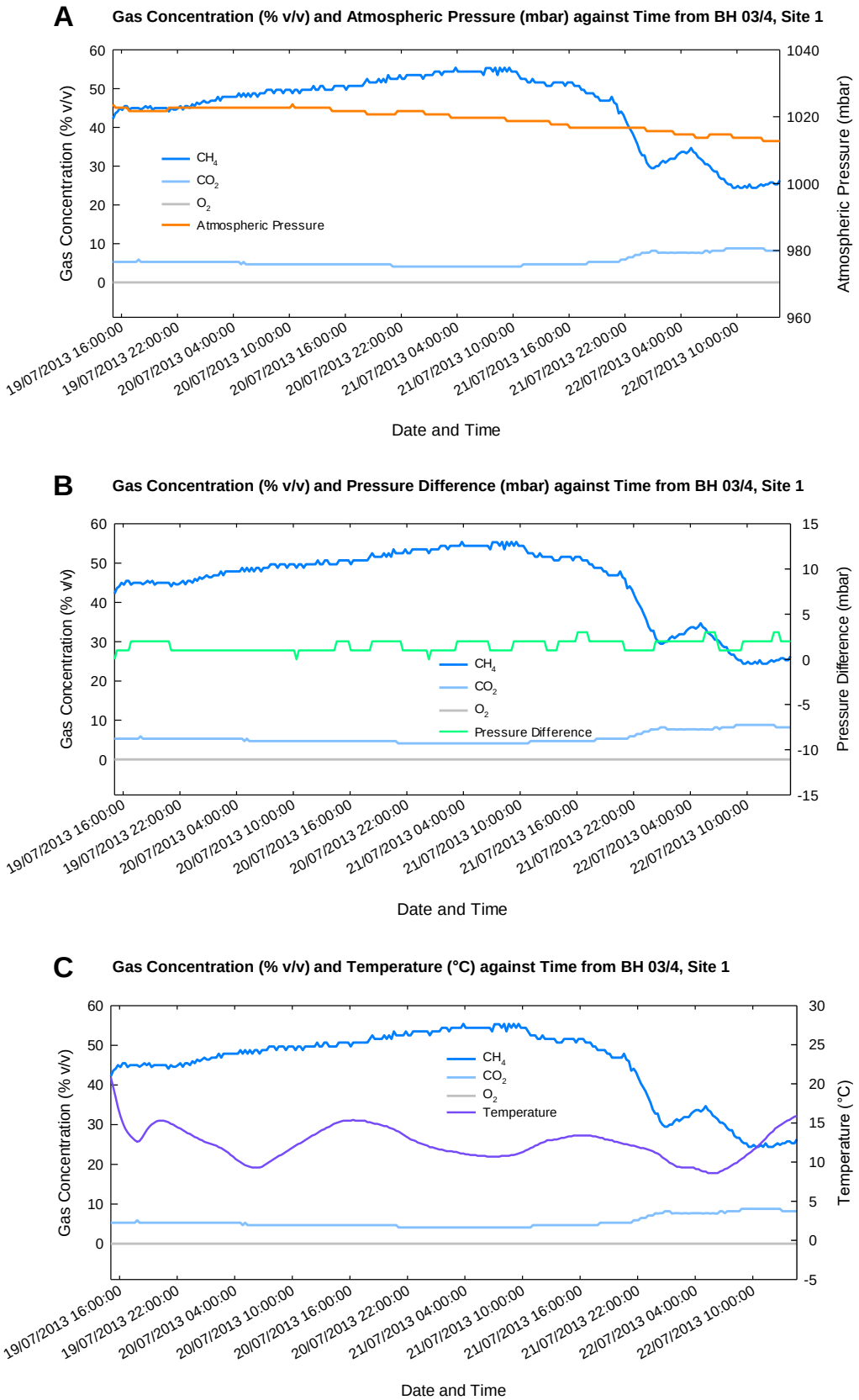

Figure H.1: Site 1 BH 03/4 High Temporal Frequency Gas Data Recorded by GasClam *000049/09/09* (19/07/2013 – 22/07/2013)

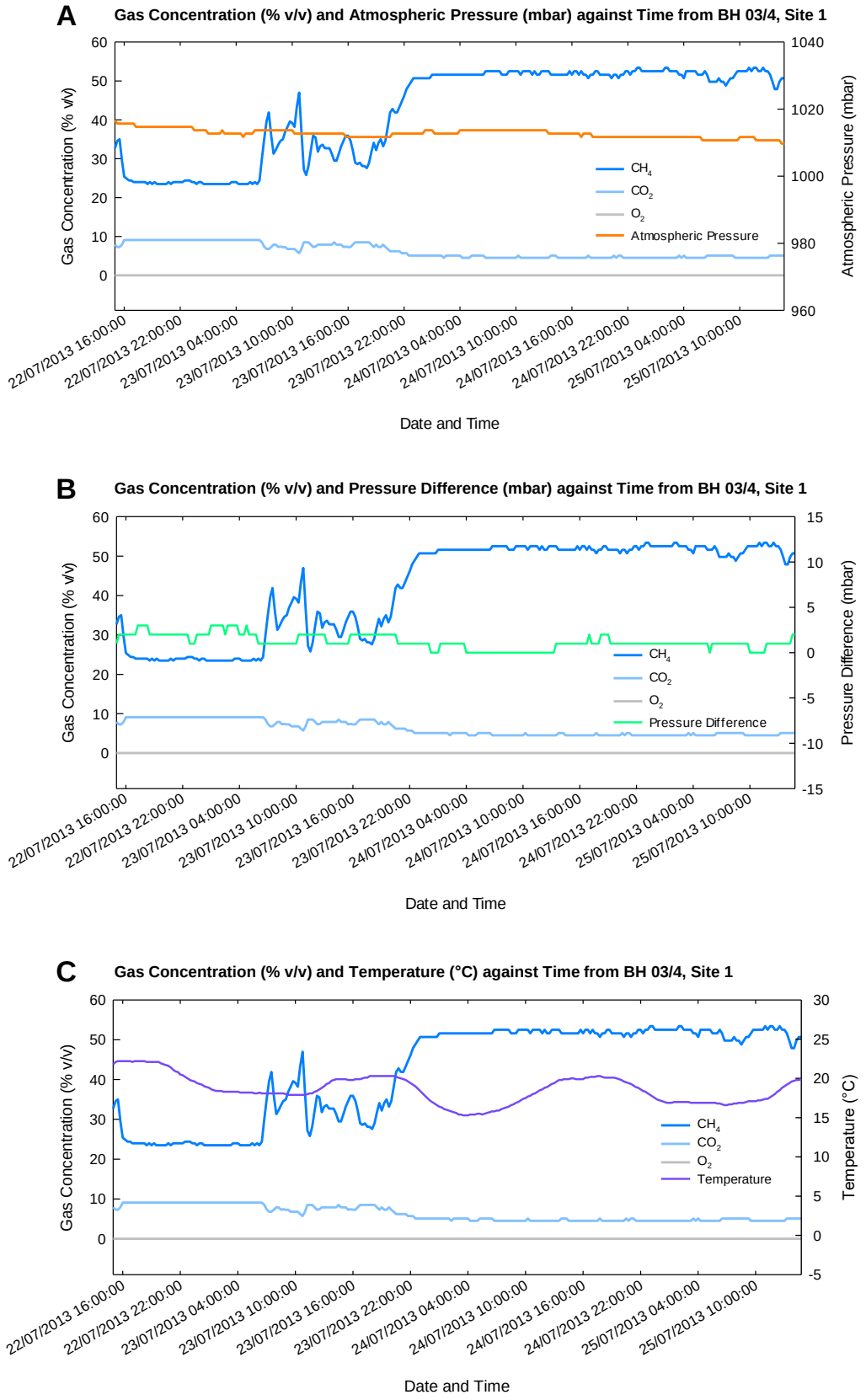

Figure H.2: Site 1 BH 03/4 High Temporal Frequency Gas Data Recorded by GasClam *000237/05/12* (22/07/2013 – 25/07/2013)

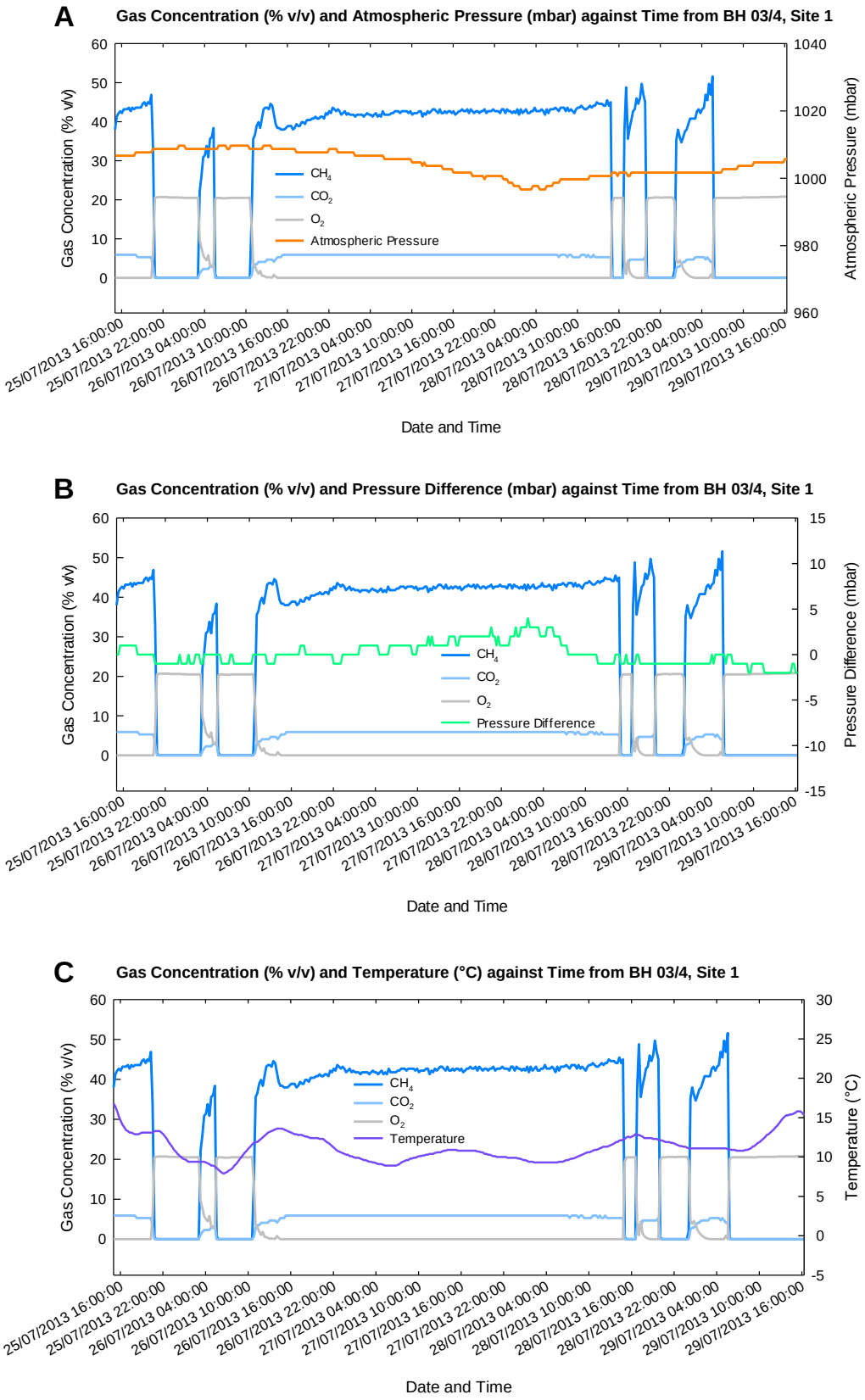

Figure H.3: Site 1 BH 03/4 High Temporal Frequency Gas Data Recorded by GasClam *000049/09/09* (25/07/2013 – 29/07/2013)

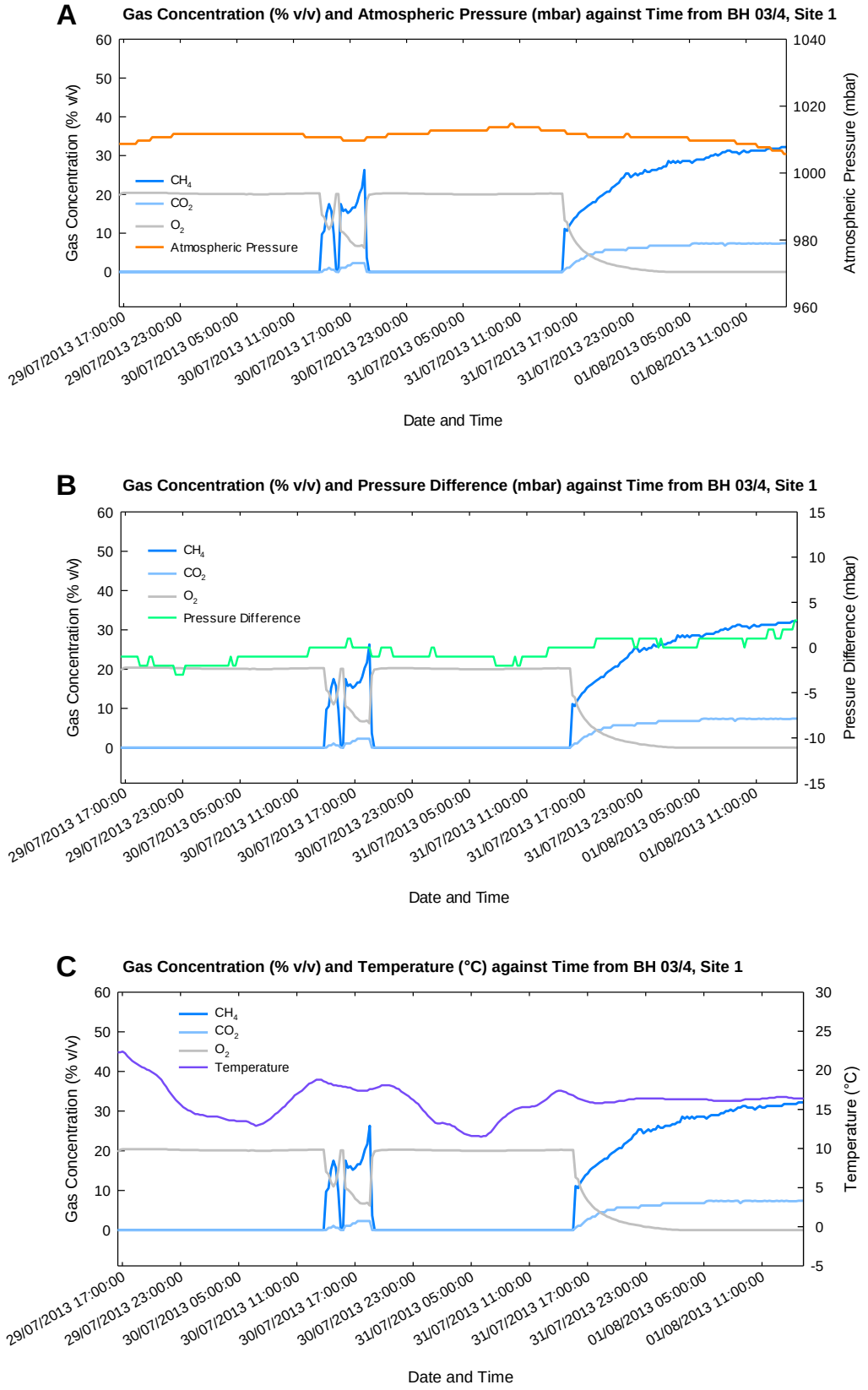

Figure H.4: Site 1 BH 03/4 High Temporal Frequency Gas Data Recorded by GasClam *000237/05/12* (29/07/2013 – 01/08/2013)

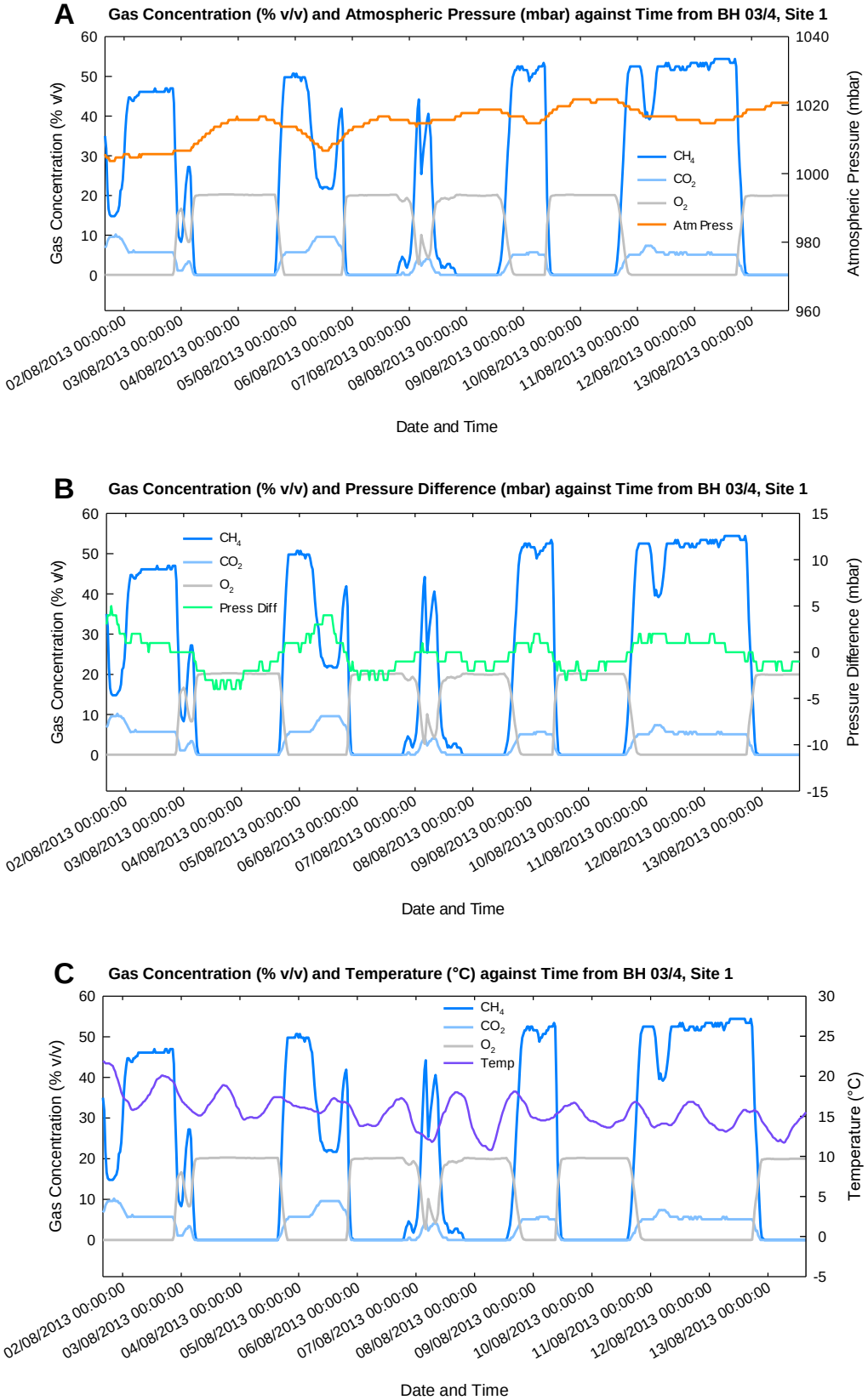

Figure H.5: Site 1 BH 03/4 High Temporal Frequency Gas Data Recorded by GasClam *000237/05/12* (01/08/2013 – 13/08/2013)

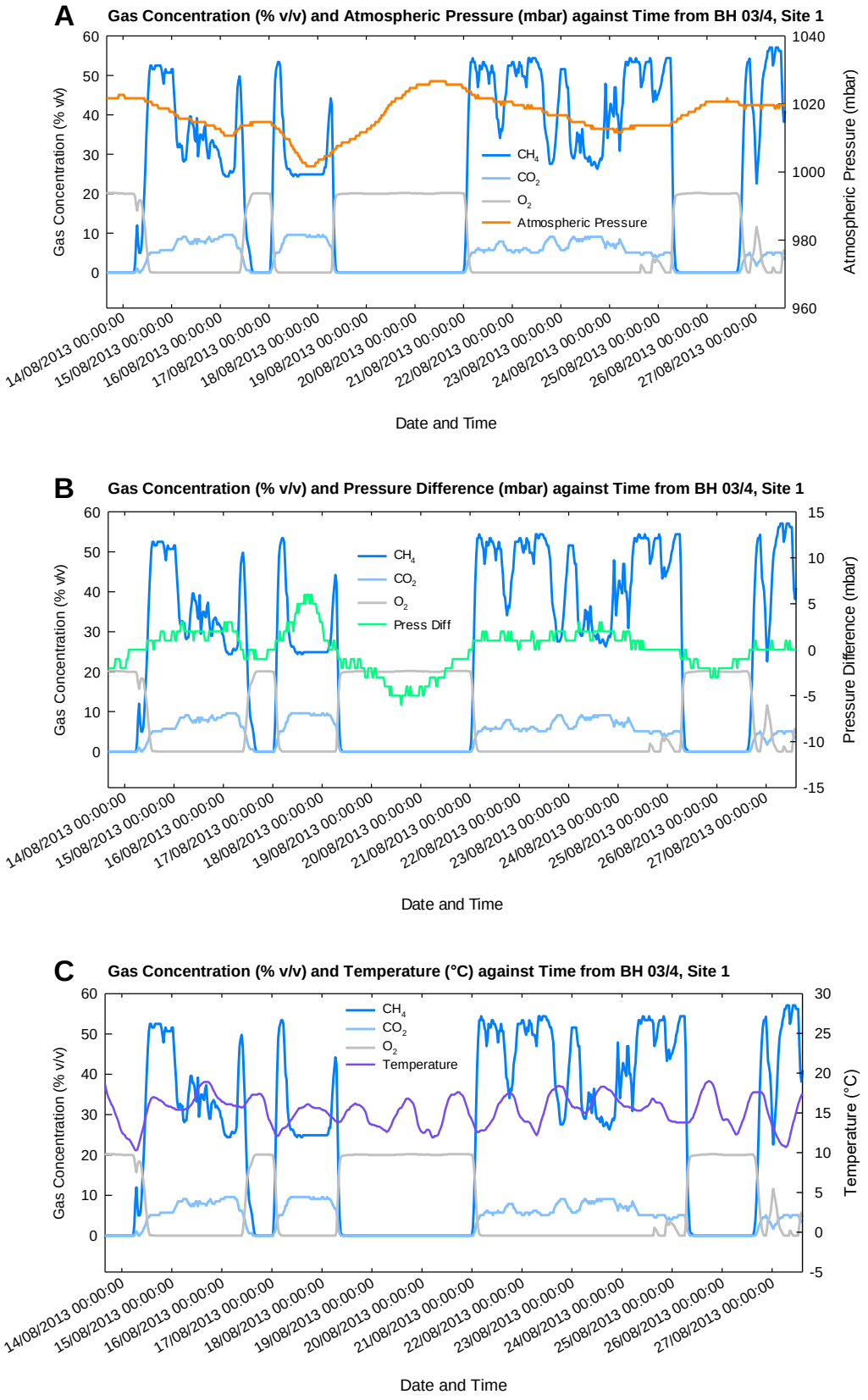

Figure H.6: Site 1 BH 03/4 High Temporal Frequency Gas Data Recorded by GasClam *000237/05/12* (13/08/2013 – 27/08/2013)

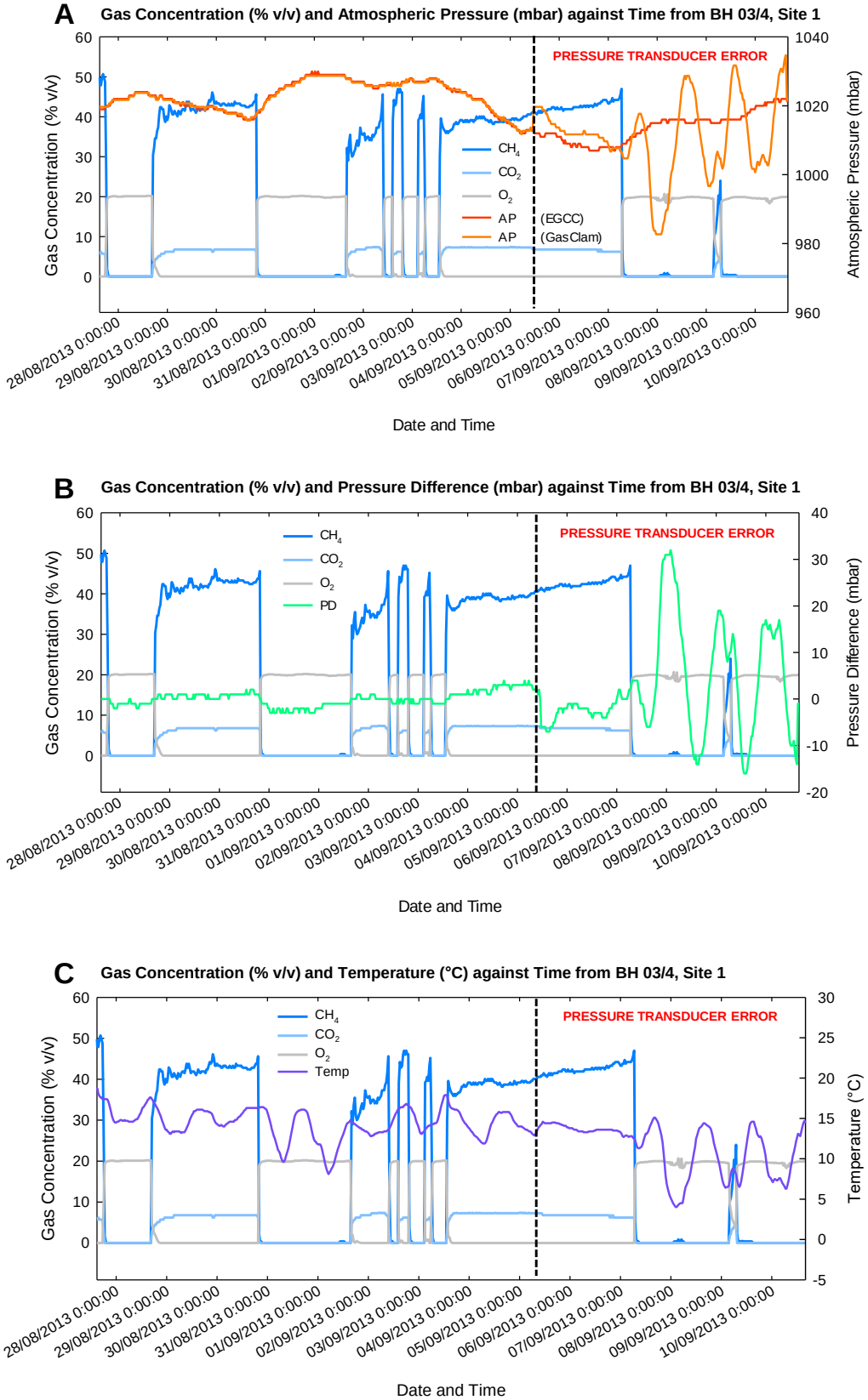

Figure H.7: Site 1 BH 03/4 High Temporal Frequency Gas Data Recorded by GasClam *000237/05/12* (27/08/2013 – 10/09/2013)

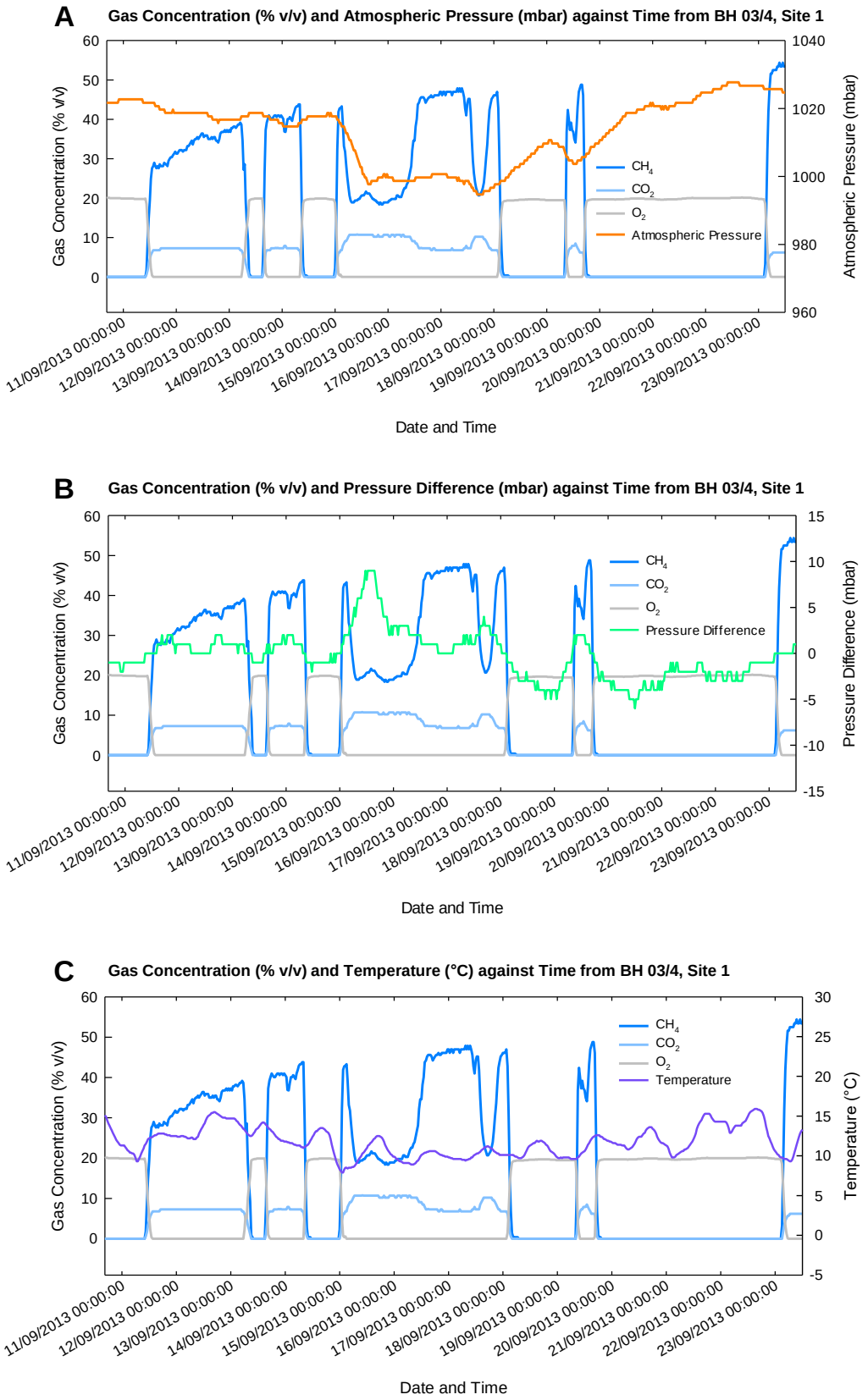

Figure H.8: Site 1 BH 03/4 High Temporal Frequency Gas Data Recorded by GasClam *000237/05/12* (10/09/2013 – 23/09/2013)

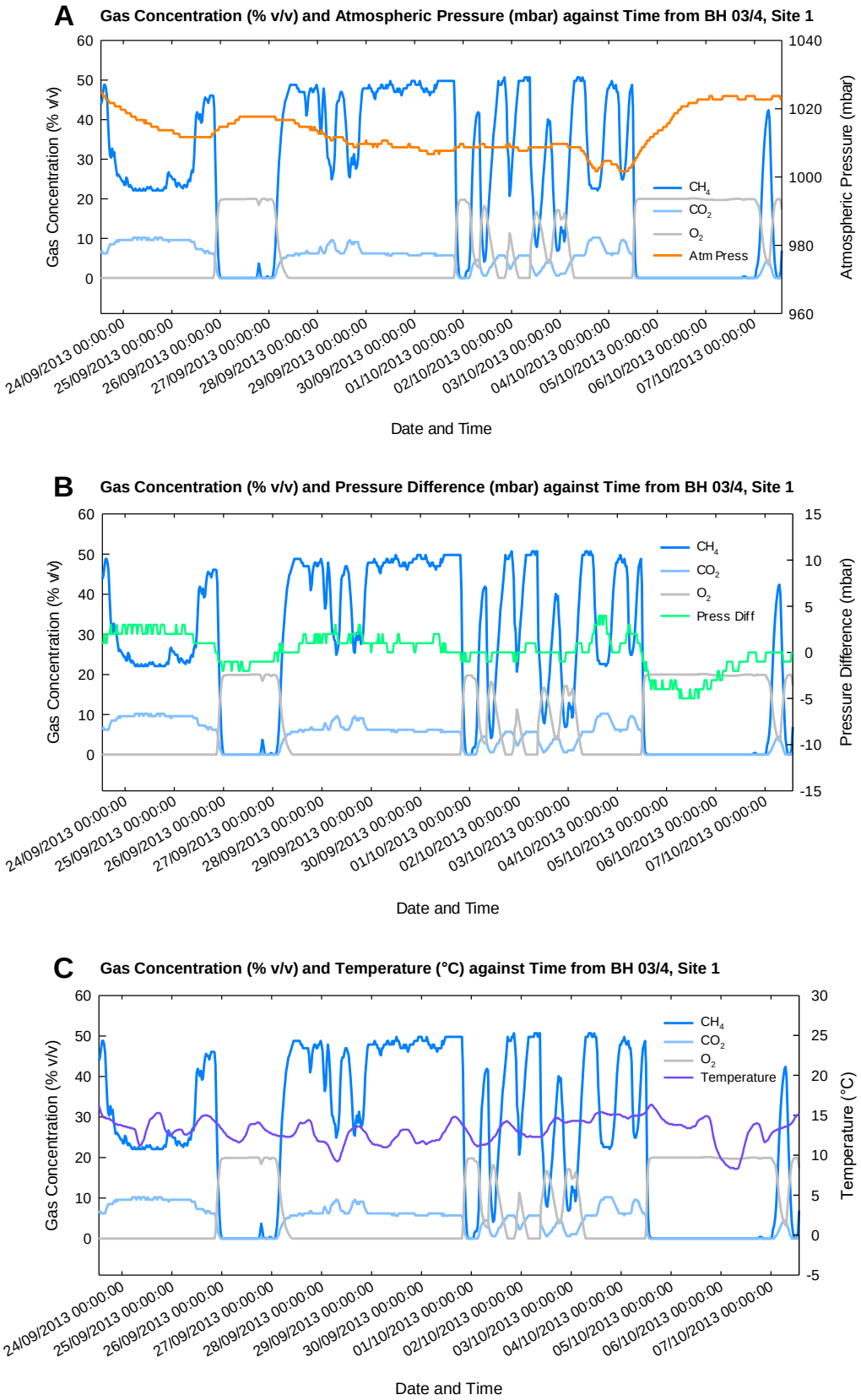

Figure H.9: Site 1 BH 03/4 High Temporal Frequency Gas Data Recorded by GasClam *000237/05/12* (23/09/2013 – 07/10/2013)

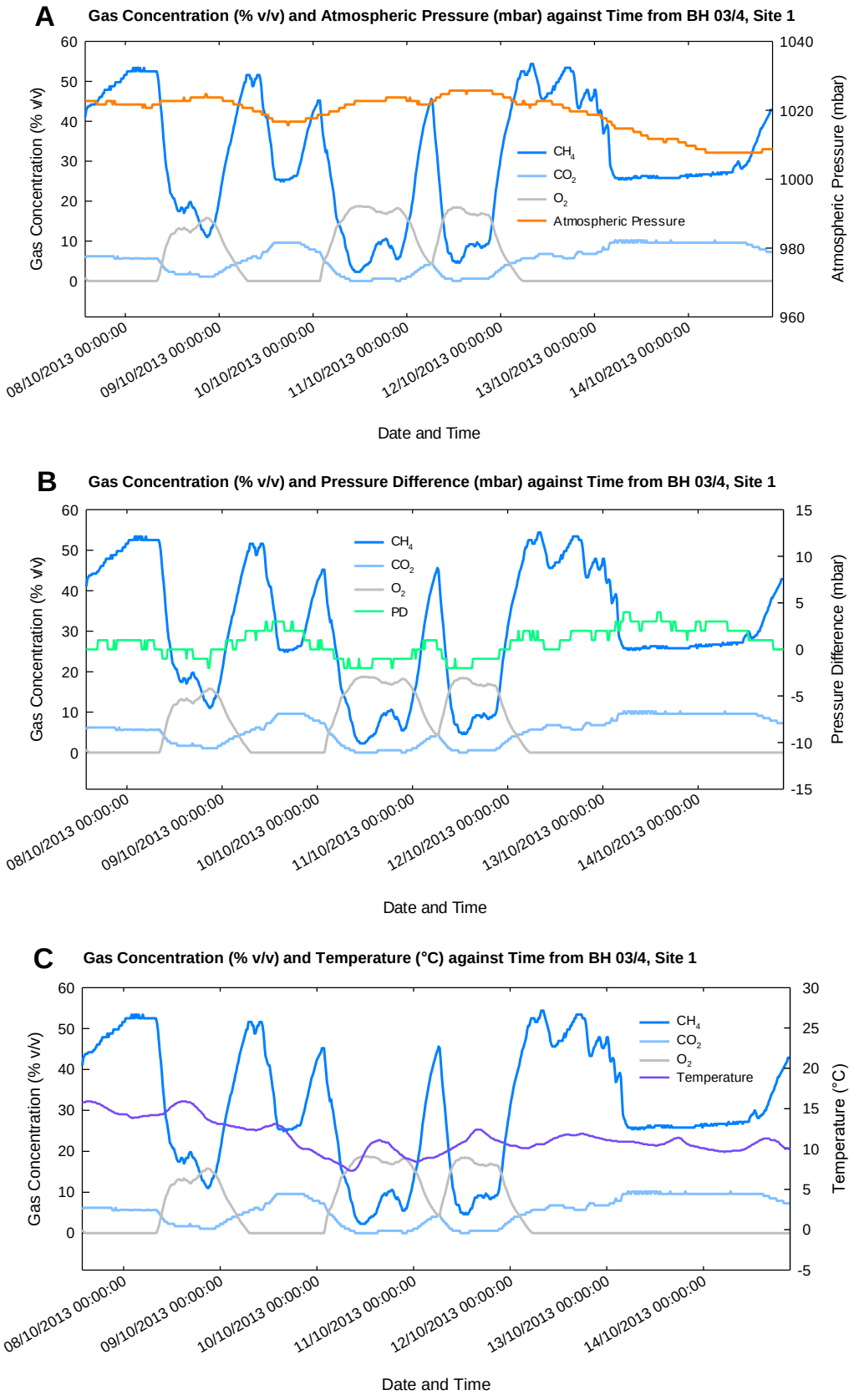

Figure H.10: Site 1 BH 03/4 High Temporal Frequency Gas Data Recorded by GasClam *000237/05/12* (07/10/2013 – 14/10/2013)

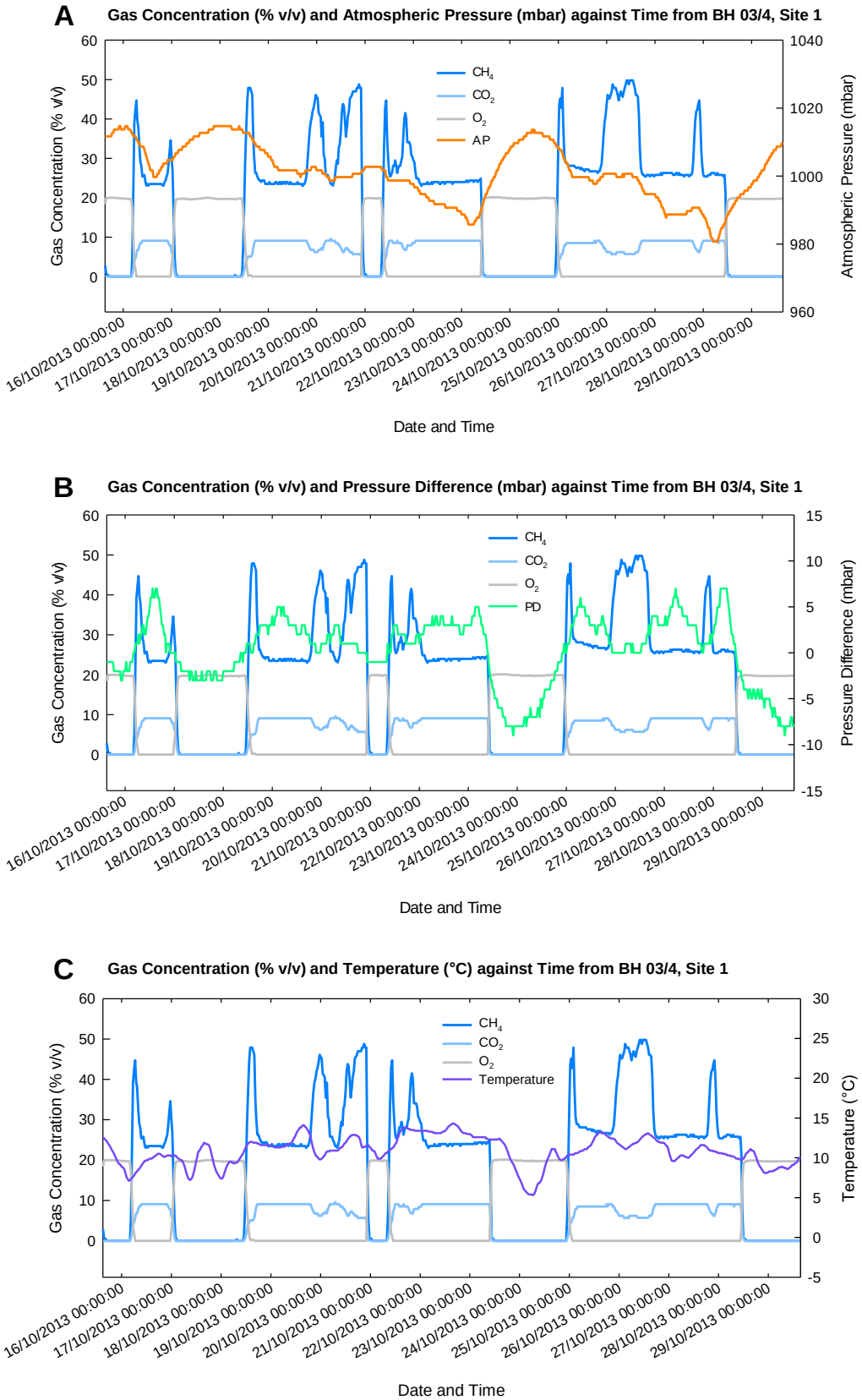

Figure H.11: Site 1 BH 03/4 High Temporal Frequency Gas Data Recorded by GasClam *000237/05/12* (14/10/2013 – 29/10/2013)

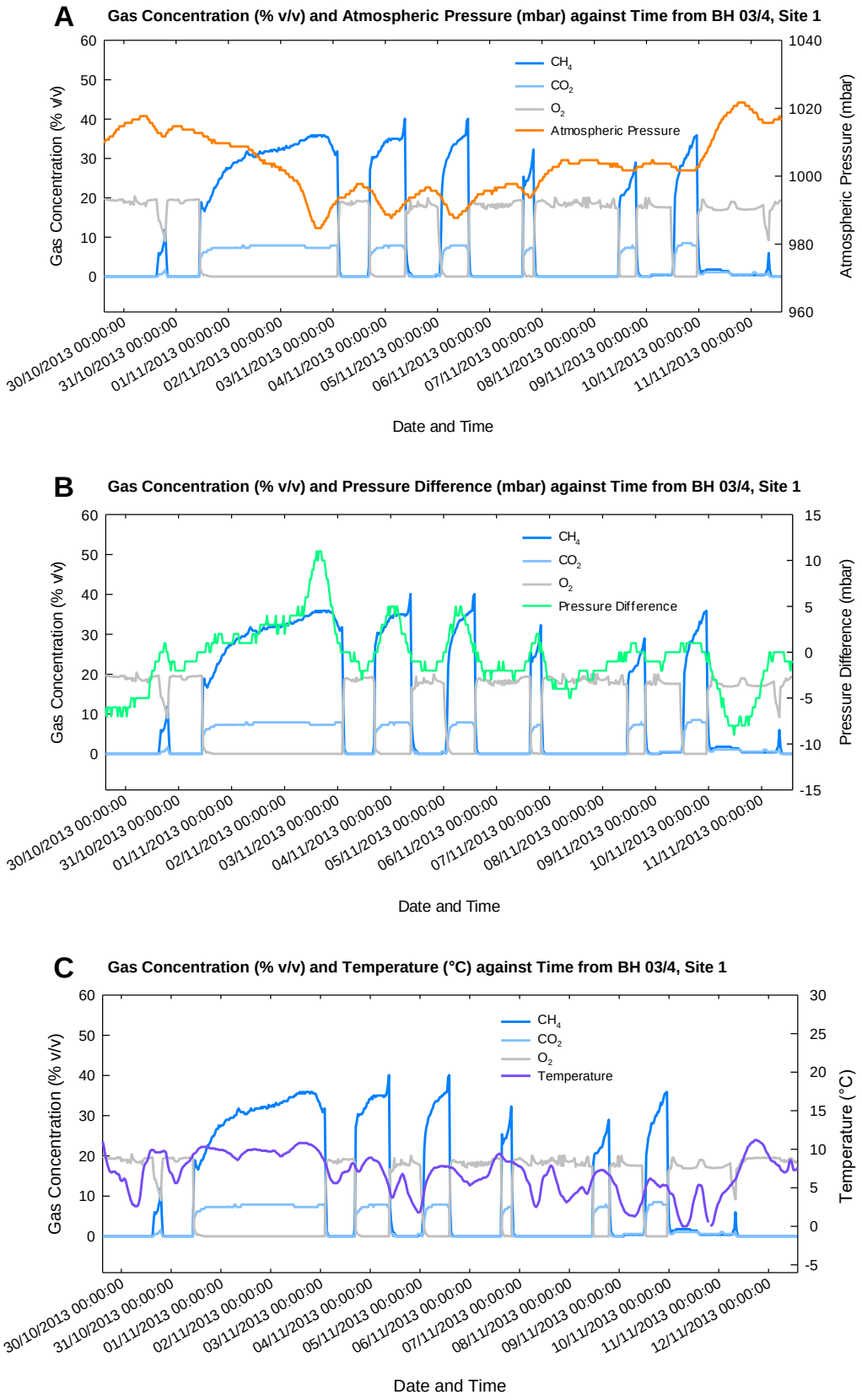

Figure H.12: Site 1 BH 03/4 High Temporal Frequency Gas Data Recorded by GasClam *000237/05/12* (29/10/2013 – 12/11/2013)

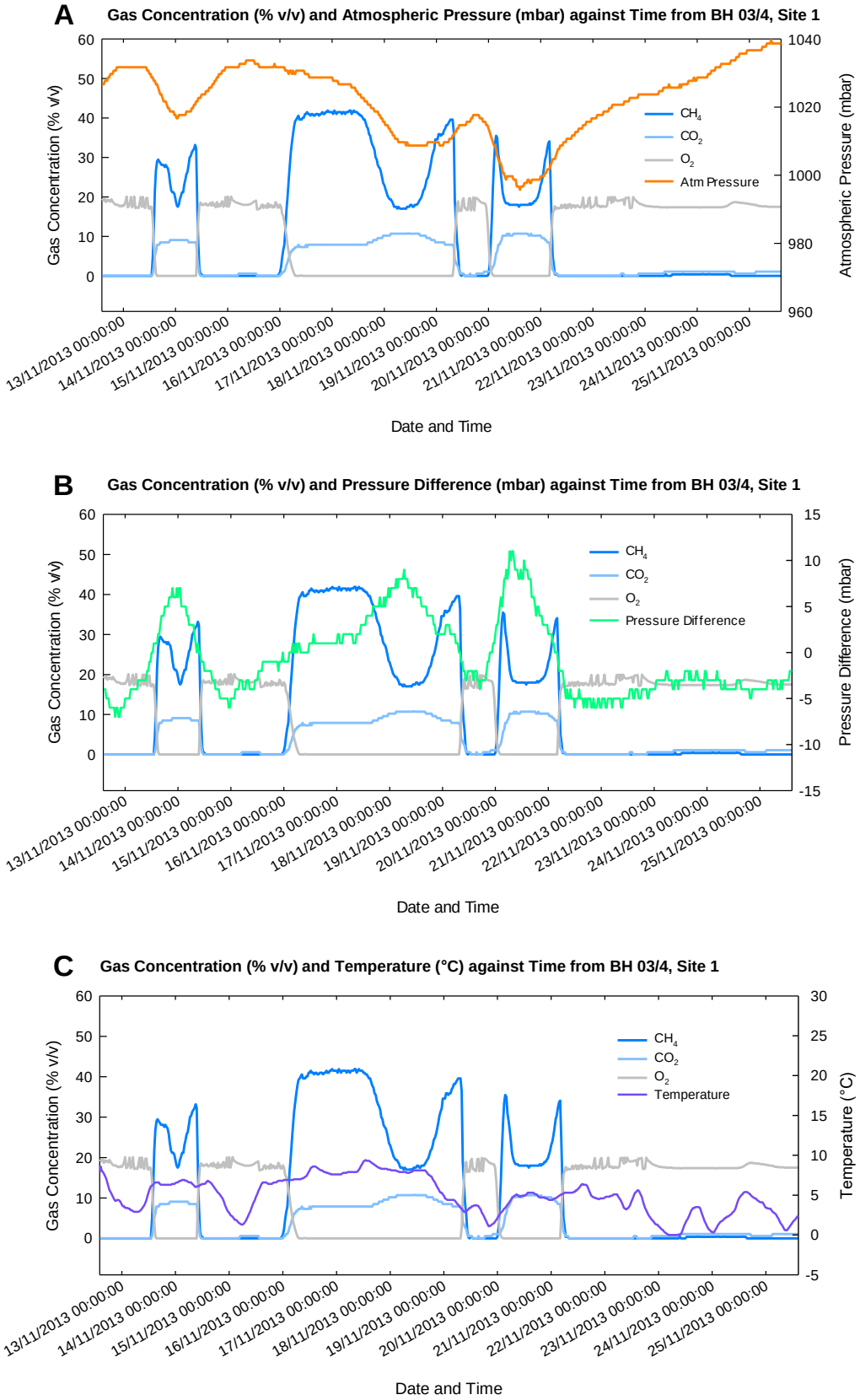

Figure H.13: Site 1 BH 03/4 High Temporal Frequency Gas Data Recorded by GasClam *000237/05/12* (12/11/2013 – 25/11/2013)

Appendix I

Site 2 High Temporal Frequency Gas Data

Time-series diagrams illustrating gas compositions for Site 2 boreholes, recorded by GasClam *000237/05/12* not primarily discussed in Chapter 5 are presented in this appendix.

BH 04

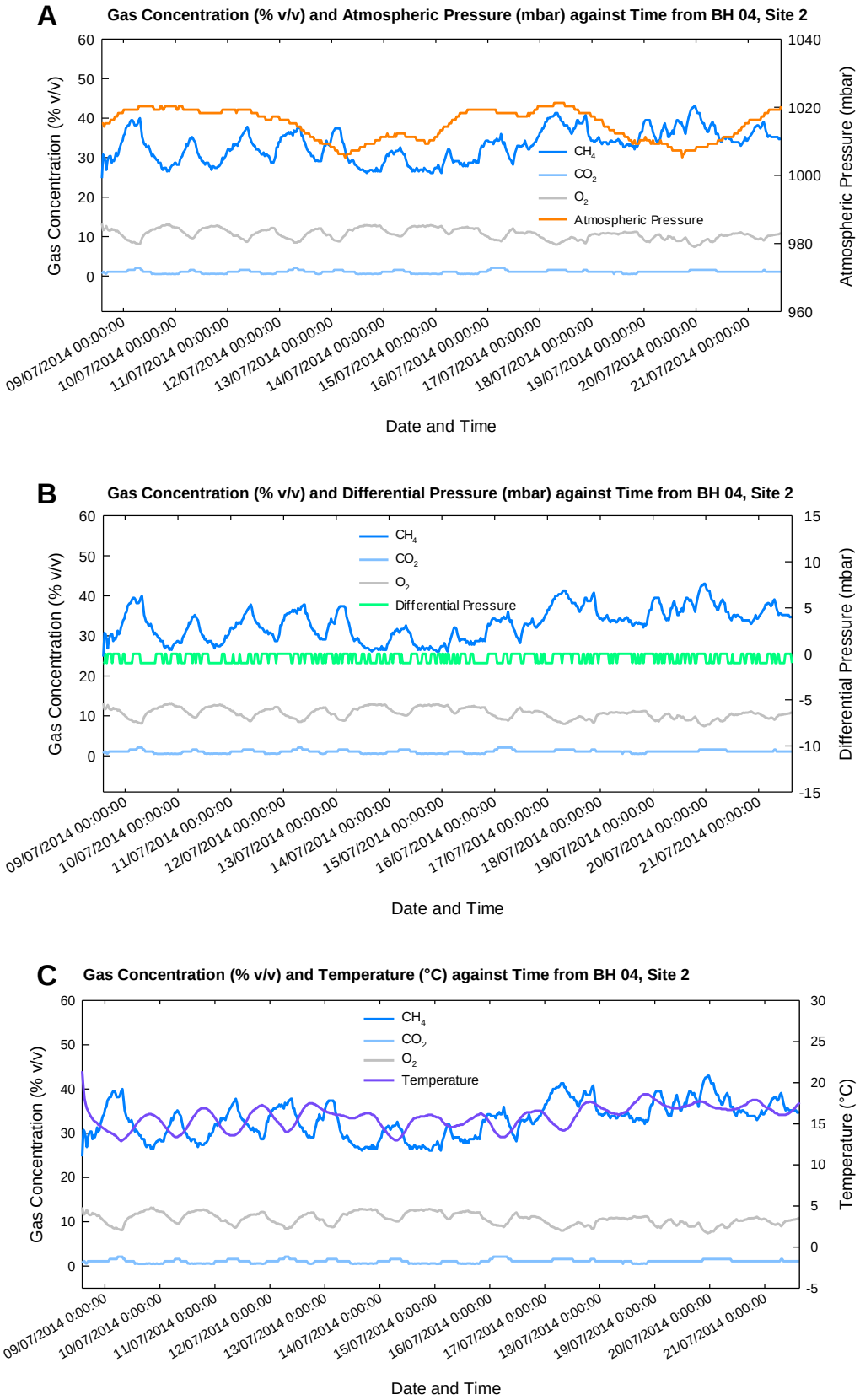

Figure I.1: Site 2, BH 04 High Temporal Frequency Gas Data (08/07/2014 – 21/07/2014)

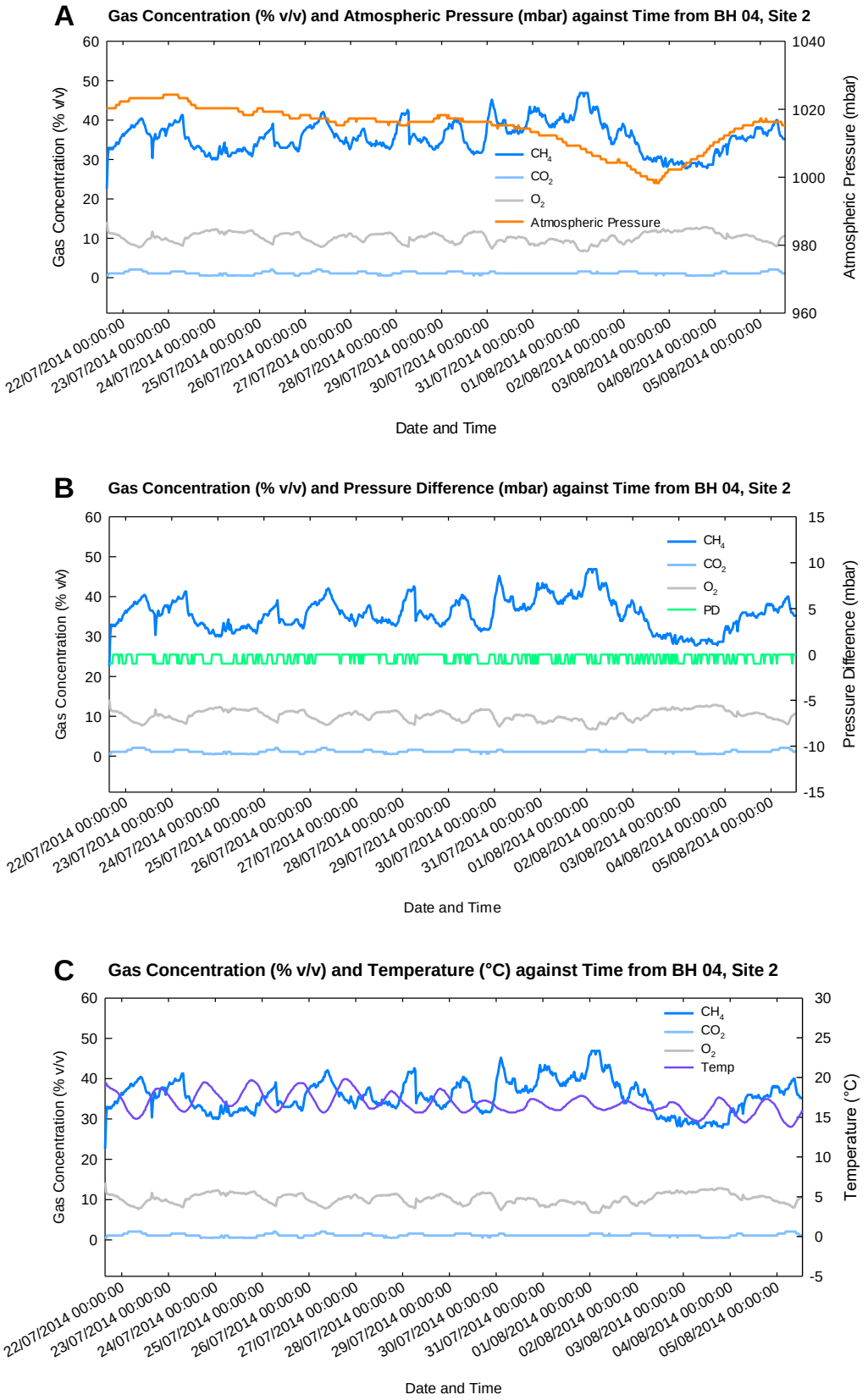

Figure I.2: Site 2, BH 04 High Temporal Frequency Gas Data (21/07/2014 – 05/08/2014)

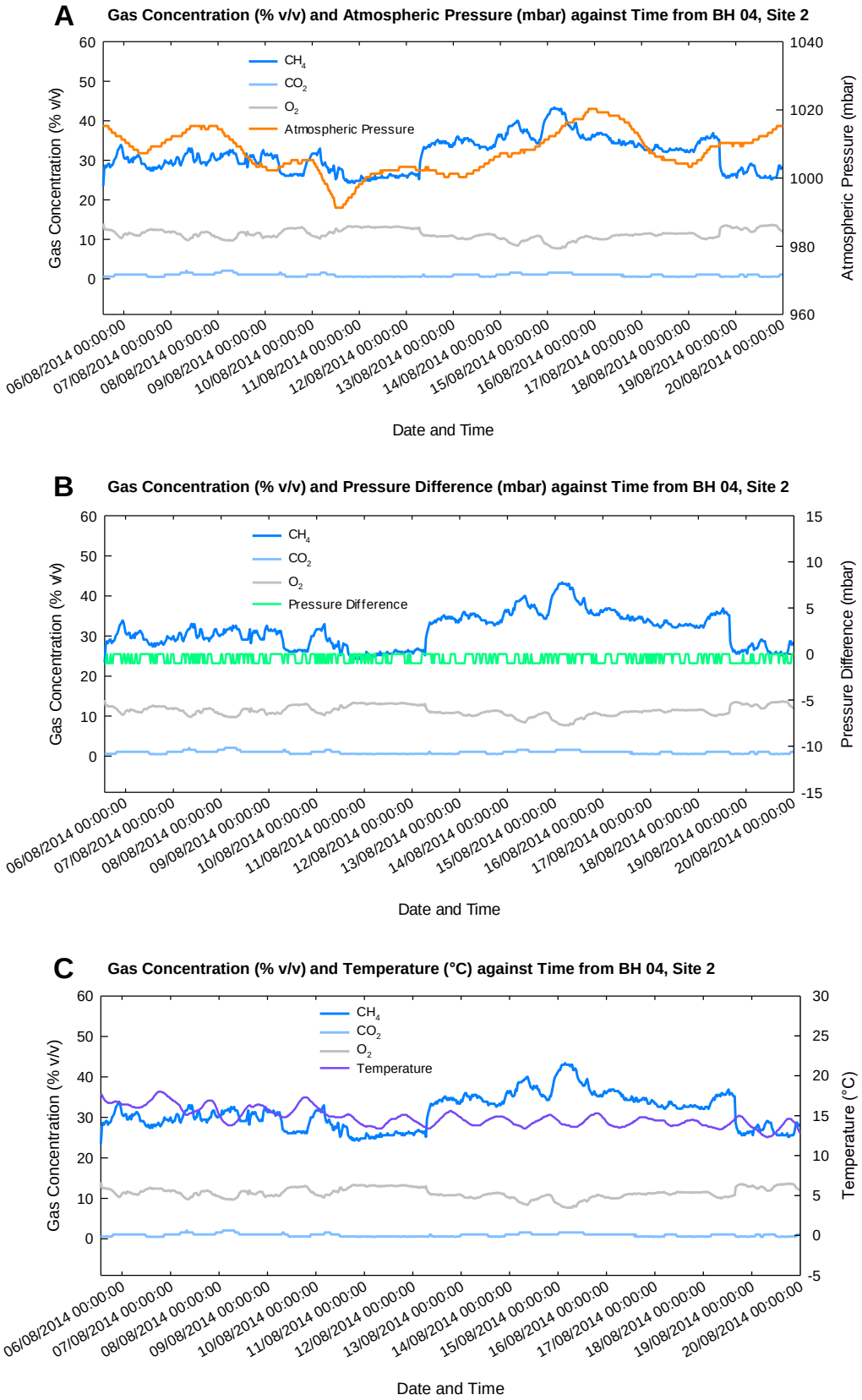

Figure I.3: Site 2, BH 04 High Temporal Frequency Gas Data (05/08/2014 – 20/08/2014)

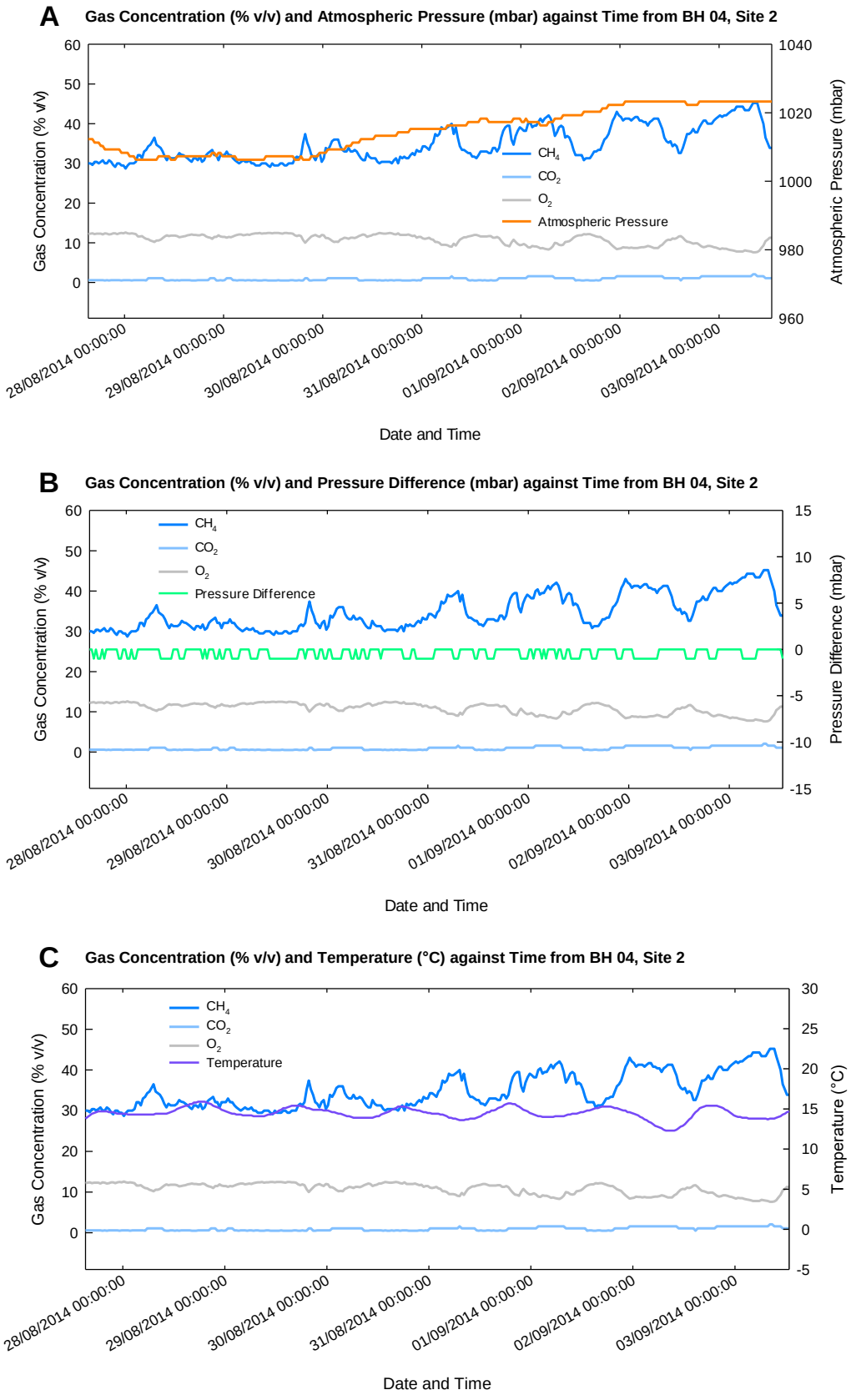

Figure I.4: Site 2, BH 04 High Temporal Frequency Gas Data (27/08/2014 – 03/09/2014)

BH 08

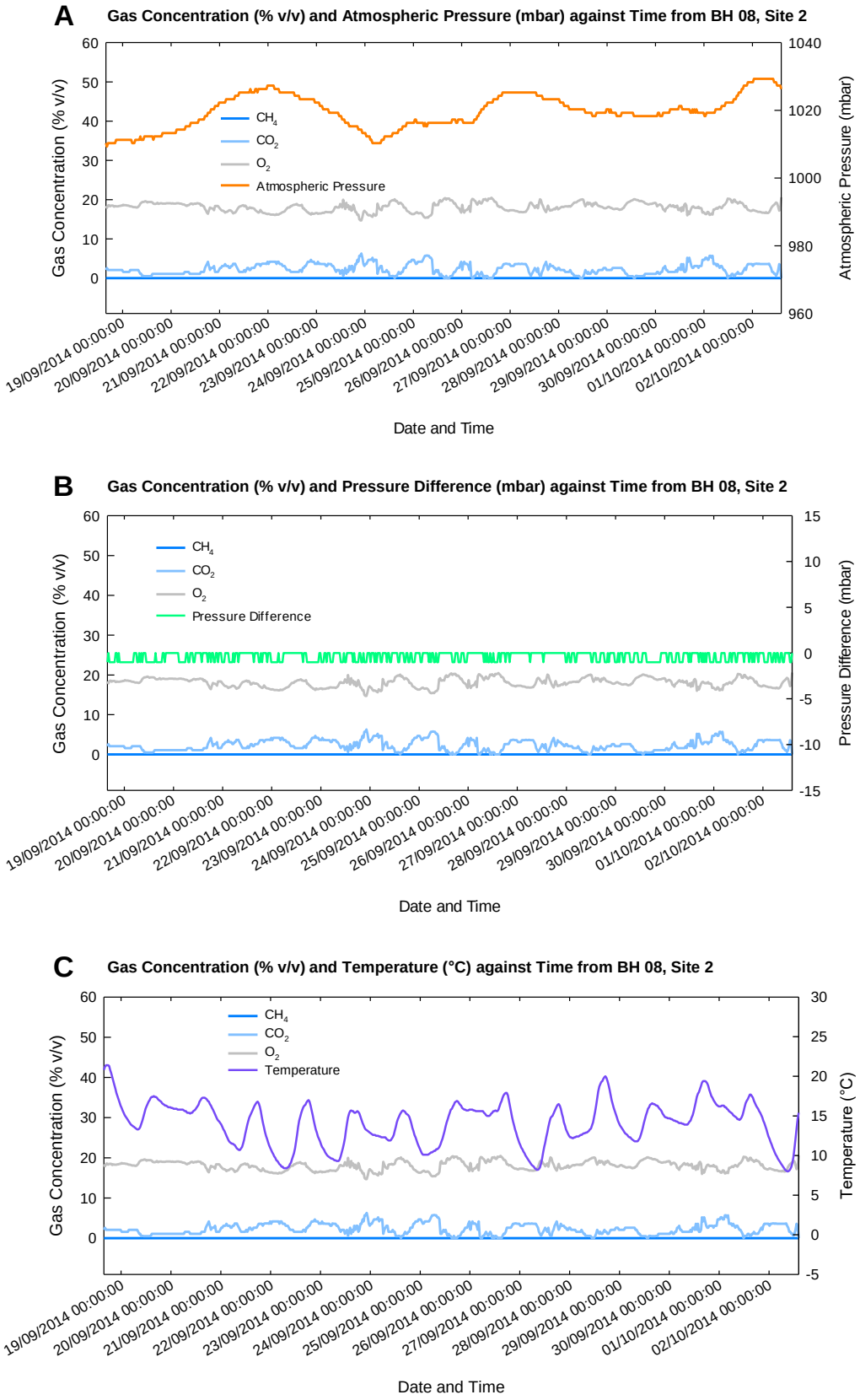

Figure I.5: Site 2, BH 08 High Temporal Frequency Gas Data (18/09/2014 – 02/10/2014)

BH 12

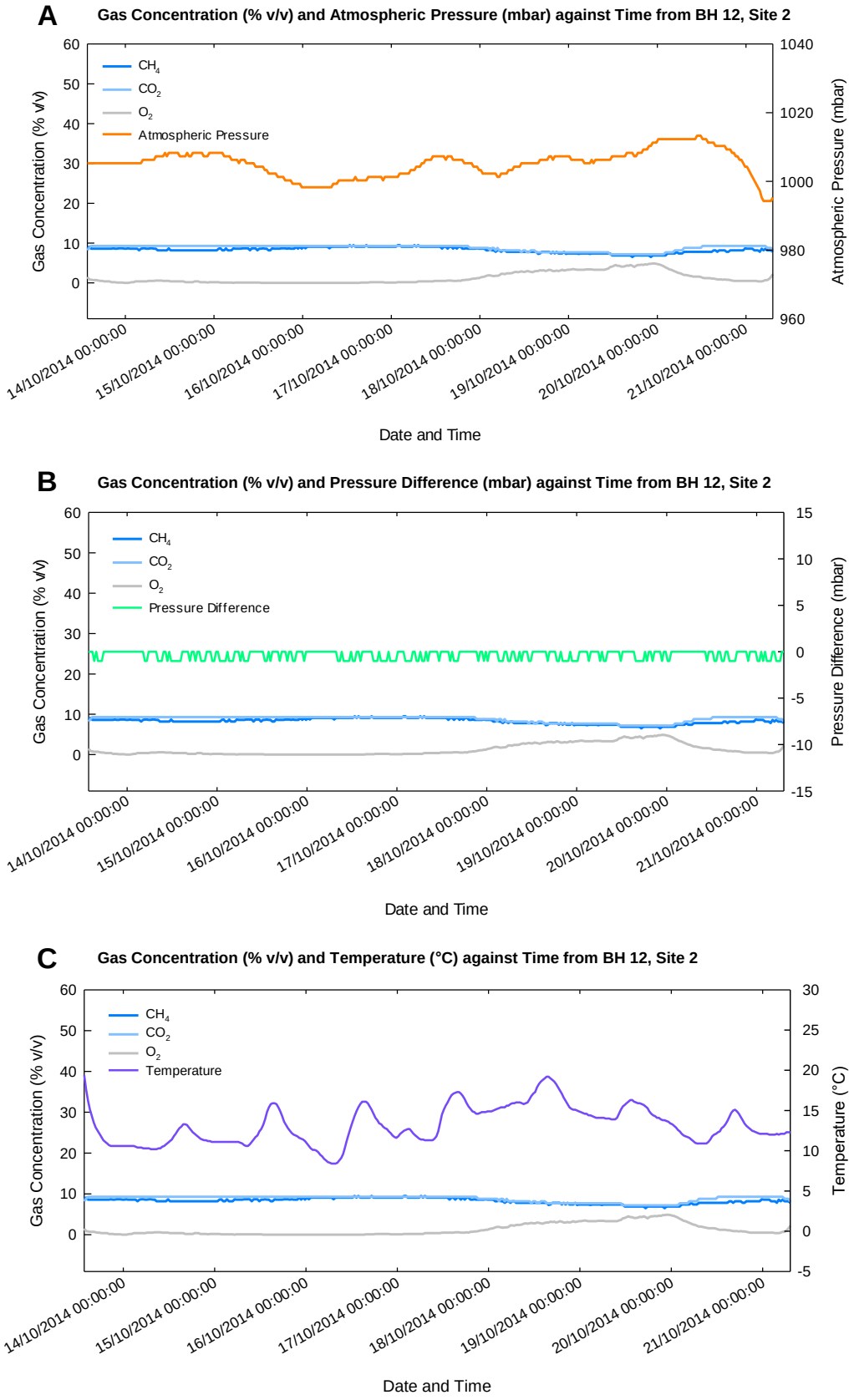

Figure I.6: Site 2, BH 12 High Temporal Frequency Gas Data (13/10/2014 – 21/10/2014)

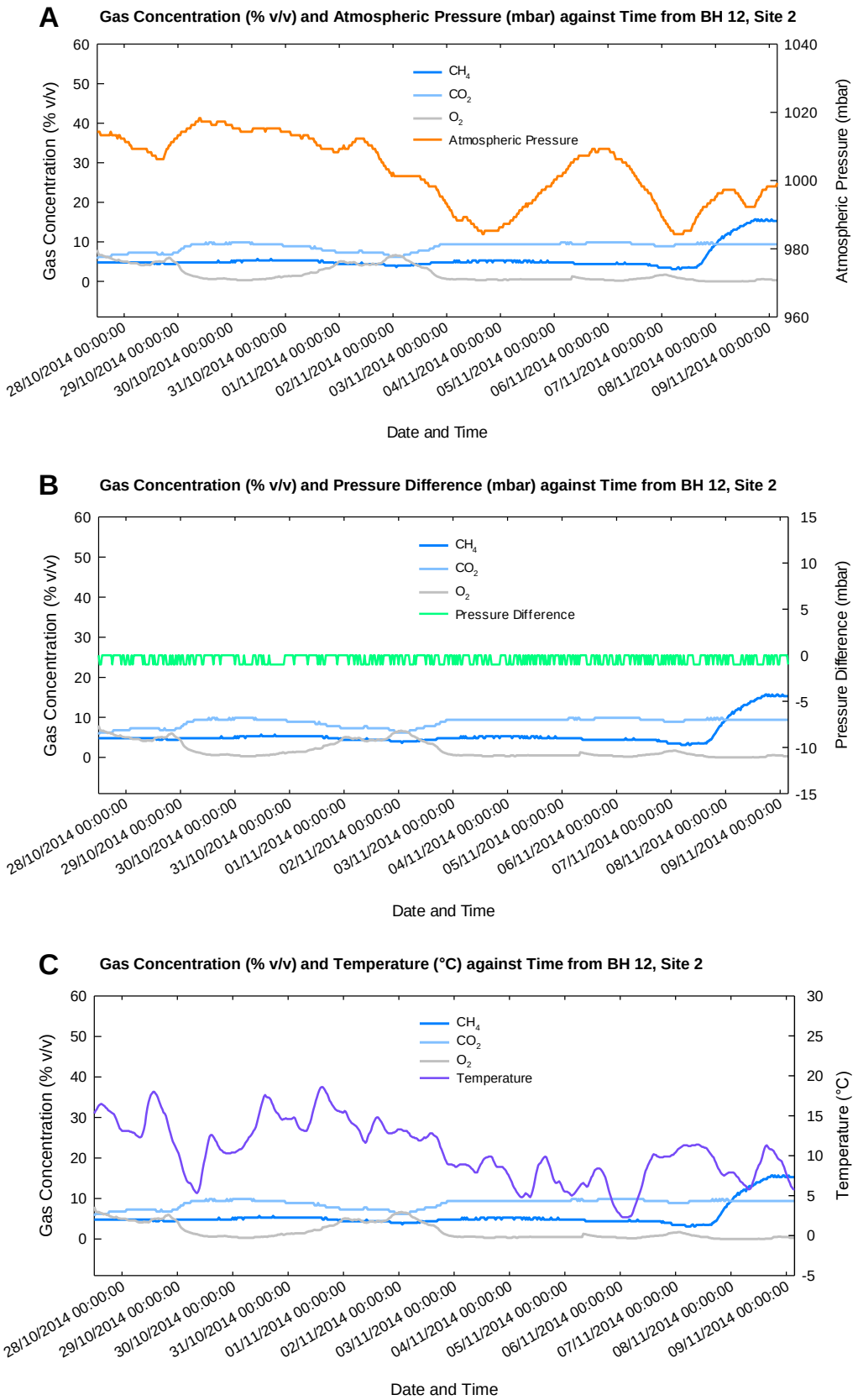

Figure I.7: Site 2, BH 12 High Temporal Frequency Gas Data (27/10/2014 – 09/11/2014)

BH 14

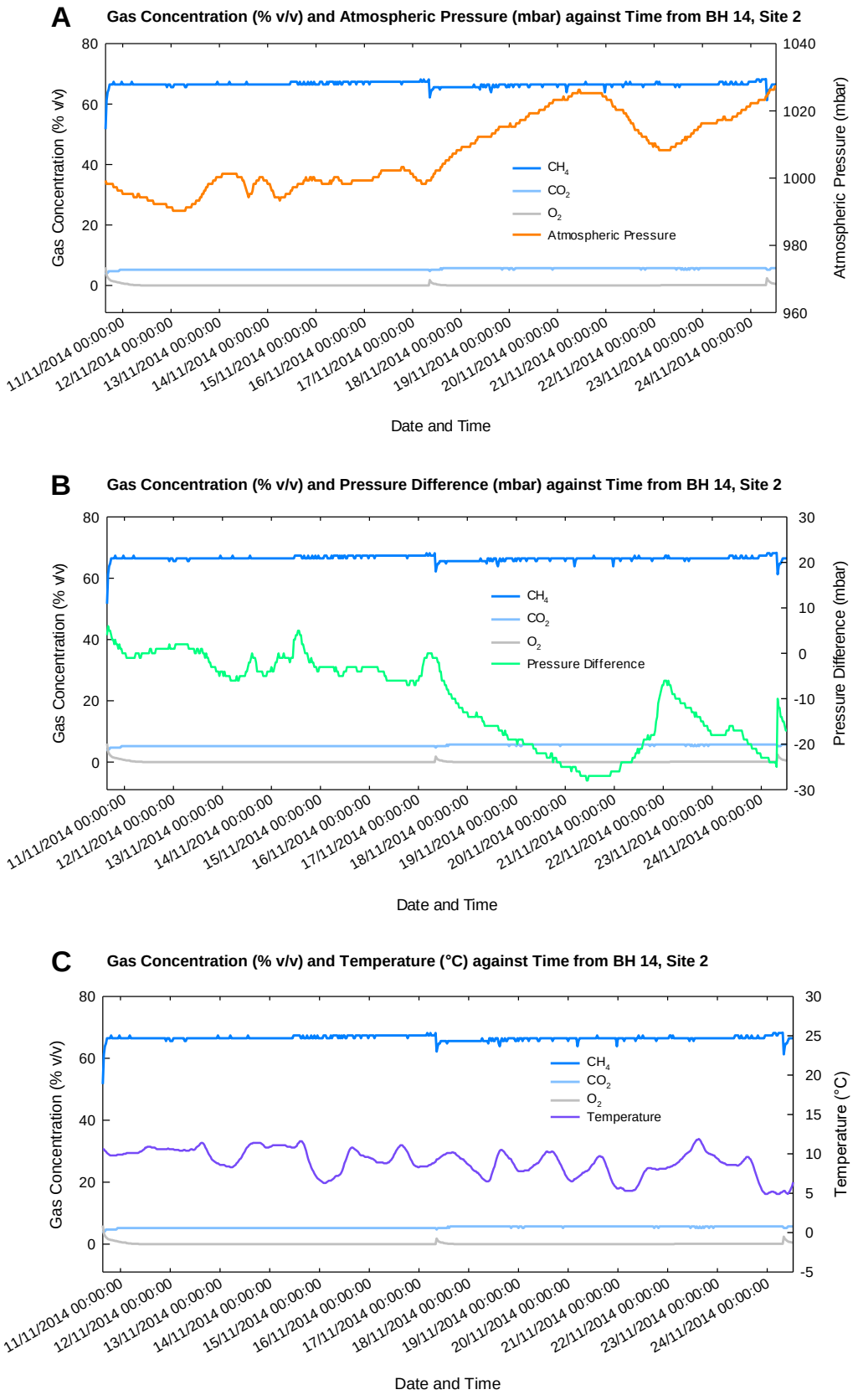

Figure I.8: Site 2, BH 14 High Temporal Frequency Gas Data (10/11/2014 – 24/11/2014)

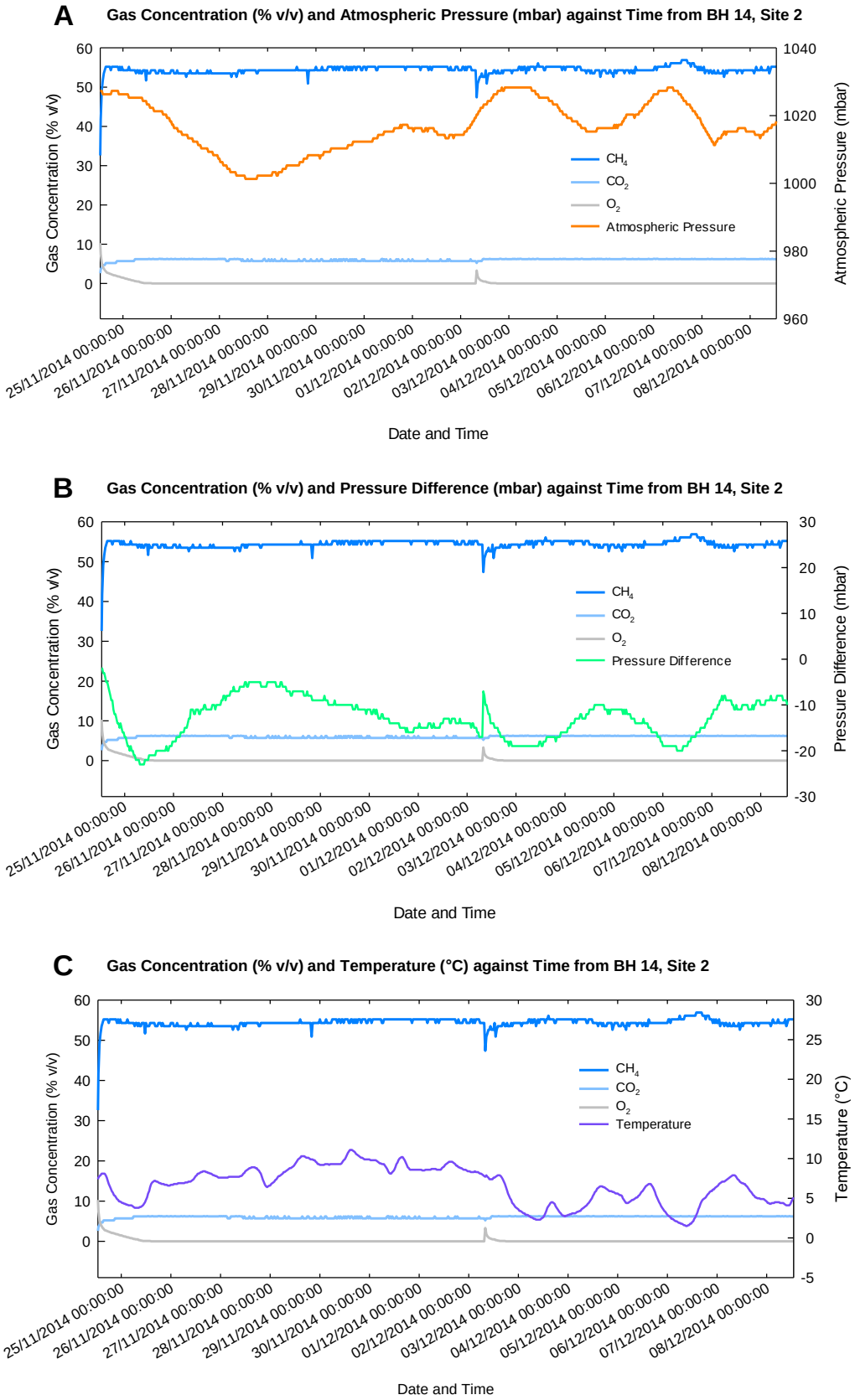

Figure I.9: Site 2, BH 14 High Temporal Frequency Gas Data (24/11/2014 – 08/12/2014)

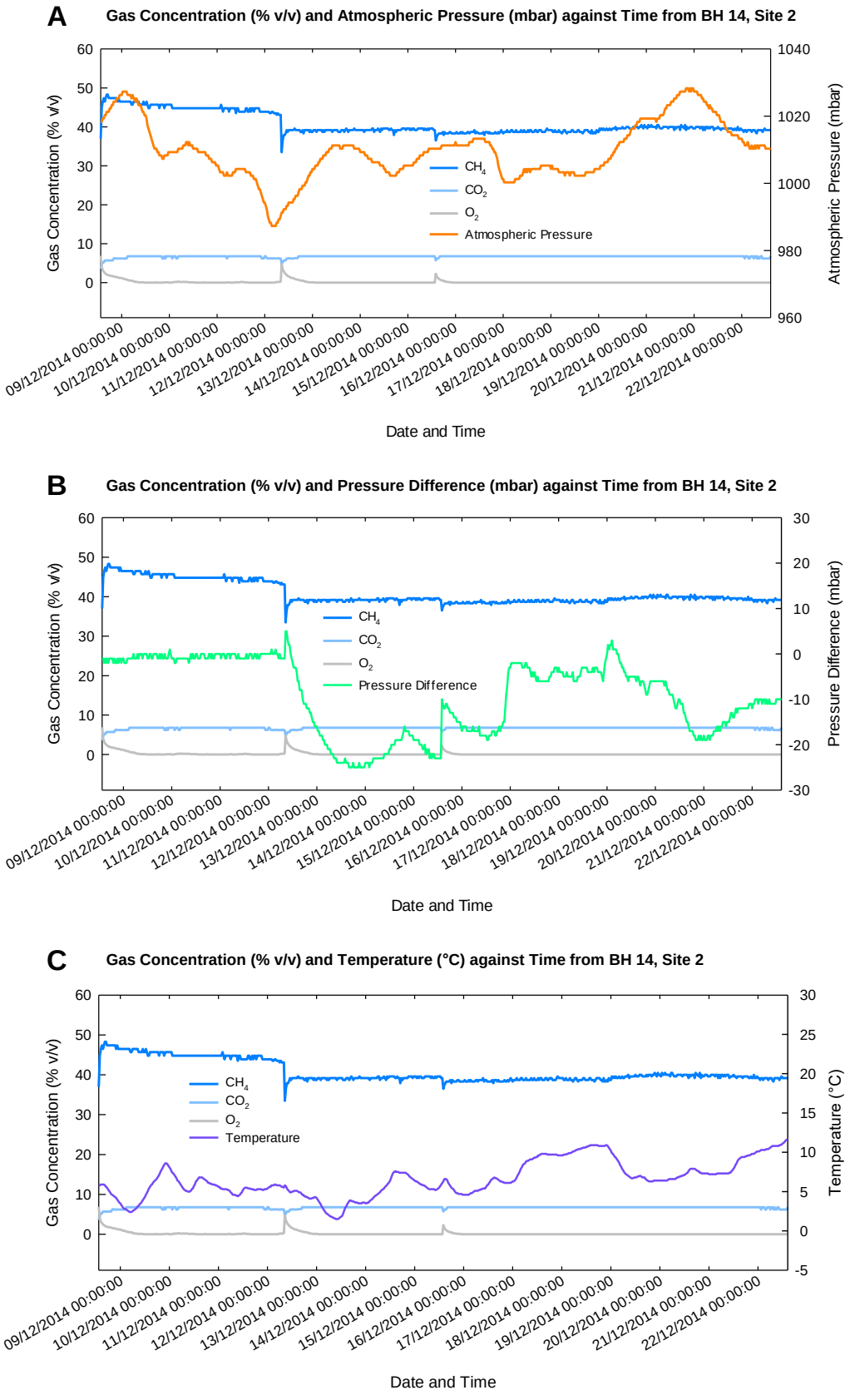

Figure I.10: Site 2, BH 14 High Temporal Frequency Gas Data (08/12/2014 – 22/12/2014)

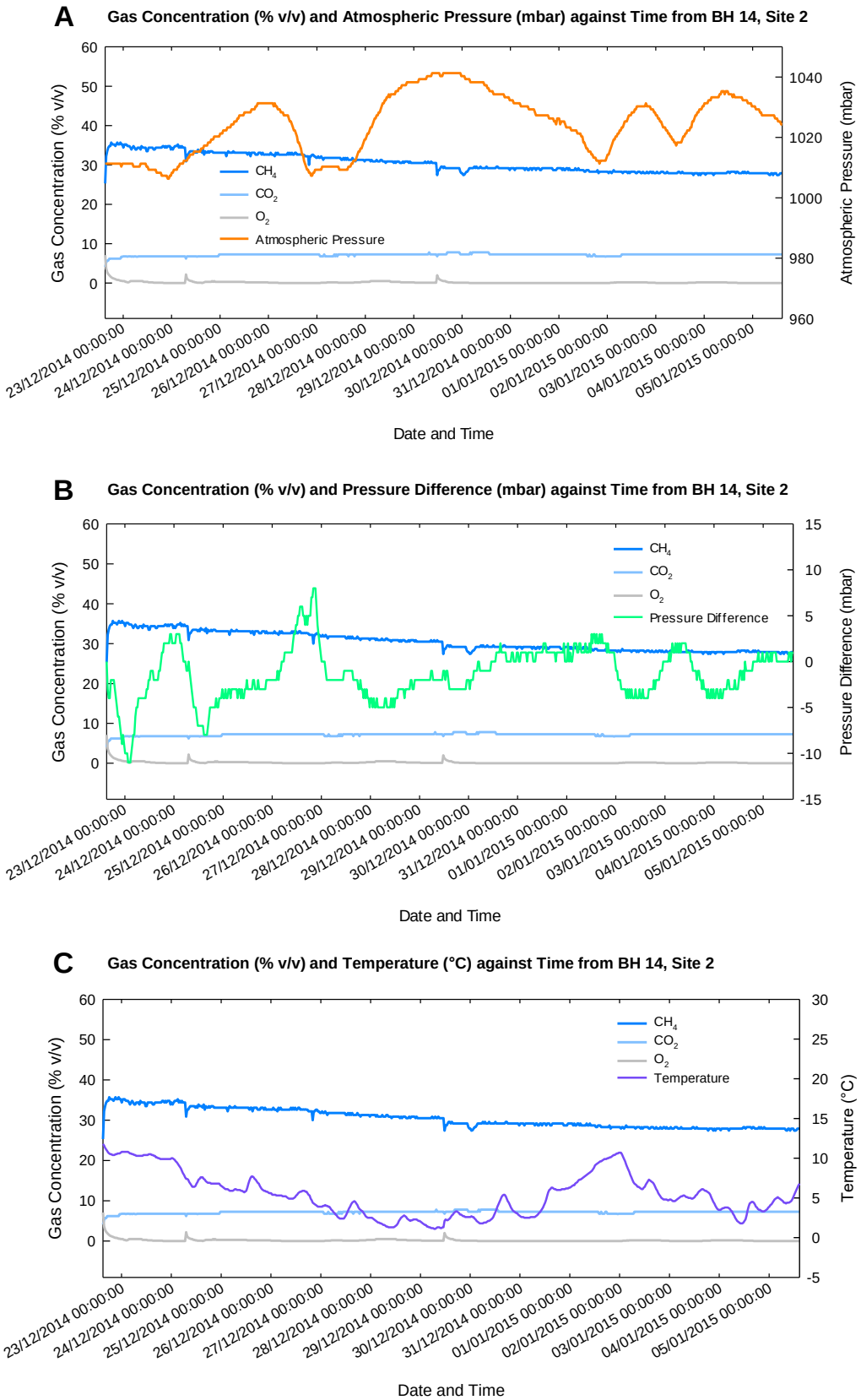

Figure I.11: Site 2, BH 14 High Temporal Frequency Gas Data (22/12/2014 – 05/01/2015)

Appendix J

Raw Stable Isotope Data

Newcastle University Raw Stable Isotope Data

For Table J.1:

- Reference Peak time = 125 & 2,910
- Reference Internal = 4.2
- Reference $^{13}\delta$C = $-37‰$

Sample ID	Amt Inj (μl)	Inj Time (s)	CH_4 Pk Time (s)	CH_4 Int	$^{13}\delta C_{CH_4}$ (‰)	CO_2 Pk Time (s)	CO_2 Int	$^{13}\delta C_{CO_2}$ (‰)
1% CH_4/CO_2 (a)	100	150	340	3.5	−43	400	3.5	−38
1% CH_4/CO_2 (b)	100	250	440	3.5	−43	500	3.5	−38
1% CH_4/CO_2 (c)	100	350	540	3.5	−43	600	3.5	−38
S2 BH 12 Smp 8 (a)	60	450	640	2.0	−48	700	8.0	−33
S2 BH 12 Smp 8 (b)	60	550	740	2.0	−48	800	8.0	−32
S2 BH 12 Smp 8 (c)	60	650	840	2.0	−48	900	8.0	−33
S2 Flare Smp 4 (a)	5	750	940	6.0	−65	1,000	3.0	+5
S2 Flare Smp 4 (b)	5	850	1,040	6.0	−65	1,100	3.0	+5
S2 Flare Smp 4 (c)	5	950	1,140	6.0	−65	1,200	3.0	+5
S2 BH 08 Smp 5 (a)	60	1,050	1,240	3.5	−55	1,300	6.5	−29
S2 BH 08 Smp 5 (b)	60	1,150	1,340	3.5	−55	1,400	6.5	−28
S2 BH 08 Smp 5 (c)	60	1,250	1,440	3.5	−55	1,500	6.5	−29
S2 BH 04 Smp 8 (a)	20	1,350	1,540	8.5	−55	1,600	2.0	−47
S2 BH 04 Smp 8 (b)	20	1,450	1,640	8.5	−54	1,700	2.0	−47
S2 BH 04 Smp 8 (c)	20	1,550	1,740	8.5	−55	1,800	2.0	−47
S2 LFC Smp 8 (a)	60	1,650	1,840	8.0	−64	1,900	5.0	+5
S2 LFC Smp 8 (b)	60	1,750	1,840	8.0	−64	2,000	5.0	+4
S2 LFC Smp 8 (c)	60	1,850	2,040	8.0	−63	2,100	5.0	+5
60% CH_4/40% CO_2 (a)	5	1,950	2,140	8.5	−44	2,200	6.0	−38
60% CH_4/40% CO_2 (b)	5	2,050	2,240	8.5	−44	2,300	6.0	−40
60% CH_4/40% CO_2 (c)	5	2,150	2,340	8.5	−44	2,400	6.0	−40
100% CO_2 (a)	5	2,250	2,440	0.0	0	2,500	9.0	−31
100% CO_2 (b)	5	2,350	2,540	0.0	0	2,600	10.0	−31
100% CH_4 (a)	5	2,450	2,640	14.0	−56	2,700	0.0	0
100% CH_4 (b)	5	2,550	2,740	14.0	−56	2,800	0.0	0
1% CH_4/CO_2	100	150	340	3.0	−43	400	3.0	−38
60% CH_4/40% CO_2	5	250	440	7.0	−45	500	4.0	−41
Mineshaft 2 Smp 4 (a)	10	350	540	8.0	−51	600	0.2	−49
Mineshaft 2 Smp 4 (b)	10	450	640	9.0	−51	700	0.2	−49
Mineshaft 2 Smp 5 (a)	10	550	740	7.0	−51	800	0.2	−49
Mineshaft 2 Smp 5 (b)	10	650	840	9.0	−51	900	0.2	−50
Mineshaft 2 Smp 6 (a)	10	750	940	8.0	−51	1,000	0.2	−46
Mineshaft 2 Smp 6 (b)	10	850	1,040	8.0	−50	1,100	0.2	−45

Sample ID	Amt Inj (μl)	Inj Time (s)	CH_4 Pk Time (s)	CH_4 Int	$^{13}\delta C_{CH_4}$ (‰)	CO_2 Pk Time (s)	CO_2 Int	$^{13}\delta C_{CO_2}$ (‰)
Mineshaft 2 Smp 7 (a)	10	950	1,140	9.0	−50	1,200	0.2	−44
Mineshaft 2 Smp 7 (b)	10	1,050	1,240	7.0	−50	1,300	0.2	−45
Mineshaft 2 Smp 7 (c)	10	1,150	1,340	8.0	−51	1,400	0.2	−45
Mineshaft 2 Smp 8 (a)	5	1,250	1,440	3.0	−50	1,500	0.2	−46
Mineshaft 2 Smp 8 (b)	5	1,350	1,540	3.0	−50	1,600	0.2	−45
Mineshaft 2 Smp 9 (a)	5	1,450	1,640	3.0	−50	1,700	0.2	−40
Mineshaft 2 Smp 9 (b)	5	1,550	1,740	3.0	−50	1,800	0.2	−45
Mineshaft 2 Smp 10 (a)	60	1,650	1,840	40.0	n/a	1,900	0.2	−46
Mineshaft 2 Smp 10 (b)	60	1,750	1,940	40.0	n/a	2,000	0.2	−46
Mineshaft 2 Smp 10 (c)	10	1,850	2,040	9.0	−51	2,100	0.2	−46
100% CH_4	5	1,950	2,140	7.0	−57	2,200	0.2	−25
100% CO_2	5	2,050	2,240	0.1	n/a	2,300	5.0	−31
North Sea Gas	5	2,150	2,340	10.0	−44	2,400	0.2	−14
10% CH_4/CO_2	5	2,250	2,440	2.0	−38	2,500	1.5	−34
Breath (a)	50	2,350	2,540	0.1	n/a	2,600	4.0	−26
Breath (b)	50	2,450	2,640	0.1	n/a	2,700	5.0	−26
1% CH_4/CO_2 (a)	100	150	340	3.5	−43	400	3.5	−38
1% CH_4/CO_2 (b)	100	250	440	3.5	−43	500	3.5	−38
1% CH_4/CO_2 (c)	100	350	540	3.5	−43	600	3.5	−38
S2 BH 04 Smp 11 (a)	20	450	640	5.0	−57	700	1.5	−47
S2 BH 04 Smp 11 (b)	20	550	740	5.0	−55	800	1.5	−47
S2 BH 04 Smp 11 (c)	20	650	840	5.0	−55	900	1.5	−47
S1 BH 03/4 Smp 10 (a)	100	750	940	1.5	−62	1,000	1.0	−49
S1 BH 03/4 Smp 10 (b)	100	850	1,040	1.5	−63	1,100	1.0	−49
S1 BH 03/4 Smp 10 (c)	100	950	1,140	1.5	−63	1,200	1.0	−49
S1 BH 03/6 Smp 4 (a)	100	1,050	1,240	0.5	0	1,300	0.5	−14
S1 BH 03/6 Smp 4 (b)	100	1,150	1,340	0.5	0	1,400	0.5	−13
S1 BH 03/6 Smp 4 (c)	100	1,250	1,440	0.5	0	1,500	0.5	−13
S1 BH 03/4 Smp 9 (a)	100	1,350	1,540	1.0	−55	1,600	1.0	−49
S1 BH 03/4 Smp 9 (b)	100	1,450	1,640	1.0	−55	1,700	1.0	−49
S1 BH 03/4 Smp 9 (c)	100	1,550	1,740	1.0	−55	1,800	1.0	−48
S1 BH 03/7 Smp 4 (a)	20	1,650	1,840	8.0	−61	1,900	3.5	−51
S1 BH 03/7 Smp 4 (b)	20	1,750	1,940	8.0	−61	2,000	3.5	−51
S1 BH 03/7 Smp 4 (c)	20	1,850	2,040	8.0	−61	2,100	3.5	−51
60% CH_4/40% CO_2 (a)	5	1,950	2,140	10.0	−44	2,200	6.0	−41
60% CH_4/40% CO_2 (b)	5	2,050	2,240	10.0	−44	2,300	6.0	−41
60% CH_4/40% CO_2 (c)	5	2,150	2,340	10.0	−44	2,400	6.0	−41
100% CO_2 (a)	5	2,250	2,440	0.0	0	2,500	9.0	−32
100% CO_2 (b)	5	2,350	2,540	0.0	0	2,600	10.0	−31
100% CH_4 (a)	5	2,450	2,640	12.0	−56	2,700	0.0	0
100% CH_4 (b)	5	2,550	2,740	12.0	−56	2,800	0.0	0
1% CH_4/CO_2 (a)	100	150	340	3.0	−43	400	3.0	−38
1% CH_4/CO_2 (b)	100	250	440	3.0	−43	500	3.0	−38
Mineshaft 1 Smp 4 (a)	5	350	540	7.0	−48	600	0.2	−10
Mineshaft 1 Smp 4 (b)	5	450	640	7.0	−47	700	0.2	−10
Mineshaft 1 Smp 5 (a)	5	550	740	7.0	−46	800	0.2	−9
Mineshaft 1 Smp 5 (b)	5	650	840	7.0	−46	900	0.2	−9
Mineshaft 1 Smp 6 (a)	5	750	940	7.0	−46	1,000	0.2	−11
Mineshaft 1 Smp 6 (b)	5	850	1,040	7.0	−46	1,100	0.2	−12
Mineshaft 1 Smp 7 (a)	5	950	1,140	7.0	−46	1,200	0.2	−13
Mineshaft 1 Smp 7 (b)	5	1,050	1,240	7.0	−46	1,300	0.2	−10
Mineshaft 1 Smp 8 (a)	5	1,150	1,340	7.0	−46	1,400	0.2	−11
Mineshaft 1 Smp 8 (b)	5	1,250	1,440	7.0	−46	1,500	0.2	−13
Mineshaft 1 Smp 9 (a)	5	1,350	1,540	7.0	−46	1,600	0.2	−13
Mineshaft 1 Smp 9 (b)	5	1,450	1,640	7.0	−46	1,700	0.2	−11
Mineshaft 1 Smp 10 (a)	5	1,550	1,740	7.0	−46	1,800	0.2	−10
Mineshaft 1 Smp 10 (b)	5	1,650	1,840	6.0	−46	1,900	0.2	−11
60% CH_4/40% CO_2 (a)	5	1,750	1,940	7.0	−46	2,000	4.0	−41
60% CH_4/40% CO_2 (b)	10	1,850	2,040	12.0	−42	2,100	6.0	−41
10% CH_4/CO_2	5	1,950	2,140	1.0	−39	2,200	1.0	−36
100% CO_2	5	2,050	2,240	0.0	0	2,300	4.0	−31
100% CH_4	5	2,150	2,340	7.0	−56	2,400	0.0	0
1% CH_4/CO_2	100	150	340	3.5	−43	400	3.0	−38
S2 BH 12 Smp 4 (a)	60	250	440	2.5	−48	500	8.0	−33
S2 BH 12 Smp 4 (b)	60	350	540	2.5	−48	600	8.0	−33
S2 BH 12 Smp 5 (a)	60	450	640	2.0	−48	700	6.0	−32
S2 BH 12 Smp 5 (b)	60	550	740	2.0	−48	800	6.0	−33
S2 BH 12 Smp 6 (a)	60	650	840	3.0	−48	900	8.0	−33

Sample ID	Amt Inj (μl)	Inj Time (s)	CH_4 Pk Time (s)	CH_4 Int	$^{13}\delta C_{CH_4}$ (‰)	CO_2 Pk Time (s)	CO_2 Int	$^{13}\delta C_{CO_2}$ (‰)
S2 BH 12 Smp 6 (b)	60	750	940	3.0	−48	1,000	8.0	−33
S2 BH 12 Smp 7 (a)	60	850	1,040	3.0	−48	1,100	8.0	−33
S2 BH 12 Smp 7 (b)	60	950	1,140	3.0	−48	1,200	8.0	−33
S1 BH 03/4 Smp 4 (a)	10	1,050	1,240	5.5	−55	1,300	2.0	−58
S1 BH 03/4 Smp 4 (b)	10	1,150	1,340	5.5	−55	1,400	2.0	−58
S1 BH 03/4 Smp 5 (a)	10	1,250	1,440	3.5	−55	1,500	2.0	−60
S1 BH 03/4 Smp 5 (b)	10	1,350	1,540	3.5	−59	1,600	2.0	−60
S1 BH 03/4 Smp 6 (a)	20	1,450	1,640	6.0	−59	1,700	4.0	−61
S1 BH 03/4 Smp 6 (b)	20	1,550	1,740	6.0	−59	1,800	4.0	−60
S1 BH 03/4 Smp 7 (a)	20	1,650	1,840	6.0	−59	1,900	4.0	−60
S1 BH 03/4 Smp 7 (b)	20	1,750	1,940	6.0	−59	2,000	4.0	−60
S1 BH 03/4 Smp 8 (a)	20	1,850	2,040	6.0	−59	2,100	4.0	−60
S1 BH 03/4 Smp 8 (b)	20	1,950	2,140	6.0	−59	2,200	4.0	−60
S2 BH 08 Smp 4 (a)	20	2,050	2,240	2.0	−54	2,300	3.0	−30
S2 BH 08 Smp 4 (b)	20	2,150	2,340	2.0	−55	2,400	3.0	−29
S2 BH 08 Smp 7 (a)	10	2,250	2,440	4.5	−56	2,500	2.0	−47
S2 BH 08 Smp 7 (b)	10	2,350	2,540	4.5	−55	2,600	2.0	−47
S2 BH 08 Smp 6 (a)	10	2,450	2,640	4.5	−55	2,700	2.0	−47
S2 BH 08 Smp 6 (b)	10	2,550	2,740	4.5	−55	2,800	2.0	−47
10% CH_4/CO_2	5	2,650	2,840	1.5	−42	2,900	1.0	−35
100% CH_4	5	2,750	2,940	7.0	−56	3,000	0.0	0
100% CO_2	5	2,850	3,040	0.0	0	3,100	6.0	−31
North Sea Gas	5	2,950	3,140	7.0	−43	3,200	0.3	−17
1% CH_4/CO_2	100	150	340	3.5	−43	400	3.5	−38
60% CH_4/40% CO_2	5	250	440	6.0	−44	500	3.5	−41
S2 BH 04 Smp 4 (a)	10	450	640	4.0	−56	700	1.0	−47
S2 BH 04 Smp 4 (b)	10	550	740	4.0	−55	800	1.0	−47
S2 BH 04 Smp 5 (a)	10	650	840	4.0	−56	900	1.0	−47
S2 BH 04 Smp 5 (b)	10	750	940	4.0	−56	1,000	1.0	−47
S2 BH 04 Smp 6 (a)	10	850	1,040	4.0	−56	1,100	1.0	−47
S2 BH 04 Smp 6 (b)	10	950	1,140	4.0	−56	1,200	1.0	−47
S2 BH 04 Smp 7 (a)	10	1,050	1,240	4.0	−56	1,300	1.0	−47
S2 BH 04 Smp 7 (b)	10	1,150	1,340	4.0	−56	1,400	1.0	−47
S2 LFC Smp 4 (a)	10	1,250	1,440	6.0	−65	1,500	4.0	+5
S2 LFC Smp 4 (b)	10	1,350	1,540	7.0	−65	1,600	4.0	+6
S2 LFC Smp 5 (a)	10	1,450	1,640	7.0	−65	1,700	4.0	+6
S2 LFC Smp 5 (b)	10	1,550	1,740	7.0	−65	1,800	4.0	+6
S2 LFC Smp 6 (a)	10	1,650	1,840	7.0	−65	1,900	4.0	+6
S2 LFC Smp 6 (b)	10	1,750	1,940	7.0	−65	2,000	4.0	+6
S2 LFC Smp 7 (a)	10	1,850	2,040	7.0	−65	2,100	4.0	+6
S2 LFC Smp 7 (b)	10	1,950	2,140	7.0	−65	2,200	4.0	+6
100% CH_4	5	2,050	2,240	9.0	−57	2,300	0.0	0
100% CO_2	5	2,150	2,340	0.0	0	2,400	4.0	−31
Breath	40	2,250	2,440	0.0	0	2,500	3.5	−27
North Sea Gas	5	2,350	2,540	8.0	−43	2,600	0.5	0
10% CH_4/CO_2	5	2,450	2,640	2.0	−37	2,700	1.0	−34

Table J.1: Raw Stable Isotope Data compiled at Newcastle University for $^{13}\delta C_{CH_4}$ ‰ and $^{13}\delta C_{CO_2}$ ‰

For Table J.2:

- Reference Peak time = 125 & 2,910
- Reference Internal = 3.5
- Reference δD = +95‰

Sample ID	Amt Inj (μl)	Inj Time (s)	CH_4 Pk Time (s)	CH_4 Int	δD_{CH_4} (‰)
60%/40% CH_4/CO_2 (a)	10	200	370	2.0	−193
60%/40% CH_4/CO_2 (b)	10	250	420	2.3	−198
60%/40% CH_4/CO_2 (c)	10	550	720	2.0	−195
60%/40% CH_4/CO_2 (d)	10	600	770	2.0	−196
100% CH_4 (a)	10	300	470	0.5	−198
100% CH_4 (b)	10	350	520	3.0	−189
100% CH_4 (c)	10	1,800	1,970	2.5	−191
100% CH_4 (d)	10	1,850	2,020	2.5	−189
100% CH_4 (e)	10	200	370	2.5	−184
100% CH_4 (f)	10	250	420	2.5	−188
S1 BH 03/7 Smp 10 (a)	100	400	570	0.5	−269
S1 BH 03/7 Smp 10 (b)	100	450	620	0.5	−149
S1 BH 03/7 Smp 10 (c)	100	300	470	0.5	−239
S1 BH 03/7 Smp 10 (d)	100	350	520	0.5	−269
S1 BH 03/7 Smp 10 (e)	100	400	570	0.5	−249
S1 BH 03/7 Smp 10 (f)	100	750	920	0.5	−260
S1 BH 03/7 Smp 10 (g)	100	800	970	0.5	−235
S2 BH 12 Smp 7 (a)	100	500	670	0.7	+67
S2 BH 12 Smp 7 (b)	100	550	720	0.7	+47
S2 BH 12 Smp 7 (c)	100	660	830	0.7	+48
S2 BH 12 Smp 7 (d)	100	700	870	0.7	+56
S2 LFC Smp 8 (a)	60	600	770	1.5	−315
S2 LFC Smp 8 (b)	60	650	820	1.5	−317
S1 BH 03/4 Smp 7 (a)	30	700	870	1.5	−284
S1 BH 03/4 Smp 7 (b)	30	750	920	1.5	−291
S2 BH 04 Smp 8 (a)	20	800	970	1.5	−177
S2 BH 04 Smp 8 (b)	20	850	1,020	1.5	−167
S2 Flare Smp 4 (a)	10	900	1,070	1.5	−322
S2 Flare Smp 4 (b)	10	950	1,120	1.5	−315
S2 BH 04 Smp 11 (a)	20	1,000	1,170	1.2	−170
S2 BH 04 Smp 11 (b)	20	1,050	1,220	1.2	−168
S2 BH 04 Smp 7 (a)	20	1,100	1,270	1.5	−167
S2 BH 04 Smp 7 (b)	20	1,150	1,320	1.5	−163
S1 BH 03/4 Smp 4 (a)	20	1,200	1,370	1.5	−295
S1 BH 03/4 Smp 4 (b)	20	1,250	1,420	1.5	−305
S1 B 03/4 Smp 4 (c)	20	2,160	2,320	1.5	−294
S2 BH 08 Smp 7 (a)	20	1,300	1,470	1.4	−169
S2 BH 08 Smp 7 (b)	20	1,350	1,520	1.4	−168
S2 BH 08 Smp 7 (c)	20	2,210	2,380	1.4	−181
Mineshaft 1 Smp 7 (a)	5	1,400	1,570	0.8	−212
Mineshaft 1 Smp 7 (b)	5	1,450	1,620	1.1	−215
Mineshaft 1 Smp 7 (c)	10	2,000	2,170	2.0	−215
North Sea Gas (a)	10	1,500	1,670	3.3	−206
North Sea Gas (b)	10	1,550	1,720	3.3	−206
North Sea Gas (c)	10	460	630	3.0	−199
North Sea Gas (d)	10	510	680	3.0	−201
Mineshaft 2 Smp 4 (a)	10	1,600	1,770	1.0	−213
Mineshaft 2 Smp 4 (b)	10	1,650	1,820	1.0	−208
Mineshaft 2 Smp 4 (c)	10	2,100	2,270	1.0	−204

Table J.2: Raw Stable Isotope Data compiled at Newcastle University for $^{13}\delta C_{CH_4}$ ‰ and $^{13}\delta C_{CO_2}$ ‰

University of California Davis Raw Stable Isotope Data

Sample ID	$^{13}\delta C_{CH_4}$ (‰)	Response (ppmv)	δD_{CH_4} (‰)	Response (ppmv)	$^{13}\delta C_{CO_2}$ (‰)	Response (ppmv)
Site 1 BH 03/4	−54.07	111,749	−307.1	115,445	−57.67	62,359
Site 1 BH 03/6	N/A	N/A	N/A	N/A	−48.92	16,231
Site 1 BH 03/7	−60.60	110,210	−238.1	147,964	−50.48	41,913
Site 2 BH 04	−53.77	134,647	−158.2	112,513	−46.74	32,196
Site 2 BH 08	−53.80	10,782	−137.3	14,182	−28.10	23,226
Site 2 BH 12	−47.06	8,651	+74.0	9,407	−32.79	34,227
Site 2 Flare	−63.58	371,269	−309.8	225,077	+6.96	144,926
Site 2 Landfill Cell	−62.12	172,458	−326.3	157,648	+6.50	120,304
Mineshaft Vent 1	−43.05	1,020,260	−202.6	1,008,411	−9.21	9,250
Mineshaft Vent 2	−49.85	256,954	−204.2	212,987	−48.81	8,270

Table J.3: Stable Isotope Ratios Measured at UC Davis Stable Isotope Facility

$^{13}CH_4$ Calibration Standards			*CD_4 Calibration Standards*			*$^{13}CO_2$ Calibration Standards*		
Standard	Measured $^{13}\delta C_{CH_4}$ (‰)	Known $^{13}\delta C_{CH_4}$ (‰)	Standard	Measured δD_{CH_4} (‰)	Known δD_{CH_4} (‰)	Standard	Measured $^{13}\delta C_{CO_2}$ (‰)	Known $^{13}\delta C_{CO_2}$ (‰)
				Check Standards				
UCDM1-new	−39.05	−39.0	UCDM1-new	−172.1	−175.0	UCDC1	−35.43	−35.40
UCDM1-new	−39.05	−39.0	UCDM1-new	−178.2	−175.0	UCDC1	−35.36	−35.40
UCDM1-new	−39.00	−39.0	UCDM1-new	−174.4	−175.0	UCDC1	−35.29	−35.40
UCDM1-new	−38.97	−39.0	UCDM1-new	−176.3	−175.0	UCDC1	−35.49	−35.40
UCDM1-new	−38.99	−39.0	UCDM1-new	−177.1	−175.0	UCDC1	−35.33	−35.40
UCDM1-new	−38.96	−39.0	UCDM1-new	−171.9	−175.0	UCDC1	−35.43	−35.40
UCDM1-new	−38.93	−39.0				UCDC1	−35.44	−35.40
UCDM1-new	−39.05	−39.0						
UCDM1-new	−38.99	−39.0						
Average	−39.00		Average	−175.0		Average	−35.39	
Std Dev	0.04		Std Dev	2.6		Std Dev	0.07	
				Calibration Standards				
Beecher	−60.91	−60.8	Beecher	−223.8	−223.2	OZ-40	−40.83	−40.81
Beecher	−61.01	−60.8	Beecher	−222.9	−223.2	OZ-40	−40.79	−40.81
			Beecher	−221.2	−223.2	OZ-40	−40.79	−40.81
043332T	−39.82	−39.8	043332T	−163.0	−160.3	OZ-10	−10.48	−10.41
043332T	−39.92	−39.8	043332T	−162.7	−160.3	OZ-10	−10.40	−10.41
			043332T	−160.5	−160.3	OZ-10	−10.40	−10.41
AH024079	−49.32	−49.3	AH024079	−175.2	−173.3	OZ-3	−3.59	−3.57
AH024079	−49.61	−49.3	AH024079	−175.0	−173.3	OZ-3	−3.60	−3.57
			AH024079	−169.7	−173.3	OZ-3	−3.57	−3.57
				Secondary Check Standards				
H iso	−23.92	−23.9	H iso	−162.3	−161.3	0.2% CO_2	−15.30	N/A
H iso	−23.89	−23.9	H iso	−162.4	−161.3	0.2% CO_2	−15.34	N/A
			H iso	−160.0	−161.3	0.2% CO_2	−15.33	N/A
L iso	−66.46	−66.5	L iso	−179.9	−178.2	Outside air	−9.01	N/A
L iso	−66.40	−66.5	L iso	−178.5	−178.2	Outside air	−8.84	N/A
			L iso	−180.0	−178.2	Outside air	−8.57	N/A
B iso	−54.67	−54.5	B iso	−278.3	−276.1	0.5% CO_2	−41.42	N/A
B iso	−54.61	−54.5	B iso	−278.9	−276.1	0.5% CO_2	−51.66	N/A
			B iso	−274.6	−276.1	0.5% CO_2	−41.39	N/A
T iso	−38.44	−38.3	NG1	−186.6	−185.1			
T iso	−38.54	−38.3	NG1	−182.8	−185.1			
NG1	−34.06	−34.2	NG2	−238.2	−237.0			
NG1	−34.62	−34.2	NG2	−235.1	−237.0			
			Scotty	−182.9	−185.0			
			Scotty	−182.1	−185.0			

Table J.4: Calibration Standards Stable Isotope Ratios Measured at UC Davis Stable Isotope Facility

Appendix K

Artificial Borehole Technical Drawings

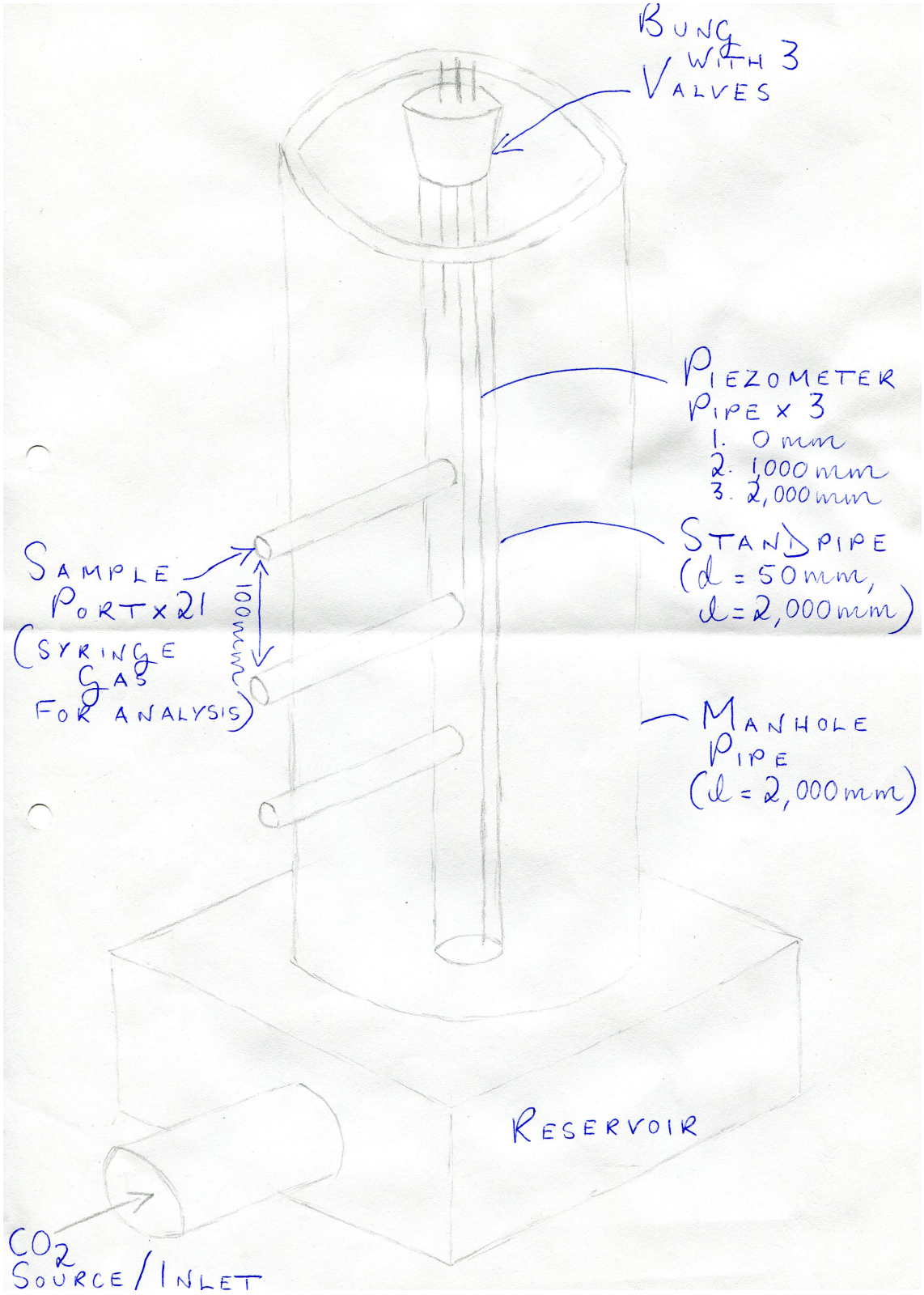

Figure K.1: Artificial Borehole Initial Concept

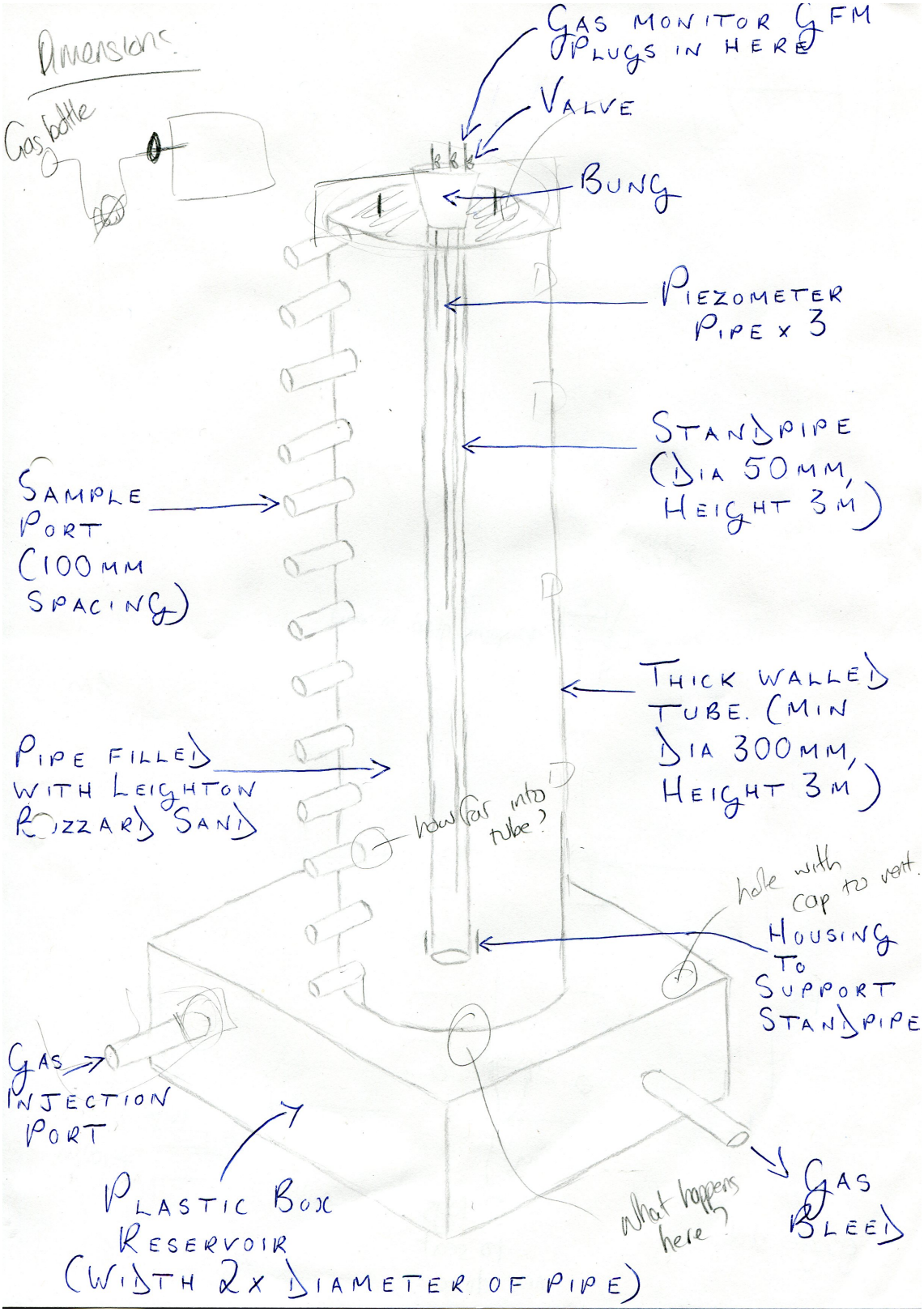

Figure K.2: Refined Artificial Borehole Design

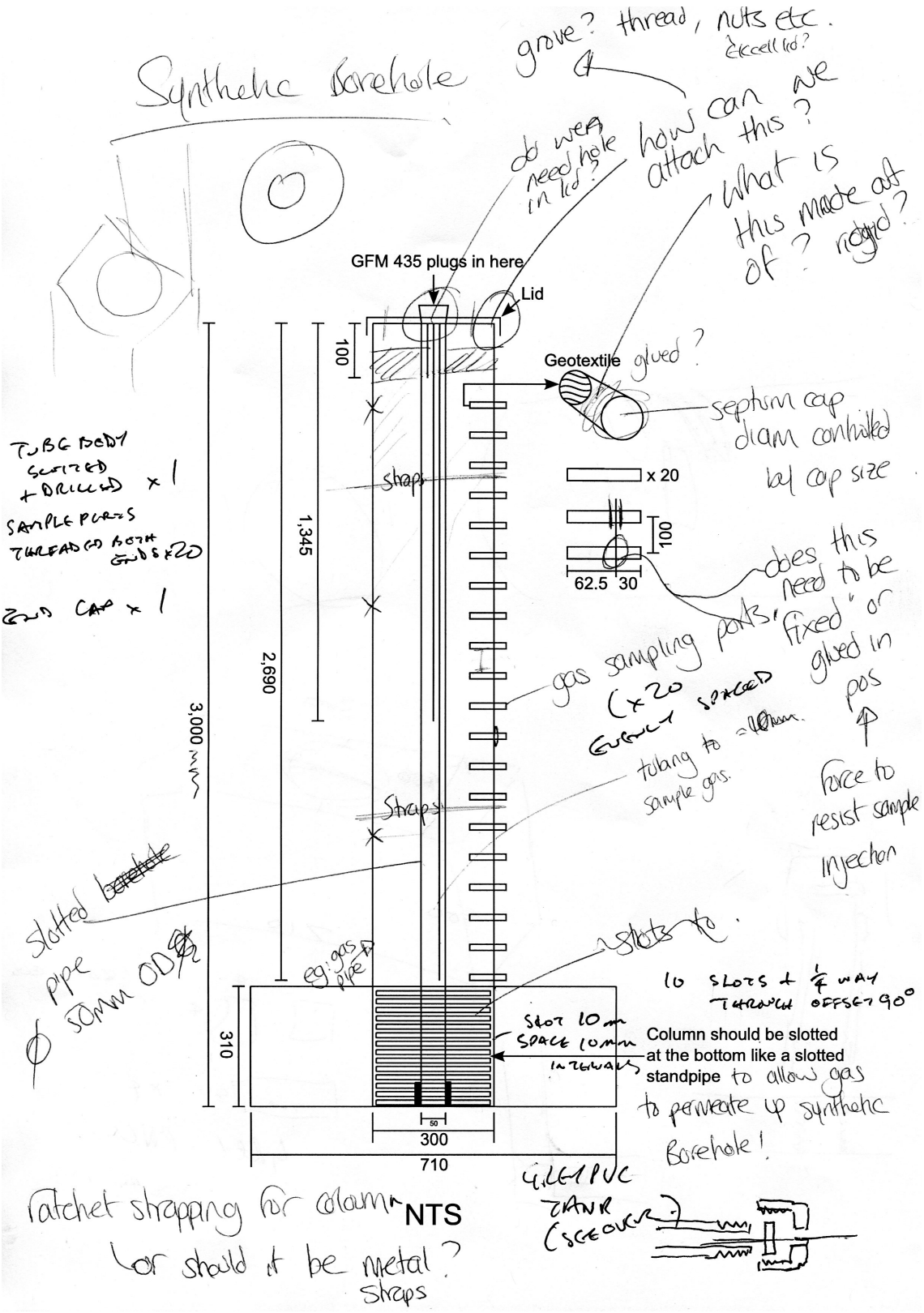

Figure K.3: Artificial Borehole Design Technical Drawing with Annotations

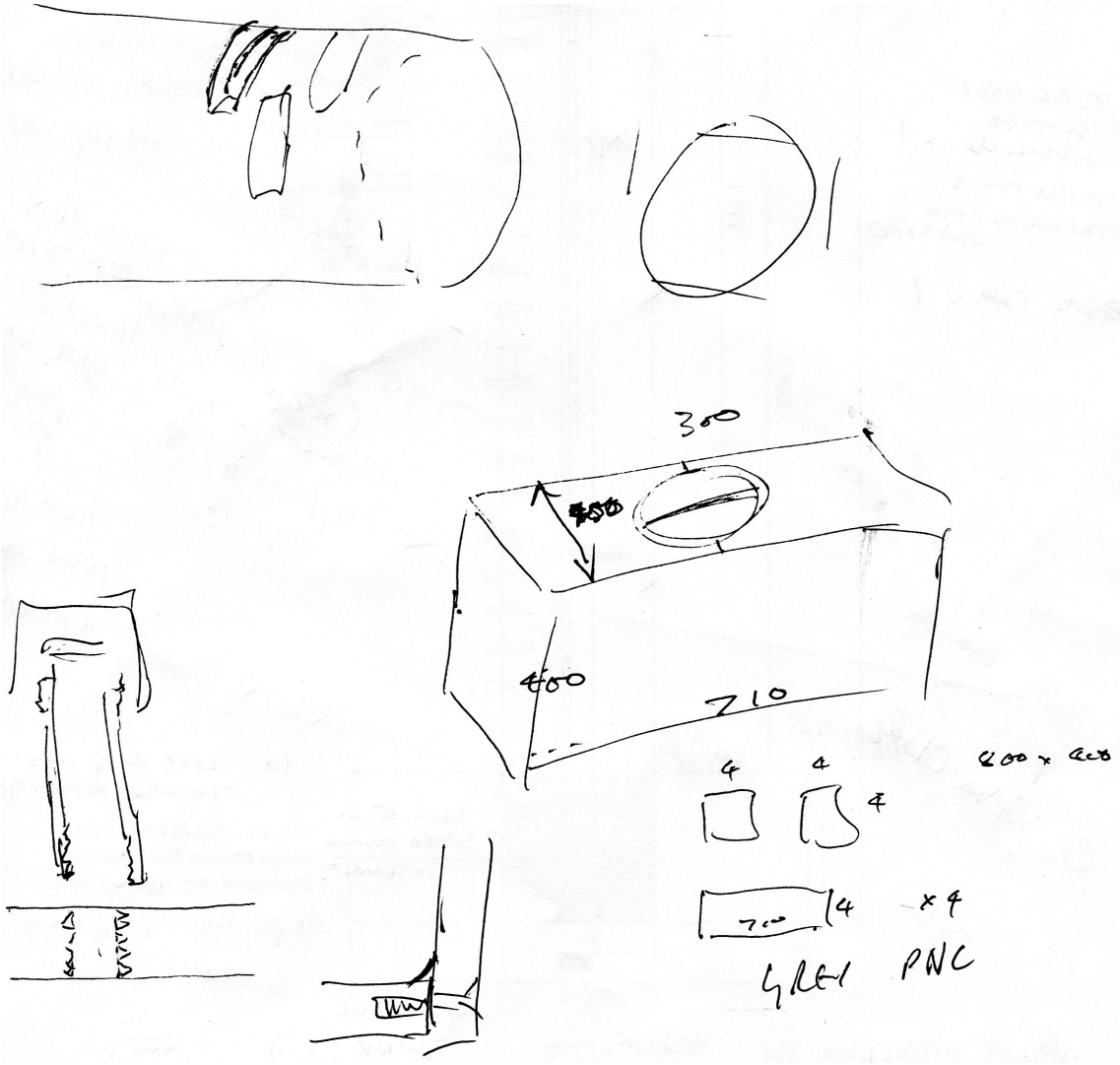

Figure K.4: Artificial Borehole Design Details

Appendix L

Artificial Borehole Ancillary Data

Artificial Borehole Performance, Temperature Change and Rejected Data

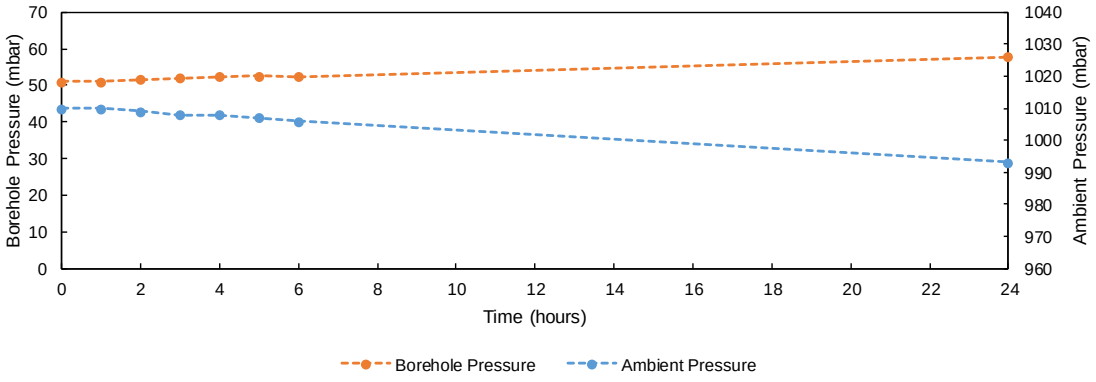

Figure L.1: Artificial Borehole Pressure Change during 100% CO_2 in Air Experiment (12/02/2015 – 13/02/2015)

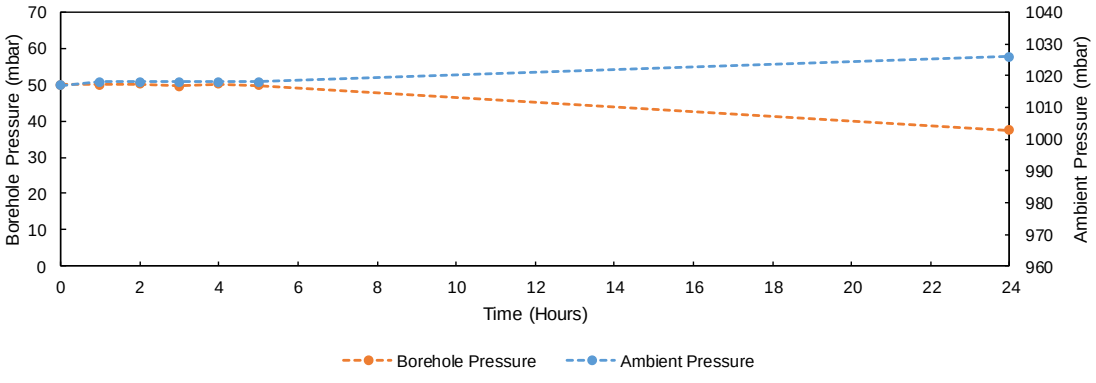

Figure L.2: Artificial Borehole Pressure Change during 20% CO_2 / 10% CH_4 in Air Experiment (17/03/2015 – 18/03/2015)

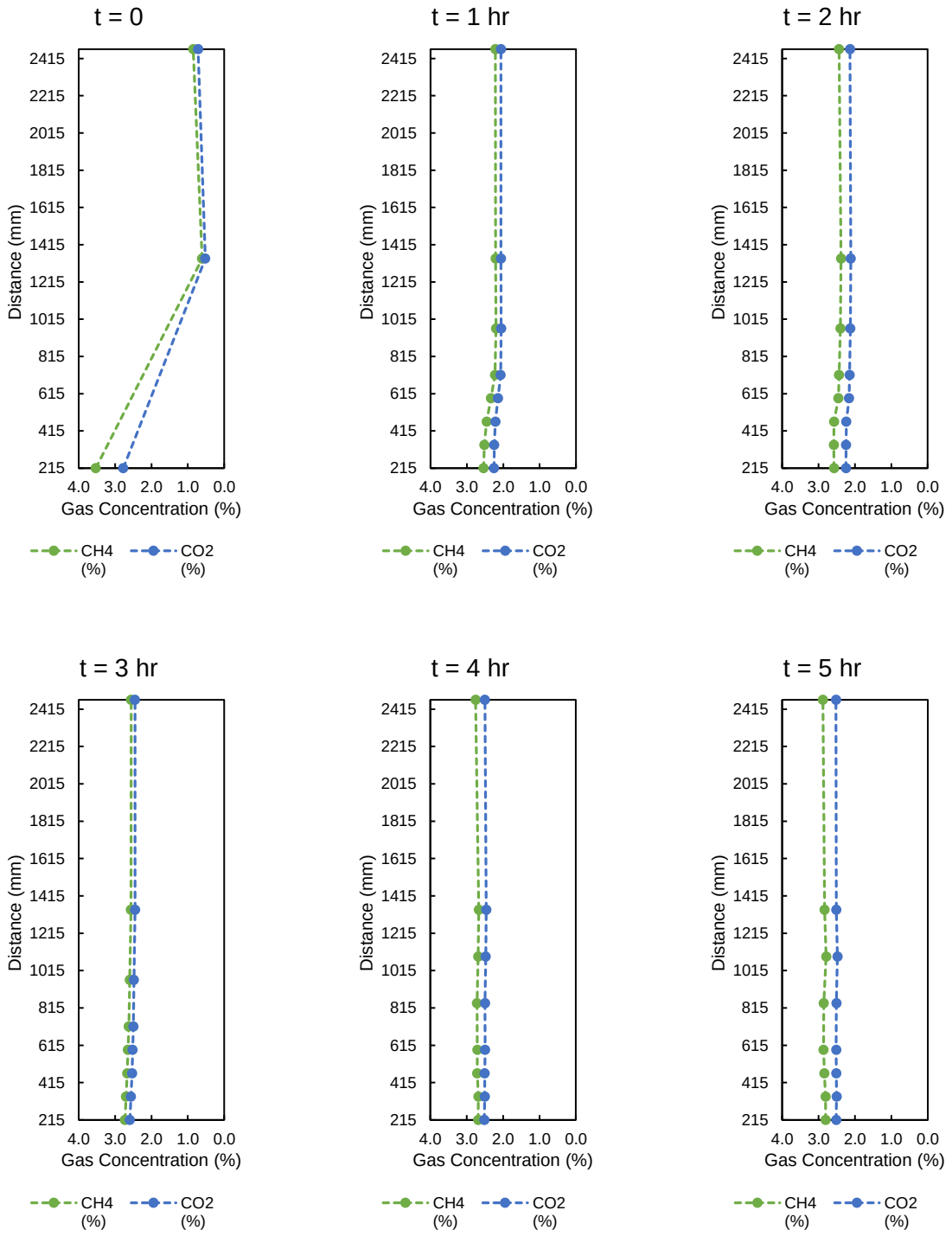

Figure L.3: Artificial Borehole 40% CO_2 / 60% CH_4 in Air Experiment Trial 1 (16/07/2015 – 17/07/2015)

The data from this experiment were rejected owing to the incorrect ratio of CH_4:CO_2 acquired from the GC-MS analysis. The expected ratio of 1.5 was not observed. It was likely that the samples had expired owing to a 2 month time lag between sample acquisition and sample analysis.

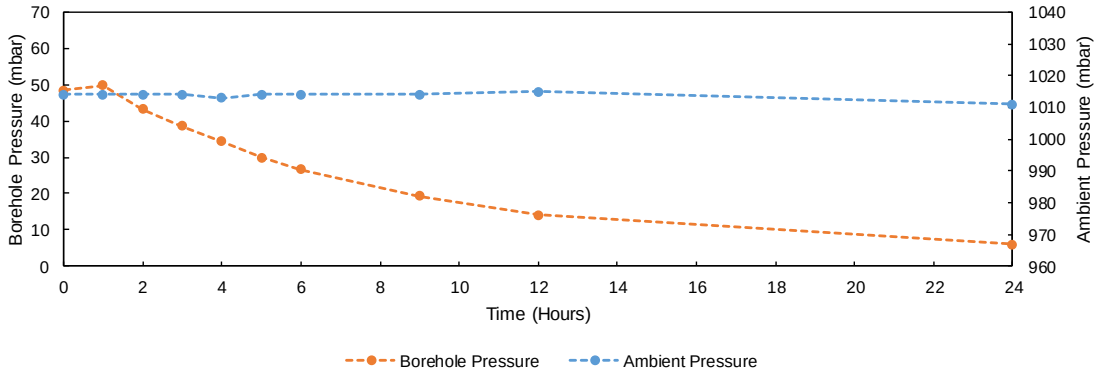

Figure L.4: Artificial Borehole Pressure Change during 40% CO_2 / 60% CH_4 in Air Experiment Trial 1 (16/07/2015 – 17/07/2015)

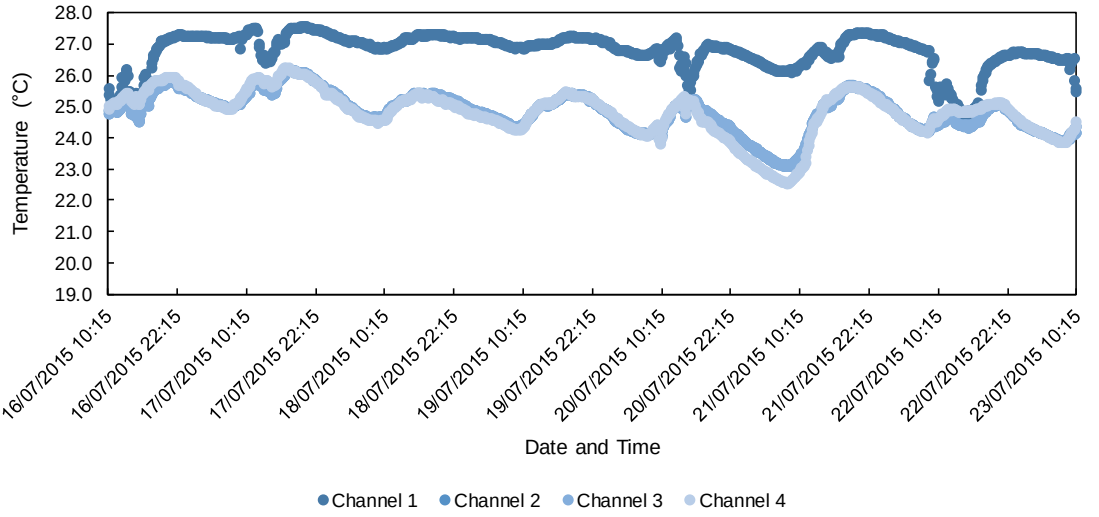

Figure L.5: Artificial Borehole Temperature Change during 40% CO_2 / 60% CH_4 in Air Experiment Trial 1 (16/07/2015 – 23/07/2015)

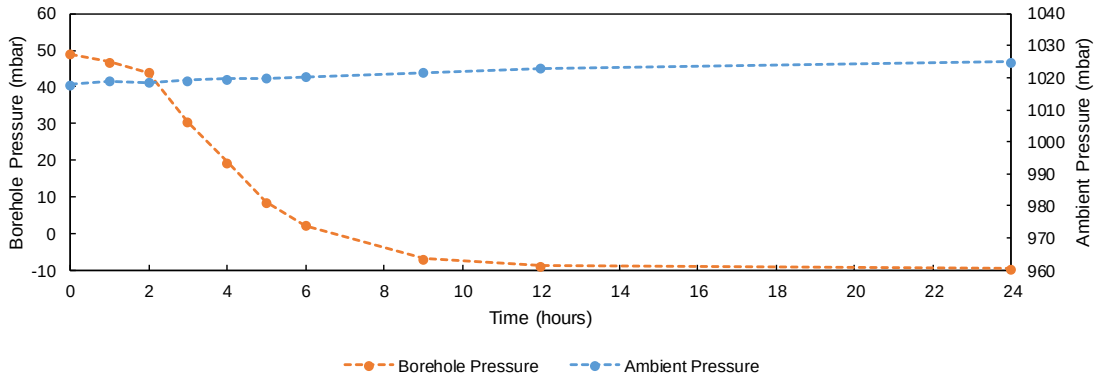

Figure L.6: Artificial Borehole Pressure Change during 40% CO_2 / 60% CH_4 in Air Experiment Trial 2 (31/08/2016 – 01/09/2016)

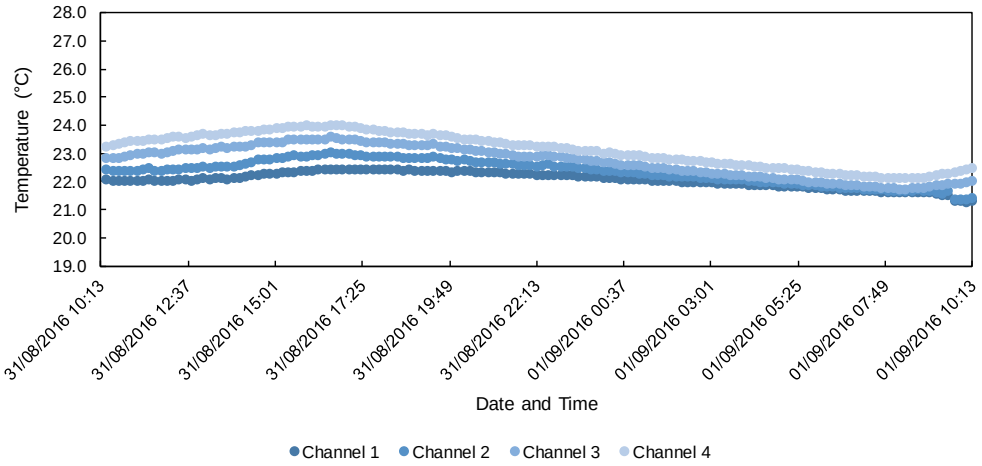

Figure L.7: Artificial Borehole Temperature Change during 40% CO_2 / 60% CH_4 in Air Experiment Trial 2 (31/08/2016 – 01/09/2016)

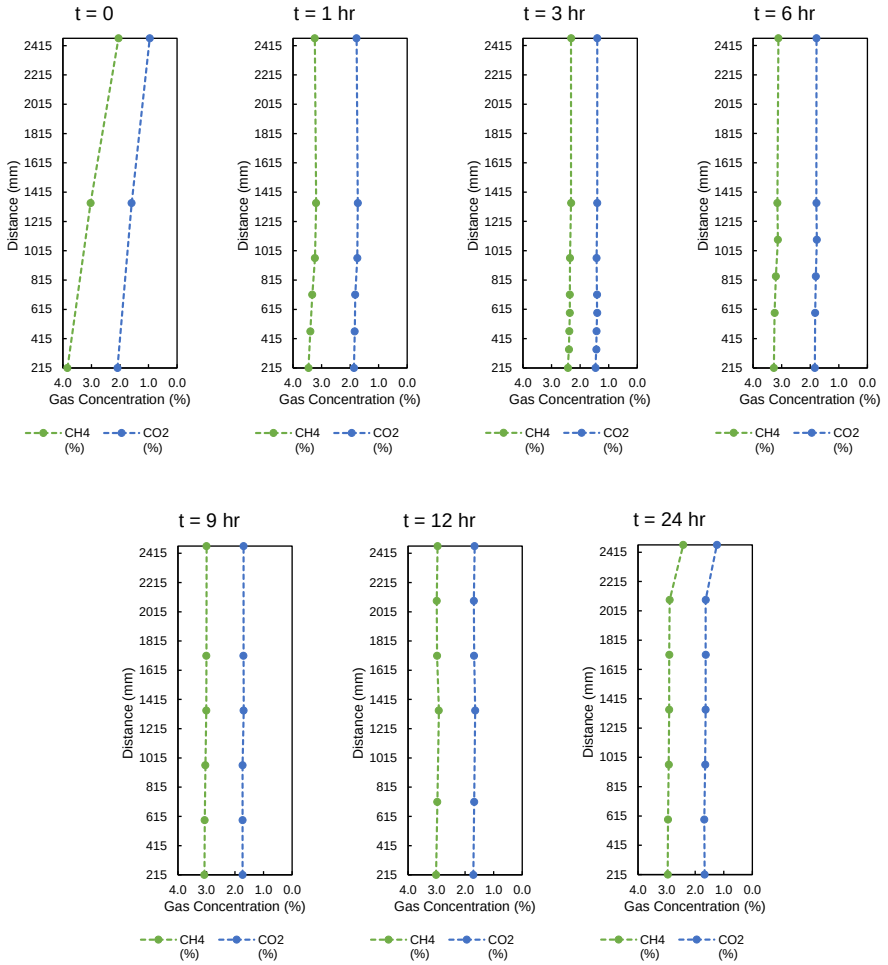

Figure L.8: Artificial Borehole 40% CO_2 / 60% CH_4 in Air Experiment Trial 3 (12/09/2016 – 13/09/2016)

The data from the 40% CO_2 / 60% CH_4 were rejected as the ratio of CH_4 to CO_2 ranged from 1.75 to 2.0. This was greater than the relative amounts of the gases injected into the reservoir. A GC-MS calibration error may have occurred.

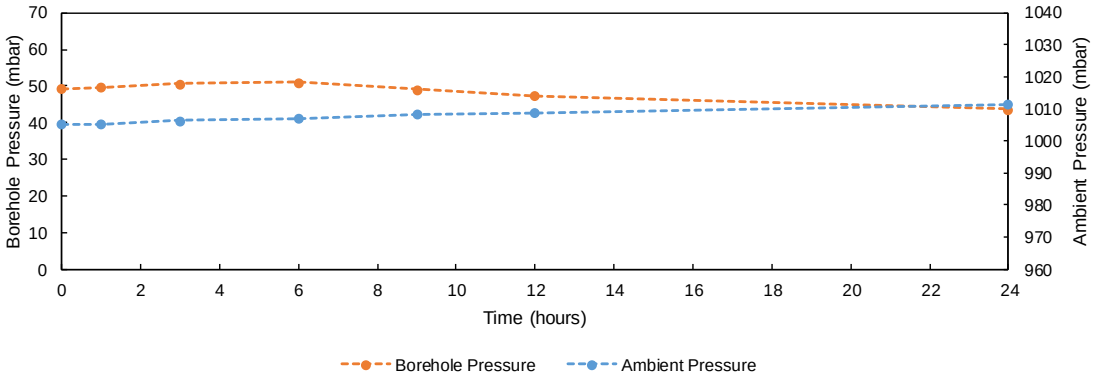

Figure L.9: Artificial Borehole Pressure Change during 40% CO_2 / 60% CH_4 in Sand Experiment (12/09/2016 – 13/09/2016)

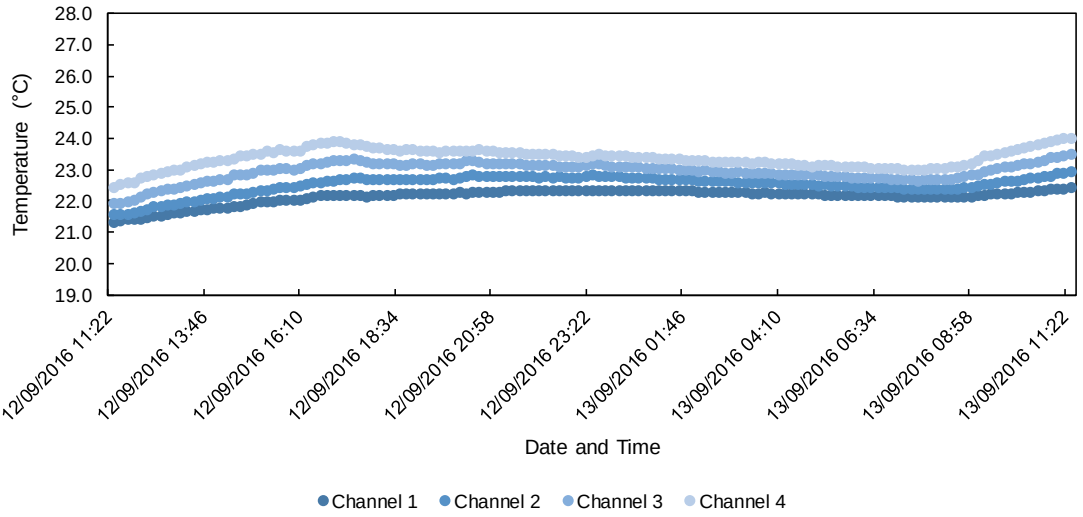

Figure L.10: Artificial Borehole Temperature Change during 40% CO_2 / 60% CH_4 in Sand Experiment (12/09/2016 – 13/09/2016)

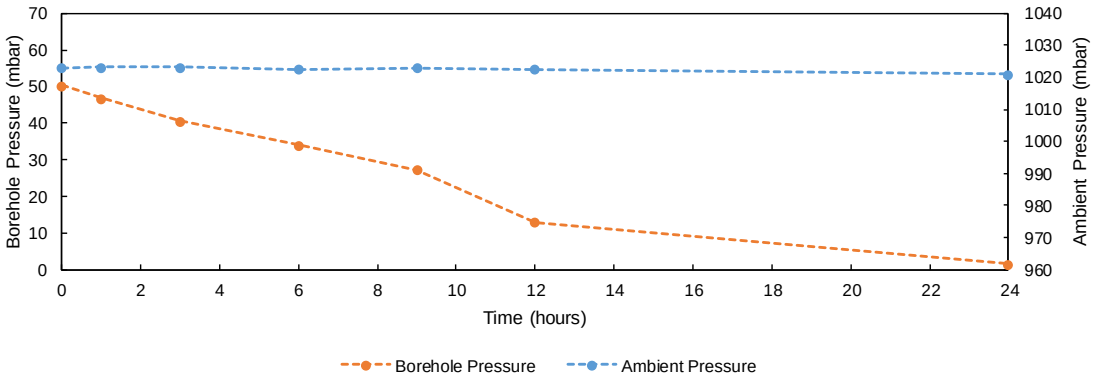

Figure L.11: Artificial Borehole Pressure Change during 40% CO_2 / 60% CH_4 in Sand Experiment (19/09/2016 – 20/09/2016)

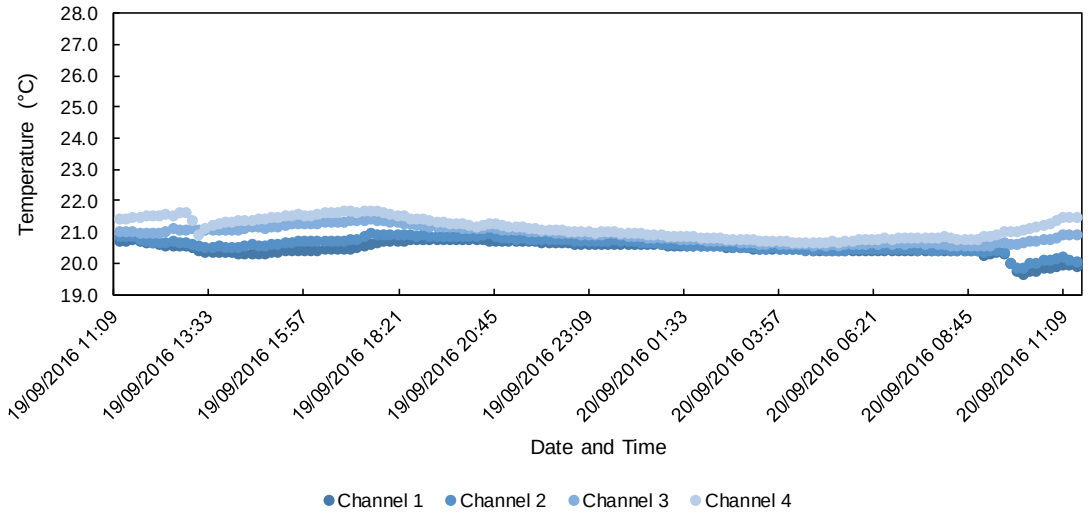

Figure L.12: Artificial Borehole Temperature Change during 40% CO_2 / 60% CH_4 in Sand Experiment (19/09/2016 – 20/09/2016)

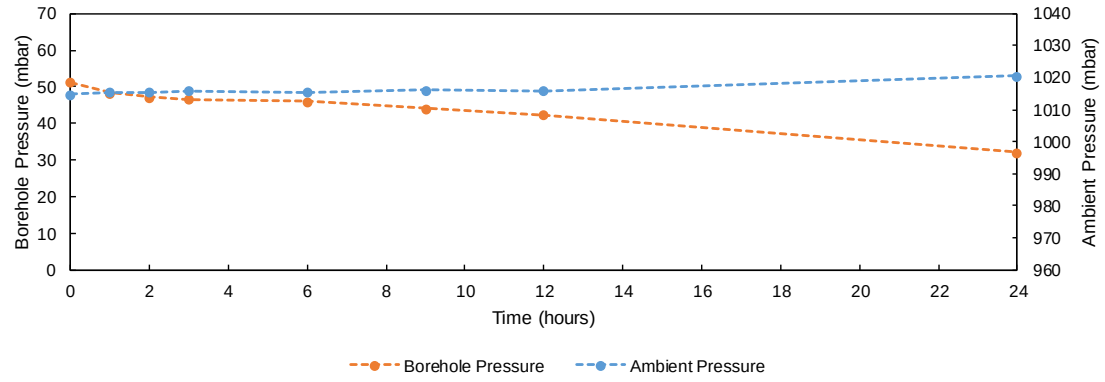

Figure L.13: Artificial Borehole Pressure Change during 100% CO_2 in Sand Experiment (22/09/2016 – 23/09/2016)

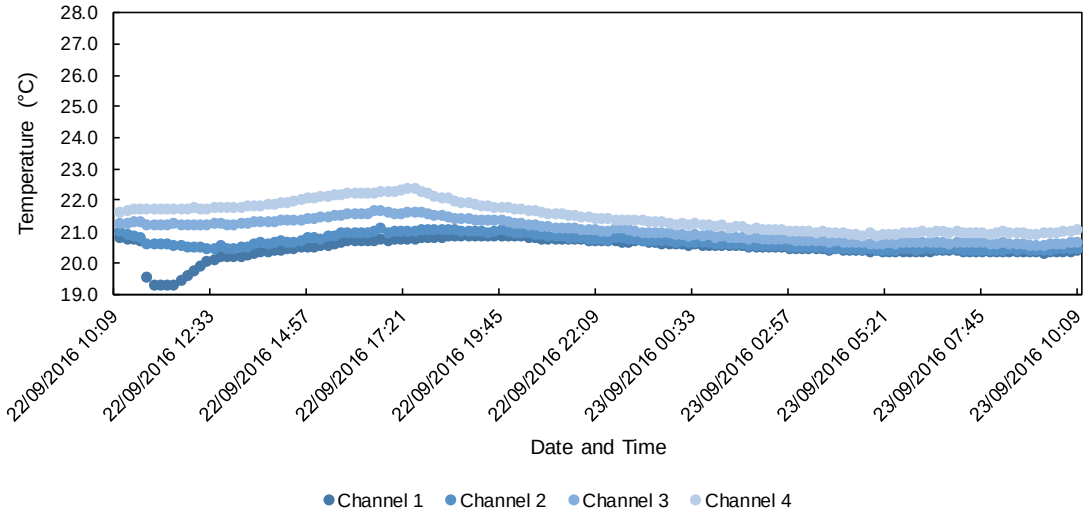

Figure L.14: Artificial Borehole Temperature Change during 100% CO_2 in Sand Experiment (22/09/2016 – 23/09/2016)

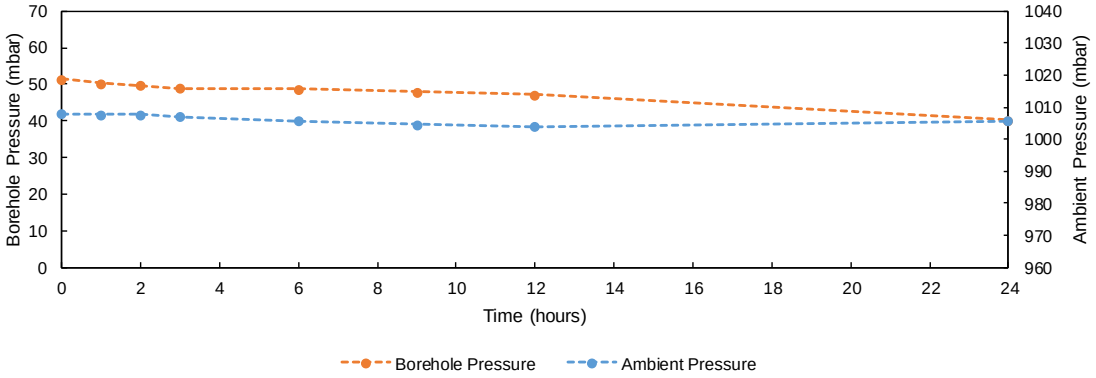

Figure L.15: Artificial Borehole Pressure Change during 100% CO_2 in Sand Experiment (24/09/2016 – 25/09/2016)

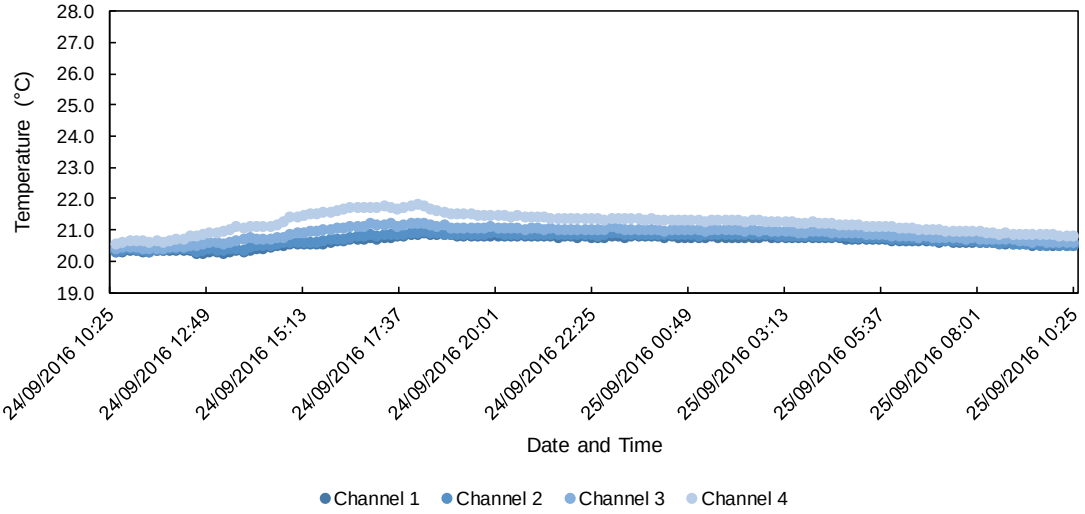

Figure L.16: Artificial Borehole Temperature Change during 100% CO_2 in Sand Experiment (24/09/2016 – 25/09/2016)

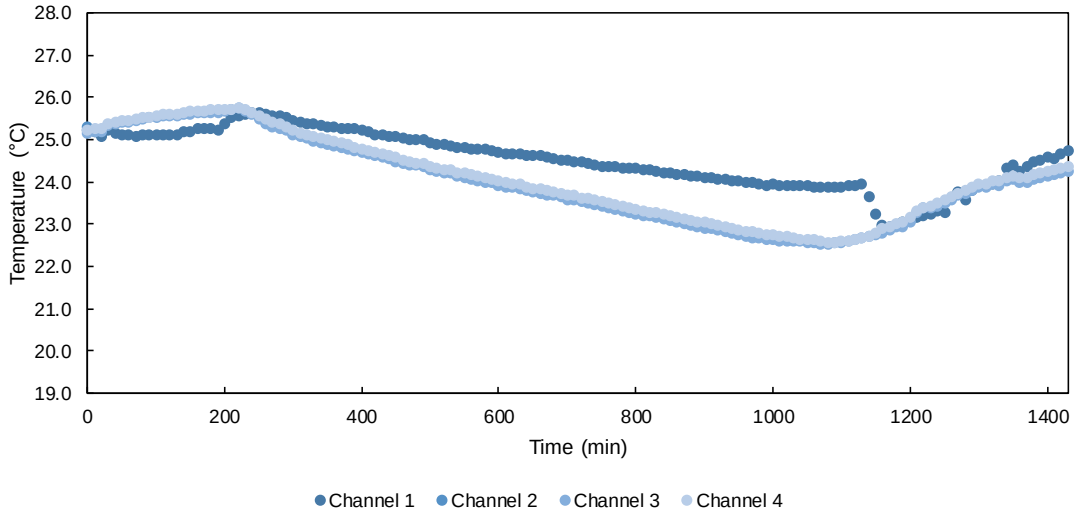

Figure L.17: Pico TC-08 Thermocouple Data Logger Calibration

Leighton Buzzard Sand Specification

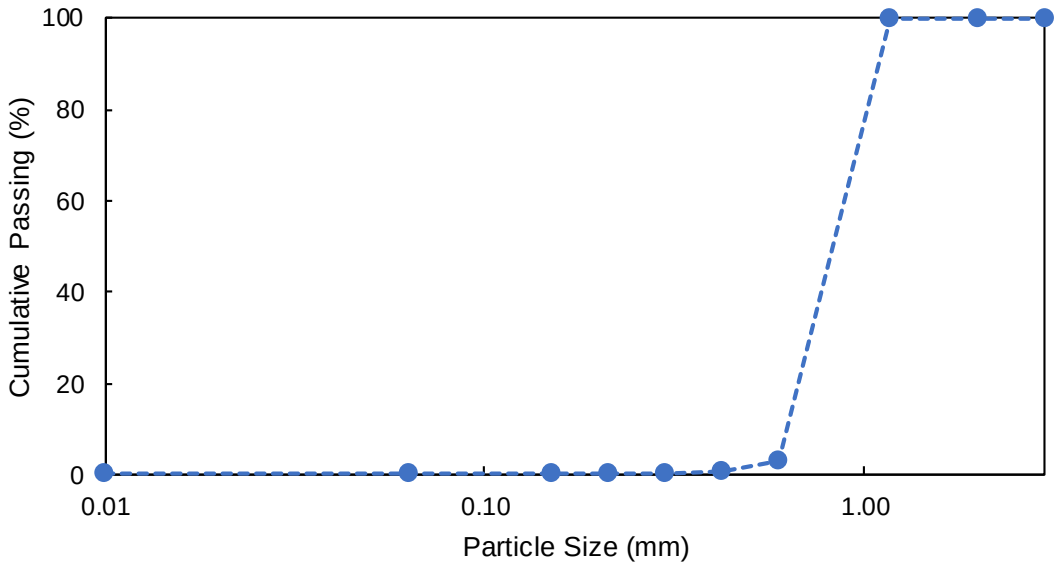

Figure L.18: Leighton Buzzard Sand Particle Size Distribution

Sample	Tray No.	Tray (g)	Tray + Wet Sand (g)	Tray + Dry Sand (g)	Diff in Mass (%)	Tray + Dry Sand (g)	Diff in Mass (%)	Tray + Dry Sand (g)	Diff in Mass (%)
Fresh Sand	1	642.6	1644.2	1636.6	0.8	1636.6	0.0	1636.6	0.0
	2	622.7	1626.2	1620.2	0.6	1620.0	0.02	1620.0	0.0
	3	645.5	1646.7	1642.7	0.4	1642.7	0.0	1642.7	0.0
Lab Sand	4	473.2	1473.3	1472.7	0.1	1472.5	0.02	1472.5	0.0
	5	286.5	1286.5	1285.9	0.1	1285.8	0.01	1285.8	0.0
	6	276.5	1277.0	1276.4	0.1	1276.4	0.0	1276.4	0.0

Table L.1: Leighton Buzzard Sand Drying Measurements

Sample	Tray No.	Tray (g)	Tray + Wet Sand (g)	Wet Sand (g)	Tray + Dry Sand (g)	Dry Sand (g)	Mass Change (g)	Moisture Content (%)	Mean / St Dev / RSD (%)
Fresh Sand	1	642.6	1644.2	1001.6	1636.6	994.0	7.6	0.76	0.59
	2	622.7	1626.2	1003.5	1620.0	997.3	6.2	0.62	0.18
	3	645.5	1646.7	1001.2	1642.7	997.2	4.0	0.40	30.6
Lab Sand	4	473.2	1473.3	1000.1	1472.5	999.3	0.8	0.08	0.07
	5	286.5	1286.5	1000.0	1285.8	999.3	0.7	0.07	0.01
	6	276.5	1277.0	1000.5	1276.4	999.9	0.6	0.06	14.4

Table L.2: Leighton Buzzard Sand Moisture Content

GC-MS Calibration Standards

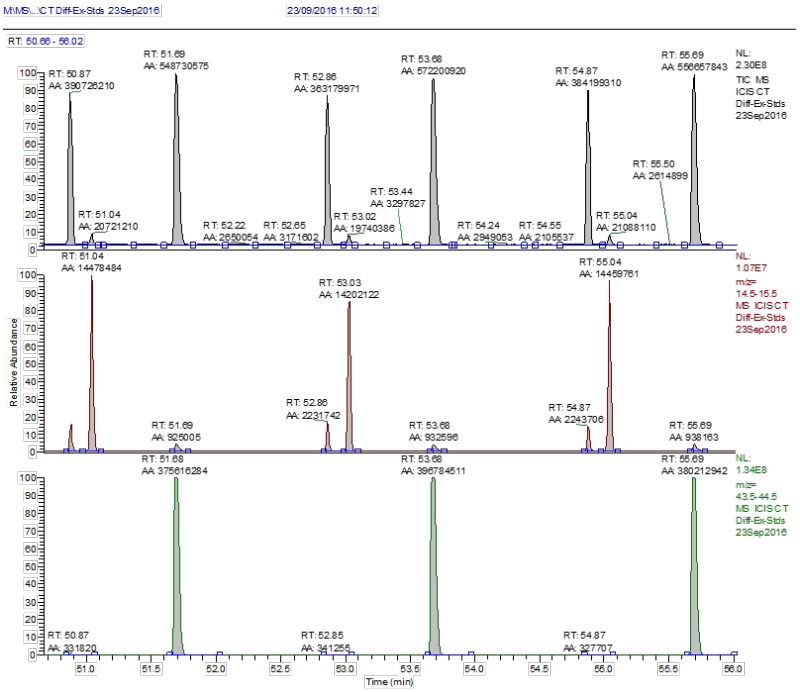

Figure L.19: 20% CO_2 / 10% CH_4 GC-MS Calibration Standard

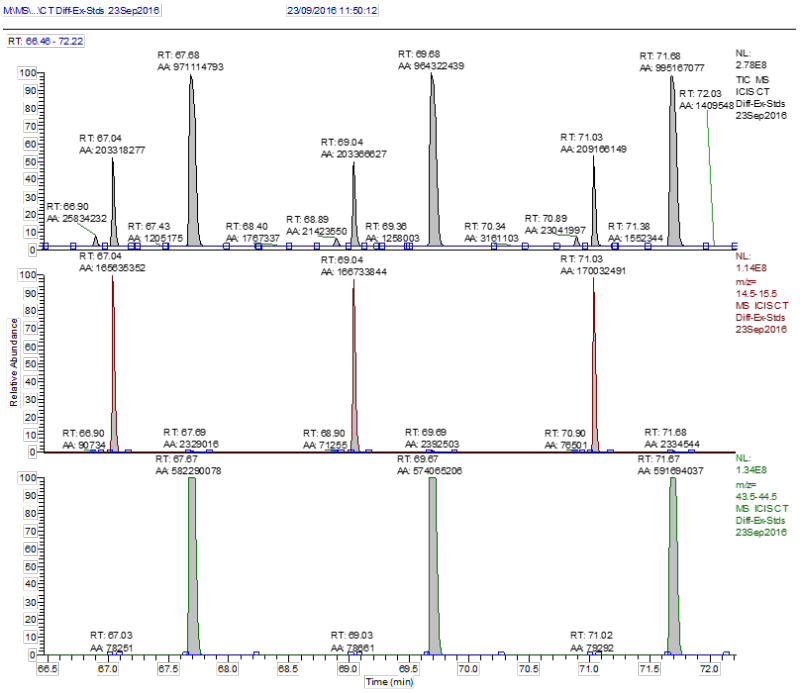

Figure L.20: 40% CO_2 / 60% CH_4 GC-MS Calibration Standard

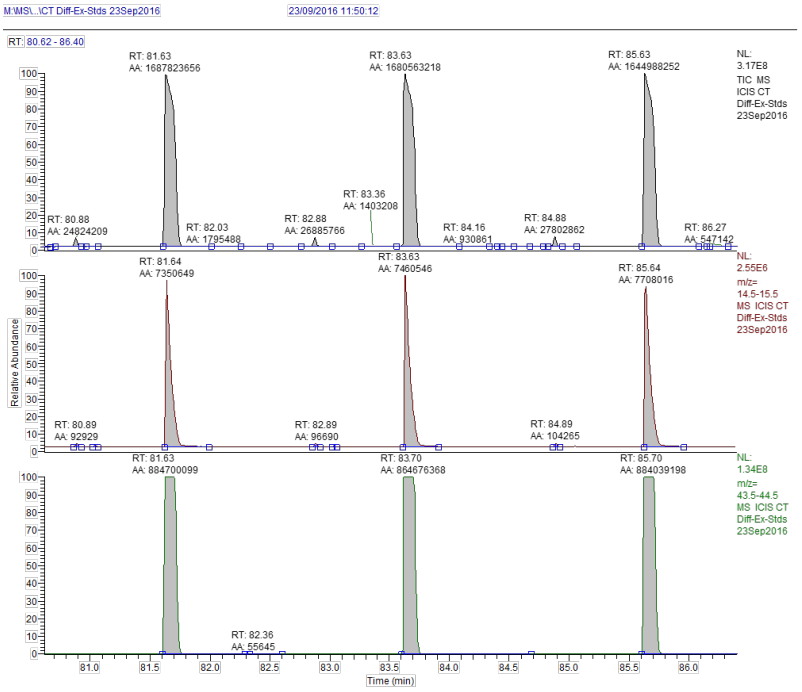

Figure L.21: 100% CO_2 GC-MS Calibration Standard

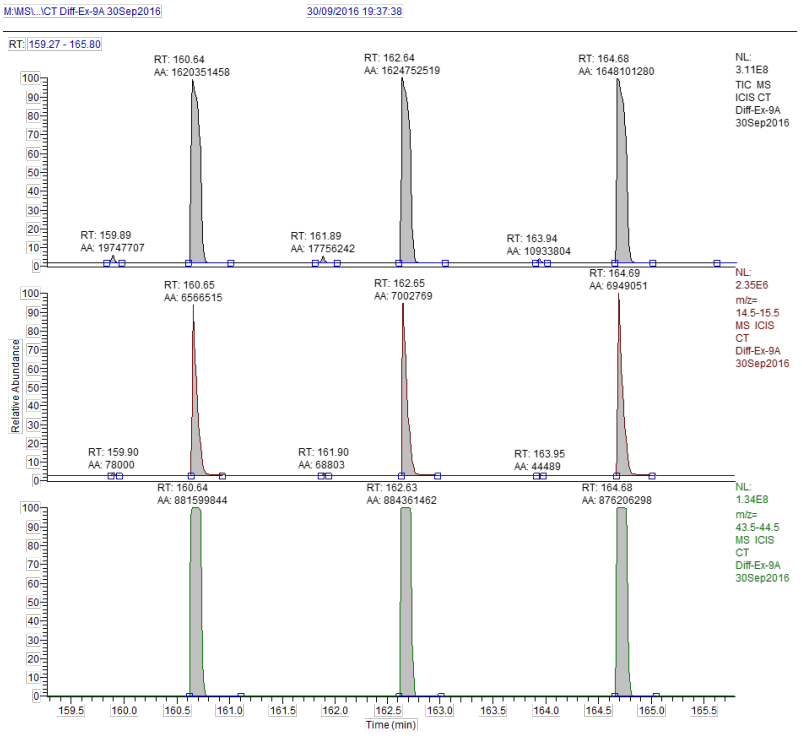

Figure L.22: CO_2 Welding Gas GC-MS Calibration Standard

GC-MS Standard Error Calculation

Methane

Sample / Standard	Peak Area			Concentration (%)		
	1,229,169	1,184,252	Mean	1.070	1.033	Mean
1% CH_4	1,169,745	39,704	St Dev	1.021	0.0327	St Dev
	1,153,842	22,923	St Err	1.008	0.0189	St Err
	15,649,826	15,832,425	Mean	10.1	10.3	Mean
10% CH_4	16,022,501	186,450	St Dev	10.4	0.107	St Dev
	15,824,948	107,647	St Err	10.2	0.0619	St Err
	165,635,352	167,467,229	Mean	60.6	61.1	Mean
60% CH_4	166,733,844	2,288,471	St Dev	60.9	0.687	St Dev
	170,032,491	1,321,249	St Err	61.9	0.396	St Err
	24,949	24,949	Mean	0.0936	0.0936	Mean
4.4.1	25,285	336	St Dev	0.0948	0.00121	St Dev
	24,613	194	St Err	0.0924	0.000699	St Err
	30,737	31,230	Mean	0.114	0.116	Mean
4.6.2	31,398	434	St Dev	0.117	0.00156	St Dev
	31,555	250	St Err	0.117	0.000903	St Err
	37,855	38,041	Mean	0.140	0.141	Mean
4.19.3	38,126	162	St Dev	0.141	0.000582	St Dev
	38,143	93.3	St Err	0.141	0.000336	St Err
	44,530	43,876	Mean	0.164	0.162	Mean
4.4.4	44,486	1,094	St Dev	0.164	0.00394	St Dev
	42,613	632	St Err	0.157	0.00228	St Err
	66,797	66,602	Mean	0.244	0.244	Mean
4.1.5	66,479	170	St Dev	0.243	0.000614	St Dev
	66,532	98.4	St Err	0.243	0.000354	St Err
	67,261	66,736	Mean	0.246	0.244	Mean
4.13.24	67,161	824	St Dev	0.246	0.00297	St Dev
	65,787	476	St Err	0.241	0.00171	St Err
	2,236,278	2,192,122	Mean	2.48	2.45	Mean
6.2.2	2,195,299	45,827	St Dev	2.45	0.0352	St Dev
	2,144,790	26,458	St Err	2.41	0.0203	St Err
	2,044,272	2,040,807	Mean	2.36	2.33	Mean
6.8.6	2,062,211	23,331	St Dev	2.35	0.0179	St Dev
	2,015,937	13,470	St Err	2.31	0.0103	St Err
	1,788,289	1,753,104	Mean	2.14	2.11	Mean
6.10.12	1,754,618	35,966	St Dev	2.11	0.0276	St Dev
	1,716,405	20,765	St Err	2.08	0.0159	St Err
	2,118,904	2,076,128	Mean	2.40	2.37	Mean
7.13.9	2,079,392	44,498	St Dev	2.37	0.0343	St Dev
	2,030,087	25,691	St Err	2.33	0.0198	St Err
	2,068,171	2,057,283	Mean	2.36	2.36	Mean
7.16.12	2,047,128	10,541	St Dev	2.35	0.00812	St Dev
	2,056,551	6,086	St Err	2.35	0.00469	St Err
	2,041,963	2,014,022	Mean	2.34	2.32	Mean
7.13.24	2,020,966	31,983	St Dev	2.33	0.0246	St Dev
	1,979,138	18,465	St Err	2.30	0.0142	St Err
	242,190	241,637	Mean	0.975	0.975	Mean
8.7.3	238,866	2,540	St Dev	0.973	0.00199	St Dev
	243,856	1,467	St Err	0.977	0.00115	St Err
	2,783,865	2,757,960	Mean	2.97	2.95	Mean
8.1.12	2,765,858	30,628	St Dev	2.96	0.0240	St Dev
	2,724,157	17,683	St Err	2.92	0.0139	St Err
	617,600	601,637	Mean	1.27	1.26	Mean
8.19.24	601,104	15,703	St Dev	1.26	0.0123	St Dev
	586,207	9,066	St Err	1.25	0.00712	St Err

Table L.3: CH_4 GC-MS Standard Error Calculation

Carbon Dioxide

Sample / Standard	Peak Area			Concentration (%)		
	16,097,648	15,918,852	Mean	1.019	1.008	Mean
1% CO_2	15,714,896	192,612	St Dev	0.996	0.0116	St Dev
	15,944,011	111,205	St Err	1.010	0.00668	St Err
	228,438,041	232,393,174	Mean	10.6	10.7	Mean
10% CO_2	232,747,818	3,790,275	St Dev	10.8	0.126	St Dev
	235,993,662	2,188,316	St Err	10.9	0.0729	St Err
	375,616,284	384,204,579	Mean	19.2	19.6	Mean
20% CO_2	396,784,511	11,134,331	St Dev	20.2	0.557	St Dev
	380,212,942	6,428,409	St Err	19.4	0.321	St Err
	582,290,078	582,683,107	Mean	43.5	43.5	Mean
40% CO_2	574,065,206	8,820,985	St Dev	42.9	0.588	St Dev
	591,694,037	5,092,798	St Err	44.1	0.340	St Err
	198,611	166,731	Mean	0.237	0.199	Mean
3.1.1	158,328	28,618	St Dev	0.190	0.0311	St Dev
	143,256	16,522	St Err	0.174	0.0180	St Err
	166,197	165,030	Mean	0.237	0.198	Mean
3.5.2	160,720	3,861	St Dev	0.198	0.00420	St Dev
	168,174	2,229	St Err	0.192	0.00242	St Err
	3,122,559	3,120,920	Mean	3.92	3.92	Mean
3.3.3	3,141,644	21,589	St Dev	3.94	0.0215	St Dev
	3,098,558	12,464	St Err	3.90	0.0124	St Err
	2,774,785	2,707,706	Mean	3.44	3.38	Mean
3.4.4	2,734,817	83,982	St Dev	3.40	0.0846	St Dev
	2,613,518	48,487	St Err	3.28	0.0489	St Err
	1,388,313	1,379,675	Mean	1.72	1.71	Mean
3.6.5	1,386,429	13,363	St Dev	1.72	0.0161	St Dev
	1,364,283	7,715	St Err	1.69	0.00932	St Err
	7,737,147	7,720,685	Mean	9.09	9.07	Mean
3.1.6	7,759,900	49,540	St Dev	9.11	0.0523	St Dev
	7,665,010	28,602	St Err	9.01	0.0234	St Err
	4,188,961	4,119,139	Mean	4.88	4.81	Mean
3.4.7	4,147,789	87,727	St Dev	4.84	0.0897	St Dev
	4,020,669	50,649	St Err	4.71	0.0401	St Err
	4,018,682	3,968,500	Mean	4.71	4.66	Mean
3.7.24	3,965,163	48,598	St Dev	4.65	0.0497	St Dev
	3,921,657	28,058	St Err	4.61	0.0222	St Err
	4,877,359	4,871,835	Mean	3.86	3.85	Mean
3.10.168	4,992,567	123,586	St Dev	3.95	0.100	St Dev
	4,745,580	71,352	St Err	3.75	0.0447	St Err
	206,562	207,199	Mean	0.187	0.187	Mean
4.4.1	208,365	1,011	St Dev	0.188	0.000772	St Dev
	206,672	584	St Err	0.187	0.000446	St Err
	258,930	258,111	Mean	0.227	0.226	Mean
4.6.2	260,128	2,528	St Dev	0.228	0.00193	St Dev
	255,275	1,460	St Err	0.224	0.00112	St Err
	305,378	304,606	Mean	0.262	0.262	Mean
4.19.3	303,033	1,363	St Dev	0.260	0.00104	St Dev
	305,409	787	St Err	0.262	0.000601	St Err
	345,505	344,266	Mean	0.293	0.292	Mean
4.4.4	347,995	4,479	St Dev	0.295	0.00342	St Dev
	339,298	2,586	St Err	0.288	0.00198	St Err
	540,609	537,835	Mean	0.442	0.440	Mean
4.1.5	536,575	2,406	St Dev	0.439	0.00184	St Dev
	536,321	1,389	St Err	0.439	0.00106	St Err
	535,278	543,800	Mean	0.438	0.444	Mean
4.13.24	551,115	7,987	St Dev	0.450	0.00610	St Dev
	545,007	4,611	St Err	0.445	0.00352	St Err
	26,692,231	26,151,459	Mean	2.28	2.25	Mean
6.2.2	26,502,687	778,286	St Dev	2.27	0.0380	St Dev
	25,259,459	449,344	St Err	2.21	0.0219	St Err

Sample / Standard	Peak Area			Concentration (%)		
	24,423,810	24,295,532	Mean	2.17	2.16	Mean
6.8.6	24,387,384	191,506	St Dev	2.17	0.00935	St Dev
	24,075,402	110,566	St Err	2.15	0.00540	St Err
	20,622,545	20,376,329	Mean	1.98	1.97	Mean
6.10.12	20,575,500	386,434	St Dev	1.98	0.0189	St Dev
	19,930,941	223,108	St Err	1.95	0.0109	St Err
	24,501,018	24,256,564	Mean	2.18	2.17	Mean
7.13.9	24,285,852	260,337	St Dev	2.17	0.0128	St Dev
	23,982,822	150,305	St Err	2.16	0.00737	St Err
	24,357,582	24,158,431	Mean	2.17	2.17	Mean
7.16.12	24,159,787	199,832	St Dev	2.17	0.00980	St Dev
	23,957,924	115,373	St Err	2.16	0.00566	St Err
	24,017,494	23,686,626	Mean	2.16	2.14	Mean
7.13.24	23,754,316	369,395	St Dev	2.15	0.0181	St Dev
	23,288,067	213,270	St Err	2.12	0.0105	St Err
	1,943,761	1,892,713	Mean	0.169	0.166	Mean
8.7.3	1,873,664	44,681	St Dev	0.165	0.00268	St Dev
	1,860,714	25,796	St Err	0.164	0.00155	St Err
	29,754,010	29,377,646	Mean	2.49	2.47	Mean
8.1.12	29,217,634	327,156	St Dev	2.46	0.0164	St Dev
	29,161,293	188,884	St Err	2.46	0.00944	St Err
	2,417,485	2,314,999	Mean	0.198	1.91	Mean
8.19.24	2,306,446	98,488	St Dev	0.191	0.00591	St Dev
	2,221,066	56,862	St Err	0.186	0.00341	St Err
	1,391,517	1,373,599	Mean	0.136	0.135	Mean
9.16.12	1,376,216	19,359	St Dev	0.135	0.00116	St Dev
	1,353,065	11,177	St Err	0.134	0.000671	St Err

Table L.4: CO_2 GC-MS Standard Error Calculation

Appendix M

Teasdale et al. (2014)

Environmental Science & Technology

Article

pubs.acs.org/est

Ground Gas Monitoring: Implications for Hydraulic Fracturing and CO_2 Storage

Christopher J. Teasdale,*[,†] Jean A. Hall,[†] John P. Martin,[‡] and David A. C. Manning[†]

[†]School of Civil Engineering & Geosciences, Newcastle University, Newcastle upon Tyne, U.K., NE1 7RU

[‡]TerraConsult Ltd, Bold Business Centre, Bold Lane, Sutton, St Helens, Merseyside, U.K., WA9 4TX

Supporting Information

ABSTRACT: Understanding the exchange of carbon dioxide (CO_2) and methane (CH_4) between the geosphere and atmosphere is essential for the management of anthropogenic emissions. Human activities such as carbon capture and storage and hydraulic fracturing ("fracking") affect the natural system and pose risks to future global warming and to human health and safety if not engineered to a high standard. In this paper an innovative approach of expressing ground gas compositions is presented, using data derived from regulatory monitoring of boreholes in the unsaturated zone at infrequent intervals (typically 3 months) with data from a high frequency monitoring instrument deployed over periods of weeks. Similar highly variable trends are observed for time scales ranging from decades to hourly for boreholes located close to sanitary landfill sites. Additionally, high frequency monitoring data confirm the effect of meteorological controls on ground gas emissions; the maximum observed CH_4 and CO_2 concentrations in a borehole monitored over two weeks were 40.1% v/v and 8.5% v/v respectively, but for 70% of the monitoring period only air was present. There is a clear weakness in current point monitoring strategies that may miss emission events and this needs to be considered along with obtaining baseline data prior to starting any engineering activity.

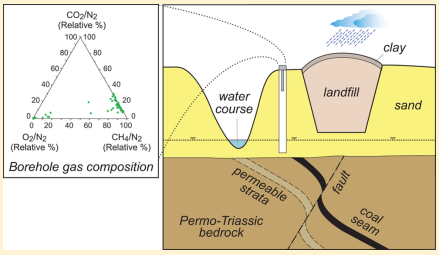

INTRODUCTION

The exchange of carbon dioxide (CO_2) and methane (CH_4) between the geosphere and atmosphere is a key component of the global carbon cycle. At the advent of industrialization, atmospheric CO_2 concentration was 280 ppm and has subsequently increased so that it now exceeds 400 ppm.[1] This figure is projected to reach 600−800 ppm by the close of the century.[1] It is believed that the rise in CO_2 concentration in the Earth's atmosphere is linked to global climate change.[2,3] As well as CO_2, CH_4 also occurs naturally in the ground. With a global warming potential (GWP) 21 times greater than CO_2,[4] its emission to the atmosphere is considered to be one of the greatest environmental challenges of the 21st Century. In addition to emissions of CO_2 from the combustion of fossil fuels, which account for the major part of the post-industrial increase,[5] CO_2 exchange between the coupled plant−soil system and the atmosphere is a major control of atmospheric CO_2.

Carbon Capture and Storage (CCS) is recognized by the Intergovernmental Panel on Climate Change (IPCC) and the United Nations Framework Commission on Climate Change (UNFCCC)[6] as a potentially important mitigation strategy against climate change due to CO_2. Geological storage is technically feasible and under favorable conditions, CO_2 may be retained for millions of years.[7,8] Nonetheless, there are accompanying risks of leaks as well as blowouts that can compromise the security of an operation.[8] Additionally, pumping CO_2 into deep geologic formations at high pressure may induce earthquakes and reduce groundwater pH, potentially enhancing contaminant mobility.[9] Monitoring for possible leaks is required to ensure the integrity of containment.

Hydraulic fracturing ("fracking") associated with the production of natural gas has been highlighted as another environmental concern.[10,11] During the process, water containing chemical additives and a physical proppant is injected into shale formations through boreholes at high pressure. Liberation of gases trapped within the shale occurs as fractures spread. There is a possibility that CH_4 may leak from the subsurface via a number of pathways. In locations where groundwater is contaminated by CH_4, there is scope for associated contamination of the overlying vadose zone.

For well-informed management of deep engineering processes that have the potential to affect greenhouse gas emissions, there is a need to understand the background levels

Received: May 23, 2014
Revised: October 30, 2014
Accepted: November 2, 2014
Published: November 3, 2014

Figure M.1: Teasdale et al. (2014) p 13610

of CH_4 and CO_2 in soils, superficial unconsolidated sediment deposits and groundwater systems and, importantly, the extent of their temporal variability. In this paper, the compositions of gases ("ground gas") within near-surface unconsolidated sands confined by a clay cover were investigated. Also, the implications of temporal variability for the design and interpretation of ground gas monitoring procedures are considered.

Emissions of gases from soils vary in their origin. Near surface fluxes of CO_2 and CH_4 from biologically active soils occur in response to microbial respiration, and occur rapidly after the formation of the gas.[12] Concentrations of CO_2 and CH_4 in soils dominated by plant roots and associated microbial systems are typically very low, below 1% v/v.[13,14] Below the biologically active soil, sedimentary geological processes produce CO_2 and CH_4, whose proportions vary according to specific geological circumstances. Natural fluxes of CO_2 and CH_4 to the atmosphere include contributions from both geological and biological sources. Artificial sources of gases within soil include sanitary landfill, where anaerobic microbial processes characteristically produce gas containing up to 70% CH_4 and 30% CO_2.[15] Once formed, geological gases migrate through permeable and fractured formations until trapped or released to the atmosphere. Similarly, gases produced in landfills migrate, laterally as well as vertically, if containment systems fail. Monitoring systems in the vicinity of landfills are designed to detect migration so that appropriate action can be taken.

Specifically considered are the compositions of gases within shallow unconsolidated sands capped by glacial till. Landfills have been constructed in these formations within the UK and monitoring regimes are in place to assess the integrity of containment. Boreholes outside landfills are used to determine gas compositions. Thus, there is access to a resource of historical monitoring data that extends back many years. CO_2 and CH_4 in the sands may be derived from sources other than landfill, including natural migration from underlying strata, in this case, coal-bearing. Given that the sites lie within an area of search for shale gas (Figure 1), it is important to understand the origin of variability in gas compositions prior to any possible future deep engineering activities. Historic periodic and recent high frequency monitoring data obtained from outside landfill sites are compared, with reference to data from a site with a similar geological setting, but distant from landfill. The use of different temporal scales of observation has major implications for the planning and interpretation of ground gas monitoring procedures, with a wide range of applications.

DEEP GEOLOGICAL SOURCES OF GAS IN THE UK

Gas is a natural component of the geological subsurface, occurring within rock pores and fractures, and migrating in response to pressure gradients (i.e., generally to the surface, unless trapped). Geological gases have a wide range of compositions, depending on their origin. The focus of this paper is on CO_2 and CH_4, which are formed naturally as a consequence of the decomposition (diagenesis) of organic matter within sediments and sedimentary rocks. In deep sediments, if geological factors are right, these gases accumulate in reservoirs which form the target of petroleum exploration. Current focus on unconventional sources of natural gas includes shale gas, tight gas and coal bed CH_4.[16] Production from these sources may require artificial fracturing, and there are concerns that "fracking" may cause gases to leak to shallow groundwater systems or to escape to the atmosphere through the soil.[17,18]

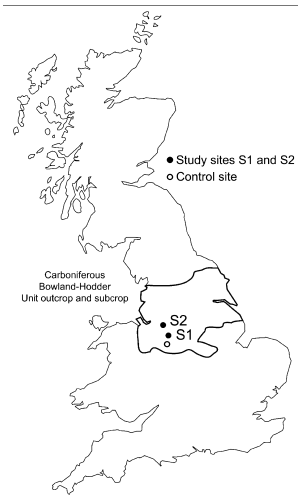

Figure 1. Outline of the Bowland-Hodder Unit outcrop and subcrop (after Andrews[23]), with monitoring locations.

In addition to considering geological gas as a resource, CCS procedures require injection of CO_2 into deep formations where it is to be stored.[19−21] Again, monitoring of ground gas compositions is required to ensure that there is no leakage from an underground store of captured CO_2.

In the UK, an evaluation of shale gas resources[22] identifies Carboniferous sequences in northern England as a priority area, and a more detailed study of the Bowland-Hodder unit is presented by the British Geological Survey.[23] Lower Carboniferous rocks that might be a source of shale gas extend from the Cheshire Basin north through Lancashire, and east to Yorkshire and Lincolnshire (Figure 1). Throughout this region, Carboniferous rocks occur at depth, beneath younger sedimentary rocks and superficial deposits, as well as outcropping.

This study considers locations (Figure 1) within the area of shale gas potential where gas monitoring data have been obtained before any investigation or exploitation of shale gas reserves. It provides baseline information that demonstrates the temporal variability of natural ground gas compositions for unconsolidated Quaternary sands capped by glacial till, which are below the root zone. These data represent ground gases that have accumulated in sands by migration from depth or by lateral movement, and that may be derived from artificial (such as landfill) or natural sources (such as coal-bearing rocks). Full details of the sites are provided as Supporting Information (SI).

DATA COMPILATION

Data Sources. Monitoring data were obtained for two landfill sites in Cheshire, UK (SI); the sites differ geologically and produce contrasting gas signatures. Site 1, a closed landfill, is situated in thick Quaternary deposits with no known

Figure M.2: Teasdale et al. (2014) p 13611

potential external (geological) source of CH_4 or CO_2. Conversely, Site 2 is situated in Quaternary deposits overlying thin Permo-Triassic bedrock, with underlying Coal Measures (Carboniferous; Westphalian) which provide a potential source of geogenic gas. Additionally, Site 2 is adjacent to a second older landfill, constructed to a lower technical specification. The Control Site was chosen at a location with similar geology to Site 1, but with no associated landfill. Details of the ground conditions at each site are given in the SI.

Historic Measurement of Gas Composition. Historically, gas composition has been measured in accordance with regulatory requirements using hand-held gas monitors, as frequently as daily (Site 2) to as infrequently as quarterly (Site 1). Measurements were made using a Geotech UK GA2000 Landfill Gas Analyzer until 2012, after which a Gas Data Ltd. GFM435 landfill gas analyzer was used. One of the limitations of changes of instrumentation over a period of several years is that data sets may not be directly comparable. Both gas monitoring instruments employ a dual beam infrared absorption method to quantify the concentration of CH_4, CO_2 and oxygen (O_2) in a flowing gas. The balance is assumed to be nitrogen (N_2). However, the instruments differ in their measurement of borehole flow. The GA2000 pressure transducer is equipped with a set resistor in order to minimize flow. It is argued that this will more closely reflect true borehole conditions as the act of opening the borehole valve will disrupt equilibrium conditions. Conversely, the GFM435 pressure transducer does not have this specification.

Measurement of Gas Composition at High Temporal Resolution. High temporal resolution data capture was achieved using a GasClam instrument, by which gas compositions can be recorded at intervals as short as 3 min.[24] The GasClam also records atmospheric pressure and temperature as well as gas composition, avoiding an additional limitation of hand-held gas monitors.[25] The instrument has, according to the manufacturer, a range 0−100% for CH_4 and CO_2, with a stated detection limit of 0.1% for both gases. In practice, observed nonzero minimum concentrations for CH_4 and CO_2 were 0.4% and 0.1%, respectively, and observed maximum values were 57.1% and 10.8% respectively.

■ ANALYSIS OF GAS MONITORING DATA

Two graphical approaches have been used to present the gas monitoring data. In the first, compositional data are compared in a ternary plot in terms of the measured CH_4, CO_2 and O_2 content normalised to N_2 (assuming N_2 to be the balance, i.e., $100 - \Sigma CH_4 + CO_2 + O_2$)). This allows the relative proportions of CH_4 and CO_2 to be compared irrespective of any dilution by air, the O_2/N_2 ratio indicating whether this has occurred and the extent to which O_2 has been removed, as N_2 can be regarded as non-reactive.[15] In a plot of this type, "end member" compositions can be identified, so that an array of observed data points can be explained as mixtures of gases from different sources, and the characteristics of one borehole can be compared with another. The second graphical approach is to show variation with time in absolute gas concentration (% v/v) measured at high frequency and how this is affected by atmospheric pressure conditions.

Monitoring Wells Near a Landfill Where There Is No Known Input from Coal-Bearing Rocks. Figure 2 shows the gas composition recorded over a period of 10 years at boreholes on Site 1. BH 1 is located on the southern boundary of the landfill (SI Figure S1), and produced a methane-rich gas

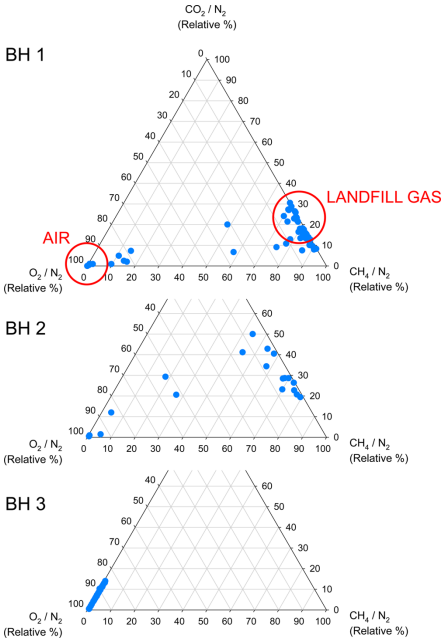

Figure 2. Gas compositions for monitoring wells on Site 1 (2003−2013), indicating (Figure 2a) expected plotting positions of landfill gas and air.

signature (70:30 CH_4/CO_2) which is attributed to landfill gas given the close proximity of the borehole to the edge of the landfill. Values recorded at 100% O_2/N_2 correspond to air. There is some evidence of mixing between landfill gas and air at this location, but this was observed on few occasions (points between the two end member compositions).

BH 2 is approximately 25 m south of the landfill perimeter, and shows a more diffuse scatter of data. There is still a strong indication of the presence of landfill gas but the proportion of CH_4 is lower (Figure 2), suggesting mixing with more CO_2-rich gas, or removal of CH_4 by biological processes. BH 3, 100 m away from the landfill, records no landfill gas (Figure 2).

High Frequency Monitoring. Gas compositions were measured at Site 1, borehole BH 1, on a 30 min sampling frequency program with the instrument vent closed to ensure that borehole conditions were not disturbed during sampling. Figure 3 shows the results of sampling for a two week period starting Monday 29th October 2013.

During this period, there were three successive rises and falls in atmospheric pressure. The falls occurred on 2nd, 3rd, and 5th November, each with similar gradients. Accordingly, with each fall, corresponding peak concentrations of CH_4 (up to 40%) and CO_2 (up to 10%) were observed, the balance being N_2. As CH_4 and CO_2 appear in the borehole, O_2 concentration decreases to 0% from atmospheric concentration (~20%). For the observed borehole, the change is very sensitive to

Figure M.3: Teasdale et al. (2014) p 13612

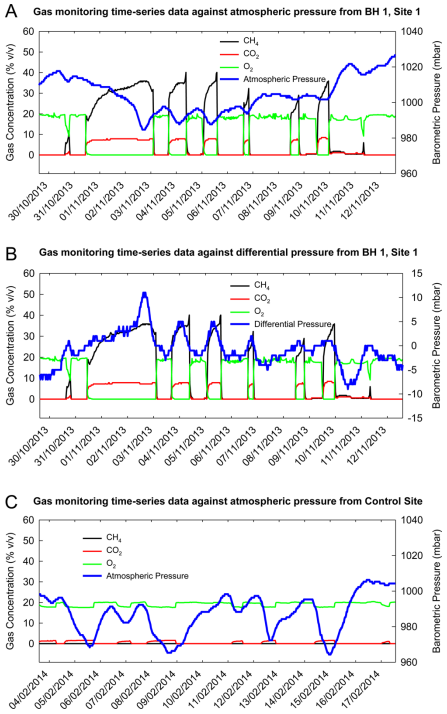

Figure 3. Gas monitoring time-series data collected from GasClam against atmospheric pressure and differential pressure (BH 1Site 1), and gas monitoring time-series data against atmospheric pressure (control site).

atmospheric pressure, usually occurring over 2−4 h and with as little as 3 mbar change in pressure. Concentrations of CH_4 and CO_2 are lower than the expected composition of landfill gas, but have not been corrected for dilution by air or N_2.

Furthermore, when the time series data are plotted against the pressure difference between atmosphere and borehole (Figure 3), it is clear that under positive pressure difference (i.e., the borehole is "blowing"), CH_4 and CO_2 are elevated within the borehole. Conversely, when negative pressure difference conditions exist, O_2 only (i.e., air) is measured in the borehole.

At the Control Site, gas monitoring data are not available for hand-held instruments. High frequency data were collected over a two week period, with the same instrument settings as at Site 1 (Figure 3). During the two week monitoring period, there were several winter storms (depressions) that crossed the UK, as shown by the pressure data. With each successive depression, the CO_2 concentration in the Control Site borehole rose to a maximum 1.3% v/v. It is assumed that this corresponds with background CO_2 that has entered the borehole from the sand formation, as a consequence of a rapid fall in atmospheric pressure. Hooker and Bannon[26] observed that typical contributions to CO_2 concentration from natural sources such as weathering of bedrock typically lie within the range 0−5% v/v. At a peak concentration of 1.3% v/v CO_2, the borehole O_2 concentration dipped to approximately 18% v/v. No CH_4 was detected. Typically, surface ground gas CH_4 concentration varies between 0.2 and 1.6 ppm (mean concentration in air); with no external source of CH_4, the concentration is not expected to exceed 0.1% v/v.[26]

High frequency data for the two-week period from BH 1 at Site 1 are plotted (Figure 4) for comparison with monitoring

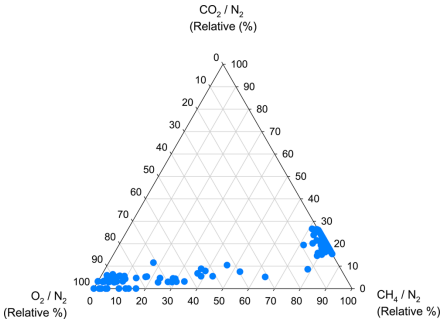

Figure 4. Ternary Plot of GasClam Data obtained from BH 1 Site 1 for the Period 29/10/2013−12/11/2013.

data for 10 years for the same borehole (as in Figure 2). In two weeks, a pattern of variation in gas composition is observed that covers the range of data observed during ten years of periodic monitoring. Additionally, mixing of air and landfill gas is more fully resolved, as demonstrated by the greater number of data points between the two end member compositions. Crucially, this demonstrates that occurrences of elevated emissions of CO_2 and CH_4 over a ten year period are much more frequent than suggested by measurement under the requirements of a normal regulatory regime.

Monitoring Wells Near a Landfill That Show Inputs to Ground Gases from Coal-Bearing Rocks. At Site 2, which overlies Coal Measures, monitoring wells are located around the landfill perimeter. From hand-held monitor generated data, the CH_4/N_2 ratio frequently exceeds 80%, suggesting a geogenic gas influence arising in two boreholes (BH 1 and BH 4). In BH 1, the array of data is consistent with mixing of air with predominantly geogenic CH_4, with some observations extending toward CO_2/N_2 that may reflect a landfill gas component.

Boreholes BH 3 and BH 4 clearly show more variable gas compositions, with CH_4/N_2 and CO_2/N_2 ratios approaching 100% (Figure 5). Compared with Site 1, where gas composition was almost exclusively air or landfill gas (with some mixing in between), boreholes at Site 2 show a more complex pattern. The complication and greater mixing of gases is most likely to be due to additional sources, and the geological characteristics of the site are consistent with the presence of geogenic gas derived from the underlying Coal Measures.

Compared with the distributions that were observed at Site 1, Figure 5 clearly shows a more CH_4-rich gas composition mixed with air. A gas with such a high CH_4 content is unlikely to be

Figure M.4: Teasdale et al. (2014) p 13613

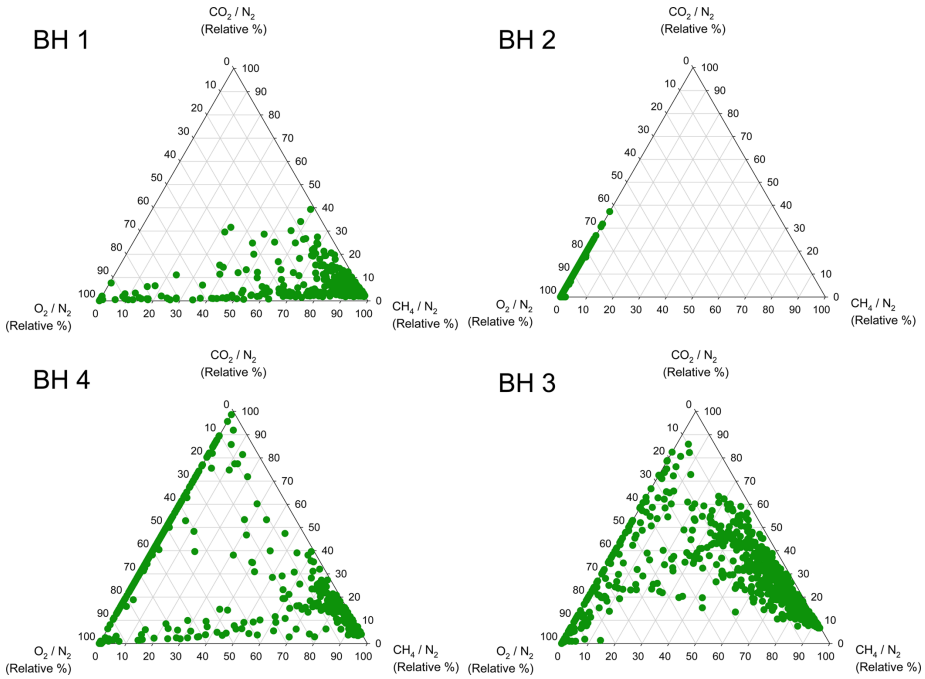

Figure 5. Gas compositions for monitoring wells at Site 2 (1998–2014).

derived from landfill (CO_2 is always present in landfill gas at these sites), and so is considered to originate from the underlying Coal Measures and to mix with landfill gas prior to entering the borehole. Migration and mixing of gas at the site can be achieved through sand lenses within glacial till, fissures and other voids (e.g., former boreholes). There is a population in the ternary diagram (Figure 5) for BH 3 around 60–70% CH_4 vs 30–40% CO_2 that likely indicates the presence of landfill gas in this monitoring well. BH 2 demonstrates a similar pattern to BH 3 at Site 1, dominated by air with a small concentration of diluted CO_2 (10–30% v/v range). Isotopic analysis of $^{13}C/^{12}C$ ratios may clarify the origin of these gases.[27] However, routine monitoring protocols exclude routine collection of these data because of cost.

DISCUSSION

The historical data measured using portable gas monitoring devices reveal patterns in gas composition that relate to the geology of the site and subsequent landfill activity, where appropriate. The high frequency monitoring of data allows temporal variability to be constrained, and indicates links with weather conditions. Taken together, these observations have significant implications for the understanding of ground gas emissions to the atmosphere with particular relevance for deep engineering activities that might perturb soil emissions, including CCS and fracking, as well as for the design of monitoring programmes

Ground Gas Emissions to the Atmosphere. Figure 6 shows a conceptual model for the migration of gas from geological and non-geological sources through different pathways to the atmosphere at locations where glacial deposits

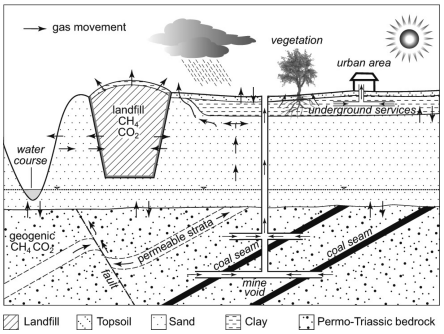

Figure 6. Conceptual model of CH_4 and CO_2 flows in the saturated and unsaturated zones.

Figure M.5: Teasdale et al. (2014) p 13614

overly coal-bearing rocks. This is a two-way process, as monitoring data clearly indicate that air enters boreholes (and other voids) in periods of high atmospheric pressure. Wherever permeable formations are exposed naturally (e.g. valley sides), air is also able to enter. Dilution of gases in a mixture by equivalent proportions occurs with the addition of one non-reactive gas component.[28] Thus, any CO_2 and CH_4 present are diluted by air (N_2 + O_2) during periods of increasing atmospheric pressure.

The sources of ground gas can be distinguished from their compositions; taking a ratio to N_2 enables the relative proportions of CH_4 and CO_2 to be determined, allowing for dilution by air. In this study, gases derived from sands overlying coal bearing rocks are shown to be richer in CH_4 than those gases derived from landfill. Historical monitoring data shows evidence of mixing of ground gas and air, to extents that vary from occasion to occasion. Observations of gas compositions at a site with neither landfill nor coal-bearing sources show that the natural ground gas is air with a small proportion of CO_2, and CH_4 below detection

In Figure 6, CH_4 and CO_2 migration may be by either advective flow or diffusion, depending on the porosity and permeability characteristics of the subsoil. The relative importance of each is not considered here, although it is evident from borehole behavior that advective flow is important in the geological materials that they penetrate.

Faults and permeable strata in the bedrock act as natural conduits for gas flow in the subsurface. Similarly, mine shafts and other voids provide man-made channels for gas to flow to the surface. In the instance of abandoned mine shafts, the height of the water table becomes an important factor in gas movement. As groundwater recharges and fills the mine void, a piston effect is achieved that drives the gas toward the surface. However, as CO_2 is 58 times more soluble in water at standard temperature and pressure (STP) than CH_4[26] a proportion of this gas may be dissolved and so removed from the system.

Examining the high temporal resolution data, it becomes clear that in addition to the potential pathways that are available to CH_4 and CO_2 in the unsaturated zone, atmospheric pressure is a key controller of gas movement. As air pressure falls, gas is released from the unsaturated zone. With increasing atmospheric pressure, air is forced into the ground, thereby producing a diluting effect on the concentration of CH_4 and CO_2. As was seen from the monitoring data, under a negative air pressure gradient, pressure in a borehole builds up and creates a positive borehole flow. In other words, the pressure in the borehole is greater than the atmosphere, giving a focused induced flow of gas from the ground to the atmosphere.

Wider Implications: Design of Monitoring Programmes. The data collected from continuous monitoring show considerable variation with time, and are consistent with the CH_4 and CO_2 data collected by hand-held meters. Using these, measurements are made at specific times/dates. If the periodicity of the sampling points is superimposed on the high frequency data series, gas composition is measured as a snapshot view of a highly variable system, and measured concentrations will vary considerably (as shown in Figures 2 and 3 in particular).

From a regulatory perspective, high temporal resolution allows a clearer understanding of the processes that are occurring in the near-surface ground gas regime. As has been noted, air pressure and depth of water table are key factors. Current UK practice is to take point measurements from all monitoring wells on a site for a minimum investigation period of 6 weeks. It is required that at least one of the point measurements needs to be taken during falling atmospheric pressure.

The data presented here show high temporal variability. The periodicity of the cycling of gases can be as short as a few hours to as long as a few days. Under current regulatory practice, two point measurements would have been made during the selected two week period shown in Figure 3. For 70% of that monitoring period, only air (N_2 + O_2) was present in the test borehole. Thus, there is a high likelihood of missing an emission event. To be certain of the ground gas regime for a site where CH_4 and CO_2 are likely to pose a hazard, a high temporal resolution data set may be required. Furthermore, a longer statutory monitoring period could be necessary to identify any longer-term seasonal variations in the ground gas regime.

Wider Implications: CCS and Hydraulic Fracturing. The monitoring data reported here demonstrate the complex behavior of gases within the vadose zone, emphasizing the highly variable nature with time of exchanges of CO_2 and CH_4 between the soil and the atmosphere. Great care needs to be taken in the interpretation of ground gas data to distinguish variation arising from meteorological controls from those arising from changes in geogenic or anthropogenic inputs, which need to be recognized in any attempt to attribute an artificial cause for an emission. It is essential that the time period for monitoring is sufficient to capture meteorological events such as a rapid reduction in atmospheric pressure, and that the frequency of sampling is small enough to determine changes arising from these. Furthermore, other practices of continuous ground gas monitoring in relation to CCS have been discussed by Schlömer et al.[29] and Schlömer et al.[30] and outline the importance of establishing baseline conditions in the vadose zone before and during operations to determine any leakages of CO_2 from geologic formations.

It is clear that from the development of a conceptual model of the ground gas regime, the principles that are applied to landfill sites are equally applicable to gas emissions from other subsurface activities including CCS and hydraulic fracturing. It is possible that leakages occur along undetected faults and fractures coupled with changes in atmospheric pressure. Without rigorous monitoring, there is potential for low intensity leakages to go undetected for prolonged periods of time.[31] For example, Klusman[32] estimated that approximately 170 tons of CO_2 was lost per annum through leakage from deep storage to the atmosphere at an enhanced oil recovery/CO_2 sequestration site at Rangely, CO. In order to establish baseline levels of CO_2, monitoring programmes are required, before injection (with respect to CCS) and continuing through operations for safety, public acceptance and model calibration.[33]

Importantly, the data presented in this paper demonstrate that ground gas compositions vary greatly with time. Conventional monitoring protocols are likely to fail to detect some emission events, and so it is important that high frequency measurements are made as part of a monitoring regime that is underpinned by a sound conceptual model of the geological characteristics of the location of interest.

Figure M.6: Teasdale et al. (2014) p 13615

■ ASSOCIATED CONTENT

Supporting Information

Additional information as noted in the text. This material is available free of charge via the Internet at http://pubs.acs.org

■ AUTHOR INFORMATION

Corresponding Author

*Email: c.j.teasdale1@newcastle.ac.uk.

Notes

The authors declare no competing financial interest.

■ ACKNOWLEDGMENTS

We thank EPSRC for financial support in the form of a DTA studentship to CJT.

■ REFERENCES

(1) IPCC. *IPCC Fourth Assessment Report: Climate Change 2007 (AR4)*; Cambridge, United Kingdom, 2007; p 996.

(2) Hansen, J.; Sato, M. Greenhouse gas growth rates. *Proc. Natl. Acad. Sci. U.S.A.* **2004**, *101* (46), 16109−16114.

(3) Hansen, J.; Johnson, D.; Lacis, A.; Lebedeff, S.; Lee, P.; Rind, D.; Russell, G. Climate impact of increasing atmospheric carbon dioxide. *Science* **1981**, *213* (4511), 957−966.

(4) Nosalewicz, M.; Brzezinska, M.; Pasztelan, M.; Sypryn, G. Methane in the environment: A review. *Acta Agrophys.* **2011**, *18* (2), 355−373.

(5) Hofmann, D. J.; Butler, J. H.; Tans, P. P. A new look at atmospheric carbon dioxide. *Atmos. Environ.* **2009**, *43* (12), 2084−2086.

(6) D'Alessandro, D. M.; Smit, B.; Long, J. R. Carbon dioxide capture: Prospects for new materials. *Angew. Chem., Int. Ed.* **2010**, *49* (35), 6058−6082.

(7) Abu-Khader, M. M. Recent progress in CO_2 capture/sequestration: A review. *Energy Sources, Part A* **2006**, *28* (14), 1261−1279.

(8) Wilson, E. J.; Johnson, T. L.; Keith, D. W. Regulating the ultimate sink: Managing the risks of geologic CO_2 storage. *Environ. Sci. Technol.* **2003**, *37* (16), 3476−3483.

(9) White, C. M.; Strazisar, B. R.; Granite, E. J.; Hoffman, J. S.; Pennline, H. W. Separation and capture of CO_2 from large stationary sources and sequestration in geological formations—Coalbeds and deep saline aquifers. *J. Air Waste Manage. Assoc.* **2003**, *53* (6), 645−715.

(10) Howarth, R. W.; Santoro, R.; Ingraffea, A. Methane and the greenhouse-gas footprint of natural gas from shale formations. *Clim. Change* **2011**, *106* (4), 679−690.

(11) Howarth, R. W.; Santoro, R.; Ingraffea, A. Venting and leaking of methane from shale gas development: Response to Cathles et al. *Clim. Change* **2012**, *113* (2), 537−549.

(12) Maier, M.; Schack-Kirchner, H. Using the Gradient method to determine soil gas flux: A review. *Agric. For. Meteorol.* **2014**, *192*, 78−95.

(13) Hirano, T.; Kim, H.; Tanaka, Y., Long-term half-hourly measurement of soil CO_2 concentration and soil respiration in a temperate deciduous forest. *J. Geophys. Res.: Atmos.* **2003**, *108* (D20).

(14) Yavitt, J. B.; Fahey, T. J.; Simmons, J. A. Methane and carbon dioxide dynamics in a northern hardwood ecosystem. *Soil Sci. Soc. Am. J.* **1995**, *59* (3), 796−804.

(15) Bergmaschi, P.; Harris, G. W. Measurements of stable isotope ratios ($^{13}CH_4/^{12}CH_4$; $^{12}CH_3D/^{12}CH_4$) in landfill methane using a tunable diode laser absorption spectrometer. *Glob. Biogeochem. Cycle* **1995**, *9* (4), 439−447.

(16) McGlade, C.; Speirs, J.; Sorrell, S. Unconventional gas—A review of regional and global resource estimates. *Energy* **2013**, *55*, 571−584.

(17) Davies, R. J. Methane contamination of drinking water caused by hydraulic fracturing remains unproven. *Proc. Natl. Acad. Sci. U.S.A.* **2011**, *108* (43), E871−E871.

(18) Davies, R. J.; Mathias, S. A.; Moss, J.; Hustoft, S.; Newport, L. Hydraulic fractures: How far can they go? *Mar. Pet. Geol.* **2012**, *37* (1), 1−6.

(19) Bachu, S. Screening and ranking of sedimentary basins for sequestration of CO_2 in geological media in response to climate change. *Environ. Geol.* **2003**, *44* (3), 277−289.

(20) Bachu, S.; Bonijoly, D.; Bradshaw, J.; Burruss, R.; Holloway, S.; Christensen, N. P.; Mathiassen, O. M. CO_2 storage capacity estimation: Methodology and gaps. *Int. J. Greenhouse Gas Control* **2007**, *1* (4), 430−443.

(21) Eccles, J. K.; Pratson, L.; Newell, R. G.; Jackson, R. B. The impact of geologic variability on capacity and cost estimates for storing CO_2 in deep-saline aquifers. *Energy Econ.* **2012**, *34* (5), 1569−1579.

(22) Department of Energy and Climate Change. The Unconventional Hydrocarbon Resources of Britain's Onshore Basins—Shale Gas. https://www.og.decc.gov.uk/UKpromote/onshore_paper/UK_onshore_shalegas.pdf (accessed October 2013).

(23) Andrews, I. J. *The Carboniferous Bowland Shale Gas Study: Geology and Resource Extimation*; British Geological Survey for the Department of Energy and Climate Change: London, UK, 2013.

(24) IonScience GasClam. Continuous Ground Gas Monitor. www.ionscience.com/products/gasclam-portable-gas-monitor (accessed 01 March 2012).

(25) Morris, P.; Todman, M.; Boult, S. *Improved Ground-Gas Risk Prediction Using In-Borehole Gas Monitoring*; Helmholtz Centre Environmental Research-Ufz: Leipzig, 2008; p 36−44.

(26) Hooker, P. J.; Bannon, P. *Methane: Its Occurrence and Hazards in Construction*; Construction Industry Research & Information Association (CIRIA); London, UK, 1993; p 137.

(27) Widory, D.; Proust, E.; Bellenfant, G.; Bour, O. Assessing methane oxidation under landfill covers and its contribution to the above atmospheric CO_2 levels: The added value of the isotope ($\delta^{13}C$ and $\delta^{18}O$ CO_2; $\delta^{13}C$ and δD CH_4) approach. *Waste Manage.* **2012**, *32* (9), 1685−1692.

(28) Romanak, K. D.; Bennett, P. C.; Yang, C. B.; Hovorka, S. D. Process-based approach to CO_2 leakage detection by vadose zone gas monitoring at geologic CO_2 storage sites. *Geophys. Res. Lett.* **2012**, *39*, 6.

(29) Schlömer, S.; Furche, M.; Dumke, I.; Poggenburg, J.; Bahr, A.; Seeger, C.; Vidal, A.; Faber, E. A review of continuous soil gas monitoring related to CCS—Technical advances and lessons learned. *Appl. Geochem.* **2013**, *30*, 148−160.

(30) Schlömer, S.; Muller, I.; Furche, M. Baseline soil gas measurements as part of a monitoring concept above a projected CO_2 injection formation: A case study from Northern Germany. *Int. J. Greenhouse Gas Control* **2014**, *20*, 57−72.

(31) Harvey, O. R.; Qafoku, N. P.; Cantrell, K. J.; Lee, G.; Amonette, J. E.; Brown, C. F. Geochemical implications of gas leakage associated with geologic CO_2 storage—A qualitative review. *Environ. Sci. Technol.* **2013**, *47* (1), 23−36.

(32) Klusman, R. W. Rate measurements and detection of gas microseepage to the atmosphere from an enhanced oil recovery/sequestration project, Rangely, Colorado, USA. *Appl. Geochem.* **2003**, *18* (12), 1825−1838.

(33) Korre, A.; Imrie, C. E.; May, F.; Beaubien, S. E.; Vandermeijer, V.; Persoglia, S.; Golmen, L.; Fabriol, H.; Dixon, T. Quantification techniques for potential CO_2 leakage from geological storage sites. In *10th International Conference on Greenhouse Gas Control Technologies*, 2011; Vol. *4*, pp 3413−3420.

Figure M.7: Teasdale et al. (2014) p 13616

Appendix N

Teasdale et al. (2015)

Theme 1. Dealing with contamination of soil, groundwater and sediment
1a. Assessment and monitoring

GROUND GAS MONITORING: EXAMINING SPATIAL TRENDS ON SHORT AND LONG TEMPORAL SCALES

Christopher J. Teasdale[1], Jean A. Hall[1], John P. Martin[2] and David A. C. Manning[1]

1. School of Civil Engineering & Geosciences, Newcastle University, Newcastle upon Tyne, UK, NE1 7RU
2. TerraConsult Ltd, Bold Business Centre, Bold Lane, Sutton, St Helens, Merseyside, UK, WA9 4TX

KEYWORDS

Carbon dioxide, methane, ground gas, monitoring, landfill, Coal Measures, high temporal frequency

ABSTRACT

Understanding the exchange of carbon dioxide (CO_2) and methane (CH_4) between the geosphere and atmosphere is essential for the management of anthropogenic emissions. In this paper an innovative approach of expressing ground gas compositions is presented, using data derived from regulatory monitoring of boreholes in the unsaturated zone at infrequent intervals (typically 3 months) with data from a high frequency monitoring instrument measuring half-hourly over periods of weeks. Similar highly variable trends are observed for timescales ranging from decades to hourly for boreholes located close to sanitary landfill sites. Additionally, high frequency monitoring data confirm the effect of meteorological controls on ground gas emissions. For a two week monitoring period, only air was present in a borehole during 70% of the data capture. There is a clear weakness in current point monitoring strategies that may miss emission events and this needs to be considered along with obtaining baseline data prior to starting any engineering activity.

INTRODUCTION

The exchange of carbon dioxide (CO_2) and methane (CH_4) between the geosphere and atmosphere is a key component of the global carbon cycle. At the advent of industrialisation, atmospheric CO_2 concentration was 280 ppm and has subsequently increased so that it now exceeds 400 ppm (IPCC, 2007). This figure is projected to reach 600-800 ppm by the close of the century (IPCC, 2007). It is believed that the rise in CO_2 concentration in the Earth's atmosphere is linked to global climate change (Hansen and Sato, 2004, Hansen et al., 1981). With a global warming potential (GWP) 21 times greater than CO_2 (Nosalewicz et al., 2011), CH_4 emission to the atmosphere is considered to be one of the greatest environmental challenges of the 21st Century. In addition to emission of CO_2 from the combustion of fossil fuels, which account for the major part of the post-industrial increase (Hofmann et al., 2009), CO_2 exchange between the coupled plant-soil system and the atmosphere is a major control of atmospheric CO_2.

Emissions of gases from soils vary in their origin. Near surface fluxes of CO_2 and CH_4 from biologically-active soils occur in response to microbial respiration, and occur rapidly after the formation of the gas (Maier and Schack-Kirchner, 2014). Concentrations of CO_2 and CH_4 in soils dominated by plant roots and associated microbial systems are typically very low, below 1% v/v (Hirano et al., 2003). Below the biologically-active soil, sedimentary geological processes produce CO_2 and CH_4. Proportions vary according to specific geological circumstances. Natural fluxes of CO_2 and CH_4 to the atmosphere include contributions from both geological and biological sources. Artificial sources of gases within soil include sanitary landfill, where anaerobic microbial processes characteristically produce gas containing up to 70% CH_4 and 30% CO_2 (Bergmaschi and Harris, 1995, Yavitt et al., 1995). Geological gases migrate through permeable and fractured formations until trapped or released to the atmosphere. Similarly, gases produced in landfills migrate laterally as well as vertically, if containment systems fail. Monitoring systems in the vicinity of landfills are designed to detect migration, so that appropriate action can be taken.

For well-informed management of deep engineering processes that have the potential to affect greenhouse gas emissions, there is a need to understand the background levels of CH_4 and CO_2 in soils, superficial unconsolidated sediment deposits and groundwater systems and, importantly, the extent of their temporal variability. In northern England, the compositions of gases within shallow

Figure N.1: Teasdale et al. (2015) p 1

unconsolidated sands capped by glacial till are specifically considered as unsaturated sands are a potential gas migration pathway. Landfills have been constructed in these formations, and monitoring regimes are in place to assess the integrity of containment, with boreholes outside the landfill to permit determination of gas compositions and so detect any migration. Thus, there is access to a resource of historical monitoring data that extends back several decades. CO_2 and CH_4 in the sands may be derived from sources other than landfill, including natural migration from underlying strata, in this case, coal-bearing. In this paper, historic periodic and recent high frequency monitoring data obtained from outside landfill sites are compared, with reference to data from a site with a similar geological setting but distant from landfill. The use of different temporal scales of observation has major implications for the planning and interpretation of ground gas monitoring procedures, with a wide range of applications. The work presented here extends material previously published by Teasdale et al. (2014).

DATA COMPILATION

Data Sources

Monitoring data were obtained for two landfill sites in Cheshire, UK. The sites differ geologically and produce contrasting gas signatures. Site 1, a closed landfill, is situated in thick Quaternary deposits with no known potential external (geological) source of CH_4 or CO_2. Conversely, Site 2 is situated in Quaternary deposits overlying thin Permo-Triassic bedrock, with underlying Coal Measures (Carboniferous; Westphalian) which provide a potential source of geogenic gas. Additionally, Site 2 is adjacent to a second older landfill, constructed to a lower technical specification. The Control Site was chosen at a location with similar geology to Site 1, but with no associated landfill and so is used as a control. Details of the ground conditions at each site can be found in Teasdale et al. (2014).

Historic Measurement of Gas Composition

Historically, gas composition has been measured in accordance with regulatory requirements using hand-held gas monitors, as frequently as daily (Site 2) to as infrequently as quarterly (Site 1). Measurements were made using a Geotech UK GA2000 Landfill Gas Analyser until 2012, after which a Gas Data Ltd GFM435 Landfill Gas Analyser was used. One of the limitations of changes of instrumentation over a period of several years is that data sets may not be directly comparable. Both gas monitoring instruments employ a dual beam infrared absorption method to quantify the concentration of CH_4, CO_2 and O_2 in a flowing gas. The balance is assumed to be nitrogen (N_2). However, the instruments differ in their measurement of borehole flow. The GA2000 pressure transducer is equipped with a set resistor in order to minimise flow. It is argued that this will more closely reflect true borehole conditions as the act of opening the borehole valve will disrupt equilibrium conditions. Conversely, the GFM435 pressure transducer does not have this specification.

Measurement of Gas Composition at High Temporal Resolution

High temporal resolution data capture was achieved using a GasClam instrument, by which gas compositions can be recorded at intervals as short as three minutes (IonScience, 2012). The GasClam also records atmospheric pressure and temperature as well as gas concentration, avoiding an additional limitation of hand-held gas monitors (Morris et al., 2008). The instrument has, according to the manufacturer, a range 0-100% for CH_4 and CO_2, with a stated detection limit of 0.1% for both gases. In practice, observed non-zero minimum CH_4 and CO_2 concentrations were 0.4% and 0.1% respectively, and observed maximum values were 57.1% and 10.8% respectively.

ANALYSIS OF GAS MONITORING DATA

Two graphical approaches have been used to present the gas monitoring data. In the first, compositional data are compared in terms of the measured CH_4, CO_2 and O_2 content normalised to N_2 (assuming N_2 to be the balance, i.e. $100 – (\Sigma\ CH_4, + CO_2 + O_2)$), in a ternary plot. This allows the relative proportions of CH_4 and CO_2 to be compared irrespective of any dilution by air, the O_2/N_2 ratio indicating whether this has occurred and the extent to which oxygen has been removed, as N_2 can be regarded as non-reactive (Bergmaschi and Harris, 1995). In a plot of this type (which is analogous to the Piper diagram in hydrogeology), 'end member' compositions can be identified, so that an array of observed data points can be explained as mixtures of gases from different sources, and the

Figure N.2: Teasdale et al. (2015) p 2

characteristics of one borehole can be compared with another. The second graphical approach is to show variation with time in absolute gas concentration (% v/v) measured at high frequency and how this is affected by atmospheric pressure conditions.

Monitoring Wells near a Landfill where there is no Known Input from Coal-Bearing Rocks (Site 1)

Figure 1 shows the gas composition recorded over a period of 10 years in boreholes at Site 1. BH 1 is located on the southern boundary of the landfill and produced a CH_4-rich gas signature (70:30 CH_4/CO_2) which is attributed to landfill gas given the close proximity of the borehole to the edge of the landfill. Values recorded at 100% O_2/N_2 correspond to air. There is some evidence of mixing between landfill gas and air at this location, but this was observed on few occasions (points between the two end member compositions).

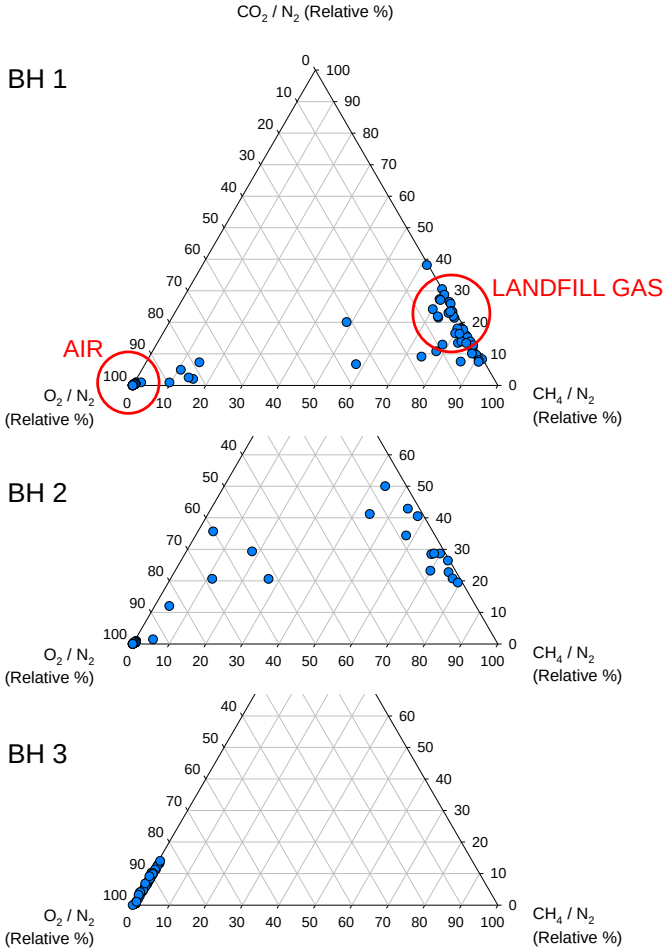

Figure 1 Gas compositions for monitoring wells on Site 1 (2004-2014), indicating (Figure 2a) expected plotting positions of landfill gas and air.

Figure N.3: Teasdale et al. (2015) p 3

BH 2 is approximately 25 metres south of the landfill perimeter, and shows a more diffuse scatter of data. There is still a strong indication of the presence of landfill gas but the proportion of CH_4 is lower (Figure 2), suggesting mixing with more CO_2-rich gas, or removal of CH_4 by biological processes. BH 3, 100 m away from the landfill, records no landfill gas (Figure 2).

High frequency Monitoring where there is no Known Input from Coal-Bearing Rocks (Site 1)

Gas compositions were measured at Site 1, borehole BH 1, on a thirty minute sampling frequency program with the instrument vent closed to ensure that borehole conditions were not disturbed during sampling. Figure 2 shows the results of sampling for a two week period starting Monday 29th October 2013.

During this period, there were three successive rises and falls in atmospheric pressure. The falls occurred on 2nd, 3rd and 5th November, each with similar gradients (average -0.8 mbar/hr). Accordingly, with each fall, corresponding peak concentrations of CH_4 (up to 40%) and CO_2 (up to 10%) were observed, the balance being N_2. As CH_4 and CO_2 appear in the borehole, O_2 concentration decreases to 0% from atmospheric concentration (~20%). For the observed borehole, the change is very sensitive to atmospheric pressure, usually occurring over 2 to 4 hours and with as little as 3 mbar change in pressure. Concentrations of CH_4 and CO_2 are lower than the expected composition of landfill gas, but have not been corrected for dilution by air or N_2.

Furthermore, when the time series data are plotted against the pressure difference between atmosphere and borehole (Figure 2), it is clear that under positive pressure difference (i.e. the borehole is 'blowing'), CH_4 and CO_2 are elevated within the borehole. Conversely, when negative pressure difference conditions exist, O_2 only (i.e. air) is measured in the borehole. This is in close agreement with the work of Czepiel et al. (2003) and Gebert and Gröngröft (2006) who determined a strong negative correlation between atmospheric pressure and CH_4 emissions over a landfill.

At the Control Site, gas monitoring data are not available for hand-held instruments. High frequency data were collected over a two week period, with the same instrument settings as at Site 1 (Figure 2). During the two week monitoring period, there were several winter storms (depressions) that crossed the UK, as shown by the pressure data. With each successive depression, the CO_2 concentration in the Control Site borehole rose to a maximum 1.3% v/v. It is assumed that this corresponds with background CO_2 that has entered the borehole from the sand formation, as a consequence of a rapid fall in atmospheric pressure. Hooker and Bannon (1993) observed that typical contributions to CO_2 concentration from natural sources such as weathering of bedrock typically lie within the range 0-5% v/v. At a peak concentration of 1.3% v/v CO_2, the borehole O_2 concentration dipped to approximately 18% v/v. No CH_4 was detected. Typically, surface ground gas CH_4 concentration varies between 0.2 and 1.6 ppm (mean concentration in air); with no external source of CH_4, the concentration is not expected to exceed 0.1 % v/v (Hooker and Bannon, 1993).

Figure N.4: Teasdale et al. (2015) p 4

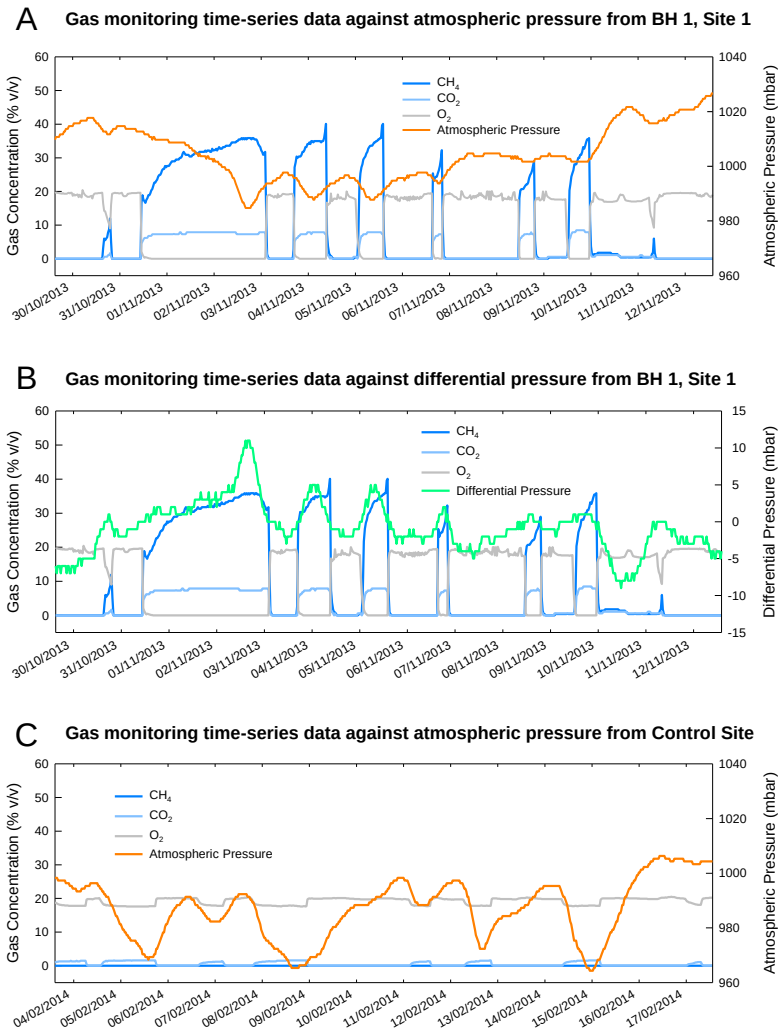

Figure 2 Gas monitoring time-series data collected from GasClam against atmospheric pressure and differential pressure (BH 1 Site 1), and gas monitoring time-series data against atmospheric pressure (Control Site)

High frequency data for the two-week period from BH 1 at Site 1 are plotted (Figure 3) for comparison with monitoring data for 10 years for the same borehole (as in Figure 1). In two weeks, a pattern of variation in gas composition is observed that covers the range of data observed during ten years of periodic monitoring. Additionally, mixing of air and landfill gas is more fully resolved, as demonstrated by the greater number of data points between the two end member compositions. Crucially, this demonstrates that occurrences of elevated emissions of CO_2 and CH_4 over a ten year period are much more frequent than suggested by measurement under the requirements of a normal regulatory regime.

Figure N.5: Teasdale et al. (2015) p 5

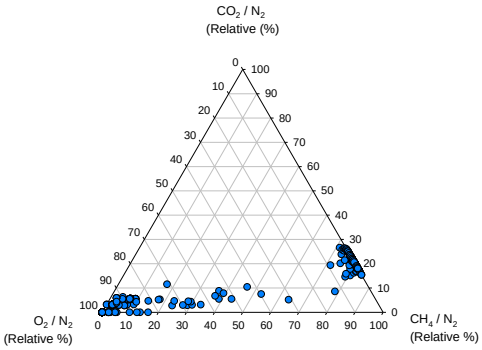

Figure 3 Ternary Plot of high frequency monitoring data obtained from BH 1 Site 1 for the Period 29/10/2013 – 12/11/2013

Monitoring Wells near a Landfill that Show Inputs to Ground Gases from Coal-Bearing Rocks (Site 2)

At Site 2, which overlies Coal Measures, monitoring wells are located around the landfill perimeter. From hand-held monitor generated data, the CH_4/N_2 ratio frequently exceeds 80%, suggesting a geogenic gas influence arising in two boreholes (BH W and BH Y). In BH W, the array of data is consistent with mixing of air with predominantly geogenic CH_4, with some observations extending towards CO_2/N_2 that may reflect a landfill gas component.

Boreholes BH Y and BH Z clearly show more variable gas compositions, with CH_4/N_2 and CO_2/N_2 ratios approaching 100% (Figure 4). Compared with Site 1, where gas composition was almost exclusively air or landfill gas (with some mixing in between), boreholes at Site 2 show a more complex pattern. The complication and greater mixing of gases is most likely to be due to additional sources associated with the geological characteristics of the site. The CH_4-rich compositions observed are consistent with the presence of geogenic gas derived from underlying Coal Measures.

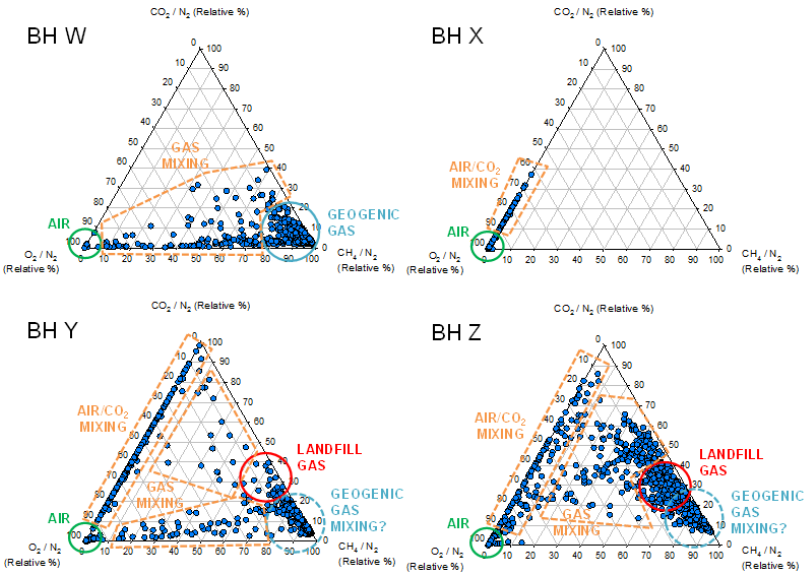

Figure 4 Gas compositions for monitoring wells at Site 2 (1998-2014)

Figure N.6: Teasdale et al. (2015) p 6

A gas with such a high CH_4 content is unlikely to be derived from landfill (CO_2 is always present in landfill gas at these sites), and so is considered to originate from the underlying Coal Measures and to mix with landfill gas prior to entering the borehole. Migration and mixing of gas at the site can be achieved through sand lenses within till, fissures and other voids (e.g. former boreholes). There is a population in the ternary diagram (Figure 4) for BH Y around 60-70% CH_4 vs 30-40% CO_2 that likely indicates the presence of landfill gas in this monitoring well. BH X demonstrates a similar pattern to BH 3 at Site 1, dominated by air with a small concentration of diluted CO_2 (10-30% v/v range). Isotopic analysis of $^{13}C/^{12}C$ ratios may clarify the origin of gases at Site 2 (Widory et al., 2012). However, cost constraints of routine monitoring protocols preclude collection of this data type.

High frequency Monitoring near a Landfill that Show Inputs to Ground Gases from Coal-Bearing Rocks (Site 2)

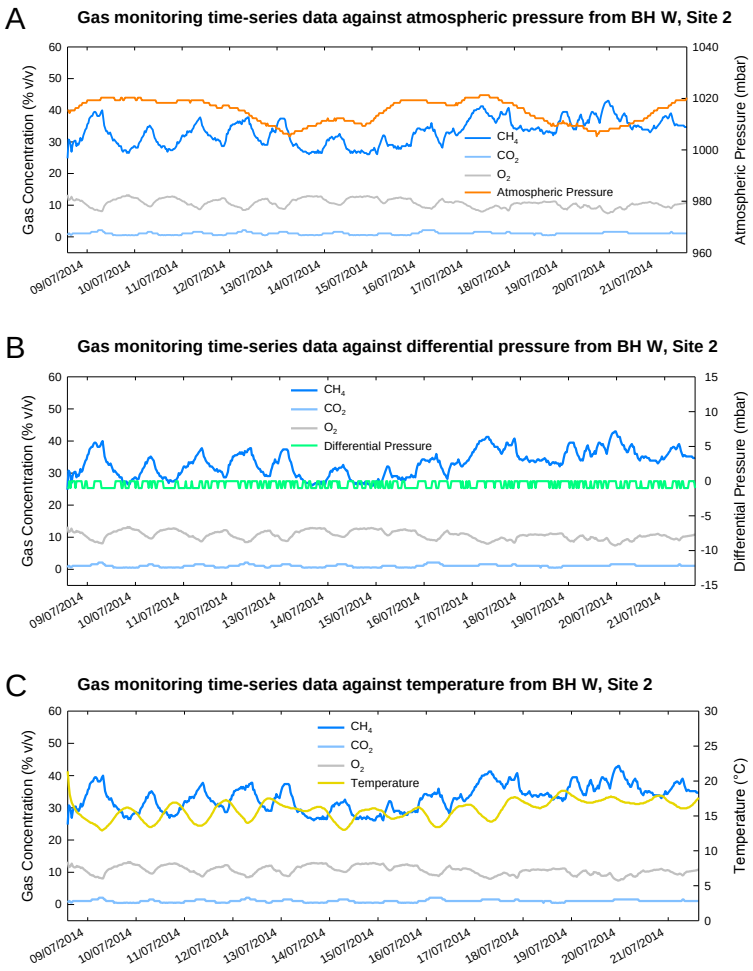

Figure 5 Gas monitoring time-series data collected from GasClam against atmospheric pressure, differential pressure and temperature at BH W, Site 2 (08/07/2014 – 21/07/2014)

Figure N.7: Teasdale et al. (2015) p 7

An immediately obvious limitation of the GasClam device is that multiple instruments are required to sample multiple boreholes simultaneously at high frequency. Data sets are not directly comparable as recordings were made during different conditions. The intended purpose is to illustrate the variability in the data, different timescales and comparisons with other sites.

Shown in Figure 5 is the variation in ground gas composition for BH W at Site 2 measured using the same protocols as at Site 1. Temperature appears to be the key influence on emissions of CH_4 and CO_2 for this monitoring well. CH_4 and CO_2 are negatively correlated with temperature while O_2 concentration is positively correlated with temperature and variability in gas composition can be ascribed to a diurnal timescale. However, the data presented here is more complex than diurnal cycling, as shown in Figure 6.

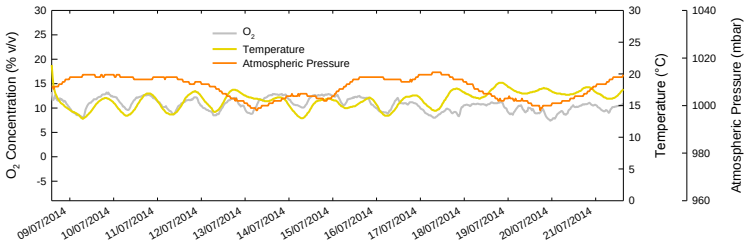

Figure 6 O_2 concentration time-series data against atmospheric pressure and temperature from BH W, Site 2 (08/07/2014 – 21/07/2014)

During periods of static high pressure (08/07/2014 – 12/07/2014), ambient temperature is the main control on gas composition and a close relationship exists that varies on a diurnal time scale. However, when atmospheric pressure decayed by 12 mbar (12/07/2014-13/07/2014), the correlation weakened, but stabilised once more when atmospheric pressure increased and stabilised at 1013 mbar on 14/07/2014. While the relationship with atmospheric pressure is less explicit for BH W, Site 2, it still has an influencing role.

As for BH 1, Site 1, that was located on the landfill perimeter, the high frequency resolution data from BH W, Site 2, may be normalised to N_2 and transformed into a ternary plot as shown in Figure 7.

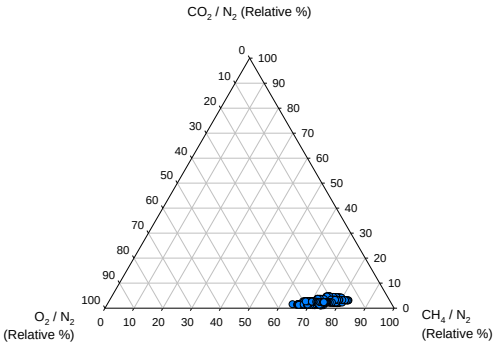

Figure 7 Ternary Plot of High Temporal Frequency Data obtained from BH W Site 2 for the Period 08/07/2014 – 21/07/2014

Unlike the point measurement data obtained over a 16 year period that shows gas composition approaching CH_4/N_2 end member concentration and a greater spread (mixing) of gases, the selected two week period consistently shows a strong CH_4 concentration (65-85%) with very little CO_2 contribution (typically less than 4%). This supports the case for a geogenic gas source.

Figure N.8: Teasdale et al. (2015) p 8

DISCUSSION

The historical data measured using portable gas monitoring devices reveal patterns in gas composition that relate to the geology of the site and subsequent landfill activity, where appropriate. The high frequency monitoring of data allows temporal variability to be constrained, and indicates links with weather conditions. Taken together, these observations have significant implications for the understanding of ground gas emissions to the atmosphere with particular relevance for deep engineering activities that might perturb ground emissions, as well as for the design of monitoring programmes

Ground Gas Emissions to the Atmosphere

Gas may migrate from geological and non-geological sources through different pathways to the atmosphere at locations where glacial deposits overly coal-bearing rocks. This is a two-way process, as monitoring data clearly indicate that air enters boreholes (and other voids) in periods of high atmospheric pressure; it will also enter permeable formations wherever they are exposed naturally (e.g. valley sides). Dilution of gases in a mixture by equivalent proportions occurs with the addition of one non-reactive gas component (Romanak et al., 2012). Thus, any CO_2 and CH_4 present are diluted by air (N_2 + O_2) during periods of increasing atmospheric pressure.

The sources of ground gas can be distinguished from their compositions; taking a ratio to N_2 enables the relative proportions of CH_4 and CO_2 to be determined, allowing for dilution by air. In this study, gases derived from sands overlying coal bearing rocks are shown to be richer in CH_4 than those gases derived from landfill. Historical monitoring data shows evidence of mixing of ground gas and air, to extents that vary from occasion to occasion. Observations of gas compositions at a site with neither landfill nor coal-bearing sources show that the natural ground gas is air with a small proportion of CO_2, and CH_4 below detection

Faults and permeable strata in the bedrock act as natural conduits for gas flow in the subsurface. Similarly, mine shafts and other voids provide man-made channels for gas to flow to the surface. In the instance of abandoned mine shafts, the height of the water table becomes an important factor in gas movement. As the groundwater recharges and fills the mine void, a piston effect is achieved that drives the gas towards the surface. However, as CO_2 is 58 times more soluble in water at standard temperature and pressure (STP) than CH_4 (Hooker and Bannon, 1993) a proportion of this gas may be dissolved and so removed from the system.

Examining the high temporal resolution data, it becomes clear that in addition to the potential pathways that are available to CH_4 and CO_2 in the unsaturated zone, atmospheric pressure is a key controller of gas movement. As air pressure falls, gas is released from the unsaturated zone. With increasing atmospheric pressure, air is forced into the ground, thereby producing a diluting effect on the concentration of CH_4 and CO_2. As was seen from the monitoring data, under a negative air pressure gradient, pressure in a borehole builds up and creates a positive borehole flow. In other words, the pressure in the borehole is greater than the atmosphere, giving a focused induced flow of gas from the ground to the atmosphere.

Wider Implications: Design of Monitoring Programmes

The data collected from continuous monitoring show considerable variation with time, and are consistent with the CH_4 and CO_2 data collected by hand-held meters. Using these, measurements are made at specific times/dates. If the periodicity of the sampling points is superimposed on the high frequency data series, gas composition is measured as a snapshot view of a highly variable system, and measured concentrations will vary considerably (as shown in Figure 1 andFigure 2 in particular).

From a regulatory perspective, high temporal resolution allows a clearer understanding of the processes that are occurring in the near-surface ground gas regime. As has been noted, air pressure and depth of water table are key factors. Current UK practice is to take point measurements from all monitoring wells on a site for a minimum investigation period. It is required that at least one of the point measurements needs to be taken during falling atmospheric pressure.

The data presented here show high temporal variability. The periodicity of the cycling of gases can be as short as a few hours to as long as a few days. Under current regulatory practice, two point measurements would have been made during the selected two week period shown in Figure 2. For 70% of that monitoring period, only air (N_2 + O_2) was present in the test borehole. Thus there is a high likelihood of missing an emission event. To be certain of the ground gas regime for a site where CH_4 and CO_2 are likely to pose a hazard, a high temporal resolution data set may be required.

Figure N.9: Teasdale et al. (2015) p 9

Furthermore, a longer statutory monitoring period could be necessary to clarify short-term diurnal trends and identify any longer-term seasonal/annual variations in the ground gas regime.

ACKNOWLEDGEMENTS

The authors would like to thank EPSRC for financial support in the form of a DTA studentship to CJT.

REFERENCES

BERGMASCHI, P. & HARRIS, G. W. 1995. Measurements of Stable Isotope Ratios ($^{13}CH_4/^{12}CH_4$; $^{12}CH_3D/^{12}CH_4$) in Landfill Methane using a Tunable Diode Laser Absorption Spectrometer. *Global Biogeochemical Cycles,* 9**,** 439-447.

CZEPIEL, P. M., SHORTER, J. H., MOSHER, B., ALLWINE, E., MCMANUS, J. B., HARRIS, R. C., KOLB, C. E. & LAMB, B. K. 2003. The Influence of Atmospheric Pressure on Landfill Methane Emissions. *Waste Management,* 23**,** 593-598.

GEBERT, J. & GRÖNGRÖFT, A. 2006. Passive Landfill Gas Emission: Influence of Atmospheric Pressure and Implications for the Operation of Methane-Oxidising Biofilters. *Waste Management,* 26**,** 245-251.

HANSEN, J., JOHNSON, D., LACIS, A., LEBEDEFF, S., LEE, P., RIND, D. & RUSSELL, G. 1981. Climate Impact of Increasing Atmospheric Carbon Dioxide. *Science,* 213**,** 957-966.

HANSEN, J. & SATO, M. 2004. Greenhouse Gas Growth Rates. *Proceedings of the National Academy of Sciences of the United States of America,* 101**,** 16109-16114.

HIRANO, T., KIM, H. & TANAKA, Y. 2003. Long-Term Half-Hourly Measurement of Soil CO_2 Concentration and Soil Respiration in a Temperate Deciduous Forest. *Journal of Geophysical Research-Atmospheres,* 108.

HOFMANN, D. J., BUTLER, J. H. & TANS, P. P. 2009. A New Look at Atmospheric Carbon Dioxide. *Atmospheric Environment,* 43**,** 2084-2086.

HOOKER, P. J. & BANNON, P. 1993. *Methane: Its Occurrence and Hazards in Construction,* London, UK, Construction Industry Research & Information Association (CIRIA).

IONSCIENCE. 2012. *GasClam® Continuous Ground Gas Monitor* [Online]. Available: www.ionscience.com/products/gasclam-portable-gas-monitor [Accessed 01 March 2012].

IPCC 2007. IPCC Fourth Assessment Report: Climate Change 2007 (AR4). *In:* SOLOMON, S., QIN, D., MANNING, M., CHEN, Z., MARQUIS, M., AVERYT, K. B., TIGNOR, M. & MILLER, H. L. (eds.) *Contribution of Working Group I to the Fourth Assessment Report of the IPCC.* Cambridge, United Kingdom.

MAIER, M. & SCHACK-KIRCHNER, H. 2014. Using the Gradient Method to Determine Soil Gas Flux: A Review. *Agricultural and Forest Meteorology,* 192**,** 78-95.

MORRIS, P., TODMAN, M., BOULT, S. & HELMHOLTZ CENTRE ENVIRONMENTAL, R.-U. 2008. *Improved Ground-Gas Risk Prediction Using In-Borehole Gas Monitoring,* Leipzig, Helmholtz Centre Environmental Research-Ufz.

NOSALEWICZ, M., BRZEZINSKA, M., PASZTELAN, M. & SYPRYN, G. 2011. Methane in the Environment: A Review. *Acta Agrophysica,* 18**,** 355-373.

ROMANAK, K. D., BENNETT, P. C., YANG, C. B. & HOVORKA, S. D. 2012. Process-Based Approach to CO_2 Leakage Detection by Vadose Zone Gas Monitoring at Geologic CO_2 Storage Sites. *Geophysical Research Letters,* 39**,** 6.

TEASDALE, C. J., HALL, J. A., MARTIN, J. P. & MANNING, D. A. C. 2014. Ground Gas Monitoring: Implications for Hydraulic Fracturing and CO_2 Storage. *Environmental Science & Technology,* 48**,** 13610-13616.

WIDORY, D., PROUST, E., BELLENFANT, G. & BOUR, O. 2012. Assessing Methane Oxidation under Landfill Covers and its Contribution to the above Atmospheric CO_2 Levels: The Added Value of the Isotope ($\delta^{13}C$ and $\delta^{18}O$ CO_2; $\delta^{13}C$ and δD CH_4) Approach. *Waste Management,* 32**,** 1685-1692.

YAVITT, J. B., FAHEY, T. J. & SIMMONS, J. A. 1995. Methane and Carbon Dioxide Dynamics in a Northern Hardwood Ecosystem. *Soil Science Society of America Journal,* 59**,** 796-804.

Figure N.10: Teasdale et al. (2015) p 10

Christopher Teasdale
c.j.teasdale1@ncl.ac.uk

GROUND GAS MONITORING

Newcastle University
School of Civil Engineering &Geosciences

Examining Spatial Trends on Short and Long Temporal Scales

Introduction

The exchange of CO_2 and CH_4 between the geosphere and atmosphere is a key component of the global carbon cycle. Emissions from the ground vary in origin. Near-surface fluxes occur due to microbial respiration. Below biologically-active soil, geological processes produce CO_2 and CH_4. Monitoring wells are used to measure these gases.

The research sites are located in north-west England, UK, above the Bowland-Hodder Unit, an area of possible shale gas exploration. Data indicate temporal variability of ground gas in Quaternary sands (unconsolidated) that are capped by glacial till below the root zone.

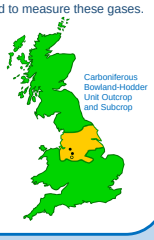

Point Measurement Monitoring

- Infrared analysis of CH_4, CO_2 and LEL (0-100%).
- Electrochemical analysis of O_2 (0-25%), CO (0-2,000 ppm) and H_2S (0-5000 ppm).
- GA2000 has since been updated to GA5000.
- Using different instruments may mean data sets are not directly comparable.
- Point measuring gases does not resolve relationship with pressure.

Geotech UK GA2000

Gas Data Ltd GFM435

Ground Gas Movement

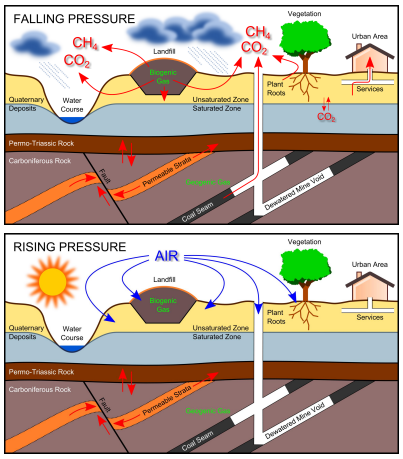

The biogenic gas component will typically generate a gas pressure that exceeds the differential pressure caused by changes in air pressure. This pressure gradient is greater when atmospheric pressure is falling. During rising pressure conditions, CH_4 will also be oxidised to CO_2 by mixing with air.

Data Analysis

Two graphical approaches are used to present gas monitoring data. In the first, CH_4, CO_2 and O_2 content are normalised to N_2 in a ternary plot. This allows the relative proportions of CH_4 and CO_2 to be compared irrespective of dilution by air. The O_2/N_2 ratio indicates whether this has occurred. Gas concentration (% v/v) measured at high frequency is plotted as a time-series in the second graphical approach.

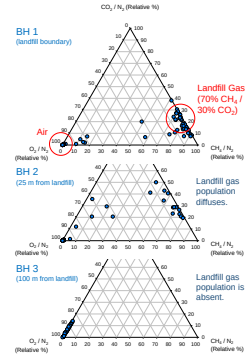

Ground Gas Compositions with increasing distance from landfill collected from point measurements over one decade (2004-2014)

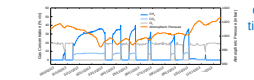

- Gas compositions for BH 1 measured at half-hourly intervals with GasClam.
- Valve closed to maintain equilibrium.
- Falls in atmospheric pressure with average gradient -0.8 mbar/hr recorded.
- Peak concentrations of 40% CH_4 and 10% CO_2 from 0% (O_2 falling to 0% from ~20%).

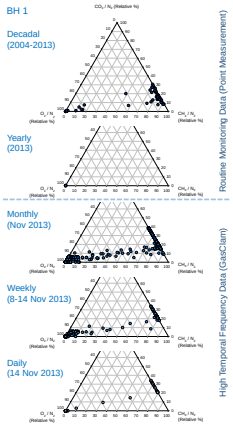

- High temporal frequency data captured by GasClam shows that gas compositions obtained from point measurement data over a ten year period can occur over much shorter time periods such as days.
- Nov 2013 data resolves the landfill gas mixing with air.
- Quarterly point measurements made with GFM435 in 2013 missed gas emission events.

GasClam time-series

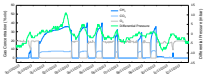

- Pressure difference between ground and atmosphere.
- Differential pressure increases as atmospheric pressure decreases.
- Positive pressure gradient results in release of gas to atmosphere.

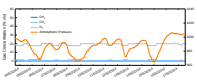

- Control Site.
- Sand quarry, no known landfill or geogenic gas sources.
- Maximum CO_2 concentration 1.3% from 0% (O_2 falling to 18% from ~20%).
- No CH_4.

High Frequency Monitoring

GasClam®

- Developed by Salamander Group, UK.
- Fully automated high temporal frequency data capture.
- Samples up to every 3 minutes, battery life of 3 months.
- Analysis of landfill gases: CH_4, CO_2, H_2S, CO and VOCs.

Summary

Current point measurement of ground gases may miss emission events. High temporal measurement resolves relationship with atmospheric pressure. Cycling of gases may occur over periods as short as a few hours to as long as a few days. Baseline data may be required prior to starting engineering activities.

EPSRC

Christopher J. Teasdale[1], Jean A. Hall[1], John P. Martin[2], David A. C. Manning[1]
1. School of Civil Engineering and Geosciences, Newcastle University, Newcastle upon Tyne, UK, NE1 7RU
2. TerraConsult Ltd, Bold Business Centre, Bold Lane, Sutton, St Helens, Merseyside, UK, WA9 4TX

TerraConsult

Figure N.11: Teasdale et al. (2015) AquaConSoil Conference Poster